GL01145

SOCIETY OF MINING ENGINEERS of AIME
345 EAST 47TH STREET, NEW YORK, N. Y. 10017

PREPRINT NUMBER
69-B-64

RELATING PELLET QUALITY TO OPERATIONAL VARIABLES THROUGH OXIDATION MEASUREMENTS

R. R. Beebe
Process Development Supervisor

M. J. Fraser
Product Development Supervisor

Marcona Corporation
One Maritime Plaza
San Francisco, California 94111

This paper is to be presented at the Annual Meeting of the American Institute of Mining, Metallurgical and Petroleum Engineers, Washington, D. C., February 16-20, 1969.

69-B-64

RELATING PELLET QUALITY TO OPERATIONAL VARIABLES THROUGH OXIDATION MEASUREMENTS

by

R. R. Beebe, Process Development Supervisor

and

M. J. Fraser, Product Development Supervisor

Marcona Corporation
One Maritime Plaza
San Francisco, California 94111

INTRODUCTION

Marcona Corporation produces about 3.5 million long tons of iron ore pellets annually on its two travelling grate pelletizing machines at San Nicolas, Peru. During 1969, these pellets will be shipped to customers in four marketing areas--Japan, the United States, Europe, and South America. All of these sales are on the open market, and product quality is a major concern.

Typical chemical, structural, and quality test results for Marcona pellets are given in Table 1.

TABLE 1. TYPICAL QUALITY OF MARCONA PELLETS

	%		%
Fe	65.4	+5/8"	3.9
Cu	0.013	-5/8" +3/8"	89.6
S	0.025	-3/8" +1/4"	3.9
P	0.009	-1/4"	2.6
SiO_2	3.90	Tumble Index (JIS +1 mm)	= 96.9%
Al_2O_3	0.96	Tumble Index (ASTM +1/4")	= 94.7%
CaO	0.38	Average Compression Strength	= 485 lb/pellet
MgO	0.80	Gakushin Swelling Index	= 13.9% (volume)

These quality levels must be maintained and improved to continue to meet the requirements of blast furnace operators throughout the world.

In all pelletizing operations, great efforts are made to relate ore characteristics and beneficiation procedures to pellet quality parameters. At Marcona, these efforts take the form of rigorous supervision and process control by the plant operators, testwork by process development personnel in Peru, review of operating data by the corporate development group, and basic and applied research at universities and contract laboratories. This paper outlines the general relationships between Marcona ore characteristics, beneficiation procedures, and pellet quality, and also describes recent work on specific relationships between the degree of pellet oxidation and other operational and quality variables.

MARCONA ORE

The Marcona ore bodies are a series of lenticular replacement deposits located 15 kilometers east of San Nicolas. A typical ore body has three main zones:(1)

(1) Oxidized and Leached Zone

Closest to the surface and of 30 meters average thickness, this zone contains mainly secondary hematite and martite. The ore is direct shipping grade, with more than 60 percent iron and less than 0.2 percent sulphur.

(2) Transition Zone

Just below the oxidized zone, this zone is about 22 meters thick. It is a result of incomplete leaching of the original ore and is a mixture of hematite and magnetite, relatively high in sulfates. It is mined as feed to a combination gravity-magnetic separation plant for production of sinter feed.

(3) Primary Zone

This zone, the source of Marcona's pellet feed, is as much as 200 meters thick. The ore is dominantly magnetite. Proven reserves total over 280 million tons containing 53-55 percent iron.

Among mineralogical characteristics of the primary ore which are potentially significant in the pelletizing process are the following:

(1) Copper and Sulfur Minerals

Minor copper is present as chalcopyrite, which is efficiently removed by magnetic separation. The fired pellets are well within copper content specifications. Most of the sulfur present is found in pyrite, but pyrrhotite has been reported. Although magnetic separation rejects pyrite, a certain amount is mechanically entrapped in the finisher concentrate. Liberation of copper and sulfur minerals at pelletizing size is excellent.

(2) Martite

This mineral, the octahedral hematite pseudomorph after magnetite, occurs in the leached and transition zones. Its importance in primary ore as a distinct mineralogical constituent is undoubtedly minor.

(3) Tremolite

This fibrous calcium-magnesium silicate tends to survive the grinding process and enter the concentrate by mechanical entrapment. Tremolite fibers, much larger in one dimension than the governing grain size, can form "fracture nuclei" in the green balls. Current practice is to run the concentrate thickener with a relatively heavy overflow to remove excessive tremolite.

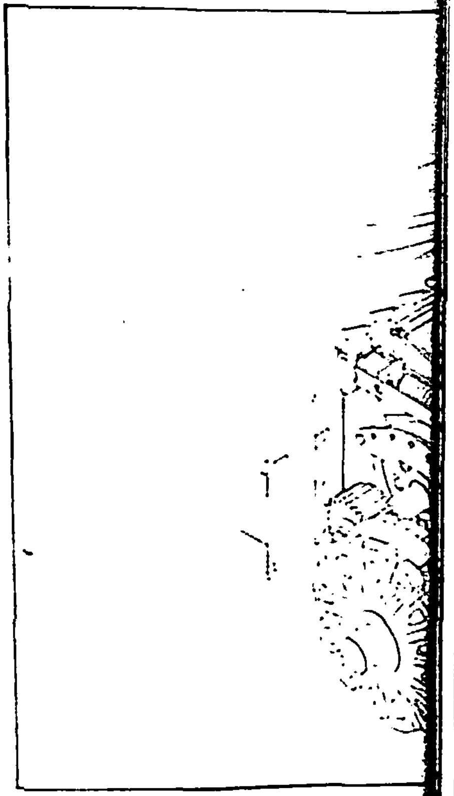

the [illegible] drive shaft, there is a
dur[illegible] the backlash or chuck
[illegible] -nging with the bra
m[illegible] in the Model 2800

accomplished with t
which engage or loc
[illegible] tical limit switches
[illegible] actions bei
[illegible] male member of th
machined hub of the
engaged with the br
[illegible] safe and positive

structures have b
[illegible] as an inte
[illegible] By so d

BENEFICIATION

Marcona's pellet feed preparation flowsheet is shown in Figure 1. Approximate grades at several points in the process are listed in Table 2.

TABLE 2. APPROXIMATE GRADES OF INTERMEDIATE AND FINAL PRODUCTS IN MARCONA PELLET PLANT*

	Fe	Fe^{++}	S	Cu	SiO_2
Rod Mill Feed	55	14.7	2.3	0.08	10.0
Cobbing Concentrate	61	17.1	1.6	0.04	5.5
Finisher Concentrate	68	18.7	0.5	0.02	2.0
Filter Cake	66.5	18.2	0.5	0.02	3.8
Pellets	65.5	1.9	0.02	0.02	4.0

*(after Ruff et al)

Marcona primary ore has exceptionally good liberation characteristics, and can yield magnetic concentrate running over 69.5 percent iron and less than 0.5 percent silica. Such a concentrate would produce oxide pellets of about 68 percent iron, however for most Marcona customers a lower iron-higher silica level has proved to be desirable for their blast furnace burdens. Present practice, therefore, is to produce pellets in the range 65.0-65.5 percent iron and 4.0 percent silica ±0.2 percent.

It is not practical merely to lower the grade of the magnetic concentrate to reach higher silica levels, because the level of copper, an important deleterious impurity, rises in a parallel fashion. The plant thus must produce a relatively high grade magnetic concentrate (i.e. about 68.0 percent iron) and bring the silica to the required level by blending in ground high silica dune sand.

About 12 pounds of bentonite per long ton of pellets is added to assist balling and drying. This addition, plus the weight change due to oxidation of magnetite, accounts for the changes in iron and silica grades between filter cake and fired pellets.

QUALITY INDICATORS

The Marcona Beneficiation Department uses a bi-hourly tumble test as one primary operating control. If the minus 1/4-inch tumble falls below 94.0 percent (ASTM procedure, 25 pound sample), the operator must take corrective action. The average compression strength, although not used as a direct operating control, provides additional quality information. Average values in excess of 440 pounds per pellet are maintained, but the operators must be concerned not only with the average compression, but also with the distribution of individual values about the average level.

Tumble and compression tests give valuable information on pellet quality, but they cannot simulate conditions in the blast furnace. Numerous reducibility and hot compression tests have been developed recently to evaluate pellets under the chemical and physical conditions found in the blast furnace itself, but no single test has achieved universal acceptance in the industry. The Gakushin swelling test developed in Japan is used by Marcona as a supplementary routine quality control procedure.(3) In the Gakushin test, pellets are reduced for one hour at 900° C by a 30 percent carbon monoxide-70 percent nitrogen gas, without being subjected to any load or movement. Although the test conditions are certainly less severe than those in the blast furnace, the results give another relative indication of pellet quality.

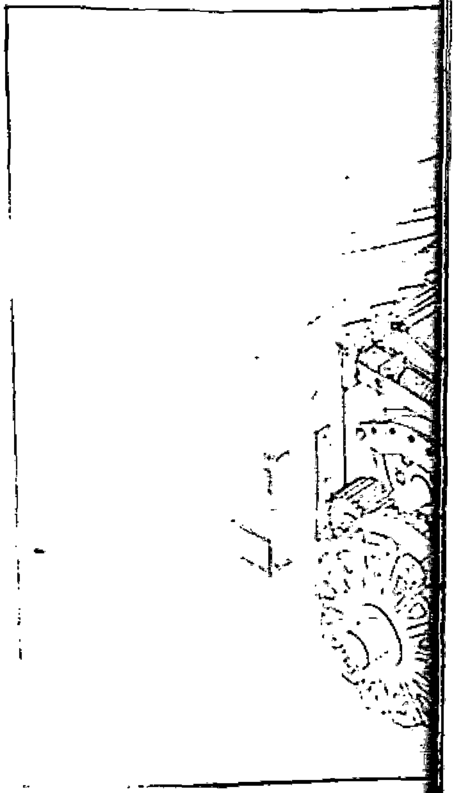

shaft, there is

backlash or chuck

with the bra

in the Model 2800

accomplished with t

engage or lo

limit switches

actions bei

the male member of th

machined hub of the

engaged with the br

safe and positive

structures have b

as an int

By so d

After the start-up of its first pelletizing line in 1963, Marcona produced pellets with about 68 percent iron and less than 2.0 percent silica. Blast furnace performance with these pellets was variable, with some operating difficulties reported.(4) As a result of various research studies, it was decided to increase the silica content to about 4.0 percent, thereby reducing the swelling characteristic of the pellets during reduction. Figure 2 illustrates the relationship between the silica content and Gakushin swelling index.

OXIDATION

The addition of silica to Marcona magnetite concentrate produces a gangue structure or slag network which tends to maintain its integrity during blast furnace reduction. The presence of this slag network, however does not eliminate the need to develop a coherent hematite structure during pelletizing. For high grade pellets (i.e. 65 percent iron and better), it is probably a truism that the better the hematite structure, the lower the gangue level required to develop stability during reduction.

The basic work of Cooke and his associates(5,6,7) defined the conditions required to form a strong hematite network in pellets made from magnetite:

(1) Oxidation of the magnetite (or at least the surface of magnetite particles) to hematite. The oxidation reaction is temperature-dependent, but the restrictive effect of secondary physical processes means that the optimum temperature range for oxidation is about 800-1000° C.

(2) Recrystallization and grain growth of hematite particles to develop interparticle bonds. Temperatures in excess of 1250-1300° C are necessary to accomplish this reaction in commercially attractive time.

The magnetite oxidation should be essentially completed before recrystallization and grain growth begin if optimum crystal structures are to be developed. These conditions are more or less effectively satisfied in the three major commercial pelletizing processes---shaft, travelling grate, and grate-kiln systems---by controlling the rate of heating through the oxidation zone. Obviously, any operational condition which upsets the heating cycle may thereby result in poor oxidation and structure development.

Most commercial pellets made from magnetite concentrates have between 0.7 and 2.5 percent ferrous iron after firing; Marcona pellets are in the 2.0-2.5 percent range. The ferrous iron level in the fired pellet is generally considered to be a good indicator of both the degree of oxidation achieved during induration and (by inference) the pellet quality. Certainly high levels of ferrous iron go hand in hand with poor quality. For example the data of Table 3 compare the tumble index, compression test and ferrous iron of an obviously underfired portion of a pellet sample with the complete sample.

there is
or chuck
with the bra
the Model 280
accomplished with
engage or lo
switches
actions bei
member of th
hub of the
with the br
safe and positive

have b
as an inte
By so d

TABLE 3. QUALITY COMPARISON: UNDERFIRED AND NORMAL PELLETS

	Underfired	Total Sample
Fe^{++}	4.8	2.3
Tumble Index (ASTM)	73.4	94.3
Compression Strength, lb/pellets	303	452
% of Total Weight	4.6	

RELATIONSHIP BETWEEN FERROUS IRON AND COMPRESSION STRENGTH

Over an extended period, operating personnel at San Nicolas observed occasional deviations in average compression strength and unexplained increases in the percentage of pellets falling below a stated minimum compression value. Studies by the operators led them to tentatively identify low compression strength with relatively high residual ferrous iron in the fired pellets. Green feed variables such as Blaine surface area, filter cake moisture, and silica content appeared to have little effect, at least within the ranges of these variables normally encountered.

Firing temperature and pattern were considered as prime possible causes of high residual ferrous iron, not only from underfiring but also from overfiring, since it is well known that hematite will revert to magnetite under certain conditions.(8, 9) Figure 3 shows the equilibrium temperature for the reversion reaction as a function of oxygen partial pressure. This relationship indicates that reversion is thermodynamically possible at the 1350-1375° C firing temperature used at San Nicolas.

Pot grate tests run in the United States suggested that hematite reversion might be the mechanism by which residual ferrous iron occurred in fired pellets. In consultation with the designers of the pelletizing machine, Marcona's operators tested several changes in firing pattern.

Although the results were something less than clear-cut, it appeared that hematite reversion was not the principal mechanism in the production units.

Effect of Sulfur on Ferrous Iron

Due to ore and operational variables, the sulfur content of the pellet feed can fluctuate from a low of 0.2 percent up to 0.8 percent or more, with most values in the 0.4-0.6 percent range. This fluctuation was not considered significant because pyritic sulfur, regardless of its amount, burned off during pelletizing and the fired pellets invariably exhibited uniformly low sulfur contents. In studying the ffects of concentrate variables on pellet quality, however, Beneficiation Department personnel began to suspect that periods of high sulfur in the concentrate coincided with periods of low or erratic compression values. This suspicion was indirectly confirmed by linear regression analyses of operating data performed on Marcona's IBM 1130 engineering computer. Residual ferrous iron was found to correlate reasonably well with sulfur content of the green feed, pelletizing machine production rate, and ferrous iron content of the green feed. This relationship is illustrated in Figure 4. Since there was some relationship between ferrous iron and compression strength, it was concluded that high-sulphur concentrate was contributing to a lower compression strength.

Sulfur dioxide resulting from the burning of pyrite had previously been recognized as a cause of corrosion in pellet machine ductwork, and data had been gathered to show sulfur dioxide concentration in exhaust gases from different sections of the Line Two machine. These data are presented graphically in Figure 5, and indicate that the zone of maximum sulfur release at windboxes 13 through 24 coincides with the preheating and early firing sections of the machine.

The optimum temperature range for pyrite oxidation is 800-900° C, similar to the optimum range for magnetite oxidation.(10) Oxygen requirements for the two process are of the same order of magnitude:

(1) Magnetite Oxidation

$$2(Fe^{++}\cdot Fe_2^{+++}O_4) + \tfrac{1}{2}O_2 \longrightarrow 3Fe_2O_3$$

and

(2) Pyrite Oxidation

$$2FeS_2 + 5\tfrac{1}{2}O_2 \longrightarrow Fe_2O_3 + 4SO_2$$

For example, to lower the ferrous iron content from 18.0 percent in the filter cake to 2.0 percent in the fired pellets requires about 516 ft^3 of oxygen (STP) per ton of pellets. To lower sulfur from 0.6 percent in the filter cake to 0.02 percent in the fired pellets requires about 200 ft^3--146 ft^3 for sulfur oxidation plus 54 ft^3 for oxidation of pyritic iron. The pyrite oxidation, furthermore, liberates about 146 ft^3 of sulfur dioxide per ton of pellets.

This analysis suggests that the concurrent processes of magnetite and pyrite oxidation compete for oxygen during the pellets' passage through the critical firing zone. The high chemical activity of the labile sulphur atom and the rapid low temperature oxidation rates of pyrite compared to iron oxides indicate that the sulphur reaction sites are more active with respect to oxygen than are ferrous iron reaction sites.(10, 11, 13) If this is true, then the sulphur oxidation reaction will dominate until most of the sulphur has been eliminated.

In addition to encouraging high ferrous iron contents by preferentially using the available oxygen supply, the sulfur may contribute to the reversion of hematite in two ways:

8

(1) The envelope of the sulfur dioxide reaction product liberated within the pellet probably reduces the oxygen partial pressure, thus lowering the temperature required for hematite reversion.

(2) The heat released by the sulfide oxidation at 900° C is about 94.9 kcal/gm mole sulfur. This heat release is higher than the equivalent from magnetite oxidation (i.e. 28.4 kcal/gm mole Fe^{++} at 900° C), and coupled with the high volumetric concentration of sulphur in pyrite particles, might well cause local superheating and encourage hematite reversion.

Although the reaction mechanisms discussed above are speculative, recent microscopic studies confirm that the residual ferrous iron content of Marcona pellets is present both as relict (unoxidized) and reversion magnetite. Relict magnetite appears dominant under conditions of high sulfur in the green feed and normally high pellet production rates.

Ferrous Iron and Other Quality Indicators

The original clue to the effect of sulfur came through recognition of the apparent correlation between residual ferrous iron and compression strength. Attempts to confirm this correlation by regression analysis of operating data have not been successful, however. It is now believed this results from the fact that there is a "plateau" effect, that is, ferrous iron values within a certain range are not directly related to compression strengths. Only when the ferrous iron level goes beyond the safe range do we experience noticeably lower compression values.

In view of its effect on compression, it was first thought that excess residual ferrous iron might also have undesirable effects on swelling and tumble indices. Further studies have shown, however, that within normal operating ranges there are no correlations between ferrous iron and these quality parameters.

CONTROL OF RESIDUAL FERROUS IRON

The most obvious method of controlling residual ferrous iron in fired pellets, simply lowering the pelletizing machine's production rate, is an entirely unsatisfactory solution from a production standpoint. Nevertheless, this course had to be taken during periods when compression strength values approached undesirable levels. The discovery that sulfur affected the residual ferrous iron content opened the way to other possible solutions, including selective mining of low-sulfur ore, installation of additional magnetic separation equipment, and installation of flotation equipment to remove pyrite from magnetic concentrates. The preliminary goal was to maintain the sulphur content of the filter cake at less than 0.4 percent sulfur.

Marcona primary ores all contain fairly uniform amounts of pyritic sulfur, a fact which limits opportunities for selective mining. This alternative, therefore, could not be considered as a satisfactory solution to the sulfur problem. Laboratory tests, however, had indicated that flotation could remove a substantial portion of the pyrite in normal finisher concentrate. The test conditions were simple and straight-forward, and encouraged the view that sulfur could be controlled by a circuit featuring minimal conditioning, short flotation time at high pulp density, and modest

---

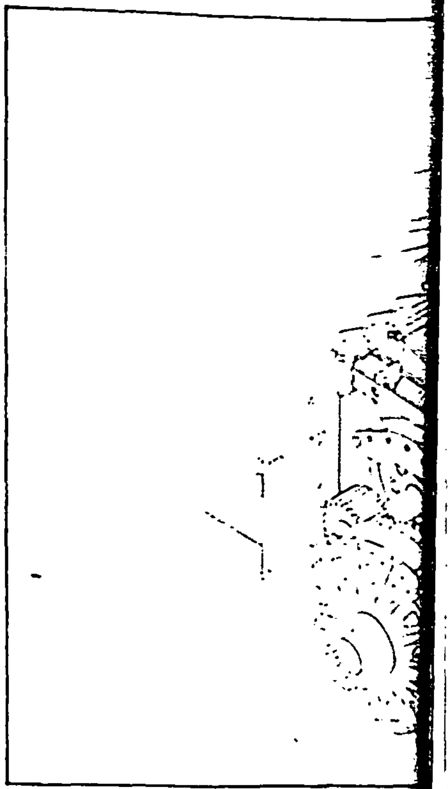

the crawler drive shaft. there is
duction in the backlash or chuc
digging or swinging with the bra
mesh removed. in the Model 280

Steering is accomplished with t
air cylinders which engage or lo
separately. Electrical limit switche
prevent both steering actions bei
taneously. The male member of t
rides on a machined hub of the
is always engaged with the b
results in a very safe and positive
ment.

Major shovel structures have b
signed to be shipped as an int
need for field machining. By so d

reagent cost, without pH or other environmental controls. A program of confirmatory laboratory tests left little doubt that flotation would be a workable solution.

During 1968, a small flotation plant was installed above the concentrate thickener to treat concentrate pumped from the magnetic plant. Figures 6 and 7 show the flotation machines and their relationship to the existing thickener and agitators. The flotation circuit allows the operators to maintain high pellet production rates when high sulfur might otherwise limit production. Continuing programs of research and testing aimed at further improving flotation results are underway. These efforts are being backed up by testwork on magnetic separation improvements which can be accomplished within the limitations of the existing plant.

SUMMARY

At Marcona, residual ferrous iron in fired pellets results in part from incomplete oxidation of magnetite. This condition, which leads to diminishment of compression strength values, correlates at high production rates with sulfur contained in the pelletizing plant feed. Analyses of ferrous iron in fired pellets as functions of feed and operational variables led directly to the conclusion that control of excess sulfur in the magnetic concentrate was required.

Of the remedies considered, flotation of pyrite from the magnetic concentrate combined with improved cleaning by additional stages of magnetic separation appears to provide the desired solution most efficiently.

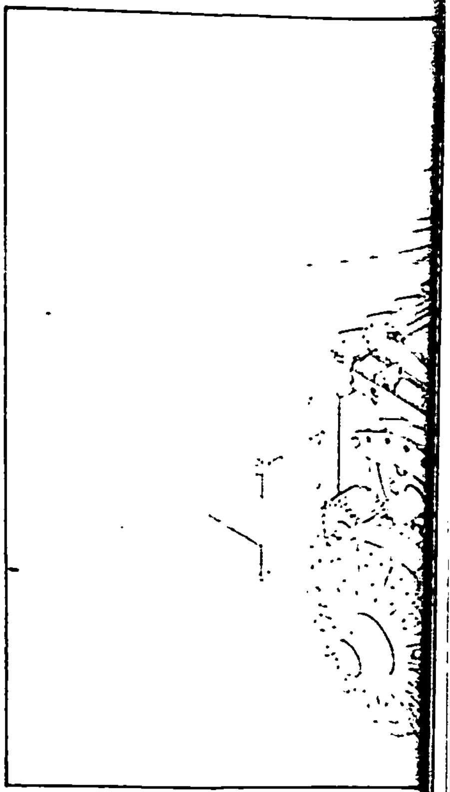

the crawler drive shaft, there is a
duction in the backlash or chuck
digging or swinging with the bra
mesh removed, in the Model 2800

Steering is accomplished with t
air cylinders which engage or loc
separately. Electrical limit switches
prevent both steering actions bein
taneously. The male member of th
rides on a machined hub of the
is always engaged with the br
results in a very safe and positive
ment.

Major shovel structures have b
signed to be shipped as an inte
need for field machining. By so do

ACKNOWLEDGEMENTS

In preparing this paper, the authors have drawn freely from the work of many talented individuals in the Marcona organization. Particular acknowledgement is due the staff of Marcona Mining Company at San Nicolas, and their Operations Manager, Dr. A. W. Ruff.

REFERENCES

1. R. Z. Legault and R. Patino, Geology and Methods of Exploration in the Marcona Mining District, X Convencion de Ingenieros de Minas del Peru, Lima, 1967.
2. A. W. Ruff, H. A. Halupka, G. E. Craig and I. A. Mozer, The Importance of Proper Feed Preparation for the Travelling Grate, AIME Annual Meeting, New York 1968.
3. M. J. Fraser and R. R. Beebe, Quality Control for the Japanese Iron Ore Pellet Market, University of Minnesota Mining Symposium, Duluth, 1969.
4. T. Hasegawa, E. Sakamoto and K. Kuroda, Blast Furnace Operation Using Marcona Pellets up to 65% in the Burden, Tetsu-to-Hagane Overseas, Vol. 5, No. 3, 1965, pp 223-242.
5. S.R.B. Cooke and T. E. Ban, Microstructure in Iron Ore Pellets, Trans. AIME, November 1952, pp 1053-1058.
6. S.R.B. Cooke and W. F. Stowasser, The Effect of Heat Treatment and Certain Additives on the Strength of Magnetite Pellets, Trans. AIME, December 1952, pp 1223-1230.
7. S.R.B. Cooke and R. E. Brandt, Solid State Bonding in Iron Ore Pellets, Trans. AIME, April 1954, pp 411-415.
8. D. M. Urich and T. M. Han, A Progress Report on the Effect of Grind, Temperature and Pellet Size Upon the Quality of Specular Hematite Pellets, Ch. 24 in Agglomeration, (Ed: W. A. Knepper), Interscience 1962.
9. L. J. Erck, Ibid., pp 663-665.
10. R. B. Thompson and W. W. Jukkola, Pyrites and Sulphide Ore Burners or Roasters, in Manufacture of Sulphuric Acid, ACS Monograph #144 (Ed: Duecker and West) Reinhold, 1959.

11. L. Himmel, R. F. Mehl and C. E. Birchenall, Self-Diffusion of Iron in Iron Oxides and the Wagner Theory of Oxidation, Trans. AIME, June 1953, pp 827-843.

12. L. S. Darken and R. W. Gurry, Physical Chemistry of Metals, McGraw-Hill, New York, 1953, p 352.

13. T. A. Henderson, The Oxidation Rates of Lump Copper-Iron Sulphides, Trans. Inst. Mining Met., Vol. 67, Pt. 1, (1957-1958), pp. 497-520.

the crawler drive shaft. there is
duction in the backlash or chuc
digging or swinging with the bra
mesh removed. in the Model 280

Steering is accomplished with t
air cylinders which engage or lo
separately. Electrical limit switche
prevent both steering actions bei
taneously. The male member of th
rides on a machined hub of the
is always engaged with the br
results in a very safe and positive
ment.

Major shovel structures have b
signed to be shipped as an int
need for field machining. By so d

Figure 1 - Marcona Pellet Feed Flowsheet

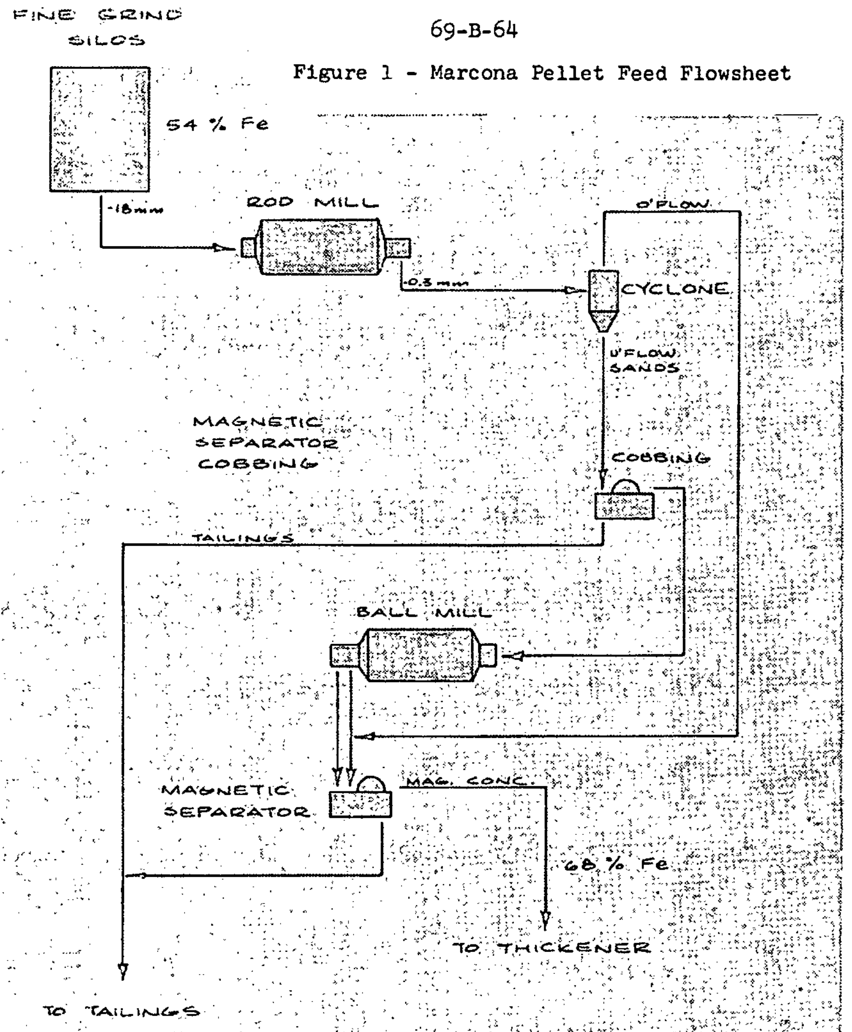

MARCONA FINE GRIND CONCENTRATE FLOWSHEET

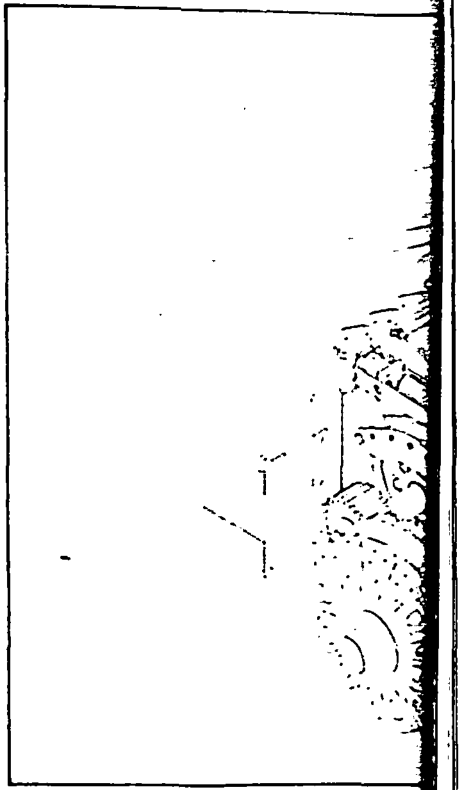

the crawler drive shaft, there is
duction in the backlash or chuck
digging or swinging with the bra
mesh removed, in the Model 280

Steering is accomplished with t
air cylinders which engage or lo
separately. Electrical limit switche
prevent both steering actions bei
taneously. The male member of t
rides on a machined hub of the
is always engaged with the b
results in a very safe and positive
ment.

Major shovel structures have b
signed to be shipped as an int
need for field machining. By so d

69-B-64

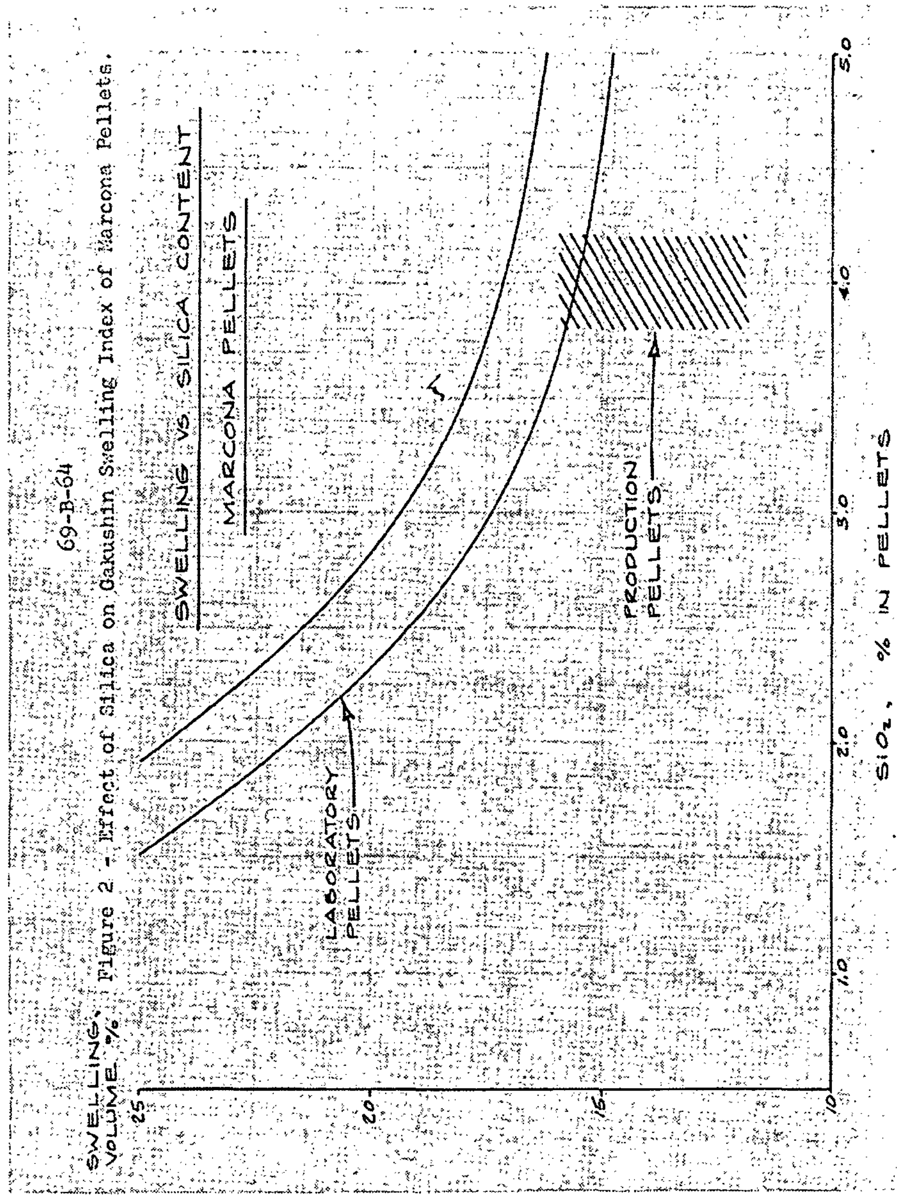

Figure 2 - Effect of Silica on Gakushin Swelling Index of Marcona Pellets.

Figure 3 - Hematite Reversion Equilibrium Temperature
and Oxygen Partial Pressure.

Figure 3 - Hematite Reversion Equilibrium Temperature and Oxygen Partial Pressure.

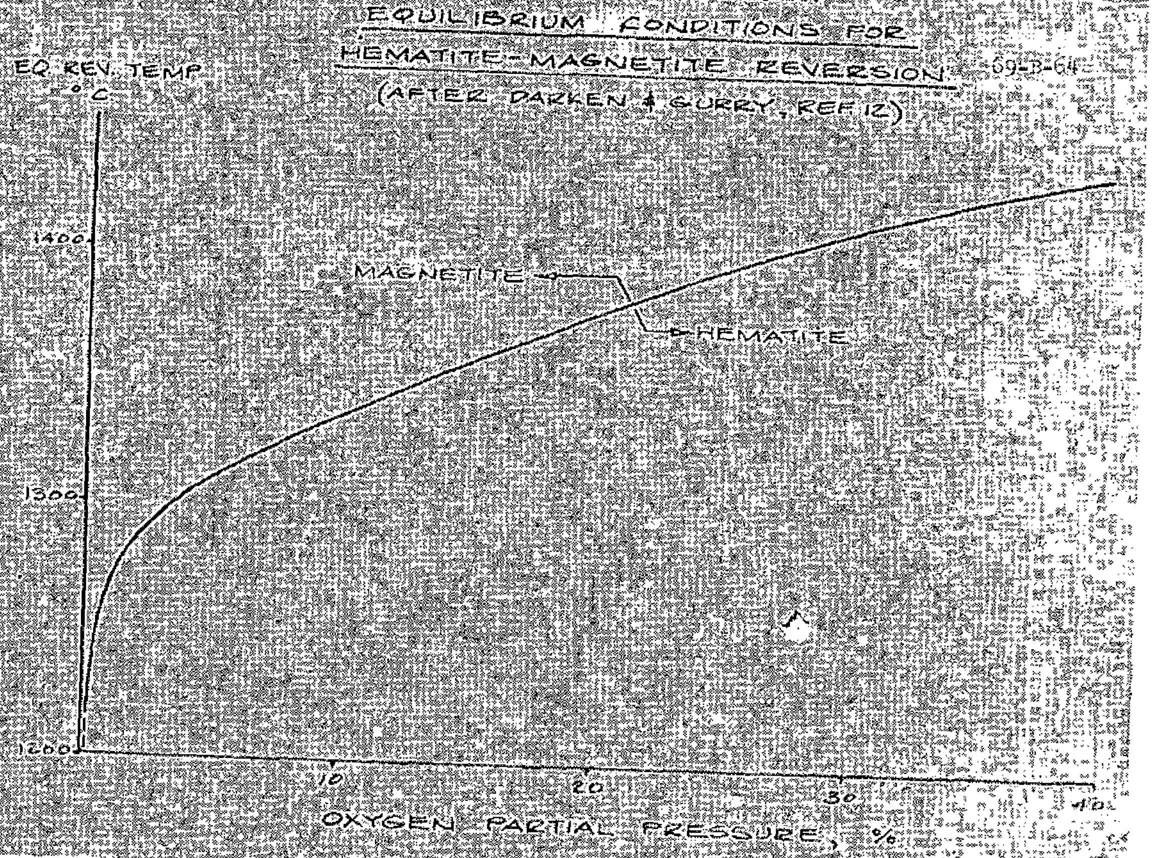

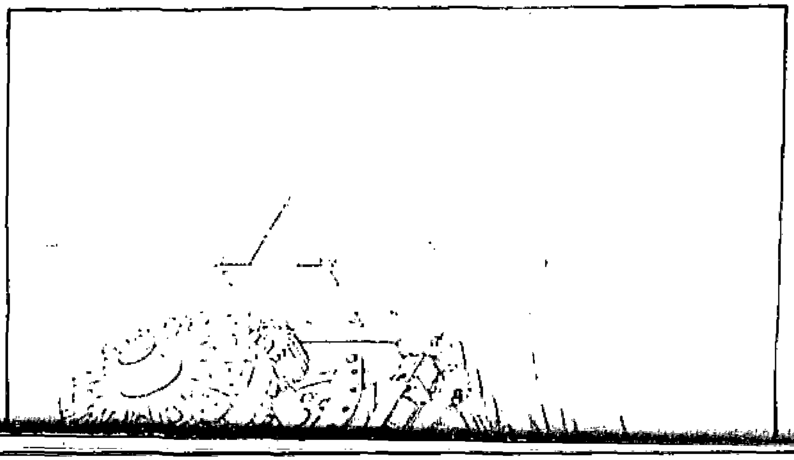

the crawler drive shaft, there is
duction in the backlash or chuck
digging or swinging with the bra
mesh removed, in the Model 2800

Steering is accomplished with
air cylinders which engage or lo
separately. Electrical limit switches
prevent both steering actions bei
taneously. The male member of th
rides on a machined hub of the
is always engaged with the br
results in a very safe and positive
ment.

Major shovel structures have b
signed to be shipped as an int
need for field machining. By so d

Figure 4 - Ferrous Iron in Marcona Pellets as a Function of Operating Rate and Filter Cake Sulfur Content.

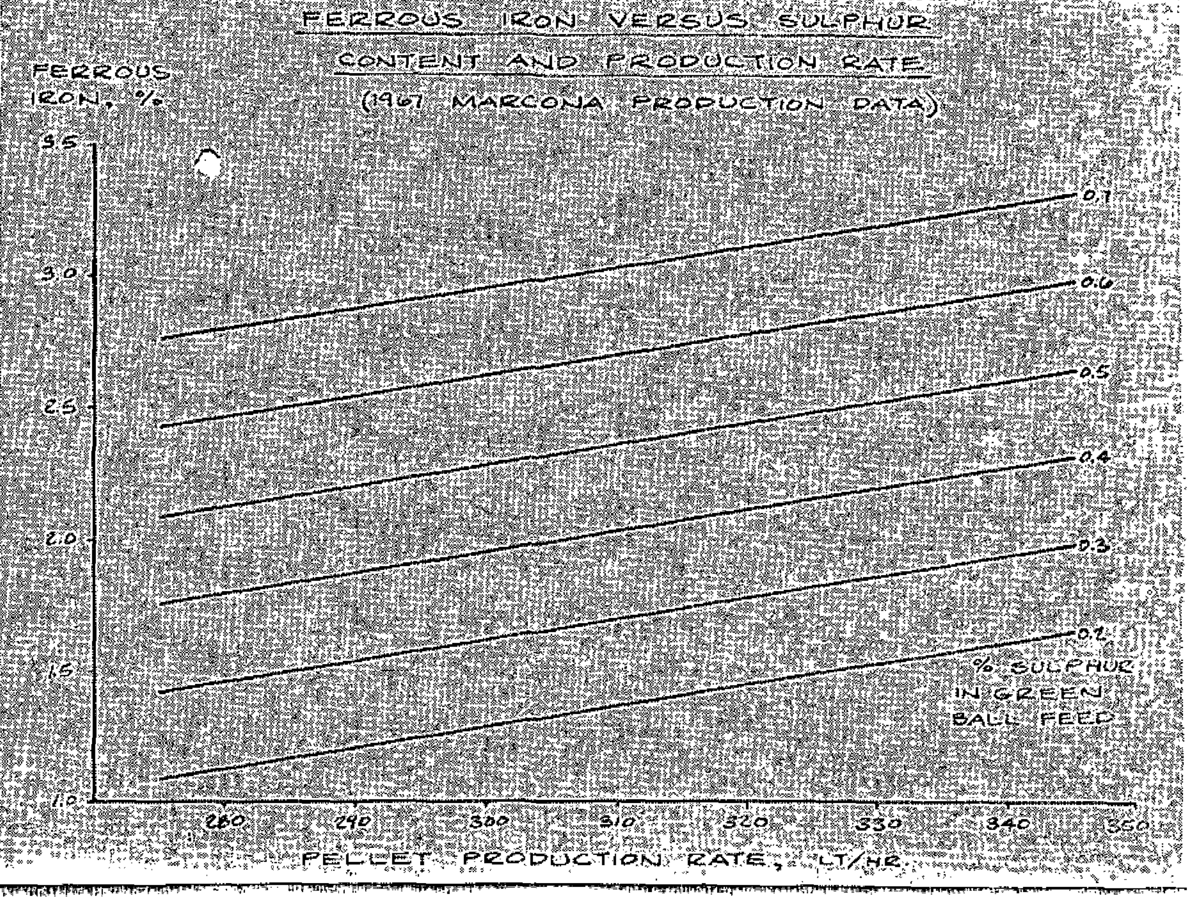

Figure 5 - Sulfur Profile, Marcona Number Two Pelletizing Machine.

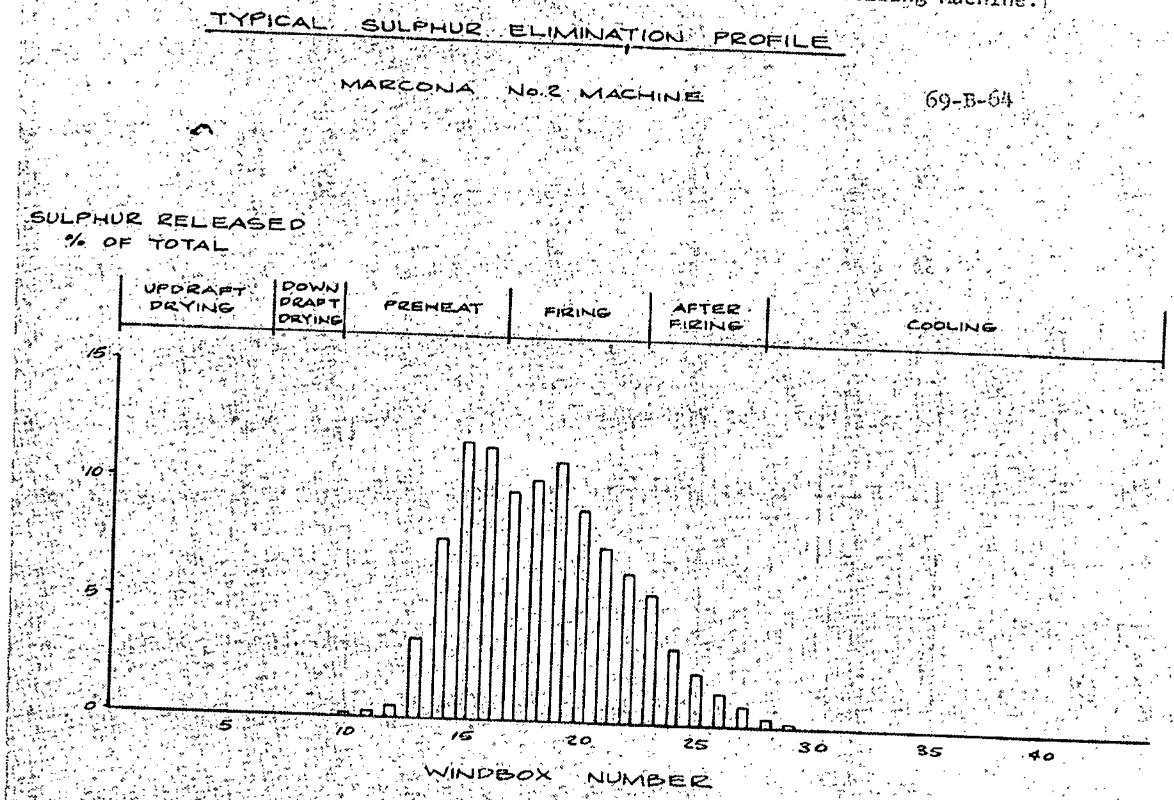

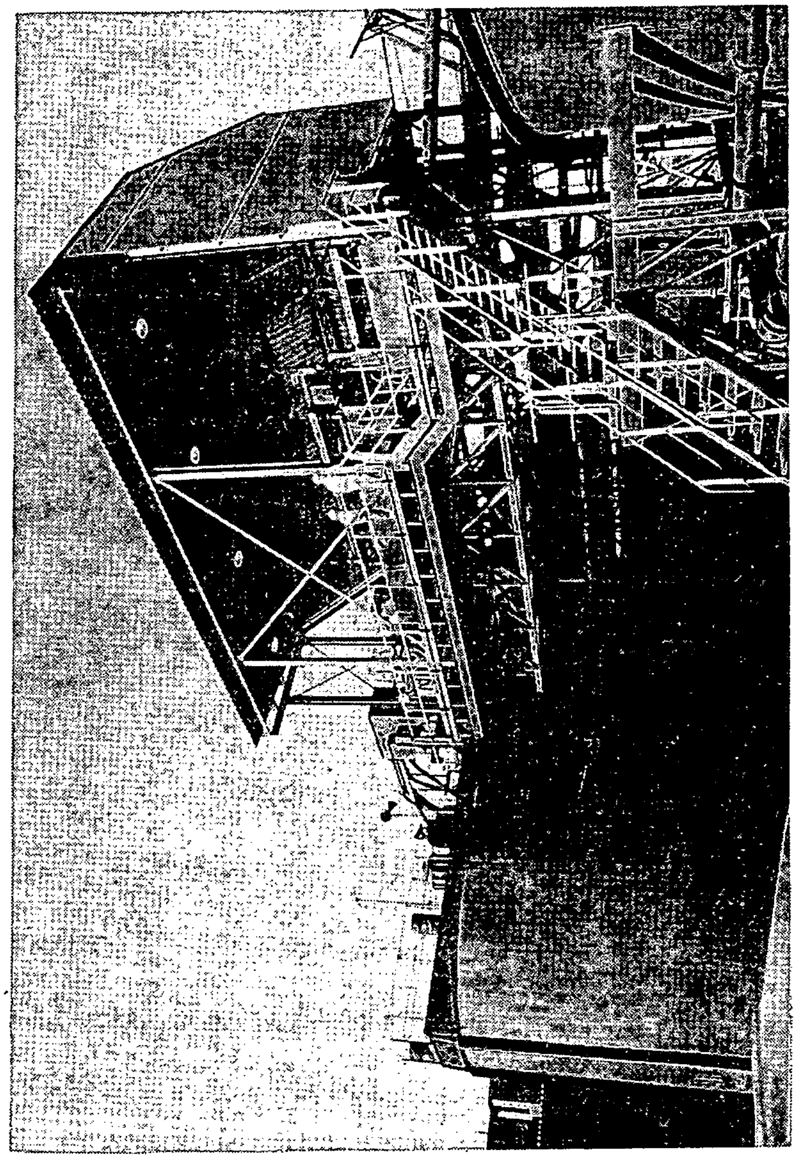

Figure 6 - Pelletizing Feed Flotation Circuit.

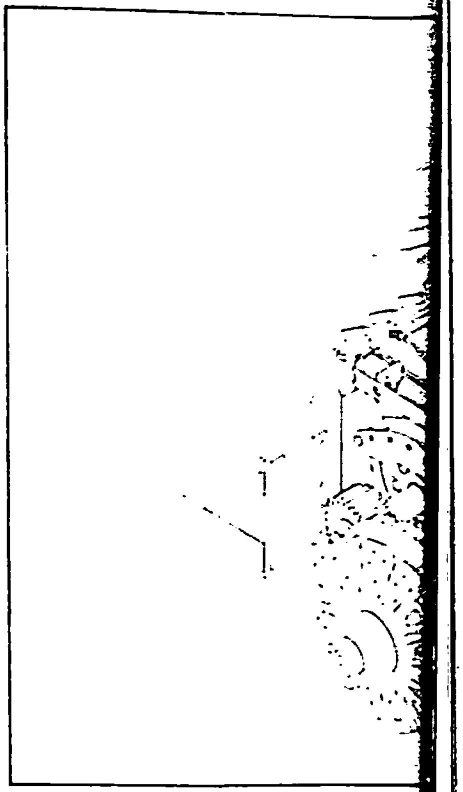

the crawler drive shaft, there is
duction in the backlash or chuck
digging or swinging with the bra
mesh removed, in the Model 280

Steering is accomplished with t
air cylinders which engage or lo
separately. Electrical limit switches
prevent both steering actions bei
taneously. The male member of th
rides on a machined hub of the
is always engaged with the br
results in a very safe and positive
ment.

Major shovel structures have b
signed to be shipped as an inte
need for field machining. By so do

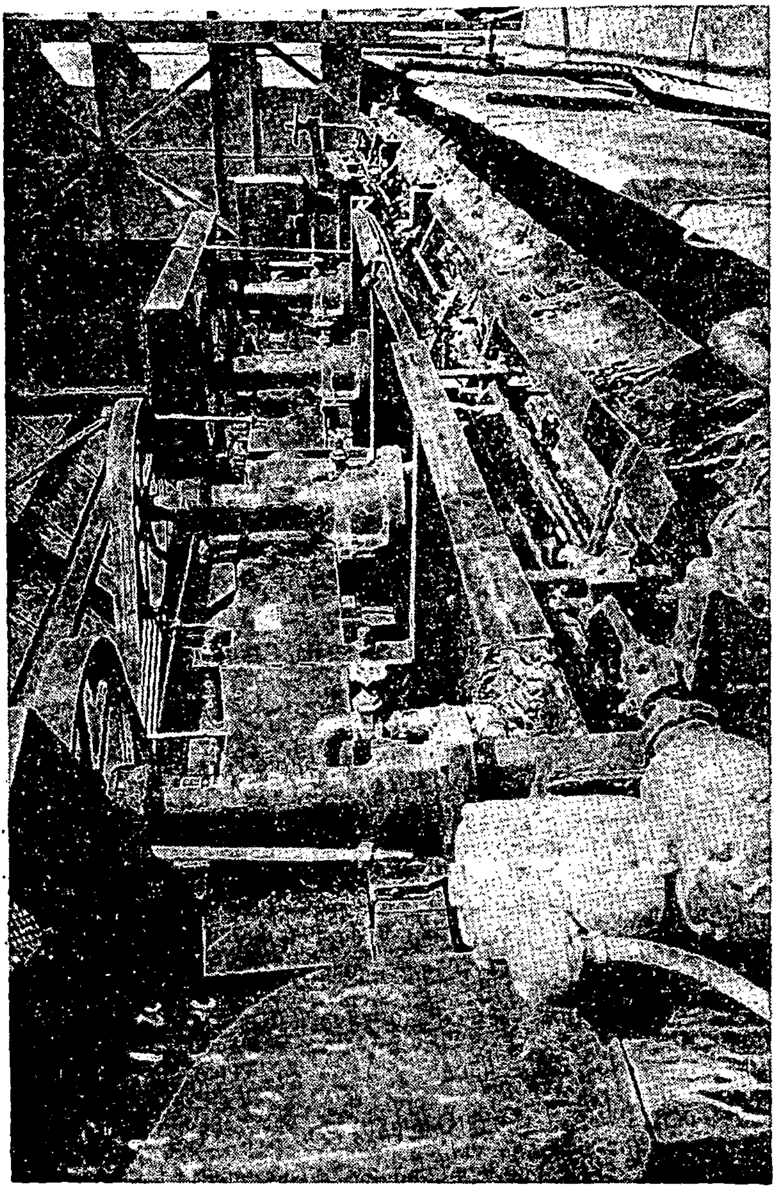

Figure 7 - Pelletizing Feed Flotation Circuit.

References

1) V V Losev: Advances of science: Electrochemistry 1969, VINITI Akad. Nauk SSSR, Moscow 1971, p. 65.
2) S Rashkov et alia: Izv. Instituta (Fiziko-Khimiya), Bulgaria 1964, 4, 97.
3) V I Lainer and N T Kudryavtsev: Principles of electroplating: Part 1, Metallurgizdat, Moscow 1953, p. 293.
4) V V Losev and A I Molodov: Dokl. Akad. Nauk SSSR 1960, 130, 111.

UDC 669.733.872

Kinetics of the autoclave dissolution of indium sulphide

G E Avakyan and I F Khudyakov (Urals Polytechnical Institute)

Summary

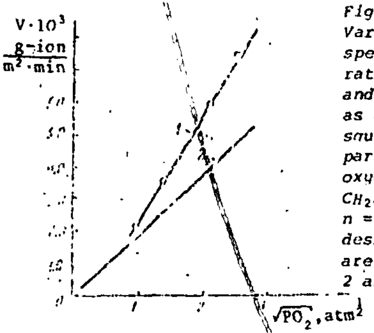

Fig.1
Variation of the specific dissolution rate of indium (1) and zinc (2) sulphate as as a function of the square root of the partial pressure of oxygen. t = 100°C, $C_{H_2SO_4}$ = 0.5 mole/1, n = 10.08 rps. The designations 1 and 2 are the same in figs. 2 and 3.

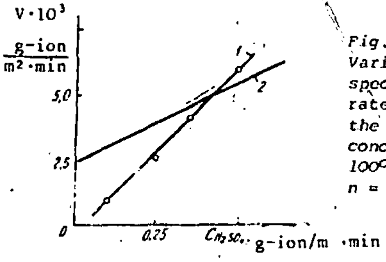

Fig.2
Variation of the specific dissolution rate as a function of the sulphuric acid concentration, t = 100°C, P_{O_2} = 5 atm, n = 10.08 rps.

Zinc concentrates and intermediate products at some concentration plants contain up to 1kg/t of indium, which is present in the zinc sulphide as an ismorphous impurity, substituting the zinc atoms in the sphalerite lattice. Autoclave leaching of zinc concentrates gives more complete extraction of the valuable components, including indium. The behaviour of indium sulphide during autoclave leaching was investigated by the rotating disc method. It was established that the dissolution rate is directly proportional to the square root of the partial pressure of oxygen. This shows that oxygen takes part in the rate-controlling stage of the reaction of the sulphide sulphur with atomic oxygen.

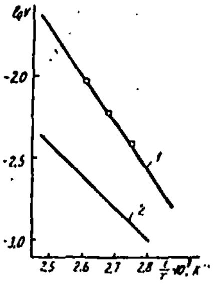

Fig.3
Variation of the specific dissolution rate as a function of the reciprocal temperature. P_{O_2} = 5 atm, $C_{H_2SO_4}$ = 0.5 mole/1, n = 10.08 rps.

The linear relation between the reaction rate and sulphuric acid concentration is similar to the relationship obtained for zinc sulphide, and the reaction is of first order in sulphuric acid. The dissolution rate of sulphides increases with increase in temperature, and the activation energy of the dissolution of indium sulphide was found to be 13 750cal/mole. Thus, comparison of the data on the kinetics of the autoclave dissolution of indium sulphide behaves similarly to zinc sulphide during leaching in sulphuric acid solutions under autoclave conditions.

Sov. Non-Fe ...
1976 v. 4 N6

UDC 669.2/8:546.719:66.074.7

Recovery of rhenium from the alkaline solutions in the desiliconizing of copper concentrates

T B Shkodina, Kh A Al'zhanova and V G Shkodin (Chemical-Metallurgical Institute, Academy of Sciences of the Kazakh SSR)

During the autoclave leaching of high-silicon Dzhezkazgan concentrates 55-60% of the silicon dioxide and 65% of the rhenium are extracted into solution¹). After regeneration the alkaline solutions contain 5mg/1 of rhenium, 130-160g/1 of sodium hydroxide and 0.1-0.6g/1 of silicon dioxide. The repeated use of recycled alkaline solutions leads to the accumulation of rhenium up to 100-150mg/1, and here the degree of leaching of rhenium from the concentrate remains practically unchanged.

The present paper gives the results from investigations into the extraction of rhenium from the desiliconizing solutions by ion-exchange sorption. There are data on the sorption of rhenium from neutral and weakly alkaline solutions²), and the known data on the possibility of the sorption of rhenium from strongly alkaline solutions are far from complete³)⁴). We tested anion-exchange resins of grades AV-17 x 8, AV-27 x 8, AMP, AV-18x, AV-182P and AV-16GS as applied to the solutions from autoclave desiliconizing. Solutions containing 160g/1 of NaOH, 0.6g/1 of SiO_2 and 0.2g/1 of Re were used. The experiments on the sorption of rhenium were carried out at room temperature under dynamic conditions by the normal method. The full dynamic exchange capacity (FDEC) of the anion-exchange resins in respect of rhenium was as follows (% on the weight of the absolutely dry resin): AV-17 x 8, 41.5; AV-27 x 8, 36; AMP, 5.7; AV-182P, 5.6; AV-18x, 3.2; AV-16GS, 0.9. All subsequent investigations on the sorption of rhenium were carried out on the AV-17 and AV-27 resins in the Cl⁻ and OH⁻ forms.

The dependence of the exchange capacity of the AV-17 x 8 resin under dynamic conditions on the rhenium concentration of the solution is shown in table 1. Since the exchange capacity of the resin in rhenium decreases by a factor of 4 with a decrease in the rhenium concentration of the solution by a factor of 10, it can be concluded that rhenium can be sorbed quantitatively from dilute solutions. In fact, a test showed that rhenium is sorbed almost completely from the solution at a concentration of 4-5mg/l.

Table 1: Effect of the initial concentration of rhenium on the capacity of the AV-17 x 8 resin in the OH^- form (0.5g of air-dry resin)

Concentration of rhenium in solution mg/l	FDEC	
	mg-eq/g	%
20	0.55	10.6
60	1.56	29.1
100	1.74	32.3
200	2.23	41.5

Desorption of the rhenium from the resins was realised with solutions of ammonium nitrate having various concentrations at room temperature under dynamic conditions. (The flow rate of the solution was 0.2ml/min). For each experiment we used 0.5g of resin saturated with rhenium. The optimum concentration of the desorbent amounted to 2g-eq/l, since the enrichment of the eluate increased little with further increase in the concentration while the conditions for the crystallisation of ammonium perrhenate from the eluate deteriorated (table 2). After elution from the NO_3^- form the resin was converted into the OH^- form with 10% sodium hydroxide solution until the NO_3^- ions had been completely eluted.

Table 2: Results from elution of rhenium from the AV-17 x 8 resin

Concentration of ammonium nitrate g-eq/l	Degree of enrichment in first fractions	Average content in first fractions of eluate g/l
1.0	47	4.7
1.5	52	5.1
2.0	63	5.7
2.5	65	5.8
3.0	80	7.2

The variation of the capacity of the AV-17 and AV-27 resins in the sorption-elution-regeneration cycles was also investigated. After eight cycles the capacity of the AV-17 x 8 resin in rhenium decreased from 41.5% to 30%. The decrease is stronger initially, and from the fourth to the eight cycle it changes little (from 36% to 31% for AV-27). This is evidently due to mechanical disintegration of the grains and to some loss of the resin during elution and regeneration.

The technique for the extraction of rhenium was checked on the solutions obtained from the autoclave desiliconising of Dzhezkazgan concentrates. After regeneration the silicate alkali solutions have the following composition g/l: 163 NaOH, 10.6 Na_2O_3, 0.59 SiO_2, 2.81 S_{tot}, 0.005 Cu, 0.005 Fe, 0.005 Pb, 0.024 Zn, 0.03 Ca, 0.2 Al, 0.004 Re. To approximate the composition of the solution to the industrial composition the rhenium content was increased to 0.18 g/l by the addition of ammonium perrhenate. The sorption was carried out in a column 1.2cm in diameter containing 10g of the AV-17 x 8 resin in the OH^- form (calculated on the dry weight). The flow rate of the solution was 2ml/min, and the full dynamic-exchange capacity amounted to 33%. The dynamic exchange capacity (to the appearance of 5mg/l of rhenium in the solution) was 27%.

The desorption of rhenium from the resin was realised with 1.5N ammonium nitrate solution, and 85% of the rhenium was eluted by 250ml of solution with an average rhenium content of 8.2g/l. The eluate was evaporated, and the ammonium perrhenate was crystallised. After washing with alcohol the product corresponded to the requirements of the state standard.

References

1) V G Shkodin et alia: The autoclave desiliconising of sulphide minerals: Ekspress-Informatsiya, Alma-Ata, Kaz NIINTI 1976, (34).
2) L V Borisova and A N Ermakov: The analytical chemistry of rhenium: Moscow, Nauka 1974, p. 209.
3) M V Darinyan and D S Gaibakyan: Rhenium: Nauka, Moscow 1964, p. 50.
4) M V Darinyan and A A Danielyan: Izv Akad. Nauk. Arm SSR Ser. Khim. 1965, (5), 462.

UDC 541.135.6

Polarisation of aluminium cathode in cerium-containing melts

V I Kober, E G Samoilov, V A Lebedev, I F Nichkov and S P Raspopin (Urals Polytechnical Institute, Department of the Metallurgy of Rare Metals)

Summary

The polarisation of solid and liquid aluminium cathodes in $KCl\text{-}NaCl\text{-}CeCl_3$ and $KCl\text{-}LiCL\text{-}CeCl_3$ melts was investigated at current densities between $1 \cdot 10^{-4}$ and $10A/cm^2$.

The polarisation curves are analysed. For the liquid aluminium cathode in the region of low current densities at the potential close to the equilibrium potential of aluminium in the melt there is an effect attributed to discharge of the aluminium ions passing into the melt on account of corrosion. At higher current densities there is a wave which is absent in melts not containing $CeCl_3$ and can be associated with the separation of cerium at the liquid aluminium cathode. Various arrests on the polarisation curve for the solid aluminium cathode are attributed to the formation of compounds of cerium with aluminium, the partial Gibbs energies of which were determined.

ease in
e is a
n the
40%) in
ls of
'most
ilphuric
solves
ct is
e of X
empera-
prefer-
40-120°C
from

xygen
activation
of cop-
lutions
nt of the
the
e of the
the
of the
y becomes
as a
of the
the
olution
energies
eristic of
rgy ex-
reduced
nt of the

-nickel

O (1)

(2)

es as the
able of

(3).

is im-

s with

increase in their concentration, particularly at low oxygen pressures. In the ammonia solutions reaction3) develops even at 40-60°C4)5)6), whereas in sulphuric acid solutions a temperature not lower than 100°C is required for appreciable development of this process. With increase in the nickel content the potential of the alloy becomes less noble, and in sulphuric acid media this promotes the following process, particularly with increased temperature:

$$(CuNi) + nCu^{2+} \longrightarrow (CuNi_{1-n})_n Cu + nNi^{2+} \qquad (4)$$

The nickel oxide formed in the initial stages of the oxidation of nickel-containing alloys only dissolves readily in the ammonia solution. Nickel oxide is formed at the atoms and complicates its further oxidation and dissolution. As a result, during treatment of the copper-nickel alloy with sulphuric acid solutions the entry of oxygen to the reaction zone and its activation involve greater energy expenditures, particularly for nickel, than in ammonia media (table 1).

Thus, the alloys investigated dissolve uniformly at the beginning of the process both in sulphuric acid and in ammonia solutions. The divalent copper ions which form are capable of oxidising the copper component of the alloy or of being reduced to elemental copper with passage of the nickel into solution (in the sulphuric acid medium). The ratio of the rates of these processes, which depend on temperature, the oxygen pressure, and the presence of a surface film (with other conditions equal) will determine the selectivity index for the dissolution of the alloys.

In sulphuric acid solutions the amount of dissolved copper (reaction 1) increases with increase in the oxygen pressure, particularly from high-copper alloys. As a result nickel passes into solution not only be reaction (3) but also by reaction (4) especially with increased temperature. During dissolution of high-nickel alloys (>40% Ni) reactions (1) and particularly (3) are retarded on account of the intense formation of the screening film, and this restricts the passage of nickel into solution under strongly oxidising conditions (P_{O_2} = 8 atm).

In ammonia solutions at low oxygen pressures the development of reactions (2) is hindered, and the role of divalent copper as oxidising agent of the copper component of the alloy increases; the copper therefore passes into solution more quickly than the nickel. With increase in the pressure (concentration) of oxygen the oxidising role of divalent copper becomes less significant, and the dissolution rates of the alloy components level out. The behaviour of high-nickel alloys approximates to the behaviour of pure nickel, which is characterised by passivation in ammonia solutions at increased oxygen pressures (3). The nickel dissolution rate therefore decreases with increase in the nickel content of the alloy, and in view of the role of divalent copper conditions are created for preferential dissolution of the copper component of the alloy.

With increase in the temperature to 80°C the copper and nickel dissolution rates from the high-copper alloys are equalised. At a higher temperature, on account of the oxygen deficiency (at P_{O_2} = const = 4 atm), the oxidising role of divalent copper increases, and this leads to increased dissolution of the copper component of the alloys. For high-nickel alloys, which are more stable to the influence ofoxygen, the activating role of the dissolved copper is retained for the whole range of temperatures.

Conclusions

1. The dissolution rate of copper and nickel from the alloy is higher than the dissolution rate of pure copper and pure nickel, particularly in sulphuric acid media.
2. Alloys containing less than 20% of Ni dissolve at the highest rate in sulphuric acid and ammonia media; The effectiveness of the use of the use of ammonia solutions increases with decrease in the nickel content.
3. To accelerate the dissolution of copper-nickel alloy it is necessary to improve the oxygen mass transfer conditions, i. e., to increase the pressure and agitation rate, particularly with t ≥90-100°C, which will substantially accelerate dissolution especially in ammonia media.
4. Nickel dissolves more rapidly than copper from alloys containing <20% Ni; The denickeling of the alloys increases with increase in the oxygen pressure and the temperature, but it is not possible to secure selective dissolution of copper.

References

1) S S Naboichenko: Zh. Prikl. Khim. 1972, **45**, (11)
2) S S Naboichenko: Zh. Prikl. Khim. 1973, **46**, (46), 1475.
3) K Shimakaga and S Morioka: Trans Inst. Mining. Met. 1971, C80, (12), 228.
4) I Halpern: J. Electrochem. Soc. 1953, **100**, (10), 421.
5) B G I Lu and W F Graydon: J. Amer. Chem. Soc., 1955, **77**, (12), 6136.
6) N Sato: J. Japan. Inst. Metals 1960, **24**, (2), 126.

Soo. Non-Fe
1976 v. 4 N3

UDC 669.334

The role of seeding in the autoclave precipitation of copper from sulphate solutions

I F Kudyakov, S S Naboichenko and S E Klyain (Urals Polytechnic Institute and Unipromed')

Data on the role of seeding in the autoclave precipitation of copper are contradictory. In papers by D Halpern et alia the homogeneous nature of the activation of hydrogen by copper ions is mentioned1). According to the data of Shaufelberger2), the catalytic effects of seeding is extremely small. The authors3) came to a similar conclusion, attributing the determining role to the homogeneous stage in the mechansim of the precipitation of copper. In the paper4) it was shown that the conditions for disproportionation of monovalent copper deteriorate and the overall rate of the process decreases with increase in the consumption rate of the seed. According to data5), the copper precipitation rate increases with increase in the consumption of the seed right up to 300% of the initial copper content at 160°C. During precipitation of copper from ammonia solutions the process rate increases with increase in the consumption and degree of dispersion of the seed, and an autocatalytic mechanism is observed1)5). The contradictory published data are largely due to the complexity of the mechanism of the process and the difficulty of controlling the concentration of monovalent copper ions, the determining role of which was confirmed by the researches of Peters et alia7).

We carried out experiments on the effect of seeding on the characteristics of the autoclave precipitation of copper from sulphate solutions in a 1 litre titanium autoclave at controlled temperature and hydrogen pressure. On the basis of previous investigations8) the agitation rate (Re = 10^4), the hydrogen pressure (P_{H_2} = 26 atm), the initial copper content (1.0 g-ion/1), the initial ammonium sulphate content (1.0-1.5mole/1), and the polyacrylamide content (0.4g/1) were taken as constant. The development of the process was monitored by periodic samples, in which the copper was determined by a volumetric method. The sampling device was provided with a filter of fine-pore sintered glass.

Copper, titanium and tungsten powders and titanium, tungsten, and chromium carbides, borides and nitrides with known specific surface were used for seeding. The materials differed in their structure and size parameters and crystal lattice imperfections, and their adsorption capacity and activity for surface recombination of hydrogen molecules were therefore different[9])

For a heterogeneous mechanism of activation of hydrogen of additives employed in increasing amounts should appreciably accelerate the precipitation of the copper. Increase in the consumption rate of the added powders by two to four times has almost no effect on the precipitation rate (table 1). With seeds having the same surface area the copper precipitation rate is fully comparable for all the powders. Somewhat higher rates were observed when molybdenum and tungsten powders were used, and these are due to their cementation capacity in relation to copper, as shown by the presence of molybdenum and tungsten and by the unchanged acid content in the final solution. At the same time, in spite of the much larger amount of seed, decrease in temperature to 120°C led to retardation of the precipitation of copper, while the experimental activation energy remained practically unchanged with variation in the consumption rate and type of seed (E_a = 25± 1.2kcal/mole). A similar effect was obtained with the carbides, borides and nitrides (specific area 1.71m^2) and even with graphite which had been activated by palladium fluoride. Microscopic investigations of the powders showed that the seeds took the form of an independent phase and were coated insignificantly with copper. Thus, the experimental data indicate the absence of an activating effect eith the various solid additions and do not confirm the heterogeneous mechanism of the process.

At the same time, with the addition of copper powder up to 100% of the copper content in the solution some increase in the rate of the process was observed in the initial period of precipitation. With the use of monodisperse fractions of powder with particle size between 0.3 and 0.01mm, possessing different surface areas, the effect of the particle size of the seed showed up for fractions finer than 0.053mm right up to the precipitation of 50-60% of the copper. Fractions finer than 0.044mm were isolated by washing with water; to eliminate oxidation of the particles dehydration and drying were undertaken just before the experiment. Experimental data on the effect of the surface are of the seed on the rate of the process are given in fig. 1.

During precipitation of the copper with two to six thickening cycles with a hydrogen pressure of 26 atm at 140°C for 40 min (in the presence of the powder obtained during treatment of the previous volume of the solution) the average rate of the process after the first cycle remained practically unchanged and amounted to 1.7± 0.02g/l.min. This is fully explainable, since after one cycle the amount of powder formed is almost equivalent to the copper content in the new portion of solution, and subsequent increase in its amount in the system does not affect the final results of the process (with unchanged mass transfer in the "gas-liquid" system).

Table 1: Values for the average rate of the process (g/l min) in the presence of seeding powders at the moment of 50 and 90% precipitation of copper (P_{H_2} = 27 atm, t = 140°C)*

Seed			v g/l min	
Name of powder	Consumption g/l	Surface m^2	50%	90%
Electrolytic copper	20.3	1.71	4.86	2.18
	38.8	3.27	5.14	2.23
	81.5	6.84	5.62	2.17
			(2.83)	(1.20)
Titanium	122.3	10.11	5.52	2.19
	47.0	1.71	5.14	2.26
	95.0	3.42	5.04	2.12
	190.0	6.84	(4.30)	(1.90)
Molybdenum	22.5	1.71	5.43	3.60
	89.0	6.84	(3.90)	(3.60)
Carbonyl tungsten	20.3	1.71	5.42	2.32
	40.6	3.42	5.40	2.32
	81.2	6.84	(2.80)	(1.44)

*) The values given in brackets were obtained at 120°C.

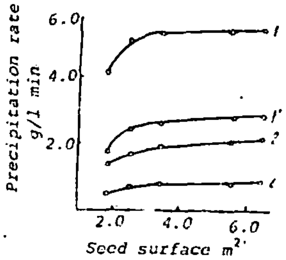

Fig.1 Relation between the average rate of the process of 50% (1',2') and 90% (1,2) precipitation and the amount of seed added; t =140°C, P_{H_2} = 26 atm, c^0_{Cu} = 71.2g/l, 70g of copper powder; $C_{(NH_4)_2SO_4}$ g/l, 1 - 0.0, 2 - 150.

Table 2 gives data on the effect of the amount of added copper powder on the kinetics of the precipitation of copper at various temperatures, hydrogen pressures and initial acidities. With increase in the amount of powder up to

Table 2: Residual content of copper in the solution (g/l) with various amounts of copper powder

Precipitation parameters			Seed consumption rate g/l	Interval between samples min				
t°C	P_{H_2} atm	$C^0_{H_2SO_4}$ g/l		5	10	15	24	40
140	28	-	0.0	36.7	24.7	15.9	7.0	3.9
			16.0	31.4	20.3	12.7	6.4	2.8
			32.0	28.6	21.0	15.3	8.3	4.4
			64.0	23.2	20.3	12.7	7.0	3.5
			96.0	22.8	20.6	13.0	7.2	4.1
150	28	-	0.0	17.7	12.9	3.8	-	-
			16.0	19.1	12.1	-	2.8	-
			32.0	19.1	11.4	4.8	1.9	-
			64.0	18.4	8.9	4.5	1.3	-
			96.0	19.7	8.3	4.5	2.9	-
140	15	20.0	0.0	55.5	49.6	41.9	28.6	19.1
			32.0	45.1	41.2	36.8	-	15.9
			64.0	42.0	*3 .4	34.0	27.9	14.8
			128.0	42.4	36.7	32.0	27.0	15.3
150	10	20.0	0.0	58.1	50.2	42.6	34.3	20.3
			32.0	48.9	42.0	37.8	27.1	15.6
			64.0	40.0	36.8	32.2	23.5	12.4
			128.0	41.9	37.0	31.0	22.0	12.7

*) Figure missing in Russian Journal.

100% of the copper content in the initial solution the copper precipitation rate is accelerated, particularly in the first 10-15 min, except for the experiment at 150°C and P_{H_2} = 28 atm. Decrease in the hydrogen pressure and temperature and increase in the initial acidity of the solution i.e. variation of the conditions which lead to a deficiency of hydrogen in the system, with a small content of copper in the solution leads to the appearance of an induction period on the kinetic curves. This induction period disappeared with increase in P_{H_2} and the copper content or with addition of copper powder (fig. 2). The presented data demonstrate the effect of metallic copper on the development of the processes involving copper and hydrogen ions.

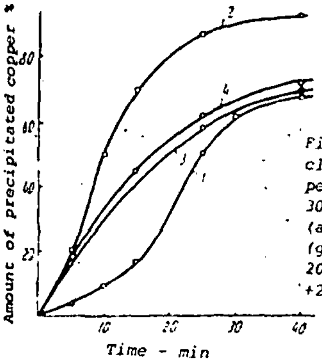

Fig.2 Kinetics of the autoclave precipitation of copper at 140°C with $C^{0}_{H_2SO_4}$ = 30g/l. Hydrogen pressure (atm) and Cu concentration (g/l): 1 - 10,20; 2 - 25, 20; 3 - 10,60; 4 - 10,20 +20g/l of seed.

It has been established[10]) that for the reaction:

$$Cu^{2+} + Cu^{0} \rightleftarrows 2Cu^{+} \qquad (1)$$

the equilibrium concentration of Cu^{+} ions is described by the equation:

$$[Cu^{+}] = \left[\frac{[Cu^{+}]}{4.575\exp\left(\frac{4650}{T} - 9.14\right)}\right]^{0.5} \qquad (2)$$

and, with other conditions equal, will decrease with decrease in the content of divalent copper ions. If it is supposed that the investigated process is heterogeneous, the rate of its development should increase with increase in the concentration of the initial compounds and also with increase in the degree of dispersion of the copper powder. Moreover, according to the stoichiometry of the reaction, the initial substances react in an equimolar ratio. The concentration of monovalent copper will therefore be determined by the content of the substance, which is present in the system in an insufficient amount (compared with the stoichiometric amount). An excess of copper powder, in particular, will affect the rate of establishment of equilibrium but not the equilibrium concentration of Cu^{+} ions.

The researches of D Halpern et alia and their data on the role of various seeds in the precipitation rate of copper indicate a determining role for the mechanism of homogeneous activation of hydrogen, the development of which is possible in the presence of copper ions through a donor or dative bond. The dissociation energy of the H-H bond amount to 62kcal/mole by the donor mechanism and a 3.4kcal/mole by the dative mechanism, and the latter was preferred for an ion with a small charge[11]). From the energy standpoint the activation of hydrogen is evidently realised through a dative bond, i.e. by monovalent copper ions.

Thus the role of the added seed amounts to an increase in the concentration of monovalent copper in the solution, which helps to accelerate the whole process by its activating effect on the hydrogen. Monovalent copper ions can also be formed by the reaction of activated hydrogen (H^{*}) with divalent copper:

$$2Cu^{2+} + 2H^{*} \longrightarrow 2Cu^{+} + 2H^{+} \qquad (3)$$

However, due to the much lower activating power of Cu^{2+} ions[12]), this process develops more slowly, particularly with a deficiency of dissolved hydrogen (e.g. with a low hydrogen pressure) and also with a low initial concentration of copper or with significant acidity, which retards the development of the direct reaction. The deficiency of hydrogen is felt at the beginning of the process, when its concentration is lower than the content of copper ions on account of its low solubility or the inadequate aerating capacity of the stirrer. It is in this case that the addition of copper powder, which leads to the formation of monovalent copper (a homogeneous catalyst for the activation of hydrogen molecules) by reaction[1]), has an appreciable positive effect.

The initial section of the kinetic curve 1 (fig. 2) illustrates the increasing rate of precipitation of copper, characteristic of autocatalytic processes. The observed relationship begins to be distorted when 50-60% of the copper has been precipitated. The autocatalytic nature of the process with a deficiency of hydrogen is due to the increasing amount of powder which forms. The amounts of powder and monovalent copper are proportional to the initial content of Cu^{+}. According to the stoichiometry of reaction (1), it is most highly developed with a Cu^{2+}:Cu^{0} ratio of 1:1, and theoretically this should occur at the moment when 50% of the copper has been precipitated; it should then decrease as a result of decrease in the concentration of Cu^{+} ions, which is confirmed in practice (curve 1, fig. 2).

Conclusions

1. The rate of autoclave precipitation of copper from sulphase solutions is indifferent to solid additions (seeds), and this confirms the homogeneous mechanism of the process.
2. A seed of copper powder helps to increase the content of Cu^{+} ions (homogeneous activators of hydrogen) in the solution.
3. The positive role of the seed (copper powder) appears under conditions which hinder the activation of hydrogen and the formation of Cu^{+} ions (insufficient concentration of dissolved hydrogen, low content of copper, high acidity in the solution).
4. The initial period of the precipitation of copper is characterised by an effect from increase in the degree of dispersion of the seed (-0.05mm) and its consumption rate (up to 100% of the content of the copper in the solution), and also by the autocatalytic mechanism of the process.

References

1) D I T Evans: Advanced extractive metallurgy: London 1967, 831.
2) F A Shaufelberger: Mining Engng. 1956, 8, (5), 539.
3) E R MacGregor et alia: Trans. AIME 1958, 212, (2), 244.
4) Z L Ratner et alia: Tr. Inst. Gipronikel', Leningrad, 1967, (32), 74.
5) A S Yaroslavtsev et alia: Tsvetnye Metally 1969, (9), 40.
6) S I Sobol' et alia: Tsvetnye Metally 1965, (1), 22.
7) E A von Hahn et alia: Phys. Chem. 1965, 69, (2), 547.
8) S S Naboichenko: Tsvetnye Metally 1971, (1), 26.
9) V A Lavrenko et alia: Zh. Prikl. Khim. 1974, (4), 763.
10) S E Klyain et alia: Izv VUZ Tsvetnaya Metallurgiya 1974, (3), 27.
11) M E Vol'pin et alia: Uspekhi Khimii 1969, 38, (4), 561.
12) W I Dunning et alia: Proc. Chem. Soc. 1960, (7). 244.

Economic Geology
Vol. 74, 1979, pp. 397-408

The Regional and Stratigraphical Context of Zechstein 3 and 4 Potash Deposits in the British Sector of the Southern North Sea and Adjoining Land Areas

DENYS B. SMITH AND ANTONY CROSBY

Abstract

Geophysical logs and cuttings records from Zechstein cycles 3 and 4 strata in boreholes in the British sector of the southern North Sea have been interpreted in the light of numerous cored boreholes through this sequence in northeast England. This interpretation shows that potash salts in the two cycles are thickest and most consistent in a belt 20 to 40 km wide parallel with and a few kilometers from the present basin margin and are here generally similar in grade to those known onshore. The potash ores in both cycles are mainly of sylvinite in onshore areas, the layered Upper Potash of the fourth cycle being rather less variable but generally of appreciably lower average grade than the Boulby Potash of the third cycle. Potash salts in both cycles are highly variable in thickness and grade in basin center areas where they have been grossly affected by diapirism of the thick second cycle salts.

Introduction and Stratigraphical Classification

ZECHSTEIN salt and potash deposits, the basis of major chemical industries in England, Germany, and Poland, occur at depth below much of the present North Sea, where they have been proved in some hundreds of hydrocarbon exploration boreholes. The salts comprise parts of four main broadly cyclic sequences (Fig. 1), those in the first (Werra) cycle being thickest in the marginal belt in which anhydrite generally predominates, while those in the second (Stassfurt) cycle are thickest in basinal areas and comprise thick sulfates (including vast amounts of polyhalite) disposed mainly peripherally to exceptionally thick chlorides. Evaporite sequences in the third (Leine) and fourth (Aller) cycles are considerably more uniform in both lithology and thickness than those of the two earlier cycles and comprise sulfates (subordinate) and chlorides (including potash salts) which together thicken progressively toward the basin center and are individually continuous far onto the surrounding shelves. The general geology of the Zechstein sequences has been summarized by Smith (1974a) and Taylor and Colter (1975) and need not be repeated.

Salts in the third and fourth Zechstein cycles, on which this paper concentrates, were profoundly disturbed in basin areas by movement of the underlying second cycle salts and in places may themselves have initiated minor diapirism. In general, however, enough undisturbed or only slightly disturbed areas are present, especially in marginal areas, for the broad outlines of the present stratigraphy and distribution of the salts to be determined and to provide some clues to their former distribution and paleogeography. It is clear that the salts thicken progressively toward the basin center and that basinward thinning of some sulfate members is more than matched by thickening of the chlorides. Both chlorides (first) and sulfates terminate abruptly toward the margin, where past or current dissolution by undersaturated groundwater is inferred. Potash salts in both the third and fourth cycles are of commercial grade, but only the Boulby Potash of the third cycle is currently being worked.

Because well cuttings (commonly not recovered or patently unrepresentative) and geophysical logs are the only record of the Zechstein third and fourth cycle evaporites beneath the southern North Sea, the key to the interpretation of the distribution and thickness of these salts lies in the well-explored area of northeast England where the margin of the evaporite basins extends for some distance inland. Details of the evaporites in these land areas will therefore be given first, in the expectation that they are typical of marginal areas around the basin, and description of the more problematical basinal sequences will follow. It should be noted, however, first, that the sequence in the northeast margin of the basin is likely to be anomalous because of extensive pre-Upper Cretaceous leaching and erosion and, second, that comparatively few boreholes were drilled in basinal areas and in most of these the salts are diapiric. English lithostratigraphic nomenclature will be employed throughout in view of the uncertainty of correlation between the English and German Zechstein potash deposits.

	Series	Groups	Formations	Cycles
PERMIAN OR TRIASSIC		Eskdale Group	Saliferous Marl	
PERMIAN	UPPER		Top Anhydrite	EZ5
			Sleights Siltstone	
		Staintondale Group	Upper Halite	EZ4
			Upper Anhydrite	
			Upgang Formation	
			Carnallitic Marl	
		Teesside Group	Boulby Halite	EZ3
			Billingham Main Anhydrite	
			Upper Magnesian Limestone	
		Aislaby Group	Fordon Evaporites	EZ2
			Kirkham Abbey Formation	
		Don Group	Hayton Anhydrite	EZ1
			Lower Magnesian Limestone	
			Marl Slate	
	LOWER		Yellow Sands & Basal Breccias	

FIG. 1. General stratigraphy of Zechstein strata in northeast England and the southern North Sea. The abbreviations EZ1 to EZ5 denote the five main evaporite cycles of the English Zechstein sequence. For correlation with Zechstein strata in Germany, see Figure 4.

Potash Deposits and Related Evaporites of the Third and Fourth Cycles on Land

The Teesside Group (EZ3)[1]

This group, the correlative of the Leine Series of northern Germany, comprises three main formations (Fig. 1); these are, in ascending order, the Upper Magnesian Limestone or Seaham Formation, the Billingham Main Anhydrite, and the Boulby Halite. The Boulby Potash is present near the top of the Boulby Halite in parts of North Yorkshire and Cleveland. Only the Boulby Halite and Boulby Potash will be specially considered here.

The Boulby Halite is widespread (Fig. 2) in northeast England and locally reaches a thickness of 80 m near the coast. Having been proved in more than 60 cored boreholes, its detailed stratigraphy and mineralogy are well known. Except in limited areas in Yorkshire it generally contains only small amounts of terrigenous material and, where fully developed near the coast, it comprises four main units (Armstrong et al., 1951; Raymond, 1953; Smith, 1971, 1973; Stewart, 1951a).

From the top they are:

D. Gray, brown, and red, generally medium-grained halite with thin beds of dark gray-green or red mudstone toward the top and with patchy sylvite near the base in some coastal districts. Parts commonly contain a distended mesh of dark gray-green or red mudstone. Small amounts of anhydrite, hematite, magnesite, and quartz are generally present. The unit is from 0 to 5.2 m thick.

C. (Boulby Potash). Sylvinite, colorless, pink, red, brown, or gray, commonly strikingly mottled, comprising a variable mixture of medium-grained and coarse-grained halite and generally secondary amoeboid sylvite in a weakly layered, distended and discontinuous, fine-grained mesh of dark gray-green carbonaceous mudstone and/or fine-grained gray anhydrite, and with beds of halitic or sylvinitic mudstone and anhydrite. Averaged KCl content is up to 45 percent (Smith, 1974b), but few data have been published. Boracite, hematite, koenenite, magnesite, pyrite, and quartz range from rare to abundant and minor carnallite is common. It is believed to pass laterally into halite of equivalent age. The unit ranges from 0 to 11 m in thickness.

---

[1] The abbreviations EZ1 to EZ5 denote the five cycles of the English Zechstein sequence. Although these cycles are probably generally equivalent to the Z1 to Z5 cycles of the German Zechstein sequence, there are several significant differences and also some doubts on the correlation.

B. *Halite*: upper part is colorless, pale gray or amber, equigranular, medium-grained, with thin laminae of fine-grained anhydrite and scattered crystals and small patches of sylvite; lower part mainly gray and brown, coarse to very coarse grained, with mudstone and anhydrite forming a discontinuous coarse mesh and some thin beds. Medium-grained granular gray halite, partly pseudomorphous after gypsum, widely forms thin beds near the base. Carnallite, magnesite, sylvite, and quartz (in higher beds) are widespread minor constituents. The unit is about 30 m thick.

A. *Halite with subordinate anhydrite*: upper part is pale gray, amber, and brown, faintly banded, generally medium grained, commonly with a discontinuous ragged mesh and some thin beds of mudstone and fine-grained anhydrite and with upright fibro-radiate pseudomorphs after gypsum in numerous layers 0.001 to 0.003 m thick; lower part is of halite (as above) and halitic anhydrite, the latter with halite pseudomorphing layers of fibro-radiate coarse-grained gypsum. Thin beds of halitic dolomite are present locally. The unit is about 15 m thick.

The Boulby Halite exhibits great lateral changes

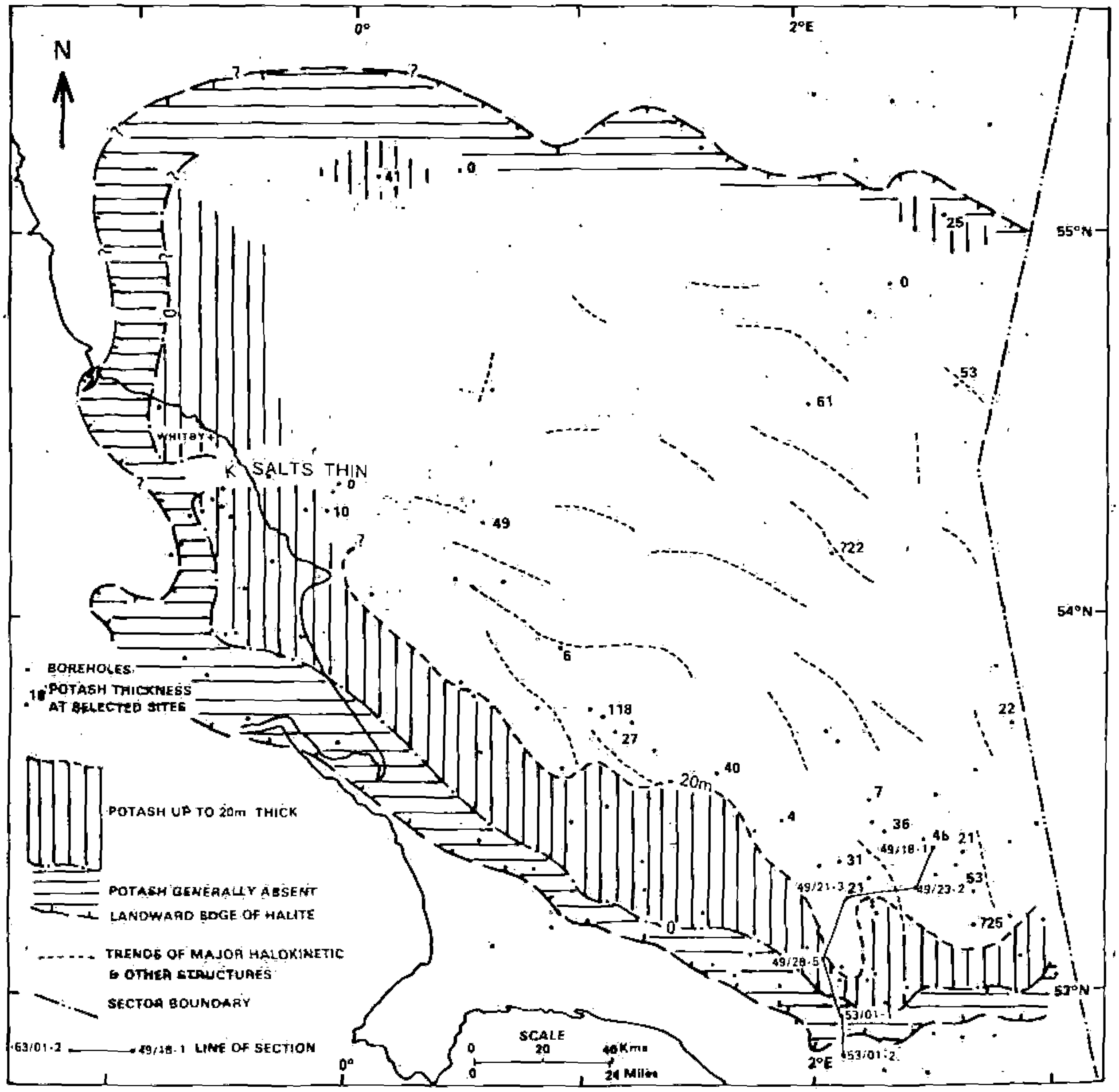

FIG. 2. Generalized distribution and thickness of the Boulby Potash in the English Zechstein Basin.

in both purity and thickness, partly because of primary lateral variations but mainly through diagenetic and tectonic effects during and after burial. These variations are superimposed on a regional, gentle, generally basinward tilt and thickening and affect the constituent units in different ways. In general units A and C have undergone the most complex diagenetic and mineralogical changes, whereas the most obvious changes in units B and C stem from plastic flow which has led to contortion and (exceptionally) local inversion. Traced westward, the Boulby Halite becomes thinner and mineralogically more simple, before terminating against an inferred solution slope; the apparent absence of residues and collapse-breccias only a few kilometers west of the margin of the halite at Teesside, northeast England, suggests that there the formation originally may not have extended far beyond its present limits. This situation may also be representative of other areas.

The complex diagenetic history of much of the Boulby Halite was revealed by the exhaustive studies of Stewart (1951a) and Armstrong et al. (1951), who demonstrated extensive replacement of the primary metastable mineral assemblages. Stewart, in particular, showed that early gypsum in the lower parts of the formation had undergone a whole series of transformations, including extensive replacement by halite and anhydrite. In the Boulby Potash the changes are even more complex, with several generations of some minerals, and little or none of the original mineral assemblage surviving. Stewart's (1956) revelation that carnallite was once the main potassium-bearing mineral in parts of this unit is especially important. Other mineralogical changes peculiar (in this area) to the Boulby Potash include first, the unpredictable presence and distribution of displacive masses and lenses up to 1 m thick of pure sylvite which have locally increased bed thickness and enhanced ore grades and, second, where the unit D is absent, have caused the local mineralization of the lower part of the Carnallitic Marl by which up to 80 percent of the rock may comprise displacive halite, sylvite, and carnallite. The presence of a mineralized zone at the base of the marl makes it difficult to identify the true top of the Boulby Potash and by occupying the place of the more competent halite of unit D could cause appreciable roof instability in mine workings. The cause and age of the mineralization are uncertain and some of it may have resulted from leaching or dehydration of the Boulby Potash during or shortly after deposition of the Carnallitic Marl.

Plastic flow in the Boulby Halite, although concentrated in the purer and mineralogically simpler halite, affects most beds. It is least apparent where a mesh of anhydrite or mudstone has hindered crystal rotation and imparted rigidity and is most apparent where anhydrite stringers in otherwise pure halite have been contorted. Flow lineation revealed by a gneissose fabric, first noted by Stewart (1951a), is widespread in units B and D wherever the formation as a whole is atypcially thick or thin and is relatively common in the Boulby Potash; beds featuring this fabric commonly contain rotated fragments of other rock types from former less ductile interbeds and locally, especially in the Boulby Potash, contain large xenolithic rafts of halitic or sylvinitic anhydrite or mudstone.

Contortion and accompanying thickness changes in the Boulby Halite in the coastal area probably stem mainly from halokinetic movements in the underlying Fordon Evaporites, but some undoubtedly result from flow induced by tectonic movement. Faults in most of the halite are apparently uncommon, possibly because of its propensity for absorbing movement by flowage and recrystallization, but are locally present in the Boulby Potash in association with sharp monoclines, rolls, and other minor dislocations. In both the Boulby Potash and the Carnallitic Marl, veins of halite, sylvite, carnallite, or rinneite (or combinations of these) up to 15 cm thick separate listric surface disposed to all angles of the bedding and are locally abundant. Sharp thickening and thinning of the Boulby Potash, and in places its complete leaching and/or pinching-out, are associated with many of the minor dislocations and most of the larger ones.

In the Boulby Halite as a whole, the sum of the many variables is insufficient to mask the essential continuity of the major subunits, and indeed some distinctive thin beds low in the formation are recognizable for considerable distances in cores and geophysical logs. In the Boulby Potash, however, the variability of thickness, mineralogy, veining, and inclination is such that it has rarely proved possible to correlate the deposit in detail even between cored boreholes a few hundred meters apart. In terms of exploration and mine working, this means that the mineralogy and stratigraphy of the orebody is unpredictable even over short distances; without supporting cores, the interpretation of geophysical logs through so variable a body is fraught with uncertainties.

The Staintondale Group (EZ4)

This group, the correlative of the Aller Series of the north German sequence, comprises four main formations (Fig. 1). Only the Upper Halite (including the Upper Potash) will be specially considered here.

The Upper Halite is slightly less extensive in northeast England than the Boulby Halite and is gen-

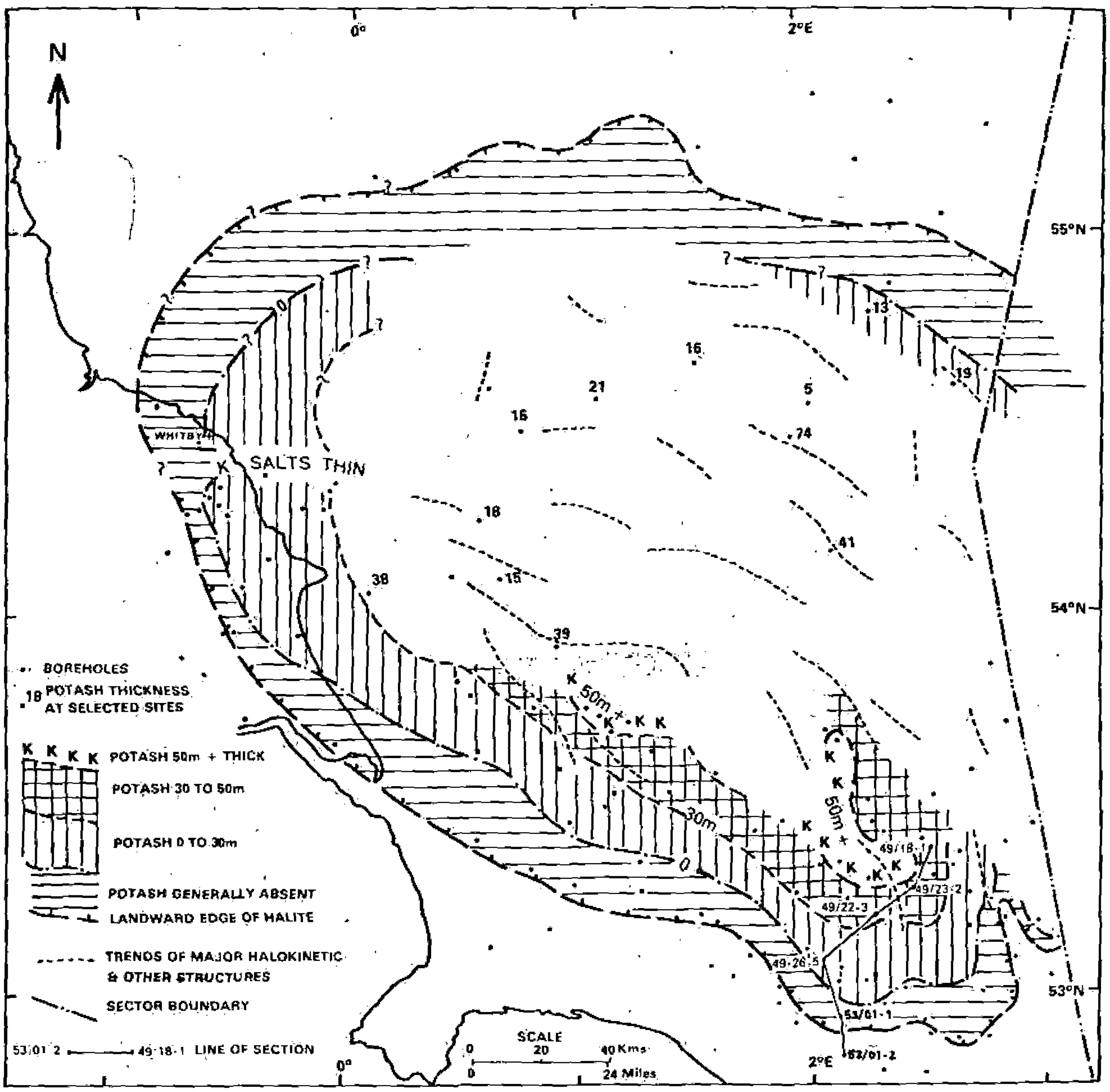

3

FIG. 3. Generalized distribution and thickness of the Upper Potash in the English Zechstein Basin.

erally somewhat thinner. From its margin (Fig. 3), inferred from its abruptness to be a solution slope, the Upper Halite thickens gently and relatively uniformly eastward to a maximum on land of about 60 m. In the coastal area of northeast Yorkshire it comprises five main units, recognizable in descriptions of several authors (Armstrong et al., 1951; Raymond, 1953; Smith, 1971, 1973; Stewart, 1951b). Except at the top of unit E and the base of unit A, boundaries are generally gradational.

From the top the units are as follows.

E. Colorless to amber, medium- to coarse-grained halite with scattered films and patches and locally a faint network of fine-grained gray anhydrite and red silty mudstone. The unit is 1.8 to 4.9 m thick.

D. Mudstone, halitic, and argillaceous or silty halite, comprising a heterogeneous, faintly layered mixture of colorless, mainly coarsely crystalline euhedral to subhedral halite, in a distended matrix of brick-red silty mudstone or argillaceous siltstone. The relative proportions of the two main components range widely and beds of almost halite-free mudstone occur. Anhydrite, hematite, magnesite, talc, quartz, and, locally in lower beds, sylvite are minor constituents. Unit D is 14 to 23 m thick.

C. (Upper Potash). Sylvinite, colorless, gray, brown, or mottled, comprising a variable mixture of medium- to coarse-grained halite and sylvite in a roughly concordant mesh of gray anhydrite and dark gray-green carbonaceous clay. Commonly divided into three or more parts by beds of halite or sylvinitic, red or gray mudstone up to 1 m thick and by beds of thinner halite and anhydrite. Averaged KCl content is up to 26 percent (Smith, 1974b), but few published data are available. Boracite, carnallite, hematite, magnesite, rinneite, talc, and quartz are generally minor constituents. Believed to pass laterally into halite and mudstone of equivalent age. The unit ranges from 0 to 8.5 m in thickness.

B. Halite: colorless, pink or amber, mainly medium-grained, equigranular, commonly weakly color-banded, and with a few laminae and thin beds of fine-grained gray anhydrite and gray or red-brown anhydritic mudstone. Local traces of a delicate distended mesh of anhydrite and/or mudstone in the upper part, where scattered patches of rinneite and sylvite are common. Hematite, magnesite, talc, and quartz are widely distributed minor constituents. Unit B ranges from 8 to 12 m in thickness.

A. Halite: colorless to pale pink, medium- to coarse-grained, faintly rhythmically color-banded, with delicate laminae of fine-grained gray anhydrite at intervals of up to 0.2 m and a few thin beds of halitic anhydrite. Halite in some rhythms near the base occurs in partly pseudomorphic courses of early upright fibro-radiate gypsum. Magnesite, rinneite, sylvite, and talc are common minor constituents, with rinneite and sylvite being locally abundant near the base. The unit ranges from 5 to 7 m in thickness.

The Upper Halite, like the Boulby Halite, is variable in both mineralogy and composition, and these variations are similarly due to both primary and secondary causes. The overall distribution and thickness of the salt, and to a large extent that of the Upper Potash, are probably primary, except where modified by dissolution, but the original mineral assemblage of unit C and to a lesser extent that of the other units has undergone complex diagenesis on a massive scale (Stewart, 1951b; Armstrong et al., 1951). Secondary thickness changes resulting from flow in the halite are most marked in units B and E, where contortion, flow lineation, and a strikingly gneissose texture are widespread. The sum of the variations, however, as in the Boulby Halite, is insufficient to obscure the overall continuity of the formation and of its individual units.

Although superficially similar to the Boulby Potash, the Upper Potash on land is considerably less variable in mineralogy and thickness. Mineralogically it differs in that it contains talc and shows no evidence that carnallite was an important primary constituent (Stewart, 1951b). But perhaps the main difference is that the Upper Potash is generally a layered body with a locally recognizable stratigraphy and with mudstone beds that may be traced for moderate distances. Although the Potash is cut by abundant minor movement planes and veins of carnallite, halite, rinneite, and sylvite, the deposit is less deformed than the Boulby Potash. Flow-lineation is uncommon in the Upper Potash.

Folds and faults in the rocks of the third and fourth cycles on land and their effect on the potash ores

The regional tectonic structure of Permian strata on land in northeast England is relatively simple with dips at the base and top generally of less than 2° and with unfaulted or sparingly faulted gentle folds commonly 2 to 5 km across and 100 to 250 m in amplitude. The top and bottom of the Permian sequence diverge eastward only slightly, mainly reflecting slight differential synsedimentary subsidence, but some strata within the sequence display considerably more complex structure. For example, the Upper Magnesian Limestone (EZ3) is appreciably more deformed and dislocated than the base and top of the Permian sequence, and greater structural complexity is also present in the Carnallitic Marl and Upper Anhydrite in the Whitby area of northeast Yorkshire. There, these two formations have been deformed into a variable much-faulted pattern by rolling folds commonly a few score meters across and with amplitudes on the order of 10 to 30 m. The cause of deformation is uncertain, although it seems likely to be a response to flow in the more ductile halite units rather than directly to external tectonic pressures. Regardless of cause, it is clear that most of the minor folds and faults in the Carnallitic Marl and Upper Anhydrite die out or diminish in the halite below and above, and that most of the movement was accommodated by flow and resulting thickness changes in units B to D of the Boulby Halite and unit B of the Upper Halite. Similar accommodation by adjoining evaporites is surmised for dislocations in the Upper Magnesian Limestone and other rigid strata lower in the sequence.

We believe that the structural variability of the Boulby Potash is greater than that of the Upper Potash mainly because the former is nearer to the most deformed part of the third and fourth cycles. In this position, it was more liable to squeezing, deformation, and redistribution or expulsion of formation fluids. Such effects also influenced the grade and thickness of the orebodies, as evidenced by the thinness or absence of the ore in the immediate vicinity of known faults and its abnormally high thickness slightly farther away. It is also evident that vein and replacive mineralization of the Carnallitic

Marl and Upper Anhydrite by carnallite, rinneite, and sylvite is most marked in areas where the Boulby Potash, though locally present, is thin or absent. In these areas we infer leaching of the potash ore and the migration of potassium and magnesium ions into fissures and interstices in the overlying mudstone and anhydrite.

A puzzling feature for which we have no satisfactory explanation is the thinness or absence of both potash beds in an irregular and ill-defined west–east belt a few kilometers south of Whitby (Figs. 2 and 3). Although this belt is generally aligned along the axis of the Cleveland anticline, the anticline is broad and gentle and seems unlikely to have radically affected the evaporites by induced flow. If there is a genetic relationship between the anticline and the belt of impoverished potash, it may be that the anticline was already active as a slightly positive feature during sedimentation. However, even though this feature decisively influenced sedimentation patterns during the Lower Permian and early Upper Permian (Smith, 1970), the narrow width of the belt—only a few kilometers—suggests a more local cause.

Potash Deposits and Related Evaporites of the Third and Fourth Cycles Beneath the Southern North Sea

Armed with the key background information from the area where the third and fourth cycle evaporites extend on land, and mindful of the erratic response of geophysical logs to the highly varied potash ores, we have attempted to establish the distribution of the halite and potash strata where they extend beneath the southern North Sea. In doing so, we are aware that the resulting maps must inevitably be generalized and subjective, and little more than vague where borehole control is scanty or lacking. Nevertheless, we believe that, particularly near the southern margin of the basin where boreholes are relatively closely spaced, the data display a considerable degree of mutual consistency and probably give a first approximation to the true distribution. As on land, the potash ores first appear some distance basinward of the margins of the halite, suggesting that this is a primary feature of their distribution. The only major exception to this is in the northeast of the basin, where sub-Upper Cretaceous erosion and solution apparently has considerably modified the primary distribution.[1] Secondary variation is presumed also to have accompanied the formation of the salt solution features described by Lohmann (1972), but no locality details are available.

Some 300 borehole records from the southern North Sea were available to the authors, but many of these were from clusters of producing wells and too closely spaced to separate at our working scale. The geophysical logs and cutting records of the remainder were carefully analyzed in the light of experience gained from the cored boreholes on land and plotted at a scale of 1 : 500,000. Those obviously affected by diapirism were ruled out first, and an approximate test for mutual consistency of an order similar to that known on land enabled us to exclude other dubious records. Isopachous lines on the resulting maps are, of course, subject to errors governed by sample size, an estimate of which may be made from the spacing of data points on Figures 2 and 3. In these diagrams we have concentrated on the thickness of the potash deposits; for isopachous lines of the halites see figure 4 of Taylor and Colter (1975).

The Teesside Group

Traced basinward the chloride evaporites of the Teesside Group thicken progressively to 60 m some 20 to 40 km from the marginal salt solution slope; we infer from averaged thickness figures that primary thickening continued beyond this, perhaps to as much as 120 m, but the evaporites in most boreholes in central parts of the basin are so variable that their original maximum thickness may only be surmised. Isopachous lines have little value in this area of widespread halokinesis.

Mainly from the evidence of geophysical logs, the Billingham Main Anhydrite and Boulby Halite are found to be continuous across the basin, and subdivisions of the latter may be traced by their distinctive signatures on electric and drilling-rate logs for long distances along the strike and for considerable distances across it (Fig. 4A). Beyond this, some subdivisions may be traced with less confidence far into the basin, where anhydrite (below) and halite make up almost the whole group.

In tracing the distribution of the Boulby Potash we have relied mainly on gamma-ray and sonic logs. The gamma-ray logs in particular show a marked deflection, permitting reasonably accurate determination of the thickness of the deposit (Fig. 2). We found that in a belt 15 to 30 km wide in the south and southwest of the basin, where data are plentiful and reasonably consistent, the Boulby Potash thickens progressively basinward to more than 20 m. In this belt, which, as onshore, may not be continuous, the potash commonly forms one-fifth to one-third of the Boulby Halite and locally forms two-thirds, but there are as many variations of thickness and grade as onshore and in some places the potash is absent; nevertheless, the trend is clear. The main problem in determining the thickness of the potash in this belt lies where unit D is absent or unrecognizable; here the Boulby Potash-Carnallitic Marl contact may be difficult to identify on geophysical logs and in these places we infer potash mineralization of unit D and of the lower parts of the Carnallitic Marl. The inferred mineralization is increasingly common farther into the basin.

On the assumption that the mineralogy of the potash ores is similar to that in Yorkshire, and on the evidence of gamma-ray deflections commonly in the range 70 to 150 API units, it seems that ore grades in the marginal belt offshore are generally within the range known onshore (up to 45% KCl) but are locally better. The presence of scattered exceptionally high gamma-ray peaks in the orebody offshore probably indicates the presence there of thick veins and lenses of pure sylvite similar to those seen in cores onshore which were associated with comparable gamma-ray responses. However, the assumption of laterally constant mineralogy may not be valid; for example, sylvinitic ores in the marginal belt may pass basinward into less diagenetically altered, more carnallitic cores. The overall KCl content probably would be unaltered by such changes.

The belt of consistent potash is succeeded basinward by a belt of about the same width (Fig. 2) in which the Boulby Potash is extremely variable in thickness and gamma-ray response. It may here comprise more than half the total thickness of the Boulby Halite and is 40 to 50 m thick in a number of boreholes. It is possible that in this belt the potash ore was originally thicker than in the more consistent belt and may have commenced formation earlier. It still, however, lies in the upper part of the Boulby Halite, a stratigraphical position suggesting broad equivalence with the Riedel Potash of northern Germany rather than with the Ronnenberg Potash. Still farther basinward, potash salts in the few boreholes not obviously affected by diapirism range from absent to very thick, vary widely in ore grade, and lie at several different stratigraphic positions; in some boreholes two or more potash beds are present. We cannot determine from available data whether this variation is primary or, as seems more likely, results from deformation such as halokinetic folding or thrusting; nor can we say whether the thickest Boulby Potash originally lay in a semimarginal belt or was thickest in the basin center. The former alternative would be more consistent with the known distribution of the Riedel Potash in Germany, but that in itself might not be a primary feature.

The Staintondale Group

Strata of this group under the southern North Sea thicken basinward more gradually and are generally thinner, less extensive, and more uniform than their counterparts in the third cycle; furthermore, diapiric salt movements affect them less and more borehole data are available than from the deeper Teesside evaporites. Even so, thicknesses are so variable that we have not attempted to draw isopachous lines in basin center areas.

In seeking to establish the pattern of distribution of the various formations in this group, we again relied mainly on geophysical logs, finding a marginal belt of reasonably consistent trends generally similar to that in the Teesside Group and a central area where data are too inconsistent for clear trends to be recognized. The Carnallitic Marl at the base of the group was found to be generally recognizable by its sharply multipeaked gamma-ray and sonic traces despite an increasing content of salts away from the margins (also noted by Taylor and Colter, 1975). The Upper (Pegmatite) Anhydrite and Upgang formations, though commonly only 1 to 5 m thick together, also show a distinctive signature on some geophysical logs. A narrow, sharp gamma-ray peak and markedly low sonic velocity at the top of Carnallitic Marl is almost ubiquitous and is probably caused by a concentration of veins of carnallite, sylvite, and rinneite such as is widespread at this level onshore. The Upper Anhydrite is commonly halite rich and/or sylvite rich and this is apparent on the geophysical logs both from land and undersea. Units A, B, and E of the Upper Halite are likewise readily traced by their distinctive log signatures and appear to change little throughout the marginal belt apart from a gentle basinward thickening and local deformation.

Unit C (the Upper Potash) and D may readily be traced in the southern marginal belt and are generally clearly separable wherever unit C is less than 10 m thick. The base of the potash is marked by a sharp step in the gamma-ray traces (Fig. 4B), and the ore itself gives a distinctive "cockscomb" trace on gamma-ray, sonic, and neutron logs. The top, too, is generally readily recognizable, so that isopachous lines may be drawn (Fig. 3) in this belt with fair confidence. As on land, there are fewer anomalies in the thickness and inferred grade of the potash ores than in the Boulby Potash and the multipeaked trace of the geophysical logs suggests that the layered structure noted onshore is widespread around the basin. Gamma-ray deflections show that some potash beds in unit C are as rich as any in the Boulby Potash, but the average grade of the whole deposit is probably lower because of the inferred mudstone and halite interbeds. Thick veins or lenses of pure sylvite appear to be uncommon in the Upper Potash in the marginal belt.

The Upper Potash in the southeast of the basin thickens basinward to more than 50 m with a consistency suggesting that the thickening is a primary feature. Judging from the geophysical logs, part of

ecu-
tash
the
ility
esis,
fore

side
of
htly
km
ated
ally

pre-
nds
sin.
our
ive.
ved

irth
le a
nar-
It
the
on-

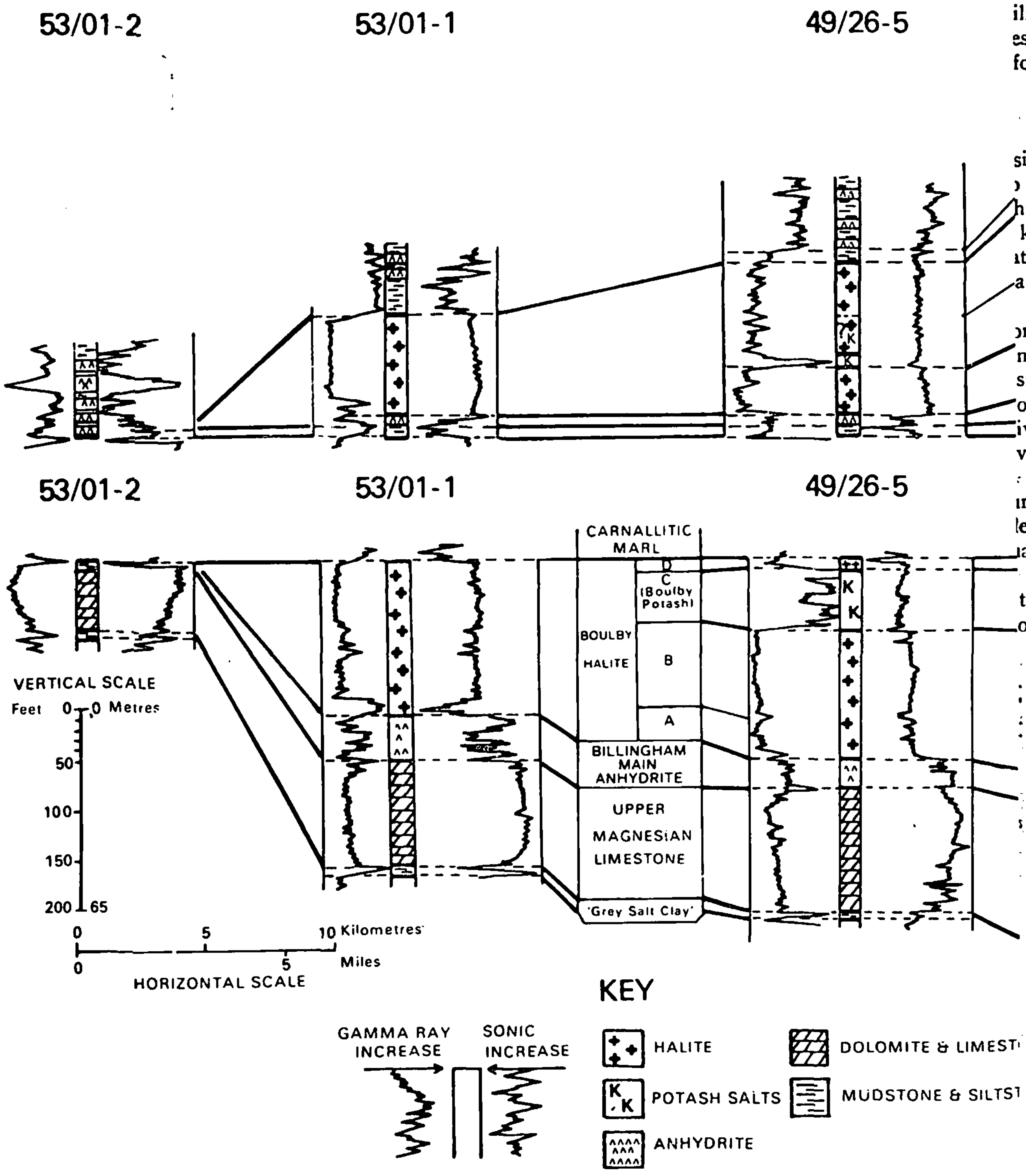

FIG. 4. Selected borel
the southern margin of th
ures 2 and 3.

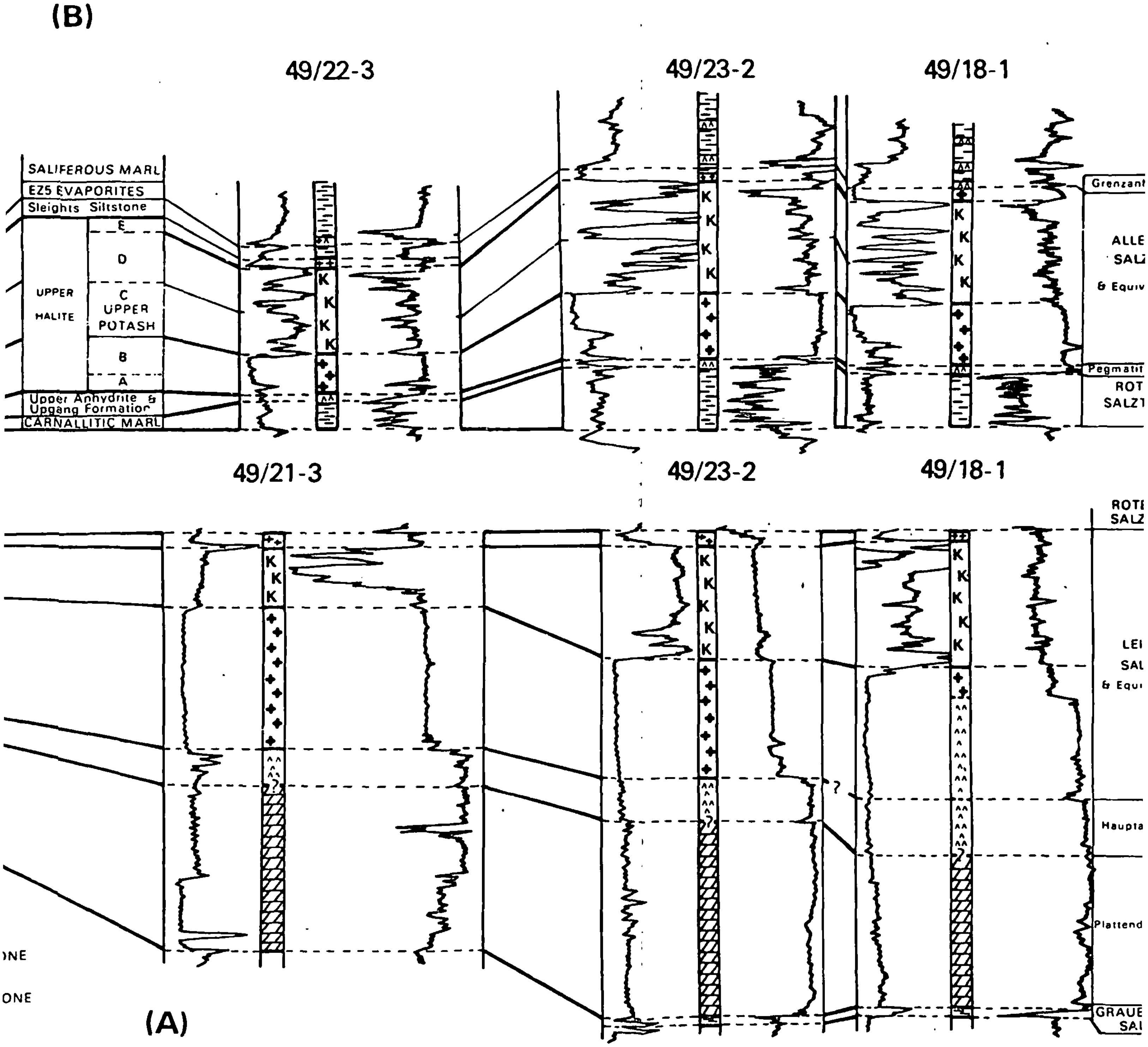

iole sections through third and fourth cycle Zechstein strata near : English Zechstein Basin. For the position of the boreholes see Fig-

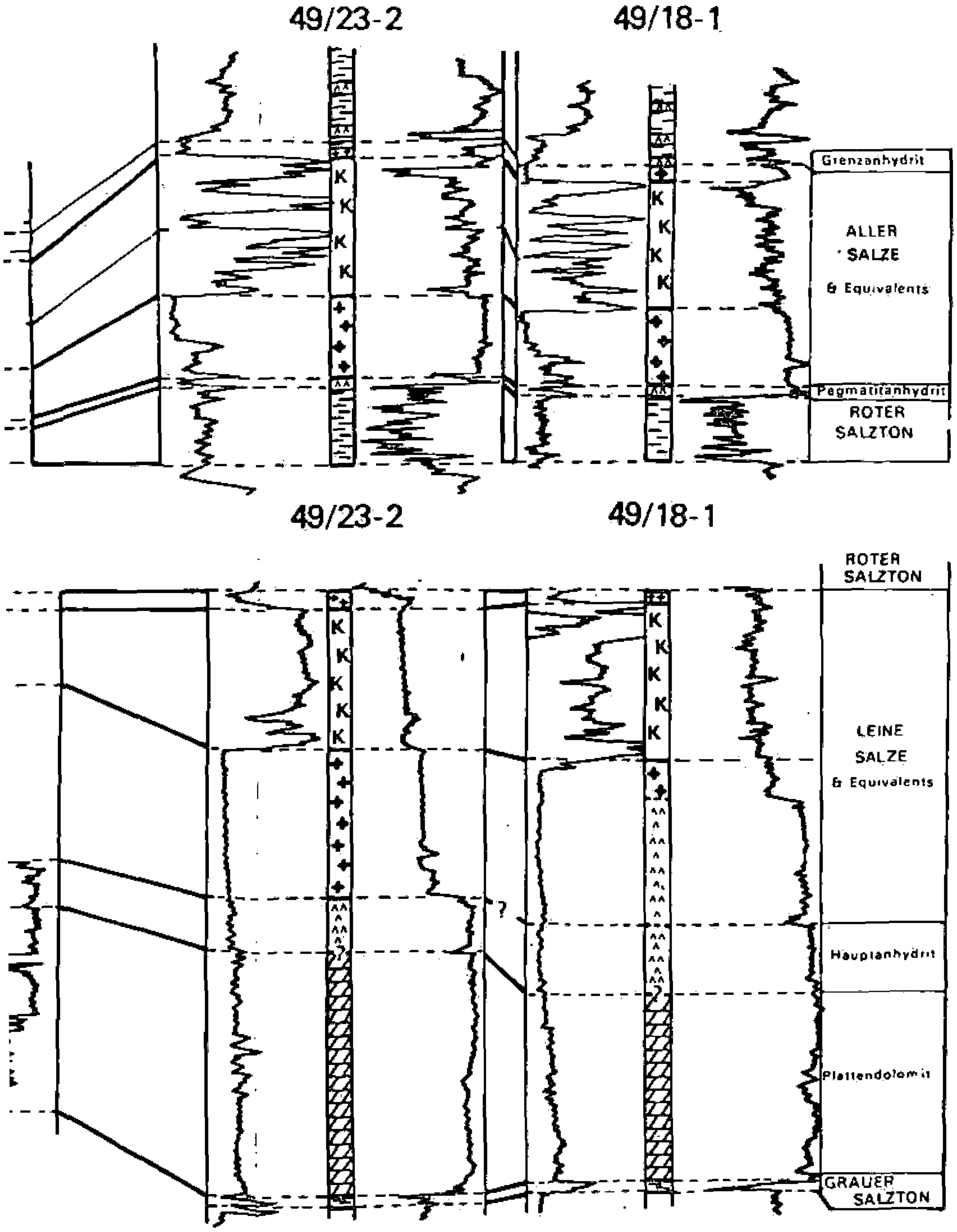

ta near
see Fig-

the thickening is probably a simple basinward expansion of unit C, but most of it, as Taylor and Colter (1975) suggested, appears to be due to the presence of abundant potash salts in unit D. In some bores where the potash-rich beds are thick it remains possible to distinguish units C and D because gamma-ray peaks in the latter tend to reach greater API unit values and to be broader and farther apart than in unit C. In other bores no such distinction is possible and units C and D merge into a thick body inferred to be of interbedded, possibly cyclic halite, mudstone, and potash. Here, as in the belt to the south, there is a tendency for geophysical logs from boreholes over limited distances to be broadly comparable (see 49/22-3 and 49/23-2 on Fig. 4B, for example), suggesting a degree of lateral continuity seldom found in the Boulby Potash. This continuity in turn suggests greater primary consistency or less complex diagenesis than in the Boulby Potash. It seems less likely in the Upper Potash than in the Boulby Potash that the marginal sylvinite grades basinward into carnallitic ore, but both carnallite and sylvite are present in unit D onshore and, on the evidence, either could predominate offshore in that unit.

A low density of boreholes limits our undestanding of the Upper Potash in basinal areas. Potash salts, where present, appear to lie mainly in unit C and are generally thinner than in the south and southwest of the basin. From this distribution it might be speculated that this is a primary feature and that the potash salts were always thickest in a belt parallel with the southwestern margin of the basin. Such a possibility has interesting connotations in terms of ore genesis, but much more reliable information is needed before it may safely be pursued.

Summary

(1) The evaporites of the third cycle Teesside Group and the fourth cycle Staintondale Group of the English Zechstein were formed in a slightly elongate arm of the Zechstein Sea about 200 km across. They were accommodated in space created by gentle synsedimentary subsidence in a generally shallow basin.

(2) In both cycles, geophysical log and other borehole information is adequate for analysis of trends only along the southwest and south sides of the basin. Data in the northwest and north is scanty and our interpretation here is correspondingly speculative. Erosion and solution are known to have removed rocks of both cycles in the northeast.

(3) Cores from rocks of the third and fourth cycles in more than 60 boreholes onshore provide a key to the interpretation of geophysical logs in marginal areas offshore, where no cores are available. It appears that the sequences in both cycles around the margins offshore are generally similar to those on-

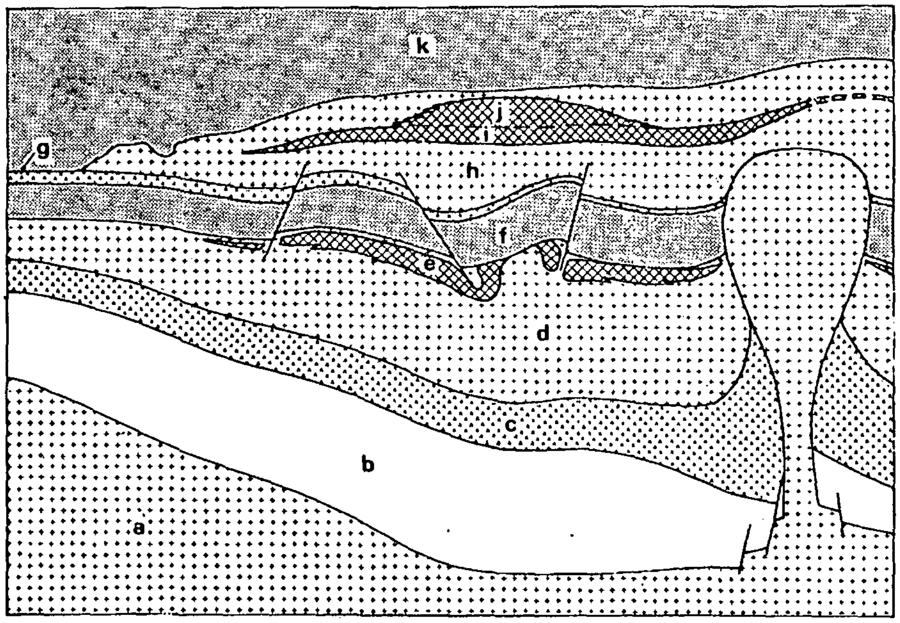

FIG. 5. Diagrammatic section of third and fourth cycle Zechstein strata near the southern margin of the English Zechstein Basin, as tentatively interpreted from borehole data. The section is about 40 km long. Key: a = Fordon Evaporites, b = Upper Magnesian Limestone/Plattendolomit, c = Billingham Main Anhydrite/Hauptanhydrit, d = Boulby Halite/Leine Halit, e = Boulby Potash, f = Carnllitic Marl/Roter Salzton, g = Upper Anhydrite/Pegmatitanhydrit, h = Upper Halite/Aller Halit, i = Upper Potash, j = Potash salts in unit D of Upper Halite, k = Saliferous Marl, 5th cycle evaporites and Sleights Siltstone.

shore and have a comparable order of variability. Fourth cycle evaporites are somewhat less extensive than those of the third cycle.

(4) Halotectonic deformation of the evaporites of both cycles is generally slight to moderate in a marginal belt commonly 20 to 40 km wide but is prevalent in central areas beyond a line corresponding roughly with the basinward limit of thick Upper Magnesian Limestone. In the marginal belt deformation is generally most apparent in the Carnallitic Marl between the two cycles and in immediately adjacent evaporites, including the Boulby Potash.

(5) The third cycle Boulby Potash is perhaps up to 40 m thick where undisturbed in the west, southwest, and south of the basin. Here it is a markedly variable but commonly high-grade ore, probably mainly sylvinitic. We cannot determine whether it occurs offshore in a series of minor subbasins as it appears to onshore or is a continuous belt. Thicknesses exceeding 40 m probably result from secondary processes, mainly flow, and scattered barren areas may reflect nondeposition, leaching, or extreme tectonic attenuation. The Boulby Potash in the halotectonically disturbed basin center areas is even more variable than in the southwest marginal belt and is commonly thinner.

(6) The less variable fourth cycle Upper Potash (i.e., unit C) is more than 20 m thick in a belt generally parallel with that in which the Boulby Potash is thickest, but abundant potassium salts apparently in the overlying argillaceous halite (unit D) occur in a belt 10 to 20 km across and the combined thickness of potash ore here exceeds 50 m. Although ore grades in individual parts of the deposit are probably equal to those in the Boulby Potash, the average grade is lower because of widespread interbeds of halite and mudstone. The Upper Potash in the basin center is commonly thinner and more variable than to the southwest.

(7) An interpretation of the present distribution and disposition of the rocks of the third and fourth cycles in the marginal belts is given in Figure 5.

Acknowledgments

The authors are indebted to British Gas, the British Petroleum Company, Candecca Resources Limited, and Home Oil (UK) Limited for permission to use data from specified boreholes onshore in the preparation of Figures 2 and 3, and to Cleveland Potash Limited and Yorkshire Potash Limited for clearance of the background information used in preparation of the text on onshore potash deposits. Brian Hains, Glyn Rhys, John Taylor, Robert Hite, and Omer Raup read the text and made many helpful suggestions. Permission to publish has been granted by the Director, Institute of Geological Sciences.

Institute of Geological Sciences
5 Princes Gate
South Kensington, London SW7 1QN,
England
September 29, 1978

REFERENCES

Armstrong, G., Dunham, K. C., Harvey, C. O., Sabine, P. A., and Waters, W. F., 1951, The paragenesis of sylvine, carnallite, polyhalite, and kieserite in Eskdale Borings Nos. 3, 4, and 6, north-east Yorkshire: Mineralog. Mag., v. 29, p. 667–689.

Lohmann, H. H., 1972, Salt dissolution in sub-surface of British North Sea as interpreted from seismograms: Am. Assoc. Petroleum Geologists Bull., v. 56, p. 472–479.

Raymond, L. R., 1953, Some geological results from the exploration for potash in north-east Yorkshire: Geol. Soc. London Quart. Jour., v. 108, p. 283–310.

Smith, D. B., 1970, The palaeogeography of the English Zechstein, *in* Rau, J. L., and Dellwig, L. F., eds., Third symposium on salt, v. 1: Cleveland, Geol. Soc. Northern Ohio, p. 20–23.

—— 1971, Possible displacive halite in the Permian Upper Evaporite Group of north-east Yorkshire: Sedimentology, v. 17, p. 221–232.

—— 1973, The origin of the Permian Middle and Upper Potash Deposits of Yorkshire: an alternative hypothesis: Geol. Soc. Yorkshire Proc., v. 19, p. 327–346.

—— 1974a, Permian, *in* Rayner, D. H., and Hemingway, J. E., eds., The geology and mineral resources of Yorkshire: Leeds, Geol. Soc. Yorkshire, p. 115–144.

—— 1974b, Evaporites, *in* Rayner, D. H., and Hemingway, J. E., eds., The geology and mineral resources of Yorkshire: Leeds, Geol. Soc. Yorkshire, p. 337–344.

Stewart, F. H., 1951a, The petrology of the evaporites of Eskdale No. 2 Boring, east Yorkshire: Part 2, The Middle Evaporite Bed: Mineralog. Mag., v. 29, p. 445–475.

—— 1951b, The petrology of the evaporites of Eskdale No. 2 Boring, east Yorkshrie: Part 3, The Upper Evaporite Bed: Mineralog Mag., v. 29, p. 557–572.

—— 1956, Replacements involving early carnallite in potassium-bearing evaporites of Yorkshire: Mineralog. Mag., v. 31, p. 127–135.

Taylor, J. C. M., and Colter, V. S., 1975, Zechstein of the English Sector of the Southern North Sea Basin, *in* Petroleum and the Continental Shelf of north-west Europe, v. 1, Applied science: Barking, England, Applied Science Publishers Limited, p. 249–263.

SUBJ
MNG
RSCD

REDUCTION OF SELENIUM COMPOUNDS DISSOLVED IN CONCENTRATED SULFURIC ACID

UDC 669.776:661.25

A. A. Zhukova, V. S. Epifanov, and L. V. Konyakhina

It is desirable in a number of processes in non-ferrous metallurgy to reduce and extract selenium from concentrated sulfuric acid without diluting it. It was discovered when studying the soption properties of bituminous coal in concentrated 92% sulfuric acid that certain grades of coal were capable of extracting the selenium dioxide dissolved in the acid completely. Apparently the selenium is reduced not by adsorption but as a result of the participation of some constituent in the coal in the reaction. The latter proposition is confirmed by the fact that in practice coke made from bituminous coal and graphite does not directly reduce selenium from 92% sulfuric acid.

Further research on the selenium reduction involved studying the reducing capacit of individual compounds found in bituminous coal [1]. The experiments were conduct under laboratory and pilot-plant conditions with 92% acid containing 0.02% dissolve selenium dioxide. The extent of selenium extraction was calculated from the acid selenium content before and after the experiment, and also by reference to the amo of selenium in the slime separated from the acid.

The acid was passed through the reactor tank in continuous experiments at a speed which ensured the necessary time for reaction between the selenium and the reducing agent, which was added to the acid before it entered the reactor. About 40 indivi substances found in bituminous coal or its primary tar have been tested for activit relative to selenium, but only some of them have the capacity to reduce selenium ef- tively (see Table).

Bituminous coal itself reduces selenium practically completely over a period of 30 min at 80°C. The product obtained may contain 12-17% Se reduced on particles of coal if the reduction process is conducted with continuous addition of fresh batche of coal and subsequent removal of slime from the reaction zone. However, if the ac is passed through a layer of coal floating in it and this layer is mixed so that th particles of elementary selenium can be "shaken off" the coal particles and carried away by the stream of acid, the selenium slime produced will contain up to 50% Se and addition of fre batches of coal can be reduced to the level necess to make up for the loss of coal with the stream of acid [2].

Reduction of Selenium from 92% Sulfuric Acid by Substances Found in Bituminous Coal, at 80°C

Reducing agent	Amount, g/100 ml of acid	% reduction in time (in min.)				Se content in slime %
		5	15	30	60	
Bituminous coal "K"	1,00	30,0	78,0	95,0	96,0	12—50
Primary coal tar	0,05	46,5	82,0	96,0	98,0	75—85
Butyl mercaptan	0,01	96,0	96,0	92,0	90,0	60—70
Cyclohexanone	0,03	17,4	85,0	91,0	92,0	85—95
Formic acid	0,10	86,0	93,0	95,0	95,0	85—95
Oxalic acid	0,10	5,0	10,0	15,0	96,5	85—95
Carbon monoxide	300 ml/min	5,0	15,0	30,0	65,0	85—95

Butyl mercaptan is very active in the process of se lenium extraction [3], but the selenium slime prod contains 30-40% S. Processing this slime to obtai mercial grades of selenium will call for complex operations, which creates considerable difficulties in practical use, apart from the toxicity of the reducing agent itself.

The rest of the reducing agents given in the Table are fairly effective and do not contaminate the selenium slime separated from the acid with impurities. The arsenic, iron, and copper compounds present in commercial sulfuric acid do not interfere with the reduction of selenium and are not themselves reduced in these circumstances. The reducing agent consumption is close to the stoichiometric amount if it is assumed that the process of selenium dioxide reduction to metal involved oxidation of the

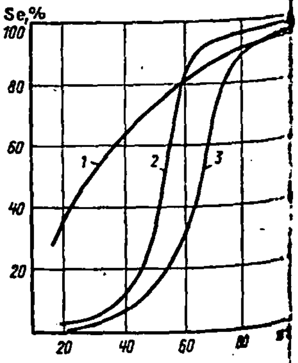

Fig. 1. Relationsh of selenium reduc tion to temperat when the followi reducing agents a used:
1 - bituminous coa
2 - formic acid;
3 - cyclohexanone.

organic reagent to carbon dioxide. The high selenium content of the slimes ensures efficient processing to obtain commercial grades of selenium.

The process temperature has a profound effect upon reduction of selenium from concentrated sulfuric acid (Fig. 1). In the case of cyclohexanone and formic acid there is a sudden increase in the degree of selenium reduction in the 50-70°C range; this is probably due to the decomposition of the reducing agent by the sulfuric acid.

The course of the kinetic curves (Fig. 2), especially at low temperatures, shows that the process is retarded initially then sharply increases in speed. This phenomenon is observed only in experiments with pure solutions of selenium in 92% sulfuric acid. However, if the experiments were conducted with addition of metallic selenium crystals to the acid or with continuous flow of fresh solution into the reactor where reduced selenium was already present, there was practically no reduction process induction period. Obviously the process was retarded by formation of a new phase (crystalline selenium).

Thus, a few minutes are sufficient for reduction of selenium with formic acid at temperatures above 50°C and for the reduction reaction to be practically complete. This is extremely important because, for example, the reduction process itself can be carried out directly on the filter where the metallic selenium is separated from the acid [4].

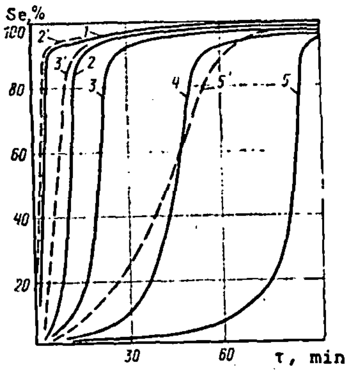

Fig. 2. Kinetic curves for reduction of selenium dioxide by formic acid according to following temperatures, °C:
1 - 80; 2,-2' - 70; 3, 3' - 50; 4 - 40; 5, 5' - 35.
Dashes indicate experiments in which metallic selenium crystals were added at the beginning.

REFERENCES

1. S. M. Grigor'ev, Processes of Fossil Fuel Formation and their Properties, Moscow, Izd-vo Akad. Nauk SSSR, 1954 262 pp., ill.
2. V. S. Epifanov, A. A. Zhukova, et al., Inventors' Cert. No. 295385, Otkrytiya Izobreteniya, Promyshlennye Obraztsy, Tovarnye Znaki, 1974, No. 17, 226.
3. V. S. Epifanov, A. A. Zhukova, and L. V. Konyakhina, Inventors' Cert. No. 295386, Otkrytiya, Izobreteniya, Promyshlennye Obraztsy, Tovarnye Znaki, 1974, No. 17, 226.
4. V. S. Epifanov, L. V. Konyakhina, and A. A. Zhukova, Inventors' Cert. No. 420235, Otkrytiya Izobreteniya Promyshlennye Obraztsy, Tovarnye Znaki, 1974, No. 25, 173.

United States Patent [19]

Pepper et al.

[11] **4,177,067**

[45] **Dec. 4, 1979**

[54] RECOVERY OF SILVER, COPPER AND ZINC FROM PARTIALLY ROASTED PYRITE CONCENTRATE BY FERRIC SULPHATE LEACHING

[75] Inventors: Terry W. Pepper, Golden; Harry G. Bocckino, Lakewood, both of Colo.

[73] Assignee: Texasgulf Inc., Stamford, Conn.

[21] Appl. No.: 897,016

[22] Filed: Apr. 17, 1978

[51] Int. Cl.^{2} C22B 11/06; C22B 15/08; C22B 13/04

[52] U.S. Cl. .... 75/104; 75/101 BE; 75/117; 75/118 R; 75/120; 423/24; 423/566; 423/571

[58] Field of Search .... 75/104, 117, 118 R, 75/120, 101 BE; 423/571, 566, 24

[56] References Cited

U.S. PATENT DOCUMENTS

240,309	4/1881	Deby	75/104
252,593	1/1882	Deby	75/104
513,490	1/1894	Emmens	75/104
1,451,734	4/1923	Irving	75/104
1,570,777	1/1926	Pike	75/113 X
2,647,827	4/1953	McGauley	75/103
2,992,894	7/1961	Hazen et al.	75/117 X
3,034,864	5/1962	Nashner et al.	423/571
3,109,732	11/1963	Goren	75/101 R
3,459,535	8/1969	Vizsolyi et al.	75/117 X
3,476,554	11/1969	Spedden et al.	75/109
3,529,957	9/1970	Kunda et al.	75/108
3,634,071	1/1972	Spedden et al.	75/109
3,640,703	2/1972	Cooper	75/101 R
3,661,563	5/1972	Spedden et al.	75/101 R
3,669,651	6/1972	Spedden et al.	75/104
3,819,797	6/1974	Spedden et al.	423/27
3,966,462	6/1976	Posel et al.	75/101 BE

Primary Examiner—G. Ozaki
Attorney, Agent, or Firm—Kenyon & Kenyon

[57] **ABSTRACT**

A process for treating a pyrite concentrate containing silver, copper and zinc to recover the metals contained therein is disclosed. The process includes the partial roasting of the concentrate to open the pyrite matrix to solution penetration followed by hydrometallurgical steps, including ferric sulphate leaching, reduction leaching, solid-liquid separation and metal extraction steps, to recover the copper and zinc separately and silver in concentrated form.

14 Claims, 1 Drawing Figure

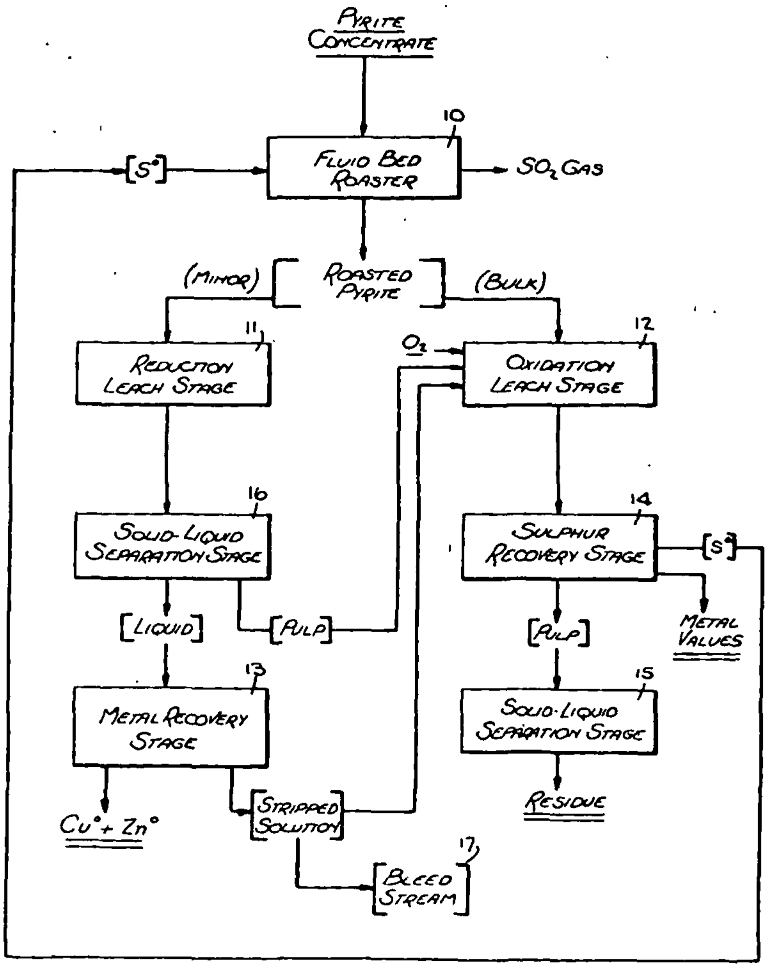

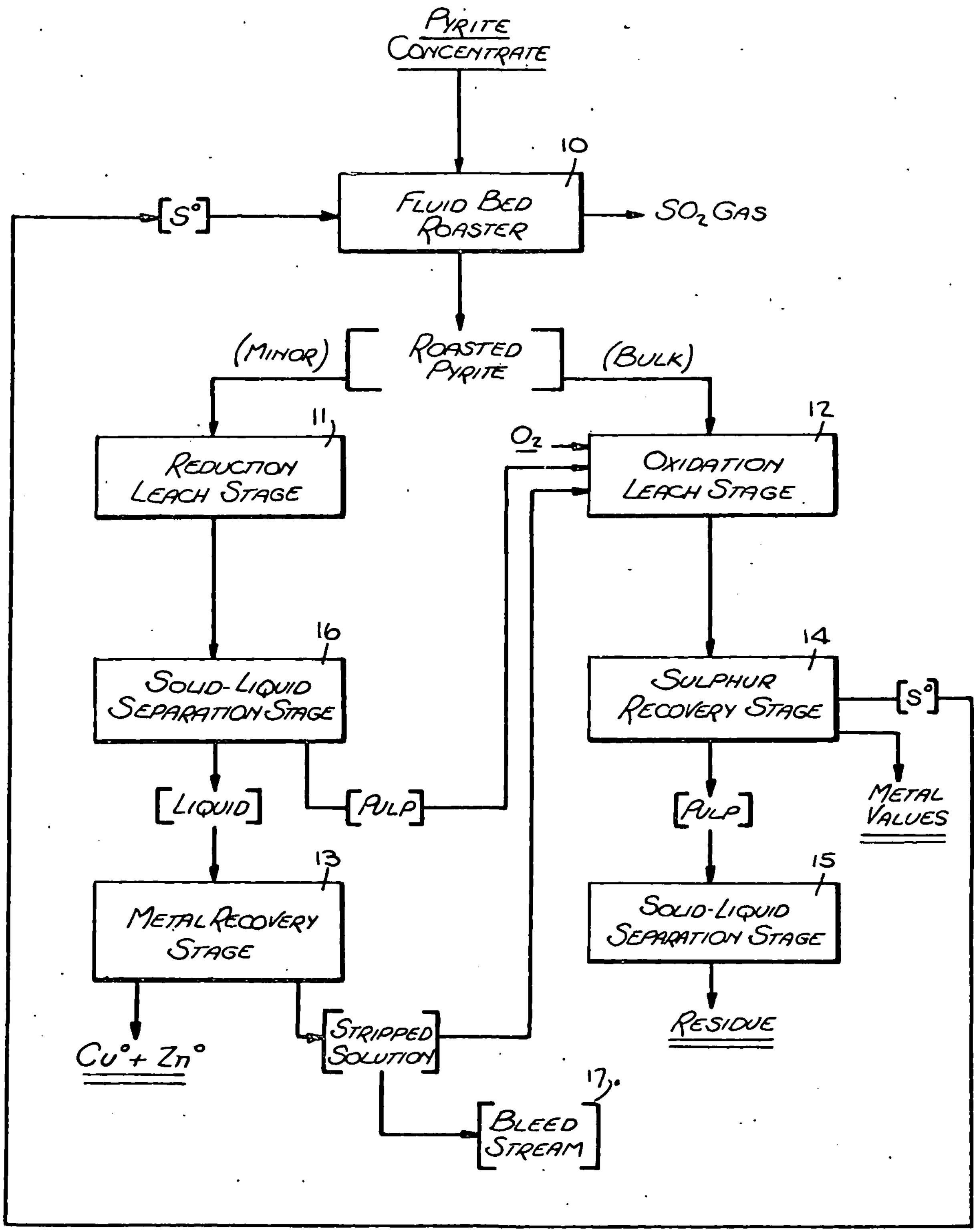
Pyrite Concentrate
10
[S°]
Fluid Bed Roaster
SO2 Gas
(Minor)
Roasted Pyrite
(Bulk)
11
Reduction Leach Stage
12
O2
Oxidation Leach Stage
16
Solid-Liquid Separation Stage
14
Sulphur Recovery Stage
[S°]
[Liquid]
[Pulp]
[Pulp]
Metal Values
13
Metal Recovery Stage
15
Solid-Liquid Separation Stage
Cu° + Zn°
Stripped Solution
Residue
17
Bleed Stream

RECOVERY OF SILVER, COPPER AND ZINC FROM PARTIALLY ROASTED PYRITE CONCENTRATE BY FERRIC SULPHATE LEACHING

BACKGROUND OF THE INVENTION

1. Field of the Invention

This invention relates to a process for treating sulphur containing ores, and more particularly, is directed to a process for recovering copper, silver and zinc from a partially roasted pyrite concentrate by ferric sulphate leaching.

2. Description of the Prior Art

In the past a variety of processes have been used for the extraction of metals and non-metals from sulphide ores. In many of these processes the sulphide ores have been subjected to concentration steps prior to recovery of specific metal values contained therein. Most of these processes suffer from the same disadvantage, in that they are incapable of recovering all the metal values in the ore using one economical process.

In addition many of the prior art processes have been limited to specific ores and concentrates which have a high concentration of the desired components to make the removal of those components economically feasible.

In a number of the above mentioned processes the sulphide ore concentrates are subjected to ferric sulphate leaching techniques to recover the metal values contained therein. Some of these processes even include a thermal decomposition of the pyrite concentrate prior to leaching. However, in many of these prior art processes the pyrite concentrate matrix is virtually unattacked by the initial heating of the pyrite and therefore a significant portion of the metal values occluded in the pyrite is lost, since they cannot be reached by the leach solution.

Lastly many of the previously mentioned processes require the use of either chloride or cyanide to extract the silver from the pyrite. Chloride ions in an oxidizing atmosphere present corrosion problems and the use of cyanide may involve problems in waste control.

The process of the present invention provides for the recovery of the metal values from a pyrite ore by opening the pyrite matrix prior to the leaching stage resulting in higher percentages of metal extraction.

Furthermore the process of the present invention allows for the complete recovery of essentially all the metal values contained in the pyrite concentrate without the use of chloride or cyanide.

SUMMARY OF THE INVENTION

The present invention relates to a method for the extraction and recovery of metals and sulphur from pyrite concentrate. In accordance with the present invention the pyrite concentrate is roasted to open the pyrite matrix to solution penetration. Subsequent to roasting the pyrite is split into two fractions, the larger of which is leached in a ferric sulphate solution. When the leaching is complete, the pulp is flashed to cool the solution and to reduce the volume of the leach liquor. Wash water is then added to the oxidation leached pulp to further cool the material and to complete the solidification of the molten elemental sulphur generated during leaching.

This elemental sulphur, now in the form of pellets, is reheated and filtered. The elemental sulphur, recovered as the filtrate, is essentially pure and is recycled to the fluid bed roaster. The filter cake which contains significant amounts of the metal values is treated for metal recovery.

The oxidation leached pulp, after sulphur removal, is flocculated, and a solid-liquid separation is accomplished by settling. The settled pulp is filtered and washed and the pulp discarded.

The solution recovered from the oxidation leach stage is then reduced by contacting it with a small amount of roasted pyrite concentrate in a reduction leach stage.

After the reduction stage is completed the pulp is flocculated and filtered. The filter cake or pulp is then returned to the oxidation leach stage to recover any metal contained therein while the solution, is treated to recover copper and zinc.

The copper is recovered from solution by precipitation with either iron or zinc while the zinc is recovered by solvent extraction and electrowinning.

Accordingly, it is an object of the process of the present invention to recover copper, silver, zinc, and lead from pyrite concentrate.

Another object of the process of the present invention is the recovery of silver from pyrite concentrate without the use of cyanide, which presents health hazards.

Another object of the process of the present invention is the production of a concentrated SO_2 gas stream for sulphuric acid production.

Another object of the process of the present invention is the recovery of silver without the use of chloride which presents corrosion problems.

Still other objects and advantages of the present invention will be apparent from the specification and attached drawing.

BRIEF DESCRIPTION OF THE DRAWING

For a fuller understanding of the invention reference is had to the following description taken in connection with the accompanying drawing wherein a flow chart of the preferred embodiment, indicating the various stages or steps in schematic form, is shown.

DESCRIPTION OF THE PREFERRED EMBODIMENT

The process of the present invention comprises treating a pyrite concentrate containing silver, copper, and zinc to recover the metals. The process involves roasting the concentrate followed by hydrometallurgical steps to recover copper and zinc separately and silver in a concentrated form.

As shown by the flow chart depicted in the drawing the process comprises seven basic steps or stages, those being: a pyrite roasting stage, an oxidation leach stage, a sulphur recovery stage, a first solid-liquid separation stage, a reduction leach stage, a second solid-liquid separation stage and a metal recovery stage.

For the purpose of clarity the process of the present invention will be described in reference to the above listed steps.

Pyrite Roasting Stage

Referring to the drawing the pyrite concentrate is introduced to fluid bed roaster **10** wherein a portion of the sulphur originally contained in the concentrate is driven off.

In order to completely open the pyrite matrix to leach solution penetration it has been calculated that at least 50% of the pyrite sulphur should be removed, however, it had been found in practice that somewhat less than 50% sulphur elimination is sufficient to allow satisfactory solution penetration to the occluded minerals. In cases where the roasting stage is also being used to evaporate water added for washing purposes, more than 50% sulphur elimination may be required to maintain the reaction temperature.

During the roasting stage exhaust gas will be generated. This gas contains very little oxygen and consists primarily of nitrogen, water vapor, sulphur dioxide, and traces of sulphur trioxide. This gas, after removal of entrained particles, may be used in the production of sulphuric acid.

It has been found that sulphur elimination of about 45% to 80% not only produces a strong SO_2 off-gas suitable for sulphuric acid production, but also opens the pyrite matrix sufficiently to allow rapid and essentially complete dissolution of the copper and zinc occluded therein by the leach solution. Sulphur elimination of 45% to 50% is preferred to leave maximal sulphur for elemental sulfur formation during leaching.

In addition to the above, the hot gases generated during roasting may be used in waste heat boilers to generate steam. However, when using waste heat boilers, about 80% sulphur elimination is preferred in order to produce maximal steam without forming ferrites in the roasted pyrite. Roasting temperatures of about 550° C. to about 700° C. are suitable to prevent ferrite formation when sulphur elimination of from about 45% to about 80% is effected.

Oxidation Leach Stage

Subsequent to roasting, the pyrite concentrate is split into two fractions the larger of which is introduced to the oxidation leach stage **12** where it undergoes oxidation in a ferric sulphate solution.

As can be seen in the drawing, two solution streams enter the oxidation leach stage. The first of these solutions is the stripped solution from the metal recovery stage **13** which acts as a lixiviant for the oxidation leaching reaction. The second solution stream introduces the pulp from the reduction leach stage and contains a small amount of reduced pregnant solution. All of the iron contained in these solutions is originally present as ferrous ion and is oxidized to ferric ion in the reaction described by the following equation:

$$2Fe^{+2}+1/2O_2+2H^+\rightarrow 2Fe^{+3}+H_2O$$

More specifically this reaction may be described for the ferric sulphate system of the present invention by the following equation:

$$2FeSO_4+1/2O_2+H_2SO_4\rightarrow Fe_2(SO_4)_3+H_2O$$

The ferric ions formed as shown above, leach the copper, zinc, and iron minerals from the pyrite as shown below:

$$CuFeS_2+2Fe_2(SO_4)_3\rightarrow CuSO_4+5FeSO_4+2S^\circ$$

$$ZnS+Fe_2(SO_4)_3\rightarrow ZnSO_4+2FeSO_4+S^\circ$$

$$FeS+Fe_2(SO_4)_3\rightarrow 3FeSO_4+S^\circ$$

Lead and silver are relatively unleached by the ferric sulphate solution.

As can be seen from the above equation the oxidation leach stage not only effects the dissolution of copper and zinc but also results in the generation of elemental sulphur. It has been found that silver in the form of silver sulphide is collected in this elemental sulphur and that higher leaching temperatures generally result in higher silver concentrates in the sulphur.

In addition to its effect on the concentration of the metals entrapped by the elemental sulphur, the leaching temperature also has an effect on the amount of the sulphur present in the leached pulp.

At temperatures greater than about 150° C. the elemental sulphur begins oxidizing at a significant rate to form sulphuric acid and as the temperature exceeds 175° C. the amount of recoverable elemental sulphur declines rapidly. At 200° C., no elemental sulphur is recovered. It has been found that a temperature range of between about 175° C. and 185° C. gives maximum silver loading of the sulphur without major loss of sulphur recovery.

In the temperature range of about 175° C. to about 185° C., the optimal oxygen partial pressure is over 120 psia, preferably 150 psia, supplied as oxygen or air. At these temperatures 20 minutes is adequate for reaction and any additional time results in reduced sulphur recovery and correspondingly reduced silver recovery. Pulp densities of up to 400 grams of roasted pyrite per 600 ml of leaching solution react satisfactorily, while pulp densities of under 100 grams of roasted pyrite per 600 ml of leaching solution result in an unsatisfactorily weak pregnant solution.

The concentration of the constituents within the oxidation leach solution will depend upon the material being leached, the reaction rate desired, as well as the limits imposed by the nature of the containment vessels. Generally it has been found when using a Kidd Creek pyrite concentrate, that the oxidation leaching stage solution will have the following composition:

Constituent	Concentration
Fe(T)	5- 30 g/l
SO_4^{-2}	40-100 g/l

The pH of this solution may vary from about 0.6 to about 1.0, however, in order to prevent acid build-up small amounts of NaOH may be added.

Sulphur Recovery Stage

At the conclusion of the oxidation leaching stage the solution is flashed to 100° C. and introduced to the sulphur recovery stage **14**. Water, used for washing the final residue and then the sulphur pellets, is added to the pulp to provide further cooling. The sulphur pellets which form at the time of cooling are next recovered by either screening or flotation. The pellets are washed on a screen with water previously used to wash the oxidation leach residue. The pellets are then heated to about 150° C., such that the viscosity of the molten sulphur is at a minimum, and filtered. Essentially pure sulphur is collected as a filtrate for recycle to the fluid bed Roaster. The filter cake containing silver and some copper and zinc is recovered for extraction of the metals contained therein. In an alternate embodiment the sulphur is recovered by dissolution in an organic solvent.

First Solid-Liquid Stage

The oxidation leach pulp, after the sulphur pellets have been removed, is subjected to a first solid-liquid separation stage **15** where it is flocculated and settled. The thickened pulp, which contains about 50% solids, is then filtered and washed. The washed residue, containing about 28% moisture, is discarded.

Reduction Leach Stage

The clear lixiviant which results from the solid-liquid separation stage is high in ferric ion. This high concentration of ferric ion concentration would result in excess reductant consumption if metal recovery were attempted. Therefore, in order to reduce the concentration of ferric ions in the solution, it is contacted with fresh roasted pyrite in the reduction leach stage **11** (not shown). The ferric ions are reduced to ferrous ions by reaction with artificial pyrrhotite contained in the partially roasted pyrite by the following equation:

$$Fe_2(SO_4)_3 + FeS \rightarrow 3FeSO_4 + S^\circ$$

The temperature of the reduction leaching stage may vary considerably, from ambient (22° C.) to the melting point of sulphur. However, over 119° C., the elemental sulphur tends to coat the particles and inhibit reactions. At 100° C., 90% ferric ion reduction can be achieved in 30 minutes with the addition of an excess of about 60% roasted pyrite concentrate. Note that for optimum results during the reduction leaching stage, oxygen partial pressure in the reaction vessel should be minimized.

Second Solid-Liquid Separation Stage

When the reduction leaching stage has been completed the reduced product is recovered and introduced to a second solid-liquid separation stage **16** where it is flocculated and then filtered. The filter cake is then recycled to the oxidation leaching stage for recovery of the residual copper and zinc, as well as the silver and sulphur, while the clear filtrate is processed to recover the copper and zinc. In an alternate embodiment the reduction leach pulp is flocculated and settled. The settled pulp is then recycled to the oxidation leaching stage.

Metal Recovery Stage

Copper may be recovered from the clear filtrate by precipitation while the zinc is recovered by solvent extraction and electrowinning. Precipitation may be carried out with a variety of metals, iron being the most common in commercial operations. Zinc may also be used if available.

As can be seen from the drawing, the stripped solution from metal recovery stage **13** is recycled to the oxidation leach stage **12**. A bleed stream **17** isolates a portion of the stripped solution to compensate for water added to the system during washing operations.

In another embodiment of the present invention the sulphur pellets recovered from the sulphur recovery stage are subjected to an additional leach stage in which the pellets are leached at approximately 135° C. to dissolve copper and zinc without major oxidation of the elemental sulphur.

Although the solution concentrations in the present invention may vary, estimated solution concentrations are given in the following table. The values for copper and zinc are based on a 30% solids leach and therefore these values would be higher if the pulp densities were increased. On the other hand the iron and sulphate analysis would be expected to remain the same if no changes were made in the pH or temperature.

FERRIC SULPHATE PROCESS
LEACHING SOLUTION CONCENTRATIONS

Solution	Cu^{+2} (g/l)	Zn^{+2} (g/l)	Fe^{+2} (g/l)	$SO4^{-2}$ (g/l)
Stripped Solution	0.00	0.1	19	76
Reduced Pregnant Solution	0.20	9.7	19	76
Pregnant Solution	0.24	11.4	15(1)	90
Diluted Pregnant Solution	0.20	9.7	13(1)	76

(1) Ferric ion (Fe^{+3})

The foregoing process may be illustrated by the following example.

EXAMPLE

Pyrite concentrate containing silver, copper, lead and zinc was roasted in a fluid bed roaster at 595° C. until approximately 44% of the sulphur contained therein was eliminated. The roasted pyrite was then subjected to a ferric sulphate leach stage. The temperature within the leach stage was 175° C. at an oxygen partial pressure of 150 psia. The pulp density within the leach stage was 30%. After 20 minutes of leaching the solution was flashed to 100° C. and the elemental sulphur generated during leaching was separated.

The following are the amounts of metals recovered from the solution and the sulphur based on the amount contained in the roasted pyrite:

	PERCENT METAL EXTRACTED (by weight)				
Product Phase	Ag	Cu	Pb	Zn	Fe
Solution	0	12	0	46	5
Sulphur	90	84	24	49	13
Total	90	96	24	95	18

The sulphur generated during the leach stage was then heated to 150° C. and filtered. The amount of sulphur recovered from the filtrate was 92.1% which was recycled to the roaster. The filter cake containing silver and some copper and zinc was then treated to recover the metal values. Listed below are the concentrations of metals recovered.

Metal Recovered From Filter Cake	Material Concentration (by weight)
Ag	18.1 OZ/T
Cu	3.22%
Pb	0.15%
Zn	19.2%
Fe	13.9%
S(T)	45.7%
S°	29.7%

The clear lixiviant which results from the solid-liquid separation of the oxidation leach solution is then contacted with a small amount of roasted pyrite in a reduction leach stage at a temperature of 100° C. for 30 minutes. The roasted pyrite addition is 1.71 g/g Fe^{+3} and the oxygen partial pressure within the reduction vessel is zero. It is found that 90% Fe^{+3} reduction was affected.

Metal extraction from the roasted pyrite is shown below:

Metal Extracted	Percent Metal Extracted (by weight)
Cu	0
Zn	54
Fe	52

The reduced pulp is then flocculated and filtered. The filtrate is processed to recover the dissolved metal valves by precipitation of copper and solvent extraction of zinc.

It will be apparent to workers skilled in this art that the foregoing process, while described with respect to certain preferred and exemplary materials and conditions, is subject to numerous other variations and alternations easily ascertainable from the description contained herein without departing from the scope and spirit of the invention as defined by the appended claims.

What is claimed is:

1. A process for the recovery of silver, copper and zinc from a pyrite concentrate, comprising the steps of:
   - (a) partially roasting the pyrite concentrate to open the pyrite matrix to solution penetration by driving off a portion of the sulphur contained therein;
   - (b) leaching under oxidizing conditions the bulk of the roasted pyrite concentrate to extract the silver, copper and zinc from therein;
   - (c) cooling the oxidation leached pulp and recovering the elemental sulphur generated during the leaching;
   - (d) heating the elemental sulphur pellets to recover silver and the portion of the copper and zinc contained therein;
   - (e) subjecting the solution resulting from the oxidation leach, containing the copper and zinc metals to a reduction leach stage wherein ferric ions contained therein are reduced to ferrous ions; and
   - (f) introducing the reduced solution from said reduction stage to a metal recovery stage wherein the copper and zinc are recovered therefrom.

2. The process of claim 1 wherein said pyrite concentrate is roasted until about 45% to about 80% of the sulphur contained therein is driven off.

3. The process of claim 2 wherein the pyrite concentrate is roasted at a temperature of from about 550° C. to about 700° C.

4. The process of claim 1 wherein the pyrite concentrate is leached using a ferric sulphate solution at a temperature of from about 150° C. to about 200° C.

5. The process of claim 4 wherein the temperature within the leach stage is from 175° C. to 185° C.

6. The process of claim 5 wherein the oxygen partial pressure within the oxidation leaching stage is about 150 psia.

7. The process of claim 5 wherein the pulp density within the oxidation leaching stage is from about 100 grams to about 400 grams of roasted pyrite per 600 ml of leaching solution.

8. The process of claim 4 wherein the oxygen partial pressure within the oxidation leach stage is over 120 psia.

9. The process of claim 1 wherein the reduction stage comprises contacting the oxidation leach solution with a small amount of freshly roasted pyrite concentrate at a temperature of from about 22° C. to about 119° C. at an oxygen partial pressure of zero.

10. The process of claim 9 which further comprises flocculating and filtering the product from the reduction stage in a solid-liquid separation stage to produce a filter cake and filtrate, said filter cake being recycled to said oxidation leach stage to recover any residual copper, zinc, silver or sulphur contained therein and said filtrate being processed to recover the metal values therein.

11. The process of claim 10 wherein the stripped solution from the metal recovery stage is recycled to said oxidation leaching stage.

12. A process for the recovery of silver, copper and zinc from a pyrite concentrate, comprising the steps of:
   - (a) partially roasting the pyrite concentrate at a temperature of from about 550° C. to about 700° C. until about 45% to 50% of the sulphur contained therein is driven off;
   - (b) introducing the majority of the partially roasted pyrite to an oxidation leach stage to extract the silver, copper and zinc values contained therein, said leaching being accomplished using a ferric sulphate solution at a temperature of about 175° C. to about 185° C. and the oxygen partial pressure within said leaching stage being about 150psia;
   - (c) cooling the oxidation leached pulp by flashing and recovering the elemental sulphur pellets generated during the oxidation stage;
   - (d) heating the elemental sulphur pellets to about 150° C., and thereafter filtering said sulphur and recovering silver and the portion of the copper and zinc in sulphur as a filter cake, and recycling the elemental sulphur filtrate to the roasting stage for SO_2 production;
   - (e) subjecting the oxidation leached solution, containing the copper and zinc to a reduction leach stage, said reduction leach stage comprising contacting the oxidation leached solution with a small amount of freshly roasted pyrite concentrate at a temperature of from about 22° C. to about 119° C. and maintaining the oxygen partial pressure within said reduction stage at zero;
   - (f) introducing the reduced solution from said reduction stage to a solid-liquid separation stage wherein said solution is flocculated and filtered to produce a filter cake and filtrate;
   - (g) processing the filtrate from said solid-liquid separation stage to recover copper and zinc and;
   - (h) recycling said filter cake from said solid-liquid separation stage to the oxidation leach stage to recover any residual copper and zinc contained therein.

13. The process of claim 12 wherein the copper contained in the filtrate produced by the solid-liquid separation stage is recovered by precipitation.

14. The process of claim 12 wherein the zinc contained in the filtrate produced by the solid-liquid separation stage is recovered by solvent extraction and electrowinning.

* * * * *

UNITED STATES PATENT AND TRADEMARK OFFICE

CERTIFICATE OF CORRECTION

PATENT NO. : 4,177,067

DATED : December 4, 1979

INVENTOR(S) : Terry W. Pepper and Harry G. Bocckino

It is certified that error appears in the above-identified patent and that said Letters Patent are hereby corrected as shown below:

Col. 3,
Lines 48, 53, 59, 61 and 63 "1/2" should be " → ".

Signed and Sealed this

First Day of *April 1980*

[SEAL]

Attest:

SIDNEY A. DIAMOND

Attesting Officer

Commissioner of Patents and Trademarks

Economic Geology
Vol. 74, 1979, pp. 315–330

A Reevaluation of the Spatial and Temporal Distribution of Sedimentary Phosphate Deposits in the Light of Plate Tectonics

Peter J. Cook and Michael W. McElhinny

Abstract

A new compilation of paleolatitudes of sedimentary phosphate deposits using worldwide paleomagnetic data confirms the hypothesis that the majority formed at low-latitude locations. A number of Jurassic and possibly some Cambrian deposits formed at intermediate latitudes (30°–50°). Phosphorites range in age from lower Proterozoic to Recent. There has been sporadic deposition of phosphate during this time, as continents drifted into low-latitude locations. It is proposed that there is no direct genetic link between periods of volcanism, orogenesis, formation of evaporites, and episodes of phosphogenesis. All these features are indirectly genetically related through plate tectonics to particular phases in the rifting and separation of continental and oceanic components of plates. In the case of diverging plates, volcanism and tectonism are an early-stage feature, evaporites intermediate-, and phosphorites late-stage features. Models are developed to explain the different sedimentary sequences that develop in north–south and east–west seaways. No model is presently available for epeiric seas.

A temporal model is also proposed to explain the distribution of phosphorus in sediments in the last 3,400 m.y. The association of phosphorus with iron and organic matter in the hydrosphere is particularly critical to the model. Even the temporal model is influenced to some extent by plate tectonics.

Introduction

Phosphorus plays a crucial role in present-day life processes and it was probably no less important in the past. Consequently, as there is now strong evidence that early forms of life existed more than 3 billion years ago, it may be assumed that phosphorus has been available, in a soluble form in the hydrosphere, for at least 3 billion years. Therefore an understanding of the global distribution of phosphorus in both space and time may ultimately lead to a far better understanding of evolutionary processes, particularly those in the Precambrian, where the fossil record is sparse. In this paper, only one aspect of the distribution of phosphorus is considered—the distribution of phosphorus-rich sedimentary rocks (phosphorites). It can reasonably be argued that most phosphorus is not tied up in phosphorites alone but in the total sediment pile. However, it is relevant to point out that the majority of phosphorites are believed to form in areas of oceanic upwelling. These areas constitute less than 1 percent of the oceanic area (Ryther, 1963), yet probably contain 50 percent of the total marine biomass. Consequently upwelling areas are of very considerable importance to our understanding of the organic geochemical evolution, despite their relatively small size. Therefore, by analogy, though phosphorites are atypical sediments, they are nevertheless likely to be of very great significance to our understanding of the phosphorus cycle and perhaps also organic geochemical evolution.

Of more immediate importance is the fact that recognition of a pattern in their spatial as well as temporal distribution will assist the search for new phosphate deposits. It is primarily for this reason that this topic has attracted the attention of a number of other authors, particularly Gimmel'farb (1958), Strakhov (1969), Sheldon (1964a), and Bushinski (1969). But in the ten years or so since this topic was last discussed in print, there has been a revolution in our understanding of many geological processes through the development of the theory of plate tectonics. Using this theory, many structural and sedimentary features and sequences can be logically explained. Therefore there is a need to attempt to develop new models for phosphogenesis using plate tectonics which will enable us to understand why a phosphorite is where it is and why particular sediments accompany it. This paper develops two such models.

General information on the majority of deposits was obtained from the third edition of the *World Survey of Phosphate Deposits* (British Sulphur Corporation, 1973) and *Old Phosphorites of Asia and their Genesis* (Bushinski, 1969). An additional general reference used is that of Liu et al. (1973). Where possible the primary sources were consulted for more precise figures on location, age, phosphorite type, and reserves. In all, data were compiled on 216 sedimentary deposits from throughout the world and ranging in age from Precambrian to Recent.

The Abundance of Phosphorites

In order to consider variations in phosphate abundance with time it was decided to attempt to determine the total amount of phosphate in deposits (expressed as metric tons of P_2O_5) without regard for whether or not that phosphate was a present or future reserve or resource. Using this sort of approach, the best figures that are arrived at are little more than approximations which provide an order of magnitude. But even with this crude approach it is only possible to provide estimates for the Phanerozoic era (Fig. 1). Total phosphate abundance for Phanerozoic deposits is on the order of 3×10^{11} metric tons of P_2O_5. The United States Bureau of Mines (1975) gives the world's measured and inferred reserves of phosphate at 8.4×10^{10} tons, but, as this figure is for ore or potential ore and not total phosphate content, there is not necessarily any significant disparity between the two sets of figures.

In addition to estimating the total phosphate content, the number of deposits (at 25 m.y. intervals) was also plotted (Fig. 1). In general, the positions of the peaks in the curve and histogram correspond fairly well, though the amplitudes of the peaks do not. The Permian peak is a prime example of this disparity and results from the fact that while there are relatively few Permian deposits, the total phosphate content is boosted considerably by the enormous deposits of the Western Phosphate Field (McKelvey et al., 1953). The location of peaks in the Mesozoic and Cenozoic is complicated by the abundance of deposits in those times, with a period of almost continuous (and major) phosphate deposition possibly extending from the Jurassic to the Oligocene, and by the relatively coarse (25 m.y.) interval used for the histogram. From these data, a number of discrete peaks can be identified as periods of phosphogenesis (Table 1). These peaks are, in general, similar to those recognized by previous workers, though the very great significance of the Lower and Middle Cambrian as a time of phosphogenesis in many parts of the world, rivaling the Permian or the Upper Cretaceous-Eocene in importance, has only become apparent in recent years. Perhaps equally important in terms of our overall understanding of the processes involved in phosphogenesis are the apparent hiatuses of phosphate deposition which occur in the Oligocene, the Triassic, and from the lower Carboniferous to the Silurian.

The data for the Precambrian deposits are too inadequate at the present time to draw anything more than a very broad and qualitative distribution pattern. As recently as 1962, Geijer argued that there was an almost total absence of phosphorites in the Precambrian. Davidson (1963) and many subsequent authors have pointed out that this clearly is not the case and that there are a large number of small Proterozoic deposits, as well as several large ones. The dating of these phosphogenic periods is

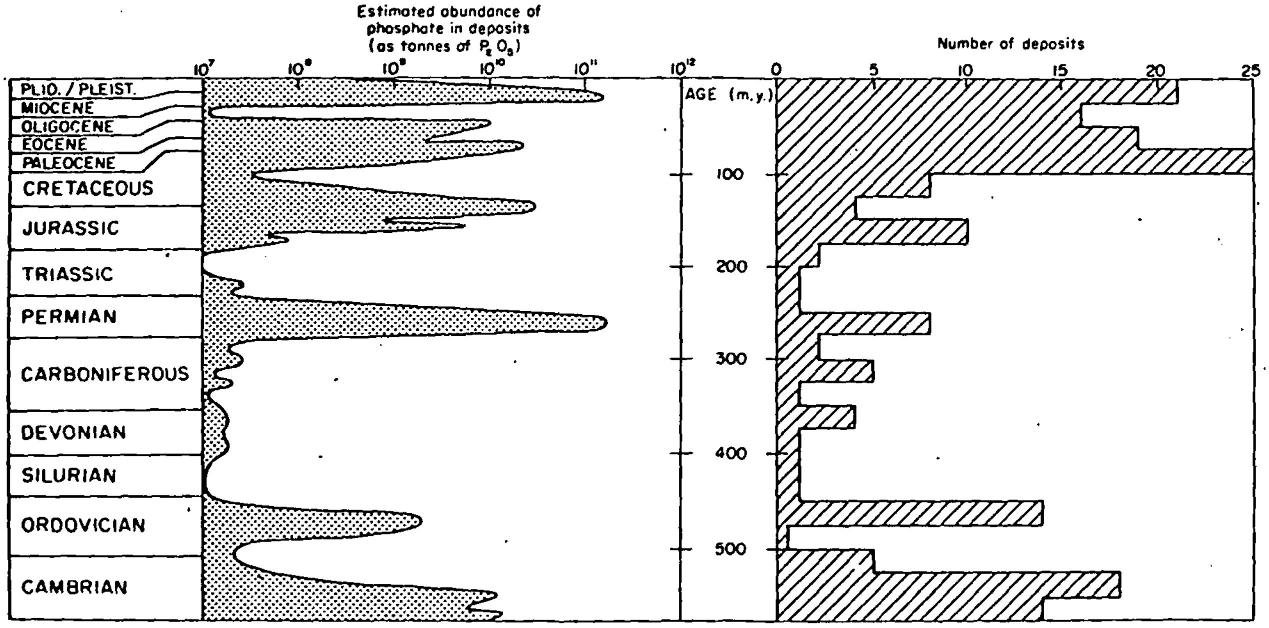

FIG. 1. Estimated abundance of phosphate (expressed as metric tons P_2O_5) in phosphate deposits throughout the Phanerozoic. The fixed time interval in the histogram is 25 m.y. It should be noted that a logarithmic scale is used for P_2O_5 abundance.

doubtful and there is clearly a need for absolute age dating of the phosphorites or their associated sediments. The most important period of Precambrian phosphogenesis appears to be in the upper Proterozoic. Whether this comprised the two peaks, upper Proterozoic I and upper Proterozoic II as indicated in Table 1, or whether there was a fairly continuous period of phosphogenesis from about 800 to about 600 m.y. and perhaps into the Cambrian, is uncertain. The status of the middle Proterozoic peak given in Table 1 is doubtful, as it is based on only two deposits—the Pogoryy and Underly phosphorites of the Yenisei Ridge with an age of about 1,600 m.y. and the phosphorites of Rajasthan with an age of 1,200 to 1,600 m.y. Both deposits have poor age control. The lower Proterozoic occurrences at around 2,000 m.y. (there are no known major deposits) have better age control and include the phosphatic sediments of the Väyrylankyla area of Finland (Laajoki and Saikkonen, 1977), Rum Jungle (Prichard and Cook, 1965), the Marquette Range of Michigan (Mancuso et al., 1975; Cannon and Klasner, 1976), the Hamersley Group of Western Australia (Morris, 1973) and, possibly, also Broken Hill, Australia (Stanton, 1972), though at present only an age of metamorphism of about 1,700 m.y. (Shaw, 1968) is available for Broken Hill.

Davidson (1963) suggests that the Slyudyanka deposits in the Baikal region of the USSR are Archean in age. Bushinski (1969) also considers that a number of small deposits in North Korea and the Inner Mongolian and Singelin districts of China may also be Archean. However, as the isotopic data in support of the inferred Archean ages are not provided, these Archean ages must be regarded as questionable for the present.

TABLE 1. Major Phosphogenic Episodes

Episode	Mean age (m.y.)	Locations
Miocene-Pliocene	14	Continental margins; *SE. USA*,[1] California, Sechura, Venezuela, Japan, Philippines
Upper Cretaceous-Eocene	65 $\left\{\begin{matrix}54^{2}\\77^{2}\end{matrix}\right.$	*W. Africa, N. Africa, Mid. East,* W. Europe, N. South America, Mexico, N. India, Ukraine, Kazakhstan, W. Australia, Pakistan, Texas, Manitoba
Jurassic	149	*Russia,* Mexico, N. South America, W. Europe, W. Australia, N. India, Pakistan, W. Canada
Permian	250	*W. USA*, Urals, Szechwan, Indochina, N. India
Ordovician	464	*Tennessee,* Ala., Ken., Central & SE. Australia, *Baltic area,* Iowa, E. Canada, Bolivia, Baikal
Cambrian	542	*Karatau, Russia, Georgina Basin, Central & SE. China, Vietnam,* S. Australia, *Chub Sugal,* Tien Shan, Sayan, Central Kazakhstan, Tennessee, E. Canada, Mauritania
Upper Proterozoic I	620	*Volta area,* Mauritania, China (?)
Upper Proterozoic II	700– 800	*China,* Central Siberia, India (?), Brazil, Central Australia
Middle Proterozoic (?)	1,200–1,600	Yenisei, *Rajasthan* (?)
Lower Proterozoic	1,800–2,200	Rum Jungle, Broken Hill, Australia (?) Michigan, Finland

[1] Regions with very large deposits are italicized.

[2] Secondary peaks may be present at about these times.

The Paleolatitudes of Phosphorites

Sheldon (1964a) was the first to point out that the paleolatitudinal distribution of ancient phosphorites matches the latitudinal distribution of young phosphorites, with both falling within 40° of the equator. Subsequently, Sheldon (1964b) and later Freas and Eckstrom (1968) applied paleolatitudes and paleogeographic reconstructions to the search for new phosphate deposits. In recent years a considerable amount of new and more reliable paleomagnetic information has become available and there is now a new understanding of plate tectonics and the movement of continents. For the purposes of this study, paleolatitudes were determined on 162 deposits from throughout the Phanerozoic, including 72 major deposits. The information presently available is inadequate for the determination of paleolatitudes for Precambrian phosphorites.

Paleomagnetic pole positions through the Phanerozoic for each of the major crustal units were determined using the methods outlined in McElhinny (1973). A set of poles was calculated adding more recent data as sumarized in McElhinny (1972) and McElhinny and Cowley (1977, 1978). If the paleomagnetic pole is situated at latitude λ_p and longitude ϕ_p, then the paleolatitude λ' of a site presently located at latitude λ_s, longitude ϕ_s, is given by:

$$\sin\lambda' = \sin\lambda_p \sin\lambda_s + \cos\lambda_p \cos\lambda_s \cos(\phi_p - \phi_s).$$

For the USSR the more recent compilations of Khramov (1971, 1973, 1975) as summarized by McElhinny et al. (1977) were used. No data are available directly for the Cambrian of China and in this case Cambrian data for North Korea were used (see McElhinny, 1973). A list of paleolatitudes calculated for each of the Phanerozoic phosphorite deposits is available from the authors on request.

Results for all deposits are summarized in Figure

2. These more complete data confirm the conclusion by Sheldon (1964a) that ancient deposits are found over a wide range of present latitudes (Fig. 2A), whereas their paleolatitudes show a narrower spread closer to the equator (Fig. 2B). This is perhaps best illustrated by the middle Paleozoic phosphorites of the Pensacola Mountains of Antarctica which are presently located at latitude 84° S (Cathcart and Schmidt, 1977) but which have a paleolatitude calculated at 39° S. The paleolatitudes of all deposits show a spread from about 0° to 70° but with a clear maximum within 20° of the paleoequator (Fig. 2B). When only the major deposits[1] are taken (Fig. 2C), the low-latitude peak is more clearly defined, with a peak between 10° and 20° from the equator. This supports the view that phosphate deposition is most abundant at low-latitude locations, with a preference for a subequatorial (10°–20°) location rather than an equatorial (0°–10°) site.

Because of the relatively large number of paleolatitude results available here, it is possible to look at latitudinal distribution for various times and also at the distribution of major and minor deposits. Paleolatitude distribution for the six time periods taken, which generally correspond with the six major periods of Phanerozoic phosphogenesis (delineated in Fig. 1) are shown in Figure 3. Because of the smaller samples for these six groups, the distribution patterns in Figure 3 are less reliable than the general distribution patterns in Figure 2. Nevertheless it would appear from these plots that the zones of phosphogenesis, while generally at low-latitude locations, have not always remained static in a near-equatorial location. There is also the suggestion of a bimodal distribution, with modes at about 10° and 40°. This is particularly evident for major deposits of the Jurassic and the Cambrian, and to a lesser extent for the Permian. The major deposits with intermediate (30°–50°) latitudes are the Jurassic deposits of Russia and the Cambrian deposits of China, although it should be stressed that Cambrian paleolatitudes for China are derived from data for North Korea and this may not be a valid extrapolation.

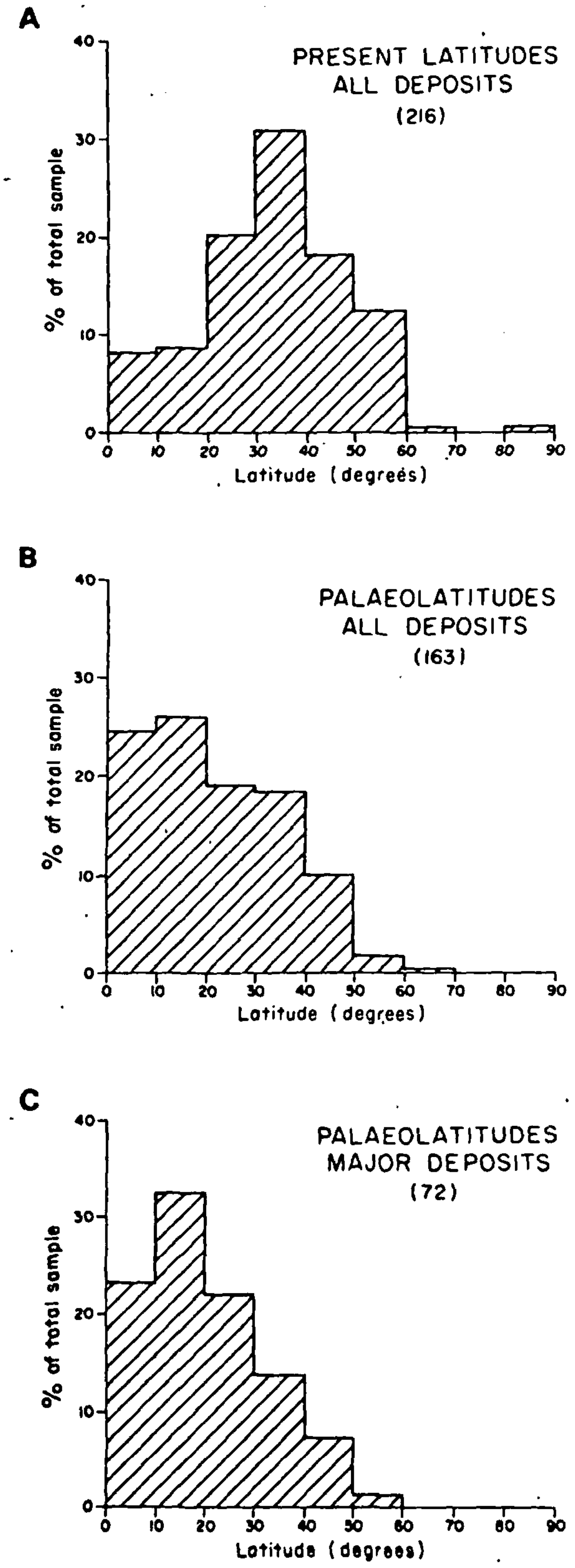

FIG. 2. The latitudinal location of Phanerozoic phosphate deposits. The number in brackets is the number of latitude values used for the compilation of the histogram.

The Spatial Distribution

The results presented previously are in general accord with those given by Sheldon (1964a). It is evident that, for phosphorite to form, the coastal portion of a continent must drift into a low-latitude location; however, some qualifications to this hypothesis need consideration. There are indications of some intermediate latitude phosphogenesis between latitudes 30° and 50°, especially in the Jurassic and

---

[1] A major deposit is regarded here as a deposit with 10 million metric tons or more of total P_2O_5, whether the ore is high grade or low grade, economic or noneconomic.

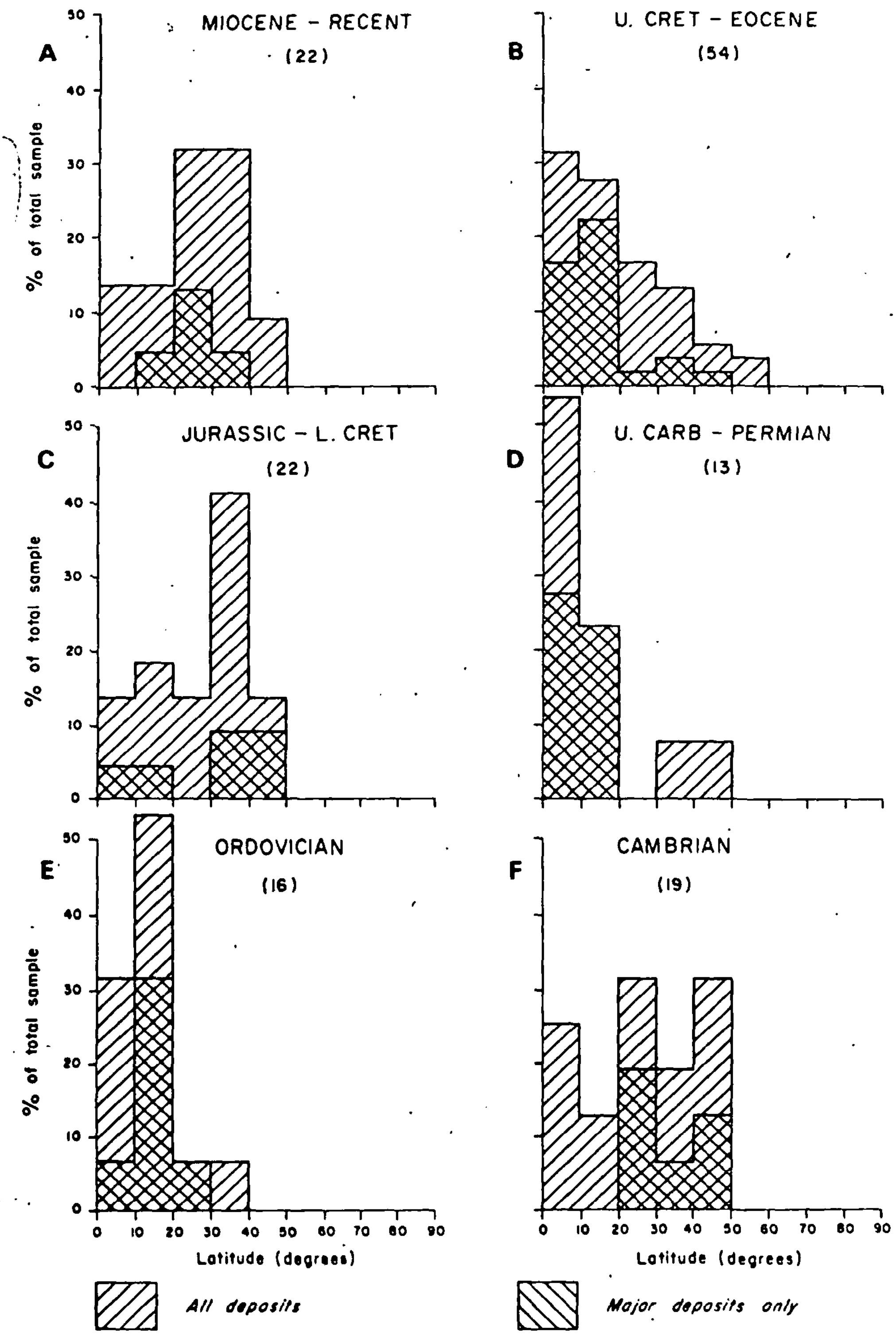

FIG. 3. The paleolatitudes of phosphorites for the six main Phanerozoic periods of phosphogenesis. The number in brackets is the number of latitude values used for the compilation of the histogram.

possibly the Cambrian, not evident from earlier compilations. Young offshore phosphorites currently are found within this latitudinal range in various parts of the world. Although none of the phosphorites at these sites are forming at the present time (Kolodny, 1969), many probably formed on these bank and ridge locations in response to dynamic upwelling as currents were forced up over topographic highs (McKelvey, 1963). Whether this explanation can be invoked for the very widespread Jurassic deposits of Russia, or the Cambrian deposits of China, is uncertain at this stage, especially as the Jurassic deposits appear to have formed under shallow-shelf conditions.

The lack of phosphorites is also dependant on the paleolatitudes of oceans and continents. The reconstructions of Smith et al. (1973) for the Devonian and lower Carboniferous show that at these times there were few coasts at low-latitude locations. Thus the apparent Silurian to Carboniferous hiatus in phosphogenesis may simply be the consequence of there being few continental/coastal areas at low latitudes. The Triassic reconstruction also suggests that there were few areas then at low-latitude locations. However, this explanation does not appear to be the case during the Oligocene and clearly there must be other reasons for the hiatus at that time.

The similarity of the fauna of the continents indicates that during the Cambrian an approximately east-west seaway extended from Australia into Asia and perhaps even into Europe, analogous to the Mesozoic Tethyan seaway (de Keyser and Cook, 1972). No accurate reconstructions are available for the Cambrian, but it is proposed here, using paleolatitude data, that the Cambrian phosphate deposits of Australia lay on the southern side of this seaway at about latitude 25° N and the Chinese and Hubsugal deposits on its northern side at about 40° N. This seaway, lying between about 25° and 40° N, then extended westward through the Karatau region, which was probably situated on its northern side. It is likely that there would have been exceptionally strong currents flowing through this narrow latitudinal seaway, producing high productivity as a result of coastal entrainment and upwelling, and particularly as a result of intense dynamic upwelling associated with topographic highs. The Cretaceous-Eocene phosphorites were similarly located in a relatively narrow east-west seaway. As we still do not understand many features of present-day oceanic circulation patterns, reconstructions of Paleozoic or Mesozoic circulation are even more speculative. Nevertheless, it is evident that just having a coast at the preferred (low) paleolatitude will not necessarily produce strong upwelling and associated phosphorites, as the continent-ocean configuration is also of primary importance. A narrow east-west seaway at a low latitude, such as the Tethyan seaway, will probably produce the strongest upwelling because of the strong westerly directed flow through it (Fig. 4A). Conversely, a narrow north-south seaway is likely to have a complex pattern of interfering current systems with little or no associated upwelling (Fig. 4C) and possibly even fairly stagnant restricted conditions (Evans, 1978). In order to have upwelling in a longitudinally directed ocean it is necessary for it to be sufficiently wide for discrete oceanic gyrals to develop. Therefore, phosphogenesis can be related to particular phases of sea-floor spreading and continental dispersal. Strong upwelling and associated phosphogenesis can take place at a juvenlie stage in a latitudinally directed seaway (Fig. 4A) but only at a farily mature stage in a longitudinally directed seaway (Fig. 4D).

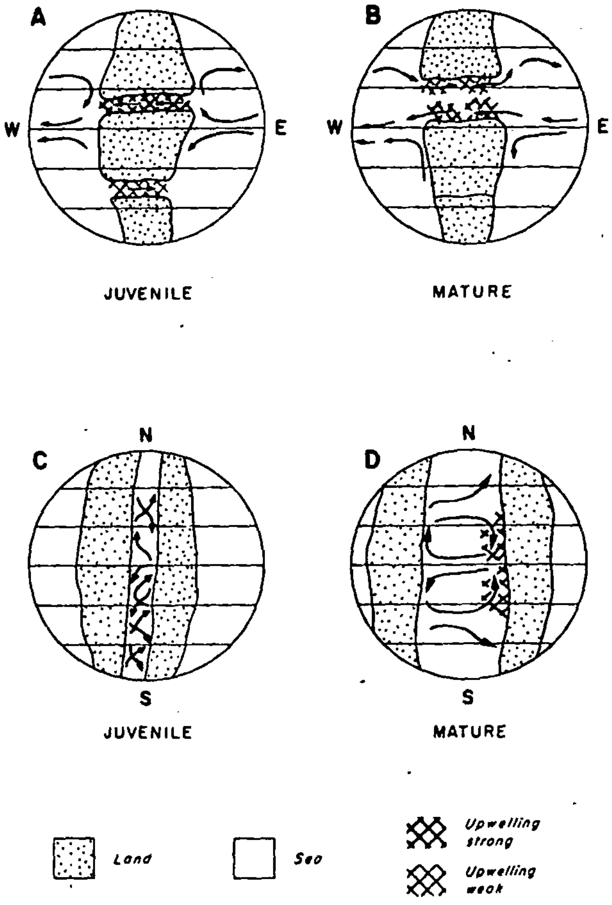

FIG. 4. Schematic representation of the likely current patterns and areas of upwelling in narrow seaways with latitudinal (A, B) and longitudinal (C, D) orientations.

The relationship between phosphogenesis and phases of continental separation and ocean formation also explains various relationships of phosphogenesis with volcanism, orogenesis, and the formation of evaporites, all of which have been invoked in the past to explain episodes of phosphogenesis. Mansfield (1940), Rooney and Kerr, (1967) and others have proposed that the formation of phosphorites is linked to volcanism either through the direct input of large amounts of volcanogenic phosphate into the sedimentary system or through the initiation of mass mortalities as a result of massive ash falls. Although both of these processes may be of some significance locally, there is no evidence that they are capable of producing large phosphate deposits. It is proposed here that the relationship is indirect. The volcanism results from the initiation of rifting which precedes the development of a seaway.

Similarly with orogenies the relationship is not a direct one, as proposed by Gimmel'farb (1958), resulting from an increased input of phosphate due to the erosion of the adjacent elevated land masses. Many orogenies and phases of phosphogenesis do seem to occur at about the same time. The Karelian (2,000 m.y.), Vyborgian (1,700–1,600 m.y.), Baikalian (540–500 m.y.), Kimmerian (170-110 m.y.), and Alpine (85-12 m.y.) orogenic cycles of Salop (1977) all appear to have phosphogenic counterparts (Table 1). However, orogeny can be a manifestation of the early stages of plate movement and the initiation of rifting which precedes the formation of a seaway or the narrowing of a broad seaway in the case of converging plates. Alternatively, it is responsible (or is associated with) the movement of a plate to a low-latitude location where the formation of phosphorites is most likely to occur. Therefore, the time interval between an orogenic phase and phosphogenesis will depend on the type and direction of plate movement. Specifically, phosphogenesis will take place at low-latitude locations: soon after the onset of plate divergence in the case of east–west rifting; some considerable time after the initiation of plate convergence (though possibly only a short time before plate collision) along an east-west axis; and a considerable time after the onset of plate divergence in the case of north–south rifting.

One of the most striking sedimentary associations is between phosphorites and evaporites. The classical example of this is provided by the Phosphoria Formation which grades laterally landward into the evaporites of the Chugwater Formation (McKelvey et al., 1959; Sheldon et al., 1967). This same association holds for many other deposits. Hite (1976) has suggested that the association between phosphorites and evaporites is a direct one, with phosphate being precipitated as a result of the interaction of phosphorus-rich continental brines and cold ocean waters. However, Brongersma-Sanders (1969) makes the important point that the process of upwelling and the associated presence of cold nearshore waters are responsible for the aridity of the hinterland and the development of coastal deserts such as the Atacama and Namib Deserts. Nevertheless, if there have been periods of global aridity due, for instance, to a broadening of the trade-wind belt, then it is conceivable that these times would have been accompanied by associated periods of phosphogenesis. In Figure 4, an attempt has been made, using mainly the compilation on world salt deposits by Lefond (1969), to plot the distribution of evaporites. As in the other compilations, the location of peaks (though not necessarily their amplitude) is reliable only for the Phanerozoic. The peak shown at about 1,000 m.y. is based on the occurrence of late Proterozoic salt deposits in Asia (Lefond, 1969) and Australia (Wells et al., 1970). The 1,800 m.y. peak is based on reports of extensive gypsum pseudomorphs in rocks of this age in Australia (Walker et al., 1977) and Canada (Bell and Jackson, 1974; Badham and Stanworth, 1977). There is also evidence of Archean evaporitic environments as old as 3,400 m.y. in the Onverwacht Group of South Africa (Lowe and Knauth, 1977). The lower and middle Proterozoic evaporite peaks do not seem to correspond with times of phosphate deposition (Fig. 5). However, the very extensive Cambrian salt deposits (possibly extending down into the uppermost Proterozoic) do appear to show a correlation, as do also the Permian evaporites. Similarly, the time of development of Tethyan Belt salt deposits corresponds to a phosphogenic period.

But to explain these correlations it is not necessary to invoke periods of global aridity; it is again essentially part of a sedimentary sequence related to plate tectonics. The evaporites result from two processes, the movement of the area into a low-latitude location, and the initiation of rifting, forming a salt basin which was partly connected to the open ocean. Whether the phosphorite is synchronous with, immediately follows, or follows many millions of years after the evaporitic phase is dependent primarily on plate movements.

The Phosphoria Formation provides the type example of synchronous phosphorites and evaporites. In this case, both sediment types formed on the east side of a broad mature ocean as the lithospheric plate moved north–south into a low-latitude location.

Some of the Cambrian phosphorites immediately overlie evaporitic units. This situation will occur when there is an east-west seaway at a low-latitude location, the evaporites occurring at the rift-valley stage and the phosphorites forming as soon as the rift is completely breached, a narrow seaway formed, and dynamic upwelling initiated. It is conceivable, in the case of a converging plate boundary, that evaporites may immediately overlie phosphorites.

From Figure 5 it is evident that the Lower Cretaceous was an important period for evaporites, but the correlation with Cretaceous phosphorites is not so well defined. The enormous Lower Cretaceous (Aptian) evaporite deposits flanking the Atlantic Ocean (Wardlaw and Nicholls, 1972) do not have

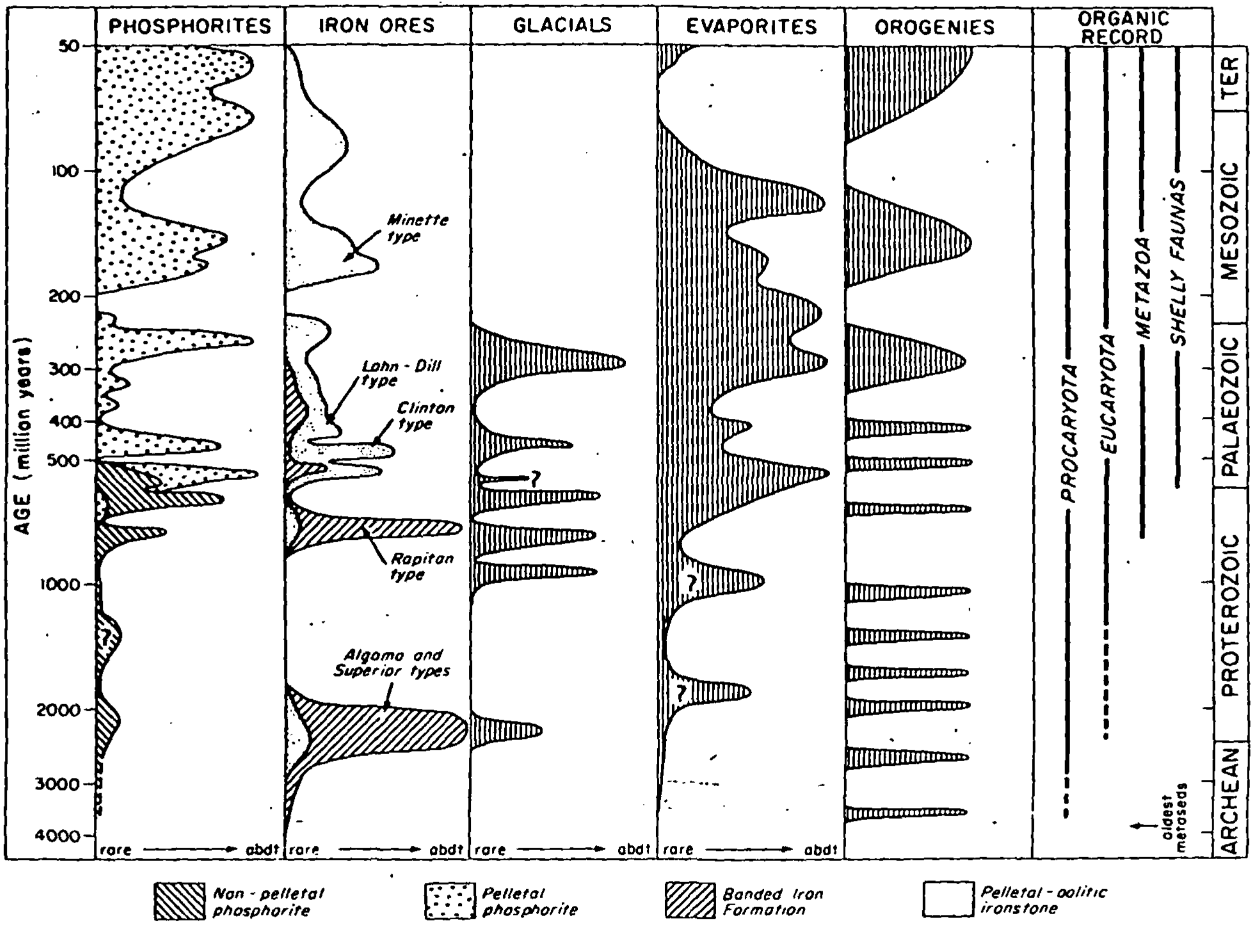

FIG. 5. The temporal distribution of phosphorites and sedimentary, organic, and tectonic events which may influence phosphogenesis. The amplitudes of peaks are schematic and probably should be regarded as being on a logarithmic scale. The time scale is logarithmic which has the effect of minimizing the Proterozoic and Archean peaks and maximizing the Phanerozoic peaks on the diagram.

any major phosphorites imediately associated with them. The evaporites formed in the juvenile stage of the north-south-oriented diverging plate boundary which was producing the ancestral Atlantic. It was not until late in the Upper Cretaceous and particularly in the middle Eocene that the Atlantic was sufficiently wide for a well-defined pattern of oceanic circulation (and associated upwelling) to develop and for phosphorites to be deposited along the west coast of Africa (Fig. 4C, D). The time between formation of the Aptian evaporites and the deposition of middle Eocene phosphorites is of the order of 55 m.y. Based on the computed spreading rates of Dickson et al. (1968) and Heirtzler et al. (1968) and the reconstruction of Smith and Briden (1977), the ancestral South Atlantic Ocean widened from about 850 km to about 3,000 km in this time. This suggests that a minimum oceanic width of about 3,000 km is necessary for the formation of major oceanic gyrals. This in turn implies that the development of phosphorites could take place anywhere from about 15 m.y. to 200 m.y., after the initiation of sea-floor spreading along a north-south axis, depending on whether a very slow (1 cm/yr) or a fast (6 cm/yr) spreading rate is taken. Therefore the phosphorite-evaporite relationship is also dependant on the rate of sea-floor spreading. In a north-south seaway the evaporites will be overlain by a thick sequence of restricted marine sediments, and then by phosphorites. Using these various disparate observations, it is now possible to develop models to explain many aspects of the distribution of phosphorites.

Spatial Models

There are probably a number of models which could be developed to explain phosphogenesis. Here, only diverging plate models are dealt with. Converging plate models would essentially be mirror images of models A and B, though the stages of continental sedimentation and rifting would be replaced by a phase of mountain building. There is clearly a need to develop models for phosphogenesis in epeiric seas and it will probably be necessary to develop separate models for pelletal and fine-grained phosphorites. The models presented here are no more than first attempts and will no doubt need to be extensively modified in the future.

Spatial Model A

1. Continental sedimentation.
2. North–south movement of lithospheric plates produces east–west rifting at a low-latitude location; some associated volcanics.
3. Large-scale development of evaporites during the stage of incomplete separation of the plates. The magnitude of the evaporites will be dependant on the nature of the rifting and the aridity of the area.
4. Complete separation of the plates and the initiation of a narrow east–west seaway. A strong westerly directed current system will produce strong dynamic upwelling and this will be associated with formation of phosphorites (e.g., the Cretaceous phosphorites of the Tethyan region).
5. As sea-floor spreading continues, the seaway becomes broader. Phosphorites may be less abundant and carbonates more abundant as the ocean water becomes warmer and upwelling becomes weaker.
6. Spreading may proceed to the stage where the northern boundary of the latitudinal sea (in the northern hemisphere) will be located within the zone of west-wind drift. This may result in high-latitude dynamic upwelling or upwelling on the northern shore as well as on the southern shore (e.g., some of the Cambrian phosphorites of China).
7. Spreading may finally proceed to the stage where both shores no longer lie within the trade and west-wind belts and consequently the area no longer constitutes a potential phosphogenic province.

Spatial Model B

1. Continental sedimentation.
2. East–west movement of lithospheric plates produces north-south rifting over a wide range of latitudes; some associated volcanics.
3. Large-scale development of evaporites during the stage of incomplete separation of the plates, particularly at low-latitude locations.
4. Complete separation of the plates and the initiation of a narrow north-south seaway but with no dominant current pattern. Ocean waters may be fairly stagnant and poorly oxygenated during this period. Organic-rich sediments may be deposited during this time.
5. As sea-floor spreading continues, the seaway will eventually become sufficiently broad (of the order of 3,000 km) that oceanic gyrals finally become established. This will lead to upwelling on the east side of the ocean and the formation of phosphorites, especially at low-latitude locations (e.g., the Eocene phosphorites of West Africa). The time between the development of evaporites and phosphorites is entirely dependant on the sea-floor spreading rate and probably ranges from 15 m.y. to more than 100 m.y. Bottom waters also become more oxygenated.
6. Eventually the stage is reached where there is just a broad ocean (rather than a seaway) with stabilized oceanic gyrals. The formation of phosphorites at any location will now be dependant on the north-south movement of the lithospheric plate, and of a coastal area, into the zone of upwelling. The formation of phosphorites will not now necessarily be preceded by an evaporitic phase; however, it is likely to grade laterally into synchronous evaporites because of the arid zone location (e.g., the Permian deposits of the Phosphoria Formation) and the formation of coastal deserts due to upwelling ocean current systems.

The Temporal Distribution

So far in this discussion it has been shown that many geological events such as volcanism, orogenesis, and the formation of evaporites are related to phosphogenesis by the processes implicit in plate tectonics. The consequences of plate tectonics on the development of phosphogenic provinces has already been outlined. Most of the peaks in phosphate abundance in Figures 1 and 5 and in Table 1 are the consequence of coasts/seaways being low-latitude locations. Conversely, some minima (such as the Silurian to Carboniferous) result from there being no coasts/seaways at low-latitude locations during these times. Until now it has been assumed that oceanic circulation and patterns of upwelling, and also the geochemistry of the oceans, has remained fairly stable. But in the short term these parameters may change locally, and in the long term they are known to be changed profoundly by events of global significance such as glacial epochs, the geochemical evolution of the oceans, and organic evolution. Even these features cannot necessarily be totally divorced from plate tectonics, for many glacial periods are the consequence of a continent drifting to a high-latitude location, and the course of geochemical and biological evolution may have been markedly affected by a change in tectonic style between the Archean and the Proterozoic or between the Proterozoic and the Phanerozoic. Similarly, if iron ores are related to upwelling then again the disposition of continents and oceans is likely to be fundamental to the presence or absence of iron ores. However, in this portion of the discussion, the main concern is on the effects of the changing geochemistry of the oceans on the deposition of phosphorites.

The oldest sediments (metasediments) known are those of West Greenland, which have an age of about 3,760 m.y. (Moorbath et al., 1973). The presence of a procaryotic fauna as far back as 3.4 billion years (Muir and Grant, 1977) indicates that phosphorus was present in the oceans in a soluble form by that time. Throughout much of the Archean there appear to have been few shelf areas. Consequently, there was little opportunity for phosphorus to concentrate. As phosphorus-bearing organisms died they fell through a large water column and the phosphorus either went back into solution or else was reincorporated into the biota. It seldom was able to reach the sea bottom and be incorporated in the ocean sediments. The development of broad shelves in the Proterozoic and Phanerozoic, presumably in response to a change in tectonic style, meant that the likelihood of phosphorus being incorporated in the sediment column was now greatly enhanced. At about 800 m.y. there was a very marked increase in the abundance of phosphorites which persists into the present time.

A number of authors such as Bushinski (1964) and Pevear (1966) have suggested that rivers are the immediate source of the phosphorus in phosphorites; however, the most generally accepted source of the phosphorus is upwelling, nutrient-rich, ocean water. The original theory of the direct precipitation of phosphate from upwelling sea water (Kazakov, 1938) has been shown to be questionable because of experimental work by Smirnov (1958) and Atlas (1975) and also by observations on the modern phosphorites off southwest Africa (Baturin, 1969, 1971) and Chile (Veeh et al., 1973). There is now evidence that a low-grade phosphorite will form diagenetically, immediately below the sediment-water interface, or in some cases by phosphatization (e.g., of glauconite) at the interface (Bremner and Willis, 1975). This is then followed by a period of mechanical reworking to form a high-grade phosphorite (Cook, 1967, 1976). Nevertheless, the originally proposed spatial association of phosphorites with upwelling areas of high productivity still appears to be valid for most deposits.

Periods of glaciation are likely to be times when the cold, deep ocean waters have enhanced concentrations of phosphorus (because the waters are colder) and when upwelling is most intense because of the greater temperature differential (Gardner, 1973). Consequently, the view that periods of glaciation are likely to coincide with times of widespread phosphogenesis has been taken in the past by a number of Soviet and Chinese geologists (see Bushinski, 1969). An association of phosphogenesis and glaciation appears to be supported by an apparent close stratigraphic association between tillites and phosphorites such as in the Georgina Basin. But this stratigraphic association is more apparent than real and there is generally a considerable time interval between the two. Nevertheless, if the distribution of glacial episodes as proposed by Williams (1975a, b) and phosphatic episodes is examined (Fig. 5), there does appear to be a fairly close correspondance between a number of events, particularly the upper Proterozoic-Paleozoic glacial episodes occurring at about 770 m.y., 615 m.y., 560 m.y., 445 m.y., and perhaps 295 m.y. and also from 26 m.y. to the present. Conversely, the major periods of phosphogenesis in the Mesozoic and early Cenozoic are totally devoid of any association with glacial episodes. Also, Burnett (1977) was able to show that the Pleistocene phosphorites off Peru and southern Chile have radiometric ages which correspond with interglacial periods, when the oceans were warmer, sea level was higher, and there was mechanical reworking (and upgrading) of the phosphorites. Gulbrandsen and Roberson (1973) give a residence time for phosphorus of 4.9×10^4 years. As the average glacial cycle has a periodicity of about 1×10^5 years, a relatively short term glacial event could modify the phosphate concentration in the oceans and hence the deposition of phosphate. There is, in addition, the inevitable problem that in older sequences the record becomes increasingly blurred so that events which appear to be synchronous may in fact have a gap of 50 m.y. or more between them. Nevertheless, there does appear to be an empirical relationship between some periods of phosphogenesis and glacial episodes, which is probably related to the associated enhanced upwelling.

Few authors seem to have considered possible correlations between episodes of phosphogenesis and iron ore deposition. Bushinski (1969) takes the view that "phosphorites and ironstones are antagonistic." This view is apparently reinforced by the fact that while 90 percent or more of the total iron ore deposits occurs in the Proterozoic (pre-750 to 800 m.y.), 90 percent or more of the total phosphorite deposits occurs in the latest Proterozoic and Phanerozoic (post-750 to 800 m.y.). Despite this, Pettijohn (1957) suggests that "the environments of phosphorite and ironstone have many factors in common." A number of phosporites are apparently associated with iron ores, such as the Tonshanto (Sinian) phosphorites of China which are interbedded with ironstones and the Tunisian phosphorites which are overlain by oolitic ironstones. However, most phosphorites are relatively low in iron and therefore it has generally been concluded that ironstones and phosphorites do indeed have little in common. But while phosphorites may be low in iron (the average Fe_2O_3

content of sedimentary phosphate rock is calculated from Smith and Lehr, 1966, at 0.63%), iron ores are not necessarily low in phosphorus, for though McKelvey (1973) gives the average P_2O_5 content of Precambrian iron ores as 0.21 percent, Phanerozoic iron ores average 1.43 percent P_2O_5. Therefore the Phanerozoic ores in particular suggest that there may be a geochemical link between the two.

The distribution of iron ores throughout time (using data from James, 1966, and Goldich, 1973) is given in Figure 5. It should be pointed out that the effect of the vertical logarithmic scale used in this diagram is to minimize the Proterozoic peaks and enhance the Phanerozoic peaks. The horizontal abundance axis which is qualitative should be regarded as logarithmic. From Figure 5 it is apparent that there are a number of similarities in the time distribution patterns of iron ores and phosphorites. The possible lower Proterozoic phosphorite peak coincides with the enormous development of banded iron-formations at about 2 billion years. The upper Proterozoic II peak (Table 1) would similarly appear to coincide with the appearance of the Rapitan-type (Yeo, 1977a, b) iron ores at about 750 to 800 m.y. Similarly in the Paleozoic, phosphogenic episodes in the Cambrian, Ordovician, the Jurassic, and the upper Eocene all appear to coincide with peaks of iron ore deposition. The two curves are clearly not entirely coincident; there is, for instance, no Miocene peak in iron ore deposition to match that of phosphorites. Similarly, there is no phosphorite peak to match the Devonian peak in iron ore formation at about 400 m.y., though the point should perhaps be made that, unlike most of the other ores, the Devonian Lahn-Dill-type iron ores are of probable volcanogenic origin and therefore somewhat atypical of most of the other sedimentary iron ores. Nevertheless there is, overall, a striking similarity of the phosphorite and iron ore distribution patterns in Figure 5.

The similarity in the two ores also extends to their morphology. As pointed out by Trueman (1971) the nonpelletal fine-grained phosphorites, variously called microsphorite, collophane mudstone, or phospholutite, are found to predominate in the Proterozoic deposits, whereas pelletal phosphorites predominate in the Phanerozoic. There is no sharp cutoff at the Precambrian-Cambrian boundary. In the Cambrian deposits of the Georgina Basin Rogers and Keevers (1976), Howard and Cooney (1976), and Howard and Hough (1979) have described very extensive deposits of these nonpelletal deposits. Riggs (1967, 1979a, b) has also described some beds of microsphorite from the Florida deposits. Nevertheless the general lack of fine-grained phosphorites in the Phanerozoic (and especially the post-Cambrian) is quite striking. Similarly, in iron ores the boundary between ore types is not razor sharp and for instance in some beds of the Superior deposits, oolitic ore is fairly common though it forms only a very small proportion of the total deposits. There are also some banded iron-formations in the Phanerozoic (O'Rourke, 1961). However, there is no doubt that, overall, pelletal and oolitic ironstones predominate in the Phanerozoic. The analogy can be taken one stage further if the ores are considered in a little more detail. The lower Paleozoic phosphorites are commonly composed of abraded fragments of phosphatic organisms (e.g., the Maardu deposits of Estonia) or calcareous organisms which have been abraded and phosphatized (e.g., the Duchess deposits of northwest Queensland). In the Permian and younger deposits, by contrast, phosphate pellets or ovules (or more rarely ooids) with obvious calcareous precurser material are much less in evidence. Similarly, the most important iron ores of the lower Paleozoic, the Clinton-types ores, are composed of ferruginized and abraded shells, whereas the Mesozoic ores which are dominated by the pelletal Minette-type ores have no clearly recognizable calcareous precursers.

But if there is an analogy between phosphorites and iron ores, the precise nature of this analogy is unclear. The generally low iron content of phosphorites demonstrates that there is certainly not a universal and intimate association between iron and phosphorus. To some extent the phosphorus content of iron ores and the iron content of phosphate rock may be somewhat understated in the literature because phosphorus is an undesirable feature of iron ore and iron is similarly an undesirable property of phosphate rock. Consequently, the "average ore" has commonly been preferentially mined to provide a low content of the undesirable minor element. Nevertheless, the total phosphorus content of many iron deposits is very large. If the average P_2O_5 content of 0.25 percent for the Dales Gorge Member (Trendall, 1968) and the total iron content 9.4×10^{13} metric tons for the Hamersley Basin (Trendall, 1973) are used, then the total P_2O_5 content of the Hamersley Group Iron Formation is approximately 5×10^{11} metric tons. This is more than the total phosphorus in most of the world's major phosphate deposits (see Fig. 1). Other iron deposits similarly contain enormous quantities of phosphorus though of course this does not mean that they are "phosphate deposits." Most of the phosphorus is associated with the iron in an adsorbed form or, perhaps, in a poorly crystalline iron phosphate phase. But in some deposits, apatite occurs as discrete laminae and thin beds. In the case of the Finnish deposits, the lanthanide distribution in the apatite (Laajoki, 1975) is very similar to that found in Phanerozoic phosphorites (Altschuler et al., 1967; Cook, 1972). Laajoki and Saikkonen (1977) regard this, and particularly the cerium deficiency, as evidence that the apatite in the iron-formations is of marine origin.

It is not the purpose of this paper to discuss the origin of iron-formations; this topic has been covered exhaustively in papers by Woolnough (1941), James (1954, 1966), Goodwin (1962), Lepp and Goldich (1964), Govett (1966), Gross (1973), Trendall (1973), and Holland (1973) to name but a few examples of the voluminous literature on this topic. The sources suggested for the iron include volcanic emanations, rivers, ground water, and the ocean. Holland (1973) shows fairly convincingly that, as suggested earlier by Borchert (1960), the most likely source for the iron is deep upwelling sea water. An upwelling environment would also serve to explain the large amount of phosphorus associated with iron ores. Though much more work is required on this topic, the rare earth patterns in apatite-rich iron ores support a marine source for the phosphorus and, by analogy, for the iron, too. Work by Berner (1973) has shown that on the East Pacific Rise phosphorus is "scavenged" by iron oxides, and apatite will not normally form as a separate mineral. Though Berner's experiments were concerned with the uptake of phosphorus by volcanogenic ferric oxides, his conclusion—that all of the phosphorus delivered to the ocean by rivers can be adsorbed by the volcanic iron of the East Pacific Rise—is important to our appreciation of just how potentially important the iron-phosphorus association is. However, the presence of apatite-rich bands in some banded iron-formations indicates that, for a limited period at least, a high P/Fe ratio prevailed in places, which enabled phosphorus to form a separate mineral phase. During the early Proterozoic, at least, the dispersal and concentration of phosphorus in marine sediments was controlled largely by the distribution of iron and the periodic upwelling of reducing iron-rich ocean waters of the type envisaged by Holland (1973). The extent to which the biota was also involved at this time is uncertain, though La Berge (1973) has shown that, despite the high degree of oxidation in the ores, there are still abundant remains of algae or bacteria in some iron ores or associated sediments, suggesting that organisms might have played a significant role at times.

It was not until later in the Proterozoic that the development of a more prolific (eucaryotic) fauna resulted in larger quantities of phosphorus being tied in the biota. This, coupled with a decrease in the iron content of the deep upwelling ocean waters, resulted in the association with iron becoming minimized to the extent that phosphorus was sufficiently concentrated in some sediments for phosphorites to form as separate deposits. The development of major phosphorites at about 700 to 800 m.y. coincided with the incoming of the Rapitan-type ores, fairly extensive glaciation, and the development of metazoans. These large-bodied organisms presented enhanced opportunity for the further biochemical concentration of phosphorus in upwelling areas. An equally fundamental change occurred at about the base of the Cambrian with the massive development of phosphorites, and particularly the occurrence of pelletal phosphorites (and to a lesser extent ironstones), on a large scale. In many cases, this is clearly linked to the development of organisms with hard parts which would abrade to form pellets. In some cases, the organisms (e.g., trilobites, inarticulate brachiopods) were originally phosphatic; in other cases, the shell fragments were phosphatized following burial. Some of the pellets may be fecal pellets, but this is probably a relatively minor component in most deposits.

Throughout the remainder of the Phanerozoic, pelletal phosphorites (and ironstones) continued to dominate. Few, if any, of the deposits result from the abrasion of phosphatic organisms because of the dominance of calcareous organisms in the post-Cambrian period. Most of the pellets, especially those in the Mesozoic-Cenozoic, show few signs of abrasion or oolitic banding and their origin still remains something of a puzzle. Davies et al. (1976) have shown that the formation of calcareous ooids is in part dependant on the formation of an organic film on the outer skin. The composition of the film is a critical feature of the process, with the presence of lipids especially important. Powell et al. (1975) found that phospholipids were a particular feature of the Phanerozoic phosphorites that they examined. It therefore appears likely that the formation of pelletal phosphorites, and by inference pelletal iron ores, is linked to a particular stage of organic evolution. Therefore, it is now possible to propose a model to explain the temporal distribution of phosphorites though, as pointed out earlier, this model, too, is in part dependant on plate tectonics and should not be viewed purely as a geochemical model.

Temporal Model

Model C

1. *3,400 m.y. or earlier:* Phosphorus present at a sufficient level in the hydrosphere that is available to the procaryotic fauna but insufficient for the formation of phosphorites.

2. *3,400 to 2,200 m.y.:* Phosphorus concentration continues to increase in the hydrosphere (by degassing and weathering) and in the biosphere. Lack of shallow seas and association with iron, and a com-

paratively small total biomass, preclude the formation of phosphorites.

3. 2,200 to 1,800 m.y: Overturn (perhaps initiated by the Gowgandra glaciation) of reduced deep ocean waters rich in iron and phosphorus. Most of the phosphorus coprecipitated with the iron in banded iron-formations but a few thin phosphorites formed. The hydrosphere may have been somewhat depleted in iron and phosphorus by the end of this period.

4. 1,800 to 800 m.y.: Gradual increase in phosphorus content of the hydrosphere, again, by weathering. More phosphorus now held in the biota, including the eucaryota, in the latter part of this period. Sufficient segregation of iron and phosphorus that some phosphorites were able to form.

5. 800 to 600 m.y.: Major glacial phases may again have triggered massive ocean overturn leading to the formation of Rapitan-type iron ores, and also phosphorites, at about 800 m.y. Some phosphorus held in the iron deposits but large amounts now tied up in the biota (including metazoans). Development of some large sedimentary phosphate deposits during this time, in response to the biotic segregation of phosphorus and oceanic upwelling (possibly intensified during glacial or associated interglacial episodes).

6. 600 to 400 m.y.: High concentrations of phosphorus in shallow waters in the early Cambrian resulted in the development of a phosphatic shelly fauna. This, coupled with the formation of an east-west low- to medium-latitude seaway, produced large-scale phosphorites (dominantly pelletal).

7. 400 to 200 m.y.: There was only minor formation of phosphorites during this period with the notable exception of the Permian. This lack of phosphorites may have resulted from an unfavorable continent-ocean configuration and relative climatic quiescence (no glaciation until the late Carboniferous-Permian), resulting in a lack of oceanic overturn.

8. 200 m.y. to present: Large-scale development of phosphorites throughout the Mesozoic and Cenozoic. Extensive sea-floor spreading, the development of a narrow east–west (Tethyan) seaway with marked dynamic upwelling, and a wide north–south (Atlantic) seaway with well-defined oceanic upwelling are important features of this period, which had a profound effect on the formation and distribution of phosphate deposits.

Summary and Conclusions

Phosphorites most commonly form at low latitudes; a few deposits form at intermediate latitudes. The absence of phosphorites at some times is due to the relative lack of coastal areas at low latitudes. Most low-latitude phosphorites formed in an arid climatic zone either in narrow east–west seaways in response to dynamic upwelling or in broad north–south seaways in response to oceanic upwelling on the east side of the ocean. The phosphorites found in shallow intracontinental epeiric seas do not fit either of these situations and remain an enigma.

Phosphorites formed sporadically during the Proterozoic and throughout the Phanerozoic as continents drifted into low-latitude locations and seaways formed. The major period of phosphogenesis was from about 800 m.y. to the present. A number of phosphogenic episodes can be recognized. The lower and middle Proterozoic peaks are of uncertain validity at the present time because of the incompleteness of the geologic record. The upper Proterozoic and Phanerozoic peaks are well defined.

Phosphogenesis is not directly related to phases of volcanism, orogenesis, or evaporites, but all are associated through plate tectonics and the processes of plate separation and convergence. Volcanism and orogenesis are involved in the initiation of rifting; evaporites in the "rift-valley" stage and phosphorites are formed once the rift valley is breached and a seaway established. Using these features it is possible to develop Model A to explain features (the nature of the sediments and their order of superposition) of east–west seaways and Model B to explain features of north–south seaways. There are important differences between the two models.

The chemistry of the oceans is of major significance to the formation of phosphorites. The distribution of iron in Precambrian seas was of great importance to the distribution of phosphorus in the hydrosphere. The two are linked because upwelling is important to the formation of both iron ores and phosphorites. Glacial periods may have been important because of the intensification of upwelling during glacial periods, and perhaps also because the onset of glaciation may have initiated oceanic overturn. Using the currently available information on the distribution of iron ore, phosphorites, and the course of organic evolution, it is possible to develop Model C for the temporal distribution of phosphorites.

Acknowledgments

We thank Lew Gustafson and Neil Williams, of the Australian National University, and the referees for their helpful comments on the manuscript. Karen Gibbs typed this paper and assisted in various ways. This paper is a contribution to Project 156 of the International Geological Correlation Program, which aims at attaining greater understanding of the distribution, nature, and origin of Proterozoic and Cambrian phosphorites.

Research School of Earth Sciences
Australian National University
Canberra, A.C.T. 2600, Australia
October 6, 1978

REFERENCES

Altschuler, Z. S., Berman, S., and Cuttitta, F., 1967, Rare earths in phosphorites—geochemistry and potential recovery, *in* Hale, L. A., ed., Anatomy of the western phosphate field: Salt Lake City, Intermountain Assoc. Geologists 15th Ann. Field Conf., p. 125–135.

Atlas, E., 1975, Phosphate equilibria in seawater and interstitial waters: Ph.D. thesis, Oregon State Univ., 154 p.

Badham, J. P. N., and Stanworth, C. W., 1977, Evaporites from the lower Proterozoic of the East Arm, Great Slave Lake: Nature, v. 268, p. 516–518.

Baturin, G. I., 1969, Authigenic phosphate concretions in Recent sediments of the southwest African shelf: Akad. Nauk SSSR Doklady, v. 189, p. 1359–1362.

—— 1971, Formation of phosphate sediments and water dynamics: Oceanology, v. 11, p. 372–376.

Bell, R. T., and Jackson, G. D., 1974, Aphebian halite and sulfate indications in the Belcher Group, Northwest Territories: Canadian Jour. Earth Sci., v. 11, p. 722–728.

Berner, R. A., 1973, Phosphate removal from seawater by adsorption on volcanogenic ferric oxides: Earth Planet. Sci. Letters, v. 18, p. 77–86.

Borchert, H., 1960, Genesis of marine sedimentary iron ores: Inst. Mining Metallurgy Trans., v. 69, p. 261–277.

Bremner, J. M., and Rickard, R. S., 1977, On the formation of phosphorite pellets: Electron Microscopy Soc. Southern Africa Proc., v. 7, p. 83–84.

Bremner, J. M., and Willis, J. P., 1975, Glauconite and phosphorites from Southwest Africa: Electron Microscopy Soc. Southern Africa Proc., v. 5, p. 127–128.

British Sulphur Corporation, 1973, World survey of phosphate deposits, 3rd ed.: London, British Sulphur Corp., 180 p.

Brongersma-Sanders, M., 1969, Permian wind and the occurrence of fish and metals in the Kupferschiefer and Marl Slate: 15th Inter-University Geol. Cong., Univ. of Leicester, Proc., p. 61–71.

Burnett, W. C., 1974, Phosphorite deposits from the sea floor off Peru and Chile: radiochemical and geochemical investigations concerning their origin: Hawaii Inst. Geophysics Rept. 4-3, 164 p.

—— 1977, Geochemistry and origin of phosphorite deposits from off Peru and Chile: Geol. Soc. America Bull., v. 88, p. 813–823.

Bushinski, G. I., 1964, On the shallow-water origin of phosphorite sediments, *in* van Straaten, L. M. J., ed., Deltaic and shallow marine deposits: Elsevier Pub. Co., Amsterdam, p. 62–70.

Cannon, W. F., and Klasner, J. S., 1976, Phosphorite and other apatite-bearing sedimentary rocks in the Precambrian of northern Michigan: U. S. Geol. Survey Circ. 746, 6 p.

Cathcart, J. B., and Schmidt, D. L., 1977, Middle Palaeozoic sedimentary phosphate in the Pensacola Mountains, Antarctica: U. S. Geol. Survey Prof. Paper 456-E, 18 p.

Cloud, P. E., 1973, Paleoecological significance of the banded iron-formation: ECON. GEOL., v. 68, p. 1135–1143.

Cook, P. J., 1967, Winnowing—an important process in the concentration of the Stairway Sandstone (Ordovician) phosphorites of central Australia: Jour. Sed. Petrology, v. 37, p. 818–828.

—— 1972, Petrology and geochemistry of the phosphate deposits of northwest Queenland, Australia: ECON. GEOL., v. 67, p. 1193–1213.

—— 1976, Sedimentary phosphate deposits, *in* Wolf, K. H., ed., Handbook of stratabound and stratiform ore deposits: Amsterdam, Elsevier Pub. Co., v. 7, p. 505–535.

Cloup, P., 1974, Evolution of ecosystems: Am. Scientist, v. 62, p. 54–66.

Davidson, C. F., 1963, Phosphate deposits of Precambrian age: Mining Mag., v. 109, p. 205–208.

Davies, P. J., Bubela, B., and Ferguson, J., 1976, The formation of ooids [abs.]: Internat. Geol. Cong., 25th, Sydney 1976, v. 2, p. 341–342.

Dickson, G. O., Pitman, W. C., and Heirtzler, J. R., 1968, Magnetic anomalies in the South Atlantic and ocean floor spreading: Jour. Geophys. Research, v. 73, p. 2087–2117.

Evans, R., 1978, Origin and significance of eavaporites in basins around Atlantic margin: Am. Assoc. Petroleum Geologists Bull., v. 62, p. 223–234.

Freas, D. H., and Eckstrom, C. L., 1968, Areas of potential upwelling and phosphorite deposition during Tertiary, Mesozoic and late Paleozoic time: New York, United Nations, Mineral Devel. Ser. 32, p. 228–238.

Gardner, J. V., 1973, Eastern equatorial Atlantic: Sea-surface temperature and circulation response to global climatic changes during the past 200,000 years [abs.]: Geol. Soc. *America Abstracts with Programs, v. 5, p. 629.*

Garrels, R. M., Perry, E. A., and Mackenzie, F. T., 1973, Genesis of Precambrian iron-formation and the development of atmospheric oxygen: ECON. GEOL., v. 68, p. 1173–1179.

Geijer, P., 1962, Some aspects of phosphorus in Precambrian sedimentation: Arkiv För Mineralogi och Geologi, v. 3(9), p. 165–186.

Gimmel'farb, B. M., 1958, Regularity of the tectonic distribution of phosphorite deposits in the USSR: Moscow, Izdatel'stvo AN SSR, v. 1. (In Russian)

Goodwin, A. M., 1962, Structure, stratigraphy and origin of iron formations, Michipicoten area, Algoma district, Ontario, Canada: Geol. Soc. America Bull., v. 73, p. 561–586.

Goldich, S. S., 1973, Ages of Precambrian banded iron-formations: ECON. GEOL., v. 68, p. 1126–1134.

Govett, G. J. S., 1966, Origin of banded iron formations: Geol. Soc. America Bull., v. 77, p. 1191–1212.

Gross, G. A., 1973, The depositional environment of principal types of Precambrian iron formations, *in* Genesis of Precambrian iron and manganese deposits: Kiev Symposium, 1970, Proc. (Earth Sciences, v. 9), p. 15–21.

Gulbrandsen, J. B., 1976, Phosphate investigations in Brazil, 1975: U. S. Geol. Survey, Open File Rept. 76–45, 25 p.

Gulbrandsen, R. A., and Roberson, C. E., 1973, Inorganic phosphorus in seawater, *in* Griffith, E. J., et al., eds., Environmental phosphorus handbook: New York, John Wiley and Sons, p. 117–140.

Heirtzler, J. R., Dickson, G. O., Herron, E. M., Pitman, W. C., and Le Pichon, X., 1968, Marine magnetic anomalies, geomagnetic field reversals and motions of the ocean floor and continents: Jour. Geophys. Reseach, v. 73, p. 2119–2136.

Hite, R. J., 1976, Possible genetic relationships between evaporites, phosphorites and iron-rich sediments [abs.]: Internat. Geol. Cong., 25th, Sydney 1976, v. 3, p. 835.

Holland, H. D., 1973, The oceans: a possible source of iron in iron-formations: ECON. GEOL., v. 68, p. 1169–1172.

Howard, P. F., and Cooney, A. M., 1976, D Tree phosphate deposit, Georgina Basin, Queensland, *in* Knight, C. L., ed., Economic geology of Australia and Papua New Guinea: Australasian Inst. Mining Metallurgy Mon. 5, v. 4, p. 273–278.

Howard, P. F., and Hough, M., 1979, On the geochemistry and origin of the D Tree, Wonarah, and Sherrin Creek phosphorite deposits of the Georgina Basin, Northern Australia: ECON. GEOL., v. 74, p. 260–284.

James, H. L., 1954, Sedimentary facies of iron-formation: ECON. GEOL., v. 49, p. 235–293.

—— 1966, Chemistry of the iron-rich sedimentary rocks: U. S. Geol. Survey Prof. Paper 440-W, 63 p.

Kazakov, A. V., 1938, The phosphorite facies and the genesis of phosphorites: Internat. Geol. Cong., 17th, Moscow and Leningrad 1937, p. 95–113.

Khramov, A. N., 1971, Paleomagnetic direction and paleomagnetic poles: Reference data for the USSR Acad. Sci., USSR, Soviet Geophys. Committee, World Data Center B, Leningrad; Issue 1, 124 p.

—— 1973, Paleomagnetic directions and paleomagnetic poles: Reference data for the USSR Acad. Sci., USSR, Soviet Geophys. Committee, World Data Center B, Leningrad; Issue 2, 88 p.

—— 1975, Paleomagnetic directions and paleomagnetic poles: Reference data for the USSR Acad. Sci., USSR, Soviet Geophys. Committee, World Data Center B, Leningrad; Issue 3, 44 p.

Kolodny, Y., 1969, Are marine phosphorites forming today?: Nature, v. 244, p. 1017–1019.

Laajoki, K., 1975, Rare-earth elements in Precambrian iron formations in Vayrylänkylä, South Puolanka area, Finland: Geol. Soc. Finland Bull., v. 47, p. 93–107.

Laajoki, K., and Saikkonen, R., 1977, On the geology and geochemistry of the Precambrian iron formation in Vayrylänklä, South Puolanka area, Finland: Finland Geol. Survey Bull., v. 292, 137 p.

LaBerge, G. L., 1973, Possible biological origin of Precambrian iron-formations: Econ. Geol., v. 68, p. 1098–1109.

Lefond, S. J., 1969, Handbook of world salt resources: New York, Plenum, 384 p.

Lepp, H., and Goldich, S. S., 1964, Origin of Precambrian iron formations: Econ. Geol., v. 59, p. 1025–1060.

Liu, Hung-Yun, Sha, Ching-An, and Hu, Shih-Ling, 1973, The Sinian system in southern China: Scientia Sinica, v. 6(2), p. 266–278.

Lowe, D. R., and Knauth, L. P., 1977, Sedimentology of the Onverwacht Group (3.4 billion years), Transvaal, South Africa and its bearing on the characteristics and evolution of the early earth: Jour. Geology, v. 85, p. 699–723.

McElhinny, M. W., 1972, Paleomagnetic directions and pole positions—XII: Royal Astron. Soc. Geophys. Jour., v. 30, p. 281–293.

—— 1973, Palaeomagnetism and plate tectonics: Cambridge, University Press, 358 p.

McElhinny, M. W., and Cowley, J. A., 1977, Palaeomagnetic directions and pole positions—XIV: Royal Astron. Soc. Geophys. Jour., v. 49, p. 313–356.

—— 1978, Palaeomagnetic directions and pole positions—XV: Royal Astron. Soc. Geophys. Jour., v. 52, p. 259–276.

McElhinny, M. W., Cowley, J. A., Brown, D. A., and Wirubov, N., 1977, A compilation of palaeomagnetic results from the U.S.S.R.: Australian Nat. Univ., Research School Earth Sci. Pub. 1268, 80 p.

McKelvey, V. E., 1963, Successful new techniques in prospecting for phosphate deposits, *in* Durston, John H., and Meiklejohn, J. J., eds., Science, technology, and development: United States papers prepared for United Nations Conf. on application of science and technology for benefit of less developed areas, Geneva, 1963, v. II, Washington, U.S. Agency Int. Devel., 355 p.

—— 1967, Phosphate deposits: U. S. Geol. Survey Bull. 1252-D, p. 1–22.

—— 1973, Abundance and distribution of phosphorus in the lithosphere, *in* Griffith, E. J., et al., eds., Environmental phosphorus handbook: New York, John Wiley and Sons, p. 13–30.

McKelvey, V. E., Swanson, R. W., and Sheldon, R. P., 1953, The Permian phosphorite deposits of western United States: Internat. Geol. Cong., 19th, Algiers 1952, v. 11, p. 45–65.

Mancuso, J. J., Lougheed, M. S., and Shaw, R., 1975, Carbonate-apatite in Precambrian cherty iron-formation, Baraga County, Michigan: Econ. Geol., v. 70, p. 583–586.

Mansfield, G. R., 1940, The role of fluorine in phosphate deposition: Am. Jour. Sci., v. 238, p. 863–879.

Moorbath, S., O'Nions, R. K., and Pankhurst, R. J., 1973, Early Archean age for the Isua Iron Formation, West Greenland: Nature, v. 245, p. 138–139.

Morris, R. C., 1973, A pilot study of phosphorus distribution in parts of the Brockman Iron Formation, Hamersley Group, Western Australia: Western Australia Geol. Survey Ann. Rept. 1972, p. 75–81.

Muir, M. D., and Grant, P.R., Micropalaeontological evidence from the Onverwacht Group, South Africa, *in* Windley, B. F., ed., The early history of the earth: London, Wiley, p. 595–604.

O'Rourke, J. E., 1961, Palaeozoic banded iron formations: Econ. Geol., v. 56, p. 331–361.

Pettijohn, J., 1957, Sedimentary rocks: New York, Harper and Row, 718 p.

Pevear, D. R., 1966, The estuarine formation of United States Atlantic Plain phosphorite: Econ. Geol., v. 61, p. 251–256.

Powell, T. G., Cook, P. J., and McKirdy, D., 1975, Organic geochemistry of phosphorites: relevance to petroleum genesis: Am. Assoc. Petroleum Geologists Bull., v. 59, p. 618–632.

Prichard, P. W., and Cook, P. J., 1965, Phosphate deposits of the Northern Territory, *in* Geology of Australian ore deposits: Melbourne, Australasian Inst. Mining Metallurgy, v. 1, p. 219–228.

Riggs, S. R., 1967, Phosphorite stratigraphy, sedimentation, and petrology of the Noralyn mine, central Florida Phosphate district: Unpub. Ph.D. thesis, Univ. Montana, 268 p.

—— 1979a, Petrology of the Tertiary phosphorite system of Florida: Econ. Geol., v. 74, p. 195–220.

—— 1979b, Phosphorite sedimentation in Florida—A model phosphogenic system: Econ. Geol., v. 74, p. 285–314.

Rogers, J. K., and Keevers, R. E., 1976, Lady Annie-Lady Jane phosphate deposits, Georgina Basin, Queensland, *in* Knight, C. L., ed., Economic geology of Australia and Papua New Guinea: Australasian Inst. Mining Metallurgy Mon. 5, v. 4, p. 251–265.

Rooney, R. T., and Kerr, P. F., 1967, Mineralogical nature and origin of phosphorite, Beaufort County, North Carolina: Geol. Soc. America Bull., v. 78, p. 731–741.

Ryther, J. H., 1963, Geographical variation in productivity, *in* Hill, N. M., ed., The sea, v. 2: New York, Interscience, p. 347–380.

Salop, L. J., 1977, Precambrian of the northern hemisphere: Oxford, Elsevier, 378 p.

Shaw, S. E., 1968, Rb-Sr isotopic studies of the mine sequence rocks at Broken Hill: Australasian Inst. Mining Metallurgy Mon. 3, p. 185–197.

Sheldon, R. P., 1963, Physical stratigraphy and mineral resources of Permian rocks in western Wyoming: U. S. Geol. Survey Prof. Paper 313-B, p. 49–273.

—— 1964a, Palaeolatitudinal and palaeogeographic distribution of phosphate: U. S. Geol. Survey Prof. Paper 501-C, p. C106–C113.

—— 1964b, Exploration for phosphorite in Turkey: a case history: Econ. Geol., v. 59, p. 1159–1175.

—— 1969, World phosphate resources: Mining Cong. Jour. February 1969, 4 p.

Sheldon, R. P., Maughan, E. K., and Cressman, E. R., 1967, Sedimentation of rocks of Leonardian (Permian) age in Wyoming and adjacent states, *in* Hole, L.A., ed., Anatomy of the Western Phosphate Field: Intermountain Assoc. Geol. 15th Ann. Field Conf., p. 1–13.

Smirnov, V. I., 1958, The problem of the genesis of phosphorites: Akad. Nauk SSSR (Geokhimiya), v. 119, p. 53–56.

Smith, A. G., and Briden, J. C., 1977, Mesozoic and Cenozoic paleocontinental maps: Cambridge, University Press, 63 p.

Smith, J. P., and Lehr, J., 1966, An X-ray investigation of carbonate apatities: Jour. Agr. Food Chemistry, v. 14, p. 342–349.

Smith, A. G., Briden, J. C., and Drewry, G. E., 1973, Phanerozoic world maps, *in* Hughes, N. F., ed., Organisms and continents through time: Palaeontology, Spec. Papers 12, p. 1–42.

Stanton, R. L., 1972, A preliminary account of chemical relationships between sulfide lode and "banded iron formation" at Broken Hill, New South Wales: Econ. Geol., v. 67, p. 1128–1145.

Strakhov, N. M., 1969, Principles of lithogenesis (translation): New York, Consultants Bureau, v. 2, 609 p.

Summerhayes, C. P., Birch, G. F., Rogers, J., and Dingle, R. V., 1973, Phosphate in sediments off southwestern Africa: Nature, v. 243, p. 509–511.

Trendall, A. F., 1968, Three great basins of Precambrian banded iron formation: Geol. Soc. America Bull., v. 79, p. 1527–1544.

—— 1973, Iron formations of the Hamersley Group of Western Australia: type examples of varved Precambrian evaporites, *in* Genesis of Precambrian iron and manganese deposits: Kiev Symposium 1970 Proc. (Earth Sciences, v. 9), p. 257–270.

Trueman, N. A., 1971, A petrological study of some sedimentary phosphorite deposits: Australia Mineral Devel. Labs. Bull. 11, p. 1–71.

U. S. Bureau of Mines, 1975, Mineral facts and problems, p. 820.

Veeh, H. H., Burnett, W. C., and Soutar, A., 1973, Contemporary phosphorites on the continental margin of Peru: Science, v. 181, p. 844–845.

Walker, R. N., Muir, M. D., Diver, W. L., and Williams, N., 1977, Evidence of major sulphate evaporite deposits in the Proterozoic McArthur Group, Northern Territory, Australia: Nature, v. 265, p. 526–529.

Wardlaw, N. C., and Nicholls, G. D., 1972, Cretaceous evaporites of Brazil and West Africa and their bearing on the theory of continental separation: Internat. Geol. Cong., 24th, Montreal 1972, Sec. 6, p. 43–55.

Wells, A. T., Forman, D. J., Ranford, L. C., and Cook, P. J., 1970, The geology of the Amadeus Basin: Australia Bur. Mineral Resources, Geology Geophysics Bull., v. 100, 221 p.

Williams, G. E., 1975a, Late Precambrian glacial climate and the earth's obliquity: Geol. Mag., v. 112, p. 441–465.

—— 1975b, Possible relation between periodic glaciation and the flexure of the galaxy: Earth Planet. Sci. Letters, v. 26, p. 361–369.

Woolnough, W. G., 1941, Origin of banded iron formations—a suggestion: Econ. Geol., v. 36, p. 465–489.

Yeo, G. M., 1977a, A new class of iron formation in the late Proterozoic Rapitan Group, Yukon and Northwest Territories [abs.]: Geol. Assoc. Canada Ann. Meeting, Program with Abstracts, v. 2, p. 56.

—— 1977b, Stratigraphy, sedimentation and geochemistry of the Rapitan Group, Yukon and Northwest Territories, Canada [abs.]: Geol. Soc. America, Programs with Abstracts, v. 9, p. 779.

THE ROLE OF STRESS WAVES AND DISCONTINUITIES IN ROCK FRAGMENTATION:

A STUDY OF FRAGMENTATION IN LARGE LIMESTONE BLOCKS

Stephen R. Winzer and Andrew P. Ritter
Martin Marietta Laboratories
1450 South Rolling Road
Baltimore, Maryland, 21227

1980

ABSTRACT

Reduced-scale blasting experiments were carried out in seven thoroughly characterized 14- to 23-metric-ton blocks of lower Ordovician Chambersburg limestone to study fragmentation under controlled conditions of timing, explosive type, and borehole geometry. High-speed motion pictures (8,300 to 14,000 images/s) were taken of the disintegration of the face, allowing resolution of events 70 to 100 μs apart, with spatial resolution of 0.25 cm. Cracks were observed to be open at the face about 400 μs after initiation of the first borehole, and their formation is consistent with the arrival time of the P wave at the free face. Rock motion at the free face is observable 200 to 300 μs following initiation of the first borehole. Fragmentation of detached pieces, which are evident 600 μs after initiation of the first explosive column, can be seen continuing throughout the remainder of the event, and is believed to be due to trapped stress waves within the detached block. Pre-existing fractures and other structural elements in the blocks serve as crack initiation sites, or re-initiate themselves. Mechanisms of fragmentation observed in the block tests can also be found in full-scale production blasting operations.

INTRODUCTION

The current state of knowledge of the mechanisms of fragmentation in explosively loaded rock is confusing and contradictory. At the same time, demand is growing for gaining more control and predictability in fragmentation of rock by explosives, both because of the increasing degree of sophistication required in extraction processes and because of increasingly stringent requirements for vibration control and noise reduction. In response to these needs, a research effort sponsored by the National Science Foundation, specifically aimed at the quarry industry but relevant to most areas using explosives to fragment rock, has been undertaken jointly by Martin Marietta Laboratories and the University of Maryland. The goals are to gain better understanding of the fragmentation mechanisms operating in explosively-loaded rock and to derive from this knowledge methods useful in production blasting situations. Some specific aspects of the mechanisms of fragmentation are reported here, along with their implications for future design of blasting rounds.

There are two broad areas for grouping theories of rock fragmentation by explosives. The theories can be grouped by the relative importance accorded to either (1) the role of the stress waves imparted to the rock by the rapid release of energy during detonation of the explosive, or (2) the role of the gases released by the detonation in creating a static stress field around the borehole, extending radial cracks, and moving the rock. The first is based on findings from military applications of explosives, and owes its early formulation to Sharpe's (1942) description of elastic wave production from spherical charges. Later work, using strain gages grouted into rock, produced records of the characteristics (amplitude and frequency) of the strain pulse created by dynamite under production conditions (Obert and Duvall, 1949, 1950; Duvall and Atchison, 1950). This work culminated in a generalized theory of the contribution of the stress wave to rock fragmentation (Hino, 1956; Duvall and Atchison, 1957; Rinehart, 1958, 1960; and others).

The second group of theories was developed from work by Porter (1961), Langefors and Kihlstrom (1963), Noren (1956), Porter and Fairhurst (1970), Persson et al. (1970), and others, and expresses the conditions under which the expansion of gases resulting from the detonation of an explosive creates a static stress field conducive to promoting the radial cracking initiated by the shock wave. Radial cracks are then extended by gas pressurization until they intersect the free face, resulting in fragmentation of the rock. More modern discussions of the role of gas pressure can be found in Hagan (1977).

There are problems with all the above theories. Later researchers (Kutter and Fairhurst, 1971; Field and Ladegaard-Pederson, 1971; and Hagan and Just, 1974) have attempted to synthesize the two general areas into one unified theory of rock breakage, but applications of these approaches to full-scale blasting operations still do not provide a full explanation of the results.

The strain (or stress) wave theory, as formulated by Hino (1956) and Duvall and Atchison (1957), relies heavily on the spall effect created by the reflection of a stress wave (the P or compressional wave) from the free face. Later modifications of the theory acknowledge the contribution of the reflected wave in modifying outgoing radial cracks (Field and Ladegaard-Pederson, 1971) and the function of the stress waves as a type of "pre-conditioner" of the rock. More modern approaches to quantification of the role of stress waves in rock fragmentation generally use a computational approach. The engineering parameters of rock are obtained in the laboratory by tests performed on small samples at high rates of loading. These data, combined with data obtained from stress gages implanted in rock in full-scale tests and with constitutive data on properties of the explosive, can be used to calculate, using wave codes, the extent of damage to the rock (Shockey et al., 1974; Grady et al., 1979; Grady and Kipp, 1979; Johnson, 1979; and others). These approaches have been successful in predicting size distribution of fragments at laboratory scale, or in approximating the damage zone in a single-hole shot with a cratering configuration in reasonably homogeneous media. However, these approaches have been somewhat less successful in larger, more complex configurations.

The work of Fogelson et al. (1959) and Persson et al. (1970) indicates that only a small percentage of the explosive energy is contained in the stress waves (3 to 10%), and it is rapidly dissipated. This finding, coupled with the results of work by Noren (1956), suggested that the stress waves could not be responsible for much of the fracturing seen in an explosive event. All of this work tended to support the role of gas pressure as a major contributor to fragmentation, however, this theory is not entirely consistent with observations. It is commonly observed (Dally et al., 1975) that only up to 12 radial cracks propagate for any distance from the borehole. Based on this observation, a typical production blast should produce a few large pie-shaped fragments, which is a conclusion that is clearly at odds with what is normally observed.

The development of both theories suffers from the same difficulty. Most of the work was done in either homogeneous Perspex or other polymeric models, or in rock specifically chosen to be as free as possible of major discontinuities. Therefore, the polymeric models and small rock samples do not reflect the condition of the rock encountered in most large-scale production situations, either prior to or during development of a blast. Very few consistently massive, joint-free rocks exist in quarries or mines. To be certain that the experimental conditions are reasonably representative of actual production situations, it is necessary to take these discontinuities into account.

To provide information on fragmentation mechanisms operating in rock masses encountered at production scales, we have undertaken studies at reduced scale that approximate production conditions. From this, we plan to identify the mechanisms of fragmentation in rock and to devise means of controlling fragmentation.

EXPERIMENTAL METHODS

The experiments were designed to be scaled-down configurations approximating those found in production blasting operations in open pit mines. The shot size was chosen to be large enough to allow use of commercial explosives approximating ANFO in performance, but to still be small enough so all the resulting fragments could be screened to determine their size distribution.

Ideally, the rock used should contain discontinuities representative of the majority of those found in a full-size production bench. To meet these requirements, we used seven 14- to 23-metric-ton blocks of lower Ordovician Chambersburg limestone. The Chambersburg is a dense (2.72-g/cm^3), fine-grained, nodular biomicrite, which is cut (at quarry scale) by one primary and several secondary joint sets. A rough "bedding" is evidenced through open or weathered surfaces 0.6- to 2.4-m apart. The blocks of limestone used in this study result from failure along primary and secondary joint sets and the weathered "bedding" surface. They range from 74 to 101 cm thick, and up to 2.1 and 3.4 m in length and width, and contain all but the major weathered discontinuities seen in the quarry.

Each block was carefully mapped, and we recorded the pattern, density, and distribution of cracks that were sufficiently open to draw in water by capillary action. The cracks on the face of each block (that portion simulating the bench face) were painted to enhance their visability in high-speed films. A typical experimental setup is shown in Figure 1.

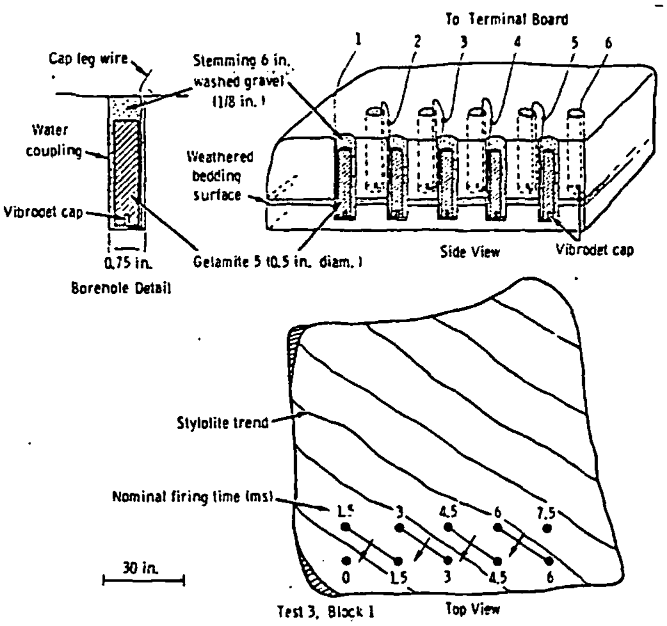

Figure 1. Schematic diagram, drawn to scale, showing a typical experimental configuration for a large block test. The firing sequence in all tests was similar, but the length of time between echelons varied. The angle between echelons and the stylolite trend varied from block to block.

The explosive used was Gelamite 5, manufactured by Hercules, Inc., of Wilmington, Delaware. This is a low-density (0.95-g/cm^3) semigelatin dynamite normally manufactured in 2.9-cm diameter, or larger, cartridges for use in pre-splitting or smooth blasting. This explosive will detonate in the 1.3-cm diameter required by the experiment, but at velocities somewhat lower than found in the production diameters. The specially manufactured cartridges were 76.2 cm long and 1.2 cm in diameter. Detonation velocities, measured by Hercules, Inc., ranged from 2,177 m/s (104-g stick) to 2,368 m/s (124-g stick). All charges were detonated with a single Hercules Vibrodet initiator placed at the lower end of the powder column. Timing was regulated by a programmable sequential blasting machine with a 450-V capacity, capable of firing ten series of initiators at intervals ranging from 400 μs to 999 ms with an error of less than 10% at 400 μs and less than 1% at 999 ms. A variety of 16-mm high-speed motion picture cameras recorded the event at image rates ranging from 8,500 to 14,000 per second. Zero time indication, for three of the tests, was achieved by placing a single initiator in the field of view of the face camera. The accuracy of this method is ± 21 μs. Further experimental details can be found in Winzer et al. (1979).

RESULTS

Seven block tests have been carried out in the series, at delay intervals of 450 μs, 800 μs, and 1.5 ms between echelons (see Figure 1). In six of the seven tests, the disintegration of the face was analyzed quantitatively by measuring the maximum length and width of the fragments and their area, and by mapping the new crack network at progressively later times in the event. These data present a time history of the fragmentation of the face of each block, which can then be compared to the bulk fragmentation obtained by screening all of the fragmented rock. Examination of the films suggests that fragmentation of the block is a continuous process, but there are two distinct periods within the event.

Early Event: Development of a Surface Fracture Network

The early portion of the event takes place between zero and about 600 μs after detonation of the first borehole (depending on the delay between boreholes), and covers the event up until distinct fragments, detached from the face, become visible. The principal differences between the disintegration patterns of the blocks in the early portion of the event are due to the difference in delay time between the holes in the pattern, and the effects of structure. Figures 2a through 2d are scale drawings showing the positions of stress waves, potential radial cracks, and cracks observed to be open on the face at 396 μs and 528 μs into the event. The delay time for this test was 800 μs, so only the first hole in the pattern had fired. The explosive column takes 238 μs to detonate, based on a velocity of 0.245 cm/μs obtained by extrapolating from velocities measured for cartridges of Gelamite 5 of a given weight. Figure 2a shows the front view, the position of the shear wave from the initial detonation of the column (at the bottom), and the P wave from the completion of detonation at the top of the column. The explosive is subsonic, detonating at about 54% of the P wave and 93% of the S wave velocity; thus, there is no shock front as would be found with supersonic explosives. The position of a hypothetical radial crack front, based on a propagation velocity of 12% of the P wave velocity [Holloway et al., 1980 (in this volume)] is shown as a cone truncated at the borehole. Cracks that can be seen as open at 396 μs are shown in the position where they appear on the face. Figure 2b is a view from the side as though the block were truncated at the borehole.

The situation at 528 μs is shown in Figures 2c and 2d. In Figures 2c and 2d, the radial crack front would just reach the bottom of the block, however, open fractures can be seen all the way to the top of the block. Close examination of the films reveals the following sequence of events, which is applicable to all blocks. Motion can be detected within 200 to 300 μs of the beginning of the detonation sequence, followed by the first indication of fracturing, usually in the bottom half of the block, about 100 μs later. Fractures in the top half of the block appear 100 to 130 μs after those in the bottom half of the block.

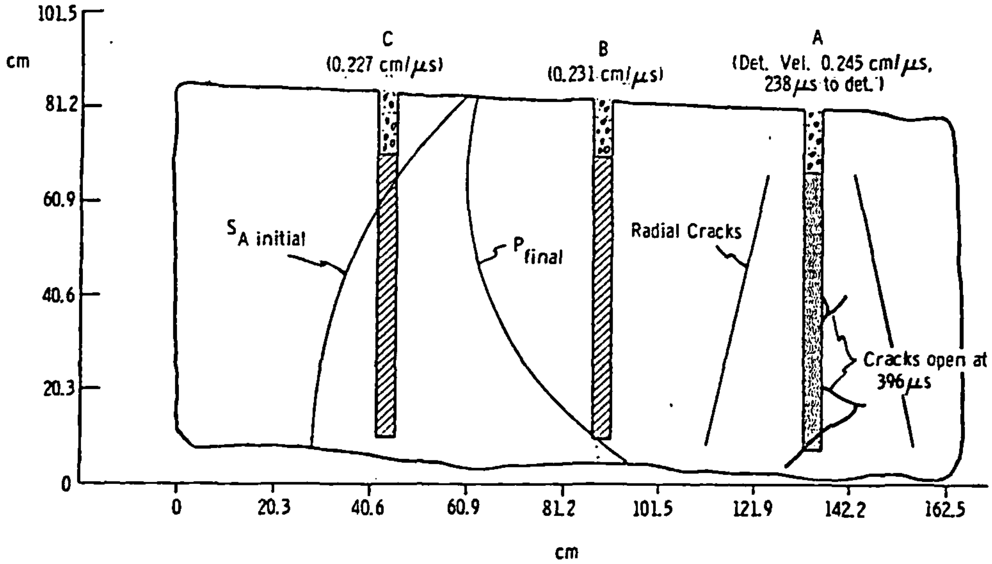

Figure 2a. Exact scale drawing of the position of the shear wave from the beginning of detonation of borehole A; the P wave from detonation of the last increment of explosive in borehole A; the position of radial cracks, based on a propagation velocity of 12% of the P wave; and cracks actually appearing at the face as seen from the front, all at 396 μs after initiation of borehole A.

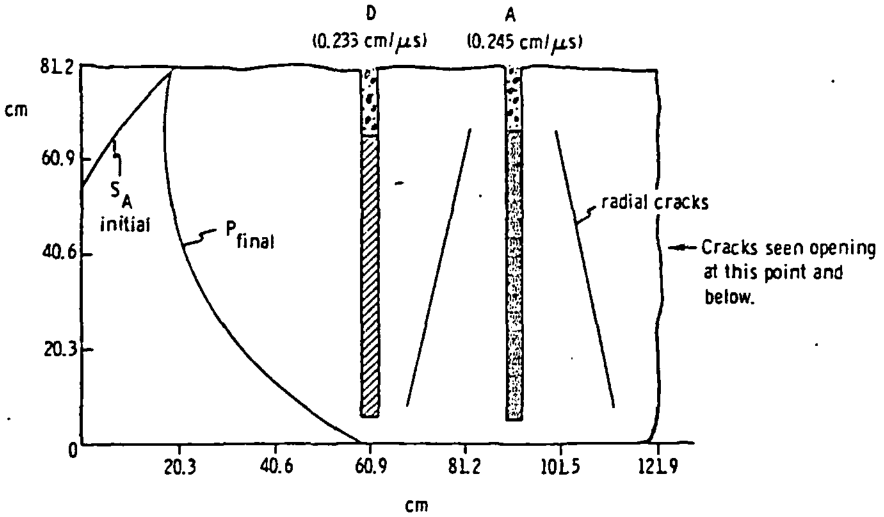

Figure 2b. Same as 2a, but viewed from the side as if the block is cut through boreholes A and D.

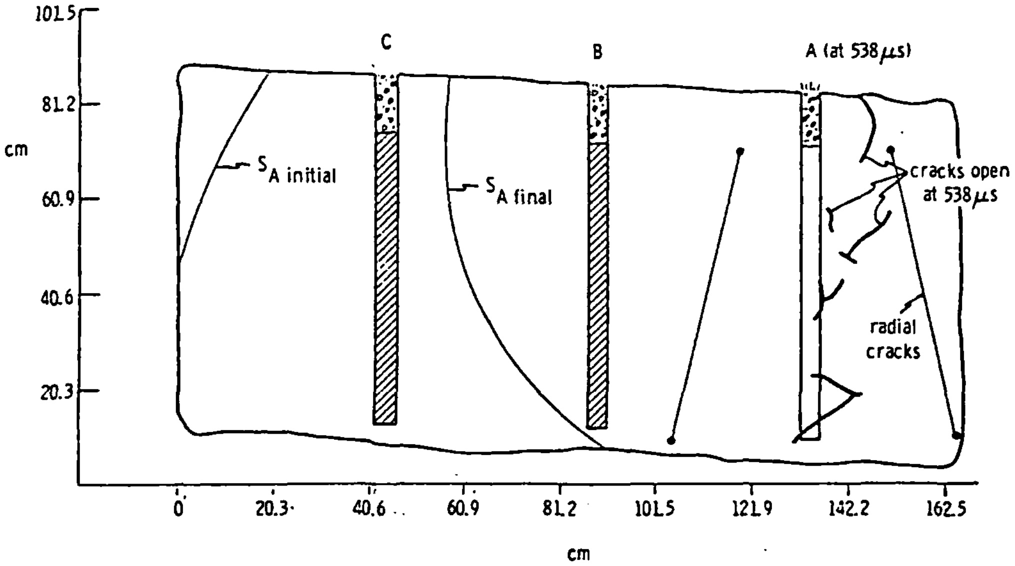

Figure 2c. Front view of same block depicted in 2a, but at 528 μs after initiation of borehole A.

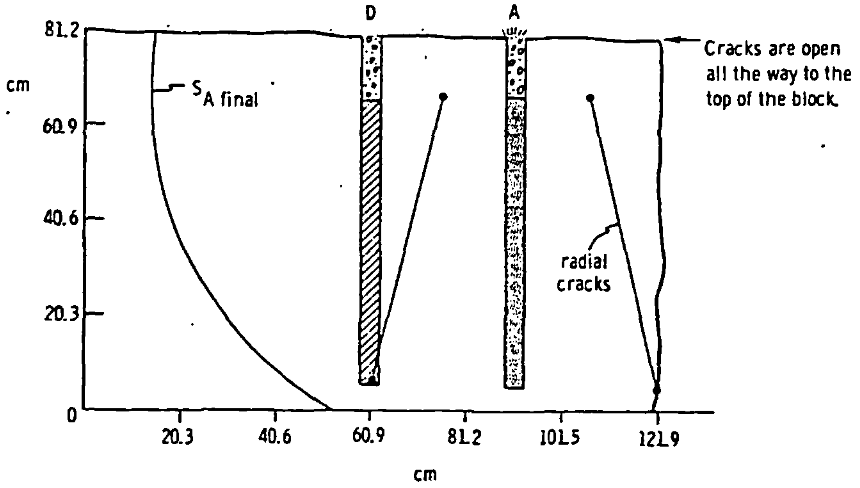

Figure 2d. Side view of same block depicted in 2a, but at 528 μs after initiation of borehole A.

Discussion

It is clear from the diagrams shown in Figures 2a through 2d that the cracks appearing at the face early in the event could not have originated from the borehole. Furthermore, these cracks are not likely of radial origin because, although they are open at least 0.5 cm, no gas can be seen venting through any of them. From the observations detailed above, and from other work on crack initiation and propagation in rock (Holloway et al., 1980), some further inferences can be drawn. The spatial resolution on the block face is about 0.25 cm for a high-contrast object. At the time the first opening cracks were seen on the surface, they were open by about 0.5 cm. Holloway et al. (1980) observed from interference patterns on the surface of explosively-loaded rock plates that the crack tip is out ahead of the point where the crack becomes visible. We can assume, therefore, that the crack arrival time at the face was prior to any visible indication of crack opening, and we can make a rough calculation of what the actual arrival time would be. The measured burden velocity in these tests averages 21.9 m/s, or about 0.0022 cm/μs. At this velocity, assuming the fragments were moving away from each other at the measured velocity, it would take 250 μs for the opening to become 0.55 cm wide. The P wave transit time is 66 μs, thus, within the error of the measurements, the crack formation is coincident with, or no more than twice the time it takes for the P wave to reach the face. This is an important observation, for Noren (1956) and Persson et al. (1970) both suggest that neither cracks nor rock motion begin before 5 to 10 times the transit time of the P wave. It is possible that these early-forming cracks are generated by the tensile stresses resulting from the reflected P wave as it travels back towards the borehole. The cracks would then be initiated at the face, and would be travelling back towards the borehole. This type of fracture has been observed by Holloway et al. (1980) in rock plates. The early cracks could also be generated at internal flaws close to the face; however, we do not have sufficient spatial or temporal resolution to resolve this question.

Late Event: Fragment Formation and Fragment Reduction

The later portions of the event begin after observation of the early-forming cracks and fragments in front of the borehole. It includes further fragment formation and detachment, and continued reduction in the size of fragments from the time of their detachment from the face through cessation of fragment motion (about 2 seconds). It is during this portion of the event that the effects of pre-existing cracks and other structural discontinuities become visible and that differences between delay times manifest themselves.

Some 130 to 400 μs after the early opening cracks are seen (Figure 2c), they begin to coalesce, defining fragments in the face to the right of the borehole. New cracks are seen between boreholes A and B. In blocks with shorter delay intervals (450-μs), the fracture pattern and fragment pattern will be developed across the entire surface of the block about 400 to 500 μs after detonation of the boreholes. The earlier fractures will be open several centimeters by this time, but no gas is seen venting through the face of any of the blocks. The open fractures define larger fragments, which are by this time detached from the face and moving well outward from it. In this early expression of fragment development, three types of fracturing can be seen. The first type includes large, continuous horizontal fractures parallel to the "bedding" in the rock. In cases where weathered bedding planes are present, gas may vent through the open plane within 1.5 ms of borehole detonation. This is the earliest expression of gas venting through the face of any of the blocks. The second type of fracture develops perpendicular to the bedding planes, and may either terminate at one of the bedding plane fractures or continue through it (Figure 3a and b). The third type of fracture is smaller (shorter) and may be oriented in any direction on the face. These cracks can be seen originating at old cracks or intersecting old cracks, or they may actually be old cracks that have re-initiated and opened (Figure 4).

Between 1.5 ms and 3 ms, depending on delay time, the entire face of the block appears to be a mass of fragments in motion. From the side camera, the face appears to be a slightly undulating mass which has moved 3 to 4 cm from its original position. In some cases, a small amount of gas may be seen venting through the base of the block, or through small parts of weathered bedding planes; but, in general, the face will be clear of gas. Most of the explosively-produced gases and steam vent through the stemming, a process which begins from 100 to 400 μs after the column has detonated.

During the period between 2 ms and loss of light, or movement of the fragments from the field of view, the fragments continue to break up. This continued breakup takes place by formation of new cracks, re-initiation of old cracks, or a combination of the two mechanisms, followed by coalescence of cracks. No collisions take place during this portion of the event; all the fragments are moving in essentially the same direction (with some divergence) at very similar velocities. This continued disintegration can be assessed quantitatively as follows: The length, width, and surface area of each visible fragment is measured through a photo-optical digitizer. Assuming that the maximum width is equal to the thickness, the weight of each fragment can be calculated from these measurements and the density of the rock. Using length as an indication of which fragments would be retained or would pass a screen of a given size, we can obtain a size distribution equivalent to that obtained by bulk screening. This quantitative analysis is done at different times in the event, and the distributions are compared. Figure 5 is a plot of the size distribution of the face of block 6, taken 3.95 and 9.21 ms after the start of the event. It shows quite clearly the decrease in fragment size with time. During the time between the two measurements, the fragments have moved 11.5 cm, based on a velocity of 21.9 m/s. This same phenomenon can be seen in all the block tests (see also Winzer et al., 1979 for earlier data).

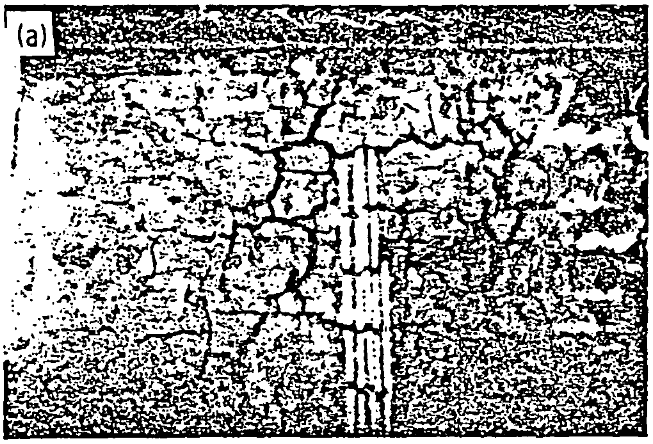

Figure 3a. Single frame taken from a 16-mm motion picture of block test 4, 1.6 ms following initiation of the first explosive column. The delay interval is 1.5 ms, so the third hole (on the right) has just fired. Note the preponderance of large horizontal fractures (these are parallel to or include bedding planes) and fractures perpendicular to them. The small dark lines on the light-colored vertical sticks are 15 cm apart.

Figure 3b. Single frame from a 16-mm high-speed motion picture of block test 6, taken 3.9 ms after initiation of the first borehole (left). This is the same block from which Figure 2 was drawn, but it is printed in reverse. Note the long, undulating horizontal fractures, some portions crossing bedding planes. Vertical fractures appear perpendicular to these cracks in the top lefthand portion of the block. Near the center of the block, note the old fracture that has re-initiated. Note also the absence of gas venting through the face. The borehole positions (solid white lines at the top and bottom of the block) are 45.7 cm apart, the block is 75 cm thick.

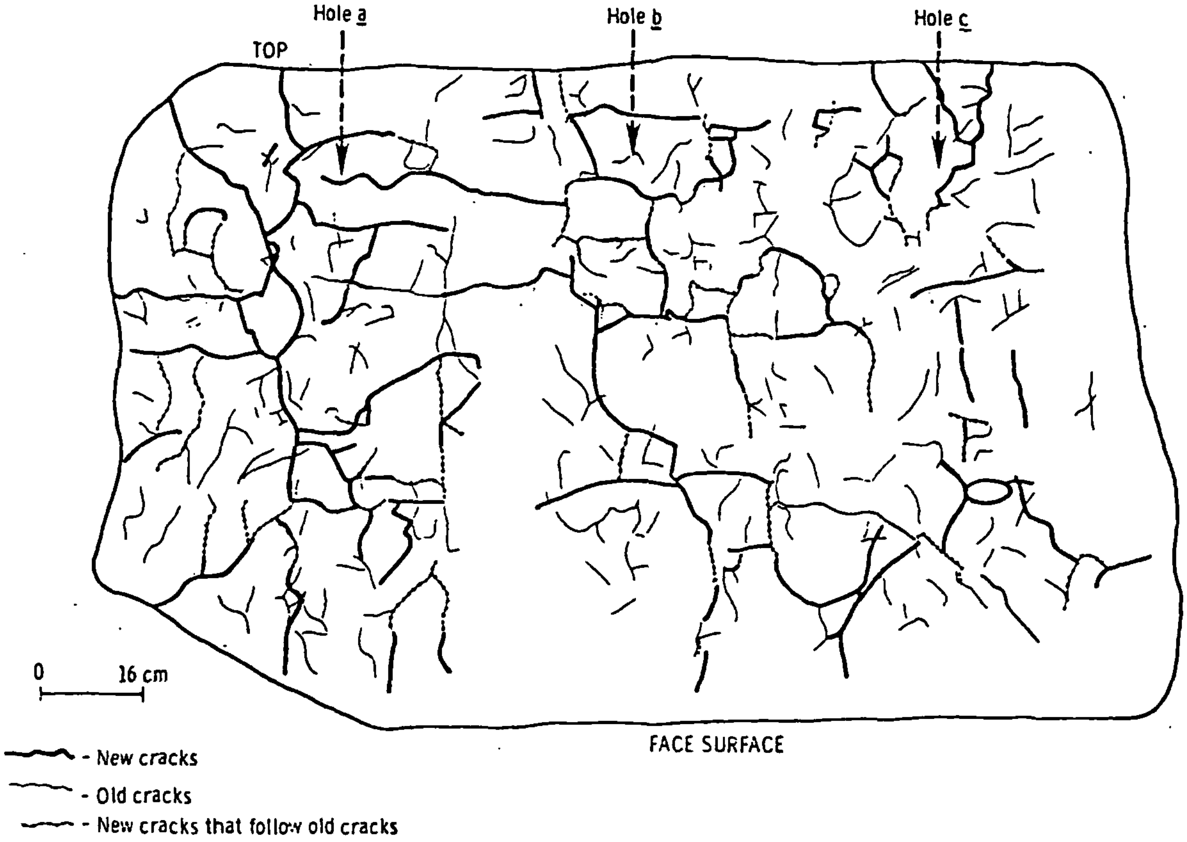

Figure 4. Diagram, traced from block test 4, showing the position of old cracks (light lines), new cracks (heavy lines), and old cracks that have re-initiated (dots over light lines). Careful examination of the figure show where new cracks have developed from old ones (perpendicular to them), and new cracks that have intersected old ones. At the time the tracing was made (up to 7 ms into the event), about 25% of the old cracks had become involved in fragmentation of the block.

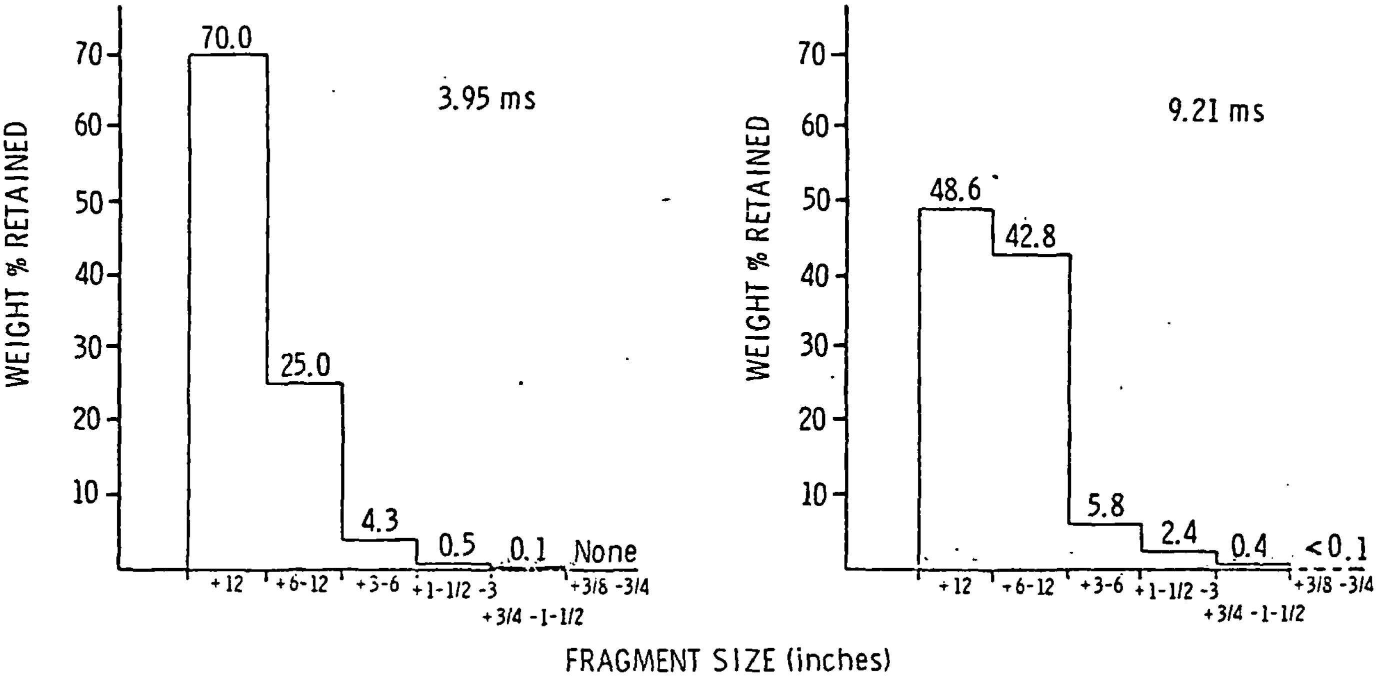

Figure 5. Histogram plots of size distributions of fragments formed by disintegration of the face, taken at 3.95 and 9.21 ms into the event.

Discussion

In the fragmentation mechanisms described by Kutter and Fairhurst (1971), Persson et al. (1970), Langefors and Kihlstrom (1963), and Hagan (1977), among others, the series of events leading to the disintegration of a mass of rock begins with initiation of radial cracks by the stress waves, and possibly with spalling of the face by the reflected stress waves, if the burden is small enough. It is followed by gas extension of radial cracks, and by acceleration of the burden by the pressure of gas built up in the borehole. As our data show, events observed between zero and 600 µs fail to confirm the early portion of the event as described by these authors. Although radial cracks do form (they can be seen in the remaining pieces of the block), they do not propagate fast enough to reach the face by the time cracks open on it. Rock at the face is in motion within 2 to 3 times the transit time of the P wave.

Observation of continued disintegration of the face also fails to confirm the mechanisms postulated by the above authors. The absence of gas venting through the majority of fractures at the surface makes it unlikely that any of the cracks are gas pressurized. Most of the gas that is generated vents through the top of the borehole, beginning very shortly after the column detonates. Thus, the borehole cannot be sustaining significant pressure for very long after the event begins. The continued disintegration of fragments detached from the surface cannot be related in any way to gas pressure, as there is no further communication possible between the borehole and the detached fragment. Two hypotheses can be put forth to explain the continued fragmentation of detached blocks. The first is that the cracks were formed during the first passage of the stress wave, and they do not become visibly open until sufficient movement has taken place. This is not the favored hypothesis because of the time it takes for a typical crack to traverse the fragment. To traverse a 15-cm thick block, a typical crack would take 272 µs, about 4.5 times the P wave velocity. A more likely hypothesis is that the fragments continue to disintegrate due to stress waves trapped in the block as it is detached from the face. If the stress intensity remains high enough, cracks will continue to propagate within the detached block, resulting in further fragmentation of the block. To put this hypothesis on firmer ground would require measurements of the degree of attenuation of the stress waves, which have not been done yet.

CONCLUSIONS

Examination of high-speed motion pictures of 14- to 23-metric-ton limestone blocks (in which miniature blasting patterns using extended column charges of low velocity explosives were fired) indicates that earlier hypotheses concerning the nature of the fragmentation process and its mechanisms need to be revised. Fragmentation of the face begins with early-forming cracks, approximately coincident with the arrival of the first stress waves. Our tests lack the resolution necessary to separate the arriving stress waves, but the opening of these early fractures is similar to fractures initiated by the reflected stress waves in rock plates (Holloway et al. 1980). Rock motion also begins much earlier than previously thought. It appears likely that this early motion could be due to the momentum transfer associated with reflection of the P wave, as discussed by Rinehart (1975).

As development of the fragment pattern continues, the role of the pre-existing structure of the pattern at the face becomes apparent. New fractures can be seen developing at pre-existing fractures, and parallel and perpendicular to "bedding" planes in the block. This type of fracturing closely approximates that found by Fourney et al. (1979) in Homalite models with flaws simulating joint and bedding planes. In the models, this type of fracturing is the result of resolved shear stresses associated with the compressive portion of the P wave as it crosses the discontinuity. We cannot confirm the mechanism, as we cannot determine which stress wave is involved, however, the pattern closely resembles that seen in the models and is consistent with the mechanism seen in the models. Concurrent with this mechanism, old cracks reactivate, or are intersected and reactivated along part of their length by new fractures. It can be presumed that these mechanisms operate within the body of the block as well, so that wherever the outgoing or reflected stress waves interact with a discontinuity, the possibility exists that it may reactivate, or serve as a site for initiation of new fractures. On the face, we have observed that from 20 to 30% of the old fractures participate in the fragmentation early in the event (up to 10 ms). It is likely that the final number is higher than this because many of the fragments separating from the face continue to break up even as they go out of the field of view, but it is not possible to assess quantitatively this contribution beyond about 10 ms into the event.

From the data we have obtained, we can say with some certainty that the stress waves play a considerably greater role than was previously thought, and that the manner in which they serve to break the rock is quite different than the mechanisms proposed earlier. The pre-existing structural discontinuities in the rock play a critical and perhaps dominant role in the overall fragmentation of the rock by interacting with the stress waves to produce new fractures or to further develop themselves. These new fractures likely result from shear stresses that developed because of the passage of the P wave over the discontinuity, and a lesser number develop in tension at the free face with the reflection of the P wave. Some spall-like fracturing, with cracks opening parallel to the face, is possible, but cannot be confirmed. Evidence for this type of failure is observed later in the event, from the side cameras. In these views, the face becomes detached from the main body of the block, forming a fragmented sheet of variable thickness (4- to 12-cm). The shear wave and the reflected P wave would intersect at about 7.6 cm into the face, within the thickness of fragments observed. However, the actual geometry is too complex to evaluate with any degree of accuracy. Any radial cracks that do form, do so quite late, and apparently do not reach the free face. Examination of the remainder of the block after tests reveals that the longest radial cracks extend some 25 to 30 cm along the remaining face, but most terminate much sooner, usually at pre-existing fractures.

Observations of production blasting operations using high-speed cinematography, and observations of fracture patterns on the faces remaining after production blasting tend to confirm the data from the block tests. Winzer et al. (1979) observed continued reduction in the sizes of fragments following detachment from the face during production blasting operations. New fractures, perpendicular to "bedding" planes, were observed in the face following blasting in limestone (Winzer et al., 1979) and similar fractures were observed developing perpendicular to major joints in granite.

The fragmentation mechanisms observed and identified in our research are of considerable importance to the design of production blasts. The structure is of paramount importance in controlling the fragmentation, even in the presence of delays (Winzer, in prep.). Activation of the mechanisms seen here is obviously critical to considerations of blast design, and further work must be done to quantify the conditions under which these mechanisms are triggered.

ACKNOWLEDGEMENTS

This research was supported by NSF grant DAR 7910285. The authors also wish to thank Mr. P. Bearzi for his assistance in the field and Mr. Ira Bain, Superintendent at Martin Marietta Aggregates' Pinesburg quarry, for his cooperation and assistance with the research effort.

REFERENCES

Dally, J.W., Fourney, W.L., and Holloway, D.C., 1975, "Influence of the containment of the borehole pressures on explosive induced fracture," Int. J. Rock Mech. Min. Sci., 12.

Duvall, W.I., and Atchison, T.C., 1950, "Vibration associated with a spherical cavity in an elastic medium," U.S. Dep. Inter., Bur. Mines, Rept. Invest. 4692.

Duvall, W.I., and Atchison, T.C., 1957, "Rock breakage by explosives," U.S. Dep. Inter., Bur. Mines, Rept. Invest. 5336.

Field, J.E., and Ladegaard-Pederson, A., 1971, "The importance of the reflected stress wave in rock blasting," Int. J. Rock Mech. Min. Sci., 8, 213.

Fogelson, D.E., Duvall, W.I., and Atchison, T.C., 1959, "Strain energy in explosion-generated strain pulses in rock," U.S. Dep. Inter., Bur. Mines, Rept. Invest. 5514.

Fourney, W.L., Barker, D.B., and Holloway, D.C., 1979, "Mechanism of fragmentation in a jointed formation," Rept. to NSF, Aug. 1979.

Grady, D.E., and Kipp, M.E., 1979, "The micromechanics of impact fracture of rock," Int. J. Rock Mech. Min. Sci., 16, 293.

Grady, D.E., Kipp, M.E., and Smith, C.S., 1979, "Explosive fracture studies on oil shale," Proc. 54th Conf. SPE (SPE 8215), p. 1.

Hagan, T.N., 1977, "Rock breakage by explosives," Proc. 6th Congr. on Gas Dynamics of Explosives and Reactive Systems, R. Inst. Technol., Stockholm.

Hagan, T.N., and Just, G.D., 1974, "Rock breakage by explosives — theory, practice and optimization," Proc. 3rd Congr. Int. Soc. Rock Mech., Denver, p. 1349.

Hino, K., 1956, "Fragmentation of rock through blasting," Q. Colo. Sch. Mines, 51, 189.

Holloway, D.C., Fourney, W.L., and Barker, D.B., 1980, "Dynamic crack propagation in rock plates," Proc. 21st U.S. Symp. Rock Mech. (This Volume).

Johnson, J.N., 1978, "Explosive produced fracture of oil shale," Los Alamos Sci. Lab. Rept. LA-7357-PR, p. 38.

Kutter, H.K., and Fairhurst, C., 1971, "On the fracture process in blasting," Int. J. Rock Mech. Min. Sci., 8, 181.

Langefors, U., and Kihlstrom, B., 1963, "The Modern Techniques of Rock Blasting," John Wiley and Sons, N.Y., 405 pp.

Noren, C., 1956, "Blasting experiments in granite rock," Q. Colo. Sch. Mines, 51, 213.

Obert, L., and Duvall, W.I., 1949, "A gauge and recording equipment for measuring dynamic strain in rock," U.S. Dep. Inter., Bur. Mines, Rept. Invest. 4581.

Obert, L., and Duvall, W.I., 1950, "Generation and propagation of strain waves in rock," U.S. Dep. Inter., Bur. Mines, Rept. Invest. 4663.

Persson, P.A., Lundborg, N., and Johannson, C.H., 1970, "The basic mechanisms of rock blasting," Proc. 2nd Congr. Int. Soc. Rock Mech., Belgrade, Yugoslavia, p. 1.

Porter, D.D., 1961, "Crater formation in plaster of paris models by enclosed charges," M.S. Thesis, Colo. Sch. Mines.

Porter, D.D., and Fairhurst, C., 1970, "A study of crack propagation produced by the sustained borehole pressure in blasting," Proc. 12th Symp. Rock Mech., Univ. Mo., Rolla, p. 497.

Rinehart, J.S., 1958, "Fracturing under impulsive loading," 3rd Annu. Symp. Mining Res., Univ. Mo. Sch. Mines Metall. Bull., 95, 46.

Rinehart, J.S., 1960, "On fractures caused by explosions and impacts," Q. Colo. Sch. Mines, 55, 155.

Rinehart, J.S., 1975, "Stress Transients in Solids," Hyper Dynamics, Inc., Sante Fe.

Sharpe, J.A., 1942, "The production of elastic waves by explosion pressure I: Theory and empirical observations," Geophys., 7, 144.

Shockey, D.A., Curran, D.R., Seaman, L., Rosenberg, J.T., and Peterson, C.F., 1974, "Fragmentation of rock under dynamic loads," Int. J. Rock Mech. Min. Sci., 11, 303.

Winzer, S.R., Montenyohl, V.I., and Ritter, A., 1979, "High-speed cinematography of production blasting operations," Min. Congr. J., 10, 46.

Restoration of Uranium In-Situ Leaching Sites

A.D. Hill, * SPE, Texas Petroleum Research Committee
I.H. Silberberg, SPE, Texas Petroleum Research Committee
M.P. Walsh, SPE, U. of Texas
W.M. Breland, U. of Texas
M.J. Humenick, U. of Texas
R.S. Schechter, SPE, U. of Texas

Abstract

In recent years in-situ leach mining has emerged as a new technology for the recovery of uranium from strata that cannot be mined economically by other means. Because the ore bodies lie within groundwater aquifers, a significant determinant in the process' viability is the requirement that such aquifers be protected from contamination. Since ammonia is one of the constituents of the leach solutions now being field tested, one environmental problem to be resolved is the removal of ammonia at the end of mining. A second related question is the fate of the ammonia that is not removed by the restoration procedure.

This paper considers the displacement and migration of ammonium cations in a flowing electrolyte with concomitant ion exchange. The ion exchange is an important feature since, during the solution mining phase, ammonium cations adsorb onto the mineral exchange sites and must be removed from these sites. A mathematical model is used to simulate this process, and the model is tested against the results of laboratory experiments. It is found that the simulations are adequate if an appropriate selection of parameters is made.

The model then is used to simulate restoration procedures and to determine the rate of migration of unrecovered ammonium in the groundwater. It is concluded that ammonium removal can be accomplished best using high concentrations of a cation that is exchanged selectively relative to ammonium cation.

Introduction

In-situ solution mining is a process rapidly being developed for the recovery of uranium from sandstone ore bodies. This mining technique is applicable when the uranium ore is too deep, too small in extent, or of too low a grade to justify using conventional mining techniques. Such ore bodies are numerous in south Texas, occurring along a broad band of the U.S. gulf coastal plain.

The solution mining process being used in Texas is primarily an alkaline leach. The sandstone ores that may be solution-mined occur in aquifers, and the uranium is in the insoluble +4 state of oxidation. To be mobilized, the uranium must be oxidized to the +6 state and then complexed with carbonate ions to form the highly soluble uranyl dicarbonate or uranyl tricarbonate ions. Thus, alkaline leach solutions contain an oxidant (usually hydrogen peroxide) and a mixture of carbonates and bicarbonates. To minimize formation damage, most solution mining now employs ammonium carbonate/bicarbonate as the carbonate source. These solutions have been found effective in dissolving the uranium minerals found in south Texas sandstone ores.[1]

However, the restoration of the mining site is also a primary consideration. Since the ore bodies that can be solution-mined occur in aquifers, government regulations require that water quality at the mining site not be degraded below the quality that existed at the inception of mining. Furthermore, the permitting procedures require that groundwater restoration be completed at one site before the next site on a particular lease may be mined.[2] Obviously, environmental aspects will be an important consideration governing the success of in-situ solution mining.

Since there are virtually no naturally occurring ammonium cations in south Texas groundwater,[3] the target ammonium concentrations at restored sites in south Texas have been set at quite small levels. The reduction of the levels of ammonium cation from the initial concentration to these required low levels is

---

*Now with Marathon Oil Co.

0197-7520/80/0008-7534$00.25

complicated greatly by the process of ion exchange. The loosely packed sandstone ores in south Texas all contain some clay minerals, usually montmorillonite,[4] which has a significant cation exchange capacity (CEC).

This report investigates the fate of ammonium cations as flow with cation exchange takes place in porous medium. The overall aim is to develop viable restoration procedures for in-situ uranium solution mining. The approach used is to model flow with cation exchange, test the model against laboratory results, and subsequently use it to identify those techniques that might prove successful in restoration. Both the fate of ammonium cation left in the mining site as it migrates downstream under the influence of groundwater flow and the behavior of the ammonium cation as restoring fluids are injected and produced will be considered.

Theory of Cation Exchange in Porous Media

Cation Exchange Equilibria

The ion exchange process can be assumed, with good accuracy, to be described locally by equilibrium relations. Malcolm and Kennedy[5] measured rates of ion exchange for several cations on different clays and found them to be rapid. Thus, over the range of fluxes normally associated with flows in porous media, an equilibrium relationship between solution and surface cations can be used instead of a kinetic description. This fact, coupled with material balances on the ionic species, will describe the phenomenon of flow with cation exchange.

The models of exchange equilibria used most extensively in describing cation exchange on clays are the Gapon equation,[6] which considers the adsorption of a cation double layer on the clay surface, and the mass action equation.[7] Various investigators have compared the behavior of these two descriptions of exchange equilibria. Paliwal[8] decided on the basis of static ion exchange studies that the Gapon equation gave slightly better agreement with experimental results than the mass action equation. Others[9,10] have concluded that the mass action equation is better. Furthermore, Laudelout *et al.*[11] stated "the diffuse layer theory (Gapon) of planar charged surfaces involves assumptions too sweeping for a valid model of cation exchange processes on the surface of a clay mineral." Based on these findings, the mass action law will be used to describe ion exchange equilibria.

Flow Equations

The equations describing flow with cation exchange have been presented by Van der Molen,[12] Reineger and Bolt,[13] Pope *et al.*,[14] Smith,[15] and Griffith[16] and will not be developed here. Material balances for the ammonium cation and the anion are as follows.

$$\frac{\partial C_{NH_4^+}}{\partial t}+\frac{\partial q_{NH_4^+}}{\partial t}=-\frac{u}{\Phi}\frac{\partial C_{NH_4^+}}{\partial x}+D_L\frac{\partial^2 C_{NH_4^+}}{\partial x^2}, \quad \ldots\ldots\ldots\ldots\ldots\ldots (1)$$

and

$$\frac{\partial C_A}{\partial t}=-\frac{u}{\phi}\frac{\partial C_A}{\partial x}+D_L\frac{\partial^2 C_A}{\partial x^2}, \quad \ldots\ldots\ldots\ldots (2)$$

where ϕ is the porosity, $C_{NH_4^+}$ is the ammonium cation concentration in solution (equivalents/L), $q_{NH_4^+}$ is the ammonium adsorbed (equivalents/L of pore volume), u is the flux, D_L is the dispersion coefficient, and C_A is the solution anion concentration (equivalents/L). Eq. 2 is written assuming that the anion does not adsorb on the mineral surfaces.

If the exchange process is assumed to be an equilibrium one, then from mass action the exchange of two monovalent cations can be approximated by

$$\frac{q_{NH_4^+}}{q_i}=K_i\frac{C_{NH_4^+}}{C_i}, \quad \ldots\ldots\ldots\ldots\ldots\ldots\ldots (3a)$$

where K_i is a constant. For a monovalent cation (NH_4^+) and a divalent cation the relationship becomes

$$\frac{q_{NH_4^+}}{q_i^{1/2}}=K_i\frac{C_{NH_4^+}}{C_i^{1/2}}, \quad \ldots\ldots\ldots\ldots\ldots\ldots\ldots (3b)$$

Furthermore, the physical requirements of electroneutrality in both the solution and on the surface demand that

$$C_i+C_{NH_4^+}=C_A, \quad \ldots\ldots\ldots\ldots\ldots\ldots\ldots\ldots (4)$$

and

$$q_i+q_{NH_4^+}=Q_v, \quad \ldots\ldots\ldots\ldots\ldots\ldots\ldots\ldots (5)$$

where C_i is the concentration of the exchanging cation, q_i is adsorbed exchanging cation per unit of pore volume, and Q_v is the cation exchange capacity (CEC). Using Eqs. 3 through 5 the term $\partial q_{NH_4^+}/\partial t$ can be eliminated from Eq. 1 leaving two coupled partial-differential equations and two unknowns. This system of equations can be solved numerically given the appropriate boundary conditions. The technique adopted[16] uses a forward time and backward space finite-difference approximation. Numerical dispersion is introduced in a controlled fashion to represent the actual dispersion. This technique is discussed by Roache.[17]

Results of Laboratory Studies

Experimental Observation

A series of column-flow experiments were performed in a 1-in.-ID, 12-in.-long stainless steel tube. The column was packed carefully (see Ref. 16 for details) with ore sampled from a batch prepared by disaggregating and thoroughly blending about 40 lbm of ore taken from a south Texas open pit mine in the Jackson formation, Karnes County, TX. Initially the ore was saturated with a 1-N ammonium chloride solution. To ensure that all of the gases were removed, the system was evacuated before admitting the ammonium chloride solution. The 1-N solution was circulated through the column for 24 hours, and then the solution concentration was reduced to 0.1 N and the effluent concentration monitored. When the

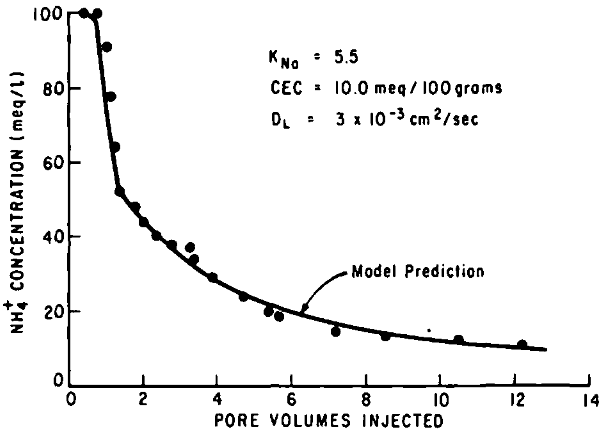

Fig. 1 – Ammonium cation elution for an initial NH_4^+ concentration of 100 meq/L and an eluting fluid concentration of 50 meq Na^+/L.

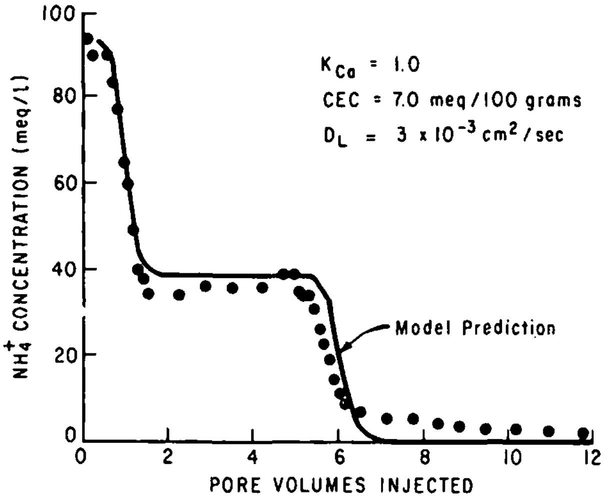

Fig. 2 – Ammonium cation elution for an initial NH_4^+ concentration of 95 meq/L and an eluting fluid concentration of 40 meq Ca^{++}/L.

effluent concentration stabilized, all of the ion exchange sites were assumed occupied by ammonium cation and the elution phase initiated.

Sodium or calcium chlorides or mixtures of the two were used to displace the sorbed ammonium cation. Chlorides were used because precipitation problems associated with divalent anions are circumvented. The effluent was collected in increments of 7 ml (about 0.1 PV) and was analyzed for sodium, calcium, and ammonium. The analytical methods are described by Hill.[16]

Frontal velocities of approximately 10 ft/D were maintained. Experiments were conducted to establish that the effluent concentrations depended only on the number of pore volumes injected and not on the fluid velocities at a fluid velocity of 10 ft/D.

Typical ammonium cation elution curves are shown in Figs. 1 and 2. No attempt was made to protect the ore samples from oxidation or from exchanging moisture with the air. These factors are known to be important for leaching studies but should not influence restoration results. The solid lines are the model predictions obtained by adjusting the mass action equilibrium constant, the dispersion coefficient, and the CEC of the ore. The dispersion coefficient was adjusted to fit the anion wave since adsorption or desorption effects are absent when this wave emerges from the column. The CEC is determined essentially by the area under the curve after 1 PV has been displaced.

The model results obtained by solving Eqs. 1 and 2 accurately reflect the experimental observations. The agreement is good even though other mechanisms such as the dissolution of calcium carbonate contribute changes to the ion exchange environment that are not accounted for in this model.[15] It is concluded that the model for flow with ion exchange is adequate.

Another observation that may be made by comparing Figs. 1 and 2 is that sodium and calcium generate different types of ammonium cation waves as the exchange takes place. In both figures, an abrupt drop in NH_4^+ cation concentration occurs at 1 PV due to the passage of the anion wave from the column. A 400 or 500 meq/L anion wave is displacing the 100 meq/L concentration initially in the core. When sodium is exchanging for ammonium cations, the effluent ammonium concentrations decline gradually throughout the rest of the run. In contrast, when calcium is the eluting cation, the ammonium cation concentration in the effluent remains essentially constant for several pore volumes after passage of the anion wave and then drops sharply. This sudden decline is evidence of the passage from the columns of the back edge of the ammonium cation wave. The difference in these two wave shapes is a result of differences in the selectivity of the clay surface for the ions involved. The calcium cation with its high charge density adsorbs preferentially with respect to the ammonium cation, whereas the ammonium cation is favored with respect to sodium. It is the selectivity that gives rise to the wave form. This fact will be an important feature in understanding the discussion that follows.

Variability of Cation Exchange Capacities

A phenomenon observed in these experiments that could be important in the restoration of a solution mining site was the different CEC exhibited by the ore tested with respect to sodium and calcium (Figs. 1 and 2).

Integrating the total amount of ammonium removed from the column when eluting with sodium yielded a value of 10 meq/100 g for the CEC. However, since this experiment was terminated while a significant concentration of ammonium cation (in excess of 10 meq/L) remained in the effluent, the value of 10 meq/100 g must be considered a low estimate. From the elution curve in the calcium run (Fig. 2) an apparent CEC of 7 meq/100 g was obtained. In this run the effluent ammonium cation concentration had reached a low level, indicating that

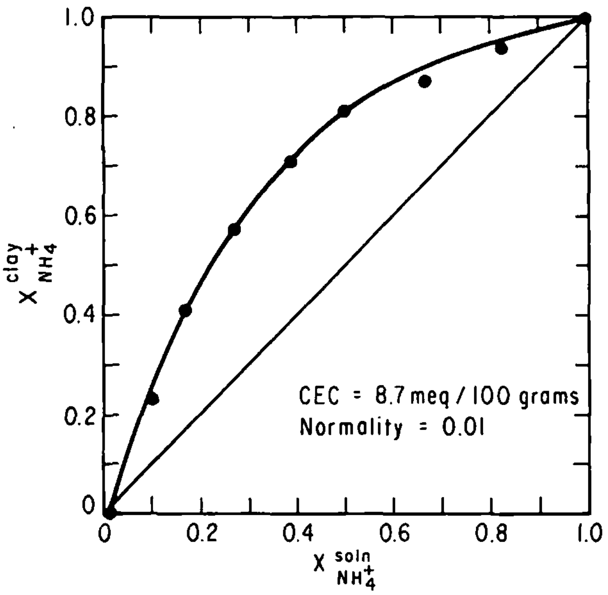

Fig. 3 – NH_4^+ – Na^+ ion exchange isotherm at 25°C.

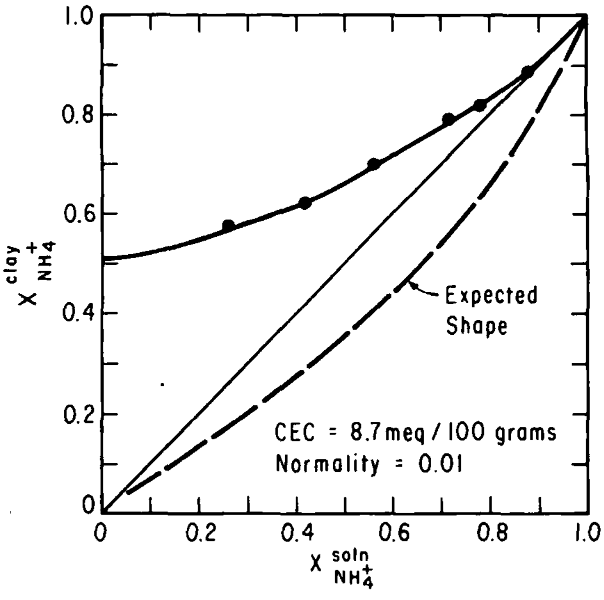

Fig. 4 – NH_4^+ – Ca^{++} ion exchange isotherm at 25°C.

the exchange reaction was virtually complete.

From the disparity in these results, it appeared that calcium was not exchanging with all of the ammonium held on the clays, while sodium was. To check this hypothesis, a run was performed in which ammonium cation was first eluted with calcium cations followed by further elution with sodium cations. It was evident that a significant portion of the ammonium held by the clays was not accessible to the calcium cations because a second ammonium cation elution wave was formed on injection of the sodium chloride solution. Integrating the two portions of the elution curve indicated that only about half of the ammonium cation present was displaced by the calcium cation.

A second verification of the phenomenon is seen in the isotherms shown in Figs. 3 and 4. These were obtained by static batch tests in which at least 24 hours were allowed for mixtures of ore and solution to come to equilibrium, but for some runs as many as 16 days were allowed. The ammonium cation in these tests is replaced step-wise by calcium or sodium cations keeping the constant normality, $N = 0.01$.

Fig. 3 shows the isotherm for ammonium-sodium. The fraction on the surface is calculated using a CEC of 8.7 meq/100 g. The results shown in Fig. 4 for ammonium-calcium reflect the inability of calcium cations to displace ammonium completely at least during a minimum of 24 hours allowed for solution equilibrium.

A possible explanation of this phenomenon would be the expansion of alternate layers of the montmorillonite structure as described by Sawhey.[18] Certain cations, particularly potassium and ammonium, are known to collapse the interlayers of montmorillonite. When calcium or magnesium was used to replace potassium in these collapsed layers, the potassium was replaced only in alternate layers, leaving half of the potassium ions unexchanged. Another possible explanation would be the presence of two clays having markedly different ion exchange isotherms.

If this process occurs during restoration, using calcium clearly would be disadvantageous even though the shape of the wave front resulting from calcium elution of ammonium is the desired one.

To date only two different ores have been studied. The second one has been obtained from the Oakville formation and did not exhibit differences in the apparent CEC when different cations were exchanged for ammonium. The second ore tested had about the same CEC as the one reported here. The difference between these two ores that gives rise to the anomalous behavior of one and not the other is not understood. Therefore, it is not possible to predict which mine sites will be susceptible to successful restoration using solutions of divalent cations without first conducting laboratory tests.

Application for Restoration

Ammonium Migration of Groundwater

Consider the hypothetical situation depicted in Fig. 5. Assuming that groundwater behaves similarly to a solution containing 8.55 meq/L of NaCl, Fig. 6 presents the ammonium profiles obtained when this groundwater invades a 200-ft mine site containing 1,000 meq/L ammonium cation, which is approximately the strength of the lixiviants now being tested. The ammonium cation moves downstream as a high concentration front until, after about 20 years for the conditions assumed, the front of the ammonium wave and the back of the anion wave (which is traveling faster) coincide. After this time the maximum ammonium concentration in solution is 8.55 meq/L. (This level may be in excess of that allowed.) The ammonium cations initially present in the solution in the mine site are now adsorbed onto the clays in the 400-ft region downstream.

It also should be noted that the anion wave is not shown in Fig. 6. This wave will continue to migrate with groundwater velocity; however, the cation now associated with the anion to maintain electrical neutrality will not be ammonium but rather that cation displaced from the clays by the ammonium now adsorbed in the 400-ft region beyond the mine site. This high-salinity wave will move downdip until it is reduced in concentration by dispersive processes.

If the initial ammonium carbonate concentration in the mine area is reduced substantially by some restoration technique, the progress of the front will be retarded greatly, as seen in Fig. 7. With an initial concentration of 200 meq/L, the ammonium has migrated only 140 ft in 35 years. Clearly, the distance that the ammonium migrates in a given time is also directly proportional to the groundwater flux. The 28 ft/yr used in all of the calculations is larger than the average of those observed in the area. The distance of migration is almost exactly halved when the flow rate is halved, since dispersion is not an important feature of these low-salinity processes.

Increasing the CEC also will retard the movement of ammonium. The example used here is for a CEC smaller than usually is found; therefore, the distance of ammonium movement shown here is an overestimate for most field situations.

The effect of the exchange isotherm can be seen by varying the equilibrium constant. By setting the value of $K<1$, the prevalent cation in the groundwater becomes selectively adsorbed in preference to ammonium. With $K=0.2$, the ammonium wave becomes sharp at the back and diffuse in the front, as shown in Fig. 8 and as predicted by chromatographic theory.

From these results of ammonium migration from an unrestored site, the following conclusions may be drawn. First, the ammonium left in solution and on the clays will migrate downstream under the influence of groundwater flow at a rate that decreases with increasing CEC and increases with increasing ammonium concentration in the site. After a period of years sufficient to allow the anion wave to pass the cation wave, the maximum ammonium concentration will be equal to the groundwater anion concentration (assumed here to be 8.55 meq/L based on 500 ppm NaCl groundwater). The maximum concentration is about 120 ppm nitrogen. This ammonium wave will continue to move downstream.

Reservoir heterogeneities in permeability and clay content will tend to make the ammonium cation wave more disperse as it migrates downstream. The assumption of a homogeneous formation probably leads to the worst possible case from the standpoint of ammonium cation migration. Nevertheless, it appears that some type of restoration is needed.

Migration With Substantial Restoration of a Mine Site

To model more realistically the fate of ammonium after a solution-mining operation, the program was used to simulate a two-step process. In the first stage, restoration fluid is injected at $x=0$ and produced at

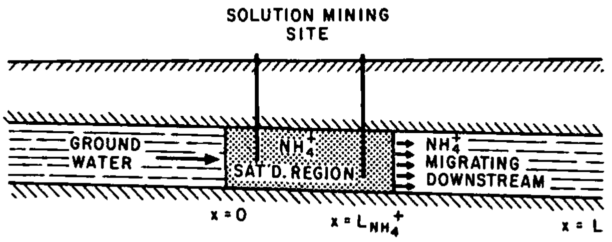

Fig. 5 – Assumed ammonium cation distribution at termination of mining activities.

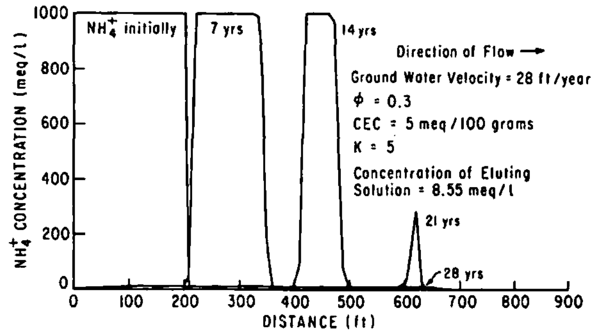

Fig. 6 – Ammonium cation migration as a function of time.

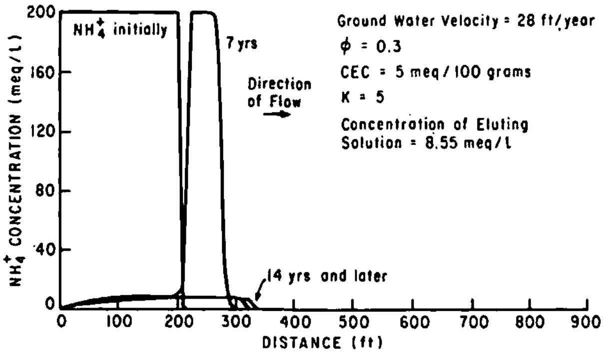

Fig. 7 – Ammonium cation migration as a function of time for an initial concentration of 200 meq/L.

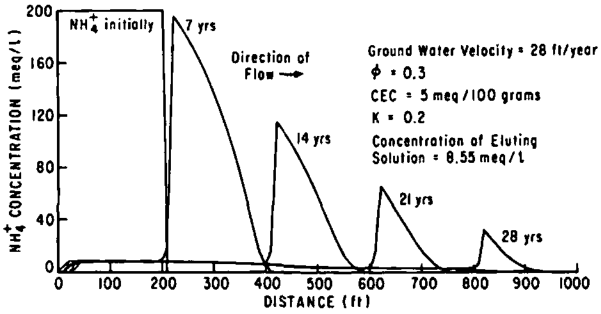

Fig. 8 – Ammonium cation migration as a function of time with preferential adsorption of the displacing cation.

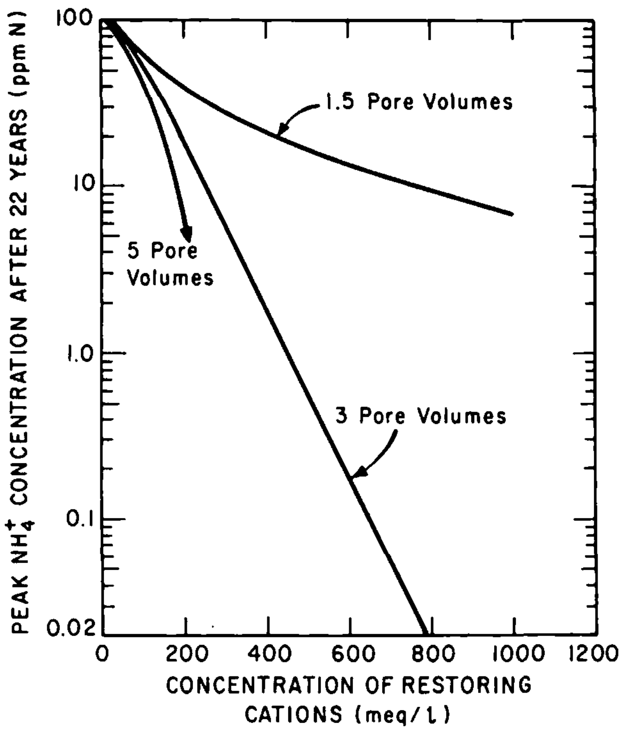

Fig. 9 – Effect of cation concentration and pore volumes of restoring fluid on the maximum ammonium cation concentration in groundwater after 22 years.

$x = L_{NH_4^+}$ (Fig. 5). Thus, during the first stage ammonium is not permitted to migrate downstream. This constraint models the restoration step as well as it can be simulated using an equation that is restricted to one spatial direction. A two-dimensional program, such as that reported by Bommer and Schechter,[19] that considers the flow patterns associated with a system of injection and production wells is required to model restoration accurately. In the present case, the restoring fluid moves in a single direction.

Following the injection of certain quantities and concentrations of a restoring fluid, the injection and production wells are shut in and the migration of the remaining ammonium determined. Fig. 9 presents a typical result. In making this calculation, it was assumed that initially the 200-ft mine site contained 200 meq/L NH$_4^+$ in solution with the clay ion exchange sites completely filled with ammonium cations. After restoring the region with 5 PV of a restoration fluid containing 200 meq/L of a cation that is not favorably attracted to the surface when competing with NH$_4^+$, the maximum ammonium concentration is always less than 10 ppm nitrogen contained in a diffuse wave that will migrate slowly downstream.

To demonstrate better the benefits of increasing both the restoration-fluid cation concentration and the number of pore volumes applied, plots have been prepared showing the peak NH$_4^+$ concentration remaining in the system after 22 years vs. these variables. Fig. 9, a graph of peak NH$_4^+$ concentration vs. the cation concentration of the fluid injected, shows the obvious conclusion that more effective restoration is obtained with a greater number of pore volumes. More important is the benefit obtained by increasing the ionic strength of the restoring fluid. Thus, it appears that one strategy for restoration might be the injection of a highly saline brine to displace efficiently the ammonium cation. The high-concentration brine will migrate in the groundwater, but its concentration will be that of the groundwater anions once the anion wave passes the cation front. After this time, a high-salinity wave will continue to migrate downstream ahead of the cation wave. To prevent the migration of this high-salinity pulse, the high-concentration brine could be displaced from the mine site as the last step in restoration.

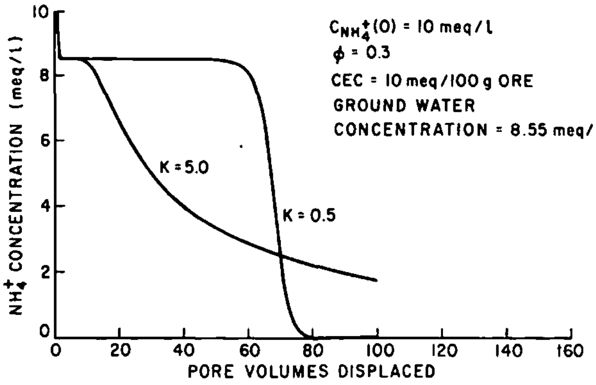

Fig. 10 – Ammonium cation concentration at a point downstream from the mined area.

Another view of ammonium cation migration is seen by observing the concentration at a fixed point within the mine zone. Fig. 10 shows the concentration at a point (arbitrarily chosen) for two different K values. With $K = 5.0$, ammonium cations are held on the surface sites preferentially to the groundwater cation. $K = 0.5$ represents preferential groundwater cation adsorption. In this plot the pore volume is defined as the fluid volume contained between the observation point and the upstream edge of the mined zone.

The ammonium cation initially has a concentration equivalent to that of the lixiviant, but after 1 PV has been displaced, the concentration in solution decreases to a level equal to the groundwater anion concentration. This decrease in concentration is seen in Fig. 10. Thereafter, more than 50 PV of displacing fluid are required to displace that ammonium cation initially contained between the observation point and the upstream side of the mined zone. Since groundwater flows are often slow, measured in feet per year, it will take considerable time to displace 50 PV from the mined zone. It is evident from these results that the ammonium cation concentration in the solution mining region will decline very slowly.

Conclusions

1. Flow with cation exchange for a two-cation system can be modeled accurately assuming local equilibrium.

2. The use of the mass action model of the equilibrium exchange reaction provides an adequate

representation of the processes involved in the elution of ammonium cation from a packed column by a second cation. The formulation provided an adequate comparison with experiments both for cations that are selectively adsorbed and for those that are not.

3. Solution containing only calcium cations may not exchange completely with an ammonium saturated one, perhaps because of alternate layer expansion of the clay structure. Solutions containing sodium have been found to displace ammonium cation completely.

4. If the exchanging cation used to displace the ammonium cation is not adsorbed selectively (as in the case of sodium), then many pore volumes of solution would be needed to restore an ammonium leach site. Ammonium cation removal is improved by using more total volume of restoring fluid and by using higher concentrations of cations.

5. The ammonium cation left after the mining site has been abandoned tends to migrate as a result of groundwater influx. The rate of migration depends on the composition of groundwater, the cation exchange capacity of the reservoir minerals, the groundwater flow rates, and the selectivity of the clays.

Nomenclature

C = concentration of ions, meq/L
D_L = axial dispersion coefficient, cm^2/s
K_i = equilibrium constant, defined by Eq. 3a for monovalent-monovalent exchange and by Eq. 3b for divalent-monovalent exchange
Q_v = cation exchange capacity per unit pore volume, meq/L

$$= \frac{\rho_{\text{solid}}(1-\phi)}{\phi} \bar{Q}_v$$

$\bar{Q}_v$ = cation exchange capacity per unit mass of ore, meq/g
q = adsorbed ions per unit of pore volume, meq/L

$$= \frac{\rho_{\text{solid}}(1-\phi)}{\phi} \bar{q}$$

$\bar{q}$ = adsorbed ions per unit mass of ore, meq/g
t = time
u = flux, cm/s
x = distance measured along axis of linear system, cm
ρ_{solid} = density of solid, g/cm^3
ϕ = porosity

Subscripts

A = anion
i = exchanging cation
NH_4^+ = ammonium cation

Original manuscript received in Society of Petroleum Engineers office Aug. 8, 1978. Paper accepted for publication March 2, 1979. Revised manuscript received June 6, 1980. Paper (SPE 7534) first presented at the SPE 53rd Annual Fall Technical Conference and Exhibition, held in Houston, Oct. 1-4, 1978.

References

1. Galichon, P., Schechter, R.S., Cowley, A., and Breland, W.M.: "Chemical Factors in In Situ Leach Mining," *In Situ* (1977) **1,** 125.
2. Taylor, W.R.: "Regulation of In-Situ Uranium Mining for Purposes of Protecting Groundwater Quality," paper presented at South Texas Uranium In-Situ Mining Symposium, South Texas Minerals Section of AIME, Corpus Christi, TX, Sept. 25-28, 1977.
3. Braswell, J., Breland, W.M., Chang, M., Hill, D., Johnson, D., Schechter, R.S., Turk, L., and Humenick, M.: "Literature Review and Preliminary Analysis of Inorgainc Ammonia Pertinent to South Texas Uranium In Situ Leach," Center for Water Resources Report #CRWR-155, EHE 78-01, U. of Texas, Austin (1978).
4. Galloway, W.E.: "Catahoula Formations of the Texas Coastal Plain: Depositional Systems, Composition, Structural Development, Groundwater Flow History and Uranium Distribution," Bureau of Economic Geology Report of Invest. No. 87, U. of Texas, Austin (1977).
5. Malcolm, R.L. and Kennedy, V.C.: "Rate of Cation Exchange on Clay Minerals as Determined by Specific Ion Electrode Techniques," *Proc.*, Soil Science Amer. (1969) **33,** 247.
6. Gapon, E.N.: "Theory of Exchange Adsorption of Soils," *J. Gen. Chem.* (U.S.S.R) (1933) **3,** 144.
7. Gaines, G.L. and Thomas, H.C.: "Adsorption Studies on Clay Minerals. II. A Formulation of the Thermodynamics of Exchange Adsorption," *J. Chem. Physics* (1953) **21,** 714.
8. Paliwal, K.V.: "Cation Exchange Equilibria in Na-K-Ca-Mg Systems of Some Clay Minerals," *J. Soil Water Conservation India* (1966) **14,** 144.
9. Griffith, T.D.: "Application of the Ion Exchange Process to Reservoir Preflushes," paper SPE 7587 presented at the SPE 53rd Annual Technical Conference and Exhibition, Houston, Oct. 1-4, 1978.
10. Hill, H.J. and Lake, L.W.: "Cation Exchange in Chemical Flooding: Part 3 – Experimental," *Soc. Pet. Eng. J.* (Dec. 1978) 445-456.
11: Laudelout, H., Von Bladel, R., Bolt, G.H. and Page, G.H.: "Thermodynamics of Heterovalent Cation Exchange Reactions in Montmorillonite Clay," *Trans.*, Farad. Soc. (1968) **64,** 1977.
12. Van der Molen, W.H.: "The Exchangeable Cation in Solids Flooded with Sea Water," *Verslagen Van Landvouwkundige Onderzoekingen* (1957) **63,** No. 17, 1.
13. Reineger, P. and Bolt, G.H.: "Theory of Chromatography and Its Application to Cation Exchange in Soils," *Neth. J. Agric. Sci.* (1972) **20,** 301.
14. Pope, G.A., Lake, L.W., and Helfferich, F.G.: "Cation Exchange in Chemical Flooding: Part 1 – Basic Theory Without Dispersion," *Soc. Pet. Eng. J.* (Dec. 1978) 418-434.
15. Smith, F.W.: "Ion Exchange Conditioning of Sandstones for Chemical Flooding," *J. Pet. Tech.* (1978) 959-968; *Trans*, AIME, **265.**
16. Hill, A.D.: "Prediction and Control of Ammonium Ion Migration After Uranium Solution Mining," Texas Petroleum Research Committee Report No. UT 78-3, U. of Texas, Austin (1978).
17. Roache, P.J.: *Computational Fluid Dynamics*, Hermosa Publishers, Albuquerque, NM (1976).
18. Sawhey, B.L.: "Selective Sorption and Fixation of Cations, A Review," *Clays and Clay Minerals* (1972) **30,** 93.
19. Bommer, P.M. and Schechter, R.S.: "Mathematical Modeling of In-Situ Uranium Leaching," *Soc. Pet. Eng. J.* (Dec. 1979) 393-400.

SI Metric Conversion Factors

ft × 3.048* E−01 = m
in. × 2.54* E+00 = cm
lbm × 4.535 924 E−01 = kg

*Conversion factor is exact.

SPEJ

Behavior of the Bagnore Steam/CO_2 Geothermal Reservoir, Italy

P.G. Atkinson, SPE, Union Oil Co. of California
R. Celati, Inst. Intl. per le Ricerche Geotermiche
R. Corsi, ENEL-Centro Ricerca Geotermica
F. Kucuk,* SPE, Stanford U.

Abstract

A commonly encountered geothermal steam reservoir consists of a gas cap overlying an aquifer. In addition to steam, the gas cap may contain substantial amounts of carbon dioxide and other noncondensable gases. A mathematical model for describing the pressure and composition histories of such reservoirs is presented. The model evaluates the change in states of a homogeneous vapor/liquid region as a mixture of steam and carbon dioxide is removed from the gas cap and as recharge water enters the liquid region.

The production history of the Bagnore steam field in Italy was evaluated using this model. It is concluded that early reservoir behavior was controlled by a blowdown of carbon dioxide in the gas cap, while long-time behavior is being controlled by water influx.

Introduction

This paper presents a lumped-parameter model of a vapor-dominated geothermal reservoir containing a significant quantity of noncondensable gas. The formulation and methodolgy presented may be applied to noncondensable gases in general. However, this work is concerned only with the effects of carbon dioxide and dissolved carbonates on the producing characteristics of a geothermal steam field.

Model calculations are compared with the observed history of the Bagnore steam field in Italy. It is concluded that the behavior of this field can be explained in terms of multicomponent vapor/liquid equilibrium considerations in conjunction with energy influx from local reservoir rocks and liquid influx from an external source.

Lumped-parameter models traditionally have been used in studies of oil and gas reservoirs. Here they are known more commonly as material balance methods[1] since material conservation is the only balance law used. The extension of such techniques to pure water/steam geothermal systems requires in principle only the addition of appropriate energy balances. This has been done by Whiting and Ramey[2] for a liquid-dominated field and by Brigham and Morrow[3] for hypothetical vapor-dominated systems. The application of such models to multicomponent geothermal systems requires again only the addition of chemical species conservation equations for each additional component. For example, Grant[4] has applied such a model to a liquid-dominated reservoir in New Zealand that contains substantial amounts of dissolved carbon dioxide.

The model described in this paper is an extension and coupling of the Brigham and Morrow and Grant models. It is an example of a class of models that may be useful for analyzing the behavior of vapor-dominated geothermal systems. This paper used the model to evaluate the production history of a gas-cap geothermal reservoir significantly affected by the presence of carbon dioxide.

Lumped-Parameter Producing-State Model

This section discusses the producing-state mathematical model. First the thermodynamic system is described, next the constituent equations of state are presented, and then the development and numerical solution of the governing equations are discussed.

Thermodynamic System

The thermodynamic model to be discussed is depicted in Fig. 1. The reservoir is considered to

---

*Now with Science Applications Inc.

0197-7520/80/0008-7132$00.25

Robert A. MacGregor
Stanrock Uranium Mines Ltd.,
Elliot Lake, Ont.

SUBJ
MNG
RUUL

Recovery of U_3O_8 by Underground Leaching

Annual General Meeting, Montreal, April, 1964
Transactions, Volume LXIX, 1966, pp. 162-166

ABSTRACT

Following several months of test work, water leaching in mined-out areas at Stanrock commenced on a production basis in February, 1963.

A combination of fast high-pressure washing and rewashing of stopes on a predetermined cycle, and the intermittent sprinkling of low-grade heaps, using both fresh water and recirculated acid water, has proved most successful. There was also a correlation of daily sampling data points to a relationship between the leach water grade and the grade of the material being washed, the leaching time and the location along the dip. An increasing tolerance for uranium by the acid-producing bacteria is also indicated.

A steady production rate of 10,000 to 12,000 lbs. of U_3O_8 per month is being maintained, with an over-all mine water grade of 0.25 lb. per ton and a pH of 2.3.

Introduction

IT has been recognized for the past several years that the action of micro-organisms on sulphide minerals results in the release of sulphuric acid, iron and other contained metals. The discovery of these bacteria resulted from investigations into the cause of acid mine drainage waters, particularly in the coal mines of Pennsylvania and West Virginia (1,2, 3).

This same bacterial activity has been the basis for the leaching of copper from large waste heaps, containing small quantities of iron and copper sulphide minerals, at open-pit copper mines in the western United States. Although leaching of copper from waste heaps had been carried out for many years, it was only recently that the true role played by bacteria was recognized. Previously, the copper was considered to have been leached by sulphuric acid produced by the atmospheric oxidation of sulphide minerals (4).

Experimental work in Portugal has shown that uranium may also be leached from its ores by the same micro-organisms, provided that sufficient pyrite is present to provide iron and sulphur. The presence of oxidizing bacteria which convert ferrous iron to ferric iron assists in the extraction of uranium by sustaining reactions which oxidize pyrite to ferrous sulphate and sulphuric acid. These bacteria thrive in acid mediums at temperatures between 20° and 30°C (5).

At Stanrock, acid mine waters resulting from apparent bacterial activity on the sulphides contained in the uranium ores were found to contain 0.038 lb. U_3O_8 per ton.

This paper deals with methods developed to increase the uranium content of the mine water by leaching ore and waste material in abandoned areas of the mine.

History

Mine waters at Stanrock, although approximately neutral for some time after the commencement of operations in 1958, became progressively more acid until they constituted a threat to the mine drainage pumps and pipelines. Similar acid mine water conditions were met with at other uranium mines in the district. Investigation showed the Stanrock mine water to contain 0.038 lb. U_3O_8 per ton. Plans were made to neutralize the mine water and pump the resulting slurry to the mill.

Investigations into the causes of mine water acidity led to the conclusion that acid mine waters were being produced by the bacterial leaching of sulphide minerals. Stanrock ores contain from 10 to 15 per cent pyrite as well as minor quantities of pyrrhotite, sphalerite and chalcopyrite. Although the bacteria have at no time been positively identified, they were assumed to exist for the following reasons:

1.—Laboratory tests show that the reaction is completely inhibited by sterilization but can be restarted by inoculation with fresh mine water.
2.—Literature on acid mine water and uranium leaching describes reactions caused by bacteria that are similar to the leaching action at Stanrock.

Pumping of the neutralized mine water slurry to the mills No. 4 neutral thickener began in September of 1960. The uranium oxide content, at this time, had risen to 0.04 — 0.05 lb. per ton.

Commencement of extensive pillar extraction in late 1961 resulted in a further increase in the U_3O_8 content of the mine water. Mine water recovery increased by 1,000 to 1,500 lbs. U_3O_8 per month. This further rise was believed to be the result of drill water from pillar mining operations becoming acid and leaching out U_3O_8 values as it percolated through worked-out areas of the mine.

Test work to develop a production method for water leaching began in December, 1962. This test work proved quite successful, and a comprehensive leaching program was begun, with four men (later increased to six) engaged in underground water leaching work. Production steadily increased to 10,000 lbs. U_3O_8 per month and has been maintained at about this figure since. *Figure 1* illustrates the rise of mine water values during this period.

Quirke Lake water, the mine's fresh water source, has shown a gradual decline in pH from 6.8 in 1958 to 5.0 in December, 1963.

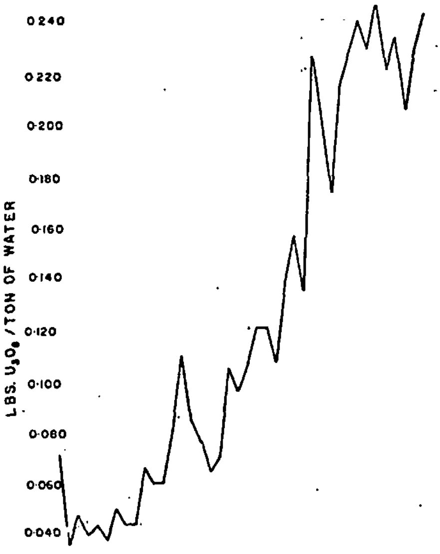

Figure 1.—Graph showing the increase in U_3O_8 content of Stanrock mine water.

Results of Test Work

The test work quickly indicated that the rapid washing of a reasonably large area with high-pressure water would give the most consistent results. Intensive washing of a small area with high-pressure water gave erratic results and appeared to kill the bacteria or wash them away. After intensive washing with high-pressure water, it requires six months or more before leaching again proceeds normally, as shown in *Figure 2.* High-pressure washing of a large area with a mixture of 50 per cent fresh water and 50 per cent recirculated acid water did not give any better results than achieved with fresh water alone, and, as the mixture had a pH of 2.7, it proved troublesome to handle.

Sprinkling of waste heaps with fresh water gave low but consistent results (0.05 to 0.15 lb. U_3O_8 per ton). Assays from these leaching streams dropped below 0.05 lb. U_3O_8 per ton in three months or less. When sprinkling was discontinued for a period of one month to six weeks, assays of 0.05 to 0.15 lb. U_3O_8 per ton could again be recovered. Attempts at sprinkling in stopes were not successful because of the rapid channelling of the water. Later test work indicated that sprinkling waste heaps with recirculated acid water gave better results (0.15 to 0.25 lb. U_3O_8 per ton). Because of the limited life expectancy of the Stanrock operation, the cost of the acid-resistant pumps and pipelines necessary to implement such a program has limited the use of acid mine water to localities where it is available by gravity flow.

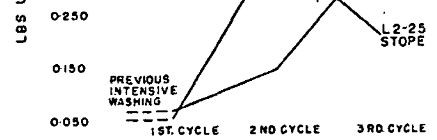

Figure 2.—Graph showing recoveries from stopes which were washed on a three-month cycle following previous intensive washing, compared with a stope which had not been washed previously.

It was apparent from the higher results (0.30 to 1.00 lb. U_3O_8 per ton) and larger volumes of water that high-pressure washing recovered uranium minerals spread over a wide area much faster and more efficiently than sprinkling. High-pressure washing is believed to give a maximum recovery because of a more thorough coverage of the area, and because the force of the water causes a scouring of the rock surfaces. Aeration of the tightly packed fine material is also believed to be an important factor. As leaching could continue as long as the bacteria were not destroyed and material remained to be leached, the high-pressure washing was set up on a cyclical basis.

Varying the length of the cycle showed that stopes re-washed within two months usually gave assays of less than 0.20 lb. U_3O_8 per ton. Re-washing stopes five to six months later usually gave results that were no better than would have been expected in three months (0.20 to 1.00 lb. U_3O_8 per ton). From these indications, the optimum cycle time for Stanrock conditions was judged to be greater than two months and less than five months. Eventually, a cycle time of three to four months was put into practice.

There are no natural water seepages in stopes. Stope walls, backs and the loose muck on the floors all appear quite dry. The humidity is, however, about 85 per cent. Average underground temperature is 64°F.

Development of a Leaching Program

The difficulties to be overcome in the development of a leaching program were:

1.—The area of the mine in which leaching was to take place had been abandoned for a year or more. Ventilation was poor and services practically non-existent.

2.—The ore and waste material from which the acid mine waters were leaching the U_3O_8 was scattered thinly over a very wide area. Small heaps resulting from small falls of ground or the storage of waste development rock, averaging less than 1.00 lb. U_3O_8 per ton, also were scattered throughout the area.

3.—Stanrock's mining operation was expected to end within a year or two. For this reason, no large expenditure was warranted and time was not available to develop or train crews in any complicated methods. For a successful operation it was imperative to develop, as quickly as possible, a fast, simple and inexpensive method of leaching.

Stanrock did, however, have several natural advantages that aided greatly in the rapid development of leaching:

1.—The Stanrock orebody is part of an extensive flat-lying bed or reef with an average dip of 15 degrees to the southwest. Thus, the mine waters were able to flow slowly for considerable distances through worked-out areas, picking up additional U_3O_8, before being collected in sumps for pumping to surface.

2.—The west or abandoned section of the mine in which leaching was to take place had been mined down dip to the southwest corner of the property, thereby providing practically unlimited natural sump capacity.

3.—Stanrock's mine drainage system had been designed to handle two to three times the volume of water actually encountered in mining operations.

In view of these conditions, the best solution to the problem appeared to be:

(a) to increase the U_3O_8 content of the water to the maximum attainable by simple and economic methods; and

(b) to increase the quantity of mine water to the maximum capacity of the mine dewatering system.

Before actual washing operations began, a complete survey was made of the area to be washed. All waste heaps, old pipelines and dangerous ground conditions were noted on a 1 in = 100 ft. plan. Pillars in the area showed no signs of failure, and only minor falls of ground were found. Some 2-inch steel pipelines remained in the north half of the area.

Plans were laid out for pipelines to be installed on every second haulageway, all stopes being accessible from main haulageways at either top or bottom entries. *Figure 3* shows the washing area, with its pipelines and waste heaps.

Using available pipe, 2-in. steel lines, with take-offs every 60 feet, were installed in the north section, with 3-in. plastic lines in the south section. Hundred-foot lengths of 3-in. plastic pipe were joined together by means of plastic inserts squeezed into the ends of the pipe

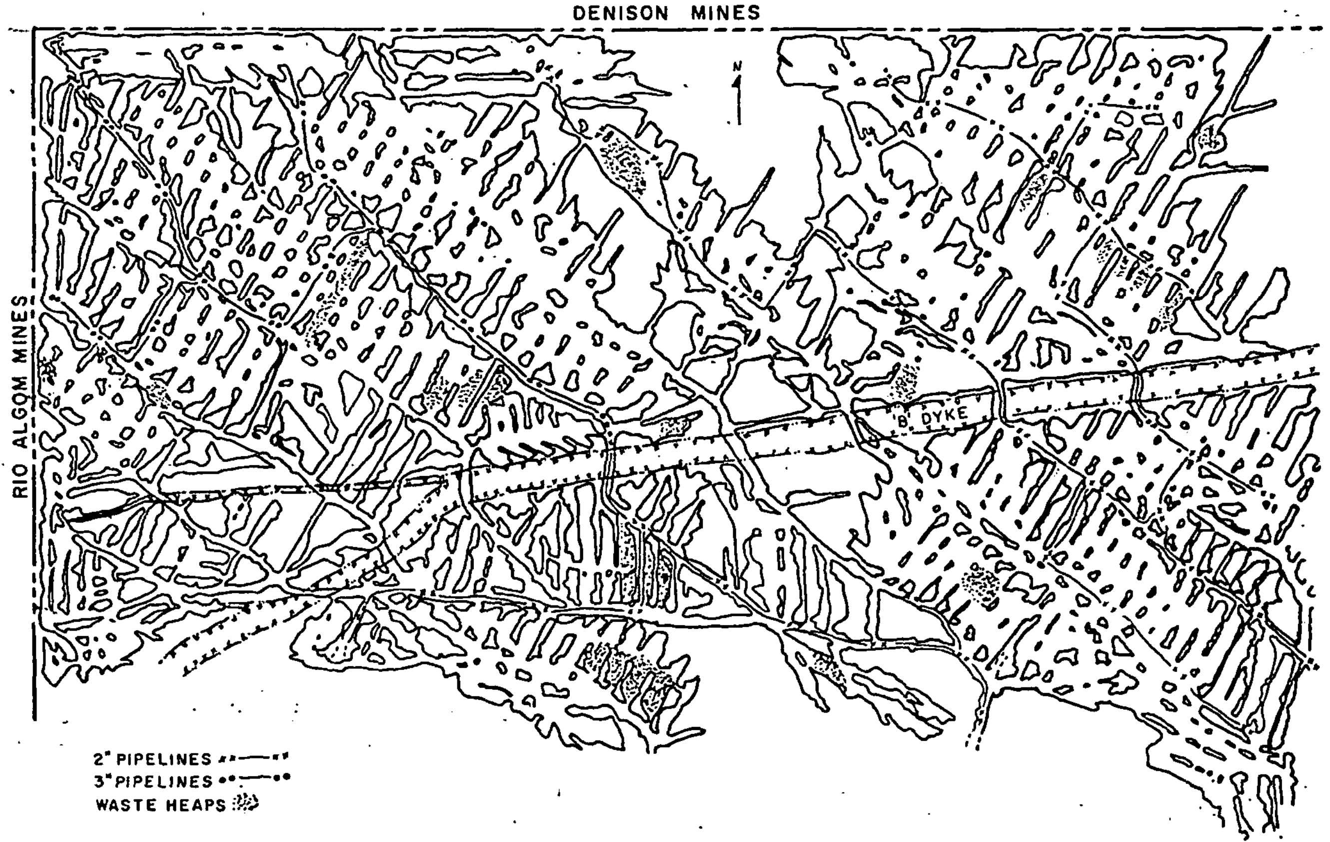

Figure 3.—Diagram showing the Stanrock leaching area.

and clamped with standard 3-in. victaulic couplings. The plastic pipe proved to be exceptionally adaptable, being light and easily moved. The clamping arrangement proved satisfactory as long as operating pressures did not exceed 75 psi, thus allowing the use of readily available standard victaulic and threaded pipe fittings for take-offs and valves.

Each crew of two men was provided with 500 feet of standard 2-in. rubber hose in 50-foot lengths, as well as the necessary valves, fittings and wrenches. Each washing hose was fitted with a tapered fire nozzle, 10 inches long, with a ½-in. nozzle opening giving a concentrated high-pressure stream of water. Crews wash two adjacent stopes per shift, washing two up-dip stopes and two down-dip stopes on alternate days to balance the water pressures of the two operations. Stopes at Stanrock are 150 feet to 250 feet long, with an average floor area of 5,000 to 7,000 square feet. Washing proceeds up dip to facilitate sampling. The rate of washing is governed by the physical characteristics of the particular stope area. The objective is to wash a large area rapidly and thoroughly with a large volume of water.

Two washing shifts per 24 hours are worked—1:00 a.m. to 9:00 a.m. and 1:00 p.m. to 9:00 p.m. This schedule allows most of the water for washing to be drawn in the period from 4:00 o'clock to 8:00 o'clock, when water is not required for regular mining operations. (Regular mining shifts are 8:00 a.m. to 4:00 p.m. and 8:00 p.m. to 4:00 a.m.). Actual washing time is 5½ to 6 hours per 8-hr. shift, the remainder being lunch, travel and set-up time.

Sprinkling of waste heaps is accomplished by spraying from perforated 1-in plastic hoses placed over the top of the waste heaps, and by spraying with various types of nozzles. These sprinkling systems are set up by the washing crews working in the areas, but, because of the lower U_3O_8 content of the water flowing from the waste heaps, the sprays are operated only when increased volumes of water can be pumped.

Sumps and pumping capacity were already adequate. However, an abandoned conveyorway, to be drained by a syphoning arrangement, was utilized as an intermediate sump to save on pumping costs. Water pumped from the west section, together with water syphoned from the conveyorway sump, flows into the main settling and clear-water sump system, where it is neutralized and pumped in three stages to a surface tank of 8,000 gallons capacity.

To avoid loss of precipitate, the neutralizing reagent is injected into the suction line of the pumps. The precipitate is carried to the mill as a slurry, there being sufficient natural agitation in the intermediate sumps to prevent settling. The neutralizing reagent is an ammonia solution, piped underground from the mill in controlled quantities. Conversion from caustic soda to ammonia neutralization in June, 1963, has resulted in a 50 per cent saving in reagent cost, and better pH control. From the surface tank, mine water slurry is pumped to the No. 4 neutral thickener in the mill, where it is treated along with the ore. Pump running time is recorded, making it possible to calculate the number of tons of water pumped to the mill daily. Indicated recovery is 94 per cent, the 6 per cent loss being mostly due to extremely fine particles being carried over in the thickener overflow.

Safety

As washing operations necessitated re-entering many areas of the mine previously considered abandoned, a complete assessment of ground conditions was necessary. A survey made of the area had already shown the old workings to be in good condition, so working in the area presented only normal

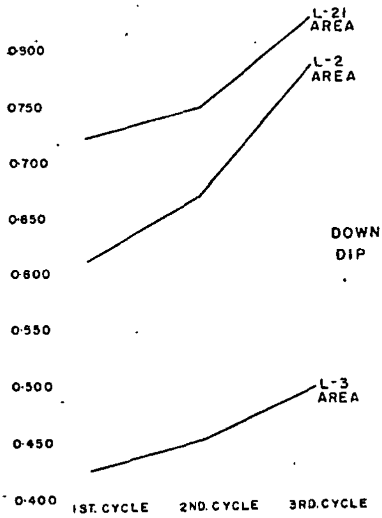

Figure 4.—Graph showing the average assays from stopes in areas L3, L2 and L21, which were washed on a three-month cycle. The U_3O_8 content is highest in areas farthest down the dip.

hazards, provided that the following rules were observed:

1.—Establish travelways and check frequently for any sign of deteriorating ground conditions.
2.—Make every effort not to disturb the existing condition of the workings.
3.—Re-establish and maintain ventilation.

There have been no serious injuries to date.

Sampling

Complete records of daily sampling results for individual stopes have been kept as a check on recoveries. These records show a steady increase in U_3O_8 content for the three washing cycles completed to date. An increasing U_3O_8 content is also noted for dip positions. The average of U_3O_8 assays for a group of stopes down the dip (as areas L-21 and L-2) is higher than for a similar group of stopes up the dip (as area L-3). (See *Figure 4*).

Table I—Average Assays of Ore-Bed and Water Obtained from Stopes Washed on a Three-Month Cycle.

(lbs. U_3O_8/ton)

Stope	Mining	Washing
L21-1	4.44	1.421
L2-38	4.26	0.963
L2-26B	3.14	0.400
L20-14	2.74	0.475
L21E-1	1.93	0.216
L3-22	1.83	0.162
L3-32	1.79	0.274

Increasing tolerance by the bacteria for uranium and other metalliferous compounds dissolved from the ore is believed to be partly responsible for the steady increase in U_3O_8 content. Leach waters contain, in addition to uranium, rare earths and thorium in considerable quantity. The rare earth content is approximately equal to the uranium content; the thorium content is approximately one-half the uranium content. Individual stopes from which higher grade ores were mined tend to give the best results and the highest assays from washing. Table I shows average mining and washing assays for a number of stopes.

Samples are collected by each man in 8-ounce plastic flasks at the beginning, mid-point and end of the washing shift. To determine the sampling location, samples were taken at 2-ft. intervals along the water channel from washing. An assay taken 2 feet from the spot where water was being hosed in the stope showed 50 per cent of the U_3O_8 content of an assay taken 100 ft. away. An assay taken 10 feet from the spot where water was being hosed in the stope had a U_3O_8 content only slightly less than an assay taken 100 ft. away. Assays taken at intermediate points showed smaller and smaller increases in U_3O_8 content as the distance from the water source increased. This showed that U_3O_8 was picked up within 10 feet of the water source and indicated that the U_3O_8 content was pre-leached and in a readily soluble form.

Samples are analysed daily by X-ray spectrograph in Stanrock's assay laboratory. It should be noted that, although all assays are quoted as U_3O_8, the exact chemical form of the uranium in the leach waters is unknown. Assay cards showing individual assays and averages for each stope are filed. Stopes showing average assays below 0.2 lb. U_3O_8 per ton for two consecutive cycles are withdrawn from the program.

A continuous sampling device at the No. 4 neutral thickener in the mill gives a daily composite sample of mine water. From the analysis of the composite sample and the tons of water pumped to the mill, a daily figure for pounds of U_3O_8 contained in the mine water is calculated.

Sampling during test work to determine optimum washing areas indicated anomalous depositions of U_3O_8 content. It was found that when two men were washing, one the up-dip half and the other the down-dip half, assays from the up-dip half of the stope consistently indicated twice as much U_3O_8 content as assays from the down-dip half. This anomalous deposition of U_3O_8 content was also found in stopes which were not open to the haulageway at the up-dip end. Circulation of water and air does not appear to affect the deposition of U_3O_8 in this particular case and is contradictory to the general working hypothesis that the best available U_3O_8 content is found farther down the dip. An opinion is offered that these micro-organisms have some degree of mobility, and that those with the greatest tolerance for uranium, being the more active, move up the dip. Table II shows sample records illustrating this phenomenon.

Table II

Table of assays and average assay from samples taken at intervals during a washing shift. Stopes were washed on a 3-month cycle. A higher assay is shown to be obtained from the top half of the stope than from the bottom half.

L18-20 Open at Top End

Samples — lbs. U_3O_8/ton of water

		1st.	2nd.	3rd.	Average
1st. Cycle		0.420	0.718	0.416	0.518
2nd Cycle		0.282	0.436	0.838	0.519
3rd. Cycle	Top	0.470	1.402	2.110	1.661
	Bottom	0.852	0.638	0.614	0.701

L18-21 Closed at Top End

Samples — lbs. U_3O_8/ton of water

		1st.	2nd.	3rd.	Average
1st. Cycle		0.512	1.112	0.996	0.873
2nd Cycle		0.134	0.434	0.132	0.233
3rd. Cycle	Top	2.332	2.298	1.408	2.013
	Bottom	1.960	1.282	0.734	1.325

Samples of fine material taken from stopes prior to washing gave assays of 3 to 4 lbs. U_3O_8 per ton. Samples of mud accumulated at the bottom of stopes following first-cycle washing showed 1 lb. U_3O_8 per ton or less. Sampling of the same mud at the bottom of stopes following subsequent washing showed an only slightly lower U_3O_8 content. The indicated recovery from fines is approximately 70 per cent from the first-cycle washing, and insignificant in subsequent cycles. Recovery, which has improved during second- and third-cycle washing, must be coming from material other than the fines.

Since the beginning of U_3O_8 recovery from mine waters in September, 1960, an estimated 148,073 lbs. of U_3O_8 have been recovered. With a 6 per cent loss in recovery, and considering the estimated U_3O_8 content of the mine water previously discarded, more than 160,000 lbs. of U_3O_8 have been leached from Stanrock workings to December, 1963. Estimated ore "lefts" or muck remaining in stopes from mining operations is 100,000 tons, containing an average 2 lbs. of U_3O_8 per ton. At least one-half the total muck remaining consists of slabs or blocks more than ½ in. thick. Recovery from mine water shows no signs of dimishing. Based on pounds of U_3O_8 produced from material available, the bacteria appear capable of leaching to depths of more than ¼ in. into both the muck remaining and the walls and floors of the stopes.

Costs

The recorded cost of the leaching program for 1963 was $33,017. The estimated recovery of U_3O_8 from mine water during 1963 was 105,622 lbs., for an indicated cost of $0.31 per lb. This cost does not include pumping or neutralization, most of which cost would accrue to the mine regardless of leaching operations. The recorded cost does, however, include $7,726 for materials (many of which consist of non-recurring items such as pipe and fittings), installation cost and labour for test work and sump installations.

Pumping costs for 1963 were $112,653, or $1.065 per lb. of U_3O_8 produced from water leaching. The pumping costs for 1962, when no leaching was being carried out were $120,657.

Assuming that such an operation could be set up with a life expectancy of two or three years, a cost of $0.25 per lb. or less appears possible if the leaching is carried out in conjunction with a regular mining operation. The cost of leaching in an abandoned mine would depend upon pumping, overhead and service costs.

Conclusions

1.—Fast high-pressure washing appears to be the most efficient method of removing pre-leached U_3O_8 minerals from old workings.

2.—The bacteria appear to develop a natural tolerance for U_3O_8 and other metalliferous compounds of the ore.

3.—The U_3O_8 content tends to concentrate down the dip.

4.—Areas of highest grade ore usually give the highest and most consistent results.

5.—The bacteria would appear to have some degree of mobility.

6.—The bacteria appear to be capable of leaching the rock to depths of ¼ in. or greater.

7.—An operating cost of $0.31 per lb. of U_3O_8 has been realized; $0.25 per lb. appears possible.

8.—Thorium and rare earth metals are also contained in the leach waters.

9.—Abandoned workings have been safely leached.

Acknowledgment

The writer wishes to thank Stanrock Uranium Mines Limited for permission to publish this paper.

References

(1) Colmer, A. R., and Hinkle, M. E., "The Role of Micro-Organisms in Acid Mine Drainage," *Science*, Vol. 106, 253-256, 1947.

(2) Temple, K. L., and Delchamps, E. W., "Autotrophic Bacteria and the Formation of Acid in Bituminous Coal Mines," *Applied Microbiology*, Vol. I, 255-258, 1953.

(3) Leathen, W. W., Kinsel, N., and Bradley, S. A., "Ferrobacillus Ferro-oxidans; A Chemosynthetic Autotropic Bacterium," *Jour. Bac.*, Vol. 72, 700-3, 1956.

(4) Bryner, L. C., Beck, J. V., Davis, D. B., and Wilson, O. G., Micro-organisms in Leaching Sulphide Minerals," *Ind. Eng. Chem.*, Vol. 46, 2587-2592, 1954.

(5) Miller, R. P., Napier, E., Wells, R. A., Audsley, A., and Daborn, G. R., "Natural Leaching of Uranium Ores," *Bull. Inst. Min. Metall.*, London, 217-254, January, 1963.

REPRINTS OF TECHNICAL PAPERS

READERS of *The Canadian Mining and Metallurgical Bulletin* are reminded that reprints of *most* of the technical papers that have been published in these pages recently are available from Institute Headquarters. The price is fifty cents each to the membership of The Canadian Institute of Mining and Metallurgy and one dollar each to non-members. Symposia and papers of exceptional length are charged at proportionately higher rates, which are available on request.

Stresses Around Boreholes in Bilinear Elastic Rock

B. C. HAIMSON
T. M. THARP
MEMBERS SPE-AIME

*THE U. OF WISCONSIN
MADISON, WIS.*

ABSTRACT

It is commonly accepted that the radial and tangential stresses around boreholes are independent of the rock elastic properties when the assumptions of linearity, homogeneity, and isotropy are made. Although rock is never perfectly linear, the stress/strain relationship can often be linearized as a first approximation, which vastly simplifies the analytical approach. However, the slope of the linear relationship in compression (E_c) *is almost always higher than that in tension* (E_t), *and this bilinear behavior can and should be incorporated in the analytical approach to any problems involving mixed stresses at a point — e.g., stresses around boreholes and cavities, stresses along the vertical diameter in a Brazilian test, stresses in uniaxially loaded rings, stresses in bent beams. The problem of a circular hole under internal pressure and hydrostatic loading at infinity has been worked out. The resulting stresses differ considerably from those obtained using the common assumption of linearity. In particular, when no external loading exists, the tangential stress* (σ_θ) *at a borehole wall is expected to equal the internal pressure* (p_i) *in the borehole* ($\sigma_\theta = p_i$). *However, the bilinear character of rock yields the expression*

$$\sigma_\theta = p_i \sqrt{E_t/E_c}.$$

The internal pressurization of hollow cylinders was suggested as a possible technique for determining tensile strength. The findings reported here dispute the suitability of the method since the tensile and compressive Young's moduli must be known in order to calculate σ_θ. *Laboratory testing shows that generally the internal pressure required to initiate rupture around a borehole is higher than the uniaxial tensile strength of the rock, in accord with the results of this paper.*

INTRODUCTION

Linear elasticity is generally assumed in both field and laboratory situations involving stress and displacement in rock. That assumption allows the direct application of a considerable body of theoretical stress solutions. Unfortunately, those solutions are only as good as the underlying assumptions, which are sometimes of questionable validity in rock.

The typical nonlinearity of the stress/strain curve in rock has long been recognized but is usually ignored. The stress/strain relationship can often be linearized as a first approximation, which vastly simplifies the analytical solution. However, the slope of the line in compression (E_c) is almost always higher than that in tension (E_t). The ratio E_t/E_c can in fact vary between 1:1 in very tight rocks, to 1:2 in some limestones, to 1:20 in weak sandstones, to 0 in no-tension soils (see Table 1).

Hence, with respect to its complete deformation spectrum, rock stress/strain relationship can at best be simplified into a bilinear curve with the point of intersection at zero stress (Fig. 1). The assumption of bilinearity can and should be incorporated in the analytical approach to any problems that involve mixed stresses at a point.

The bilinear assumption has been employed by a number of investigators to represent this behavior. Burshtein[1] and Fairhurst[2] have derived bilinear stress formulas for rectangular beams in flexure, and Adler[3] has done the same for beams of circular and more general cross-sections.

These efforts cover only a few of the many cases in which both tensile and compressive stresses exist. The emphasis of the present paper is on bilinear stress equations for thick-walled cylinders. Possible important applications include stress around wellbores, hydraulic fracturing (in which the

TABLE 1 — YOUNG'S MODULI IN TENSION AND COMPRESSION

Rock Type	E_t (10^6 psi)	E_c (10^6 psi)	E_t/E_c
Westerly granite[8]	2.5	10.5	0.24
Austin limestone[6]	1.7	2.3	0.74
Carthage limestone[6]	5.1	9.2	0.55
Indiana limestone[7]	1.6	3.9	0.41
Georgia marble[8]	3.4	6.1	0.56
Tennessee marble[8]	7.7	11.1	0.69
Russian marble[1]	1.3	3.0	0.43
Star Mine quartzite[8]	11.0	11.0	1.00
Arizona sandstone[6]	1.7	6.6	0.26
Berea sandstone[8,9]	.6	3.4	0.18
Millsap sandstone[6]	0.1	1.9	0.05
Tennessee sandstone[6]	0.2	2.4	0.08
Russian sandstone[1]	1.7	8.3	0.21

Paper (SPE 4241) was presented at the SPE-AIME Sixth Conference on Drilling and Rock Mechanics, held in Austin, Tex., Jan. 22-23, 1973.

[1] References listed at end of paper.

tangential stress at failure is tensile and the radial stress is compressive),[4] pressure tunnels, and the hoop-stress tensile test.[5]

Bilinearity may be important also in the Brazilian and ring indirect tension tests and in the case of underground excavations such as tunnels or other regular and irregular openings in which tensile stresses may occur. These latter problems are probably not amenable to analytical solutions. They could, however, be solved by the finite-element technique, and in view of the results already obtained for simpler cases, such a solution may be a worthwhile effort.

THEORY

GENERAL

As stated above, in almost all the problems involving rock, the assumption of linearity is made — i.e., the rock is assigned unique Young's modulus (E) and Poisson's ratio (μ) values. The same E, μ values are ordinarily used regardless of the stress configuration. Since it has been established that for most rocks the slope of the stress/strain curve in tension is markedly different from the one in compression, a behavior that can be simplified to no better than a bilinear curve, four parameters should be determined for each rock: E_t, μ_t for tension, and E_c, μ_c for compression. If all the stresses at a point are compressive, only E_c, μ_c should be used; if all the stresses are tensile, only E_t, μ_t should be used. But if both tensile and compressive stresses are generated, all four parameters are involved.

For the latter case, the strain/stress relationship is (assuming for example that σ_1, σ_2, are compressive, σ_3 is tensile)

$$\varepsilon_1 = \frac{1}{E_c}\sigma_1 - \frac{\mu_c}{E_c}\sigma_2 - \frac{\mu_t}{E_t}\sigma_3$$

$$\varepsilon_2 = -\frac{\mu_c}{E_c}\sigma_1 + \frac{1}{E_c}\sigma_2 - \frac{\mu_t}{E_t}\sigma_3$$

$$\varepsilon_3 = -\frac{\mu_c}{E_c}\sigma_1 - \frac{\mu_c}{E_c}\sigma_2 + \frac{1}{E_t}\sigma_3 \quad . \; . \; . \; . \; (1)$$

where ϵ_1, ϵ_2, ϵ_3, and σ_1, σ_2, σ_3 are principal strains and stresses, respectively.

From the theory of elasticity it is remembered that by considering the potential of elastic forces[10] the number of elastic constants can be reduced because of the symmetry of the stress coefficient matrix. Thus, the coefficient of σ_3 in the first of Eqs. 1, for example, is equal to the coefficient of σ_1 in the third of Eqs. 1; that is,

$$\frac{\mu_c}{E_c} = \frac{\mu_t}{E_t} \quad . \; . \; . \; . \; . \; . \; . \; . \; . \; . \; . \; . \; . \; . \; . \; . \; . \; (2)$$

Hence, only three of the four elastic parameters are independent.

Examples of situations in which both compressive and tensile stresses exist at a point are numerous. The more important cases are those of stresses around wellbores, boreholes, tunnels and other underground openings, in bent beams, and in Brazilian and ring test specimens. In this paper, only the simple case of stresses around circular openings will be considered.

STRESS AROUND A CIRCULAR OPENING IN BILINEAR ROCK

The method of approach in determining stresses or displacements in bilinear rock is simple. The theory of stress and the theory of strain are entirely unaffected by the bilinear characteristics. In those regions where all stresses are tensile or compressive, the existing solutions hold (remembering to use the appropriate E, μ). It is only in the regions where mixed stresses (both compressive and tensile) exist that new stress calculations are needed if $E_c \neq E_t$.

In calculating the stresses around cylindrical openings in bilinear elastic rock, the method used by Jaeger[11] to solve the cylindrical pressure vessel problem has been closely followed, with the exception of replacing his unique E, μ by the appropriate E_t, E_c, μ_t, μ_c.

The problem is that of calculating the stresses in a hollow cylinder $r_i < r < r_e$ (r is the radius measured from the axis of cylinder) subjected to hydrostatic pressures on both the inside and the outside surfaces.

The equation of equilibrium for this case of axial symmetry is given by

$$\frac{d\sigma_r}{dr} + \frac{\sigma_r - \sigma_\theta}{r} = 0 \; . \; . \; . \; . \; . \; . \; . \; . \; . \; . \; . \; . \; . \; (3)$$

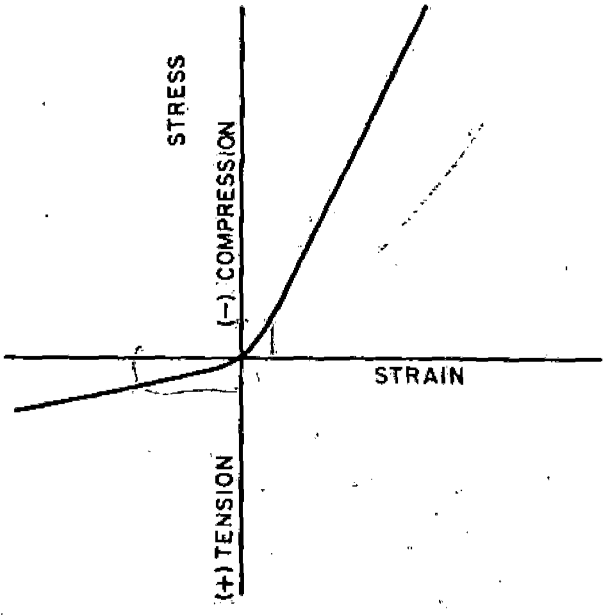

FIG. 1 — TYPICAL STRESS-STRAIN RELATIONSHIP FOR ROCK IN TENSION-COMPRESSION.

in both the plane-strain and plane-stress cases. σ_r, σ_θ, σ_z are the radial, tangential, and vertical stresses acting in the cylinder.

The displacements are purely radial and vertical ($s_\theta = 0$), and the components of strain are given by

$$\epsilon_r = \frac{ds_r}{dr};\ \epsilon_\theta = \frac{s_r}{r};\ \epsilon_z = \frac{ds_z}{dz}\quad ,\ .\ .\ (4)$$

where ϵ_r, ϵ_θ, ϵ_z are the radial, tangential, and vertical components of strain; s_r, s_θ, s_z are the respective displacements.

The strain/stress relationships considering the case in which both tensile and compressive stresses are developed, and keeping in mind that the tangential stress is then definitely tensile, are

$$\epsilon_r = \frac{1}{E_c}\sigma_r - \frac{\mu_t}{E_t}\sigma_\theta - \frac{\mu_z}{E_z}\sigma_z$$

$$\epsilon_\theta = \frac{1}{E_t}\sigma_\theta - \frac{\mu_c}{E_c}\sigma_r - \frac{\mu_z}{E_z}\sigma_z$$

$$\epsilon_z = \frac{1}{E_z}\sigma_z - \frac{\mu_c}{E_c}\sigma_r - \frac{\mu_t}{E_t}\sigma_\theta\quad ,\ .\ .\ .\ (5)$$

where μ_z, E_z are the elastic constants corresponding to the type of stress acting in the z direction, which at this point in unknown.

Two cases are now considered. If the configuration is one of plane stress — i.e., $\sigma_z = 0$ — and use is made of Eqs. 2 and 4, the first two Eqs. 5 become

$$\frac{ds_r}{dr} = \frac{1}{E_c}(\sigma_r - \mu_c\sigma_\theta)$$

$$\frac{s_r}{r} = \frac{1}{E_t}(\sigma_\theta - \mu_t\sigma_r)\ .\ .\ .\ .\ .\ .\ .\ .\ (6)$$

If the case is one of plane strain — i.e. $\epsilon_z = 0$ — the third Eq. 5 becomes

$$\sigma_z = \mu_z(\sigma_r + \sigma_\theta)\ ,\ .\ .\ .\ .\ .\ .\ .\ .\ .\ (7)$$

and by incorporating this result in the first two Eqs. 5 the strain/stress relationships become

$$\frac{ds_r}{dr} = \frac{1-\mu_c\mu_z}{E_c}\sigma_r - \frac{\mu_c}{E_c}(1 + \mu_z)\sigma_\theta$$

$$\frac{s_r}{r} = \frac{\mu_c}{E_c}\left(\frac{1}{\mu_t} - \mu_z\right)\sigma_\theta - \frac{\mu_c}{E_c}(1 + \mu_z)\sigma_r$$

$$.\ (8)$$

Solving for σ_r and σ_θ in the plane stress case, using Eqs. 6, one obtains

$$\sigma_r = \frac{E_c}{1-\mu_c\mu_t}\frac{ds_r}{dr} + \frac{E_t\mu_c}{1-\mu_c\mu_t}\frac{s_r}{r}$$

$$\sigma_\theta = \frac{E_c\mu_t}{1-\mu_c\mu_t}\frac{ds_r}{dr} + \frac{E_t}{1-\mu_c\mu_t}\frac{s_r}{r}\ .\ .\ .\ .\ (9)$$

In plane strain, use of Eq. 8 will yield

$$\sigma_r = \frac{E_c}{S}\frac{1-\mu_t\mu_z}{\mu_t}\frac{ds_r}{dr} + \frac{E_c(1+\mu_z)}{S}\frac{s_r}{r}\ ,$$

$$\sigma_\theta = \frac{E_c(1+\mu_z)}{S}\frac{ds_r}{dr} + \frac{E_c(1-\mu_c\mu_z)}{S\mu_c}\frac{s_r}{r}\ ,$$

where

$$S = \frac{1}{\mu_t}(1-\mu_t\mu_z)(1-\mu_c\mu_z) - \mu_c(1+\mu_z)^2$$

$$.\ (10)$$

Replacing σ_r and σ_θ in Eq. 3 with Eqs. 9, we obtain the following plane-stress equilibrium condition:

$$\frac{d^2s_r}{dr^2} + \frac{1}{r}\frac{ds_r}{dr} - \frac{E_t}{E_c}\frac{s_r}{r^2} = 0\ .\ \ .\ .\ .\ .\ (11)$$

For the plane-strain case, the equation of equilibrium becomes

$$\frac{d^2s_r}{dr^2} + \frac{1}{r}\frac{ds_r}{dr} - \frac{1-\mu_c\mu_z}{1-\mu_t\mu_z}\frac{E_t}{E_c}\frac{s_r}{r^2} = 0.$$

$$.\ (12)$$

The differential Eqs. 11 and 12 are both of the following type:

$$\frac{d^2s_r}{dr^2} + \frac{1}{r}\frac{ds_r}{dr} - k^2\frac{s_r}{r^2} = 0\ .\ \ .\ .\ .\ .\ (13)$$

The general solution for Eq. 13 is

$$s_r = Ar^k + Br^{-k}\ ,\ .\ .\ .\ .\ .\ .\ .\ .\ .\ .\ (14)$$

where k^2 is the coefficient of s_r/r^2 in Eq. 13, whose value is given by

$$k^2 = \frac{E_t}{E_c}\ .\ .\ .\ .\ .\ .\ .\ .\ .\ .\ .\ .\ .\ .\ (14a)$$

for plane stress, and

$$k^2 = \frac{1-\mu_c\mu_z}{1-\mu_t\mu_z}\frac{E_t}{E_c}\ .\ .\ .\ .\ .\ .\ .\ .\ .\ .\ (14b)$$

for plane strain. A and B are constants determined by the boundary conditions. Strains calculated from Eq. 14 satisfy the compatibility conditions.

The radial and tangential stresses for the plane-stress case can now be rewritten using Eqs. 9 and 14.

$$\sigma_r = \frac{E_c}{1-\mu_c\mu_t}\left[(k+\mu_t)Ar^{k-1}-(k-\mu_t)Br^{-k-1}\right]$$

$$\sigma_\theta = \frac{E_t}{1-\mu_c\mu_t}\left[(1+k\mu_c)Ar^{k-1}\right.$$

$$\left.+(1-k\mu_c)Br^{-k-1}\right]. \quad \ldots\ldots\ldots (15)$$

For the plane-strain case, using Eqs. 10 and 14,

$$\sigma_r = \frac{E_c}{\mu_t S}\{[k+\mu_t+\mu_t\mu_z(1-k)]Ar^{k-1}-$$

$$-[k-\mu_t-\mu_t\mu_z(1+k)]Br^{-k-1}\}$$

$$\sigma_\theta = \frac{E_t}{\mu_t S}\{[1+k\mu_c-\mu_c\mu_z(1-k)]Ar^{k-1}-$$

$$-[1-k\mu_c-\mu_c\mu_z(1+k)]Br^{-k-1}\} \quad . (16)$$

CASE 1 — σ_θ TENSILE THROUGHOUT

The general boundary conditions for the case where σ_θ is tensile throughout the thickness of the cylinder are

$$\sigma_r = -p_e \quad \text{at} \quad r=r_e$$

$$\sigma_r = -p_i \quad \text{at} \quad r=r_i.$$

where

$$p_i > \frac{r_i^2+r_e^2}{2r_i^2}\,p_e \quad \ldots\ldots\ldots\ldots (17)$$

A and B in Eq. 15 or 16, depending on the state of stress, can now be evaluated. By replacing A and B by their values, Eqs. 15 and 16 become

$$\sigma_r = \frac{p_i r_i^{k+1}-p_e r_e^{k+1}}{r_e^{2k}-r_i^{2k}}\,r^{k-1}-$$

$$-\frac{r_i^{k+1}\,r_e^{k+1}(p_i r_e^{k-1}-p_e r_i^{k-1})}{r_e^{2k}-r_i^{2k}}\,r^{-k-1}$$

$$\sigma_\theta = \frac{p_i r_i^{k+1}-p_e r_e^{k+1}}{r_e^{2k}-r_i^{2k}}\,kr^{k-1}+$$

$$+\frac{r_i^{k+1}r_e^{k+1}(p_i r_e^{k-1}-p_e r_i^{k-1})}{r_e^{2k}-r_i^{2k}}\,kr^{-k-1}$$

$$\ldots\ldots\ldots\ldots\ldots\ldots\ldots\ldots (18)$$

where the value of k depends on the state of stress. Note that in linear elasticity $k = 1$ and Eqs. 8 become the classical solution to the thick cylinder problem.[11]

Often, the region of interest is the vicinity of the cylindrical hole. The stresses at $r = r_i$ are

$$\sigma_r = -p_i$$

$$\sigma_\theta = k\,\frac{p_i(r_e^{2k}+r_i^{2k})-2p_e r_i^{k-1}r_e^{k+1}}{r_e^{2k}-r_i^{2k}}\,.$$

$$\ldots\ldots\ldots\ldots\ldots\ldots\ldots\ldots (19)$$

In the case of $p_e = 0$, the condition on p_i is $p_i > 0$ (Eq. 17) and the stresses at $r = r_i$ become

$$\sigma_r = -p_i$$

$$\sigma_\theta = kp_i\,\frac{r_e^{2k}+r_i^{2k}}{r_e^{2k}-r_i^{2k}}\,. \quad \ldots\ldots\ldots (20)$$

If moreover, $r_e \to \infty$, Eqs. 20 reduce to

$$\sigma_r = -p_i\,,$$

$$\sigma_\theta = kp_i\,. \quad \ldots\ldots\ldots\ldots\ldots (21)$$

Eq. 19, 20, and 21 yield tangential stresses that are significantly different from those calculated from linear elastic relations. As stated above, k can have either of the two values given by Eq. 14a or Eq. 14b, depending on the state of stress. As the stress/strain relationship departs from the linear ($k = 1$) into the bilinear, the value of k decreases ($0 < k < 1$). Moreover, for the same rock, k for the plane-strain case is always lower than k for plane stress, since $1 - \mu_c\mu_z < 1 - \mu_t\mu_z$. This relation is correct whether μ_z is compressive or tensile because $\mu_c > \mu_t$. Also, the ratio $1 - \mu_c\mu_z/1 - \mu_t\mu_z$ is in the range of 0.90 to 1.00 for all practical values of μ_c, μ_t. Hence, by using $k = \sqrt{E_t/E_c}$ (Eq. 14a) for both plane stress and plane strain, one obtains the exact solution for the first case and a slightly conservative one for the second case. Although the sacrifice of accuracy is extremely limited, use of the plane stress k considerably simplifies matters in the plane-strain case, since knowledge of the Poisson's ratio values is no longer required. In addition, the necessity to check whether μ_z is compressive or tensile is thus eliminated.

CASE 2 — σ_θ TENSILE AND COMPRESSIVE

The general boundary conditions for the case where σ_θ is tensile throughout a portion of the cylinder thickness and compressive otherwise are

$$\sigma_r = -p_e \quad \text{at} \quad r=r_e,$$

$$\sigma_r = -p_i \quad \text{at} \quad r=r_i,$$

where

$$\frac{2r_e^2}{r_i^2+r_e^2}\,p_e < p_i < \frac{r_i^2+r_e^2}{2r_i^2}\,p_e,$$

$$\sigma_\theta = 0 \quad \text{at} \quad r=R$$

where

$$r_i < R < r_e \quad . \; . \; . \; . \; . \; . \; . \; . \; . \; . \; . \; . \; . \; (22)$$

Two regions must be distinguished. From Eq. 22, σ_θ is tensile in region $r_i < r < R$, and in region $R < r < r_e$ it is compressive. σ_r remains compressive throughout.

In region $r > R$ the distribution of the stresses is found by using the classical linear solution for a thick cylinder and the condition of Eq. 22, since both σ_r and σ_θ are compressive,

$$\sigma_r = \frac{-r_e^2 p_e}{r_e^2+R^2}\left(1+\frac{R^2}{r^2}\right)$$

$$\sigma_\theta = \frac{-r_e^2 p_e}{r_e^2+R^2}\left(1-\frac{R^2}{r^2}\right) \quad . \; . \; . \; . \; . \; . \; . \; (23)$$

In region $r_i < r < R$ the bilinear state (Eq. 15 or 16) holds, with the boundary conditions as given by Eq. 22. For reasons explained above, only the plane-stress solution will be treated:

$$\sigma_r = -p_i\left(\frac{r_i}{r}\right)^{1-k} \frac{\left(\frac{R}{r}\right)^{2k}+1}{\left(\frac{R}{r_i}\right)^{2k}+1},$$

$$\sigma_\theta = kp_i\left(\frac{r_i}{r}\right)^{1-k} \frac{\left(\frac{R}{r}\right)^{2k}-1}{\left(\frac{R}{r_i}\right)^{2k}-1} \quad . \; . \; . \; . \; . \; . \; (24)$$

The solution of Eq. 23 or Eq. 24 is a function of the unknown R. This value can be determined by noting that at $r = R$ the radial stress as determined by Eq. 23 should be equal to that determined by Eq. 24:

$$-\frac{2r_e^2 p_e}{r_e^2+R^2} = -\left(\frac{r_i}{R}\right)^{1-k} \frac{2}{\left(\frac{R}{r_i}\right)^{2k}+1}\,p_i \; . \quad (25)$$

The value of R obtained from Eq. 25 can then be used to determine the stresses around the cylindrical hole.

DISCUSSION OF RESULTS

The results obtained are directly applicable to laboratory tensile testing by means of the hoop-stress and to field problems related to pressure tunnels, wellbores under pressurized mud, hydraulic fracturing, or any situation in which a tensile strain is developed around a cylindrical hole. The effect on the radial and the tangential stresses due to the bilinear behavior of rock is significant and is illustrated for a number of specific cases in Figs. 2 through 5. The most important departure from the linear case is that rock Young's moduli are required in calculating the stresses. The linear solution does not necessitate knowledge of material properties.

Fig. 2 shows the distribution of stresses for both the linear and the bilinear cases in a finite-thick cylinder. At $r = r_i$ the bilinear tangential stress is lower than the value predicted by linear theory and this could be, at least in part, the reason for the unusually high tensile strength values in hoop-stress testing. What makes the hoop-stress tensile testing unattractive, however, is that because of bilinear

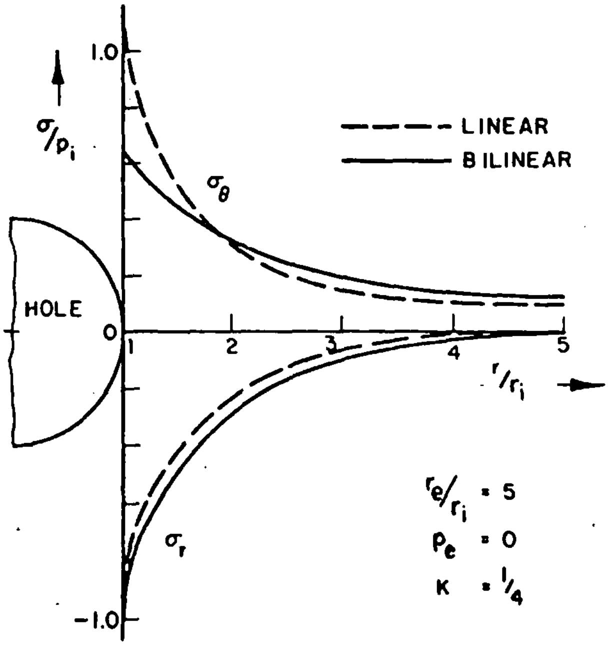

FIG. 2 — RADIAL AND TANGENTIAL STRESS DISTRIBUTION IN A THICK HOLLOW CYLINDER FOR CONDITIONS AS GIVEN.

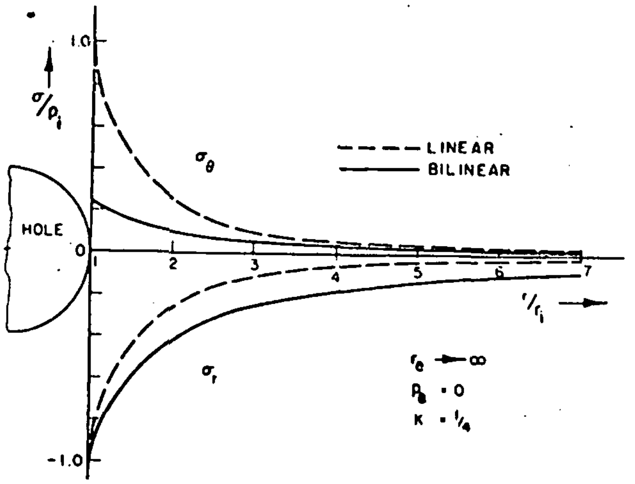

FIG. 3 — RADIAL AND TANGENTIAL STRESSES AROUND A WELLBORE FOR CONDITIONS AS GIVEN.

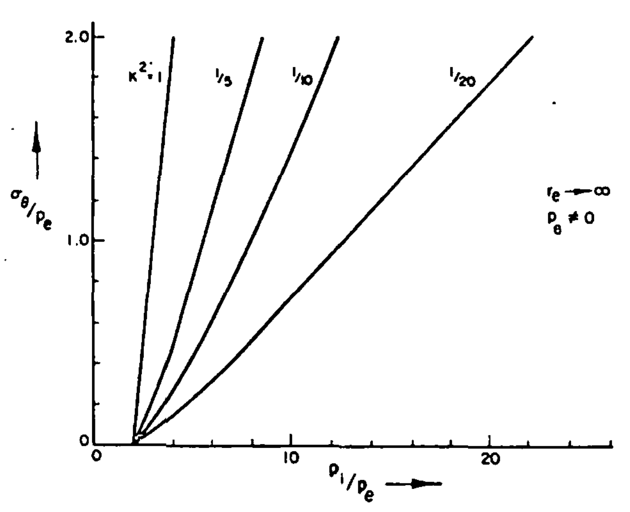

FIG. 4 — TANGENTIAL STRESS AT WELLBORE WALL VS WELLBORE PRESSURE FOR DIFFERENT E_t/E_c VALUES AND $p_e \neq 0$.

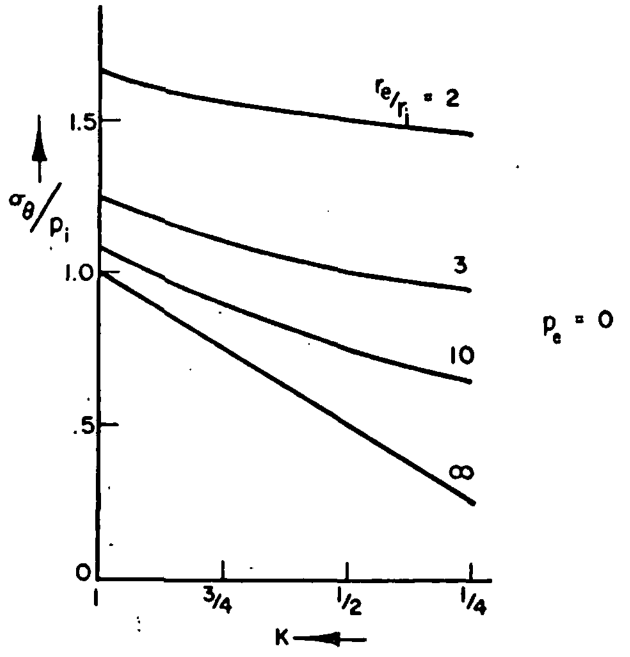

FIG. 5 — TANGENTIAL STRESS AT INNER HOLE WALL VS k FOR DIFFERENT r_e/r_i RATIOS.

behavior the two Young's moduli for the rock must be determined before the tensile strength can be calculated.

Fig. 3 is similar to Fig. 2 except that $r_e \to \infty$. The drop in $\sigma\theta$ at $r = r_i$ as a result of rock bilinearity is most severe. In the particular case shown ($k = 1/4$), the tangential stress is only one-quarter of that expected from linear theory. In a less severe case, like $k = \sqrt{1/2}$, the discrepancy is close to 30 percent. A list of k values and respective tangential stresses is given in Table 2. Note that the difference between plane stress and plane strain is very slight.

Fig. 4 depicts the changes in $\sigma\theta$ at $r = r_i$ as a function of p_i for different values of k when $p_e \neq 0$. Again the discrepancy between the linear case ($k = 1$) and the bilinear range is remarkable.

Fig. 5 reveals the drop in tangential stress with respect to k for different r_e/r_i ratios. The trend is toward higher-than-expected tensile strength if linear behavior is assumed.

A few specific results of tangential stresses for the case of $r_e \to \infty$, $p_e \neq 0$, are given in Table 3. The calculation of these stresses necessitated a computer program to determine R (Eq. 25). The resulting discrepancies from the commonly used linear solution are clearly impressive. For example, the tangential stress at the wellbore wall in a hard sandstone ($E_t/E_c = 0.5$) is approximately one-half the expected value from classical linear solutions.

In general, the tangential stresses around holes as developed according to linear elasticity appear to be deceptively high. Numerous examples can be cited in the literature where the tensile strength as determined in the laboratory by internal pressurization of a hollow cylinder was *significantly* higher than expected, owing to the assumption of linearity in calculating the tangential stress.[4,5,12]

TABLE 2 — STRESSES AROUND A BOREHOLE UNDER $p_e = 0$ (FOR DIFFERENT RATIOS OF E_t/E_c)

	$\sigma\theta$ at $r = r_i$	
E_t/E_c	Plane Stress ($\times\ p_i$ psi)	Plane Strain $\mu_c = 0.25$ ($\times\ p_i$ psi)
1.00 (linear)	1.00	1.00
0.67	0.82	0.80
0.50	0.71	0.69
0.34	0.58	0.56
0.25	0.50	0.49
0.20	0.45	0.44
0.10	0.32	0.31
0.05	0.22	0.22

TABLE 3 — STRESSES AROUND A BOREHOLE FOR WHICH $r_i = 12$ IN., $p_e = 1{,}000$ PSI, $p_i = 5{,}000$ PSI

	Plane Stress		Plane Strain $\mu_c = 0.25$	
E_t/E_c	R (in.)	$\sigma\theta$ (psi)	R (in.)	$\sigma\theta$ (psi)
1 (linear)	24	3,000	24	3,000
0.67	25.2	2,211	25.3	2,174
0.50	26.0	1,762	26.1	1,715
0.05	29.4	221	29.4	208

CONCLUSIONS AND RECOMMENDATIONS

1. Rock is nonlinear in its elastic behavior. When linearized for purposes of mathematical analysis, the slope of the stress/strain curve is most often higher in compression than it is in tension. A recalculation of the stresses around a circular hole based on the assumption of bilinearity reveals severe discrepancies between the stresses developed and those expected from linear elastic solutions.

2. In bilinear rock, unlike in linear rock, stresses around circular holes are a function of the material's elastic properties.

3. As a result of Conclusion 2, the use of the hoop-stress method to determine the tensile strength of rock appears rather impractical, since it requires knowledge of rock properties in tension and compression.

4. The results obtained can be applied to calculations of allowable pressures in wellbores (during drilling or hydraulic fracturing), pressure tunnels, and boreholes. These pressures are always higher than expected from linear elasticity.

5. In view of the reported results, other indirect methods of measuring tensile strength, like the Brazilian, the ring, and the beam tests, should be reconsidered. These methods employ loading configurations that result in mixed stresses and therefore require the use of the bilinear assumption.

6. The obtained results for wellbores justify the recalculation of stresses wherever both tensile and compressive stresses are generated, such as in storage cavities, mining excavations, and tunnels.

NOMENCLATURE

E = Young's modulus
E_c = Young's modulus in compression
E_t = Young's modulus in tension
E_z = Young's modulus in direction z
k^2 = the ratio E_t/E_c
p_i,p_e = inner and outer pressures
r,θ,z = radial, tangential, and vertical cylinder coordinates
r_i,r_e = inner and outer radii of a thick cylinder
R = radial distance from central axis of cylinder to the point where $\sigma_\theta = 0$
s_r,s_θ,s_z = radial, tangential, and vertical displacements
$\epsilon_1,\epsilon_2,\epsilon_3$ = principal strains
$\epsilon_r,\epsilon_\theta,\epsilon_z$ = normal strains in cylindrical coordinates
μ = Poisson's ratio
μ_t = Poisson's ratio in tension
μ_c = Poisson's ratio in compression
μ_z = Poisson's ratio in direction z
$\sigma_1,\sigma_2,\sigma_3$ = principal stresses
$\sigma_r,\sigma_\theta,\sigma_z$ = normal stress in cylindrical coordinates

ACKNOWLEDGMENT

This work was supported in part by the API, Research Project 147.

REFERENCES

1. Burshtein, L. S.: "Rock Strength Under Axial Tension and Flexure," *Fizico-Teknicheskie Problemy* (1967) 53-61.
2. Fairhurst, C.: "Laboratory Measurements of Some Physical Properties of Rock," *Proc., Fourth Symp. Rock Mechanics* Bull. 76, Mineral Ind. Experiment Station, Pennsylvania State U., University Park (1961).
3. Adler, L.: "Double Elasticity in Drill Cores Under Flexure," *Intl. J. of Rock Mech.*, Mineral Science (1970) 357-370.
4. Haimson, B.: "Hydraulic Fracturing in Porous and Nonporous Rock and Its Potential for Determining In-Situ Stresses at Great Depth," Report to the Missouri River Div. Corps of Engineering, Contract DA-25-066-NEG-14, 764.
5. Hardy, H. R., Jr., and Jayaraman, N. I.: "Hoop-Stress Loading — A New Method of Determining the Tensile Strength of Rock," *Soc. Pet. Eng. J.* (June 1972) 246-252; *Trans.*, AIME, Vol. 253.
6. Perkins, T. K., and Krech, W. W.: "The Energy Balance Concept of Hydraulic Fracturing," *Soc. Pet. Eng. J.* (March 1968) 1-12; *Trans.*, AIME, Vol. 243.
7. Haimson, B. C.: "Aspects of Mechanical Behavior of Rock Under Static and Cyclic Loading — Part B," *Annual Report* (March 1972) and *Semi-Annual Report* (Sept. 1972) to USBM Contract H-0210004-ARPA.
8. Determined in the rock mechanics laboratories of the U. of Wisconsin, Madison (unpublished).
9. Krech, W. W.: Personal communication (1972).
10. Filonenko-Borodich, M.: *Theory of Elasticity*, English ed., Peace Publishers, Moscow (1963) 88-89.
11. Jaeger, J. C.: *Elasticity Fracture and Flow*, Metheun & Co., Ltd., London (1962) 125-126.
12. Haimson, B. C., and Edl, J. N., Jr.: "Hydraulic Fracturing of Deep Wells," paper SPE 4061 presented at SPE-AIME 47th Annual Fall Meeting, San Antonio, Oct. 8-11, 1972.

***

N11, 1975

SORPTION OF ARSENIC FROM AQUEOUS SOLUTIONS BY FERROUS SULFIDE

UDC 622.7:628.34

Yu. O. Grigor'ev, N. G. Tyurin, O. G. Perederii, and N. N. Pustovalov

At a number of copper smelters, the concentration plant effluents and discharges from chemical production processes containing arsenic enter the same slime storage pond. The arsenic appears in the recirculating water when the overflow from such a pond is used as a recirculating supply source.

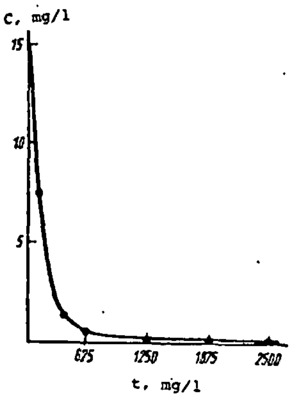

Fig. 1. Effect of sorbent mass upon residual arsenic concentration. Initial arsenic concentration 15 mg/liter; pH 7, τ = 20 min.

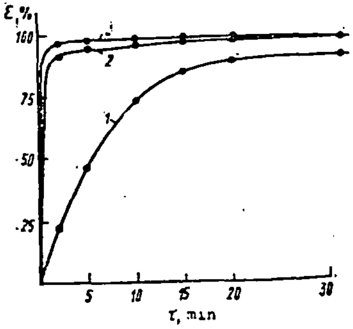

Fig. 2. Kinetics of arsenic extraction from solution by ferrous sulfide. Initial arsenic concentration 15 mg/liter; pH = 7. Sorbent concentration, g/liter: 1) 0.625; 2) 1.25; 3) 2.5.

Sampling the flotation tailings liquid phase under industrial conditions at the Krasnoural'sk Concentration Plant, which uses as a water supply slime pond outflows containing up to 60 mg/liter As (mainly in trivalent form), showed a reduction in the arsenic concentration under flotation conditions: in the bulk cycle the arsenic residual concentration is 0.15 mg/liter and 0.03-0.07 mg/liter in the selective cycle, which is in accordance with the public health norms.

It was assumed that the arsenic might be sorbed on sulfide minerals under flotation conditions.

Special investigations were undertaken to reveal the mechanism of the reaction between arsenic anions and sulfide minerals in an aqueous medium.

All the investigations were conducted with artificially produced sulfides, and with ferrous sulfide in particular, to avoid the possibility of undesirable effects from the impurities which exist in natural minerals. It was assumed in addition that when the optimum process characteristics were ascertained the method would be important in its own right, as a method of removing arsenic from non-ferrous metallurgy enterprise effluents.

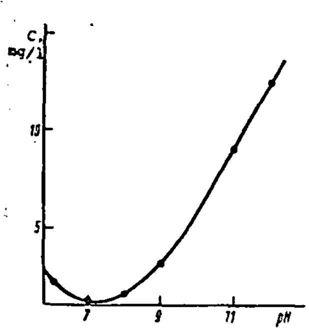

Fig. 3. Effect of pH upon residual arsenic concentration. Initial arsenic concentration 15 mg/liter; sorbent concentration 0.625 g/liter, τ = 10 min.

Ferrous sulfide was synthesized on the basis of ferrous sulfate and sodium thiosulfate in an alkaline medium, subsequently washing out the fine crystalline precipitate corresponding to FeS (Fe 64%, S 36%). The experimental method was as follows. The artificially prepared ferrous sulfide (FeS) was added to 400 ml of the initial solution of trivalent arsenic with a concentration of 15 mg/liter, with mixing at a high rate. The solution residual arsenic concentration was found by photometry, using silver diethyldithiocarbamate in pyridine solution [1].

It follows from Fig. 1 that even very small amounts of sulfide (30-15 mg per mg As) reduce the arsenic concentration to 1-2 mg/liter, and 500-1000 mg of sulfide purify the solutions (where FeS:As = 170), to the maximum permitted concentration.

The experimental curves (Fig. 2) indicate that there are two arsenic sorption stages: a rapid stage, in which most of the material is sorbed, and a slow stage which, when complete, brings the system into equilibrium.

In our view, the arsenic sorption process is in accordance with the equation

$$Fe_2S_2O_3(OH)_2 + 2AsO_2^- \rightleftarrows Fe_2S_2O_3(AsO_2)_2 + 2OH^-.$$

Thus arsenic must be a competing anion relative to the collector ions. It is known that substantial concentrations depress the flotation process [2]. It was established by experiment that the presence of up to 50 mg/liter of arsenic in the recirculating water at the Krasnoural'sk Concentration Plant did not have an adverse effect upon copper-zinc ore flotation figures.

A study of the effect of pH (Fig. 3) upon the extent of purification showed that the best results were achieved in the 6.5-7.5 pH range. This may be the result of changes in sulfide surface properties at various pH values. Elementary sulfur is formed on the mineral surface in an acid medium. This is confirmed by the fact that at pH 5-5.5 synthesized lead, zinc, and cadmium sulfides contain up to 1% elementary sulfur and do not sorb arsenic, even when air is bubbled through at high rates.

The investigations showed that sulfide minerals are sorption-active in relation to trivalent arsenic.

REFERENCES

1. A. K. Babko and A. T. Pilipenko, Photometric Analysis. Methods of Determining Non-Metals, Moscow, Khimiya, 1974, 257 pages, illustrated.

2. A. M. Gaudin, Principles of Flotation, Moscow, Gosgortekhizdat, 1963, 614 pages, illustrated.

1977 v.18 N1

SEPARATION OF ARSENIC FROM COBALTIFEROUS SOLUTIONS

UDC 669.778

L. I. Pimenov, R. N. Dudin, and I. F. Khudyakov

The removal of arsenic from cobaltiferous solutions is usually combined with iron removal. Up to the present there has been no single opinion as to the mechanism of arsenic precipitation.

A range of investigations to study conditions for arsenic separation have been carried out in the department of metallurgy of heavy non-ferrous metals at the S. M. Kirov Urals Polytechnical Institute by I. F. Khudyakov and E. Z. Kharitidi. They showed that thorough (98.5-99.5%) purification of solutions was possible when trivalent iron sulfate is added up to an Fe:As ratio in the solution of not less than 2:1.

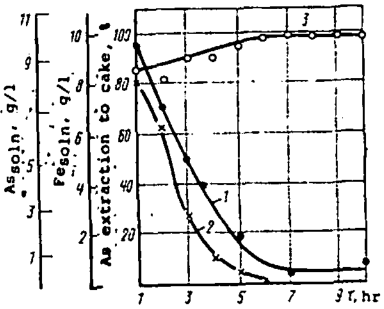

Fig. 1. Changes in As content (1) and Fe $^{+}$ content (2) of solution and in As extraction into cake (3) according to duration of oxidation with atmospheric oxygen.

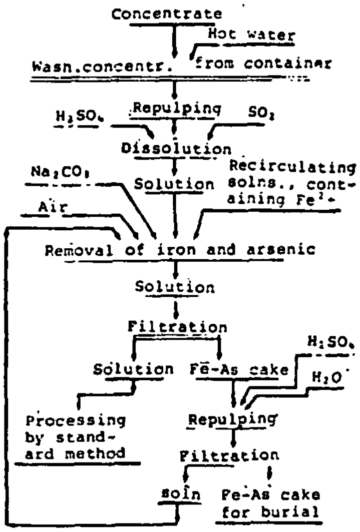

Fig. 2. Flow chart for processing concentrates containing arsenic.

Introduction of bivalent iron ions with subsequent oxidation by air or oxygen over a period of 1 hr ensures the removal of 92% As with air oxidation and 96-97% when oxygen is used.

The oxidation time, the ratio of iron to arsenic in the initial solution, the hydrogen ion concentration, and coprecipitation of valuable constituents into the ion-arsenic cakes are the most important indices in the operation of arsenical purification. Identifying the optimum parameters is therefore an urgent problem in processing concentrates containing arsenic.

Combined Results of Extraction of Elements into Filtrate, %

Element	Without repulping	With repulping at pH	
		3.0	3.5
Cobalt.	93,20	96,40	96,36
Nickel.	92,30	95,80	95,70
Copper.	68,80	83,40	83,00
Iron.	2,09	3,07	2,48
Arsenic	0,30	1,00	0,74

These patterns were studied under Urals Nickel Combine conditions, with actual solutions obtained from dissolving production concentrates. A proportional relationship between the Fe and As content and arsenic extraction into cake was found when studying the effect of the Fe:As ratio in the solution (Fig. 1).

Removal of arsenic at pH = 3.5 and t = 40° C was 85% at Fe:As = 1:1 and 94% at Fe:As = 2. Increasing the pH to 4.5 increased arsenic extraction into cake to 93% at Fe:As = 1:1, to 98% at Fe:As = 2:1, and to 99% at Fe:As = 4:1.

Reducing the acidity of the solution at the end of precipitation increases the extent of arsenic removal from the solutions. In these circumstances, however, there are increased losses of valuable metals with the precipitated cake.

Raising the temperature from 40-50 to 80° C causes some reduction in the extent of arsenic removal from the solutions, due to acceleration of the back reaction of arsenic compound dissolution.

The data obtained formed the basis of industrial technology for arsenic separation from cobaltiferous solutions (Fig. 2).

Acid repulping of the cakes (see Table) substantially increases the extraction of non-ferrous metals into the finished product and so reduces irrecoverable losses of

Technology News

FROM THE BUREAU OF MINES
UNITED STATES DEPARTMENT OF THE INTERIOR

Technology News provides information on the results of the Bureau of Mines Mining Research Program. It is published to encourage the transfer of this information to the mining industry, and its application in commercial practice. A free subscription may be obtained by writing to the Technology Transfer Group, Bureau of Mines, 2401 E. St. N.W., Washington, D.C. 20241.

No. 56, October 1978

Single Borehole Mining of Uranium Ore

Objective

To mine uraniferous sandstone in an economically feasible and environmentally compatible manner without placing men underground.

Approach

Uraniferous sand is remotely extracted through a single borehole by cutting into the ore around the borehole with a high pressure water jet, and pumping the resulting slurry to the surface.

How It Works

A 16-inch-diameter borehole is drilled from the surface down into the buried mineral deposit, and the mining tool is installed. High pressure water is released as a jet from a nozzle in the mining tool to erode the ore, forming a slurry that flows to the bottom of the cavity. The slurry is drawn into inlets located near the bottom of the drill string. See drawing.

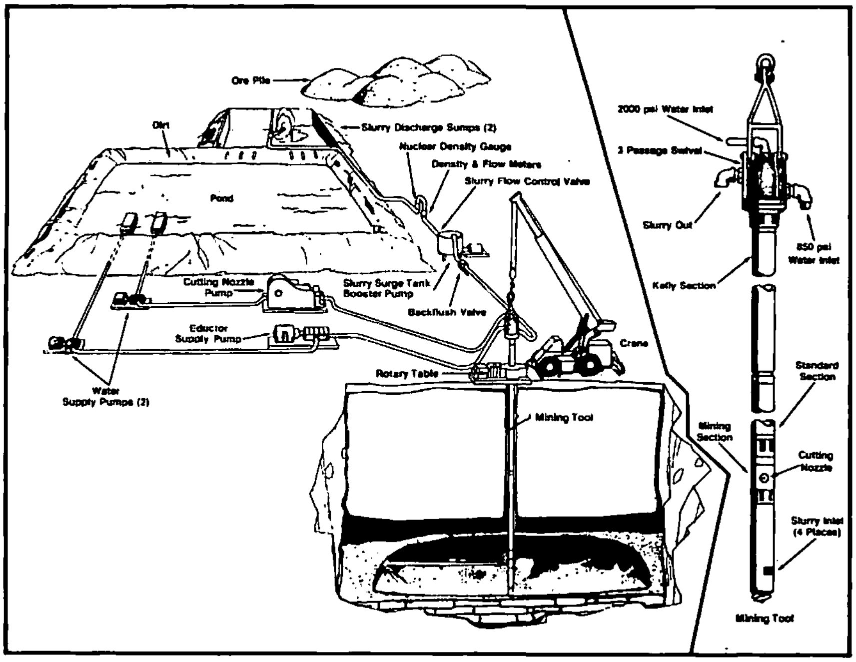

System and tool for single borehole slurry mining.

After being pumped to the surface, the slurry is weighed, metered, and checked for radioactivity. It is then deposited into one of a pair of sumps. Water collecting in the sumps drains into an adjoining pond for reuse. Thickened ore in the sumps is removed and placed in piles.

The mining tool consists of a 12-inch-diameter drill string and accessories, that is tipped with a mining section. This section has an auger at the bottom. Four slurry inlet holes and the eductor are located above the auger, and the single cutting nozzle is located near the top of the mining section.

A kelly section on the surface is connected to the mining section by lengths of standard pipe. The kelly section along with all the sections below it, can be rotated by means of the rotary table. Rotation is used to auger down into the broken ore in the borehole; it also allows the water jet to be turned.

Above the rotatable kelly section, there is a non rotating swivel section which is suspended from a crane. The swivel section contains two water inlets and one water outlet. These are connected to three annular passages, which in turn connect through the standard section to the mining section.

The underground system is powered by two sources of high pressure water on the surface. Water from a 2,000 psi pump is released from the cutting nozzle to erode the ore. Water from an 800 psi pump drives the eductor used to suck slurry from the mined cavity into the return flow.

The eductor was adopted for drawing off the slurry after repeated failures of pumps installed at the bottom of the drill string. The eductor, a low-efficiency, venturi section device has the overriding advantage of no moving parts. No failures or problems have occurred while pumping the abrasive uraniferous sandstone slurry or other slurries.

System benefits include:

1. Precludes health and safety problems of underground mining.
2. Ore fragmentation and transportation are a single continuous process.
3. Small or erratic deposits can be mined.
4. Production begins without underground development.
5. Crushing and grinding are unnecessary.
6. Environmental impacts are minimal. No overburden is removed. Groundwater quality is normally not impaired.

Test Results

This slurry borehole mining system is an outgrowth of Bureau of Mines research begun during 1973. Starting in July 1976 a coal mining design, built by Flow Industries to Bureau specifications, was tested for six weeks. Testing took place near Wilkenson, Washington on property of the Donald Hume Association, under a cooperative agreement with the Bureau. The first design was not economically feasible for coal mining, but analysis suggested that a higher output (40 tons per hour) system would be. Coal applications of this research are now responsibility of DOE.

To adapt the system to mining uranium-ore-bearing sandstone, the cutting pressure was reduced from 4,000 psi to 1,500 psi, and the flow was increased from 200 gpm to 1500 gpm. A second generation system was built incorporating a new nozzle and turning vanes, both designed by TRW corporation under a Bureau of Mines contract.

The improved system was successfully tested for six weeks beginning in July 1977. Testing took place at Nine-Mile Lake in Natrona County, Wyoming on property of the Rocky Mountain Energy Corporation under a cooperative agreement with the Bureau. During this testing ore was cut at horizontal distances of up to 25 feet and an average rate of 8 tons per hour. A total of 350 tons of uraniferous ore were mined from a 10-foot-thick seam at depths of 75 to 100 feet.

Testing of methods to prevent environmental damage should be completed this month. Two problems, subsidence of the ground above the mined cavity and the radioactivity of the ore tailings, are being attacked by injecting the ore tailings back into the hole. Future work includes evaluation of the effectiveness of this method for other minerals.

This mining system was developed by the Bureau of Mines through in-house research and contract research. The project officer is Dr. George Savanick of the Bureau's Twin Cities Mining Research Center.

Patent Status

The U.S. Department of the Interior is not applying for a patent on the borehole mining tool. The Department does hold a patent on a backwashing system that is often used with this tool. That system was invented by John B. Cheung and Earll M. Murman.

For More Information

Drawings and specifications are available. Requests should be addressed to:

Technology Transfer Officer
Bureau of Mines
Twin Cities Mining Research Center
P.O. Box 1660
Twin Cities, MN 55111

17th U.S. Symposium on Rock Mechanics,
Snowbird, Utah, Aug 25-27, 1976.

Chapter 24

SOME CONSIDERATIONS IN THE DESIGN OF BLASTS FOR IN SITU COPPER LEACHING

1976

by

Dennis V. D'Andrea,[1] William C. Larson,[2]
Peter G. Chamberlain,[1] and James J. Olson[3]

ABSTRACT

Blasts designed for in situ copper leaching must produce adequate fragmentation and permeability for successful leaching. Copper recovery depends to a large extent on the particle size distribution created by the blast, the permeability in the blast-fractured zone, and the ability to maintain solution flow with a minimum amount of channeling. This paper presents the results of Bureau of Mines experiments where core drilling was used before and after blasting to establish the degree of fragmentation. Data are presented from tests at the Sierrita mine of Duval Corp., and also from tests at the Emerald Isle mine of El Paso Mining and Milling Co. Copper recovery is predicted from fragment size distribution data using a computer model. Data from several blasts are used to show how predicted copper recovery is related to powder factor.

INTRODUCTION

Obtaining maximum copper recovery within a reasonable time is the most important requirement for successful in situ leaching. Copper recovery depends on the ore body mineralization, the degree of fragmentation produced by blasting, the permeability of the broken ore, the chemical characteristics of the leach solution, and the leach solution circulation system. Although all of these factors have significant effects on copper recovery, the blast design is the most important variable under the control of the mine operator. Blasting must adequately fragment the ore and produce a particle size distribution that is suitable for good leaching. The blasting must also increase permeability such that the leach solution can continue to contact the broken ore, with a minimum amount of channeling, for the life of the operation.

This paper describes a method of designing blasts for in situ leaching based on fragment size distribution measurements obtained from drill core taken before and after a series of test blasts. Bureau of Mines fragmentation experiments at the Sierrita mine of Duval Corp., near Tucson, Ariz. (2, 4) and at the Emerald Isle mine of El Paso Mining and Milling Co. near Kingman, Ariz. (1) are summarized. Copper recovery is predicted using a computer program and the results of fragment size measurements and laboratory leaching tests.

BLASTING TESTS

The Sierrita mine test was a nine-hole blast detonated with blasthole spacings of 15, 20, and 25 feet and powder factors of 1.13, 0.64, and 0.41 lb/ton, respectively. These blastholes were 9 inches in diameter and 110 feet deep. The Emerald Isle mine blasts were detonated in two test areas. The Phase I test area involved ore exposed in the pit bottom. Seven 8.375-inch-diameter blastholes 47 feet deep, spaced 25 feet apart, were used with a powder factor of 0.78 lb/ton. The ore fragmented in the Phase II test at the Emerald Isle mine was under 205 feet of overburden and extended to 277 feet. Two blasts were detonated in the Phase II area, the first with seven 9-inch-diameter blastholes spaced 20 feet apart with a powder factor of 0.95 lb/ton, and the second with three 9-inch-diameter blastholes spaced 18 feet apart with a powder factor of 1.47 lb/ton. The second Phase II test blast was detonated in an effort to improve the fragmentation in the area broken by the first blast.

CORE DRILLING

Core holes were drilled before and after blasting with an NQ double-barrel wireline system using drilling mud. The drill core produced was about 2 inches in diameter. Drilling into ore broken by blasting presented no major problems and was accomplished with return circulation of drill mud. The core drilling process did, however, create additional fracturing of the core, resulting in a finer fragment size distribution than was actually present in the blasted ore.

RESULTS OF FRAGMENT SIZE MEASUREMENTS

Table 1 lists the results of drill core measurements. The quartz monzonite porphyry ore at the Sierrita mine was more highly fractured initially than the Gila Conglomerate ore at the Emerald Isle mine. The Sierrita mine preshot core data are the average of three holes, and both the postshot 25-foot and the 20-foot spacing data are the averages of two holes. The Emerald Isle mine preshot core data are the average of two holes, one in the Phase I area and the other in the Phase II area. Preshot core from the Phase I and Phase II areas did not differ significantly so these two core holes were combined. Unfortunately a postshot core hole was not drilled in the Phase I test area at the Emerald Isle mine. However, a postleach core hole was drilled in this area after completion of an in-place leaching test.

Figure 1 shows the fragment size distribution curves for the Sierrita ore, and Figure 2 is a similar plot for the Emerald Isle ore. These curves were obtained by least squares fitting of the Weibull distribution function to the actual size data. The average size data listed in Table 1, based on 50 percent passing, were obtained using the curves shown on Figures 1 and 2.

---

[1] Geophysicist.
[2] Geologist
[3] Supervisory mining engineer.
All authors are with the Twin Cities Mining Research Center, Bureau of Mines, U.S. Department of the Interior, Twin Cities, Minn.

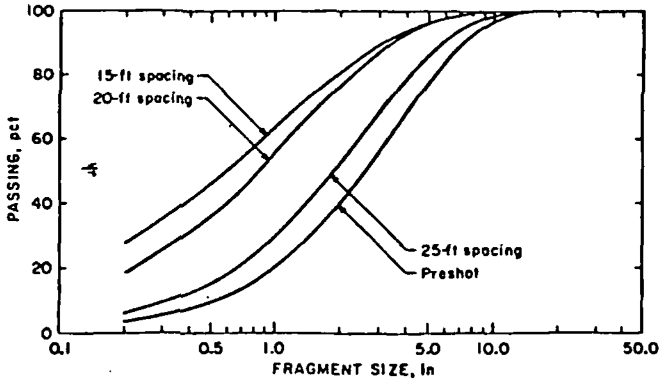

FIGURE 1. - Fragment size distribution curves for Sierrita ore.

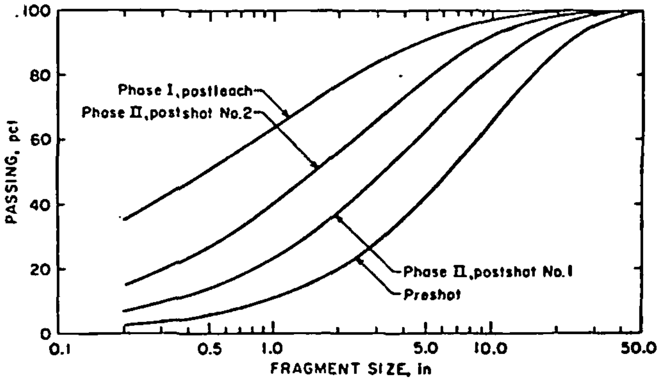

FIGURE 2. - Fragment size distribution curves for Emerald Isle ore.

COMPUTER-PREDICTED COPPER RECOVERY

Copper recovery was calculated from the size distribution data using a computer program developed by Madsen, Wadsworth, and Groves (3). This computer program, based on a mixed kinetics model, assumes that bulk solution transport is not rate controlling. Circulation of leach solution around each particle is assumed to be sufficient to maintain the necessary chemical reactions. In actual practice, however, the leach solution does not contact all of the ore because of channeling and permeability variations within the ore body so that this computer model will overestimate copper recovery values. Laboratory leaching tests were run to determine the two constants required as input to the computer program. These constants depend on the type of ore being leached and on the characteristics of the leach solution (primarily the pH).

Figure 3 shows the predicted copper recovery versus time for the Sierrita ore. These curves are based on leaching with sulphuric acid at a pH of 2. Figure 4 shows predicted copper recovery for the Emerald Isle ore based on leaching with sulphuric acid at a pH of 1.5. (These pH values were selected because laboratory leaching tests were run at these levels.) Although the measured fragmentation was better in the Sierrita ore, the predicted copper recovery was not as high as for the Emerald Isle ore owing to differences in pH and leaching characteristics of the ore.

Figure 5 is a plot showing predicted and actual copper recovery versus time for the Emerald Isle Phase I test area, which was leached in-place for 117 days. The actual copper recovery was much less than the predicted recovery, because (1) the computer model has limitations that result in overestimating the copper recovery, and (2) the drilling process created additional breaks and fracturing of the drill core resulting in a finer indicated size distribution than the true in situ size distribution. However, the procedure of coring and predicting copper recovery used in this paper does have value in establishing an upper limit on the predicted copper recovery.

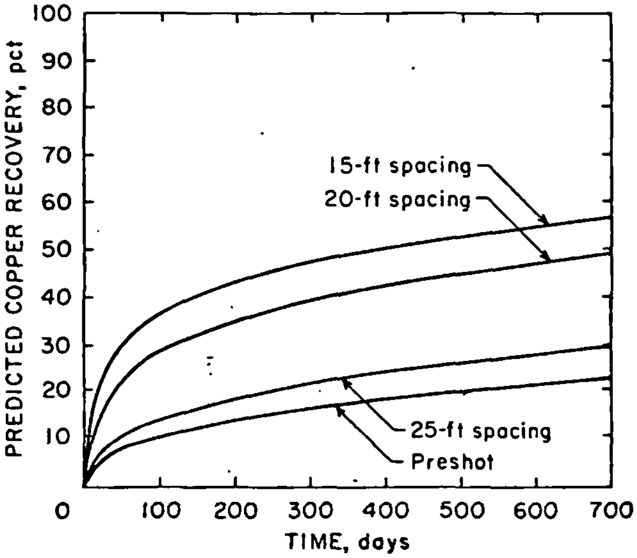

FIGURE 3. - Predicted copper recovery versus time for Sierrita ore.

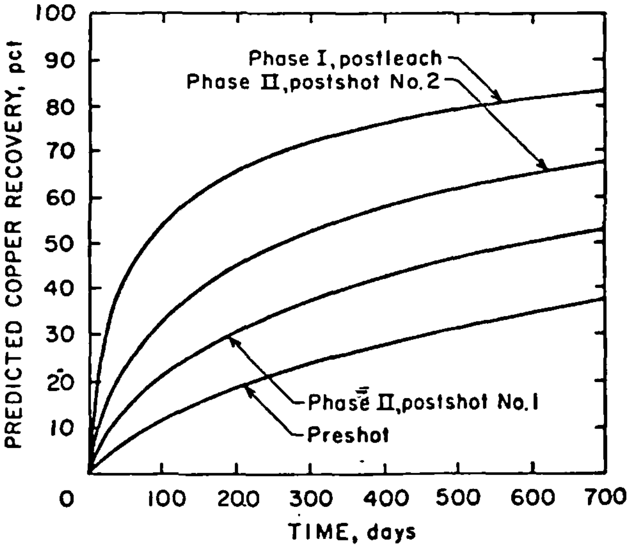

FIGURE 4. - Predicted copper recovery versus time for Emerald Isle ore.

TABLE 1. - Drill core data

	Emerald Isle			
	Preshot	Postleach, Phase I	Postshot 1, Phase II	Postshot 2, Phase II
Core run, ft	70.6	54.0	43.7	77.5
Core length recovery, pct	90	35	83	67
RQD, pct	68	11	40	31
Average size, in. (50% passing)	6.4	0.5	3.1	1.5
Largest piece, in	33	9	20	16
	Sierrita			
	Preshot	Postshot, 25-ft spacing	Postshot, 20-ft spacing	Postshot, 15-ft spacing
Core run, ft	117.5	113	105.5	110.5
Core length recovery, pct	98	79	52	37
RQD, pct	37	24	10	10
Average size, in. (50% passing)	2.6	1.9	.9	.6
Largest piece, in	17	11	9	9

TABLE 2. - Powder factor and predicted copper recovery

Location	Powder factor,[1] lb/ton	Predicted copper[2] recovery, pct
Sierrita		
Preshot	0.00	23
Postshot, 25-ft spacing	.41	30
Postshot, 20-ft spacing	.64	49
Postshot, 15-ft spacing	1.13	56
Emerald Isle		
Preshot	0.00	38
Phase II, postshot 1	.95	54
Phase II, postshot 2	2.42[3]	68
Phase I, postleach	.78	83

[1] Powder factor (lb/ton) = $1814 \frac{Pe}{P_r} \left(\frac{D}{S}\right)^2$

where

Pe = specific gravity, explosive
P_r = specific gravity, rock
D = blasthole diameter, ft
S = blasthole spacing, ft

for ore in powder column zone only

[2] Predicted recovery after 700 days of leaching.

[3] Powder factor of 2.42 is the sum of powder factors for two blasts with powder factors of 0.95 and 1.47.

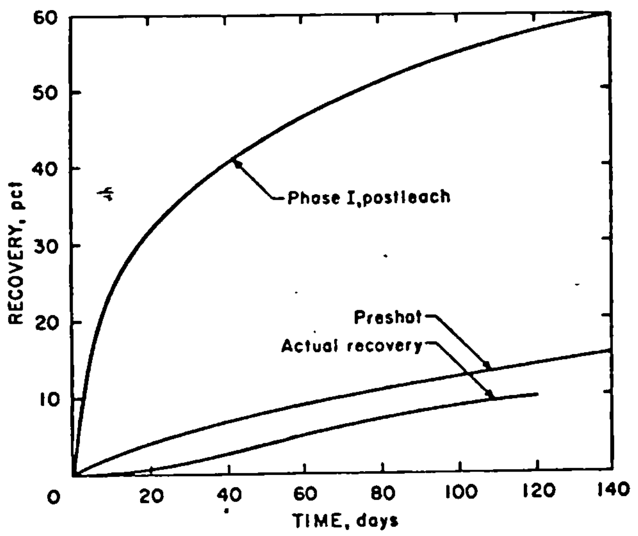

FIGURE 5. - Comparison of actual and predicted copper recovery for Emerald Isle ore.

If this upper limit is below that required for economic success, the deposit being investigated should not be leached in-place. With the use of improved drilling techniques utilizing a triple-tube core barrel with a split inner tube and the development of improved computer models for predicting copper recovery, the accuracy and reliability of predicting copper recovery by coring into blasted ore will be greatly improved.

PREDICTED COPPER RECOVERY VERSUS POWDER FACTOR

Table 2 lists the powder factors for each blast and the associated predicted copper recovery. The powder factor listed for the Emerald Isle Phase II, postshot 2 blast of 2.42 lb/ton is the sum of the individual powder factors for the two blasts that were detonated in the Phase II area with powder factors of 0.95 and 1.47 lb/ton. Figure 6 is a plot showing how predicted copper recovery increases with increasing powder factor. The Sierrita data and the Emerald Isle Phase I data are for blasts that broke ore from some depth to the surface. The Emerald Isle Phase II blasts were detonated under 200 feet of overburden, and the plot of these data indicates a slower rate of increasing predicted copper recovery due to the effects of overburden confinement. In actual practice the economic advantages of improved recovery due to better fragmentation with higher powder factors would have to be weighed against the greater drilling and blasting costs necessary for higher powder factors.

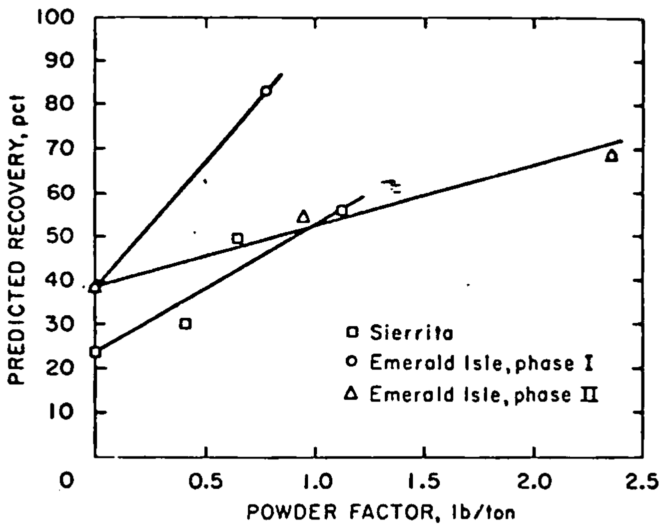

FIGURE 6. - Predicted copper recovery versus powder factor.

CONCLUSIONS

Core drilling before and after blasting is very useful in measuring the change in fragment size distribution created by blasts for in situ leaching. The upper limit of copper recovery can be predicted from the results of the fragmentation size distribution analysis and laboratory leaching tests using computer models. These methods can be applied to several small test blasts to estimate the relationship between predicted copper recovery and powder factor for a particular ore body. This combined information is valuable in establishing the in situ leaching potential of a copper ore body and in designing large blasts for in situ leaching.

REFERENCES

1. D'ANDREA, D.V., R.A. DICK, R.C. STECKLEY, and W.C. LARSON, 1974, A Fragmentation Experiment for In Situ Extraction, Proceedings, Solution Mining Symp., AIME Annual Meeting, Dallas, Tex., Feb. 25-27, 1974, pp. 148-161.

2. D'ANDREA, D.V. and S.M. RUNKE, 1976, In Situ Copper Leaching Research at the Emerald Isle Mine, Proceedings of the Society of Mining Engineers, AIME Fall Meeting, Denver, Colo., Sept. 1-3, 1976. (To be published.)

3. MADSEN, B.W., M.E. WADSWORTH, and R.D. GROVES, 1975, Application of a Mixed Kinetics Model to the Leaching of Low-Grade Copper Sulfide Ores, Trans. AIME, v. 258, pp. 69-74.

4. STECKLEY, R.C., W.C. LARSON, and D.V. D'ANDREA, 1975, Blasting Tests in a Porphyry Copper Deposit In Preparation for In Situ Extraction. BuMines RI 8070, 57 pp.

In Monograph On Rock Mechanics Applications in Mining
W. S. Brown, S.J. Green, W.A. Hustrulid, editors
Soc. Mining Engrs. of AIME, New York, 1977
17th Symposium on Rock Mechanics,
Snowbird, Utah 1976

Chapter 24

SOME CONSIDERATIONS IN THE DESIGN OF BLASTS FOR IN SITU COPPER LEACHING

by

Dennis V. D'Andrea,[1] William C. Larson,[2]
Peter G. Chamberlain,[1] and James J. Olson[3]

ABSTRACT

Blasts designed for in situ copper leaching must produce adequate fragmentation and permeability for successful leaching. Copper recovery depends to a large extent on the particle size distribution created by the blast, the permeability in the blast-fractured zone, and the ability to maintain solution flow with a minimum amount of channeling. This paper presents the results of Bureau of Mines experiments where core drilling was used before and after blasting to establish the degree of fragmentation. Data are presented from tests at the Sierrita mine of Duval Corp., and also from tests at the Emerald Isle mine of El Paso Mining and Milling Co. Copper recovery is predicted from fragment size distribution data using a computer model. Data from several blasts are used to show how predicted copper recovery is related to powder factor.

INTRODUCTION

Obtaining maximum copper recovery within a reasonable time is the most important requirement for successful in situ leaching. Copper recovery depends on the ore body mineralization, the degree of fragmentation produced by blasting, the permeability of the broken ore, the chemical characteristics of the leach solution, and the leach solution circulation system. Although all of these factors have significant effects on copper recovery, the blast design is the most important variable under the control of the mine operator. Blasting must adequately fragment the ore and produce a particle size distribution that is suitable for good leaching. The blasting must also increase permeability such that the leach solution can continue to contact the broken ore, with a minimum amount of channeling, for the life of the operation.

This paper describes a method of designing blasts for in situ leaching based on fragment size distribution measurements obtained from drill core taken before and after a series of test blasts. Bureau of Mines fragmentation experiments at the Sierrita mine of Duval Corp., near Tucson, Ariz. (2, 4) and at the Emerald Isle mine of El Paso Mining and Milling Co. near Kingman, Ariz. (1) are summarized. Copper recovery is predicted using a computer program and the results of fragment size measurements and laboratory leaching tests.

BLASTING TESTS

The Sierrita mine test was a nine-hole blast detonated with blasthole spacings of 15, 20, and 25 feet and powder factors of 1.13, 0.64, and 0.41 lb/ton, respectively. These blastholes were 9 inches in diameter and 110 feet deep. The Emerald Isle mine blasts were detonated in two test areas. The Phase I test area involved ore exposed in the pit bottom. Seven 8.375-inch-diameter blastholes 47 feet deep, spaced 25 feet apart, were used with a powder factor of 0.78 lb/ton. The ore fragmented in the Phase II test at the Emerald Isle mine was under 205 feet of overburden and extended to 277 feet. Two blasts were detonated in the Phase II area, the first with seven 9-inch-diameter blastholes spaced 20 feet apart with a powder factor of 0.95 lb/ton, and the second with three 9-inch-diameter blastholes spaced 18 feet apart with a powder factor of 1.47 lb/ton. The second Phase II test blast was detonated in an effort to improve the fragmentation in the area broken by the first blast.

CORE DRILLING

Core holes were drilled before and after blasting with an NQ double-barrel wireline system using drilling mud. The drill core produced was about 2 inches in diameter. Drilling into ore broken by blasting presented no major problems and was accomplished with return circulation of drill mud. The core drilling process did, however, create additional fracturing of the core, resulting in a finer fragment size distribution than was actually present in the blasted ore.

RESULTS OF FRAGMENT SIZE MEASUREMENTS

Table 1 lists the results of drill core measurements. The quartz monzonite porphyry ore at the Sierrita mine was more highly fractured initially than the Gila Conglomerate ore at the Emerald Isle mine. The Sierrita mine preshot core data are the average of three holes, and both the postshot 25-foot and the 20-foot spacing data are the averages of two holes. The Emerald Isle mine preshot core data are the average of two holes, one in the Phase I area and the other in the Phase II area. Preshot core from the Phase I and Phase II areas did not differ significantly so these two core holes were combined. Unfortunately a postshot core hole was not drilled in the Phase I test area at the Emerald Isle mine. However, a postleach core hole was drilled in this area after completion of an in-place leaching test.

Figure 1 shows the fragment size distribution curves for the Sierrita ore, and Figure 2 is a similar plot for the Emerald Isle ore. These curves were obtained by least squares fitting of the Weibull distribution function to the actual size data. The average size data listed in Table 1, based on 50 percent passing, were obtained using the curves shown on Figures 1 and 2.

---

[1] Geophysicist.
[2] Geologist
[3] Supervisory mining engineer.
All authors are with the Twin Cities Mining Research Center, Bureau of Mines, U.S. Department of the Interior, Twin Cities, Minn.

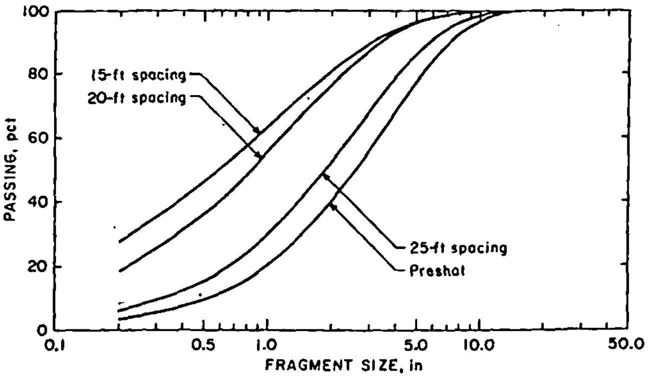

FIGURE 1. - Fragment size distribution curves for Sierrita ore.

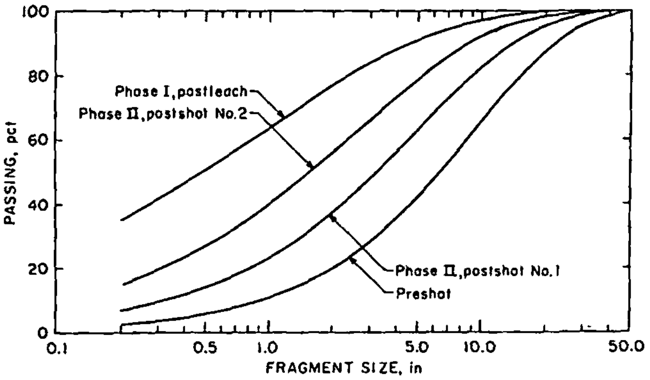

FIGURE 2. - Fragment size distribution curves for Emerald Isle ore.

COMPUTER-PREDICTED COPPER RECOVERY

Copper recovery was calculated from the size distribution data using a computer program developed by Madsen, Wadsworth, and Groves (3). This computer program, based on a mixed kinetics model, assumes that bulk solution transport is not rate controlling. Circulation of leach solution around each particle is assumed to be sufficient to maintain the necessary chemical reactions. In actual practice, however, the leach solution does not contact all of the ore because of channeling and permeability variations within the ore body so that this computer model will overestimate copper recovery values. Laboratory leaching tests were run to determine the two constants required as input to the computer program. These constants depend on the type of ore being leached and on the characteristics of the leach solution (primarily the pH).

Figure 3 shows the predicted copper recovery versus time for the Sierrita ore. These curves are based on leaching with sulphuric acid at a pH of 2. Figure 4 shows predicted copper recovery for the Emerald Isle ore based on leaching with sulphuric acid at a pH of 1.5. (These pH values were selected because laboratory leaching tests were run at these levels.) Although the measured fragmentation was better in the Sierrita ore, the predicted copper recovery was not as high as for the Emerald Isle ore owing to differences in pH and leaching characteristics of the ore.

Figure 5 is a plot showing predicted and actual copper recovery versus time for the Emerald Isle Phase I test area, which was leached in-place for 117 days. The actual copper recovery was much less than the predicted recovery, because (1) the computer model has limitations that result in overestimating the copper recovery, and (2) the drilling process created additional breaks and fracturing of the drill core resulting in a finer indicated size distribution than the true in situ size distribution. However, the procedure of coring and predicting copper recovery used in this paper does have value in establishing an upper limit on the predicted copper recovery.

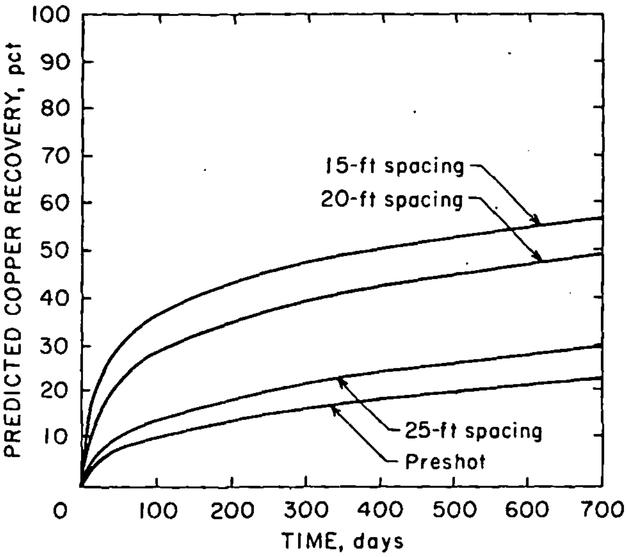

FIGURE 3. - Predicted copper recovery versus time for Sierrita ore.

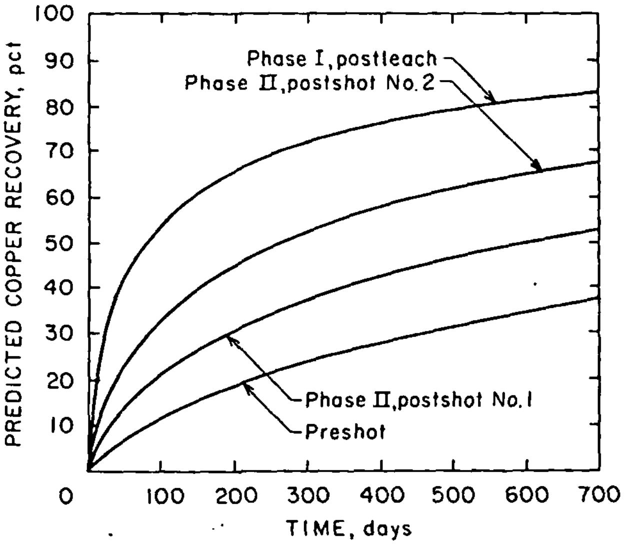

FIGURE 4. - Predicted copper recovery versus time for Emerald Isle ore.

TABLE 1. - Drill core data

	Emerald Isle			
	Preshot	Postleach, Phase I	Postshot 1, Phase II	Postshot 2, Phase II
Core run, ft............	70.6	54.0	43.7	77.5
Core length recovery, pct....................	90	35	83	67
RQD, pct................	68	11	40	31
Average size, in......... (50% passing)	6.4	0.5	3.1	1.5
Largest piece, in........	33	9	20	16
	Sierrita			
	Preshot	Postshot, 25-ft spacing	Postshot, 20-ft spacing	Postshot, 15-ft spacing
Core run, ft............	117.5	113	105.5	110.5
Core length recovery, pct...................	98	79	52	37
RQD, pct................	37	24	10	10
Average size, in........ (50% passing)	2.6	1.9	.9	.6
Largest piece, in.......	17	11	9	9

TABLE 2. - Powder factor and predicted copper recovery

Location	Powder factor,[1] lb/ton	Predicted copper[2] recovery, pct
Sierrita		
Preshot	0.00	23
Postshot, 25-ft spacing	.41	30
Postshot, 20-ft spacing	.64	49
Postshot, 15-ft spacing	1.13	56
Emerald Isle		
Preshot	0.00	38
Phase II, postshot 1	.95	54
Phase II, postshot 2	2.42[3]	68
Phase I, postleach	.78	83

[1] Powder factor (lb/ton) = $1814 \frac{Pe}{P_r} \left(\frac{D}{S}\right)^2$

where

Pe = specific gravity, explosive
P_r = specific gravity, rock
D = blasthole diameter, ft
S = blasthole spacing, ft

for ore in powder column zone only

[2] Predicted recovery after 700 days of leaching.

[3] Powder factor of 2.42 is the sum of powder factors for two blasts with powder factors of 0.95 and 1.47.

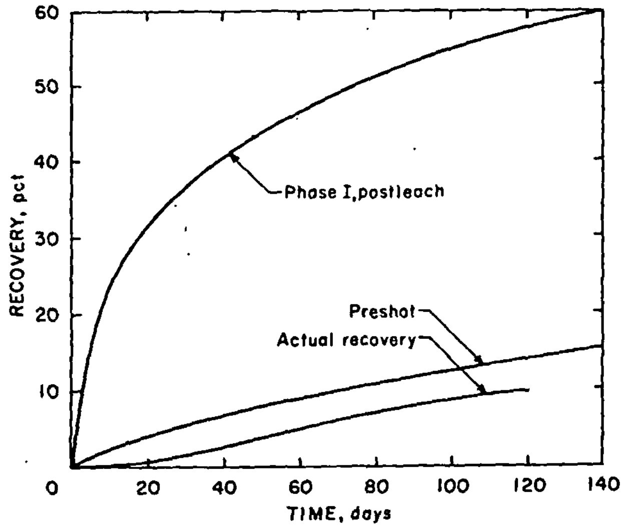

FIGURE 5. - Comparison of actual and predicted copper recovery for Emerald Isle ore.

If this upper limit is below that required for economic success, the deposit being investigated should not be leached in-place. With the use of improved drilling techniques utilizing a triple-tube core barrel with a split inner tube and the development of improved computer models for predicting copper recovery, the accuracy and reliability of predicting copper recovery by coring into blasted ore will be greatly improved.

PREDICTED COPPER RECOVERY VERSUS POWDER FACTOR

Table 2 lists the powder factors for each blast and the associated predicted copper recovery. The powder factor listed for the Emerald Isle Phase II, postshot 2 blast of 2.42 lb/ton is the sum of the individual powder factors for the two blasts that were detonated in the Phase II area with powder factors of 0.95 and 1.47 lb/ton. Figure 6 is a plot showing how predicted copper recovery increases with increasing powder factor. The Sierrita data and the Emerald Isle Phase I data are for blasts that broke ore from some depth to the surface. The Emerald Isle Phase II blasts were detonated under 200 feet of overburden, and the plot of these data indicates a slower rate of increasing predicted copper recovery due to the effects of overburden confinement. In actual practice the economic advantages of improved recovery due to better fragmentation with higher powder factors would have to be weighed against the greater drilling and blasting costs necessary for higher powder factors.

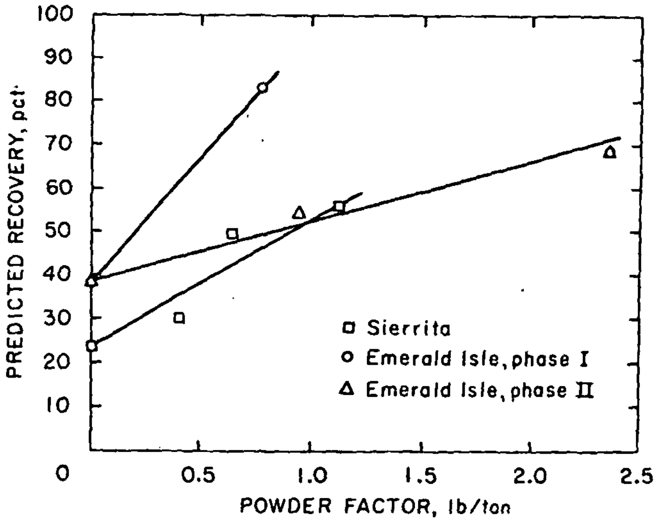

FIGURE 6. - Predicted copper recovery versus powder factor.

CONCLUSIONS

Core drilling before and after blasting is very useful in measuring the change in fragment size distribution created by blasts for in situ leaching. The upper limit of copper recovery can be predicted from the results of the fragmentation size distribution analysis and laboratory leaching tests using computer models. These methods can be applied to several small test blasts to estimate the relationship between predicted copper recovery and powder factor for a particular ore body. This combined information is valuable in establishing the in situ leaching potential of a copper ore body and in designing large blasts for in situ leaching.

REFERENCES

1. D'ANDREA, D.V., R.A. DICK, R.C. STECKLEY, and W.C. LARSON, 1974, A Fragmentation Experiment for In Situ Extraction, Proceedings, Solution Mining Symp., AIME Annual Meeting, Dallas, Tex., Feb. 25-27, 1974, pp. 148-161.

2. D'ANDREA, D.V. and S.M. RUNKE, 1976, In Situ Copper Leaching Research at the Emerald Isle Mine, Proceedings of the Society of Mining Engineers, AIME Fall Meeting, Denver, Colo., Sept. 1-3, 1976. (To be published.)

3. MADSEN, B.W., M.E. WADSWORTH, and R.D. GROVES, 1975, Application of a Mixed Kinetics Model to the Leaching of Low-Grade Copper Sulfide Ores, Trans. AIME, v. 258, pp. 69-74.

4. STECKLEY, R.C., W.C. LARSON, and D.V. D'ANDREA, 1975, Blasting Tests in a Porphyry Copper Deposit In Preparation for In Situ Extraction. BuMines RI 8070, 57 pp.

SITE CHARACTERIZATION OF JOINT PERMEABILITY USING THE HEATED BLOCK TEST

By M. Voegele, E. Hardin, D.

Terra Tek, Inc., S

Proceedings of the 22nd U.S. Symposium on Rock
Mechanics: Rock Mechanics from Research to Application
held at Mass. Inst. of Tech., June 28-July 2, 1981
compiled by H.H. Einstein

INTRODUCTION

The isolation of nuclear waste in a mined rock repository poses unique problems in site characterization. The ultimate barrier to radionuclide migration to the biosphere is the joints and major discontinuities that are pervasive at least to several kilometers depth. Modelling the potential effects of these joints on near-field conditions requires that the thermal, mechanical and hydraulic properties of joints are coupled. Acquisition of joint data is therefore a more demanding problem than at any previous time.

Tunneling and mining experience, physical models (Barton and Hansteen, 1979) and numerical models (Voegele 1978, Wahi et al. 1980) demonstrate the possibility of significant shear displacement along joints exposed by an excavation. This process is enhanced by anisotropic stress distributions, by transient thermal loading and by dynamic loading from earthquakes. If the relevant joints are rough, with high wall strength, stability will not necessarily be reduced by the shearing process since roughness-induced dilation will lock the joints in some finite displaced position. The only serious consequence of this process is the joint aperture strain. Permeability may be enhanced around the repository and shaft. According to the present studies a significant shear displacement may be as little as 0.2 mm.

Model studies of flow in a rough joint replica sheared at very low stress reported by Maini (1971), indicated that joint permeability could increase as much as one order of magnitude in the first 2 mm of shear displacement, and a further one order of magnitude in the next 4 mm of shear displacement. Although these effects would be reduced at realistic levels of normal stress, their influence could have important influence on repository sealing requirements.

The effect of temperature on joint permeability has not been an area of extensive research, although this deficiency is rapidly being adjusted. Tests by Nelson (1975) on single fractures in sandstone subjected to a relatively low confining pressure (0.1 MPa) indicated initial increases in permeability to 60°C, followed by significant reductions when increasing the temperature further to 100°C. In-situ tests conducted in Stripa granite by Lundström and Stille (1978) using water temperatures of 10°C and 35°C indicated a 50% reduction in joint permeability, despite the reduced viscosity of water at the higher temperature. Unfortunately there was no coupling of permeability measurements with the full-scale and time-scaled heater experiments, and no possibility of controlling the total normal stress acting across the joints during the flow tests.

Ambient tests of joint permeability as a function of normal stress or aperture have been widely reported There appears to be considerable discrepancy in the interpretation of results. Some authors (e.g. Witherspoon et al. 1979a) have suggested that the cubic law relating aperture and flow rate is valid even for rough fractures in intimate contact. Other authors (e.g. Kranz et al. (1979) and Walsh (1981)) have explained the measured flow reductions caused by tortuosity and roughness, by a modification to the law of effective stress.

The possibility of a scale effect on joint permeability has been suggested by Witherspoon et al. (1979b). At present, the data base is too limited and diverse to make definite conclusions. It is often unreasonable to try to compare the permeabilities of rough, fresh artificial fractures (a typical test configuration) with weathered natural joints of different roughness, since the degree of aperture closure under a given stress level will vary in each case. Recent work (Barton, 1981a) suggests that scale dependent joint permeability will probably not be a significant factor under conditions of pure normal closure, but will be observed when shearing occurs. This is due to the scale-dependent dilation that occurs when joints of different length are sheared, as shown in a major test program reported by Bandis (1980).

HEATED BLOCK TEST

The pressing need for large scale coupled thermo-mechanical-hydraulic test data prompted Terra Tek's current 8 m^3 block test, performed under contract with the Office of Nuclear Waste Isolation. The site is located in gneiss, about 150 metres underground in a test adit in the Colorado School of Mines experimental mine in Idaho Springs.

The 2x2x2 metres block is located in the floor of the test adit. Loading is applied on four vertical sides with flatjacks. The base is attached to the surrounding rock mass. The vertical sides of the specimen were formed by line drilling. The extreme hardness of the quartz lenses in the gneiss caused unexpected difficulties with hole alignment, and diamond coring of the slots was required.

The surface of the block is instrumented with some 30 pairs of Whittemore bolts for recording strain and/or displacement across joints, four Irad strain metres, and five surface strain gauge rosettes. Deformation occurring across the block as a whole is registered with horizontal DCDT rod extensometers. Deformations within the block are monitored with MPBX borehole extensometers. Stress levels are monitored using a variety of instruments. Four vertical holes are used for cross-hole dynamic modulus determination. Data acquisition is accomplished by means of a computer controlled system which stores the readings on magnetic tape and is supplemented by manual readings of certain instruments.

A unique feature of the test facility is the line of heaters crossing the center of the block, shown schematically in Figure 1. The nine boreholes contain linear heaters, equally spaced 40 cm apart. The combination of heaters and flatjacks has permitted joint permeability to be measured under normal stress or combined shear and normal stress, at any rock temperature in the range 12°-74°C. At the highest temperature the rock reaches 140°C in the heater plane. The block was subjected to a variety of load and temperature paths as detailed in the test matrix shown in Figure 2.

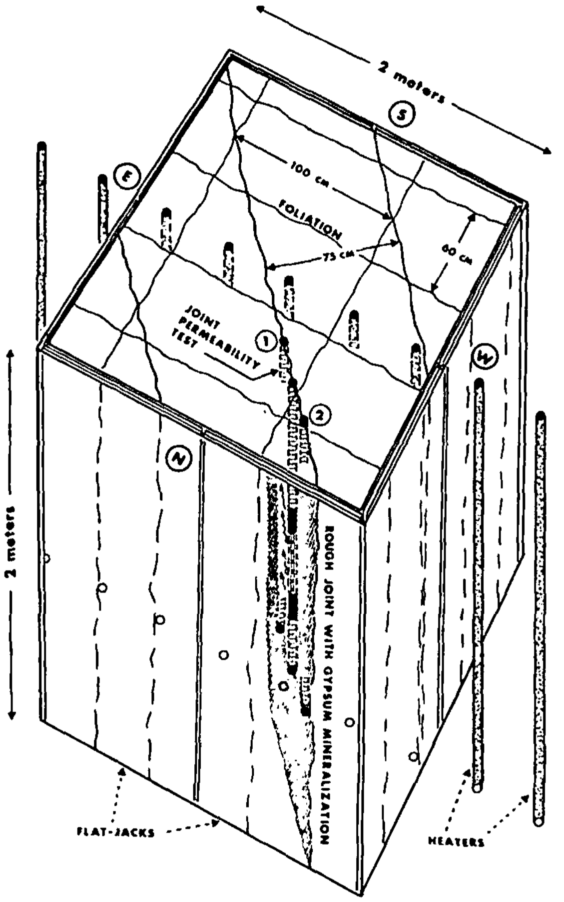

FIGURE 1. Schematic view of test block showing the line of heaters, the permeability test location, and the mean joint frequency and orientation.

The major mineralized diagonal joint (Figure 1) chosen for permeability testing was subjected to pure normal stress under the equal biaxial load cycles. Under the two uniaxial tests the joint was subjected to proportional shear and normal stress, with a shear reversal between the N-S and E-W tests.

SUMMARY OF BLOCK STRUCTURE AND JOINT PROPERTIES

Joint mapping in the roof and walls of the test adit surrounding the block reveals three sets of significant joints (i.e. continuity >2 metres). Each is steeply dipping or vertical. The mean spacing of the three sets is shown schematically in Figure 1. The block size index (ISRM 1978) is approximately 75 cm, the volumetric joint count approximately 4.8 joints/m^3 (medium size blocks), and the RQD approaches 100%. Significant horizontal or sub-horizontal jointing is not in evidence. There are probably at least 30 discrete, interlocked blocks of rock within the 8 m^3 test block.

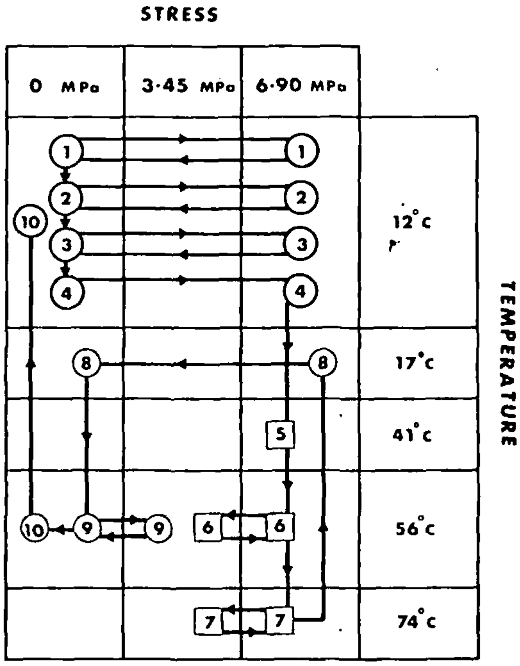

FIGURE 2. Test matrix for the present series of block tests.

1. Equal biaxial, cycle to 6.9 MPa
2. N-S uniaxial, cycle to 6.9 MPa (AMBIENT)
3. E-W uniaxial, cycle to 6.9 MPa
4. Equal biaxial, load to 6.9 MPa

5. Equal biaxial, 41°C
6. Equal biaxial, cycle, 56°C (HEATING
7. Equal biaxial, cycle, 74°C AND COOLING
8. Equal biaxial, unload, 17°C CYCLES)
9. Unconfined, 50°C, and 55°C cycle
10. Unconfined, ambient

When interpreting the test results and attempting to extrapolate our results to other environments, it is helpful to have a quantitative characterization of the jointing that can be used in numerical modelling. For this reason, extra care was taken with characterization of the set of diagonal joints, which were the subject of this study.

The diagonal joints are hydrothermally altered, with gypsum mineralization and iron staining of the joint walls. By contrast the foliation joints show little evidence of alteration or weathering. The roughness of all the joints was recorded in numerous locations using a 15 cm long contour gauge, and was also measured over longer base lengths. Visual estimation of the joint roughness coefficient (JRC) using Barton and Choubey's (1977) set of profiles, was supplemented with self-weight tilt tests of jointed pieces of drill core (Figure 3). These cores were obtained from the permeability test holes, which were drilled down the plane of the major diagonal joint. The various estimates of JRC were converted to natural block size values using the methods derived by Bandis et al. (1981).

The compressive strength of the joint walls (JCS) was measured with a Schmidt hammer. The diagonal joints proved to be markedly weaker than the other two

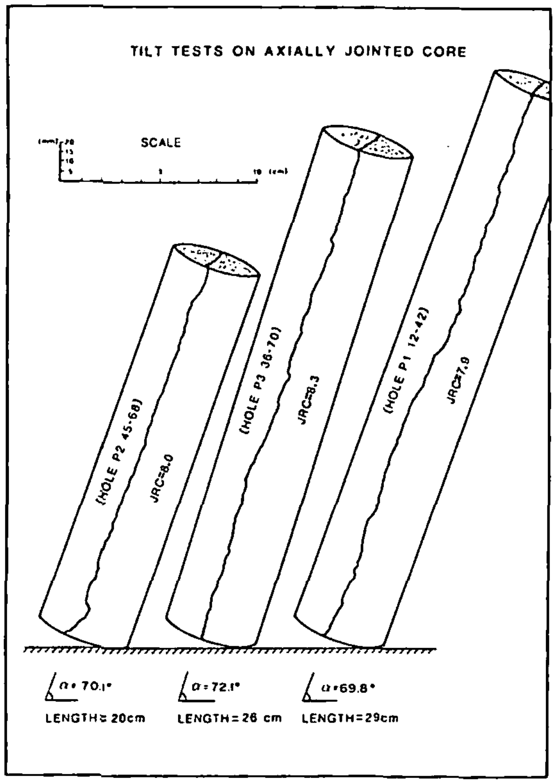

FIGURE 3. Characterizing the diagonal joints drilled from the three permeability test holes, P1, P2 and P3.

joint sets, due to alteration. These values were again converted to natural block size values.

Significant properties for interpretation of joint strength and deformability are listed below:

	Estimated full-scale values		
	JCS	JRC	ϕr
Diagonal joints	50-65 MPa	6.7-10.0	25°

Peak friction angles (ϕ') for the diagonal joints which are loaded in shear during the uniaxial tests, are given by the following equation (Barton and Choubey, 1977):

$$\phi' = \text{JRC} \log (\text{JCS}/\sigma_n') + \phi_r \qquad (1)$$

where σ_n' = effective normal stress
ϕ_r = residual friction angle

These parameters are used to model the complete shear stress-displacement and dilation behavior of joints (Barton, 1981b). Other recent work by Bandis (1980) has shown that JCS and JRC also control the normal stiffness and closure of joints. Consequently, the joint permeability measured during the various load paths will also depend on these parameters.

MECHANICAL CONSTRAINTS OF A CONTINUOUS BASE

The two metre cube of rock was isolated from the surrounding rockmass on four sides, but the base was continuous. Analysis showed that for deformation in the elastic range, the upper 80% of the block would be essentially unaffected by a continuous base, i.e. down to a depth of some 160 cm, strains would be uniform.

During uniaxial loading the high shear stresses developed on the diagonal joints tend to deform the block beyond the elastic range. However, this initial tendency is strongly resisted by the stiffening behavior of the underlying rock mass. In effect, only a portion of each diagonal joint is subject to shear, making shear resistance high. Figure 4 indicates the estimated range of peak shear strength, assuming that the base of the block was a frictionless boundary. The N-S and E-W uniaxial load paths shown in the same figure did not cause gross shearing along the diagonal joints due to the restraint of the continuous base. In reality the strength envelopes should be displaced several MPa to represent the cohesive, stiffening effect of the underlying rock mass.

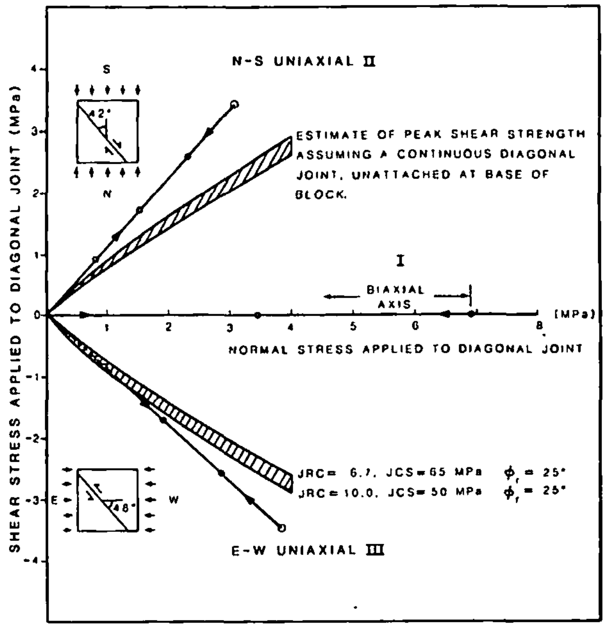

FIGURE 4. Comparison of biaxial and uniaxial load *paths with the shear strength of the diagonal joints,* assuming the block was bounded by a frictionless base.

The measured shear displacements experienced by the major diagonal joint during the N-S and E-W uniaxial load paths are shown in Figure 5. The N-S test is the first shearing event, and it is resisted by an initial shear stiffness of 4.8 MPa/mm. This increases rapidly as shear displacements approach 0.2 mm. Despite these mechanical constraints, joint permeability was clearly affected by these aperture strains, small as they appear.

JOINT PERMEABILITY AS A FUNCTION OF STRESS

Joint conductivity was monitored by injecting water along the major diagonal joint. This was done utilizing double packers located in a central hole drilled coaxially down the joint (Figure 1). The flow section was at a depth interval of 66-109 cm. Flow rates were monitored at the bottom of parallel boreholes drilled each side of the vertical injection hole. Hole No. 1 was 18.5 cm from the injection hole, hole No. 2 was 24 cm in the opposite direction.

Analysis of the drill core recovered from these holes indicates that due to its roughness and local undulations, the diagonal joint is not intersected by hole No. 2 in the depth interval 70-130 cm. Flow rates were correspondingly low towards this hole, and at

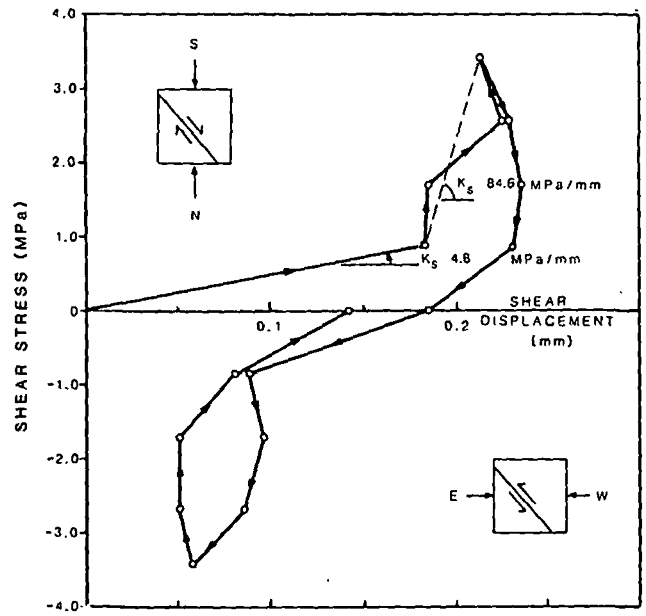

FIGURE 5. Shear displacement of the diagonal test joint is limited by the continuous base. Reversal is only partial during E-W loading.

some stress levels the flow rate fell below measurable levels (i.e., <0.001 cm^3/sec). Consequently only the flow rates towards hole No. 1 are analyzed here. It is estimated from the core analysis that a section of the injection interval (95-105 cm) is non-conducting, and a section of observation hole No. 1 (103-109 cm) also non-conducting, due to the undulating joint passing outside the boreholes locally. This means that the measured flow rates may be some 10-15% less than representative for the joint as a whole.

The flow rate was measured by a depth indicator installed in the observation holes. The pressure gradient was assumed to be approximately linear, and equal to the injection pressure divided by the distance between the two holes. Injection pressures used in the ambient tests were 0.14, 0.24 and 0.34 MPa (20, 35 and 50 psi).

Figure 6 summarizes the results of the first three ambient permeability tests. The numbers 1 through 8 indicate the order of testing. Theoretical smooth wall apertures (e) and permeabilities ($e^2/12$) can be calculated from the following well known equation for linear flow between parallel plates:

$$q = \frac{de^3}{12\mu} \cdot \frac{dP}{dy} \qquad (2)$$

where dP/dy = pressure gradient
μ = absolute viscosity (1.24x10^{-5} gm.sec/cm^2 at 12°C)
d = width of flow path
q = flow rate

Table 1 summarizes the most significant data from the three first ambient tests.

The permeability of the joint when it was virtually unloaded by drilling four slots round the sides of the block, was equivalent to that of a smooth wall aperture (e) of 60.7 microns. Each of the three ambient load paths reduced this to between 27.1 and 30.3 microns at the highest stress level. Subsequent biaxial loading to 6.9 MPa prior to heating the block also produced an equivalent aperture of the same magnitude; 30.0 microns. The relationship between these theoretical smooth wall aperture changes, and the change of real joint aperture measured during the various load cycles is discussed later.

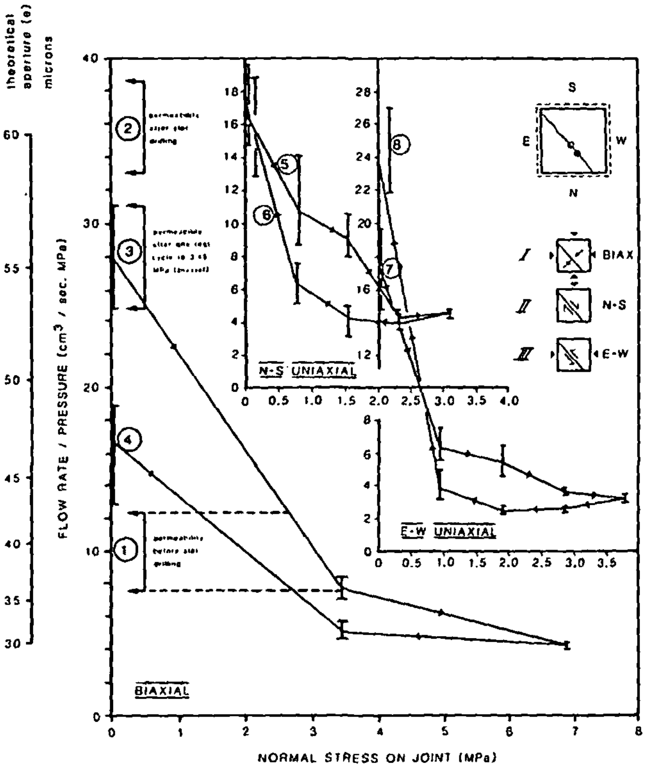

FIGURE 6. Effect of normal stress on flow rate and on the theoretical smooth wall aperture (e) (1 micron = 0.001 mm). Ambient tests.

Table 1

Stress Dependency of Joint Permeability
Rock Temperature = 12°C

Stresses on Joint σ_n (MPa)	τ (MPa)	e (micron)	K (darcys)
Pre-slot drilling (in-situ stress)		38.6	124
Post-slot drilling			
0	0	60.7	307
1. Biaxial			
0	0	55.7	259
6.9	0	29.7	73.5
0	0	46.9	183
2. N-S uniaxial			
0	0	46.9	183
3.1	3.4	30.3	76.5
0	0	47.6	189
3. E-W uniaxial			
0	0	47.6	189
3.8	3.4	27.1	61.2
0	0	52.7	231

1 micron = 0.001 mm; 1 darcy = 10^{-8} cm^2

JOINT PERMEABILITY AS A FUNCTION OF STRESS AND TEMPERATURE

The rock temperature gradients established during the various heating cycles were monitored with 80 thermocouples located in boreholes throughout the block. The rock temperature at the permeability test interval was interpolated from two thermocouples located 50 and 75 cm from the heater plane. Twenty-one days heating at an output of 500 watts per borehole heater, established a quasi-steady state gradient, giving a rock temperature of 55° at the test interval. A further twelve days at 700 watts per heater increased this to 74°C. Cooling to near-ambient temperature (17°C) took 33 days.

Various flow tests were performed to investigate the effect of mismatching the rock temperature and the water temperature at the injection side of the test. It was found that the calculated smooth-wall flow apertures (e) were more consistent when the rock temperature was used to estimate the viscosity of the water, in place of the injection water temperature. There was evidence for suspecting that cold water injected into a hot rock joint caused aperture increase. Efforts were therefore made to preheat the water to the rock temperature. A mismatch of 5° or 10° did not appear critical since the heat capacity of the rock, combined with the slow flow rates, were sufficient to guarantee flow temperatures equal to rock temperatures.

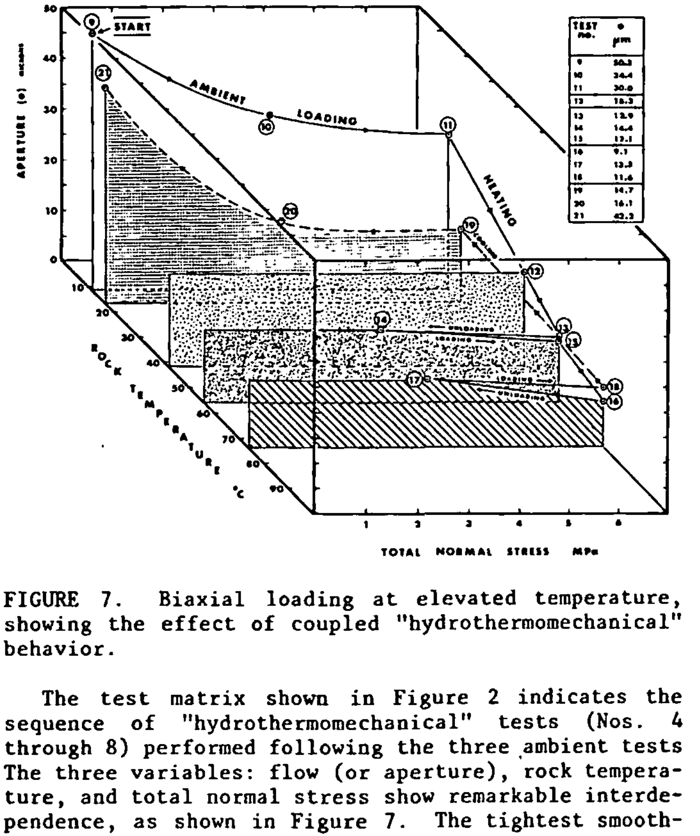

FIGURE 7. Biaxial loading at elevated temperature, showing the effect of coupled "hydrothermomechanical" behavior.

The test matrix shown in Figure 2 indicates the sequence of "hydrothermomechanical" tests (Nos. 4 through 8) performed following the three ambient tests The three variables: flow (or aperture), rock temperature, and total normal stress show remarkable interdependence, as shown in Figure 7. The tightest smooth-wall aperture of 30.0 microns achieved at ambient temperature (12°C) and under a total normal stress of 6.9 MPa was reduced to 18.3 μm at 41.4°C and to 9.1 μm at 73.6°C. Thus increased temperature alone reduced joint permeability by an order of magnitude from 75 darcys to 6.8 darcys.

This remarkable reduction of flow aperture (which could not possibly be achieved at ambient temperature without exceptionally high stress levels) is interpreted as improved mating of the opposed joint walls. The diagonal joints are quite rough, and they were undoubtedly formed at elevated temperature, though how high is uncertain. A roughness profile of a joint measured at ambient temperature will not exactly match a profile measured while the joint is at elevated temperature, due to thermal expansion. Our elevated temperature and pressure partially recreate formation conditions. The improved mating of the asperities is almost maintained by pressure alone during cooling, probably due to the high shear strength of the tightly mated walls. Significant lack of fit was not re-established until the aperture rebounded from 16.1 to 42.2 μm, which occurred somewhere between 3.45 MPa and 0 MPa (points 20 and 21 in Figure 7).

The inversion of the load cycle at 74°C (points 16, 17 and 18) is further evidence that temperature may have a more powerful influence on aperture (e) than pressure. After unloading to 3.45 MPa, a reloading to 6.9 MPa was insufficient to "reclose" the joint to the same extent. The table below suggests that the scatter of flow data is insufficient to invalidate this conclusion, despite the diminuitive apertures involved.

Table 2

Sample of Experimental Scatter From Three Sets of Flow Data

Test No. (Figure 7)	Mean e (μm)	Range (μm)	σ_n (MPa)
16	9.06	8.6-9.8	6.90
17	13.5	13.1-14.1	3.45
18	11.6	11.5-11.7	6.90

The final sequence of heated flow tests shown in Figure 2 (Nos. 9 to 10) were conducted on the unconfined side of our loading matrix. The starting point was No. 21 on Figure 7, with T = 16.5°C, σ_n = 0 MPa and e = 42.2 μm. This aperture increased to 48.2 μm at 50.5°, presumably due to the thermal expansion of the roughness profile, which was not in this case in intimate contact with its mating half due to the absence of confinement. The aperture (e) returned to 41.9 μm at 55°C. A load cycle to 3.45 MPa (equal biaxial) at 56°C induced significantly better fit, with (e) closing to 17.5 μm. The subsequent unconfined test allowed the aperture to rebound to 36.5 μm. It appears that the "hydrothermomechanical" closure effect is only achieved when there is coupling of both temperature and pressure. This is quite logical when conditions under which joints were formed are visualized.

COMPARISON WITH REPORTED DATA

Witherspoon et al. (1979b) considered that the four thick curves shown in Figure 8 were potential evidence of a scale effect on fracture permeability. Our in-situ ambient data for the natural mineralized joint shows close agreement with the Pratt et al. (1977) in-situ data for a joint in granite, and apparently lends support to this scale effect hypothesis.

However, several aspects of the hypothesis are suspect. Chief of these is the attempt to compare artificial, unweathered tension fractures (Iwai, 1976 and Witherspoon et al., 1977) with natural weathered joints. Bandis (1980) has shown that joint apertures tend to be larger when joints are weathered, with low

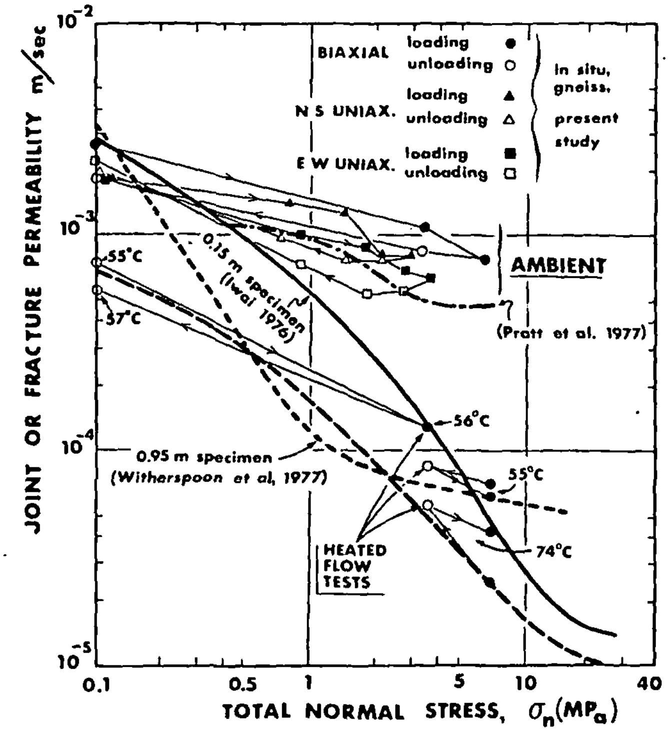

FIGURE 8. Comparison of ambient and heated flow tests performed in the present block test, with data presented by Witherspoon et al. (1979b).

JCS values. In addition, the closure measured under a given level of normal stress is found to depend on the values of JCS, JRC and the initial aperture. Weathered joints and artificial fractures are therefore likely to exhibit different permeability-stress relationships even at the same scale, unless their properties (JRC, JCS) are matched. Temperature "matching" is also important.

Intuitively, samples of different size taken from the same joint would not seem likely to exhibit different permeabilities if subjected to the same normal load paths, since pure normal closure is likely to depend on the properties of the small steeply inclined asperities at all scales.

However, when shearing of the joint is an added variable, the scale dependent properties of JRC and JCS must be considered (Bandis et al., 1981). The reduction of these two parameters with increasing sample size immediately introduces a potential permeability scale effect. The reason for this is seen in Figure 9, which illustrates the recent development of dilation modelling for different joint sample sizes taken from the same joint (Barton, 1981b). Increasing the size of sample causes delayed dilation, and seems sure to guarantee a major scale effect on permeability if significant shearing occurs.

An extremely interesting point emerges from the comparison of joints and artificial fractures shown in Figure 8. The artificial fractures were generated and presumably flow-tested at nearly the same ambient conditions in the laboratory. In contrast, the natural joints in gneiss and granite were undoubtedly formed at elevated temperature and pressure. Our results show that when joints are flow-tested at elevated temperature and pressure, mating of the joint walls apparently approaches the degree of mating achieved

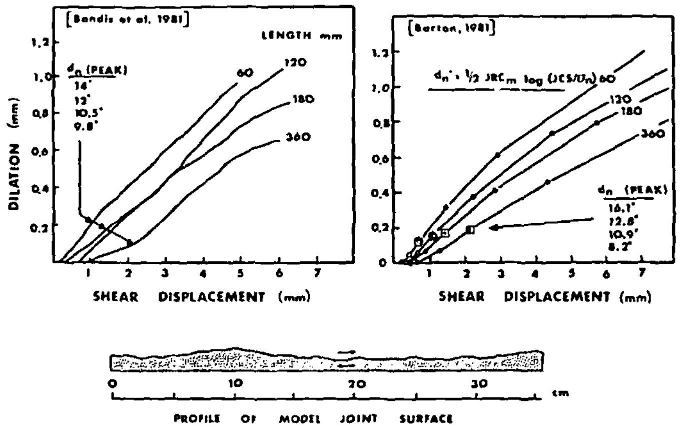

FIGURE 9. The delayed dilation exhibited by larger samples of the same joint (Bandis et al., 1981) suggests scale dependent joint permeability when shearing occurs.

when flow-testing an artificial fracture at its formation temperature.

ROUGHNESS AND TORTUOSITY EFFECTS

In many of the joint or fracture permeability tests reported in the literature, the true joint aperture is unknown. Results are therefore expressed as in this study, by an equivalent smooth wall aperture (e) derived from equation 2, or from an equivalent formulation for radial flow. This "cubic law" formulation was derived for open, non-contacting, smooth parallel surfaces.

In a recent article, Walsh (1981) utilizes the analogy of heat flow in a sheet with non-conducting cylindrical inclusions, to deduce that the permeability K_1 of a joint with points of contact is related to K_0 of an equivalent joint with an unhindered flow path as follows:

$$\frac{K_1}{K_0} = \frac{1 - A_1/A_0}{1 + A_1/A_0} \qquad (3)$$

where A_1 = area of contact points
A_0 = total area of joint

An analysis of contact area measurements by Iwai (1976), Barton and Choubey (1977) and Bandis (1980) indicates that a simple estimate of A_1/A_0 both for normal closure and limited states of shear is as follows:

$$A_1/A_0 \cong \sigma_n'/JCS \qquad (4)$$

where σ_n' is the effective normal stress applied across the joint.

This simple model predicts linear increases in contact area with load, which agrees with a more complicated formulation by Walsh and Grosenbaugh (1979).

According to equations 3 and 4, tortuosity effects alone would result in about 20% reduction of permeability for our altered mineralized joint, when tested under an equal biaxial stress of 6.9 MPa. The combination of tortuosity and roughness results in the smooth wall aperture (e) being smaller than the real aperture (E). By similar reasoning, changes in either parameter (Δe, ΔE) will not be of equal magnitude. Results for $\Delta E/\Delta e$ measured in the present block tests are compared with E/e reported in the literature in

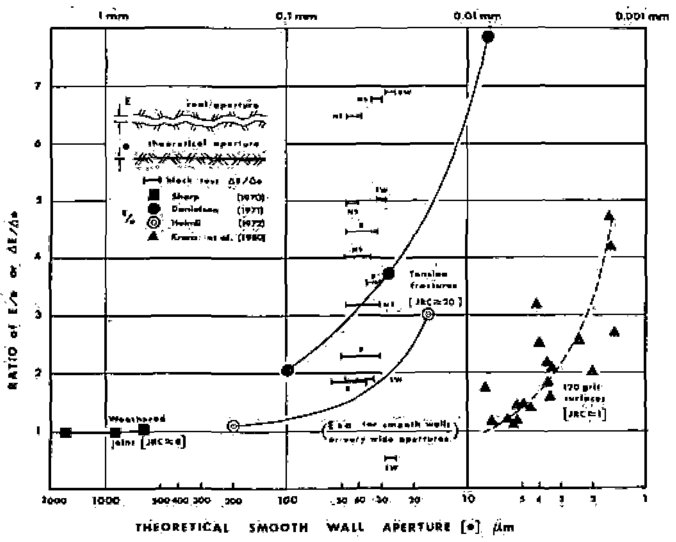

FIGURE 10. Losses due to tortuosity and roughness expressed as the ratio E/e. In-situ block test results are compared with data reported in the literature. B = biaxial, NS = uniaxial, EW = uniaxial.

Figure 10. The mean value of ΔE/Δe for our biaxial tests was 3.0, for a mean value of e = 40 μm.

The flow losses due to tortuosity and roughness and the observation of load path dependence has been interpreted by Kranz et al. (1979) and Walsh (1981) as evidence that the law of effective stress may not apply to flow through fractured rocks. The foregoing evidence that E/e ≧ 1 for rough "closed" joints would appear to be a more reasonable and correct explanation. A recent article by Witherspoon et al. (1979a) has suggested that the cubic law (e = E) does hold even for "closed", rough fractures down to e = 4 μm. Their conclusions are contrary to the above findings, and may have been influenced by the mathematical technique used to estimate the true apertures, which were not measured directly.

CONCLUSIONS

1. A mineralized joint in gneiss, loaded normally in an 8 m^3 biaxially loaded block, exhibited a fourfold reduction in permeability when loaded from 0 to 6.9 MPa, under ambient conditions (12°C). A subsequent loading test at 74°C to the same stress, produced a thirty-fold reduction in permeability. Increased temperature alone, with no change in the 6.9 MPa normal stress, reduced permeability tenfold. Temperature does not appear to have a positive effect on joint permeability when the joint is unconfined.

2. It appears important to test joints at elevated temperature during repository characterization, since the mating of joint walls may be artificially limited by ambient testing.

3. Uniaxial loading of the block caused 0.25 mm shear displacement of the test joint. This caused sufficient aperture strain (dilation) to increase the permeability a few percent. The continuous base of the block prevented further shear, dilation and permeability increases under the stress applied.

4. Comparison of measured changes in joint aperture (ΔE) with calculated changes in the smooth wall aperture (Δe), indicates that E/e > 1 for rough, "closed" joints. This is presumably due to the combined effects of tortuosity and roughness, which may be particularly marked for the case of mineralized joints.

5. Excavation and thermally-induced shear strain and the resulting joint dilation seem likely to enhance permeability in the immediate vicinity of a repository. Outside this zone the thermal pulse might have a positive effect in reducing joint permeability. Further studies are recommended for resolving this important question.

ACKNOWLEDGEMENTS

The heated block test was funded by DOE through the Office of Nuclear Waste Isolation, under Contract No. E512-04700. The support of Mr. R. Robinson, Mr. R. Cudnick and Mr. W. Ubbes is gratefully acknowledged. The project could not have been completed without the support of the Colorado School of Mines, in particular Dr. W. Hustrulid and his students, and Mr. H. Gadbury, manager of the CSM experimental mine. Special acknowledgement is also made to Terra Tek's field crew. Terra Tek's consultants Bill Brace and Howard Pratt made significant contributions to the success of the tests. The opinions expressed in the paper are not necessarily those of DOE or ONWI.

REFERENCES

BANDIS, S., 1980, Experimental studies of scale effects on shear strength, and deformation of rock joints, Ph.D. Thesis, Univ. of Leeds, 385 p.

BANDIS, S., LUMSDEN, A., BARTON, N., 1981, Experimental studies of scale effects on the shear behavior of rock joints, Int. J. Rock Mech. Min. Sci. and Geomech. Abstr., (in press).

BARTON, N. and CHOUBEY, V., 1977, The shear strength of rock joints in theory and practice, Rock Mechanics, Springer, No. 1/2, pp. 1-54.

BARTON, N. and HANSTEEN, H., 1979, Very large span openings at shallow depth: deformation magnitudes from jointed models and F.E. analysis, Proc. 4th Rapid Excavation and Tunneling Conference, Atlanta, Ch. 77, pp. 1331-1353.

BARTON, N., 1981a, Some scale dependent properties of joints and faults, NSF/UCB Workshop on Large Volume Experimentation, Geophysical Research Letters (in press).

BARTON, N., 1981b, Modelling rock joint behavior from in-situ block tests: implications for nuclear waste repository design (in preparation for ONWI).

DANIELSEN, S.W., 1971, Joint permeability, thesis (in Norwegian), Norwegian Technical University, Trondheim.

HEIMLI, P., 1972, Water and air leakage through joints in rock specimens, (in Norwegian), Fjellsprengningsteknikk, Bergmekanikk, Oslo 1972, pp. 137-142.

ISRM, 1978, Suggested methods for the quantitative description of discontinuities in rock masses, International Society for Rock Mechanics, Int. J. Rock Mech. Min. Sci. and Geomech. Abstr., Vol. 15, pp. 319-368.

IWAI, K., 1976, Fundamental studies of fluid flow through a single fracture, Ph.D. Thesis, University of California, Berkeley, 208 pp.

KRANZ, R.L., FRANKEL, A.D., ENGELDER, T. and SCHOLZ, C.H., 1979, The permeability of whole and jointed Barre granite, Int. J. Rock Mech. Min. Sci. and Geomech. Abstr., Vol. 16, pp. 225-234, and Erratum, Vol. 17, pp. 237-238.

LUNDSTROM, L. and STILLE, H., 1978, Large scale permeability test of the granite in the Stripa mine and thermal conductivity test, Lawrence Berkeley Laboratory, LBL 7052, SAC-02, 33 pp.

MAINI, T., 1971, In-situ hydraulic parameters in jointed rock -- their measurement and interpretation, Ph. D. Thesis, Imperial College, London, 312 pp.

NELSON, R.A., 1975, Fracture permeability in porous reservoirs: an experimental and field approach, Ph.D. Thesis, Texas A & M University, 171 pp.

PRATT, H.R., SWOLFS, H.S., BRACE, W.F., BLACK, A.D. and HANDIN, J.W., 1977, Elastic and transport properties of an in-situ jointed granite, Int. J. Rock Mech. Min. Sci. and Geomech. Abstr., Vol. 14, pp. 35-45.

SHARP, J.C., 1970, Fluid flow through fissured media, Ph.D. Thesis, Imperial College, London, 181 pp.

VOEGELE, M.D., 1978, An interactive graphics based analysis of the support requirements of excavations in jointed rock masses, Ph.D. Thesis, Univ. of Minnesota.

WAHI, K.K., TRENT, B.C., MAXWELL, D.E., PYKE, R.M., YOUNG, C. and ROSS-BROWN, D.M., 1980, Numerical simulations of earthquake effects on tunnels for generic nuclear waste repositories, Science Applications Inc., SAI-FR-126, Vols. I and II.

WALSH, J.B. and GROSENBAUGH, M.A., 1979, A new model for analyzing the effect of fractures on compressibility, Journal of Geophysical Research, Vol. 84, No. B7, pp. 3532-3536.

WALSH, J.B., 1981, Effect of pore pressure and confining pressure on fracture permeability (in press).

WITHERSPOON, P.A., AMICK, C.H. and GALE, J.E., 1977, Stress-flow behavior of a fault zone with fluid injection and withdrawal, Mineral Engineering Report No. 77-1, University of California, Berkeley.

WITHERSPOON, P.A., WANG, J.S.Y., IWAI, K. and GALE, J.E., 1979a, Validity of cubic law for fluid flow in a deformable rock fracture, Lawrence Berkeley Laboratory, LBL-9557, SAC-23, 28 pp.

WITHERSPOON, P.A., AMICK, C.H., GALE, J.E. and IWAI, K., 1979b, Observations of a potential size-effect in experimental determination of the hydraulic properties of fractures, Lawrence Berkeley Laboratory, LBL-8571, SAC-17, 15 pp.

SEPARATION OF COPPER-NICKEL SOLUTIONS BY SORPTION AND SOLVENT EXTRACTION

UDC 66.933 + 669.243

M. D. Ivanovskii, G. V. Sedel'nikova, and V. S. Strizhko

Solutions of complex composition containing (in g/liter) ∿ 40 Cu, ∿ 30 Ni, and 120-150 H_2SO_4 are formed when processing secondary copper. Constant removal of nickel by removing part of the copper electrolyte for nickel sulfate crystallization is essential for succesful copper electrolysis. The method used at present for processing copper-nickel solutions is not effective enough, because it involves heavy losses of copper, nickel, and sulfuric acid.

Two methods of processing copper-nickel solutions are suggested in the present work: copper extraction with oxime OMG from copper-nickel solutions which have been previous stripped of sulfuric acid and sorption of copper with ANKB-2 ampholyte directly from the copper electrolyte.

In view of the impossibility of extracting copper from strongly acid solutions (120-150 g/liter H_2SO_4) with known extractants, sulfuric acid was extracted from the copper electrolyte as a preliminary step with trialkylphosphine oxide (TAFO) to pH 1.5; copper was then extracted with alkanophenoxime OMG. The trialkylphosphine oxide showed high extractive capacity (Fig. 1); reextraction of sulfuric acid from TAFO with water is comparatively easy, whereas reextraction from amines is difficult. Complete regeneration of TAFO was achieved in five reextraction stages with a ratio of organic to aqueous phase o:a = 1:1 and in seven stages with o:a = 2:1. The reextract H_2SO_4 content was 70-140 g/liter.

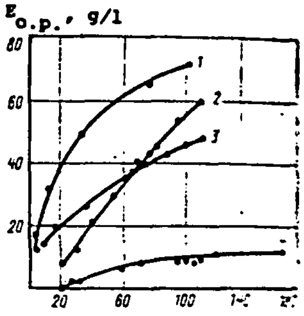

Fig. 1. Isothermal lines for extraction of sulfuric acid by various compounds: 1 - TOA; 2 - TAFO; 3 - mixture of secondary and tertiary amines; 4 - tributyl phosphate (TBF) ($E_{o.p}$ - is the capacity of the organic phase).

Copper was extracted from the acid copper-nickel solutions with alkanophenoxime OMG. The extractant has good kinetic indices: equilibrium is established in the system in 2-4 min. The optimum OMG concentration in kerosone is 30% for extraction from solutions containing 30-40 g/liter Cu.

The extractive capacity of OMG depends upon the pH of the sulutiôn. For concentrated sulutions (30-40 g/liter Cu) the pH at which extraction commences is 1.5, which corresponds to a copper electrolyte H_2SO_4 content of 5 g/liter. Copper was reextracted from the saturated organic phase with sulfuric acid solutions. The copper is completely extracted in two stages by a solution of 200 g/liter H_2SO_4.

The results obtained made it possible to separate the copper-nickel solution into three components, which can be processed by the generally known methods. Stripping an actual copper electrolyte containing 32 g/liter Cu, 28.6 g/liter Ni, 120 g/liter H_2SO_4 and traces of impurities resulted in a reduction in the sulfuric acid concentration to 5 g/liter or pH 1.5. i.e., to the pH at which copper extraction commences. The sulfuric acid concentration in the reextract was ∿ 140 g/liter.

After five stages of counterflow copper extraction the residual copper content of the raffinate was < 0.01 g/liter; the raffinates has pH values of 1.5-2.0. The nickel concentration in the sulution remained unchanged. A counterflow reextraction routine with o:a = 3:1 and a number of stages n = 2 yielded reextracts containing 28-30 g/liter Cu and 154-157 g/liter H_2SO_4.

The sorption variant of copper-nickel solution separation does not call for a reduction in the sulfuric acid content of the initial sulution, because ANKB-2 ampholyte is capable or sorbing copper from strongly acid solutions, up to 450 g/liter H_2SO_4 (Fig. 2). This ampholyte, which contains picolinic acid groups, is produced by chemical conversion of copolymer 2,5-methylvinylpyridine with divinylbenezene. The presence of functional groups with opposite charges in the resin structure ensures a high level of copper sorption due to complexing.

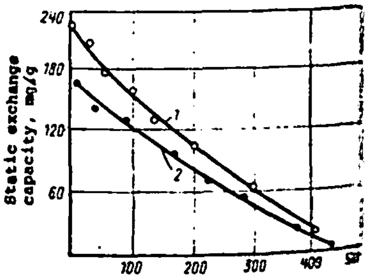

Fig. 2. Relationship of capacity of ANKB-2 for copper to solution H_2SO_4 content at a copper concentration (in g/liter) of: 1 - 10; 2 - 5

The static exchange capacity of ANKB-2 in sorption of copper from a solution with a concentration of 40 g/liter Cu and 120 g/liter H_2SO_4 is 170 mg/g. The ampholyte is not selective enough relative to copper: nickel is absorbed in addition to copper. Where copper and nickel are present together the factor $D_{Cu/Ni} = 16.2$. The high sorportion capacity of the ampholyte in strongly acid media leads to difficulties in copper desorption[1]. The saturated resin was regenerated with highly concentrated eluent solutions (up to 740 g/liter H_2SO_4). Under these conditions only 93% Cu was desorbed in one desorption stage. The low level of copper desorption from the ampholyte is apparently due to the strength of the complex formed between copper and the resin functional groups. Electrodesorption of copper from ANKB-2, i.e., desorption with a simultaneous deposition of copper on a cathode[2], was used to increase the extent of copper desorption from the resin. In these circumstances *copper extraction increased by 20% compared with ordinary desorption.*

The possibility of using ANKB-2 for soption of copper from actual copper-nickel solutions was investigated. Counterflow sorption with a phase volume ratio $V_{res}:V_{sol} = 1:2$ and a number of stages n = 4 yielded raffinates containing (in g/liter) 0.1-0.3 Cu, 21-23 Ni, and 110-117 H_2SO_4, which can be sent for nickel sulfate production; the saturated resin can be sent for copper separation by desorption or electrodesorption.

Solvent-extraction and sorption methods of separating copper-nickel solutions with high extraction indices have a number of advantages over the existing scheme.

1. Removal of nickel from the copper electrolyte improves electrolysis indices and the quality of the electrolytic copper.
2. Returning the $CuSO_4$ eluates to the main electrolysis cells will increase the yield of electrolytic copper.
3. Thorough removal of copper will increase nickel extraction into nickel sulfate.

---

[1] L. E. Slobtsov, B. N. Laskorin, V. N. Goldobina, et al, Tsvetnye Metally, 1973, No. 9, 15-16.

[2] G. V. Sedel'nikova, M. D. Ivanovskii, and V. S. Strizhko, Tsvetnye Metally, 1975, No. 1, 13-14.

SORPTION DEACIDIFICATION OF SOLUTIONS TO ELIMINATE ARSENIC

UDC 661.183.12:669.337.131

S. V. Bereza, N. Ya. Lyubman, L. A. Lukonina, and L. I. Mekler

To remove arsenic from copper electrorefining solutions, these are treated with titanium salts [1] and also neutralized with lime [2] or copper [3]. When the solutions are neutralized with lime a bulky precipitate forms which is difficult to filter or settle out. This method of removing arsenic involves a high consumption of lime and irreversible metal losses due to coprecipitation, mechanical entrainment, and sorption by the surface of the gypsum.

The solution should be treated with copper granules when it is sent for vitriol production. However, if arsenic removal from the electrolyte as such is required, this method is relatively ineffective.

The most acceptable methods of achieving the desired reduction in acid concentration are the reagentless methods, by which solution acidity can be reduced without bringing in additional impurities (metal cations).

One of the most effective methods, which is suitable for deacidification of highly concentrated sulfuric acid solutions, is the selective sorption of acid [4] in the process of sulfate-bisulfate exchange on anion-exchange resins [5].

$$R_2^+SO_4^{2-} + HSO_4^- + H_3O^+ \rightleftharpoons 2R^+HSO_4^- + H_2O,$$

where R is the anion-exchange resin polymer base. In concentrated sulfuric acid solutions this equilibrium shifts to the right, and to the left in dilute solutions. If a concentrated solution of sulfuric acid which also contains metal ions (spent electrolytes, vitriol production solutions, washing acids) is passed through an anion-exchange resin layer in SO_4^{2-} form, fairly thorough separation of the sulfuric acid and the metal salts can be achieved.

The separation is based on the difference in sorption interaction between the constitutents of the mixture and the sorbent. In this case the anion-exchange resin has a much greater affinity for bisulfate ions than for metal cations (Cu^{2+}, Ni^{2+}, Zn^{2+}, etc.), so that a solution of salts containing practically no acid can be obtained at the exit from the column. The acid can be eluted from the resin with water.

The dispersion of arsenic on passing strongly acid electrolyte through an anion-exchange resin (e.g., AV-17-8) layer should be examined separately. It was demonstrated in [6] that arsenic acid at various pH values is sorbed by an anion-exchange resin in the form of various anions (according to the stages of dissociation):

$$\underset{pH<4.2}{H_3AsO_4 \rightleftharpoons H_2AsO_4^-} \rightleftharpoons \underset{pH=4.2\div 9}{HAsO_4^{2-}} \rightleftharpoons \underset{pH=9\div 14}{AsO_5^{3-}}.$$

On passage of the solution, practically complete deacidification is achieved in the exchange zone, the solution pH rises to 4-5, and thus conditions favorable for arsenic sorption are created.

In addition, when the solution pH in the resin zone rises favorable conditions are created for formation of copper and nickel arsenates, which are precipitated on the resin as a molecular-dispersed deposit.

In the process of acid elution, fairly concentrated solutions sufficient for the practically complete desorption of arseniferous anions and for the solution of metal arsenates are formed over the height of the sorbent layer.

Thus the process of sorption deacidification of solutions is accompanied by partial elimination of arsenic from them, the latter being present mainly in eluates and precipitate. The proportion of arsenic in the precipitate rises as the degree of neutralization increases and the acid concentration in the initial solution is reduced.

We tested this simple and effective method of solution deacidification by sorption with simultaneous separation of arsenic in the purification of copper-nickel solutions from electrolytic and vitriol production at the Balkhash Mining

Results of Deacidification of Spent Electrolyte (pilot-plant results, g/liter)

Initial solution				Deacidified solution				Eluate			
H_2SO_4	Cu	Ni	As	H_2SO_4	Cu	Ni	As	H_2SO_4	Cu	Ni	As
95,5	59,8	15,6	12,3	18,5	48,3	13,6	2,52	25,0	0,95	0,37	2,57
79,5	77,0	13,8	7,7	14,1	62,0	12,3	2,10	30,0	1,90	—	2,30
110,0	58,0	16,2	23,2	18,0	49,0	15,3	4,75	30,0	1,27	0,59	8,40
103,0	74,0	16,1	8,3	23,8	65,8	14,6	1,12	34,2	1,27	0,58	2,92
81,0	51,5	16,7	9,9	13,7	42,8	14,7	2,00	27,4	1,27	—	1,65

and Metallurgical Combine. The experiments were carried out under laboratory, pilot-plant, and full-scale industrial conditions. In all cases, the electrolyte solution was passed through a layer of anion-exchange resin at a speed of 5 specific volumes per hour with elution by water at the same speed. The commercial anion-exchange resin AV-17-8, previously converted to the sulfate form, was used as the sorbent. It is apparent from the Table that there is fairly complete separation of acid and metals in the process of sorption deacidification. The copper and nickel in the deacidified solution alter slightly in content, the arsenic concentrating predominantly in the eluates. Elimination of arsenic from the process in the form of acid eluates containing relatively small amounts of non-ferrous metals is incomparably easier and economically more advantageous than its elimination from initial solutions, because in this case, the metal losses are not great.

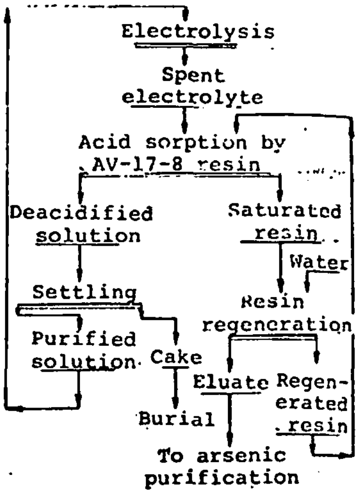

Flowsheet for arsenic removal from spent electrolyte.

It is possible to remove all of the arsenic from the solutions in one cycle, but the reduction of the arsenic concentration in the deacidified solutions in this case is quite acceptable for practical purposes.

The investigation formed the basis for the proposal of a flowsheet (see Figure above) for arsenic removal from spent electrolyte by deacidification with a view to the return of the purified electrolyte to the process.

REFERENCES

1. A. K. Sharova, A. P. Shtin, and E. N. Ketova. USSR Patent No. 186404. Byull. Izobr. i Tov. Znakov, 1966, No. 19, p. 20.
2. V. Z. Grigoryan. Tsvetnye Metally, 1972, No. 3, pp. 54-56.
3. L. I. Mekler, L. S. Borodina, L. N. Gulenko, and S. F. Akhmetov. Tsvetnye Metally, 1972, No. 12, pp. 57-61.
4. S. V. Bereza, N. Ya. Lyubman, Yu. N. Svyadoshch, et al. Ion-Exchange in Hydrometallurgy and Purifying Waste Waters. Alma-Ata, 1972 (Kazmekhanobr, vol. 10), pp. 72-80.
5. K. A. Krause, F. Nelson, and J. F. Baxter. J. Amer. Chem. Soc., 1953, vol. 75, No. 11, pp. 2768-2772.
6. S. I. Pol'kin, V. D. Dyatlov, and V. F. Andrianov. Izv. Vuz. Tsvetnaya Metallurgiya, 1971, No. 6, pp. 70-73.

8) A N Krasil'nikov: Mikrobiologiya 1969, 28, (4), 19.
9) A G Vologdin: Izv. Akad. Nauk SSSR. Seriya Geologich. 1947, (3).
10) J E Zajic: Microbiol. Biogeochemistry. Academic Press, New York - London 1969.
11) V G Aleksandrov and M I Ternovskaya: Silicate effective fertiliser. Moscow VINITI 1968.
12) Zh. P Teshich and D I Mar'yanovich: Ref. Zh., Delo 1971, Series D, (6).
13) W H Huang and W D Keller: Nature Phys. Sci. 239, (96), 149.

Tsvetnye Metally, 1974

SDT

SUBJ
MNG
SDT

Selectivity of dialkyl thiocarbamates in the flotation of minerals and extraction of metals

A V Glembotskii and Yu P Savintseva (State Institute of Rare Metals)

Since there are no systematic data on the flotation and extraction characteristics of reagents with one and the same functional group in the literature, we undertook a detailed investigation of the behaviour of dialkyl thiocarbamates in the flotation of minerals and the extraction of metals, as illustrated by the Z-200 reagent:

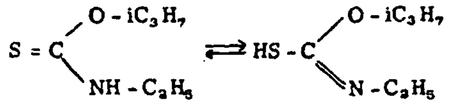

The Z-200 reagent is poorly soluble in water; in an acidic medium (up to pH = 7) it exists in the neutral thione form, and in an alkaline medium it changes partly into the thiol form[1]). This characteristic of thiocarbamates makes it possible to follow the behaviour of Z-200 in the extraction of metals and flotation of minerals as a function of the form in which the reagent is present in the solution.

For this purpose we studied the extraction of Cu(I) and Fe(III) and the flotation of sulphide minerals containing them. The effect of the pH of the solution (with sulphuric acid for the acid medium and sodium hydroxide for the alkaline) on the extraction of copper and iron by the Z-200 reagent is shown in fig. (a). Copper only begins to be extracted appreciably at pH > 7 under conditions of conversion of the reagent into the chelating thiol form. Iron is not extracted over the whole pH range of the solution. Earlier we established [2]) that Z-200 extracts Cu(I) only from solutions of hydrohalic acids; copper is not extracted from sulphuric, nitric and hypochlorous acid solutions. Thus, the extraction of copper in a weakly alkaline medium indirectly indicates reaction of Z-200 with copper by a chelate mechanism under these conditions.

It must be emphasised that Fe(III) is hardly extracted into solution at all, irrespective of the type of acid and the form of the Z-200 reagent. By analogy with the extraction of iron, Z-200 does not react chemically with FeS_2 and floats it extremely weakly (fig. b). In contrast to xanthate, for example, the chemisorption of which on pyrite gives rise to a jump of the electrode potential of the mineral to 200mV, in the presence of Z-200 there is no change in the electrode potential of FeS_2, and the reagent is easily desorbed from the surface by washing with water (fig. b, c). For $CuFeS_2$ in the weakly alkaline region (pH = 7.5) an increase is observed in the amount of attached reagent (fig. b), and there is a maximum jump in the potential of the mineral (fig. c). Here the attachment of the reagent is extremely strong; less than 50% of the Z-200 is desorbed by washing the mineral with alcohol. This demonstrates the chemical character of the adsorption of Z-200 on $CuFeS_2$ and, evidently, the chelate form of attachment of the thiocarbamate.

For the extraction of metals by neutral reagents in the form of co-ordination solvated compounds it is necessary that the donor atom of the extractant should give a strong bond with the metal and be able to compete with the inorganic ligand (e.g. sulphate ion) for a site in the co-ordination sphere of the metal.

For the flotation of minerals the interaction of the reagents with the surface through van der Waals forces promotes an increase in the adsorption of the reagent and hydrophobisation of the mineral. This feature explains the strong attachment of Z-200 to $CuFeS_2$ in an acidic medium and the flotation of the mineral, in spite of the weaker chemical interaction between them compared with the alkaline medium. The predominantly physical character of the attachment of Z-200 to $CuFeS_2$ in an acidic medium is confirmed by the ready desorbability of the reagent from the surface when the sulphide is washed with alcohol (fig. c).

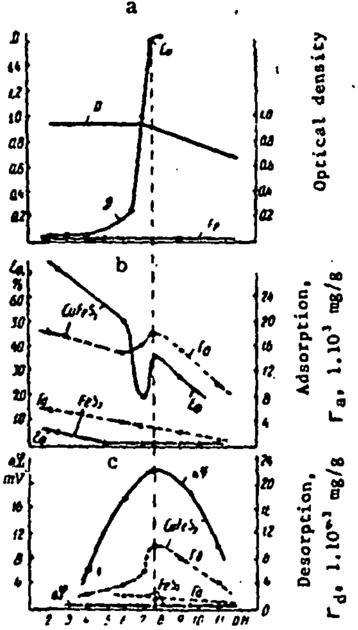

Fig. The effect of the pH of the solution on the extraction of Fe(III) and Cu(I) ions by chloroform in the presence of Z-200 (a). Extraction of the minerals during flotation and adsorption of Z-200 on them for solutions with various pH values (b). Variation of the electrode potential of the sulphides in the presence of Z-200 and the amount of Z-200 not desorbed from the surface of the minerals by alcohol for solutions with various pH values (c). The dashed line indicates the region in which the Z-200 exists in the thione form (pH <7.5) and in both the thione and thiol forms (pH >7.5).

Since the Z-200 reagent has found wide use in the flotation of various sulphide ores, it is expedient to compare its selectivity in the extraction of metals and the flotation of minerals. Data from investigation of the extractability of a large number of metals by the Z-200 reagent from solutions in hydrohalic and other mineral acids are summarised in the table.

A relationship was found between the distribution coefficient (D) of the metals and the concentration of the acids over a wide range. Here solutions of salts of the metals labelled with radio-active isotopes at concentrations of 10^{-6} - 10^{-8} g-ion/litre were used. The resuls shows that the nature and concentration of the acid have a large effect on the effectiveness and selectivity of the extraction of the metals.

In the presence of Z-200 metals which form stable halide complexes (Ag, Hg, Au, Tl, Cu) are extracted well from solutions of hydrohalic acids with chloroform. Very high selec-

Results from extraction of metals with 0.05 M solution of Z-200 in chloroform

Inorganic ligand HL	Concn.of HL HL g-ion/l	Readily (1) and poorly (2) extracted elements	
		D>5	D<0.1
		1	2
Chloride (KCl + 2.5 M H_2SO_4) or HCl	0.05-9	Ag	Au, Zn, Cd, Ga, In, Tl, Pb, Sb, Bi, Se, Te, W, Fe, Co
	0.05-6	Hg	
	6-9	Cu	
Bromide (KBr + 2.5 M H_2SO_4) or HBr	0.3 -1.0	Ti	Zn, Cd, Ga, In, Pb, Sb, Bi, Te, W, Fe, Co
	0.3 -3.3	Au	
	0.3 -3.3	Se	
	0.01-2	Ag	
	0.01-0.5	Hg	
	5-6	Cu	
Iodide (KI + 2.5 M H_2SO_4) or HI	0.01-1	Ti	Zn, Cd, Ga, Bi, W, Fe, Co
	0.3 -3	Au	
	0.3 -3.3	Se	
	0.1 -5	Cu	
	<0.1	Ag	
	<0.1	Hg	
Perchlorate $HClO_4$	0.05-6	Ag	Cu, Zn, Cd, Ga, In, Tl, Pb, Bi, Se, Te, Mo, W, Sb, Fe, Co
	0.05-6	Hg	
Nitrate HNO_3	0.1 -5	Ag	Cu, Zn, Cd, Ga, In, Tl, Pb, Bi, Se Te, Mo, W, Sb, Fe, Co
	0.1 -5	Hg	
Sulphate H_2SO_4	1 -10	Ag	Cu, Zn, Cd, Ga, In, Tl, Pb, Bi, Se, Te, Mo, W, Sb, Fe, Co
	1 -10	Hg	

tivity is obtained during extraction from nitric and sulphuric acid solutions. Only silver and mercury are extracted quantitatively over a wide range of concentrations of acids, particularly sulphuric (1-10M). It should be emphasised that cobalt, nickel, lead and zinc, in addition to iron, are not extracted at all under all the investigated conditions, and they can therefore be easily separated from silver, gold and a series of other metals.

A characteristic feature of Z-200 in the flotation of ores is its extremely weak collecting action on pyrite during effective flotation of copper sulphates and zinc-blende activated with copper. The high selectivity of Z-200 in the separation of copper sulphides from lead sulphide in an acidic medium and the effectiveness of its collecting action in the flotation of silver-containing ores are also noted ³).

Conclusions

1. As illustrated by thiocarbamates, it was shown that the selectivity of reagents with an identical functional group is retained without substantial changes in the extraction of metals and in the flotation of minerals containing like metals.
2. Investigation of the flotation characteristics of Z-200 made it possible to propose this reagent as an effective and selective extractant for chalcophilic metals (metals of class b in the Arland-Chatt classification).
3. Investigation of the extraction characteristics of Z-200 made it possible to discover certain features of the action of thiocarbamates in the flotation of minerals. A satisfactory explanation was found for the specific nature of the reaction of Z-200 with copper sulphide in an alkaline medium.

References

1) A K Livshits et alia: Tsvetnye Metally 1968, (2).
2) Yu A Zolotov et alia: Dokl. Akad. Nauk SSSR 1973, 209, (4), 909.
3) L Ya Shubov et alia: Reagents conditions in the flotation of non-ferrous metal ores at foreign plants: Tsvetmetinformatiya, Moscow, 1966, p. 21.

UDC 622.7

Effect of certain factors on the variation of the volume inside the mill in a grinding plant

P Susskii, V I Shilov and Z V Uteush (Khar'kov Engineering-Construction Institute)

Summary

One of the most important parameters affecting the processes taking place in a mill is the volume V occupied by the grinding medium and the material being ground. The grinding process inevitably generates causes of a natural character leading to an increase in V. This involves primarily the wear of the lining, the wear of the grinding medium, variation in the volume of the grinding medium, and other factors. The article is devoted to the production of an analytic relationship between the factors affecting V.

SORPTION EXTRACTION OF ANTIMONY FROM COPPER ELECTROREFINING SOLUTIONS

UDC 669.75.053:661.886

N. Ya. Lyubman, G. K. Imangazieva, A. U. Makhmudova, and E. A. Simkin

Antimony is one of the most harmful impurities in the electrolytic refining of copper, substantially reducing the quality of the cathode copper and adversely affecting the course of electrolysis. However, copper electrorefining solutions, which normally contain up to 0.6-0.7 g/liter Sb, can become an additional source for the production of this scarce and valuable metal. Until recently, however, no effective solution could be found to this problem because of the extraordinarily complex composition of the electrolyte and because appreciable losses of its principal constituents in the purification process could not be permitted.

The sorption method, using a highly-selective ion-exchanger which extracts only antimony from the solution has great potential in this case. Research on choosing such a sorbent had led to the development of a method of synthesizing a complexing ion exchanger of macroporous structure containing pyrocatechol radicals as active groups (PK-S ion exchanger). The synthesized ion exchanger is highly specific in relation to antimony and extracts it quantitatively from sulfuric acid solutions. For example, the PK-S ion exchanger sorbs up to 400 mg/g Sb (calculated as absolutely dry weight) from a solution with the composition (in g/liter) 0.8 Sb, 17.1 As, 52.0 Cu, 22.3 Ni, 1.8 Fe, and 140 H_2SO_4.

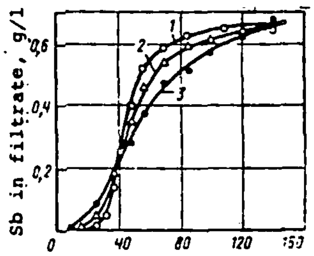

Fig. 1. Elution curves for antimony sorption at various filtration speeds, spec. vol/hr: 1 - 10; 2 - 30; 3 - 60.

Large scale tests were conducted using the PK-S ion exchanger under the conditions prevailing at the Balkhash Mining and Metallurgical Combine. The installation consisted of two ion exchange columns 90 mm in diameter and 220 mm high, each of which was loaded with 1 liter of ion exchanger (ratio of depth of sorbent layer to diameter 1.8:1) having a grain size of 0.4-0.8 mm. The columns were connected to one of the lines in the electrolysis shop, in which electrolyte of the following composition (in g/liter) was circulating: 0.68 Sb, 9.1 As, 43.0 Cu, 15.5 Ni, 1.8 Fe, and 170 H_2SO_4. The electrolyte temperature was 60°C.

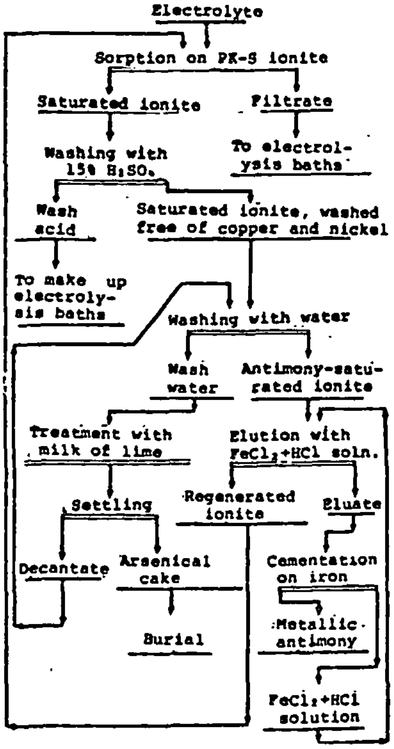

Fig. 3. Diagram of antimony extraction from copper electrolyte.

The elution curves for antimony sorption on the PK-S ion exchanger are given in Fig. 1. The total dynamic exchange capacity up to breakthrough depends upon the filtration rate. Transition from a filtration speed of 10 spec. vol/hr to 30 spec. vol/hr leads to a 1.2-fold reduction in capacity up to the breakthrough and passing the solution through at a rate of 60 spec. vol/hr halves the capacity up to breakthrough.

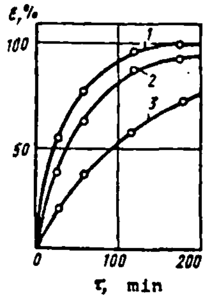

Fig. 2. Kinetic curves for antimony sorption at various filtration speeds, spec. vol/hr: 1 - 60; 2 - 30; 3 - 10. (ε - is the extent of utilization of ion-exchanger capacity for antimony, % of the maximum achieved under the given conditions.

The certain amount

of washing away of sorption capacity characteristic of a speed of 30 spec. vol/hr can be disregarded, because it is accompanied by acceleration of the antimony extraction by over 1.5-fold (Fig. 2).

Thus, feeding the initial solution through at a speed of 30 spec. vol/hr combines a high process speed with maximum utilization of the sorption capacity of the ion exchanger.

After saturation, the ion exchanger contained (in mg/g) 315 Sb, 239 As, 167 Cu, and 35 Ni; no Fe was found.

Unlike antimony, the impurity elements (As, Cu, Ni) enter the ion exchanger phase mainly as a result of physical sorption and can be removed from the sorbent fairly completely by washing with sulfuric acid and water.

After treatment with sulfuric acid and water, the ion exchanger contained (in mg/g of dry sorbent) 301 Sb, 31 As, 17 Cu. No Ni nor Fe were found.

The wash acid, which contains (in g/liter) 0.1 Sb, 0.9 As, 1.8 Cu, and 0.4 Ni, can be used to make up the electrolysis baths, and the wash water, containing (in g/liter) 0.07 Sb, 1.6 As (no Cu, Ni, nor Fe were found) can be used as recirculating solution after purification with lime and clarification.

The antimomy was eluted with reagents containing chlorides. Hydrochloric acid solutions of various concentrations, as well as solutions of various chlorides acidified with hydrochloric acid, were tested as eluents.

It was established that the degree of elution was governed by the acidity of the eluent and the chloride ion concentration in it; excess of chlorides is essential to suppress the great affinity of antimony for the ion exchanger active groups, and acidity is necessary to increase the stability of the antimony chloride complexes.

The greatest elution effect (98.6% antimony extraction from the ion exchanger) is maintained by using 15-17% HCl, producing eluates containing > 20 g/liter Sb. Antimony oxide containing (in %) 0.4 As, 0.003 Bi, 0.0005 Cu (no Ni nor Fe were found) was separated out from these solutions by dilution with water at 60°C.

A disadvantage of using hydrochloric acid is the difficulty of processing the eluates. The evolution of antimony from its chloride solution in the form of oxychloride by dilution with water with subsequent hydrolysis to oxide is very attractive in its simplicity. However, this involves heavy and practically irrecoverable losses of hydrochloric acid, because subsequent concentration of the dilute HCl to its initial concentration is technically difficult. The electrolyte processing of chlorides eluates is also difficult, because of the instability of available anodes in chloride media.

A solution containing 20% $FeCl_2$ and 5% HCl proved to be a convenient eluent, because it can be used repeatedly in processing eluates by cementation. Passing 15 specific volumes of this solution through gives a 91.3% degree of elution.

It was established that reduction with metallic iron led to the thorough separation of antimony from these eluates in the form of a cement residue containing 91-93% metallic antimony. The regenerated solutions produced in these circumstances are practically identical to the initial eluent in composition. The desorbents are readily processed in this way, and the composition of the recirculating eluent is corrected by the periodic addition of HCl solution in amounts corresponding to the process losses of solution.

25 sorption-elution cycles were conducted using a hydrochloric acid solution of bivalent iron chloride as the eluent, obtaining stable and reproducible results in antimony extraction from copper electrolyte from the Balkhash Mining and Metallurgical Combine. Following extraction of the antimony, the filtrate yielded satisfactory cathode deposits when used as the electrolyte in copper electrorefining.

The developed technology (Fig. 3) has been adopted for pilot-plant checking at the Balkhash Combine. The Kazmekhanobr Institute has designed and is building an installation which will process $\sim$ 600 m^3 of electrolyte daily with a reduction in the antimony concentration of from 0.6-0.7 to 0.10-0.15 g/liter for the pilot-plant tests.

The relationships of the electrolytic separation of metals in molten salts

A D Pogorelyi, I V Aleksanyants, A N Kokoev, N V Lazarev and A E Suanov (North-Caucasian Mining-Metallurgical Institute - Department of General Metallurgy)

Summary

Algorithms are formulated for calculation of the results from electrolytic separation of two-component systems in melts. With data on the composition of the raw material and electrolyte and on the physicochemical characteristics of the system being separated it is possible to predict the course of and the results from the electrolysis process.

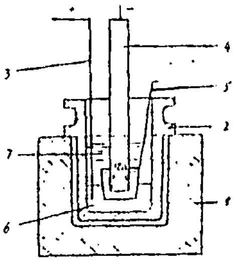

Fig.1

Experimental electrolysis cell for work with melts. 1) thermostat; 2) quartz crucible; 3) anode lead; 4) cathode; 5) container for cathode product; 6) anode melt; 7) electrolyte.

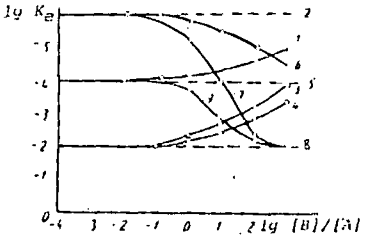

Fig.2 The dependence of K_e on the composition of the anode,metal for $K = 0.01$ and for various metal valencies: m for A, n for B. 1 - $m = 3, n = 2$; 2 - $m = 3, n = 3$; 3 - $m = 3, n = 1$; 4 - , $= 2, n = 1$; 5 - $m = 2, m = 2$; 6 - $m = 2, n = 3$; 7 - $m = 1, n = 3$; 8 - $m = 1, n = 1$, 9 - $m = 1, n = 2$.

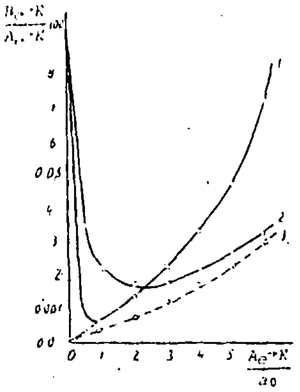

Fig.3 The variation of the composition of the cathode metal: 1 - instantaneous values of the content of B (%) in the cathode product; 2 - % of B in the cathode product of the normal operation; 3 - % of B in the cathode product of the normal operation. The dotted line shows the results for the initial operation, the solid lines show the results for the normal operation.

experiments

Sov. Non-Fe metals Research v6, N3, 1978.

yes

UDC 669.2

Selective extraction of copper from iron-containing solutions

G B Illyuvieva and Le-Nai-Fyong (Leningrad Mining Institute - Department of General and Physical Chemistry)

To increase the degree of utilisation of ore material is one of the pressing problems of mining and metallurgical industry in the tenth five-year plan. At the same time between 5 and 20% of the total balance reserves of non-ferrous metal ores is lost during processing, and a considerable amount of the metals is carried away by the mine waters[1][2].

The capital costs for the extraction of copper from such materials, for example, are approximately three times lower than the cost of its production from ores of new deposits. The most rational method for the extraction of copper from balance ores and wastes is underground and heap leaching, which have been widely developed abroad[2]. One of the complex problems of the industrial application of these processes is isolation of the copper from the obtained low-concentration solutions containing considerable amounts of iron. The presence of iron reduces the effectiveness of the use of such widely known processes as cementation, extraction, and sorption, increasing the consumption rate of the cementate and extractants and reducing the useful capacity of the sorbents.

Investigations showed that it is possible to use the flotation method for selective extraction of copper from such solutions. The advantages of this method include its high rate, the possibility of using apparatus widely used by industry (mechanical or pneumatic flotation machines), the almost complete regeneration of the collector, and the recycling of the solutions even in bacterial leaching[3][4].

The investigations were carried out on model sulphate solutions containing 0.5g/l Cu and 1.0g/l Fe(III). The flotation machine (volume 150 and 1800ml). The necessary pH value in the solution was created by the addition of sodium hydroxide or sulphuric acid and was measured by potentiometry with a glass electrode and an LPU-1 potentiometer. The following materials were used as precipitant-collectors: xanthates, petroleum sulphides and sulphoxides, caroxylic and hydroxamic acids.

All the tested reagents successfully float copper from its solutions in a specific range of pH values and with some of them (petroleum sulphides, carboxylic and hydroxamic acids) at concentrations below the equivalents. The flotation of iron(III) takes place under approximately the same conditions, whereas the flotation of iron(III) is considerably less effective and takes place at different pH values. This determines the possibility of selective separation of copper and iron (III). In the simultaneous presence of both metals in solution, however, their behaviour changes significantly, and with the majority of reagents (xanthates, naphthenic and hydroxamic acids) selection is almost absent.

rlier investigations[5]) the possibility of selective tion of iron(III) from solutions containing non-ferrous by means of high-molecular-weight acids of the series was demonstrated. However, such a process es the need for additional consumption of the collector, makes the use of flotation for the extraction of cop- profitable. The widely employed hydrolytic isolation leads to considerable losses of copper as a result of pitation and sorption[6]).

his makes it necessary to seek a method for the sel- flotation of copper. The process was therefore rea- the following way. Carboxylic acids were first erted into sodium salts by mixing with equivalent s of a 1.0N solution of sodium hydroxide at 80-90°C. solutions were diluted to the required concentration 0.25N) with hot water and divided into portions. Before duction into the flotation equipment the solution was d where necessary (stearate, palmitate). The con- ption of the reagent is determined by the copper con- . The first portion at the rate of 0.5 of the equivalent t of copper is delivered to a solution having a pH of 1.8-2.0 directly in the flotation equipment, where ation is realised for 10-15 min.

re, as a result of hydrolysis, the sodium salt of the ctor is converted fully into the acid, which forms an endent highly dispersed solid (palmitate, stearate) quid (oleate, naphthenate) phase. A 1.0N solution of hydroxide is then added to the solution in portions, the pH value is increased to 5.6-6.1, after which the tion is continued for a further 10-15 min. Here the hydroxide is precipitated and gradually converted into ture of complex hydroxides, possessing a consider- ly lower specific surface and sorption and reaction cap- y. This process can be represented by the following me:

$$n[Fe(H_2O)_{6-x}(OH)]^{(3-x)+} \rightarrow [Fe_n(H_2O)_{n(6-x)}(OH)_{nx}]^{n(3-x)+} \rightarrow$$

$$\rightarrow [Fe_n(H_2O)_{n(6-x)}O_{ny}(OH)_{n(x-y)}]^{n(3-x)+} + nyH^+$$

The reaction of the solid phase which forms with the col- lector depends on its state of aggregation. Where it is re- presented by a finely dispersed liquid phase (oleic, naph- thenic acid), hydrophobisation of the surface occurs if the collector is a solid phase (stearic, palmitic acid), and its reaction with iron hydroxides hardly occurs at all. Here partial saponification of the collector occurs, and the anions which form interact with the copper cations, forming a carboxylate, which passes into the froth product during subsequent flotation. For complete extraction of the copper in the flotation process a further amount of the collector, calculated so that the total amount is equivalent to the amount of copper, is added. The results from the experiments (table 1) show that with liquid acids (naphthenic, oleic) selection is absent, and when solid acids of close molecular weight (palmitic, stearic) are used the selectivity is fairly high and the copper is extracted almost completely into the froth product.

The presence of even small amounts of liquid acids (e.g. synthetic fatty acids of the C_7-C_9 fraction) completely destroys the selection. This explains the absence of selection when technical fatty acids of the C_{17}-C_{20} fraction (solid), containing low-molecular fractions as impurity, are used (table 1).

Table 1: The results from the flotation of copper and iron by various carboxylic acids. Delivery of the collector in two equal portions *)

Collector-acid	State of aggregation at 25°C	pH value during addition of collector		Extraction into froth product %	
		Portion I	Portion II	Copper	Iron
Naphthenic	liq.	1.7	5.6	93.4	~100.0
Oleic	liq.	1.9	5.9	~100.0	~100.0
Palmitic	solid	1.9	6.2	90.0	13.3
Stearic	solid	2.0	5.4	98.0	14.0
Stearic	solid	2.0	5.9	96.5	10.0
Stearic, 90% +	solid				
Synthetic fraction C_7-C_9 10%	liq.	1.9	7.1	98.6	92.5
Aliphatic synthetic fraction C_{17}-C_{20}	solid	1.8	6.1	~100.0	~100.0
Stearic (regenerated)	solid	2.0	5.9	94.1	16.5

*) Consumption of the collector in an amount stoichiometric with the copper.

Flotation with stearic acid and its salts was investigated in greater detail. With the addition of an amount of sodium stearate equivalent to the copper in one portion at a pH value of 6.4 both metals are extracted completely into the froth product, as expected. With the addition of the same amount of collector to a solution with a pH value of 2 selection is observed, and the best results are secured *by the addition of collectors in two equal portions (table 2).* Analogous results can be obtained with an alcohol solution of stearic acid, where the character of the processes does not change; when added to an acidic aqueous solution, stearic acid forms a finely dispersed solid phase (table 2).

The accuracy of the ideas about the nature of the processes which occur is confirmed by the results from *potentiometric titration, phase analysis of the flotation products,* and investigation of their IR spectra. Whereas complete saponification of the stearic acid in the aqueous phase occurs at pH 8.2-8.5, in the presence of copper ions the formation of stearates occurs at pH > 4 and is complete at pH 5.8-6.0, and this is due to displacement of the equilibrium:

$$HR_{solid} \rightarrow HR_{soln} \rightarrow H^+ + R^- \xrightarrow{Cu^{2+}} CuR_{2\,solid}$$

Table 2: The results from flotation with stearic acid and its salts

Composition of collector	Solvent	Flotation conditions						Extraction into froth product %	
		First stage		Second stage		Total consumption of collector	pH of tailings		
		pH	Consumption of collector	pH	Consumption of collector			Copper	Iron
Sodium stearate	Water	6.4	1.0	-	-	1.0	6.9	100.0	100.0
Sodium stearate	Water	2.0	1.0	6.3	0	1.0	6.7	89.2	36.4
Sodium stearate	Water	2.0	0.5	5.5	0.5	1.0	5.9	96.5	10.0
Sodium stearate	Water	2.1	0.5	5.4	0.5	1.0	5.7	98.0	14.0
Sodium stearate	Water	2.0	0.25	6.0	0.75	1.0	6.0	91.8	13.5
Sodium stearate	Water	1.9	0.75	5.9	0.25	1.0	5.9	90.8	15.3
Sodium stearate	Water	1.8	0.25	5.9	0.25	0.5	5.9	78.2	13.0
Sodium stearate	Water	1.9	0.37	6.1	0.37	0.75	6.1	82.3	13.5
Stearic acid	Alcohol	5.9	1.0	-	-	1.0	6.1	88.0	13.0
Stearic acid	Alcohol	2.3	1.0	-	-	1.0	6.0	85.5	10.0
Stearic acid	Alcohol	2.0	0.5	5.9	0.5	1.0	6.1	95.0	0.0
Stearic acid	Alcohol	2.0	0.5	5.5	0.5	1.0	5.9	96.5	10.0

*) The consumption of the collector is given in fractions of the stoichiometric amount for copper.

as a result of the formation of the poorly soluble copper carboxylate and its withdrawal into the froth. The presence of solid stearic acid in the acidic solution (pH = 2) does not affect the formation of the oxides and basic salts of iron.

The flotation products obtained under optimum conditions do not contain free stearic acid. The froth product, into which more than 98% of the collector is extracted, represents neutral copper stearate with hydroxides and basic salts as impurity. The cell product consists of hydroxides and basic salts of iron with iron stearates as impurity ($R^-:Fe^{3+}$ ratio 0.004). The aqueous phase of both products in the form of a transparent solution containing sodium sulphate in an amount equivalent to the copper and iron and not more than 20mg/l of stearate is separated by settling (about 90% of the volume of the cell product and 50% of the froth) and can be returned to leaching. (By special tests it was established that the activity of the thiobacillus ferro-oxidans bacteria is not destroyed in this solution).

The solid phase of the cell products is easily filtered. The air-dry precipitate is a mixture of hydroxides and basic salts of iron and corresponds to the overall formula $Fe_4(SO_4)(OH)_{8-10}$. The solid phase of the froth product is also easily separated by filtration. After dissolution in a 30% hot solution of sulphuric acid and cooling the stearic acid is separated by filtration and returned to flotation. The filtrate is a solution of copper sulphate, the concentration of which is 20-25 times greater than the initial. This solution also contains a certain amount of iron, which is higher the higher its content in the initial solution. Final separation of the iron from the concentrated solution can be realised successfully, for example, by cation-exchange extraction with naphthenic or fatty acids⁷).

By experiments it was established that milk of lime can be used in addition to sodium hydroxide for neutralisation of the solution. The basic scheme for the treatment of low-concentration iron-containing solutions is shown in the figure.

Conclusions

1. A method is proposed for selective extraction of copper from an iron-containing solution with low concentration by flotation with the use of aqueous solutions of the salts of solid carboxylic acids as precipitant-collectors.

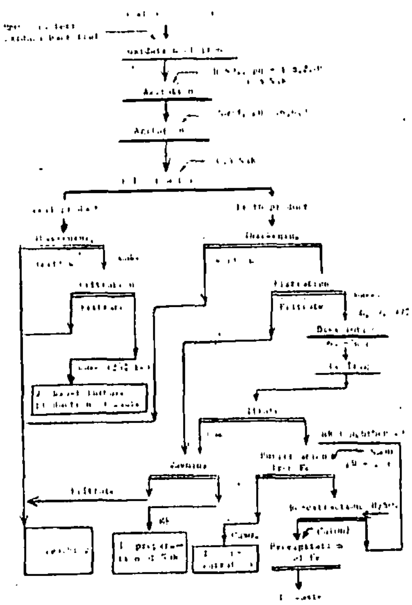

Fig. Basic technological scheme for the treatment of low-concentration solutions containing copper and iron.

2. From the combined results from flotation trials, potentiometric titration, and investigation of the phase composition of the flotation products an explanation is given for the mechanism of the processes.
3. The process can be realised with standard equipment, with regeneration of the collector and recycling of the aqueous phases.

References

1) S I Kuznetsov et alia: Introduction to geological microbiology: Izd. Akad. Nauk SSSR 1962.
2) B M Sobol' and P V Khodov: Gornyi Zhurnal 1963, 9, 1.
3) S F Kuz'kin and A M Gol'man: Flotation of ions and molecules: Nedra 1971.
4) G I Karavaiko: Advances in microbiology: Nauka, Moscow 1970, (6).
5) T F Poltaranina: Zapiski LGI 1963, 42, (3).
6) V V Yatsuk et alia: Tr. VNIITsvetmet 1968, (12).
7) G V Illyuvieva et alia: Zapiski LGI 1970, (3).

UDC 669.2/8; 669.24.046.43(088.8)

Phase and structural changes in the charge and the dynamics of the release of gases during segregation roasting of pyrrhotite calcines

A K Orlov, I N Piskunov and N M Telyakov (Leningrad Mining Institute - Department of the Metallurgy of Heavy and Noble Metals)

The subject of the investigations was pyrrhotite calcine obtained by oxidative roasting of pyrrhotite concentrate which had been previously pelletised to a particle size of -400+160μ in a fluidized-bed furnace at 750-800°C. According to chemical analysis, the calcine contained the following %: 2.8Ni, 0.218Cu, 0.073Co, 58.68Fe, 0.185S, 2.24SiO_2, 0.91MgO. The experiments on segregation roasting were carried out with 100g of calcine, to which the necessary amounts of calcium chloride of particle size -100μ were added in a rotary tubular reactor¹) made either of porcelain or of stainless steel. In order to observe the variation in the material composition of the charge, the particle size of the metallic phase, and the behaviour of the calcium chloride during heating of the charge and holding at the segregation roasting temperature 2-6-g samples of the material were taken from the reactor at 10-15 min intervals. The "chlorine" content of the charge and the amount of water soluble nickel and iron chlorides were calculated from the results of analysis of an aqueous extract obtained during leaching of the sample with water. Where necessary the residue after leaching was also analysed.

The material composition of the samples was studied on a Dron-05 Xray diffractometer and under a Neofot-2 microscope. In the second case polished sections inserted into bakelite were prepared. In some of them the number of grains of metallic phase with various sizes was counted (on an area of the section 15mm in diameter). Some samples were investigated on a Cameca MS-46 Xray microanalyser. The apparatus for segregation roast¹) in the experiments on the dynamic release of gases was supplemented by a bubbler containing water, in which hydrogen chloride contained in the gas flow was absorbed. A check showed that carbon dioxide was absorbed little in the bubbler. The amount of residual gases emerging from the reactor was determined by a gas meter, and the contents of oxygen, carbon monoxide, and carbon dioxide were determined by a gas analyser of the GKhP-3M type.

Material analysis of the initial calcine showed that the pre-

Solvent Extraction for Copper Recovery—Some General Considerations

By M. J. Cahalan

Paper read at the inaugural meeting of The Solvent Extraction Group on October 28, 1966)

PERHAPS the most important potential application for solvent extraction in the mining and metal extraction industries is in the recovery of copper from dilute solutions.

Most of the world's copper is obtained from sulphide ores which are treated by flotation to yield a concentrate from which copper is obtained by pyrometallurgy. Mineral deposits generally contain considerable tonnages which are too low in copper to be economically mined. In an underground mining operation such material is mostly left in place but in open cast operations, large tonnages may be excavated and dumped nearby in order to gain access to ore which can be mined and processed profitably.

Natural oxidation of sulphide ores, aided by bacteriological action, readily leads to dissolution of copper in a sulphate solution. The result of this natural process has been known for centuries and copper has been recovered from the solutions on a commercial scale for about 100 years, but only in the last 10 years or so has our understanding of the mechanisms and rate controlling factors been developed.

Imperfect though our knowledge is at the present time, heap leaching of dumps of what was hitherto regarded as waste from copper mining operations is now established commercial practice. Such leaching is not confined to waste dumps and indeed a somewhat similar process has been operated since early this century in Spain, Portugal and the South West United States, but the process has now become much more significant in the overall world picture of copper availability and production. Currently it is estimated that approaching 150,000 tons per annum of copper is recovered in this way (from a free world production of around 5m tons) and it is not unrealistic to say that the figure could be increased five fold within the next 10 years.

Recovery from solution is universally effected by the classical method of cementation with iron. Improvements have been made in the art, science and engineering—much scrap iron has been replaced by shredded detinned cans, or iron powder prepared by hydrogen reduction of iron oxide. One elegant approach even uses reduction of copper smelting slags high in iron to obtain a precipitant which provides some additional copper recovery. The general process is shown in Fig. 1.

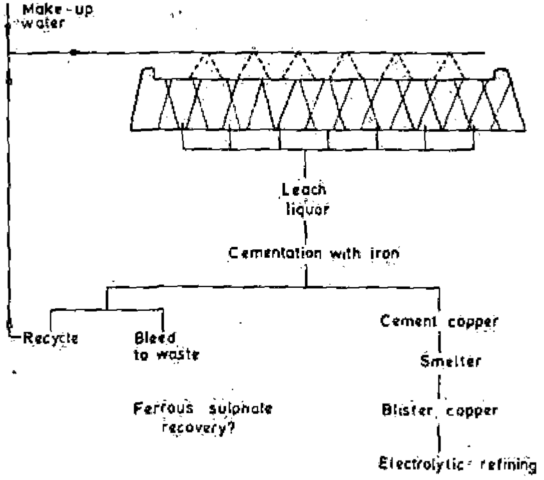

FIG. 1.—*Conventional heap leaching*

The cost of precipitation by these methods is still high, despite increased mechanisation and better control techniques. There is the minimum stoichiometric requirement of iron (0·89 lb Fe per lb Cu) and the presence of ferric sulphate, necessary for successful leaching, is an added consumer of iron so that in practice the consumption is usually nearer 1·5 lbs. This has added disadvantages in many cases where recirculation of the solution after precipitation to leaching dumps is desirable, since increasing iron content raises many problems in leaching.

Precipitated copper obtained by cementation still has to be redissolved and electrodeposited or smelted and refined to yield a marketable product. It is not a particularly attractive material for handling because of its fineness and the difficulty of washing it free from acid, so that direct recovery of copper from solution in a form suitable for handling has obvious attractions.

Solvent extraction with its very low labour requirement offers the prospect of a convenient method of recovery well suited to the large volumes of solution to be handled.

General Process Concept

Electrodeposition of copper from sulphate solution containing 10—100 g.p.l. of free H_2SO_4 is well established practice. However, it is not a practical proposition for solutions containing much less than 10 g.p.l. Cu and particularly at low copper concentrations the presence of significant amounts of iron has a markedly adverse effect on current efficiency, due to oxidation-reduction reactions.

Solvent extraction offers a means of selective extraction from the dilute leach liquor with back extraction (stripping) into a concentrated sulphate/sulphuric acid solution which becomes the electrolyte for electrodeposition to the metal. There is the added attraction that electrodeposition of copper liberates

H_2SO_4 which can be recycled to back extraction thus reducing chemical reagent costs, (see Fig. 2). For such a process, chemicals used are limited to making up for losses in circulation.

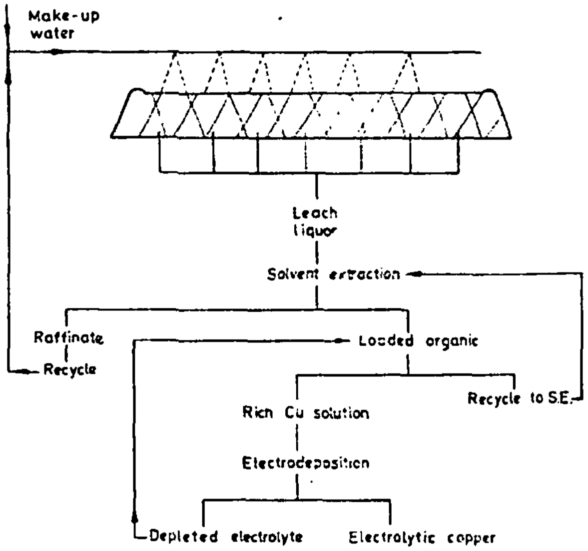

FIG. 2.—*Heap leaching with solvent extraction*

Two purely technical questions arise in comparing this process concept with the conventional flow sheet shown in Fig. 1. First, is the recycle of raffinate containing traces of organics likely to have an adverse effect on the leaching process, and second, is the organic entrainment in the back extract going to electrolysis likely to affect electrodeposition? Investigations into the first have shown that some extractants have a toxic effect on the bacteria important in accelerating the leaching process, notably on thiobacillus thiooxidans, so that care must be exercised in this regard. On copper electrodeposition, there is little likelihood of insurmountable problems arising from organics in the electrolyte.

If the concept is viable, what are the prospects of developing a commercially attractive process? The key is availability of a suitable extractant and it now appears that at least one acceptable extractant will be available.

Solutions to be Treated

The types of solutions to be considered for copper recovery range widely in analysis. Present leaching practice should give copper concentrations in the range 1 to 5 g.p.l. Iron contents could conceivably be as high as 10 g.p.l. in a cyclic process but might in practice be limited to 3 g.p.l. Ideally, all the ferric iron should be reduced in leaching while passing through the heap in accordance with one assumed reaction:

$$2Fe_2(SO_4)_3+CuFeS_2\longrightarrow 5FeSO_4+CuSO_4+2S$$

Note, however, that this is not necessarily the dominant reaction and our present understanding is that direct oxidation of chalcopyrite leading to approximately equal concentration of copper and iron in solution, is dominant in natural leaching processes. With copper minerals low in iron, for example, chalcocite, Cu_2S, the iron problem is much reduced. As far as solvent extraction is concerned, however, it must be assumed that ferric iron may be present.

The pH must be in the region of 2·5—3·0 during leaching for best extraction rates and selectivity for copper. In some cases a significant amount of free H_2SO_4 may be present.

Solvent Requirements

The ideal extractant should operate at the natural pH of the copper solution, be selective for copper (and particularly it should not extract iron), strip without undue difficulty with sulphuric acid, have a low water solubility and be non-toxic to thiobacillus thiooxidans (the most important bacterium in the natural leaching process). Preferably it should operate with a cheap diluent like kerosene and should itself be stable over a temperature range of 0—80°C.

Price is not a primary consideration because if an extractant meets the requirements stated above satisfactorily, particularly with respect to water solubility, its loss in processing will be sufficiently small to be an acceptable cost. Similarly, ability to operate effectively at the low natural pH of the leach liquors would normally be expected to lead a fairly low organic loss (compared with the marked tendency to emulsion formation at near neutral and alkaline pH's).

Solvents Examined

Carboxylic acids have been examined fairly thoroughly at Warren Spring Laboratory and elsewhere as possible extractants for copper. They are cheap and readily available, but suffer the serious disadvantage in this context that significant copper extraction takes place only above pH 4 and iron in concentrations exceeding a few milligrams per litre interferes with extraction.

Versatic acids (synthetic carboxylic acids marketed by Shell) suffer much the same disadvantages although one modification—Versatic 9—can operate with solutions containing iron by extracting it before copper extraction.

A modified carboxylic acid, α-bromo lauric acid—has been developed by Israel Mining Industries. With its more acidic character, it can extract copper at a somewhat lower pH—around 3·3—an improvement over other carboxylic acids.

All carboxylic acids suffer the disadvantage that hydroxyl ions stoichiometrically equivalent to the metal recovered must be consumed in extraction. Even using limestone, as it seems possible to do with α-bromo lauric acid, this alkali cost would normally be unacceptable in recovering copper from leach liquors, especially those containing free acid.

A few years ago, General Mills introduced an α-hydroxyoxime under the trade name of LIX-63 for recovery of copper from solution. It is particularly suited to recovery from ammoniacal solutions of the type obtained from oxide copper ores by conventional ammonia leaching (in closed vessels) as distinct from the field of major commercial interest—natural leaching of open heaps of sulphide ores. The reagent has useful properties—particularly low water solubility and high specificity for copper, but suffers from inability to extract copper at pH below 3·0.

More recently, the same company has developed another reagent—LIX-64—which is described as a mixture of 2-hydroxybenzophenoximes—which like all the foregoing reagents is also used diluted with kerosene. It is outstandingly specific in action and extracts copper from solution in the presence of substantial amounts of iron (ferrous or ferric) and in general appears to satisfy all the basic requirements for the treatment of leach liquor.

Possible disadvantages at first sight are its relatively low loading capacity (2·5 g.p.l. Cu for a 10%solution in kerosene compared with about 20 g.p.l. for carboxylic acids of the same percentage concentration in kerosene) and rather sluggish stripping characteristics with sulphuric acid. However, such disadvantages are more apparent than real, as consideration of the suggested flow sheet (Fig. 2.) shows. The low loading requires a larger inventory of solvent, but this is in any case a small cost in relation to that of overall processing. The slow stripping requires more contact time and hence larger equipment, but this cost too is likely to be relatively unimportant in the overall picture.

A further operating consideration is that in treating a dilute solution with an extractant capable of a high loading, an internal recycle of organic would normally be desirable to maintain a low phase ratio (organic/aqueous) which is generally considered necessary to minimise organic entrainment in the raffinate. Thus, with the low loading of LIX-64, phase ratios close to 1:1 are obtainable without recycling, resulting in desirable simplicity in plant which will be handling very high throughputs.

In electrodeposition, circulation of electrolyte is a necessity and cycling of electrolyte, partially depleted in copper, to back extraction (stripping) achieves this requirement. However, it may be desirable to use some internal recycle as well.

Process Economics

An estimate put forward by those associated with the development of LIX-64 suggests that for a leach liquor containing 1-2 g.p.l. Cu, the total cost of solvent loss, electricity and incidental chemicals usage—approximately £25 per ton of metal produced—should be less than the cost of recovering copper by cementation. From the estimated plant cost data given from the same source, it seems that solvent extraction plant for 10 tpd of metal recovered would cost about £150,000 leading to a depreciation charge of £4–5 per ton of copper. If the above claims are substantiated, a rapid adoption of the process is to be expected.

Solvent loss was estimated in the range of 0·05–0·12 gallons of mixed solvent per 1000 US gallons treated (that is about 0·7 lbs/1000 Imp gallons). If this very low loss is confirmed in practice, the relatively high price of the LIX-64 reagent ($2·25 lb) is of little significance.

Comparison with naphthenic acid and its corresponding requirement of alkali (as caustic soda) for extraction is instructive—the naphthenic acid route would involve an alkali cost of approximately £40 per ton of copper recovered and about £1 per ton for organic reagent. Depreciation would not be markedly different.

Summary and Conclusions

The economic incentive to develop an effective solvent extraction process is a major one, primarily for the copper producers.

A very promising reagent has been developed and process engineering studies can be expected to proceed rapidly.

With the very large volumes of solution to be processed, control of organic phase loss will be important and research and development on this aspect will probably be intensified. Of particular interest will be the ability of the solvent to treat solutions containing a variety of metal ions, silica and suspended matter. These problems are likely to provide a searching test of chemical engineering skill.

LONG SERVICE AWARDS TALK

Speaking at a Long Service Awards Ceremony on March 30, Dr P. W. Reynolds, a deputy chairman of ICI Agricultural Division had some hard things to say about sub-contractual engineering work on some of ICI's new plants.

"Most of you will know," he said "that we have built a new ammonia plant at Immingham to supply Fisons, who have waited for long enough for the product. The plant was ready for use last Christmas, but steam mains blew at the joints; a packaged boiler refused to steam; boiler feed pumps collapsed one after the other; safety valves stuck in the open position or broke their springs, until at last we got to the turbine only to discover that the expansion of the pipework moved the turbine out of line. All this has now been corrected and the turbine is running today, but it has involved three months delay because of inefficient engineering which had nothing whatever to do with the processes of ammonia synthesis technology."

Comparing Japanese engineering with that encountered by ICI Dr Reynolds said "A plant almost identical to that at Immingham, built by the same contractors on the basis of the same 'know-how,' but involving 99% of equipment made in Japan, came up to flowsheet output in 17 months from signing the contract. At Immingham we have reached 33 months and we have not made ammonia yet."

He concluded, however, that he had absolute confidence in the plants that the Division had built and he looked forward to the time when ammonia was exported from the Tees rather than imported.

SOLVENT EXTRACTION OF GALLIUM FROM HYDROCHLORIC ACID SOLUTIONS USING A MIXTURE OF HIGHER ALCOHOLS

UDC 669.871

I. N. Sakharova, Yu. I. Ostroushko, and I. V. Muzalevskaya

Solvent extraction from hydrochloric acid solutions by ethers, ketones, tertiary amines, aliphatic monocarboxylic acids, and H-tributylphosphate is an effective method of gallium separation; however, most of these extractants are expensive and not readily available.

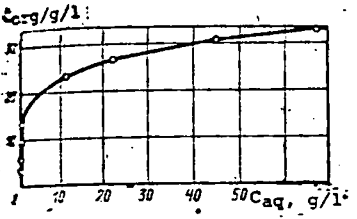

Gallium extraction isotherm.

An analysis is made in the present work of the possibility of using a mixture of higher alcohols as an extractant for gallium; the mixture is a waste product of isooctyl alcohol production and costs 400 rubles/ton.

Experiments were carried out with a mixture of higher alcohols of the following composition, %: light alcohols 1, $C_{12}H_{25}OH$ 75, $C_{16}H_{33}OH$ 21, and H_2O 1; boiling range of mixture 215-250° C, flash point 118° C, self ignition point 260° C, explosion hazard limits 0.8-3.3%, and density at 20° C 0.856 g/cm³.

Extraction from gallium chloride solution was carried out in glass extractors with mechanical mixing at ~ 200 rpm. The phases were separated by centrifuging. The phase ratio in all the experiments was kept at 1 : 1. The initial solution gallium content was ~ 0.44 g/liter.

A study of the effect of the hydrochloric acid concentration (from 1 to 10N) on gallium extraction with the mixture of higher alcohols showed that the highest percentage extraction of gallium into the organic phase (99.9%) was achieved in the range of hydrochloric acid concentrations from 6 to 9N. The maximum distribution coefficient value exceeds 500.

It was also established that equilibrium was quickly reached in the water-organic system, after 2-5 min of mixing.

The isotherm for gallium extraction from 8.5N hydrochloric acid solutions (see Fig.) was plotted with a phase contact time of 5 min. The distribution coefficients for gallium in the region remote from saturation are fairly large. Maximum capacity of the extractant for gallium is 33 g/liter, which is 0.11 g-mole per mole of higher alcohol mixture.

The effect of aluminum and iron on gallium extraction was studied. The results indicate the possibility of extremely effective gallium and aluminum separation by solvent extraction from hydrochloric acid solutions using a mixture of higher alcohols over a wide range of relationships between these elements (see Table).

Effect of Aluminum Concentration in Initial Solution on Extractability of Gallium

Ga init, g/l	Al init, g/l	D^{*}_{Al}	D^{*}_{Ga}	K^{*}	Ga extraction, %
0,77	16,4	0,045	91,8	$2{,}04 \cdot 10^3$	98,9
0,50	6,43	0,021	229,0	$1{,}09 \cdot 10^4$	99,6
0,56	1,40	0,261	661,0	$2{,}53 \cdot 10^3$	99,8
0,54	0,21	1,620	105,0	$6{,}48 \cdot 10^2$	99,8

*D is the distribution coefficient; K - the Ga-Al separation coefficient

According to the published data, trivalent iron is readily extracted by organic solvents containing oxygen; no experiments on Fe^{3+} extraction were therefore carried out. Study of bivalent iron extraction from 8.5N HCl solution showed that Fe^{2+} was not extracted by this mixture of higher alcohols.

The gallium was reextracted with water from solutions with a gallium concentration in the organic phase of 4.24 g/liter, phase contact time being 5 min. It was established that Ga was extracted into the reextract practically completely in one contact (99.7%) at low phase ratios (up to W : O = 1 : 5). An increase in the hydrochloric acid concentration in the reextract prevents a possible increase in the phase ratio. This can be avoided by adding the appropriate amount of alkali. Thus gallium extraction was 81.7% in reextraction with water (W : O = 1 : 8), the acidity of the reextract being 3.5N, but in reextraction with a 2N solution of NaOH (phase ratio W : O = 1 : 10) gallium extraction from the organic phase is 99.9%.

The results of organic phase analyses for alkali metals showed that there is no extraction of these elements under the given conditions. Metallic gallium is obtained after electrolysis of the alkaline reextracts.

SORPTION EXTRACTION OF NICKEL AND COBALT FROM AMMONIA-CARBONATE PULP

UDC 669.243:(729.1)

L. E. Slobtsov, Ventura Errera, Esteban Alfonso, Oswaldo Granda Ibarra, and Pablo Escobar

The existing technology at the Nicaro Plant[1] has a series of shortcomings:

- low extraction to solution of nickel (75-80%) and especially of cobalt (10-20%). due to incomplete reduction during roasting, coprecipitation with iron hydroxide during leaching, and incomplete washing the metals free of tailings;
- the extended period of pulp treatment (about 72 hours) and the associated large amount of apparatus required, due to the use of extensive thickening processes during leaching and washing operations.

It was established in research by Laskorin and others [2, 3] that sorption from ammonia-carbonate pulps makes possible a 5% increase in nickel extraction, a 20% increase in cobalt extraction, and a sharp drop in ore-treatment time.

To meet the specific problems arising under Cuban conditions, it was necessary to use a sorbent which possessed satisfactory sorption properties and regenerated well with a concentrated ammonia-carbonate solution. In this case, one can process a commercial eluate by distillation to produce a nickel carbonate and by regeneration of the reagents (see Figure). These requirements are met by a new sorbent, synthesized in the USSR, having a high mechanical strength and a low swelling coefficient (2.4 mg/g). Its capacity depends strongly on the NH_3 and CO_2 content in the solution. When the NH_3 concentration is increased from 10 to 80 g/l and the CO_2 concentration from 5 to 40 g/l, the nickel content in the swollen resin is lowered from 24 to 7 g/l (when there is 2.5-3 g/l in the original solution). At the anticipated reagent concentrations in the liquid phase of the pulp (40-50 g/l NH_3 and 20-25 g/l CO_2), 11-13 g/l Ni would be in the resin. If the NH_3 content were higher than 140 g/l and the CO_2 content higher than 70 g/l, no nickel would be sorbed at all. Consequently, solutions with that composition would be used for nickel desorption.

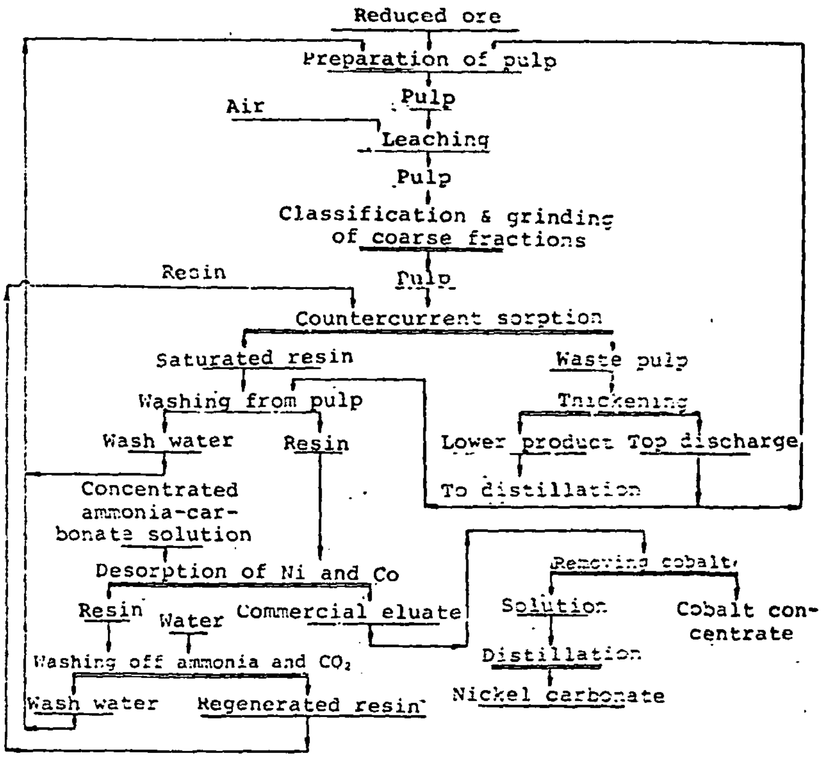

Flowsheet for the extraction of nickel and cobalt from reduced ore with the use of sorption.

First of all, a study was made of the effect that ore-leaching conditions (reagent concentration and the l:s ratio) have on sorption-process indices.

The composition of reduced ore samples used in the tests was 1.38% Ni, 0.106% Co, 40.6% Fe_{tot}, 2.4% Fe_{met}, and 12.9% MgO. The relative content of soluble metals, determined by controlled leaching (the so-called QT* sample) is 74.9% Ni and 61.8% Co.

---

[1] Clara Alonso, Marta Velasquez, Gilberto Rodriguez, and Amansiya Garcia participated in the experimental part of the work.

* Test conditions with the QT sample: 100 g of the ore batch; l:s ratio 14; 130 g/l NH_3 and 65 g/l CO_2; air flow rate 630 l/kg ore; mixing time 3 hours; mixer rotation rate 300 rpm.

We note that metal extraction to solution is lower under industrial conditions than in sample QT: it comes to 2-3% Ni and 45-50% Co.

Leaching was performed in one stage, using a laboratory turboaerator with air supplied in an amount 150 liters per kg of reduced ore. Leaching time is 1 hour. Reagent concentration is within 20-40 g/l NH_3 and 10-20 g/l CO_2. The liquid:solid ratio is 3:1 and 4:1.

The leached ore contained 6-7% of +0.15 mm and 81-83% of size -0.074 mm. Considering the requirements for apparatus arrangements to conduct the sorption process, it is necessary to grind the coarse sizes in such a way that its content in the pulp did not exceed 2%.

Effect of Leaching Conditions on Sorption-Treatment Indices for Reduced Ore

Test conditions and results	Test number			
	1	2	3	4
Leaching of reduced ore				
Solid:liquid ratio	4	4	4	4
Content in starting solution, g/l:				
of ammonia	20,0	30,0	40,0	40,0
of CO_2	10,0	15,0	20,0	20,0
Extraction from ore to soln., % of				
Ni	55,1	61,3	71,3	64,4
Co	2,9	8,9	14,7	7,6
Countercurrent sorption from pulp:				
Volumet ratio of pulp:resin flows	8,0	6,7	5,7	4,4
Extraction from ore to resin, % of:				
Ni	75,2	76,3	78,3	78,6
Co	34,9	43,7	54,5	49,9
Increase of Ni extraction to resin compared with QT sample, %	0,3	1,4	3,4	3,7
Reduction of Co extraction to resin compared with QT sample, %	26,9	18,1	7,3	11,9
Rated content in resin, g/l of:				
Ni	18,3	15,6	13,6	13,7
Co	0,65	0,69	0,73	0,67

Sorption was conducted with mechanical mixing. Fresh resin was used in the tests in which the ammonia-form granules were 0.2-1.6 mm in size. The resin and pulp were separated on a screen in which the hole size was 0.4 mm. Each test was stopped at the point where it reached the predetermined countercurrent cycle.

The following sorption conditions were determined after preliminary tests: the number of stages (8) and the pulp-resin contact period in each test (30 min). In order to conduct sorption under identical conditions, calculations were made of the relationship between the resin and pulp flows, on a basis which calculated the complete resin capacity for nickel at 80% with the given reagent concentration. This was the cause of the different flow relationships in the tests.

It follows from the data given in the Table that the reagents content in the leached solution and the l:s ratio have a strong influence on metals passage to solution during leaching; at the given conditions, the extraction of nickel -- and especially of cobalt -- to solution was low. Subsequent sorption from the pulp substantially increases extraction due to the effect of sorption leaching. In particular, nickel extraction to resin will even exceed its extraction, obtained in sample QT. Conditions for preliminary leaching have only a small effect on the sorption extraction of nickel, but their influence is much stronger with respect to cobalt extraction. Therefore, proceeding from the goal of effecting a maximum extraction of both nickel and cobalt, ore should be leached at a l:s ratio of 4:1, using a solution containing 40-50 g/l NH_3 and 20-25 g/l CO_2. It is possible to have a still further increase in reagent concentration and to increase extraction; however, due to the sharp drop in resin capacity it is important to increase the resin flow and its simultaneous charging.

In order to check the stability of the resin properties and to study the behavior of the impurities. an extended test was made including 10 cycles of resin circulation.

The composition of the reduced ore sample was 1.53% Ni, 0.09% Co, 38.1% Fe_{tot}, 2.0% Fe_{met}, 21.0% Fe^{2+}, and 11.8% MgO. The relative content of the soluble metals (sample QT) was 81.2% Ni and 60.3% Co.

Every day, the ores were leached, countercurrent sorption conducted, and the resin regenerated with a strong ammonia-carbonate solution. Daily indices for all of the operations were stable.

The ores were leached for an hour in a turboaerator at a l:s ratio of 4:1 with an air-flow rate of 150 l/kg ore. The leached solution was prepared with use of circulation solutions (clarified solution following thickening of exhausted pulp and the wash waters of the regeneration cycle). The leached solution contained 40.4 g/l NH_3, 24% CO_2, 0.08% Ni, and 0.005% Co. Extraction to solution during leaching was 60.9% Ni and 10.3% Co.

Sorption conditions were as follows: number of stages - 8; contact time at each stage - 30 min; ratio of pulp:resin flows - 4.

In the liquid phase of the spent pulp, the content was 0.036 g/l Ni, 0.014 g/l Co, 20.3 g/l NH_3, and 18.5 g/l CO_2. The solid phase contained 0.30% Ni, 0.045% Co, and 40.8% Fe.

Extraction from ore to resin was 81.3% Ni and 52.3% Co, i.e., it was 0.1% higher for nickel and 8.0% lower for cobalt than in sample QT.

In test 3 (see the Table), conducted under the very same conditions, the increase in nickel extraction was much greater than in sample QT. This can probably be explained by the use of fresh resin in the test, rather than the recirculated resin containing undesorbed metals.

The average metals content in the saturated resin was as follows: 11.0 g/l Ni, 0.55 g/l Co, 0.65 g/l Mg, 0.002 g/l Zn, 0.07 g/l Cu, and 0.09 g/l Fe.

The resin has stable sorption properties and no impurities accumulate in it.

The resin was regenerated under dynamic conditions with a solution containing 135 g/l NH_3 and 73 g/l CO_2. The filtration rate was 2 vol. per vol. resin per hour. 10 volumes of eluted solution passed through each volume of resin. Moreover, 10 fractions of eluate (per volume) were selected; the two first of these were used as commercial fractions and the remainder used in the subsequent desorption cycle. The average degree of desorption was 94.75 Ni, 88% Co, 94.2% Mg. 100% Cu, and 100% Zn.

CONCLUSIONS

1.Sorption from pulps makes it possible to attain a 2-3% increase in nickel recovery and a 38-42% increase in cobalt recovery.

2. The selected resin grade possesses stable sorption properties and is satisfactorily regenerated with a concentrated ammonia-carbonate solution.

3. The total period during which the pulp remains with the sorption operation is 4 hours, as acompared with 72 hours in existing technology.

REFERENCES

1. J. Castellanos. In: Metalurgia Extractiva de los Minerales Oxidados de Niquel la Habana. Instituto Cubano del Libro, 1972, p. 151.
2. B. N. Laskorin. In the book: Separating Metals with Similar Properties. Moscow, Metallurgizdat, 1962, pp. 11-14.
3. B. N. Laskorin and I. A. Logvinenko. In the book: Extraction and Sorption in the Metallurgy of Nickel, Cobalt, and Copper. Moscow, Tsvetmetinformatsiya, 1970, pp. 81-83.

N6, 1975

METALLURGY

HEAVY NON-FERROUS METALS

SOLVENT EXTRACTION PROCESSES IN NON-FERROUS METALLURGY

UDC 669.2.053.4.068

G. P. Giganov and T. I. Yarinova

Solvent extraction is becoming particularly important as a process for the separation, concentration, and purification of metals in the course of development of hydrometallurgical methods.

At present the view is widely held abroad that the use of solvent extraction methods in hydrometallurgy is profitable when the metal to be produced has a price equal to or higher than the price of copper.

Solvent extraction processes are developed mainly in application to clarified solutions. Apart from these, new solvent extraction processes are being developed which include the following: extraction from extremely dense pulps or pastes; metal extraction by an extractant enclosed in granules of porous hydrophobic material, so called granule extraction; combined solvent extraction-decantation extraction of metals; direct separation of metals from extractants by treating the extract with hydrogen under pressure at an elevated temperature.

During the last three years 115 patents have been issued relating to the solvent extraction of metals from aqueous solutions, practically all of them for metals which are more expensive than copper.

Production of Heavy and Noble Metals. The replacement of the copper cementation method by solvent extraction has been widely discussed abroad in recent years. It is known that there are six plants in operation and six plants under construction or being designed at which a solvent-extraction technology is being or will be used in the process of copper production (Table 1). They all use the reagent Lix 64 N as an extractant. A plant in the Republic of South Africa (Rustenberg) uses a tertiary carboxylic acid of Versatic 911 type as an extractant to separate copper and nickel [1].

The plant at El Paso (USA) is particularly interesting, because it processes mother liquors from the copper sulfate crystallization operation during evaporation concentration of refining plant electrolyte [1,2]. The

Table 1
Data on Plants Producing Copper by Solvent Extraction

No.	Plant, firm, country	Raw material	Output, tons per day	Observations
1	Bluebird, Ranchers Dev. Corp. USA (Arizona)	Dilute sulfuric acid solutions from oxidized ore leaching	18,2	First plant in world for solvent extraction of Cu
2	Bagdad Copper Corp, Bagdad USA (Arizona)	Same	18,2	Cost of solvent extraction unit equal to cost of electrolysis shop Stainless steel mixer-settlers
3	Casa Grande*, Capital Wire and Cable Co USA (Arizona)	Solutions from ammonia leaching of cement copper and Cu-scrap	18,2	Regenerated ammonia returned to leaching process
4	El Paso Sec. Corp. USA (Texas)	Acid Cu-Ni solutions from electrolysis waste	18,2 Cu 0,454 Ni	Intermed. adjustment of pH for copper; Ni extraction from raffinate after addition of NH_3
5	Johnson-Matthey Co., London (Gt Brit)	Cu- and Ni-sulfate solutions	Unknown	
6	Metal Chem.*, USA (Arizona)	Solutions from leaching of Cu-scrap	Unknown	Diluent perchlorethylene. Settlement rate 6.45 $\text{lit}/(m^2\cdot\text{sec})$
7	Nchanga Consolidated Copper, Chingola, Zambia	Solns. from sulfuric-acid leach. of tailings & other low-grade material	182	Plant in prestart period
8	Anaconda Co. Anaconda, USA (Montana)	Solns. from ammonia leaching of 25% sulfide concentrat	100	Arbiter-process Plant in prestart period
9	Anaconda Co. Twin Buttes, USA (Arizona)	Dilute solns. from sulfuric-acid leaching of oxidized ore	100	Plant under construction; opening in 1975
10	A new plant at Sahuarita, USA (Arizona)	Unknown	Unknown	Plant under construction; opening in 1976
11	Cie de Cobre, Chuquicamata Chile	Solns. from sulfuric acid leaching of oxidized ores	200	Plant construction agreement signed
12	New plant at Nchanga Con. Cop., Zambia	Solutions from processing ore in Kansanshi underground mine	70	Plant under construction; opening in 1977

* Plant temporarily closed

initial solution contains copper (70-90 g/liter), nickel, iron, aluminum, etc. The solution is neutralized with ammonia to pH = 2.0 and the copper is extracted, after which the raffinate is neutralized to pH = 9.0, the precipitated hydroxides of iron and aluminum are filtered off, and nickel is extracted.

The wide-ranging discussion on the economics of the Lix extraction-copper electrolysis process has made it desirable to make an economic comparison of this process with the cementation-smelting technology [3]. The labor and capital inputs in solvent extraction-electrolysis are made good by the exclusion of expenditure on the smelting of cement copper and the purchase of iron scrap, and by the reduced outgoings on sulfuric acid and on manning the installation. Expenditure on making up the losses of extractant makes up 10-14% of total expenditure. However, certain plants already have experience in the use of extractant flotation to cut down these losses [1].

It is assumed that the solvent extraction process will be even more economical in future because the price of scrap is constantly rising and the price of extractant is falling.

Apart from the synthesis of new and more selective extractants for copper, research is in progress on improving the process technology.

The following processes proved to be promising:

Lix ectraction of copper from dilute acid solutions without electrolysis, including acid reextraction, evaporation concentration of the reextract and copper sulfate crystallization, production of metallic copper by reduction with hydrogen at 300° C (the process has been put forward for industrial implementation);

deposition of copper in powder form from the organic phase by reduction with hydrogen, eliminating the reextraction operation and a number of others. The process is at the development stage [3].

Apart from the problem of processing solutions from the leaching of low-grade copper material, the processing of solutions from sulfide concentrate leaching (which depends to a large extent on the method of leaching) is an important problem. In the processing of ammonia solutions the problems of selecting a more efficient extractant to ensure ease of reextraction and the production of a reextract suitable for the electrolysis of copper do not arise. Therefore the use of Lix extraction of copper shows the greatest promise at present in combination with the Arbiter process [3,5].

Considerable interest is aroused by the nitrate leaching process for sulfide concentrates, as a result of which a copper sulfate solution suitable for direct electrolysis [6] or for the extraction of copper or nitric acid can be produced.

A technology has been suggested in the USSR for processing solutions obtained as a result of heap, underground, and bacterial leaching using extractants of the hydroxyoxime class [7]. The synthesized extractant OMG (from the alkanophenonoximes) has a number of advantages over Lix 64 N: it extracts copper in the more acid region, blends better with hydrophobic organic diluents, and has twice as much capacity for copper. The extractant has been tested at the Almalyk Mining and Metallurgical Combine. By comparison with the cementation method, copper extraction can be increased by 10% and operating costs are reduced by 15-20%.

Further expansion of the use of solvent extraction technology in copper production in the USSR is envisaged, along the lines of developing integrated flowcharts for processing sulfide copper-zinc and copper-nickel concentrates and middlings including the following: autoclave leaching or roasting of initial raw material, metal separation by solvent extraction, electrolysis, autoclave production of powders.

An industrial installation is in operation at the nickel plant in Kristiansand (Norway) for the removal of iron by solvent extraction with tributylphosphate and of cobalt with triisooctylamine from nickel sulfate-chloride solutions produced in the so-called Hybinett process [8]. The same plant has an industrial solvent-extraction installation for the removal of nickel from cobalt; it was designed on the basis of laboratory tests, bypassing the stage of pilot plant testing.

The construction of a high-output plant using the Norwegian plant system is planned in Canada [9]. A plant is also being built in Canada for the solvent-extraction separation of nickel and cobalt from sulfate solutions obtained by leaching waste from the new IPC Plant at Copper Cliff [1]; the extractant is di-2-ethylhexylphosphoric acid. There are pilot plants in operation in the United States processing deep-sea manganese concretions, with solvent extraction of nickel, cobalt, and copper. The extractants used are Kelex 100 for nickel and copper and triisooctylamine for cobalt.

The following have been recommended for industrial implementation:

the Canadian method of processing previously reduced nickel-cobalt ore by chlorination in sea water with subsequent solvent extraction of the metals from solution;

the American process of obtaining nickel from low-grade laterite ores, with solvent extraction of the nickel from ammonia-carbonate solutions using Lix 64 N extractant and subsequent nickel electrolysis [3]. Cobalt is separated out in the process of reextraction with sulfuric acid;

the American process of producing high-purity nickel from solutions obtained from leaching nickeliferous raw material, using extraction by α-hydroxyoxime and subsequent electrolysis without cathode diaphragms [10].

In the USSR, an industrial solvent-extraction installation is in operation at the Noril'sk Combine producing high-purity cobalt, using carboxylic acids [11].

In the Republic of South Africa, a process for solvent extraction of zinc from pickling solutions from hot galvanizing has been developed and tested in an experimental installation [12]. The appropriate plant is nearing completion near Johannesburg.

In the USSR, a process has been introduced for the solvent extraction of cadmium from sulfate solutions obtained from lead dust processing [13]. The cadmium is extracted by tributylphosphate in the form of an iodide complex.

Table 2
Industrially Adopted Solvent Extraction Processes for Rare Metals

Metal	Initial material	Extractant	Country, plant
Tantalum, niobium	Various materials, hydrofluoric-nitric solutions	MIBK	USA, most plants
	Slag from tin smelting	MIBK	Japan, Isihara Sange Plant
	Columbite-tantalite ore	TBF	India
	Various materials, hydrofluoric-sulfuric solutions	TBF	USSR
Zirconium hafnium	Thiocyanate solutions	MIBK (MEK or alchol addit.)	USA
	Nitrate solutions	TBF	USA
	Sulfuric acid solns.*	TOA	USA
	Hydrochloric acid sol solutions	Ethyl acetate	USSR
Scandium	Waste solutions from uranium production	D2EGFK (di-2-ethylhexylphosphoric acid)	USA
	Hydrochloric acid solutions from leaching tin-production slags	D2EGFK	USA
Thallium	Sulfate solutions from leaching lead dusts	TBF (iodine solution)	USSR, UKSTsK
	Zn-Cd production middlings*	D2EGFK	USSR, UKSTsK
Tellurium	Te concentrates from Pb production	TBF	USSR
		TAA	USSR
Indium	Sulfate solns. from Zn production	D2EGFK	USSR
	No data	No data	USA, Molybdenum Corp. plants
	Bastnasite concentrr	D2EGFK	Same
	No data	No data	USA, plants of American Potash and Chem. Corp.
All rare-earth metals	Hydrochloric and nitric solutions	TFB (alkylphosphoric acid)	USSR
Tungsten	Tungstite and scheelite concentrates	No data	USA
	Molybdenum concentrates*	Commercial TAA (C,-C, fract.)	USSR
Rhenium	Copper-molybdenum concentrates	Isoamyl alcohol	France, plant in Bertolus
	Sublimates from Cu concentrate smelt.	Same	Polish Peop. Rep. plant in Legnica
	Washing acid from sulfuric acid shop	Tertiary amines	USSR
	Solutions from wet dust trapping	Same	USSR
	Solutions from dust leaching	» »	USSR

*Solvent extraction tested under production conditions.

In the development of hydrometallurgical methods for processing oxidized manganese ores in Canada a study is being made of the possibility of solvent extraction of zinc from the solutions with a mixture of di-2-ethylhexylphosphoric acid and tributylphosphate.

The application of solvent extraction technology to the production of other heavy metals is still at the development stage.

Much attention has recently been devoted to the solvent extraction and separation of noble metals.

The solvent extraction method developed in the United States for the extraction and purification of gold from noble metal concentrates produced in the form of anode mud in the electrorefining of copper and nickel is used abroad on an industrial scale [14]. The extractant is dibutylcarbitol, which extracts gold selectively and in quantity from chloride solutions in the presence of platinum metals.

Production of Light Metals. A solvent extraction process for the production of high-purity beryllium oxide from acid sulfate solutions obtained from leaching low-grade ores is in use on an industrial scale at the Delta Plant in the United States [13]. A process of electrochemical leaching (after treating the ore with oxalic acid) and solvent extraction has also been developed to extract beryllium from the ores.[1]

Strontium is obtained from liquid waste from nuclear fuel processing by solvent extraction with a mixture of di-2-ethylhexylphosphoric acid and tributylphosphate [15]. Solvent extraction is used in the production of electrolytic magnesium to remove calcium from concentrated magnesium chloride solutions [16].

Aluminum is obtained by solvent extraction from waste solutions following copper cementation, using monododecylphosphoric acid; the crystalline salt is salted out from the reextract by passing hydrogen chloride through it [17]. The technique is recommended for the extraction of aluminum from copper mine waters in the United States.

Methods have been developed for the removal of iron, zirconium, and titanium from aluminum solutions using an amine[2] or a quaternary ammonium compound.[3]

Production of Rare Metals. Solvent extraction processes have found their widest application in the production of rare metals, where they have become vital technological operations. The main developments in this field have been in the USSR and in the United States. Solvent extraction under industrial conditions is used in the production of tantalum and columbium, zirconium and hafnium, scandium, yttrium, and the rare earth elements, thallium, tellurium and indium, tungsten, molybdenum, and rhenium.

The solvent extraction processes for the production and separation of rare metals which have been implemented under production conditions have been described quite extensively in the literature (Table 2).

Apparatus. Installations of mixer-settler type and rotating and pulsating columns have given good accounts of themselves in the field of apparatus design. Preference is given to mixer-settlers in solvent extraction installations with high throughput capacity and a small number of separation stages. Economic considerations obviously impose limitations on the use of existing high-output centrifuges. There have been tendencies toward using wet cyclones, which maintain a high output for a small volume of apparatus.

The principal manufacturers of equipment for solvent extraction processes are the United States (General Mills and Denver Equipment), the USSR, and the German Democratic Republic.

In correlating Soviet and foreign methods of using solvent extraction technology in non-ferrous metallurgy it must be stated that there have been considerable achievements in this field. A series of solvent extraction methods have been developed for the separation, concentration, and production purification of metals from various solutions (including complex solutions) or low-grade raw material which are acceptable to industry. Certain methods have already been put into practice on an industrial scale, yielding appreciable savings; others are being prepared for adoption.

A large number of selective extractants have been tested and synthesized within the framework of fundamental research. However, only a few of them have found industrial applications, for technological and (above all) economic reasons.

The development of new, highly selective extractants will permit fundamental changes in the hydrometallurgical processing practice for ores and concentrates. In addition, it will become possible to use hydrometallurgical methods for those ore materials which are at present unprofitable.

REFERENCES

1. D. S. Flett, Ingenieursblad, 1972, 41, No. 15-16, 424-431 [Ekspress-Informatsiya VINITI. Tsvetnaya Metallurgiya, 1972, No. 43, 14-30].
2. S. N. Abramishvili and N. V. Sinel'shchikova, Tsvetnaya Metallurgiya (Byull. In-ta "Tsvetmetinformatsiya"), 1974, No. 14, 34-37.
3. D. S. Flett, Trans. Inst. Min. and Met., 1974, 83, March, 30-38 [Ekspress-Informatsiya VINITI. Tsvetnaya Metallurgiya, 1974, No. 31, 1-9].
4. Metal Trans., 1973, 4, No. 5, 1429-1430.
5. A. A. Tseidler, Tsvetnye Metally, 1974, No. 12, 69-71.
6. J. Prater, P. Queneau, J. Thomas, and T. Hudson, Min. Engng., N.Y., Dec. 1971, 23, 67, Abstract.
7. I. I. Zeger, N. A. Vinogradova, L. V. Kovalenko, et al., Inventors' Certificate No. 392133, Otkrytiya, Izobreteniya, Promyshlennye Obraztsy, Tovarnye Znaki, 1973, No. 32, 61.

---

[1] U.S. Patent No. 3441405, 1969.

[2] U.S. Patent No. 3323865, 1967.

[3] U.S. Patent No. 3473919, 1969.

8. E. Wigstol and K. Frouland, *Ingenieursblad*, 1972, 41, No. 17, 476-486 [*Ekspress-Informatsiya VINITI. Tsvetnaya Metallurgiya*, 1972, No. 48, 1-26].
9. *Eng. and Min. J.*, 1971, 172, No. 2, 23.
10. *Eng. and Min. J.*, 1973, 174, No. 9, 200.
11. V. F. Borbat, in: Solvent Extraction and Sorption in the Metallurgy of Nickel, Cobalt, and Copper, *Moscow, Tsvetmetinformatsiya*, 1970, pp. 26-27.
12. A. K. Haines, T. N. Tunley, T. E. Riele, et al., *J. S. Afr. Inst. Min. and Met.*, 1973, No. 4, 149-157 [*Ekspress-Informatsiya VINITI. Tsvetnaya Metallurgiya*, 1974, No. 12, 23-27].
13. V. A. Kuznetsov, Metallurgy of the Non-Ferrous and Rare Metals, Review of Science and Technology, Metallurgy Series, Issue 6, *Moscow, Izd-vo Akad. Nauk SSSR*, 1973 (Institute of Scientific Information), pp. 56-135.
14. B. F. Rimmer, *Chem. and Ind.*, 1974, No. 2, 63-66 [*Ekspress-Informatsiya VINITI. Tsvetnaya Metallurgiya*., 1974, No. 17, 12-15].
15. J. le Bouhellec and E. Henry, *Note CEA*, 1971, No. 1419, 258-265.
16. *Chem. and Engng. News*, 1967, 45, No. 34, 54-56.
17. D. R. George and R. E. Tame, *J. Metals*, 1969, 20, No. 9, 59-63.

RARE METALS AND SEMICONDUCTORS

SORPTION EXTRACTION OF RHENIUM AT THE BALKHASH MINING AND METALLURGICAL COMBINE

UDC 669.849

L. I. Mekler

Sorption schemes for rhenium extraction from industrial solutions of various compositions have been developed and adopted at the Combine, in collaboration with the Institute of Metallurgy and Concentration, Academy of Sciences of the Kazakh SSR and Kazmekhanobr.

The sulfuric wash acid formed during the wet cleaning of converter gases on the way to sulfuric acid production is the principal source of rhenium in the copper smelting production cycle.

The wash acid (20-30% H_2SO_4), in which rhenium is present as $HReO_4$, is diluted with water, left to stand, and decanted to separate the slimes; these become commercial lead cake after being washed free of acid and neutralized with soda. The wash water is combined with the wash acid, bringing the sulfuric acid content to 5-10%.

Rhenium is selectively extracted from these solutions by an adsorption-ion exchange technique (Fig. 1a). The solutions, which contain (g/liter) from 0.02 to 0.1 Re, 5-7 Zn, 0.1-0.2 Cd, 0.1-0.2 Bi, 0.3-0.5 Cu, 0.4-0.6 F, 0.5-0.7 As, 0.1-0.2 Fe, 0.1-0.2 Ca and Mg, and 0.4-0.6 Cl, are fed first to carbon columns, and the rhenium is adsorbed on KAD activated carbon. The acid solutions after adsorption contain < 2 mg/liter Re and go to waste.

After the carbon has become saturated with rhenium (its capacity is 1-2%) it is washed with 8-10 volumes of water and the rhenium is desorbed as $NaReO_4$ with hot (85-90° C) 1% soda solution. The batch of carbon can be used in 40-50 cycles, after which it is replaced. Since the soda desorbates contain a very small amount of molybdenum and the rhenium and sulfates ratio < 1 : 5 these solutions do not require special purification. The desorbates, which contain 1-2 g/liter Re, 3-6 g/liter sulfates, and a certain amount of iron and molybdenum, are acidified with hydrochloric acid to pH = 4-5 and fed to ion-exchange columns containing AN-21 low-basicity anion-exchange

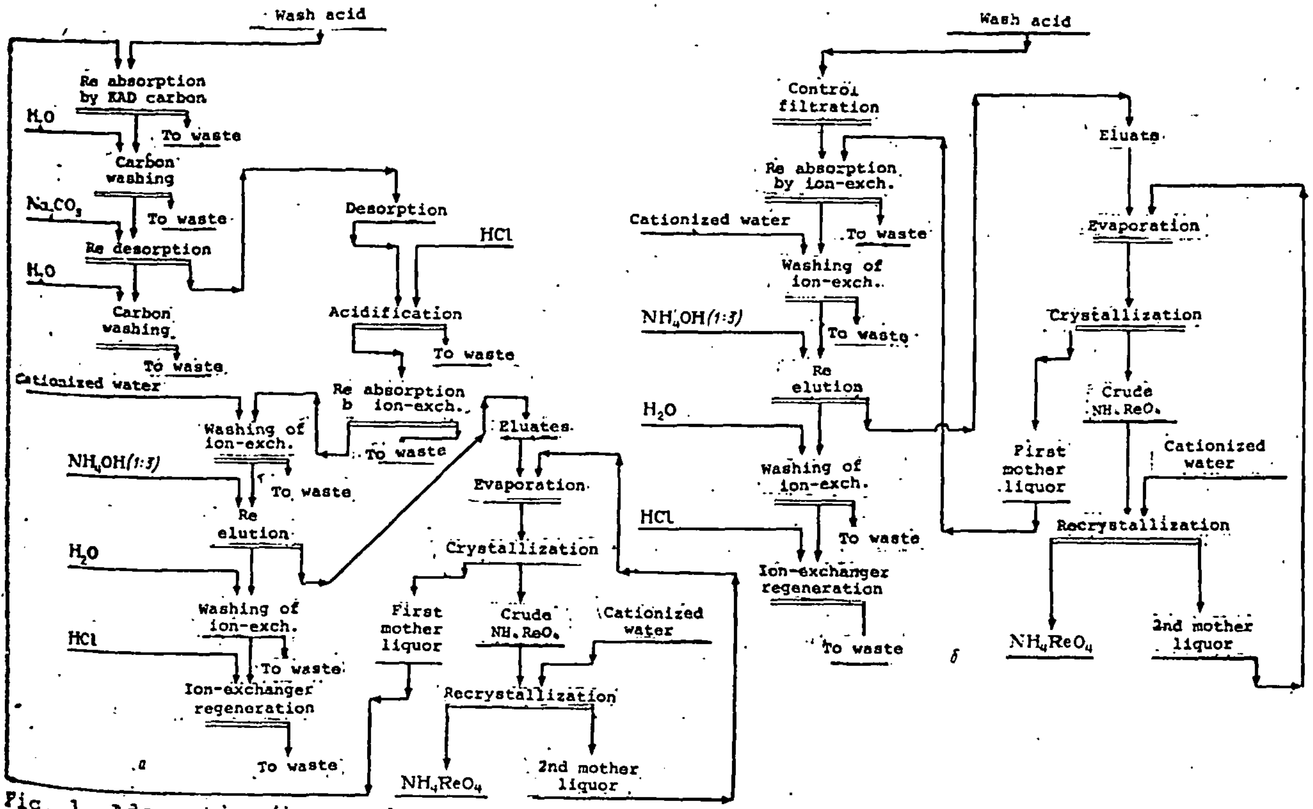

Fig. 1. Adsorption/ion-exchange scheme (a) and proposed scheme (b) for extraction of rhenium from sulfuric wash acid.

resin with secondary and tertiary amines as its ionogenic groups. The anion-exchanger is regenerated first with hydrochloric acid and simultaneously converted to chloride form. Rhenium is sorbed on the anion-exchanger as ReO_4^- when the rhenium-bearing solutions are passed through the column of AN-21 at a specific load of ≯ 3^{1}/hr (not more than three volumes of solution per volume of anion-exchanger per hour).

The low-basicity anion-exchangers absorb predominantly rhenium, molybdenum, sulfates, and chlorides from the industrial solutions. The chlorides and sulfates do not interfere with ammonium perrhenate production by subsequent crystallization because the ammonium sulfate and chloride remain in the mother liquor, by virtue of their high solubility.

The dynamic exchange capacity of the anion-exchanger for rhenium is 20-30%. After saturation with rhenium, the anion exchanger is washed with 10-12 volumes of cationized water to eliminate possible cations and the rhenium is eluted with 2-2.5N NH_3. The first batches of eluate, which contain up to 0.2 g/liter Re, are returned to the adsorption system because of possible contamination by impurities. Subsequent eluate solutions (containing on average 5-7 g/liter Re) are concentrated by evaporation to 80-90 g/liter Re and the hot solution is filtered. During evaporation concentration in metal apparatus the molybdenum is reduced and comes down as a precipitate which is easily filtered out. The leaner eluates and the first wash solutions containing ammonia are collected in a separate vessel for subsequent elution.

The first crystals of ammonium perrhenate separate out from the concentrated eluate after cooling to 10° C; they are contaminated by ammonium sulfate, because the anion-exchanger absorbs perrhenate and sulfate ions to approximately the same extent.

The first mother liquors contain > 100 g/liter sulfates and ~ 5 g/liter Re; these solutions are returned to the carbon absorption cycle. The first crystals of crude ammonium perrhenate are recrystallized twice, the third mother liquor being used in the first recrystallization and water in the second.

The second mother liquor from the first recrystallization, contaminated with sulfates and containing 25-30 g/liter rhenium, is returned to the evaporation cooling stage with the eluate. During evaporation concentration in the next operation, the excess of sulfates is taken out for adsorption with the first mother liquor from the crude perrhenate. When this dissolves in the third mother liquor there are no additional losses of rhenium because the liquor is already saturated with perrhenate. The third ammonium perrhenate crystals are washed with alcohol to remove traces of ammonium sulfate and possible admixtures of phosphorus. After drying, the salt contains ≮ 69.4% rhenium and is up to standard in terms of 13 limiting impurities. Rhenium extraction from the wash acid into the commercial product is ~ 95%.

In collaboration with the Institute of Metallurgy and Concentration, Academy of Sciences of the Kazakh SSR, and Kazmekhanobr, the Combine has developed a method for the extraction of rhenium from wash acid solutions by direct ion exchange using AN-21 low-basicity anion-exchanger, bypassing the stage of rhenium concentration on carbon (Fig. 1b). The essentials of the method are as follows. After control filtration, sulfuric acid solution containing rhenium is fed to columns containing AN-21 exchange resin in chloride form at a specific loading of up to 5 volumes of solution through 1 volume of resin per hour.

The resin is saturated when the rhenium breakthrough after the first column (using three columns in series) is equal to the rhenium concentration in the acid solution coming to the sorption process and the rhenium breakthrough after the third column ≯ 2 mg/liter.

After saturation with rhenium, the resin is washed with water to remove excess acid to pH = 5-6 and the rhenium is eluted with ammonia solution at a concentration of 1 : 2 or 1 : 3.

The lean rhenium eluates are used in secondary elution and the rich eluates are concentrated by evaporation to 65-70 g/liter Re. The first crystals of crude ammonium perrhenate are precipitated from the cooled evaporated solution and subsequently recrystallized.

After rhenium elution and washing with water, the resin is regenerated with hydrochloric acid (1 : 1) to convert it to its initial chloride form. The resin is ready for re-use after washing out the excess hydrochloric acid with water (to pH = 4-5).

Pilot-plant and experimental industrial tests have been carried out on the method of direct ion exchange for rhenium extraction from wash acid.

Structural improvements had to be made to the ion-exchange columns in order to bring this method into use. Apparently the most acceptable version involves pulsation apparatus or continuous sorption columns with pneumatic discharge.

Mother liquors after precipitation of calcium molydbate and sulfuric acid solutions from wet cleaning of exhaust gases from the fluidized-bed furnace roasting substandard molybdenum concentrates for processing in the molybdenum plant hydrometallurgy shop are sources of additional rhenium and molybdenum production.

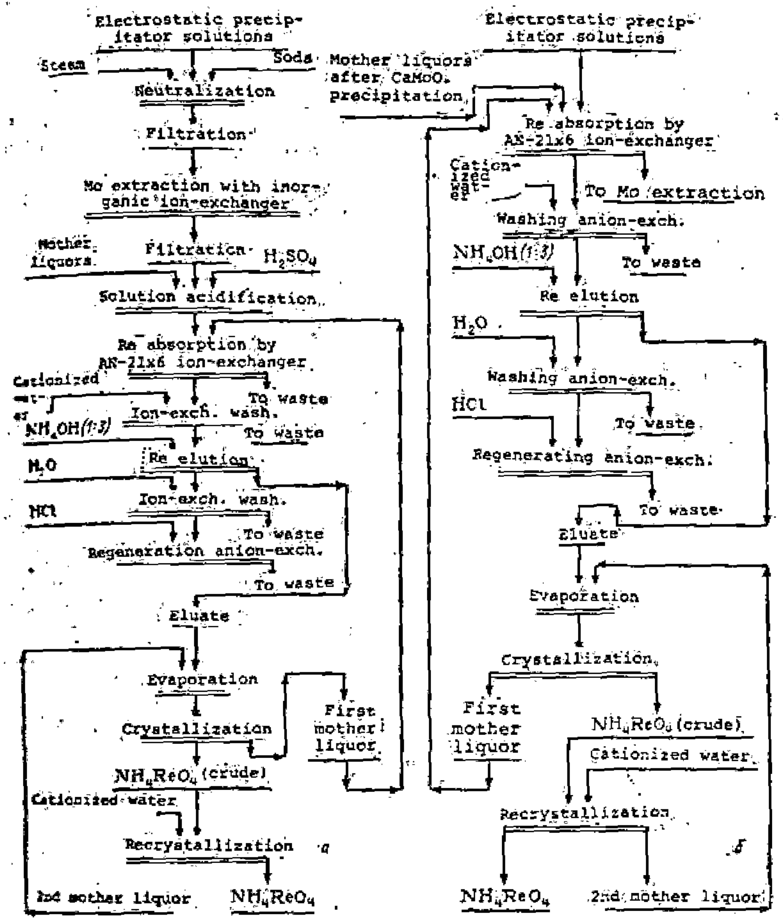

Fig. 2. Improved scheme (a) and proposed scheme (b) for rhenium extraction from molybdenum production solutions.

The sulfuric acid solutions from wet cleaning of gases from the fluidized-bed furnace roasting substandard molybdenum concentrates are the main source of rhenium production in the molybdenum production cycle at the Balkhash Combine. Their composition (g/liter) is 0.3-0.6 Re, 4-17 Mo, 40-80 H_2SO_4, 0.6 Cu, 1.0 Fe, 0.05 As, and 0.7 Cl. The flowsheet for rhenium extraction from these solutions which was in use until 1970 was very complex.

Previous investigations had established the possibility of rhenium extraction from molybdenum shop gas-cleaning solutions by ion exchange using AN-21 anion-exchange resin. Capacity of the resin for rhenium was 8.5% (by mass). The rhenium was eluted with a 1 : 3 ammonia solution at room temperature.

It was decided on the basis of good laboratory results to carry out pilot-plant tests of the new technology in the molybdenum plant hydrometallurgy shop. Moderately cross-linked AN-21×6 anion-exchange manufactured by the Kemerovo Chemical Industry Research Institute was used in the tests.

The AN-21×6 resin was loaded into an industrial ion-exchange column and mother liquors stripped of molybdenum with AN-1 resin and containing 15-30 mg/liter Re and 50-100 mg/liter Mo were fed in. Solutions from wet gas cleaning and dust trapping containing 350-450 mg/liter Re and 50-100 mg/liter Mo after appropriate treatment (removal of molybdenum with inorganic ion-exchanger and acidification to pH = 3) were fed to the resin after the column filtrate rhenium content went beyond the process norms. Saturation proceeded at a specific loading of 1-2.5^{1}/hr. Under these conditions the filtrate rhenium content (breakthrough) fell to zero and the capacity of the resin for rhenium reached 8-10% (by mass). The rhenium was eluted with 2N NH_3 at a specific loading of 0.5-1^{1}/hr. Commercial-grade ammonium perrhenate to GOST requirements was obtained from the ammonium eluates after concentration by evaporation, crystallization, and recrystallization.

The new rhenium extraction technology, brought into use in October 1970 (Fig. 2a), yields ammonium perrhenate while bypassing the potassium perrhenate precipitation stage and excluding the operations of rhenium adsorption on carbon modified with methylene blue, rhenium desorption with 1% soda solution at 90° C, concentration evaporation of the soda desorbates and precipitation of potassium perrhenate with potassium chloride, dissolving, acidification, and sorption by AN-2F anion-exchanger. The degree of rhenium extraction rose by more than 2% as a result of using the new technology.

In spite of the considerable simplification obtained by using AN-21×6 anion-exchanger to extract rhenium from solutions containing molybdenum, the technology has substantial disadvantages: the necessity for neutralization of electrostatic precipitator solutions and removal of molybdenum from them by an inorganic ion-exchanger which partly absorbs rhenium. The separation of molybdenum and rhenium when they are present together in acid solutions is therefore a matter of great urgency.

As has been stated above, two methods are used at the Balkhash Combine to Separate rhenium and molybdenum, based upon preliminary extraction of molybdenum from the solutions with AN-1 anion-exchanger and an inorganic ion-exchanger, The principal disadvantages of the methods are the substantial losses of rhenium sorbed by the ion-exchangers and the complexity of the technology.

Further research was carried out to develop a simple and effective technology for separating rhenium and molybdenum. Laboratory studies with synthetic and with industrial solutions established that the strongly cross-linked low-basicity AN-21×16 anion-exchanger gave practically complete separation of rhenium and molybdenum at pH = 3-0.5. This is because AN-21×16 behaves like a molecular screen relative to rhenium and molybdenum, absorbing rhenium completely and not absorbing molybdenum.

Pilot-plant tests were carried out with standard industrial equipment in the hydrometallurgy shop at the Balkhash Combine, using solutions of the following composition, g/liter: 0.62 Re, 10.5 Mo, and 62.5 H_2SO_4.

The tests were carried out with electrostatic precipitator solutions only, because at the time of the tests there was no pipework which could be used to feed the mother liquors to the ion-exchange column after treatment with AN-1.

Fifty kg (air-dry weight) of AN-21×16 anion-exchanger manufactured by the Kamerovo Chemical Industry Research Institute were loaded into the ion-exchange column. The specific loading during sorption was kept at the 2^1/hr level. The filtrate was analyzed for rhenium and molybdenum every hour. After the ion-exchange column, filtrates containing < 5 mg/liter were sent to the existing hydrometallurgical circuit for leaching molybdenum calcine from fluidized-bed roasting of molybdenite concentrates, and those containing > 5 mg/liter were recirculated. It was established during operation that molybdenum was hardly sorbed at all by the ion-exchanger and practically all of it passed into the filtrate. Two saturation and elution cycles were carried out. In all, 18.8 m^3 of electrostatic precipitator solutions were passed through the ion-exchanger.

When the sorption process was completed, the anion-exchanger was washed with condensate to pH = 4, then with cationized water to pH = 5. Elution was carried out with a 1 : 4 ammonia solution at a specific loading of 0.7^1/hr. The rhenium eluates were evaporated to a density of 1.1 g/cm^3 and crystals of crude ammonium perrhenate were obtained on cooling to 4° C. The mother liquors were sent for processing by the existing technology and the crude perrhenate was recrystallized. The ammonium perrhenate produced was in accordance with the GOST (All-Union State Standard) for AR-1 grade.

The pilot-plant tests demonstrated the substantial advantages of the new method (Fig. 2b) for extraction of rhenium from molybdenum-bearing solutions over the existing method.

The use of AN-21×16 makes it possible to extract rhenium from electrostatic precipitator solutions in the molybdenum plant hydrometallurgy shop in one stage, excluding treatment of the solutions with soda, live steam, calcium chloride, inorganic ion-exchanger, and sulfuric acid; consequently the process becomes much simpler and cheaper and rhenium extraction is increased. According to the test results, using AN-21×16 anion-exchanger in the molybdenum plant hydrometallurgy shop increases rhenium extraction by a minimum of 3% by comparison with the existing technology.

Extraction of molybdenum from waste water from the molybdenum plant using ionic flotation was introduced at the Balkhash Combine in the first half of 1972; filtrates from AN-21×16 anion-exchanger containing < 5 mg/liter Re will be sent to the above installation for recovery of molybdenum and acidification of the alkaline waste water.

Staff from Kazmekhanobr and the Combine have developed a technology for extraction of rhenium from ammonium eluates by electrodialysis which was tested under pilot-plant conditions in 1973, to reduce mechanical losses of rhenium at the stage of ammonium perrhenate production and ammonia regeneration. The investigations showed that crystalline ammonium perrhenate could be produced by electrodialytic concentration of eluates with practically complete recovery of ammonia. The installation (Fig. 3) is based on labyrinth-type electrodialyzers with MK-40 and MA-40 ion-exchange membranes. The installation also includes a mechanical filter, a tank for the initial solution, tanks for the first- and second-stage diluates, tanks for the first- and second-stage concentrates, a cation-exchange column, a device for cooling and filtering the second-stage concentrate, circulation pumps, a controllable direct current source, and monitoring instruments. Ammonium eluates (1.2-1.5N) containing 2-3 g/liter Re were processed in the installation, which operated on the circulation principle. While the eluates were being processed the solution temperature increased to 30-50° C, preventing formation of ammonium perrhenate crystals in the process of concentration. In the first stage the rhenium concentration in the diluate was brought to 0.05-0.08 and in the concentrate to 17-22 g/liter; the respective figures for the second stage were 2-3 and 40-50 g/liter. The first-stage diluate, the ammonia concentration of which was reduced by 3-5% in all, was used for elution of rhenium from ion-exchange columns containing AN-21. The second-stage diluate was combined with the initial eluate on the way to the electrodialysis installation. The second-stage concentrate was cooled to 15-20° C and the precipitated ammonium perrhenate crystals were separated out. The mother liquor (containing 20-22 g/liter Re) was continuously circulated in the installation concentrate circuit and the ammonium perrhenate separation operation was repeated when the solution rhenium content reached 45-50 g/liter.

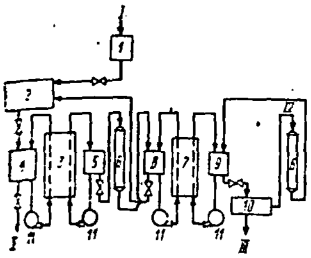

Fig. 3. Line diagram of industrial electrodialysis installation: 1) mechanical filter; 2) initial solution tank; 3) first-stage electrodialyzer; 4) tank for first-stage diluate; 5) tank for first-stage concentrate; 6) ion-exchange column containing cation-exchanger; 7) second-stage electrodialyzer; 8) tank for second-stage diluate; 9) tank for second-stage concentrate; 10) cooling and filtration unit for second-stage concentrate; 11) circulation pumps; I) initial solution; II) rhenium elution; III) ammonium perrhenate; IV) mother liquor.

The first-stage concentrate was passed through an ion-exchange column containing cation-exchanger KU-2×8 in NH_4-form at a speed of 5 specific volumes per hour to remove impurity cations from the process solutions (the resin was regenerated by consecutive treatment with 5% H_2SO_4 and 10% NH_3).

The pilot-plant tests on electrodialytic processing of rhenium-bearing eluates showed that crystalline ammonium perrhenate could be produced from sulfuric wash acid in a continuous closed circuit: sorption - elution - electrodialysis with recirculation of ammonia in the process. The method was brought into use in 1974, and makes it possible to recover ammonia and to reduce mechanical losses of rhenium.

Work is constantly in progress at the Combine to improve the sorption processes and apparatus.

It has been established in collaboration with the staff of Kazmekhanobr in laboratory and pilot-plant tests that porous anion-exchangers of AN-21 type substantially reduce ammonia consumption in elution and increase dynamic exchange capacity. Industrial tests on this anion-exchanger were therefore carried out in 1974 and it was adopted for extraction of rhenium from sulfuric wash acid and from molybdenum plant solutions.

Combine specialists have been working to increase the dynamic exchange capacity of porous ion-exchange resins. It has been established that exposure to magnetic fields during sorption increases the dynamic exchange capacity by 2.5-3 times. This method is now under test in the shop.

We have tested a low-basicity anion-exchanger synthesized by specialists at the Central Asian Non-Ferrous Metallurgy Enterprise Design Research Institute for extraction of rhenium from sulfuric wash acid and molybdenum production solutions. The new resin showed good sorption and kinetic properties: its total dynamic exchange capacity is approximately twice that of the AN-21 anion-exchanger now in use. Pilot-plant tests will be carried out when a batch of the resin is received.

Combine specialists have developed a technology for the production of AR-O grade perrhenate which includes cation removal from the solutions with standard cation-exchangers and have tested it under pilot-plant conditions.

A series of projects has been completed to improve methods of extracting rhenium from ion-exchanger resins using organic and inorganic reagents and mixtures, substantially intensifying the elution of rhenium and increasing the degree of rhenium extraction into the finished product.

All the sorption columns for rhenium extraction have been redesigned at the instance of Combine staff. The new column design makes it possible to remove mechanical suspensions clogging the sorbent during the sorption process and to increase the output of the apparatus.

N6, 1975

SOLVENT EXTRACTION REAGENTS FOR HYDROMETALLURGY

UDC 669.2:542.61

Yu. A. Zolotov

Finding highly effective and available solvent extraction reagents is a matter of great importance in view of the extended utilization of solvent extraction in hydrometallurgy.

The requirements imposed on solvent extraction reagents for laboratory (e.g., analytical) use and for industrial applications coincide at certain points, but in general they differ substantially. These are the principal requirements imposed on reagents:

1) selectivity;
2) high extractive power relative to the required constituent;
3) chemical and radiational stability;
4) ready availability and low cost;
5) a high level of solubility in the organic phase and low solubility in the aqueous phase, and low losses with the aqueous phase;
6) a high capacity relative to the constituent to be extracted;
7) high extraction period;
8) ease of reextraction of the valuable constituent and the possibility of reagent regeneration;
9) low toxicity and low fire and explosion risks.

In the case of analytical solvent extraction reagents the most important items on this list are selectivity and extractive power, and to a lesser extent stability, availability, and solubility. The remaining points are less important. In hydrometallurgy all the points are of vital importance. Up to the present there is apparently not one solvent extraction reagent which would meet all the requirements listed. For example, tributylphosphate is an excellent reagent but it is not selective. Some of the new reagents containing sulfur for the chalcophilic metals are good on almost all points except for ease of reextraction, and so on. This circumstance (and not this alone) leads to the view that one should not speak of good solvent extraction reagents in general. There may be excellent reagents for a specific task, for example, for the extraction of a given metal, or better reagents from a particular class of compounds. The significance of the individual points in the list of requirements alters greatly according to the problem to be solved. Thus high extractive power, selectivity in relation to particular metals, and radiational stability are important in the extraction of plutonium in radiochemical production; less attention is paid to the cost of the reagents. However, in the solvent extraction of copper in hydrometallurgy the requirements of selectivity, low reagent losses in the extraction process, and ease of reagent regeneration come first.

Let us dwell in greater detail on some of the reagent requirements which have been enumerated.

Selectivity. Highly selective solvent extraction reagents are very rare. We have become accustomed to regarding as good solvent extraction reagents not so much the selective reagent as the reagent which selectively extracts the required metal under given conditions, for example, at a prescribed acidity or in the presence of a masking substance. It is vital from the practical standpoint to find these conditions. Almost all past successes in solvent extraction were achieved in precisely this way. No one would call tributylphosphate or trioctylamine highly selective solvent extraction reagents, but no one would deny their importance.

Nonetheless selective reagents are very necessary. Their use cuts down the number of operations and simplifies metal recovery. The use of selective reagents would have greatly facilitated the adoption of solvent extraction in non-ferrous metallurgy. On this basis, selectivity is put at the head of the list of requirements imposed on reagents.

The general principal which can be used as the basis in constructing selective solvent extraction reagents is that of ensuring maximum compatibility between the properties of the central atom and those of the reagent methods. The problem of selectivity can be solved by approaching it from two viewpoints: from the direction of the central atom and (here coordination chemistry is the decisive factor) from the direction of the reagent (taking account of achievements in organic chemistry). This, of course, is an arbitrary distinction. How one might attempt to ensure this compatibility was considered previously in [1]. There are two new works which may be mentioned which have a bearing on this publication.

The first work is about increasing selectivity by extraction of coordinately solvated neutral complexes containing inorganic ligands (for example, halides) and molecules of neutral sulfur-bearing extractant in their inner sphere [2].

Metals can be extracted in the form of three classes of compound by neutral solvent extraction reagents: as covalent coordinately unsolvated compounds of $GeCl_4$ type, as complex acids or their salts, and as coordinately solvated neutral (mixed) complexes; $ScCl_3$.3 tributylphosphate will serve as an example of the latter. Extraction of the molecular halides $AsBr_3$ and $GeCl_4$ is the most selective, but such compounds are few. Of the two remaining groups, the neutral mixed complexes deserve greater attention from the point of view of selectivity. Both complex acids and neutral mixed compounds can be extracted only in the presence of solvent extraction reagents having donor atoms, but the functions of these atoms differ. In the extraction of complex acids protonization, the formation of a cationic hydrate-solvate, is required of the reagents, whereas in the extraction of mixed complexes the reagent must give a strong link with the metal directly. In most cases solvent extraction reagents containing oxygen willingly carry out both tasks; they can be protonized and they can enter the inner sphere of many metals. If, therefore, both complex acids and mixed neutral complexes can be formed simultaneously in a system they will all be extracted by reagents containing oxygen; selectivity will be low. For example, tributylphosphate extracts iron, gallium, and many other elements from chloride solutions together with scandium.

However, the situation will change if solvent extraction reagents containing sulfur are used. Sulfur readily enters the inner sphere of chalcophilic metals (silver, mercury, bismuth, the platinum metals, gold), but shows little inclination toward protonizing. This makes it possible to intercept the extraction of complex acids at once, and selectivity rises sharply.

Table 1
Classification of Metal Ions According to Changes in the Stability of their Halide Complexes in the Series $F^- - I^-$

Class of metal ions	Metal ions
Class A (strong acids)	Alkali, alkali earth, and rare-earth metals, Be, Mg, Mn (II), Al, Sc, Fe (III), As (III), Ga, Cr (III), Co (III) In, Ti (IV), Zr, Th, Ge, Sn (IV), Nb, Ta, U (V), V (IV)
Class B (weak acids)	Cu (I), Ag (I), Au (I), Tl (I), Hg (I), Pd, Pt (II), Cd, Hg (II), Tl (III), Au (III), Pt (IV), Tc (IV)
Elements with intermediate properties	Sn (II) Cu (II), Ni, Pb, Rh (III), Ir (III), Sb (III), Bi

Thus in a chloride solution containing gold, iron, and gallium only the gold forms an extractable neutral complex ($AuCl_3$.S) in the presence of extraction reagents containing sulfur; the iron and the gallium give anionic chloride complexes. Neither the iron nor the gallium will be extracted when a solution of a compound containing sulfur in an inert diluent, for example, benzene, is used as the extractant.

In general form we have the following:

$$MX_n^{m-n}+pS \rightleftarrows MX_mS_p+(n-m)X^-,$$

where M is the metal, X is the inorganic ligand, and S is the neutral extractant. The state of the reaction is determined by the stability of the links between the metal and X and S and by stereochemical requirements, by the compatibility of X and S in the inner sphere.

The entry reaction of extractant S may proceed even further, as far as the formation of various ionic associations, including associations with a metal containing no inorganic ligands at all.

Diphenylthiourea (DFTM, I), isopropylethylthionocarbamate (Z-200, II), etc., were studied as reagents containing sulfur; they are extremely selective reagents for particular metals:

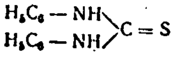

$$\begin{matrix} H_5C_6-NH \\ H_5C_6-NH \end{matrix}\!\!>C=S$$

I

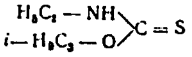

$$\begin{matrix} H_5C_2-NH \\ i-H_7C_3-O \end{matrix}\!\!>C=S$$

II

Diphenylthiourea has been used for a number of purposes, for example, for group concentration of the platinum metals [3]. Extraction is from 6M HCl after heating the aqueous solution with tin chloride (II); the DTFM is added to the aqueous phase. Zinc, iron (III), cobalt, nickel, and manganese do not affect extraction; copper reduces the extraction of the platinum metals somewhat, but is removed from the extract by EDTA and ammonia solution. This method utilizes both the specific reaction between the platinum metals and DFTM and kinetic factors: the increased lability of complexes containing $SnCl_3^-$ ion, and the slow decomposition reaction of the platinum metals-DFTM complexes with ammonia and EDTA at the reextraction stage.

The second work makes it possible to assess the nature of the metal links with X and S to indicate to some extent the most suitable solvent extraction reagent on this basis. The subject is the utilization of the principle of strong and weak acids and bases, Pearson's principle. In accordance with this principle, strong acid metals give stable complexes with strong bases and weak acid metals give stable complexes with weak bases (Table 1). Separation of metal ions into strong and weak acids almost coincides with the well-known Sidgwic Arland-Chatt classification in coordination chemistry.

Alkali and alkali earth metals, elements from group III in the periodic system, Ti, Zr, Hf, Cb, and Ta, actinides and lanthanides, etc., are classified as group A metals according to Arland-Chatt or as strong acids according to Pearson; Ag, Cu(I), Au(I) and Au(III Tl, Hg, Te, Cd, and the lower states of oxidation of the platinum metals belo to group B, or to the weak acids.

The strong bases include extractants with active oxygen and nitrogen atoms; the weak bases include those with active atoms of sulfur and phosphorus (III). The strength of inorganic ligands may also be assessed qualitatively; thus in the case of halides it decreases from F^- to I^-.

If the series of changes in strength for metals, solvent extraction reagents, and inorganic anions is known, the preferential nature of the reaction in the solvent extraction system can be evaluated. Such an analysis has been made in relation to metal halide complexes.

The most important factor now in the problem of selectivity is extensive fundamental research into the factors which determine selectivity: the electron structure of the reacting constituents, stereochemical

Table 2
Flotation Reagents of Interest for Solvent Extraction

Technical name	Type of compound	Formula
Xanthates	Xanthates	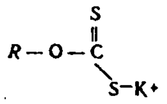
Aerofloats	Dialkyldithiophosphates	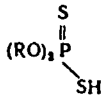
Dialkyldithio carbamates	Dialkyldithiocarbamates	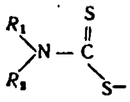
DTK	Tertiary dodecyltrithiocarbamate	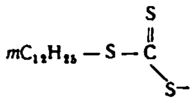
ITK, Z-2000	O-isopropyl - N-alkylthiocarbamate	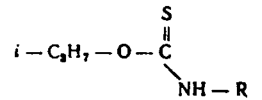 ($R = CH_3$, HTK, $R = C_2H_5$, $Z = 200$)
Dialkyldixanthogenides (AB-1)	Dialkyldixanthogenides	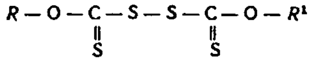 $R-O-\underset{\underset{S}{\|}}{C}-S-S-\underset{\underset{S}{\|}}{C}-O-R^1$
Allyl xanthates	Allyl xanthates	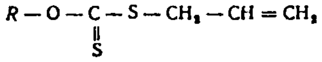 $R-O-\underset{\underset{S}{\|}}{C}-S-CH_2-CH=CH_2$
Thiurams	Tetraalkyl thiuram disulfides	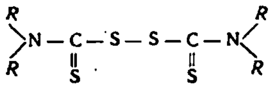
Thiourea derivatives	Thiourea derivatives	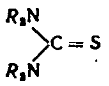
Captax	2-mercaptobenzothiazole	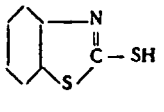
IM-50	Alkylhydroxamic acids	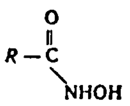
ANP cationic collector	Primary amine hydrochlorides	—

factors, etc. This does not, of course, exclude an empirical search based on the study of the great mass of potentially interesting compounds with a view to finding selective solvent extraction reagents for a particular metal among them. This is the path at present being followed in the intensified search for selective solvent extraction reagents for copper. After the now widely known Lix reagents, which are α- and β-oxyoximes, had been patented in the United States a competition began in the hope of finding equivalent compounds which were more freely available. The Lix reagents belong to a group of copper-selective reagents which have long been known to analytical chemists. The most commonly used reagents in this group are α-benzoxime and salicylaldoxime.

Analytical chemists' experience is extremely valuable in the search for selective extractants of industrial significance. In 1972, at a symposium in Belgium on the use of solvent extraction in metallurgy, one of the major contributors, Spitzer from Holland [4], observed: "It is safe to say that solvent extraction involves no magic. Many if not all of the reactions at present in use have been described, at least in principle, in various handbooks of inorganic analytical chemistry, which are still full of valuable suggestions for those who are attempting to create 'new' selective extractants for metals." There is every reason to agree with this conclusion.

However, let us return to the list of basic requirements for solvent extraction reagents. Various correlations are of importance in assessing the extractive capacity of reagents in a homologous series. Much has been published on this topic, especially by A. M. Rozen.

Let us consider the availability [5,6] of reagents from two points on the list.

It is very tempting to use as solvent extraction reagents compounds produced in large quantities for other purposes. Such compounds include flotation reagents, rubber vulcanization accelerators, oil additives, and pesticides.

The collector reagents which are worthy of attention for solvent extraction are indicated in Table 2. Among these we studied reagent Z-200 and DFTM (on approximately 20 metals from various media), dibutyldithiophosphate and thiurams (for copper). Captax and its disulfide Altax were also studied. Reagent Z-200 is of undoubted interest for various purposes. Dibutyldithiophosphate ensures selective separation of copper from iron, cobalt, nickel, and other metals from weakly acid solutions.

Table 3
Pesticides of Interest for Solvent Extraction

Compound	Formula
Alkylthiocarbamates	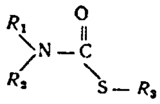
Thiazolthion	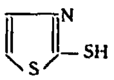
N-alkylamidothiophosphates (or phosphates)	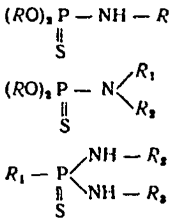
Thiophosphoric acid esters	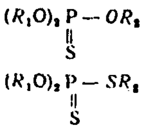 $(R_1O)_2\underset{\underset{S}{\Vert}}{P}-OR_2$ $(R_1O)_2\underset{\underset{S}{\Vert}}{P}-SR_2$

The other group of potential solvent extraction reagents is the pesticides, for example, herbicides or insecticides. The alkylthiocarbamates and dialkyldixanthogenides already mentioned, certain metal-dithiocarbamate compounds, and the compounds given in Table 3 can be used in this capacity.

The salts of dialkyldithiophosphoric acid formed with certain metals, etc., are used as oil additives.

A detailed study of thiophosphoric acid amides was made in our laboratory. One of them (III) is of interest for the selective extraction of copper:

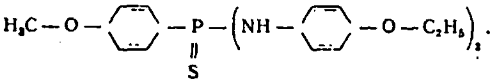

III

It extracts copper from a solution with pH = 2 against a background of iron, cobalt, and cadmium; 2-mercaptobenzothiazole and the mononaphthenic acids are of interest for the same reason. The latter are not being produced as yet, but they may become freely available because they can be produced without difficulty from naphthenic acids, which are in fact waste products in the refining of petroleum. Thionaphthenic acids are suitable for the separation of selenium and tellurium [7], and of nickel and cobalt (only cobalt is extracted from the ammonia solution) [8].

The monothionaphthenic acids belong to the group of reagents of petroleum origin. Apart from them the group includes mercaptans, sulfides, and sulfoxides produced by oxidation of sulfides.

The sulfoxides and sulfides are now the subject of much attention. A symposium was held at Novosibirsk in 1972 on the utilization of these compounds as solvent extraction reagents [9]. The possibilities of sulfides in relation to the number of extractable metals are limited, but on the credit side they are extremely selective as regards mercury, silver, gold, and palladium. The selectivity of sulfoxides is extremely low, but their potential availability and ability to compete with tributylphosphate are attractive.

REFERENCES

1. Yu. A. Zolotov, Izv. Sibirsk. Otdel. Akad. Nauk SSSR, Seriya Khimicheskikh Nauk, 1971, No. 9, Issue 4, 3-10.
2. Yu. A. Zolotov, I. V. Seryakova, G. A. Vorob'eva, and A. V. Glembotskii, Dokl. Akad. Nauk SSSR, 1973, 209, 909-912.
3. G. A. Vorob'eva, Yu. A. Zolotov, L. A. Izosenkova, et al., Zhurnal Analiticheskoi Khimii, 1974, 29, 497-505.
4. E. L. T. M. Spitzer, in: International Symposium Solvent Extraction in Metallurgical Processes, Antwerp, 1972, pp. 16-20.
5. D. S. Fleft, ibid., pp. 22-29.
6. A. V. Nikolaev and A. V. Fokin, Zhurnal Vsesoyuzn. Khim. Obshch. im. D. I. Mendeleeva, 1970, 15, 364-369.
7. Yu. A. Zolotov and A. A. Alekperova, Zhurnal Analiticheskoi Khimii, 1971, 26, 131-133.
8. A. A. Alekperova, R. A. Alekperov, and Yu. A. Zolotov, Zhurnal Analiticheskoi Khimii, 1970, 25, 2283-2286.
9. Izv. Sibirsk. Otdel. Akad. Nauk SSSR, No. 7, Issue 3, 3-104.

SOME FACTORS IN THE DESIGN OF HEAP LEACHING OPERATIONS

George M. Potter

ABSTRACT

This report reviews and discusses some factors in the design of heap leaching operations using dilute alkaline cyanide solutions to dissolve gold and silver from relatively coarse ores. Some of the requirements for laboratory and pilot work to permit reliable scale-up for plant design are presented. The influences upon design of such factors as ore reserves, available terrain, crushing requirements, ore preparation, pad materials, leaching solution strengths, solution application rates, and precious metals recovery methods are briefly outlined. Alternative methods of recovering the precious metals from solution and their subsequent smelting to a doré bullion and some factors affecting choice of method are reviewed. The role of activated carbon in gold-silver recovery and various means of recovering the metals from subsequent stripping operations are discussed. Other viable precious metal recovery methods, including Merrill-Crowe zinc dust precipitation and soluble sulfide precipitation of silver, are described. A few notes on some recent published plant capital costs are mentioned.

FOR PRESENTATION AT THE
PRECIOUS METALS SYMPOSIUM
OF THE
NORTHERN NEVADA SECTION
OF
SME/AIME
IN COOPERATION WITH THE
NEVADA BUREAU OF MINES AND GEOLOGY
AND THE
NEVADA DIVISION OF MINERAL RESOURCES
SPARKS, NEVADA
NOVEMBER 17-19, 1980

TABLE OF CONTENTS

SOME FACTORS IN THE DESIGN OF HEAP LEACHING OPERATIONS

George M. Potter

INTRODUCTION

During the late 1960's the mining industry became interested in the U.S. Bureau of Mines' efforts to develop the gold-silver heap leaching process. In the decade 1970-1980, successful commercial heap leaching applications increased. The process provides a relatively low-capital means of processing treatable ores with reasonable operating costs. Present gold and silver prices compared to capital and operating costs favor the continued growth of the heap leaching method.

The heap leaching process (Figure 1) is defined as the percolation leaching of relatively coarse gold-silver ore piled on an impervious surface. To date, dilute alkaline cyanide solution is the lixiviant of choice. However, other leaching reagents such as thiourea and hypo have been suggested, although not currently used in heap leaching practice to my knowledge. Ores may be mine run in size or crushed as fine as about 3/8-inch (1 cm.). Gold and silver-bearing solutions draining from the heaps may be processed in activated carbon columns to recover (adsorb) the metals followed by stripping and metal recovery, or treated by the Merrill-Crowe zinc dust precipitation method. All solutions are generally recycled to the leaching step, and the heap leaching system is relatively easy to control from the environmental viewpoint.

A number of helpful references from the Bureau of Mines, consultants, and industrial sources describing heap leaching are available in the literature. A selected list of references is attached, and these valuable references and supplementary personal communications have been instrumental in preparing this report.

The flexibility of the heap leaching process should be emphasized. Plants may be very simple, comprising leaching of uncrushed ore on a locally-obtained clay lined pad and shipment of gold and silver recovered in the form of loaded carbon or zinc precipitates; such a plant would have a relatively low capital investment. More elaborate plants for larger ore bodies and available financing may be planned to include crushing, cyclic pad use, and doré gold-silver recovery. The general planning is similar in each case.

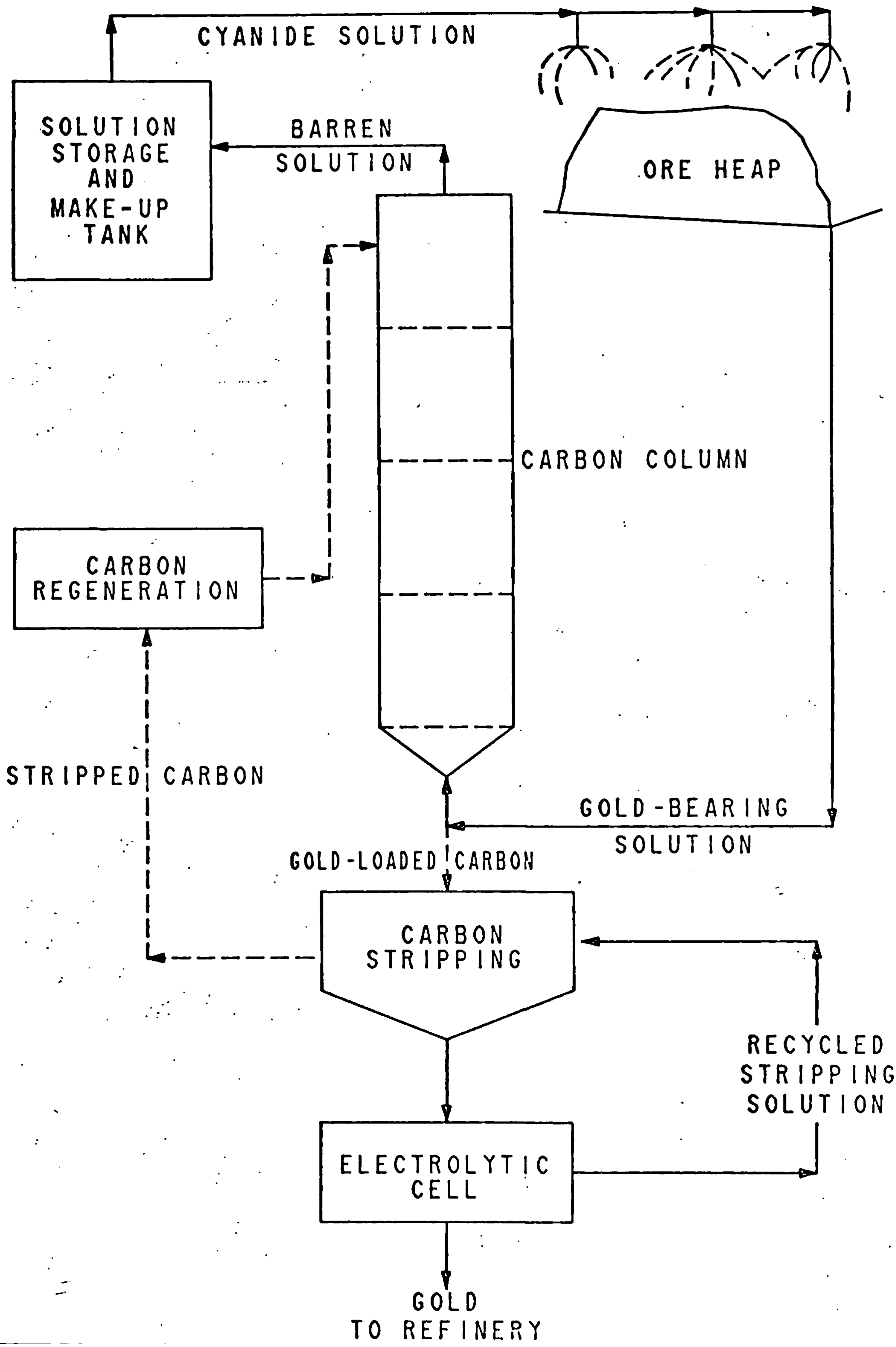
CYANIDE SOLUTION
SOLUTION STORAGE AND MAKE-UP TANK
BARREN SOLUTION
ORE HEAP
CARBON COLUMN
CARBON REGENERATION
STRIPPED CARBON
GOLD-BEARING SOLUTION
GOLD-LOADED CARBON
CARBON STRIPPING
RECYCLED STRIPPING SOLUTION
ELECTROLYTIC CELL
GOLD TO REFINERY

The purpose of this paper is to outline some key factors in the design of heap leaching operations and how they are applied to develop a design for a working operation. Individual design requirements and local construction costs vary so much that no attempt has been made to list detailed costs. A few general comments on costs are included.

OREBODY, RESERVES, PROCESS EVALUATION, AND PRELIMINARY FEASIBILITY STUDY

The evaluation of a given mine ore reserve in terms of tonnage, grade, and process amenability is a basic prerequisite for any process design including heap leaching. As mine sampling of a new or unknown orebody proceeds, preliminary metallurgical tests should be made concurrently so that continuously updated information on ore process response is available. By the time the ore body is reasonably well defined, preliminary cost feasibility studies should be made to determine profitability obtainable by various process alternatives using several assumed metals prices and process conditions. Thus, the first step in design is a feasibility study to enable:

1. Decision to continue with the project
2. Selection of an appropriate process (assumed to be heap leaching in this case)
3. Estimation of a tentative allowable budget for mine and process plants under assumed conditions
4. Determination of the estimated life of the operation, tonnage rate per day, yearly tonnage, ore grade, and metals recovery.

PERMITS, SERVICES, AND ENVIRONMENTAL FACTORS

The availability and cost of power, water, and other services have a large influence on design and should be studied early. Similarly, operating permits and the effect of environmental regulations upon design should be outlined promptly because of their key role in design or proceeding with design. For example, environmental requirements in tailings storage might influence the choice of pad design as to cyclic or one-time use, as well as the design of the storage area. The climate notably affects design through effect on the annual operating time under part-time freezing conditions, and the need for insulating and heating buildings and process units.

TOPOGRAPHICAL MAPS AND PLOT PLAN

The best available topographical maps will already have been used to some extent in the preliminary feasibility study and are essential in preparing a plot plan. The final design of a heap leaching operation is greatly influenced by the topography and location of the leaching pads. Pad size, type, and pumping costs are linked to available areas and elevations. The location of solution reservoirs and the process plant is likewise a critical design decision.

DETAILED METALLURGICAL TESTING FOR SCALE-UP

The ore mineralogy and rock permeability affect the amenability of ores to the heap leaching process. Treatable ores should be porous, competent, and satisfactorily low in cyanide and oxygen consuming substances. The gold and silver particles should be clean and fine in size. The clay content must be low enough so that permeability in a leaching heap can be maintained, or else the ore may be agglomerated as outlined in recent USBM work [10]. Each ore deposit presents different characteristics, so that detailed laboratory and pilot tests are required to determine the optimum flowsheet in each case. Tests may be made in bottle rolls, small columns, large columns, and actual heaps of various sizes. The use of all these methods as keys to scale-up and design is recommended, as outlined in the following discussion.

1. Preliminary tests in bottles and small columns are helpful in showing response to cyanidation at sizes up to 3/8-inch (1 cm) or so.

2. Larger column tests are a reliable guide to scaled up operations. Columns may be thought of as a core in the center of a large leaching heap, with the same access to solution and oxygen. The column diameter should be four times the largest rock size to avoid undue wall effects. Some essential design factors obtainable from columns include the following:

   - amount of solution needed to saturate the ore
   - amount of solution that drains from saturated ore
   - amount of moisture retained by drained ore
   - size of crushing versus leaching time
   - optimum cyanide strength and consumption

- choice of alkali (frequently lime), strength, alkali consumption, pH
- solution and wash application rate
- height of the leaching ore column
- amount of time of draining and washing
- oxygen content of effluent
- feasibility of countercurrent leaching and/or washing

3. Pilot heap tests are used to verify most of the factors listed under column tests and also to provide information on some physical factors of heap construction and leaching. However, heaps smaller than 500 tons or so, unless very shallow, have an excessive slope area compared to the level part of the heap and may mislead on oxygen availability. Heaps supplement columns by indicating:

    - mode of applying solution (sprinklers, wigglers, drip, etc.)
    - confirmation of solution application rate
    - physical factors of heap construction
    - general confirmation of column test factors
    - compaction under leaching conditions

4. Laboratory and pilot gold and silver recovery tests by the activated carbon, Merrill-Crowe zinc dust precipitation, soluble sulfide, and other methods are helpful supplements to column and heap leaching tests. However, the selection of the recovery method from leaching solutions is finally based upon economic analysis of the probable solution flow and analysis, together with experience.

DEVELOPMENT OF THE METALLURGICAL FLOWSHEET AND DESIGN

Each ore body differs in important respects from others. Therefore, the flowsheet and plant design must be based upon individual tests as previously outlined. Nevertheless, there are a number of common factors derived from operational experience that are summarized in the following sections.

1. THE MINE PLANT

The mining method for heap leaching has usually been open pit. Mines vary so much that the type and size of equipment cannot be specified here but adequate maintenance (usually at the property) is absolutely essential whether contract mining or company-operated. Ore sampling and assaying facilities near the mine are a requisite for grade control. The degree of mechanization such as conveyor belt ore and waste handling is tied to ore reserves and the available investment budget.

2. THE ORE PREPARATION

The optimum degree of ore crushing (if any) will have been determined by laboratory and pilot tests. High prices of gold relative to general cost indices usually favor relatively fine crushing to improve ultimate recovery and shorten the leaching cycle. Most ores not containing excessive clay will percolate fairly well when crushed as fine as 3/8-inch (1 cm) or so. Ores presenting percolation problems may be agglomerated by USBM-suggested techniques [10], and cyanide and alkali may be added during agglomeration. A properly sized agglomerating drum might be chosen, or sufficient agglomeration might be accomplished by sprays and mixing at belt transfer points. The complexity of the crushing plant is dictated by leaching size requirements and available budget. Jaw or gyratory primary and cone crusher secondary and tertiary stages are typical if finer crushing is needed. Screening practice is standard. The selection of equipment sizes is in accordance with tonnage requirements, with suitable maintenance time available. Dust control is essential. Dust slurries from control may be pumped onto the leaching heaps.

3. ORE SAMPLE AND WEIGHT

Many heap leaching feeds are "spotty" in gold and silver content (contain relatively coarse values). Automated sampling to provide a large bulk sample of ore to each pad is recommended. Probably the bulk sample will typically be crushed and reduced in weight by a secondary automatic sampler at least once before going to preparation and assay. Spotty head samples should be analyzed on the basis of a 5- to 10-kilogram weighed lot, processed by gravity, cyanidation, fire and atomic absorption assay for a calculated combined head value. A weighing device should record total weight to each pad. Hand moisture samples are common. The design should not skimp on sample plant or weighing control, usually placed just before the delivery point to the pads whether a truck bin or a belt. Small properties may sample by hand.

4. DELIVERY OF ORE TO PAD AND HEAP CONSTRUCTION

Ore is delivered to the pad by truck or belt, depending upon individual cost analysis of capital and operating factors. Heaps up to 14 to 16 feet (4 to 5 meters) deep may be built without driving a truck over the heap; trimming is provided by a front-end loader. Trucks may be 50 ton (45 metric tons) units or larger and loaders about 8 yards (6 cubic meters). Deeper heaps may be built without running trucks over the main bulk of the ore by pushing dumped ore with a dozer or loader. Ripping of machine-compacted surfaces (if any) is recommended. Heaps may also be built by conveyor belt delivery and tripper distribution from a bridge unit. In all cases, the optimum depth of the heap should have been verified by full-height column tests.

5. PAD DESIGN

The choice of pad material, pad size, and design must be determined by local factors in each case. Some key elements in the selection are available area, length of the leach cycle, maximum practical height of the leaching heap, availability of local clays, local construction costs, and availability of tailing storage areas. Pads may be built for one-time or cyclic use. Environmental regulations, likewise, have a critical influence on design, as does available capital and estimated materials (ore and residue) handling costs.

Hot rolled asphalt is probably the material of choice for cyclic use. The design is based upon the heaviest load to be carried per vehicle tire, usually the front-end loader. A 2-inch (5 cm) layer of asphalt, followed by a rubberized seal coat, then 5 or 6 inches (10 to 15 cm) of hot rolled asphalt has been successful for loaders to 8 yards or so (6 cubic meters). Earthen foundations should follow best preparation practice in grading and compaction; slopes are generally at least 3 degrees in two directions to provide for solution recovery in a parallel ditch. An inter-pad curb to provide solution isolation and sampling capability from each leaching unit is a great operational help. Maximum heap depth to avoid running trucks over the heap is probably 15 to 16 feet (about 5 meters) in the case of truck/loader preparation. If trucks run over the heap, the heap should be ripped. In the case of bridge-loaded pads the height may be maximum efficient leaching depth.

Clay linings of 18 inches (46 cm) thickness or so placed on a prepared earthen foundation may be suitable for single-use pads. The particular clay proposed for use should be tested for leakage in the laboratory using the same alkalinity and water as planned for production. Even a small leakage at the present price of gold is very painful. Plastic membrane-lined drainage may be used.

Reinforced plastic membranes can be used for single-use pads. Graded, compacted bases should be covered with about 6 inches (15 cm) of rock-free cushioning sand to help avoid puncture. The membrane strips are joined in the field, then covered with an additional layer of cushioning fine gravel or sand. Butyl plastic of 30 mil (0.8mm) thickness, reinforced with glass fiber, has been used successfully. Drainage canals may also be plastic-lined.

In all cases, bore holes should be angled under each pad to detect any possible leakage.

6. APPLYING SOLUTION AND WASH

Solutions are delivered to the pads by centrifugal pumps via steel or plastic pipe headers that may be buried, insulated, and/or heat-traced for freezing climates. Conservative design indicates relatively large pipes to reduce friction losses and pumping costs. Distribution to the ore heap by sub-headers is usually in plastic pipe with a gradient toward the main headers and thus drainable in case of freezing weather.

Solution application is usually sufficient at 0.002 to 0.005 gpm/sq. ft. (.0014 to .0034 liters/sec./sq. meter). Higher rates of application simply dilute the grade of the pregnant solution. Steady flow appears satisfactory in most cases. Although pregnant solutions may show increased value after a period of "rest", cumulative production usually falls on a steady flow curve, provided that solutions have enough oxygen and cyanide at all times.

Both "wigglers" (short lengths of surgical gum tubing) and various mechanical sprays have proved satisfactory for applying leach solutions. Depending on pressure, wigglers may cover a 30-foot (9 meter) radius and mechanical sprays a larger radius. Spray types providing larger drops favor conservation of cyanide, water, and heat. More work is needed to define spray drop sizes and also to apply water- and heat-conserving solution applying devices such as drip tubes.

For best washing efficiency, several fresh water washes should be applied with draining periods between if time permits. Allowable water washing is governed by evaporative and tailing-retained losses, and all makeup should be applied to the washing heaps to promote washing efficiency.

Solutions may be recycled to dumps to build up the grade, provided that soluble losses in the residues do not increase because of washing problems.

7. SOLUTION RECOVERY AND STORAGE

Pregnant solutions and wash draining from heaps flow by gravity in plastic, asphalt, or otherwise-lined ditches and steel or plastic pipes to storage. The storage tank or pond should be large enough to retain 24 hours of gravity drainage from saturated dumps plus a maximum estimated rainfall in the event of extended power failure. Asphalt, concrete, plastic-lined, and clay-lined storage reservoirs have been used satisfactorily.

8. GOLD AND SILVER RECOVERY PLANT

Alternative methods of recovering gold and silver from cyanide leach solutions include carbon adsorption, zinc dust (Merrill-Crowe) precipitation, ion exchange, direct electrowinning, soluble sulfide precipitation, and aluminum dust precipitation. Most heap leaching operations use carbon or zinc dust methods for treating the leach solutions, although the application of sodium sulfide to precipitate silver from carbon stripping liquors has received favorable attention.

The choice of carbon columns versus zinc dust precipitation should be based upon a capital and operating cost analysis plus consideration of metallurgical efficiency. Probably very large volumes of low grade solutions containing mainly gold may be treated most economically in carbon columns. Rich solutions in comparatively small volume or solutions involving a large daily production of silver should be considered for zinc dust precipitation and compared with the carbon and other systems on a cost/efficiency basis. As to other methods, any applications of direct electrolysis to recovery of gold and silver would be favored by small volumes of rich solution. Ion exchange resins, combining high precious metal loadings and ease of stripping, may be developed. The carbon and zinc dust systems are considered more fully in the following sections.

(a) Carbon System

Experience indicates that the expanded-bed, multiple stage carbon column is an efficient, low cost device for recovering gold and silver from large and small volumes of solutions. The general theory of preparing adsorption isotherms and cascade design has been treated by the U.S. Bureau of Mines [11]. In practice, countercurrent flow in five or more columns is advisable for obtaining high loadings and low barrens. Minus 10-plus 28-mesh carbon (12 x 30 in the carbon industry) provides the best compromise of flow rate and rapid adsorption. Coconut carbon is a good standard; other carbons may be judged on comparative adsorption, durability, and price. The solutions fed do not have to be clarified.

Column design is featured by orifice plate bottoms, bottom-fed upward flow of around 15 gpm/square foot (600 liters/sq. meter) and a working height of 5 feet (1.5 meter) or more above the orifice plate. Carbon when at rest occupies 24" to 30" (0.6 to 0.67 meter) of depth in the column, and weighs about 60 to 75 pounds per square foot (290 to 365 kg/sq. meter). Bed expansion is influenced considerably by solution temperature and resulting viscosity, but fortunately the carbon system is not very sensitive to the amount of expansion. Much helpful material on multiple compartment adsorption was developed by the U. S. Bureau of Mines for ion exchange adsorption of uranium [18].

Individual carbon columns may be superimposed in the form of one multi-stage vertical column. Such a design has considerable advantage if floor space is at a premium. Otherwise an open cascade design of individual columns may be considered. The open design features overflow launders on each tank leading to a feed pipe entering below the orifice plate on the following stage.

A trash screen, 20- to 35-mesh should be placed ahead of the first adsorption column. A "safety" screen with 35-mesh openings should be in circuit after the last column to catch any floating carbon.

Carbon is conveniently moved from stage to stage by hydraulic eductor. Fresh carbon is fed to the last stage, from which barren solution returns to the heap.

(b) Merrill-Crowe Zinc Dust System

Merrill-Crowe plants were once a standard item, but as a package are now available (to my knowledge) from only one U.S. firm (the State of Maine Mining Company, Tombstone, Arizona). They may be custom-designed and manufactured on the basis of a flowsheet comprising precoated clarification filter(s), deaeration unit, zinc dust feeder, precipitate filter, and accessory pumps. The solution fed to a Merrill-Crowe clarifier should not exceed 50 to 100 ppm total solids to avoid undue cleaning requirements. Manufacturer's filter design recommendations should be followed throughout.

9. THE PROCESSING OF RECOVERY-PLANT PRODUCTS

(a) Loaded Carbon

Several alternatives are available for recovering gold and silver doré from loaded carbon:

(1) Direct sale to a smelter. This has the advantage of requiring no capital investment for carbon treatment and is a viable possibility, particularly for smaller operations. Of course, the carbon itself is sacrificed.

(2) Stripping with 1 percent NaOH, 0.1 to 0.2 percent NaCN at a temperature near boiling (90°C). Conical bottomed cylindrical tanks are used, and solutions are percolated at the rate of 10 to 12 gpm per short ton of carbon (0.7 to 0.8 liters/sec. per metric ton). Effluent solutions are usually electrowon, and the solutions returned to the stripping cycle. Some 48 to 72 hours should be allowed to strip carbon loaded typically with from 150 to 400 troy oz. (5100 to 13700 ppm) of gold plus silver down to less than 3 ounces (100 ppm).

(3) The addition of alcohol (say 10 percent of ethanol or propanol) to a 1 percent NaOH, 0.1 to 0.2 percent NaCN solution enables stripping to be accomplished in less than 8 hours at temperatures of 60°C or so and may reduce the need for subsequent carbon regeneration. Seven to 10 bed volumes of strip solution plus wash should suffice. However, alcohol is flammable, explosive, and toxic and the system must be safely designed. At least one experienced company ("NUCON") has a packaged design for handling an alcohol system that recovers most of the alcohol for reuse.

(4) Gold and silver may be stripped from loaded carbon in less than 8 hours with 1 percent NaOH, 0.1 to 0.2 percent NaCN at temperature of 120 to 130°C under a pressure of 70 psig (5 kg/sq. cm.) using 7 to 10 bed volumes of stripping plus wash solutions.

(5) Either the pressure or the alcohol system produces very rich solutions. They may be electrowon to recover doré. Electrolytic cells feature fiber reinforced plastic construction with stainless steel anodes and cathode frames loaded with mild steel wool.

Voltages are on the order of 2.5 to 3.5 volts per cell and amperages consistent with 30 percent current efficiency for gold, rising to 40 percent or more for high silver solutions.

Alternatively, stripping solutions may be treated with zinc dust or by chemical precipitation to provide a filterable precious metal product.

A scheduled "bleed" of stripping solution, adjusted to each operation to control impurities, is fed very slowly (to avoid inhibiting adsorption) back to the recovery plant adsorption columns.

Smelting of either gold zinc precipitates or steel wool cathodes is readily accomplished in crucible furnaces to avoid higher dust losses in direct fired units. A No. 125 silicon carbide crucible unit should readily handle

200 ounces of doré per day. The generally larger bulk of silver operations would probably favor consideration of a small reverberatory-type furnace. Fluxes are standard; for example, a borax, niter ($NaNO_3$), silica mixture. Scrubbers on furnace gases are essential. Slag crushing, removal of metallics by screening, and shipment of accumulated slags to a smelter are common steps.

(b) Zinc Precipitates

As outlined under zinc-precipitated values in stripping liquors, zinc precipitates may be smelted in a crucible or small reverberatory unit with standard fluxes. Doré is recovered and a shipping slag produced.

In many cases, refining of doré to pure gold and silver is referred to established refining concerns, and the doré is shipped to such companies.

10. BARREN SOLUTION STORAGE AND REAGENT FEEDING

Barren solution effluent from the precious metal recovery plant should be stored in a reservoir of about the same size as the pregnant solution storage. Reagent makeup is conveniently done in the barren storage. Suitable storage for alkali and cyanide, and mixing and feeding facilities, should be provided nearby. For larger properties, if lime is used, a ball-mill slaker is convenient, followed by a closed loop pulsed feeder. Loop feeders are also satisfactory for caustic (if used) and cyanide. Reagent control and feeding is standard practice.

11. INSTRUMENTATION

For larger properties an automatic head sample and recorded weight of ore to the pads are highly desirable. If the leached residue is removed from the pads, some form of hand sampling is indicated, because automated sampling would be very costly. Residues left on pads would have to be sampled by boring.

The best and most reliable available solution flow instrumentation should be installed on leaching solutions to and from the recovery plant coupled with automatic or hand samples for grade analysis. Usual pH control is needed whether manual or automatic. Dissolved oxygen meters and/or chemical tests are required at least periodically. Titrations are made for alkali and free cyanide by standard methods.

For gold and silver solution assays, the AA (atomic absorption) method is convenient. Solution samples should be extracted into ketone for reading or else a deuterium arc light source correction should be provided for direct reading.

12. MAINTENANCE OF CARBON ACTIVITY

Sooner or later carbon looses activity because of contamination with organic materials (such as oils), calcium carbonate, and other impurities. Provisions should be made to wash stripped carbon with dilute nitric acid followed by several water washes. (If hydrochloric acid were used, it would be corrosive to the kiln in subsequent reactivation). The carbon should then be washed with dilute (1 percent) NaOH, drained damp, and reactivated by heating to 630°C for 1/2 hour. A rotary kiln, indirectly fired, is convenient for the purpose. Carbon should be screened to remove fines and presoaked at least 12 hours before reuse.

13. MATERIALS OF CONSTRUCTION

- As noted before, asphalt is a good pad material and does not interfere with carbon adsorption. Local clays, if tested, may be suitable for pads. Reinforced plastics are also satisfactory if protected from punctures and tearing. Other materials such as concrete, etc., are possible alternatives.

- Non-galvanized steel, plastic, and asbestos cement may be used for piping.

- Reinforced concrete is satisfactory for pump boxes and rectangular tanks.

- Steel tanks serve for alkaline cyanide.

- Rubber lined, stainless steel, or some plastics could be used for acid washing carbon.

- Brass, bronze, zinc, copper cannot be used.

- Stainless steel stripping vessels, piping, and valves are recommendable (316 preferred).

- Fiber-reinforced plastics may be used for electrolytic cells.

BIBLIOGRAPHY

1. Bhappu, R.B., and F.M. Lewis, "Gold Extraction from Low-Grade Ores - Economic Evaluation of Processes", Mining Congress Journal, Vol. 61, No. 1, 1975, pp 38-41.

2. Chase, Clement K., William S. Ransom, and Donald L. Simpson, "The Glitter Gets Better - The Two Year Record of Gold Heap Leaching at Smoky Valley Mining Div. - Copper Range Company, Round Mountain, Nevada", presented Annual Meeting AIME, Feb. 24-28, 1980, 4 pp.

3. Cho, E.H., S. N. Dixon and C.H. Pitt, "The Kinetics of Gold Cyanide Adsorption on Activated Charcoal", AIME/TMS Metallurgical Transactions B, Volume 10B, June 1979, pp 185-189.

4. Crabtree, E.H., Jr., V.W. Winters, and T.G. Chapman, "Developments in the Application of Activated Carbon to Cyanidation", Trans. AIME, Vol. 187, Feb. 1950, pp 217-222.

5. Davidson, R.J., "The Mechanism of Gold Adsorption on Activated Charcoal", Journal of The South African Institute of Mining and Metallurgy (November 1974), pp 67-76.

6. Duncan, D.M., and T.J. Smolik, "How Cortez Gold Mines Heap Leached Low Grade Ores at Two Nevada Properties", EMJ, July 1977, pp. 65-69.

7. Heinen, H.J., and Bernard Porter, "Experimental Leaching of Gold From Mine Waste", U.S. Bureau of Mines, Report of Investigation 7250, 1969, 5 pp.

8. Heinen, H.J., D.G. Peterson, and R.E. Lindstrom, "Gold Desorption from Activated Carbon with Alkaline-Alcohol Solutions", World Mining and Metals Technology, MMIJ/AIME, Vol. 1, 1976, Weiss (Editor), p 551.

9. Heinen, H.J., D.G. Peterson, and R.E. Lindstrom, "Processing Gold Ores Using Heap Leach-Carbon Adsorption Methods", U.S. Bureau of Mines, Information Circular 8770, 1978, 21 p.

10. Heinen, H.J., G.E. McClelland, and R.E. Lindstrom, "Enhancing Percolation Rates in Heap Leaching of Gold-Silver Ores", U.S. Bureau of Mines, Report of Investigation 8388, 1979, 20 p.

11. Hussey, S.J., H.B. Salisbury, and G.M. Potter, "Carbon-in-Pulp Gold Adsorption From Cyanide Leach Slurries", U.S. Bureau of Mines, Report of Investigation 8368, 1979, 22 pages.

12. Kappes, D.W., (adapted from) "Heap Leaching is Small Miner's Golden Opportunity", Soc. of Mining Engineers, Mining Engineering, February 1979, pp 136-138.

13. Merwin, R.W., G.M. Potter, and H.J. Heinen, "Heap Leaching of Gold Ores in Northeastern Nevada", presented at Annual AIME Meeting, Washington, D.C., February 16-20, 1969, Preprint 69-AS-79.

14. Potter, G.M., "Recovering Gold From Stripping Waste and Ore by Percolation Cyanide Leaching", U.S. Bureau of Mines, Technical Paper 20, December 1969, 5 pp.

15. Potter, G.M., and H.B. Salisbury, "Innovations in Gold Metallurgy" Mining Congress Journal, July 1974, pp 54-57.

16. Ross, J.R., and D.R. George, "Recovery of Uranium From Natural Mine Waters by Countercurrent Ion Exchange", U.S. Bureau of Mines, Report of Investigation 7471, 1971, 17 p.

17. Ross, J.R., H.B. Salisbury, and G.M. Potter, "Pressure Stripping Gold From Activated Carbon", presented at Annual AIME Meeting, Chicago, Illinois, February 26-March 1, 1973.

18. Traut, D.E., I.L. Nichols, and D.C. Seidel, "Design Requirements for Uranium Ion Exchange from Ammonium Bicarbonate Solutions in a Fluidized System, U.S. Bureau of Mines, Report of Investigation 8280, 1978, 27 p.

19. White, Lane, "Heap Leaching Will Produce 85,000 oz./Year of Doré Bullion for Smoky Valley Mining", EMJ, July 1977, pp 70-72.

20. Zadra, J.B., A.L. Engel, and H.J. Heinen, "Process for Recovering Gold and Silver From Activated Carbon by Leaching and Electrolysis", U.S. Bureau of Mines, Report of Investigation 4843, 1952, 32 pp.

SORPTION OF GOLD FROM CYANIDE SOLUTIONS BY COPPER SULFIDES

UDC 669.21.053.4

A. S. Chernyak and O. V. Ovchinnikova

The copper minerals present in certain gold ores have an adverse effect upon the cyanidation process.

The essential features of this phenomenon are now being examined from two viewpoints [1,2].

1. The copper combines with CN^- ions to form the complex anions $Cu(CN)_3^{2-}$ and $Cu(CN)_2^-$, reducing the free cyanide concentration and so retarding the gold dissolution process. However, in copper-bearing gold ore cyanidation practice increasing the cyanide concentration above that necessary for formation of $Cu(CN)_4^{3-}$ does not give sufficient gold dissolution speed. In addition, this approach does not entirely agree with thermodynamic calculation results [3].

2. The adverse effect of copper upon the speed of gold dissolution is due to the formation of films on the gold grain surfaces resulting from adsorption of $Cu(CN_3^{2-}$ by the metal surface or formation of compounds of $AuCu(CN)_2$ type. However, studying the surface of gold disks after contact with copper-bearing cyanide solutions by local x-ray spectral analysis (using a Kameka MS-46 microanalyzer) did not reveal copper on the surface of the disks [4].

Thus the available data on the effect of copper compounds upon the gold dissolution process are extremely contradictory.

Having regard to the fact that heavy metal sulfides may participate in heterogeneous ion-exchange reactions [5] and that gold may be precipitated from cyanide solutions by sulfides of iron [6] and cadmium [7], the authors of the present paper assumed that dissolution of gold during its extraction from ores containing copper sulfides is accompanied by a secondary process, sorption of the dissolved gold by those sulfides.

Results obtained during the reaction of auriferous cyanide solutions with analytical-grade copper sulfide and a mixture of minerals[1] (chalcocite and bornite) are given below.

The experiment was carried out under static conditions at room temperature, the ratio of copper sulfide (g) to solution (ml) being 1:50. Cyanide was not added in the process of solution-sulfide contact (this leads to dissolution of the sulfides). "Blank" experiments, i.e., using cyanide solution not containing gold, were included in each series. A synthetic solution of single-constituent composition in terms of metal was used for study. As a rule the gold concentration in the solution varied from 4.24 6.13 mg/liter. The extent of gold precipitation was defined by reference to the difference in concentration in the solution before and after contact with the sulfide. The solution was analyzed by the atomic absorption method. The presence of gold in the solid phase was monitored by qualitative and semiquantitative spectral analysis. The free cyanide and protective alkali content of the initial solutions was de-

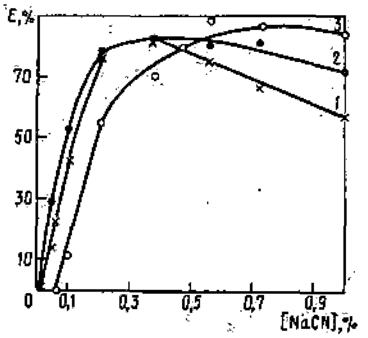

Relationship of degree of gold absorption (E) by copper sulfide to cyanide concentration in starting solution. Duration of solution contact with sulfide: 1 - 3 hr; 2 - 24 hr; 3 - 48 hr.

Table 1
Effect of Cyanide Concentration Upon Gold Adsorption from Solutions in Contact with Copper-Bearing Materials
(τ = 3 hr)

Concentration in solution			Degree of Au precipitation, %
initial		after contact with minerals	
NaCN, %	Au, mg/l	Au, mg/l	
0,01	4,24	4,10	3,30
0,05	4,46	3,46	22,67
0,19	4,42	2,75	37,78

Table 2
Relationship of Gold Extraction to Solution-Copper Sulfide Contact Time (initial solution - 6.13 mg/l Au, 0.38% NaCN, 0.05% protective alkali in terms of CaO)

Contact time, min	Solution contents after sorption				Au adsorption from solution, %
	Au, mg/l	NaCN, %	alkali, %	Cu, mg/l	
1	1.18	0.07	0.08	1360	80,75
3	1.09	0.05	0.07	1480	82,23
5	1.23	0.04	0.07	1560	79,95
8	1.15	0.02	0.08	1650	81,24
10	1.07	0.018	0.08	1650	83,03
15	1.20	0.016	0.08	1650	80,42
35	1.38	0.014	0.09	1650	77,46
60	1.08	0.008	0.09	1740	82,38

---

[1] Spectral analysis did not show any gold in the minerals.

termined by the generally accepted methods [8]. The free cyanide content of the copper-bearing solutions was established having regard to the recommendations in [9].

Study of the relationship between the extent of gold adsorption by copper sulfides and the cyanide concentration in the initial solution (see Figure and Table 1) showed that increasing the cyanide concentration leads to an increased extent of gold adsorption. In these circumstances over 80% of gold is extracted as a result of solution-sulfide contact for a period of 3 hr at an initial cyanide concentration of 0.37%. Some reduction in the extent of gold adsorption when the cyanide content is increased (see Figure, curves 1 and 2) is caused by the secondary dissolution of adsorbed gold by the fairly strong cyanide solutions. Increasing the auriferous solution-copper sulfide contact time to 48 hr leads to an increase in gold adsorption from 60 to 87% at the same cyanide concentrations (see Figure, curve 3).

The difficulties which arise in determining free cyanide in copper-rich solutions made it impossible to trace the changes in the solution free cyanide contents with sufficient accuracy. However, it was observed that the alkali concentration in the solutions increases after sorption, which is in accordance with data on the chemical mechanism of the process of sulfide dissolution in cyanide solutions [1].

It was established when studying the effect of auriferous solution-copper sulfide contact time upon gold adsorption from cyanide solutions (Table 2) that over 80% of gold is sorbed in a period of 1 min in spite of the presence of free cyanide in the solution; however, there is a reduction in the free cyanide concentration in these circumstances.

Prolonged copper sulfide contact with rich gold solutions ensures the production of a fairly high solid phase gold content. Thus the gold concentration in the auriferous solution fell from 148 to 69 mg/liter as a result of contact with copper sulfide (solid-to-liquid ratio 1:100, 0.78% NaCN, 0.12% CaO) for a period of 10 days. The copper sulfide capacity for gold calculated from these data was 7.84 mg/g. Semiquantitative spectral analysis established that the solid phase gold content was ~ 0.6%. X-ray phase analysis proved to be unsuitable for studying the process of gold sorption by copper sulfide because the extent of gold sorption is below the level of sensitivity of the method.

CONCLUSIONS

In leaching gold from ores which include soluble copper sulfides, low gold extraction is largely due to a secondary process: sorption of dissolved gold by the copper sulfides. The mechanism of gold absorption from cyanide solutions by copper sulfides is worthy of special study.

REFERENCES

1. I. N. Maslenitskii and L. V. Chugaev, Metallurgy of the Precious Metals, Moscow, Metallurgiya, 1972, 367 pages, illustrated.
2. I. N. Plaksin, Metallurgy of the Precious Metals, Moscow, Metallurgizdat, 1958, 366 pages, illustrated.
3. L. D. Sheveleva and I. A. Kakovskii, Tsvetnye Metally, 1976, No. 1, 77-79.
4. V. T. Lebedeva, Yu. M. Chikin, I. K. Skobeev, and L. L. Zav'yalova, Tsvetnye Metally, 1973, No. 1, 75-76.
5. V. V. Vol'khin and B. I. L'vovich, Zhurnal Prikladnoi Khimii, 1976, 49, No. 9, 1961-1965.
6. L. D. Sheveleva, A. A. Golovin, T. T. Tatarinova, et al., Izv. Vuzov, Tsvetnaya Metallurgiya, 1976, No. 3, 79-82.
7. I. I. Kalinichenko and P. A. Sokolova, in: Analysis Methods for Ferrous and Non-Ferrous Metals, Sverdlovsk, Moscow, Metallurgizdat, 1953, pp. 105-111.
8. V. I. Zelenov, Methods of Studying Auriferous Ores, Moscow, Nedra, 1973, 231 pages, illustrated.
9. I. K. Skobeev, Proceedings of Irkutsk State Rare Metals Industry Research and Design Institute, Issue 8, Moscow, Metallurgizdat, 1959, pp. 230-238.

1977 v 18 No 8

SORPTION OF GOLD FROM CYANIDE SOLUTIONS WITH ELECTRON-ECHANGE RESIN

UDC 669.213.3.068

V. A. Khomutnikov, G. Ya. Druzhina, and V. T. Gorbunova

Electron exchange is one of the elements involved in solving the problems of reducing gold losses when metal is extracted from cyanide solutions.

Compared with the iron-exchange sorption now being used in industry, redox sorption gives more thorough demetallizing of cyanide solutions and pulps and so reduces gold losses with effluents [1].

There is no direct published evidence of reduction of complex ions to metal on electron-exchange resin. Not particularly convincing evidence of sorption by the electron-exchange mechanism is available for silver only [2].

Synthetic cyanide solutions were used to study the process of redox sorption of gold and secondary metals by resin. The latter was a styrene and divinylbenzene copolymer with active S-bearing groups; its redox potential is -0.67 V [3].

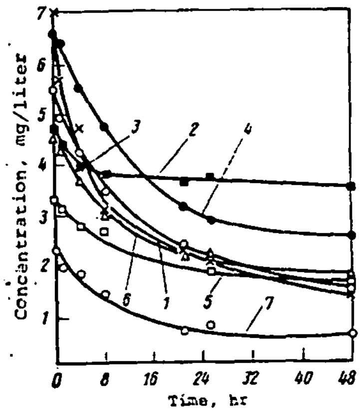

Fig. 1. Sorption curves: 1 - Au; 2 - Fe; 3 - Cu; 4 - Ni; 5 - Co; 6 - Ag; 7 - Zn.

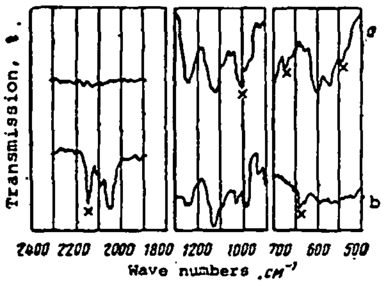

Fig. 2. Infrared spectra of initial resin (a) and of resin exposed to gold-bearing cyanide solution (b).

Electron Diffraction Parameters of Saturated Resin

Resin saturated in terms of Au		Gold according to ASTM		
I	d, Å	I/I₀	d, Å	hkl
10	2.36	100	2.355	111
5	2.04	52	2.039	200
3	1.42	32	1.442	220
2	1.23	—	1.230	311

The experiments were conducted under static conditions; the resin charge was 25 mg per 500 ml of cyanide solution. The metal concentration was determined by spectrophotometry by reference to calibration curves. An SF-16 spectrophotometer and one-centimeter quartz cells were used.

Zinc and silver cyanide complexes do not absorb light in the accessible ultraviolet and visible regions of the spectrum; the silver and zinc concentration in the corresponding solutions was therefore measured by the atomic absorption method. The nature of the curves for changes in metal concentration indicates that the process of element extraction by the resin in time is similar to sorption on ion-exchange resins: to establish equilibrium in the system, the resin must be kept in contact with the solution by mixing for a period of over 48 hr (Fig. 1). A period of about 20 hr should be adopted as the optimum duration of redox sorption; metal extraction during this period is fairly complete. The relative rate of element extraction by the resin can be assessed from the slope of the sorption curves. Gold is sorbed most quickly, followed by copper, nickel, silver, zinc, cobalt, and iron.

The resins (initial and gold-saturated) were analyzed by infrared spectroscopy and electron diffraction to reveal the sorption mechanism (the infrared spectra were recorded on a UR-20 spectrometer relative to wave numbers).

The resin infrared spectra (Fig. 2) pointed to the following conclusion: the $S_2O_3^{2-}$ group in the initial resin becomes an SO_4^{-} group in the saturated resin, i.e., $S^{2-} - 8e \to S^{+}$ oxidation occurs in the process of metal extraction. This is confirmed by the following changes in the saturated resin spectrum compared with that of the initial resin.

1. The characteristic band for the $S_2O_3^{2-}$ group, 669 cm⁻¹ in the initial resin, shifts to 645 cm⁻¹; this is the characteristic band for the SO_4^{2-} group in the saturated resin.

2. The band near 1000 cm^{-1} in the spectrum of the initial resin, characteristic of $S_2O_3^{2-}$, is very weak in the saturated resin.

3. The 541 cm^{-1} band characteristic of $S_2O_3^{2-}$ disappears from the saturated resin spectrum [4, 5].

There should be a reduction of Au^+ from the cyanide complex to metal at the same time as the oxidation of sulfur. It was possible to reveal the crystalline structure of the gold in the resin by electron diffraction. The interplanar spacings calculated from the microelectron diffraction pattern from the saturated resin coincide with the American (ASTM) card-index data for metallic gold (see Table).

The appearance in the saturated resin infrared spectrum of the 2148 cm^{-1} band characteristic of the gold cyanide complex indicates simultaneous sorption by the ion-exchange method.

The infrared spectroscopy method was also used to analyze resins exposed to cyanide solutions of secondary metals (Ag, Cu, Zn, Fe, Ni, and Co) and to "blank" sodium cyanide solutions.

The following bands were observed in the infrared spectra [4, 5]: 2097 cm^{-1}, characteristic of $[Ag(CN)_3]^{2-}$ and $[Ag(CN)_4]^{3-}$; 2060 cm^{-1} and 2100 cm^{-1} for the CN group; 2095 cm^{-1} for $[Cu(CN)_3]^{2-}$; 2075 cm^{-1} for $[Cu(CN)_4]^{3-}$; 2050 cm^{-1} for $[Fe(CN)_6]^{3-}$; 2117 cm^{-1} for $[Fe(CN)_6]^{3-}$; 2055 cm^{-1} and 2150 cm^{-1} for $[Zn(CN)_4]^{2-}$; 2124 cm^{-1} for $[Ni(CN)_4]^{2-}$, and 2130 cm^{-1} for $[Co(CN)_6]^{3-}$, indicating sorption by the ion-exchange mechanism.

No electron-diffraction analysis of the resins saturated with secondary metals was made. The presence of an electron-exchange mechanism of secondary element extraction by the redox resin is proved indirectly by changes in the infrared spectrum bands characteristic of the $S_2O_3^{2-}$ group analagous to the changes in gold extraction.

Infrared spectroscopy and electron diffraction methods have revealed lelectron exchange and ion-exchange mechanisms in sorption of gold from cyanide solutions by redox resin. The microelectron diffraction pattern for resin saturated in gold-bearing cyanide solution indicates that metallic gold is present in it, and the infrared spectrum indicates the presence of the complex anion $[Au(CN)_2]^-$ and a sulfur oxidation reaction.

REFERENCES

1. G. Ya. Druzhina, A. A. Batsuev, and V. A. Khomutnikov, Tsvetnye Metally, 1976, No. 5, 85-86.
2. A. B. Davankov and E. V. Zambrovskaya, Izv. Vuzov, Tsvetnaya Metallurgiya, 1959, No. 3, 82-86.
3. Yu. Yu. Lur'e, Handbook of Analytical Chemistry, Moscow, Khimiya, 1971, 454 pp.
4. K. Nakamoto, Infrared Spectra of Inorganic and Coordinate Compounds, Moscow, Mir, 1966, 411 pp.
5. F. A. Miller and C. H. Wilkins, Analytical Chemistry, 1952, 24, No. 8, 1253-1265.
6. M. D. Ivanovskii, M. A. Meretukov, V. D. Potekhin, and L. S. Strizhko, Izv. Vuzov, Tsvetnaya Metallurgiya, 1974, No. 2, 36-42.

1976 v.17 N/10 TSVETNYE METALLY / NON-FERROUS METALS

SUBJ
MNG
SGFO

SORPTION OF GOLD FROM ORE HEAP LEACHING SOLUTIONS USING ACTIVATED CARBON

UDC 669.213:661.183.2

G. G. Mineev, G. Ya. Druzhina, and G. A. Stroganov

BAU grade activated charcoal was used for processing the solutions, as having one of the highest capacities for gold [1]. The carbon was tested in comparison with AM-2B ion-exchange resin, which is used industrially for gold extraction from cyanide pulps.

The auriferous cyanide solutions were passed through systems of consecutive columns containing fixed layers of sorbents at a speed of 5 m/hr; the flow of solution into the sorbent was 50 liters/sec. The effective capacity of the column was 0.25 liters, its diameter was 23 mm, and the depth of the sorbent layer was 600 mm.

The composition of the solutions entering the sorption process from ore leaching varied somewhat in time; on the whole the variation was toward a reduction in the gold content. During the test period the concentrations of constituents in these solutions varied as follows, g/m³: Au from 12 to 3, Zn from 5.4 to 4, Cu from 3.0 to 2.2, Fe from 1.8 to 1.6; the solutions contained $\sim$ 0.02% NaCN and had a pH value of 8-9.

Comparative Data on the Capacity and Selectivity of Gold Sorption for BAU Carbon and AM-2B Anionic Exchange Resin

Sorbent	Concentration in initial solution (average), g/m³				Content in saturated sorbent, g/kg							Au/Σ impurities ratio in sorbent
	Au	Zn	Cu	Fe	Au	Zn	Cu	Fe	Ni	Co	Σ impurities	
Solution from leaching off-grade ore												
BAU	10	5,4	3,0	1,8	8,0	1,0	0,2	0,6	0,04	Tr.	1,8	4,4
BAU	5,4	5,0	1,8	0,9	9,2	0,1	0,1	1,5	0,04	0,1	1,8	5,1
AM-2B	6,1	4,8	2,4	1,4	13,9	19,0	2	2	0,7	0,08	24	0,58
Solution from leaching crushed gold ore												
BAU	2,7	0,05	101	0,8	1,3	0,06	29,2	1,5	0,03	Tr.	30,8	0,04
BAU	2,4	0,05	109	0,8	1,4	0,05	56,2	1,6	0,02	»	57,9	0,024
AM-2B	2,5	0,05	105	0,8	1,6	0,10	104	6,3	0,12	0,08	110,6	0,014

The crushed gold ore solutions were stable in composition, with the following average content (in g/m³): 2.5 Au, 105 Cu, 0.8 Fe, and 0.004% NaCN. The pH value was 7.

Samples were taken periodically from the solutions leaving each column in the system. The solutions were analyzed by the atomic absorption method. The low gold contents were measured after preliminary extraction with isoamyl alcohol; this increased the sensitivity of the atomic absorption method of analysis for gold to 0.005 mg/liter.

Solution from heap cyanidation of off-grade ore was used to saturate two columns each containing 67 g of activated carbon and one column containing 100 g of AM-2B resin. Solutions from leaching crushed gold ores were used to saturate 67 g of activated carbon and 100 g of AM-2B resin.

The results of experiments obtained with the two types of solution (fairly pure solution from leaching off-grade ore and solution contaminated with copper from leaching crushed gold ores) are shown in the Table. The BAU carbon has 1.2-1.7 times less capacity for gold than AM-2B, but its gold contents are fairly high. Thus the capacity reaches 9 g/kg for a solution containing $\sim$ 5 g/m³ Au. The carbon is considerably superior to the resin in selectivity toward gold: the ratio of the valuable element (Au) to total impurities (Cu, Zn, Fe, Ni, Co) in the saturated carbon is 2.8 times higher than the ratio in the resin.

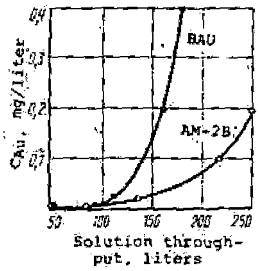

Course of gold sorption from off-grade ore heap leaching solutions.

Reduced capacity gives rise to increased Au contents in the outgoing solutions[1] from carbon sorption in the region of carbon shortage: less than 0.2 kg per 100 liters of solution (see Fig.). However, activated carbon, like ion exchange resin, removes gold from the solutions to trace levels (less than 0.005 mg/liter) when the ratio of sorbent to solution is sufficient: $\sim$ 0.2 kg or more per 100 liters of solution. This was reflected in the results of solution demetallization during the first two days of sorption.

The process of sorption by activated carbons proceeds at a higher rate than sorption

---

[1] At equal sorbent loads of 200 g each; for carbon these are the solutions from the third column, for resin the solutions from the second column.

by the ion-exchange resins, because the carbons have a highly developed surface. Thus the sorption time when the pulps are treated with carbon is 3-4 hr [2], whereas treatment with ion-exchange resins requires several times longer.

It is preferable to desorb precious metals from activated carbons by using hot water with a low calcium ion content, after preliminary treatment with solutions of potassium or sodium carbonates (as yet this method has been tested only under laboratory conditions [3]), or with hot alkaline cyanide solutions (this method is used in industry [2-7]).

The test results make it possible to recommend the method of gold sorption from solutions using activated carbons for industrial testing.

REFERENCES

1. K. B. Lebedev and N. I. Taskin, Tsvetnye Metally, 1973, No. 8, 71-73.
2. Z. A. Tauzhnyanskaya, Tsvetnaya Metallurgiya (Bull. Inst. Tsvetmetinformatsiya), 1973, No. 5, 27-28.
3. R. I. Davidson, J. South Afr. Inst. Min. Metal., November, 1974, 75, No. 4, 67-76.
4. Donald T. Delicate, World Mining, May, 1974, 27, No. 5, 32.
5. Kenneth B. Hall, World Mining, November, 1974, 27, No. 12, 44.
6. A. J. Gilmore, Canad. Mining J., 1969, 90, No. 6, 78-80.
7. V. M. Kuz'minykh, N. G. Tyurin, and A. A. Nikulova, Zh. Prikl. Khim., 1969, 42, No. 9, 2006-2010.

from which

$$\frac{d\eta}{dt} = \frac{b\eta}{M}$$

where M is the factor for conversion from decimal to nature logarithms.

The rate of variation of the viscosity of the slime charges with variation in temperature must clearly be related to the ratio of the amounts of solid and liquid phases in the sinter. The phase composition of the sinter predetermines the absolute value of the viscosity at a given temperature.

In our experiments the sum of the amounts of $Al_2O_3 + SiO_2$ in the charge varies little. Consequently, the ratio of the solid and liquid phases must depend largely on the ratio $(Na_2O_{free} + CaO_{free})/Fe_2O_3$, and also on the rate of the dissolution of the high-melting components of the sinter in the liquid phase.

It is possible that the rate of variation of the viscosity on the linear section is determining during evaluation of the temperature range of the plastic state. Thus, the viscosity curves can be used to determine the sintering temperature and range. The temperature corresponding to the beginning of deformation must be considered to be the temperature of the beginning of sintering, while the temperature at which the viscosity begins to vary according to a linear law is the temperature of the end of sintering.

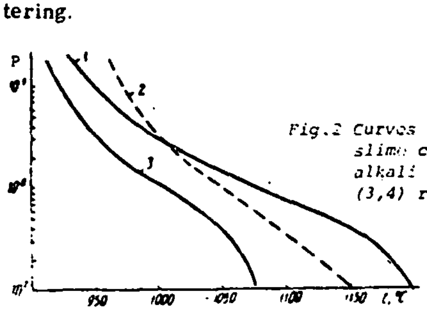

Fig.2 Curves for the viscosity of slime charges with various alkali (1,2) and limestone (3,4) ratios.

We studied the effect of the addition of 50% of a clay fraction and 15% of the high-alumina slag from the Aktyubinsk ferroalloy works on the viscosity of the slime charge of the Pavlodar aluminium works (charge 5, table 2). The viscosity curves are given in fig.3.

The form of the viscosity curves is similar to that obtained earlier (fig.2). and this shows that the phase transformations are equivalent. The addition of the clay fraction (fig.3, curve 1) extends the range of the plastic state into the region of high temperatures and leads to an increase in the melting point (1260°C) and an extension of the sintering temperature range. The addition of the high-alumina slag (fig.3, curve 3) reduces the range of the plastic state in relation to the designed slime charge (curve 2) and shifts it into the region of reduced temperatures, leading to fusibility of the charge. The beginning of plastic deformations for all the investigated charges (with and without additions) lies in the region of 900-950°C.

It is clear that the temperature range of the plastic state in slime charges can be altered and shifted into the region of high temperatures by means of the appropriate addi- This must extend the sintering temperature range and a positive effect on the operation of revolving sintering furnaces.

References

1) I Ya Zalkind et alia: Naladochnye i Éksperimental'nye Raboty ORGRÉS, Gosénergoizdat 1952, (3).

2) V F Pavlov: Author's Abstract of Thesis (in Russian), Moscow 1961.

3) I Ya Zalkin et alia: Naladochnye Éksperimental'nye Raboty ORGRÉS, Gosénergoizdat 1950, (1).

4) N V Solomin: Zh Tekhnicheskoi Fiziki 1945, XV, 11.

UDC 541.183.12 + 547.27

Sorption of gallium, indium, and aluminium from mixed sulphuric acid solutions by anion-exchange resin AV-17

A V Plyusin (Deceased), E I Kazantsev and N P Pyatin (Urals Polytechnical Institute. Department of the Metallurgy of Rare Metals)

There is hardly any information on the sorption behaviour of gallium, indium, and aluminium in sulphuric acid solutions, containing nonaqueous solvents. However, investigation of such processes in sulphuric acid solutions is of considerable interest, since sulphuric acid is widely used in the production, purification, and analysis of these elements[1]. The sorption of gallium, indium, and aluminium on anion-exchange resin AV-17 from aqueous-nonaqueous sulphuric acid solutions was therefore investigated in the present work.

The sorbability of the metal ions was investigated as a function of the concentrations of sulphuric acid and the organic solvent in the system. The concentration of the acid was varied from 0.1 - 2N, and the proportion of the nonaqueous component was varied between 0 and 80 vol.% In order to trace the effect of a series of saturated alcohols and also ketone on the sorption of the elements methyl, ethyl, and isopropyl alcohols and acetone of chemical purity or of analytical grade were used in the work. The AV-17 ion-exchange resin was used in the SO_4 form with a particle size of 0.25-0.5 mm, and it was washed from iron and soluble impurities. The experimental procedure was similar to that described earlier[2]. The desorption of the sorbed ions was realised in 2N sulphuric acid.

The results from the experiments (expressed in terms of the logarithms of the distribution coefficient D as a function of the H_2SO_4 concentration) are given in fig.1. The distribution coefficient was determined by means of the equation

$$D = \frac{X}{100 - X} \cdot \frac{V}{P}$$

where: X = percentage of the metal sorbed by the resin
V = volume of the solution ml
P = weight of the resin g

Aluminium, gallium, and indium ions are not sorbed from aqueous sulphuric acid solutions because the stability of the negatively charged complexes of the investigated metals is low. The addition of an organic solvent leads to dehydration of the ions, which assists the formation of more stable complexes, and the ions of the investigated elements begin to be sorbed on the resin. At the same time, the sorption of the metals occurs as a rule at large concentrations of the nonaqueous solvents, where their dehydrating effect appears most strongly. For this reason the sorbability of the elements increases with increase in the content of the organic component of the system. On the other hand, the sorbability of the elements decreases with increase in the sulphuric acid concentration, and this is due to increase in the sulphuric acid concentration, and this is due to increase in the competing effect of the sulphate ions.

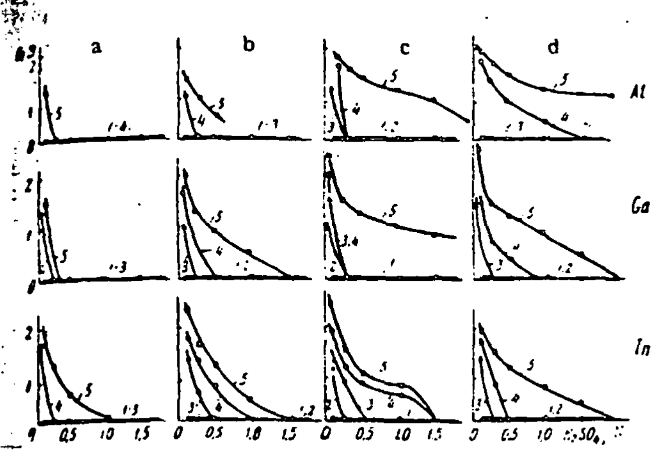

Dependence of log D during the sorption of aluminium, gallium and indium by the AV-17 ion-exchange resin in the SO_4 form on the sulphuric acid concentration in the presence of organic solvents: a) methanol; b) ethanol; c) isopropyl alcohol; d) acetone. Content of organic solvent vol.%: 1 - 0, 2 - 20, 3 - 40, 4 - 60, 5 - 80.

With increase in the molecular weight of the alcohol and with increase in the content of the organic solvent (fig. a-d) the sorption of the elements on the resin is observed over a wider range of acid concentrations. Thus, aluminium is sobred from solutions containing 80% of methanol only in the acidity range of 0.1 to 0.25N. In the presence of 60 and 80% ethanol all the aluminium remains in solution at H_2SO_4 concentrations of 0.25 and 1N respectively. Variation in the concentration of the acid and organic solvents has a similar effect on the sorption of gallium and indium.

The elements investigated begin to be sorbed with various contents of the solvents. The sorption of gallium and indium begins with lower concentrations of the non-aqueous component than sorption of aluminium. For example, in the presence of methanol the sorption of aluminium begins only with an alcohol concentration of 80, while the sorption of gallium and indium begins with an alcohol concentration of 60%. This is explained by the different susceptibilities of the elements to complex formation. Since the latter increases from aluminium to indium[3]), indium forms the most stable complexes with a large negative charge. Its sorbability is therefore highest on an anion-exchange resin, whereas the opposite behaviour is observed on a cation-exchange resin[2]). In the general case the investigated elements can be arranged in the following order of decreasing sorbability on the anion-exchange resin AV-17: In(III) > Ga(III) > Al(III).

The stability and composition of the complexes in one or the other solvent are different and depend on the stability of the solvates formed with the given solvent. The less stable the solvates the solvent forms with the element, the more stable the complexes. Solvents with similar values for the dielectric constants (acetone and isopropyl alcohol) have different effects on the complexing reactions in the solution. Complexes are formed most readily in acetone. This effect is explained by the low energy of solvation of the metal ions in this solvent[4]). The alcohol C_3H_7OH can form a coordination bond with the cation through the unshared electrons of the oxygen and forms an analogous bond with the anion through the hydrogen atom. There is strong interaction between the alcohol and the ions entering into the composition of the complex. Acetone, however, can only form a coordination bond with the cation through the unshared electrons of the oxygen. (The presence of a double bond facilitates the reaction).

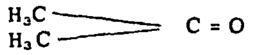

$$(H_3C)_2C=O$$

In this case the bond between the central atom and the ligand is stronger than in alcohol. In aqueous-organic sulphuric acid solutions, where the complexing process are substantially developed, the solvents can be arranged in the following order of decreasing effect on the sorption of the elements: Acetone > isopropyl alcohol > ethanol > methanol.

The effect of the nature of the solvent on the sorption of indium ions should be noted in particular. As shown by our investigations on the sorption of aluminium, gallium, and indium by the KU-2 cation-exchange resin in organic solutions of sulphuric acid[2]), indium is solvated by acetone to a much greater degree than the other investigated elements. Here the formation of complex associates is observed as a result of resolvation processes. This leads to the result that the sorbability of indium on the anion-exchange resin in the presence of acetone is less than from solutions containing isopropyl alcohol. Thus, for indium, acetone and isopropyl alcohol change places in the order of increasing effect of the nature of the solvent on the sorption of the metal ions.

Optimum conditions for the separation of aluminium and gallium are observed in a 0.1N solution of sulphuric acid containing 40% of acetone and 60% of water. Under these conditions the separation factor for this pair of ions is 50.

Conclusions

1. The sorption of aluminium, gallium, and indium ions on AV-17 anion-exchange resin was investigated from sulphuric acid solutions containing methyl, ethyl, and isopropyl alcohols and acetone.
2. It was found that the elements investigated are not sorbed on the resin from aqueous solutions of sulphuric acid. The addition of the nonaqueous solvent assists the sorption of gallium, indium, and aluminium.
3. It was shown that the sorbability of aluminium, gallium, and indium increases with increase in the content of the organic solvent and decreases with increase in the sulphuric acid concentration. The separation factor for aluminium and gallium is highest (50) in 0.1N sulphuric acid containing 60% of water and 40% of acetone.

References

1) M N Zyryanov and A P Nadol'skii: Principles of the technology of the production of trace elements. Metallurgizdat Moscow 1968.
2) E I Kazantsev et alia: Izv Vuz *Tsvetnaya Metallurgiya* 1970, (4), 48.
3) K B Yatsimirskii et alia: Instability constants of complexes. Izd Akad Nauk SSSR Moscow 1959.
4) A M Golub and V A Kalibabchuk: Zh Neorgan Khim 1966, (11), 590.

UDC 669.2

Investigation of the deposition of tungsten from its hexachloride

B S Lysov, A N Tumanov and V N Anikin

It is well known that great difficulties arise in the reduction of tungsten from its hexachloride with hydrogen owing to the development of homogeneous reactions at temperatures above 600°C[1]). In order to lessen the homogeneous reactions the process was carried out at reduced temperatures (600-700°C)[1]) or with a reduction of the total pressure[2]). In[3]) an improvement in the characteristics of the process at atmospheric pressure and at temperatures of 800 - 900°C

SOCIETY OF
MINING ENGINEERS
OF
AIME
CALLER NO. D, LITTLETON, COLORADO 80123

PREPRINT
NUMBER

81-32

THE PRODUCTION OF SUPER-GRADE IRON ORE CONCENTRATES AT LKAB

Per-Martin Sandgren

LKAB
Stockholm, Sweden

Alrik Anttila

LKAB
Malmberget, Sweden

For presentation at the AIME Annual Meeting
Chicago, Illinois - February 22-26, 1981

The Production of Super-Grade Iron Ore Concentrates at LKAB

Abstract. LKAB's ores have specific mineralogical properties that make them especially suitable for the production of super-grade concentrates. Conditions are particularly good for this purpose at Malmberget, where a concentrate for high-purity sponge iron production has been produced for many years. Until 1978 the approximate assay was 71.2 % Fe and 0.45 % SiO_2.

Since then the assays have been improved by process modifications to approximately 71.5 % Fe and 0.20 % SiO_2. Scope exists for still further improvement.

In recent years the production of fractioned concentrates has been started. The material lies within the size range 74-125 µm and the approximate chemical analysis is 71.4 % Fe and 0.30 % SiO_2. Other special products are under discussion.

The Malmberget ores are also suitable for the production of high-purity direct reduction pellets with a SiO_2 content below 1 %.

The LKAB Group

LKAB, standing for Luossavaara Kiirunavaara Aktiebolag, is a 100 percent state owned corporation with iron ore mining and processing as its primary field of activity. Wholly-owned subsidiaries are involved in energy sources, sulfide ores, tungsten ores, industrial minerals etc. Founded in 1890, the corporation now has some 7 800 employees, of whom 7 300 work in the iron ore operation.

The Iron Ore Operation

The iron mines are situated in Lapland, north of the Arctic Circle as shown in Figure 1. Here, in the extreme north of Sweden, iron ore has been mined since the late eighteenth century.

Three mines are in production at present. They are Kiruna, Svappavaara and Malmberget, with output capacities of around 19, 4 and 8 million metric tons per year (mmtpy) respectively (Figure 2). The products include lump ore, sinter fines, concentrates and pellets and are railed to LKAB's harbours at Narvik, Norway, and Luleå, Sweden, for onward shipping, and to the Luleå steelmill. The ore reserve is estimated at 4 trillion (4×10^{12}) metric tons, over 90 % of which is magnetite and the remainder hematite. The ores are described as apatitic ores, though the phosphorus content varies widely. The normal range is 0.5-1 % P, and therefore all the ore is concentrated in one way or another.

The Malmberget Operation

The Malmberget ore field consists of some twenty more or less separate orebodies (Figure 3). About 85 % of the ore is magnetite and the rest hematite. The ores have a pronouncedly coarse crystalline structure and run about 50 % iron and 0.6 % phosphorus (with side rock dilution included).

Until 1927 the ores were worked by surface mining. Today they are mined underground, mainly by sub-level caving.

The Ores: The ores consist of coarse crystalline magnetites and hematites liberated at a grind of 0.2-1 mm. The gangue and country rock minerals include felspar, quartz, mica and apatite. Since apatite contains phosphorus and felspar and mica contain alkali, the ore has to be concentrated as far as possible. Since the ore is of coarse crystalline structure, with loose grain boundaries and with very few objectionable inclusions in the magnetite grains, concentrates of a very high degree of purity can be produced. Thus it is possible to make super-grade and special concentrates with a purity approaching the theoretical Fe content of the magnetite. For very high-grade products it is necessary to separate the purest particle fractions in the concentrating process by special screening and classifying operations as illustrated by Figure 4.

Plant and Production: There are five ore processing works at the Malmberget Mine, namely: a cobbing plant for magnetite, a concentrating plant for magnetite, a concentrating plant for hematite, and a shaft furnace plant and a straight grate plant for pelletizing.

The total input capacity is about 13 mmtpy crude ore, corresponding to an output of about 8.5 mmtpy ore products. The input in 1980 was about 9.5 mmt crude ore, which yielded some 3.4 mmt sinterfeed, 3.1 mmt pellets and 0.26 mmt concentrate for the direct reduction of iron powder, plus a certain quantity of other special concentrates.

The production schedule for magnetite can be briefly described as follows (see also Figure 5).

The ore is crushed to <350 mm underground, to <100 mm in a secondary crushing stage after hoisting, and to <25 mm in the cobbing plant. In the cobbing plant the ore is preconcentrated from approximately 48 % to 54 % Fe on a dry belt low-intensity magnetic separator.

The preconcentrate proceeds to the magnetite concentrating plant, where it undergoes wet grinding and wet low-intensity magnetic separation.

After rod mill grinding the primary concentrate is classified into a coarse and a fine product. Part of the coarse material is re-separated to give a <1.5 mm sinterfeed assaying 68.6 % Fe, 0.03-0.05 % P and 2.4 % SiO_2. The remainder of the coarse product is reground in a ball mill and re-separated to give a <0.25 mm sponge iron concentrate grading 71.5 % Fe, 0.004 % P and ≤0.2 % SiO_2. The fines fraction of the primary concentrate is also used to prepare pellets feed by ball mill grinding and magnetic separation, giving a grind of 70 wt-% <44 µm and an approximate assay of 71.2 % Fe, 0.003 % P and 0.45 % SiO_2.

Production of Super-grade Concentrates

Super-grade concentrate is to be understood to mean concentrates with a SiO_2 content less than 0.5 % as the major impurity. The products manufactured on an industrial scale in 1980 were:

pellets feed, with 71.3 % Fe and 0.45 % SiO_2, for the production of direct reduction pellets for the Hyl and Midrex processes;

sponge iron concentrate, with 71.6 % Fe and 0.20 % SiO_2, for the Höganäs sponge iron process;

dried special concentrates for use as catalysts in the chemical industry etc.;

dried, classified special concentrates for the copying industry;

screened special fines for treating oil-contaminated water.

Other products have been prepared experimentally on laboratory scale, e.g. for battery electrodes, for direct reduction to steel sheets, etc.

In any mineral dressing process the quality of the final concentrate will depend on the quality of the heads, assuming the plant does not have a great deal of excess capacity. We are now working on improvements to the cobbing process (Figure 6). For the large-scale production of pellets feed and sinter feed only the 10-25 mm fraction is cobbed, while the <10 mm material is added directly to the heads entering the concentrating process. For the sponge iron concentrate, on the other hand, the entire 0-25 mm fraction is cobbed.

In a future process all the heads to the concentrating process will be cobbed, raising the grade of the concentrate from the present 54 % Fe to 59 % Fe at the same iron recovery.

In the concentrating plant we process the preconcentrates into finished concentrates and pellets feed. In producing feed for blast furnace pellets we use a flowsheet which achieves a SiO_2 content of about 0.75 %, while for direct reduction pellets we are at present reducing the SiO_2 content to 0.45 % by a slight modification of the flowsheet.

In the future we plan to reduce the slag content of the direct reduction pellets still further, but development in this direction has to take place in stages in collaboration with the direct reduction mills. We have also studied the feasibility of cleaning concentrates of pellets feed grind by flotation, whereby the SiO_2 content could be reduced to $\leq$0.1 %.

The table in Figure 7 shows analyses of concentrates and pellets of various degrees of purity.

Since 1979 we have been using the improved cobbing method in the manufacture of sponge iron concentrate and other medium-grind special concentrates. In the concentrating plant we use a flowsheet (see Figure 8) in which the preconcentrate is classified and the coarse fraction reground and concentrated to $\leq$0.2 % SiO_2. The improved cobbing stage thus results in an improvement in the final product. For example, the iron content has been raised from 71.2 % to 71.5 % and the SiO_2 content reduced from 0.45 % to 0.20 %. There is scope for still further reduction of the impurities in the product by continued process development if the market demands it and if the relation between the market price and the production cost permits.

Concentrates grading 0.10-0.15 % SiO_2 could be made by flotation cleaning.

The production plant for sponge iron concentrate for the Höganäs process is also used for the basic stages in making other special products. The catalyst concentrate requires continued dry treatment and sometimes special control of the ore flow from the mine. The product for the copying industry requires classifying, screening and drying.

Other products have been prepared on laboratory and pilot plant scale for special applications requiring very high-grade concentrates. See further Figure 9. The purest product that has been developed is intended for the fabrication of electrodes for Ni-Fe batteries, a typical assay being 71.9 % Fe, 0.02 % SiO_2 and 0.002 % P. The theoretical iron content of magnetite is 72.4 %, implying that this product is over 99 % pure with respect to Fe.

Market Aspects

The market for direct reduction pellets is growing fast. Since LKAB's ores are especially well suited for the production of DR feed with a high Fe content we are looking forward to a continuation of this development. The trend seems to be particularly promising for the direct reduction pellets with basic additions that LKAB is now producing.

The Höganäs sponge iron method for the production of iron powder is officially used at only two mills, Höganäs AB in southern Sweden and Hoganes, Riverton, USA. The total market for the special concentrate for this process is now 300 tmtpy. This method of making iron powder is presumably cheaper than the production of atomized powder, so a positive trend may be expected if sufficiently clean concentrates can be made to produce a high-quality iron powder.

In Sweden new crude iron processes are being developed whereby iron ore concentrates are reduced to iron by a melt reduction method without agglomeration. Relatively fine concentrates can be used, which implies that the melt reduction feed may consist of the same type of super-grade concentrates as the sponge iron concentrate for the Höganäs process. A development along these lines would bring considerable growth in the market for super-grade concentrates.

The synthesis of liquid fuels from coal, shale, peat etc. in the future would probably mean a big upswing in the market for catalyst concentrates.

The market for classified super-grade magnetite concentrates for copying purposes has developed within the past two years. In 1980 it amounted to around 700 metric tons and it is expected to double every three years in the immediate future.

The market for other special products and their development potential are unknown as yet. Super-grade iron ore concentrates have been tried for purposes such as direct reduction to steel sheet, pigments, electronic components, battery electrodes etc., but these applications are still in the research stage.

Development Potential

The development potential of magnetite concentrates of various grinds have been pretty thoroughly studied at LKAB. Relatively coarse concentrates with 80 wt-% finer than 0.5 mm (k_{80} = 0.5 mm) can be concentrated to between 70 and 71 % Fe. while a grind of k_{80} = 0.13 mm gives concentrates with around 71.5 % Fe and 0.10-0.15 % SiO_2 and k_{80} = 0.06 mm yields concentrates with 71.7 % Fe and $\leq$0.1 % SiO_2. These results can be achieved on industrial scale.

The concentrating characteristics and potential of hematite products are less well known, but we are working to advance our knowledge here too. It is probable that the Malmberget ores can be used to make hematite concentrates grading 68-69 % Fe and approx. 0.5 % SiO_2 by high-intensity magnetic separation, while flotation concentrating can give concentrates with about 0.25 % SiO_2.

It will be apparant from these remarks that LKAB's Malmberget operation is blest with ores that are rather unique in the possibilities they offer for making super-grade concentrates. This is why we are putting a great deal of effort into the development of treatment methods that will turn these special properties to the best advantage and are looking forward to a growth in the demand for high-grade concentrates and pellets.

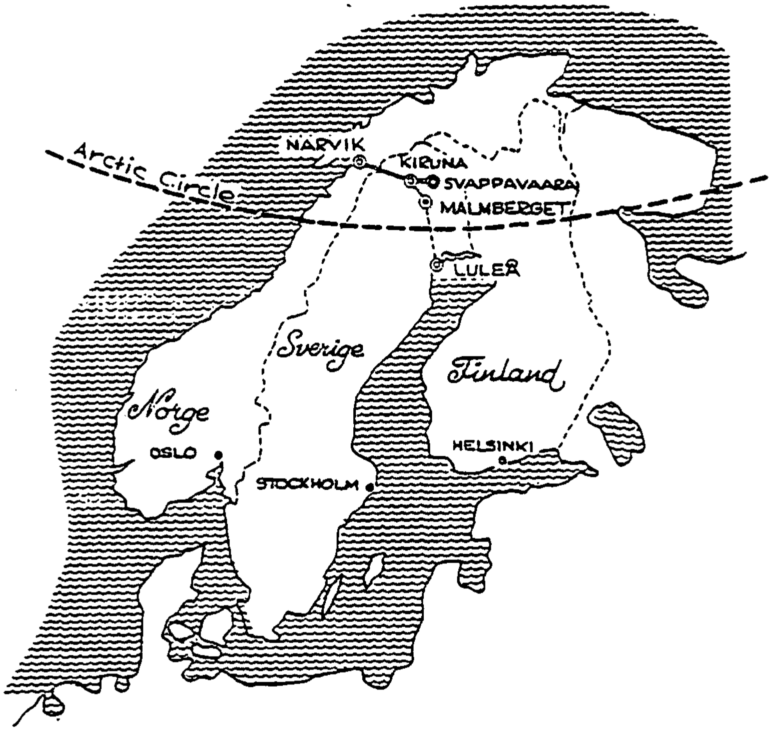

Fig.1.

LKAB:s MINES AND HARBOURS

	KIRUNA	MALMBERGET	SVAPPAVAARA
HIGH P ORE			
Lump ore	4.5		
Fines	6.0		
LOW P ORE			
Lump ore	2.0		
Fines	3.0	5.0 (-1.0)	1.0
PELLETS			
Blast furnace Direct reduction	3.5	3.0 (+1.0)	3.0
SPECIAL CONC.		0.3	
TOTAL	19.0	8.3	4.0
PRODUCTION SPAN*	17-23	8 - 9	3 - 4

*) INDICATES PRODUCTION VARIATIONS DUE TO ACTUAL SALES SITUATIONS

Fig. 2. PRODUCTION CAPACITY (Mtpy) AT LKAB

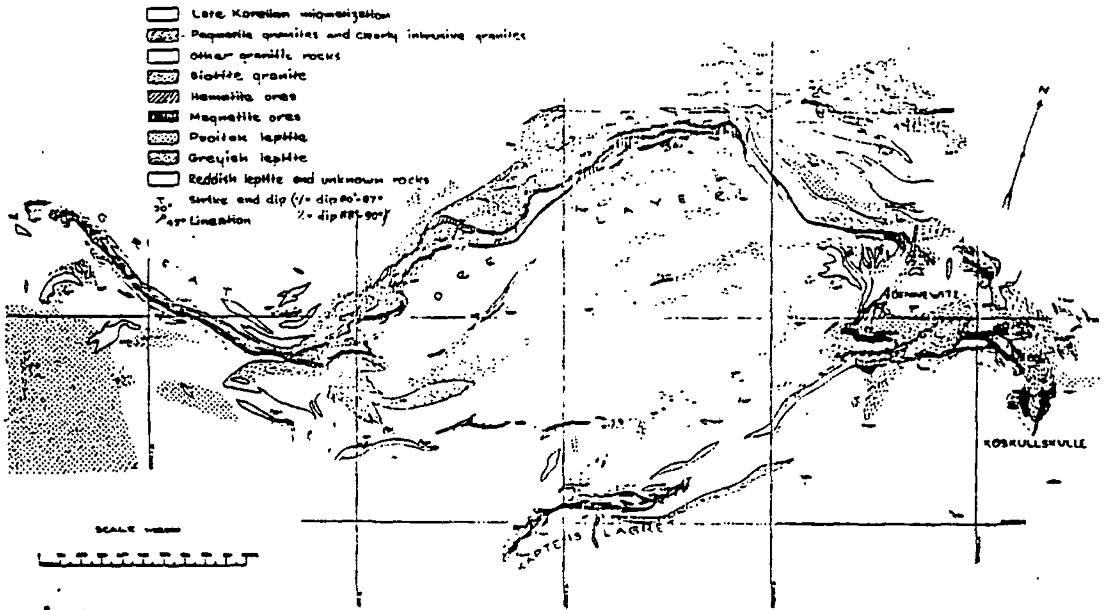

Fig. 3

THE MALMBERGET IRON ORE FIELD

Geological map of the 250 m level.
Compiled at LKAB Malmberget by S. [illegible]

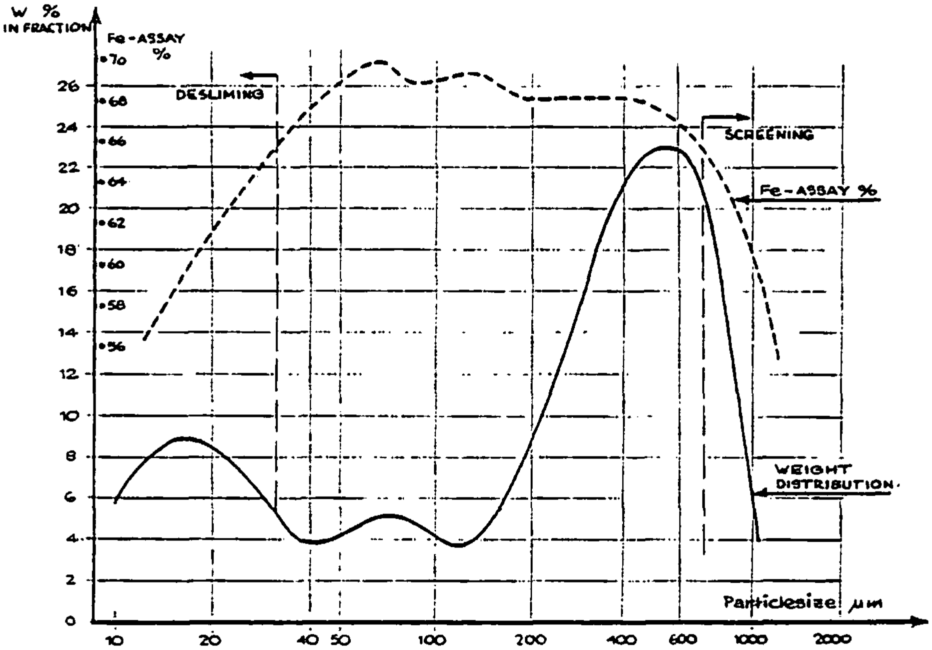

Fig. 4. Fraction analyses on primary concentrate

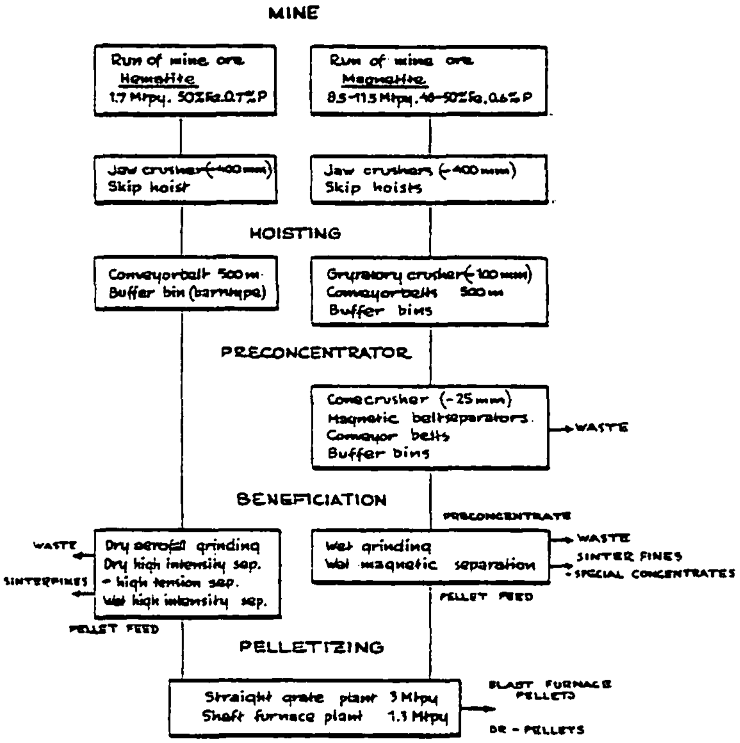

Fig. 5. IRON ORE PROCESSING AT LKAB MALMBERGET

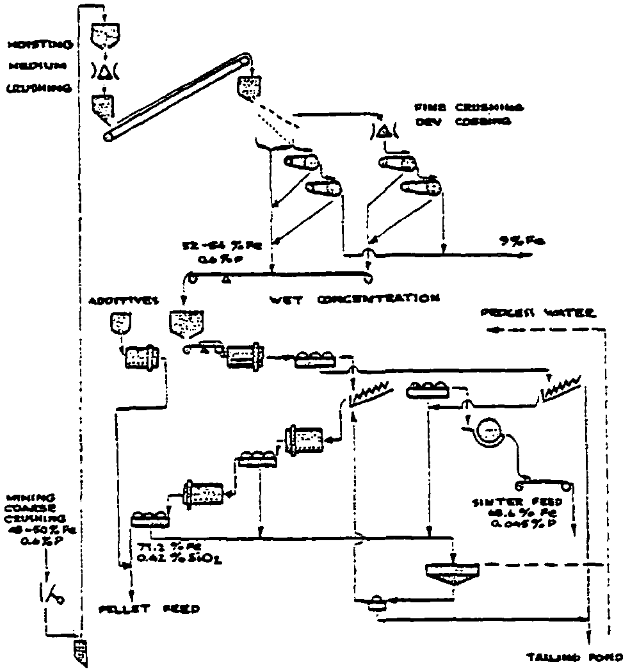

Fig.6.

TREATMENT OF MAGNETITE ORE AT LKAB MALMBERGET

5 LINES. TOT. CAPACITY 1600 TPH. PRODUCTS.
PRODUCTION OF SINTER FEED AND PELLET FEED.

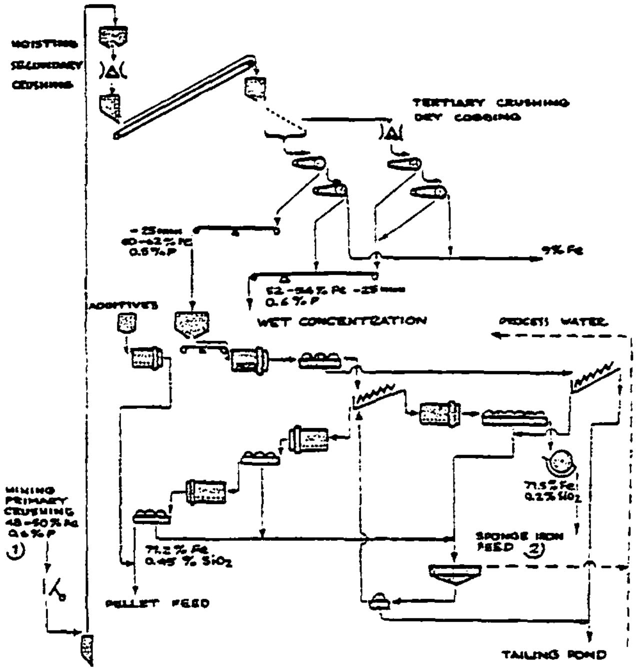

REMARKS: ① High quality crude is selected for special concentrates.

② This material is selected for production of special-concentrates. The final process consists of classifiers, microscreens, separators, dryer and packing machine. In the future will flotation possibly be added.

Fig.7.

TREATMENT OF MAGNETITE ORE AT LKAB MALMBERGET

PRODUCTION OF SPONGE IRON CONCENTRATE.

	SINTER FEED		SPONGE IRON FEED			PELLET FEED			SUPER CONC
Fe %	68.6	69.5	71.2	71.5	71.6	70.7	71.1	71.3	71.7
P %	0.045	0.035	0.006	0.004		0.008	0.007	0.006	0.003
SiO_2 %	2.4	1.8	0.45	0.20	0.10-0.15	0.80	0.45	0.35	≤ 0.1
Ca %	0.45	0.40	0.08	0.05			0.18		
Mg %	0.55	0.50	0.25	0.25			0.25		
Al_2O_3 %	0.70	0.65	0.25	0.20			0.40		
TiO_2 %	0.38	0.38	0.30	0.17			0.30		
V_2O_5 %	0.22	0.22	0.20	0.19			0.22		
Na_2O %	0.49	0.14	0.04	0.012	0.02	0.06	0.04	0.03	0.01
K_2O %	0.07	0.06	0.02	0.03	0.01	0.04	0.03	0.02	0.01
K80 µm	500			130			60		
-1mm Cumw %	97								
-0.5 ---	80			100			100		
-0.1 ---	14			70			92		
-0.07 ---	10			57			83		
-0.04 ---	5			38			68		

OTHER PRODUCTS ARE: Fractioned concentrate with 10w%-74µm and 100w% -150µm.

Fractioned concentrate with 15w%-0.5mm and 100w% -1.5mm.

Dryed and sacked specialconcentrates.

Fig.8: PRESENT AND POSSIBLE FUTURE DATA ON CONCENTRATES

	BLAST FURNACE PELLETS		DIRECT REDUCTION PELLETS	
	ACID	SELF FLUXED	ACID	DOLOMITE FLUXED
Fe %	66.2 - 66.6	63.0	68.6 - 68.8	67.7 - 68.2
Fe^{++} %	- 0.4	- 0.4	≤ 0.4	≤ 0.4
P %	0.01	0.01	0.01	0.01
SiO_2 %	3.8	3.0 - 3.1	0.8 - 0.6	0.9 - 0.6
CaO %	0.10	3.7	0.2	0.8 - 0.5
MgO %	0.2	1.5	0.2	0.2
Al_2O_3 %	0.5 - 0.3	0.8 - 0.7	0.3 - 0.2	0.3 - 0.2
Na_2O %	0.05 - 0.04	0.05 - 0.04	0.05 - 0.03	0.05 - 0.03
K_2O %	0.06 - 0.03	0.03 - 0.02	0.03 - 0.02	0.03 - 0.02
CaO/SiO_2		1.2		0.9
Compr. strength	≥ 250	≥ 280	≥ 250	≥ 280

Fig: 9.

PRESENT AND FUTURE DATA ON PELLETS FROM MALMBERGET

SUBJ
MNG
SHDL

Simulation of Heap and Dump Leaching

by Dr. Alan P. Prosser*

The metallurgical results to be obtained from a heap leaching process, or the environmental consequences of the natural weathering of mine dumps, are difficult to forecast reliably. The method of the future will surely be computer simulation, but there are difficulties to be overcome before meaningful results can be achieved. The author invites those who could potentially benefit as users of such programs to become involved with their development.

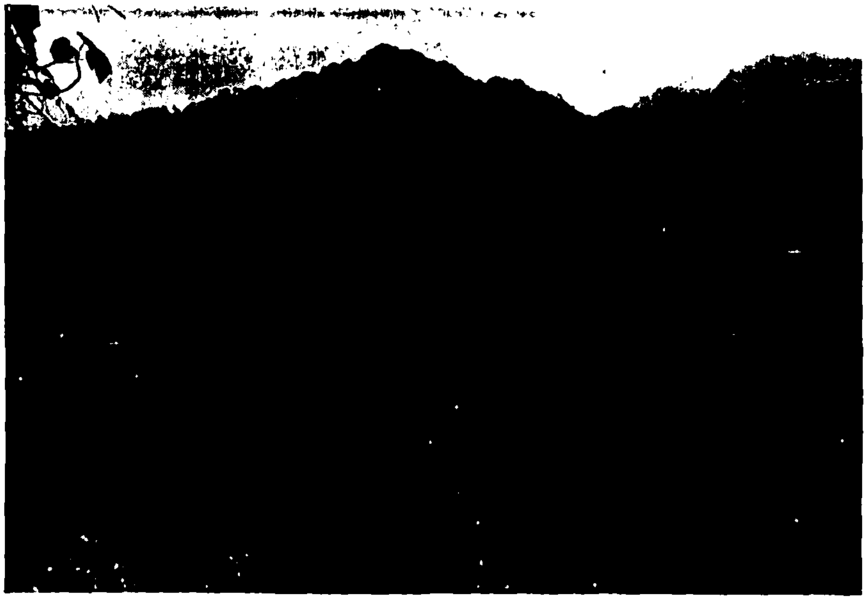

Dumps of very low-grade ore and barren rock at Bougainville, expected to grow to many hundreds of millions of tonnes before the mine closes.

SUPPOSE a process engineer has before him a proposal that many millions of tonnes of very low-grade copper-bearing rock are to be dumped near a mine site and leached to recover the copper. He knows that the recovery plant can be profitable only if the concentration of copper in the solution from the dump exceeds a certain minimum, say 0.5 g/l Cu. Clearly, a vital question he must answer is how much of the copper in the dump can be recovered before the concentration falls below that critical value. Providing the answer is not too discouraging he will want to know how the recovery can be increased by selection of appropriate operating conditions for the leaching process. As the copper recovery extends over many years he must know the answer with some certainty before the dumps and recovery plant are built.

The process engineer has a mining engineer colleague who is concerned with the development of the new mine. The waste rock from the mine contains minerals, such as sulphides, which are expected to weather and release heavy metal ions into the local water system. The government pollution control agency is demanding an assurance that rainwater emerging from the waste rock dumps will contain less than, say, 5 mg/l of copper, manganese, etc. for the next 100 years at least. That is a long time; should the assurance be given and then proved wrong the company would be at risk of some costly actions.

These are two problems typical of a sort met by an increasing number of people in the metalliferous mining industry. The usual way of starting to deal with problems of this nature is to rely on past experience, plus some elementary physics and chemistry, to obtain approximate answers. (Not that it would be described in those terms.) Later a programme of tests would be carried out to reduce the uncertainty in the answers. Of course, to lessen the risk of an inaccurate answer the tests would be made realistic by reproducing the real process, as far as possible, on a reduced scale.

A major problem soon appears if one attempts to deal with the above situations in this way. The dump leaching and weathering processes involve much larger amounts of material and continue for much longer periods of time than the normal test programme. It is unrealistic to recommend that a test dump of a few hundreds of thousand tonnes be built and the concentration of metals in the solution be followed for several years before any further action is taken in developing the project. Even if it is argued that a vertical core of the dump is nearly identical to any other core and, therefore, it is feasible to conduct column leach tests, this strategy does not reduce the time scale. What is done all too often is to reduce the size of the lumps of rock put into the column leach test and thereby speed up the process — but by what factor? And what assurance is there that some other characteristic or phenomenon has not been changed as well as the time scale?

In more formal terms the difficulty is that these leaching processes are complex in terms of their mineralogy, chemistry, fluid flow and, perhaps, energy flow, *and take 1,000 to 10,000 times longer* than the other sorts of process that are normally encountered, such as leaching in an agitated tank, flotation, comminution and roasting. (Some of the peculiar characteristics of heap leaching and dump leaching processes are illustrated in the figures.) A way must be found to reduce the time scale by a controlled factor and with the assurance that no other aspect of the process has been changed.

Simulation

Nowadays, there is a choice of two ways. The first is to formally analyse

---

*Dr. Prosser is Senior Lecturer in Chemical and Extractive Metallurgy at The University of New South Wales, Australia.

the process, reduce the scale by calculated changes in each parameter and run a programme of empirical tests. The alternative is to simulate and accelerate the process in a computer program. Both methods are dependent on having a model of the process — a shorthand way of describing the accumulated knowledge obtained from practical experience, experimental investigation and theoretical analysis put together in a valid form. The computer simulation has some advantages over the scaled-down experimental simulation and is steadily replacing it for problems of this sort.

Once the program has been written and tested thoroughly — and it is conceded that this is a lengthy and demanding task — it can be used to produce results far faster than any experimental method. The consequence is that a much wider range of variations can be investigated in a short period of time. The effects of variables can be studied singly or in any desired combination with virtually no constraints. Imagine trying to obtain samples with identical mineralisation and proportions of copper spread through the range of 0.02% to 0.2%. Or trying to obtain samples covering all combinations of three proportions *each* of chalcopyrite, galena, sphalerite, pyrite and calcite. Furthermore, if the computer program has been prepared in the appropriate form it can be used for many problems of the type described in the opening paragraphs.

Of course, there are disadvantages to the computer simulation. It can only reveal the consequences of those characteristics and phenomena of the ore-process system that have been included in the model. The consequences of unsuspected or deliberately omitted phenomena will never be revealed by the simulation. This is no worse than the appearance of artefacts or the suppression of genuine effects as a consequence of invalid scale-down in testwork programmes. We have learnt how to survive the latter risk; we should be able to survive the former as well. At least it should be easier to determine whether some observed phenomenon has been validly included in a computer program or not.

The technical literature contains descriptions of several models from which computer programs have been developed by the authors.[1-6] These reports do not contain the programs in detail. Therein lies the first hurdle to be surmounted by anyone intending to use one of the computer simulations to help solve the sort of problem described in the opening paragraphs. It is necessary to locate the authors and persuade them to run their simulation for the problem in hand. In principle it is possible to obtain the program and set it up on another computer. Unfortunately, this rarely works well in practice because the program has not been prepared for use by other people and substantial adaptation is required. So far no group has developed its program to the point that it is a marketable software package. There seems to be no reason why this should not come about in the future when the demand warrants the effort.

Information required

Whether the process is controlled leaching of a dump with recovery of valuable components or natural weathering with release of dissolved salts the process phenomena are similar. The principal ones are chemical reactions between several minerals and the reactants carried in by water and air; the bulk flow patterns of the water and air; the transport of the reactants to and the products from the reactive minerals; and the generation and transfer of heat within the ore mass. Murr has provided an excellent summary of the experimental observations made on the many specific phenomena that occur in the leaching of sulphide-bearing ore masses[7]. That is the base of accumulated knowledge from which the computer simulations have been developed.

No simulation encompasses all of the phenomena that have been observed. One should be aware of the phenomena included not only because a simulation yields results related only to those phenomena but also because the information required as input to the simulation is prescribed by them.

Substantially different materials are often put into a dump.

The information that could be required (depending on the phenomena included) is:

1) the chemical conditions in the water and air, including the concentrations of potential acids, bases, redox reagents, precipitating agents (e.g. phosphates and silicates) and microbial species; the diffusion coefficients of the dissolved species;
2) the identity of *all* minerals that are likely to react, including those that are expected to react only slowly; the proportion of each mineral; the

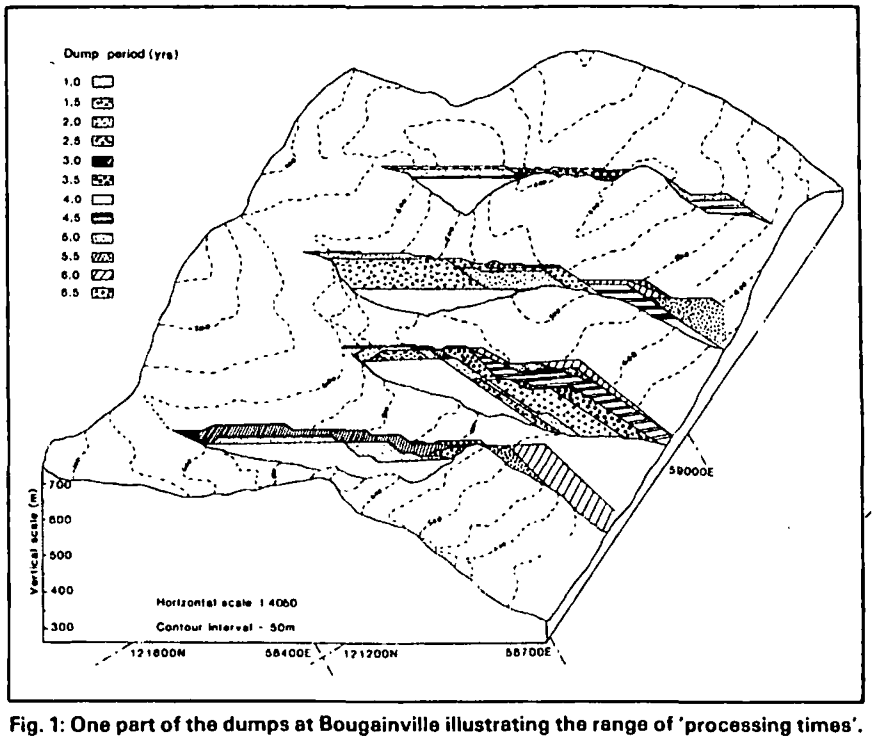

Fig. 1: One part of the dumps at Bougainville illustrating the range of 'processing times'.

distribution of each mineral if it is far from random; variations laterally and vertically; the approximate rates of the reaction between the fully liberated minerals and the other reactants;

3) the expected lump size distribution (from direct measurement, fracture spacings or blasting data); the existence or possible formation of layers of fine or compacted material; segregation of sizes; the open porosity of the lumps; the history or planned sequence of dumping; the dump geometry;
4) the flowrate of the leach liquor; points of input and output; the underlying topography; the permeability of the dump to air; rates of evaporation; seasonal variations;
5) the heats of the chemical reactions; the rates of heat transfer by convection and conduction.

The principal equations used in one of the simpler models[5,6] are

$$3/2 - \phi - 3/2(1 - \phi)^{2/3} = k_i^2 t/6 \quad (1)$$

$$k_i^2 = \frac{11CMD}{n\varrho \alpha R^2 \tau} (\varepsilon_0 + \frac{\varrho \alpha}{\varrho_r}) \quad (2)$$

$$0 < \phi < 1 \quad (3)$$

where ϕ is the recovery of the component in the solution as a function of time, t, and C is the reagent concentration, M the molecular weight of the reacting mineral, D the diffusion coefficient of the reagent, n the number of moles of reagent consumed per mole of reactive phase, ϱ the density of the lumps, α the proportion of reactive mineral, R the lump size (radius), τ the tortuosity of the pores, ε_0 the open porosity of the lumps and ϱ_r the density of the reacting mineral. Although the parameters in these equations take on a more complex form when more than one reacting mineral, more than one reagent, a distribution of lump sizes and some other characteristics are included, there is no substantial change in the form of the equations nor the type of information required.

Information produced

All simulations are capable of giving the proportion of the mineral(s) reacted as a function of time. From these data the mass of product per unit time and the concentration of the dissolved species in solution as a function of time can be readily calculated from the total mass, the assay and the solution flowrate. With appropriate input data and some modification of the programs it is possible to simulate the effects of fluctuations in the rate of irrigation, for instance.

Each result has an error associated with it, i.e. there is uncertainty as to how close the result will be to the performance of the real, full-scale process. The uncertainty arises from three sources, viz:

1) the phenomena that have been omitted from the simulation;
2) the accuracy with which the equations represent included phenomena over the range simulated;
3) the accuracy of the values used for the various parameters.

The significance of the uncertainty depends on the particular application of the simulation.

There are four tasks to which the simulations can be applied effectively at the present time, viz:

a) planning testwork
b) designing operating conditions
c) predicting future process performance, and
d) using past experience with other ore-process systems.

Planning testwork

In these early days of the simulations it is still necessary to carry out a programme of testwork. Typically, a testwork programme should determine how the concentration of the dissolved species changes with time and how that concentration is affected by lump size distribution, the proportion of the valuable mineral, the proportions of other reacting minerals (and other variations in the rock mass), the concentration of the reagent, etc. Vital information required before the commencement of a testwork programme includes the minimum number of necessary tests, the number of samples to be tested and how the samples are to be selected. Also, with the time-scale problem in mind, it would be valuable to know when to stop a test so that the performance is adequately determined without continuing longer than necessary.

Simulation runs for a variety of values of the variables can give most helpful guidance on all of these points. For example, the effects of other oxygen and cyanide consuming minerals on the rate of gold extraction and an uneven distribution of gold between the lumps are illustrated in Fig. 2[8]. As the combined effect of these two characteristics of gold ores corresponds to a hundred-fold range of rates — from one extreme of fast recovery to the other extreme of unacceptably slow recovery — it is clearly necessary to obtain test data to determine where a particular ore falls in that range. Furthermore, the simulation demonstrated that changing the flowrate of the cyanide solution, or its concentration would be of little help.

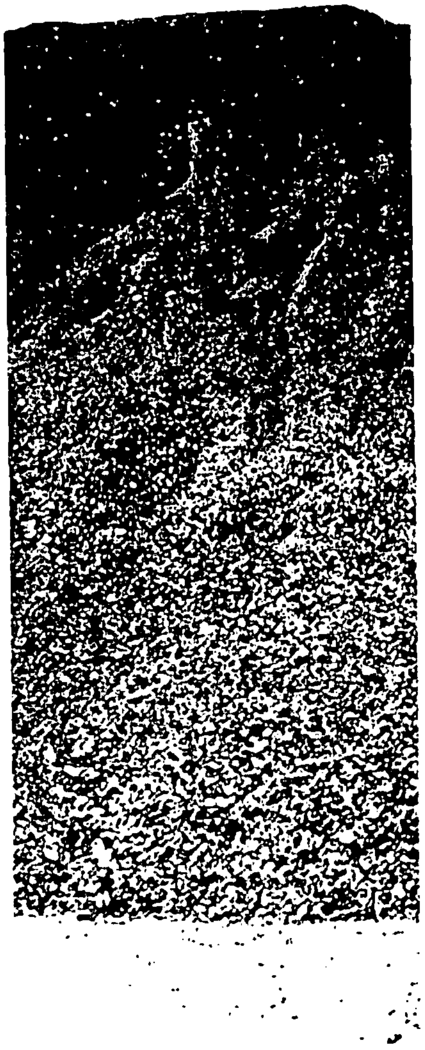

Large lumps segregate to the bottom of a dump as a result of dumping procedures. The effect of this segregation is uncertain.

In the writer's experience a number of unexpected results have been obtained from simulation. Some indicate the importance of some variable, e.g. the distribution of the gold between lumps; others indicate the relative lack of significance of other variables, e.g. the lump size distribution[6]. In hindsight the abandonment of some tests too early has been demonstrated[9]. A common deficiency of empirical testwork is often the limited number of samples examined *separately*; it is not unusual to combine samples before a test. By using the simulation to restrict the time for any one test more samples can be tested in a prescribed length of programme. The optimum programme is determined mainly by the variations in the rock mass. The greater the variation the more extensive the programme should be and the more valuable the simulation will be in planning the programme.

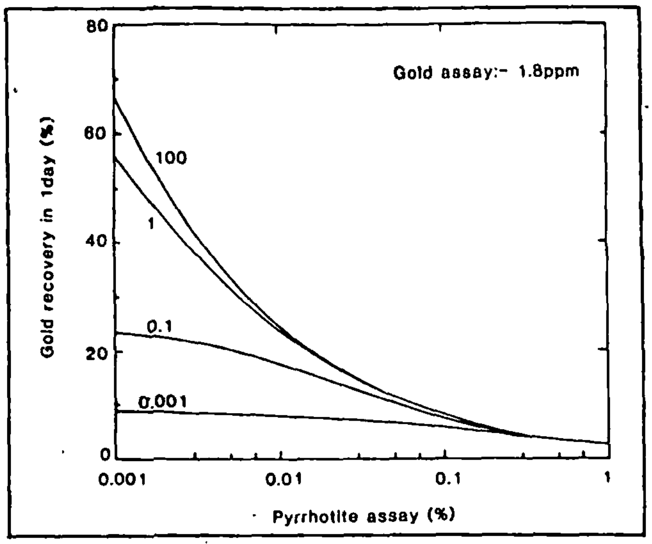

Fig. 2: Simulated effects of a competing mineral (pyrrhotite) and an uneven gold distribution on rate of gold extraction in cyanide heap leaching. Figures against curves are % of lumps containing gold, for a constant mean assay.

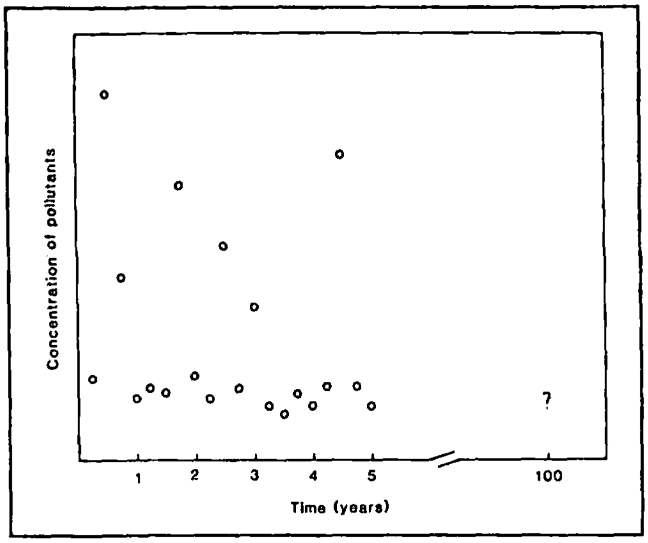

Fig. 3: Some typical data for pollution in water emerging from mine waste dumps, illustrating the difficulty of long-term prediction.

Having a good idea of the results of a programme of tests before starting them is most helpful. If the results come out as expected, one proceeds with confidence; if they come out different from expectation, one's attention is immediately focussed and the progress of the next test is closely examined for evidence of unsuspected phenomena.

Designing operating conditions

Simulations can be used for determining the effects of options in the operating procedures in the same way as for planning testwork. They indicate the likely consequences of various operating methods at full scale, e.g. changing lump size, dump geometry, rate of irrigation, breaks in irrigation, concentration of reagent, compaction and mixing or segregation of different ore-types. The number of variables considered tends to be greater for full-scale operations than for column leach tests, hence a comprehensive model is potentially the more useful. However, the comprehensive simulations rely on data obtained from the full-scale operation or at least a large-scale experimental simulation. They cannot be used with certainty to determine *beforehand* the effects of variables associated with the construction stage e.g. lump size and compaction.

Predicting performance

Fig. 3 illustrates the results that may be obtained when the leaching process occurs naturally with no control over the chemical and fluid flow phenomena. The concentration of salts in the effluent fluctuates dramatically. This could be the situation when a mine closes and the dumps are left unattended. The question is what will be the concentration in 100 years time. Extrapolation of the best straight line through those points, from 5 years to 100 years, is obviously going to give an answer of little value. If one argues that the concentration must decrease with time and draws (literally or figuratively) a downward sloping line the result is not much better. Clearly, it is necessary to have some understanding of why certain concentrations are much higher than others. Extrapolation is then a matter of deciding by how much the extraordinary values will change with time and, perhaps, by how much the 'normal' low values will change. Simulation of the natural leaching process is the formal, quantitative way of extrapolating existing data on the basis of some understanding of the complex phenomena involved.

Heap or dump processes can take anything from 50 days (gold heap leaching) to over 100 years (generation of pollutants) to reach 'completion'. Consider an example in the middle of this range, which takes 10 years to complete, and in which the chemistry and fluid flow phenomena are under control as a result of maintaining constant solution inputs. Because the process is exceptionally slow there is a need to forecast results well ahead of current operations. This calls for extrapolation over a distance on the time scale up to 20 times the length of existing knowledge. Not only is it worthwhile knowing the predicted performance but it is also worthwhile knowing the possible error in that result. The computer simulation can be of considerable assistance in producing the latter information.

Each simulation uses values for several ore-process variables, such as mineral assays and reagent flow-rate. Each of these values has a range of uncertainty associated with it. Numerous combinations of values, falling within the nominated ranges, will give an acceptable fit to the existing data. If the extrapolation is made for each of those combinations a set of values is obtained for the output concentration, or some other output. The range encompassing that set indicates the uncertainty in the predicted concentration.

In this way, the sensitivity of the concentration (or other output variable) to particular ore-process variables is revealed and can be used to focus attention on those variables which give rise to the most uncertainty. Suggestions and opinions about the uncertainty can be tested objectively and quantitatively. Once again, the simulations can reveal the unsuspected importance of some variables.

The nature of the simulation itself has an important bearing on the value of the results for predicted performance. The simulation that gives the best fit to the existing data by curve-fitting does *not* necessarily give the most valuable prediction. It can underestimate the uncertainty in the predicted results, to the extent that the actual result is excluded from the feasible range. This point is explained later when selection of the simulation is discussed.

Using past experience

Past experience has always been an important input to the business of deciding what to do and how to do it in mineral processing. Unfortunately, it is almost always a qualitative, semi-empirical and subjective input. The comprehensive models that are being developed for the leaching processes provide an excellent framework with which to make better use of the past experience of different people. An example will illustrate how.

A great deal of uncertainty still exists about the flow of solution through a dump. However, many people who have observed one or more of these operations over a period of time have some comments to make about solution flow. Their *combined* observations could form a useful input to the development of these models.

For instance, three (hypothetical) reports on quite different processes could supply the following information:

Case A. The dumps contained little sandy material and no clay. There were no problems in maintaining normal flow through the dump; all solution entered the dump quickly; no pools on the surface lasted more than an hour once irrigation ceased. Good recovery of the metal (∼70%) was achieved after 5 years.

Case B. A small proportion of the material was very fine after blasting. The flow through the dump gradually decreased over the first year or so; the concentration fell to an unacceptable level after two years when only about 30% of the metal had been obtained. Some fine material collected in low areas on the top surface and led to shallow pools that took a day to clear.

Case C. The ore was known to contain a few percent of clayey material. Flow through the dump was never good and almost stopped after a few months; the solution that came out was fairly concentrated but the recovery was less than 1% per year after the first few months.

These three reports when put together give a consistent and useful guide to the effect of fines. (Perhaps it is too much to expect such consistency!) They could be used to assign approximately only 20% of the dump accessible to solution when it contains a few percent of clay, through 50% accessible when there is the same proportion of sandy material, to 100% accessible when the dump is substantially free of any fine material. Although those figures are crude approximations and neglect the effect of the distribution of the fine material they are useful inputs to the simulation. Without information of this sort or better the effect of fine materials would have to be omitted altogether from the simulation. Clearly, that is a worse approximation.

Further development

Further developments are assured; the technique is too useful to be neglected. The only doubts concern how quickly, by whom and in what directions.

The types of developments that are required are as follows:

1. Incorporation of further phenomena and characteristics — either through a new development or by combining useful features of two or more simulations. Two phenomena that are not yet adequately incorporated are the catalytic action of microbial components and the effects of fine materials on flow; but there are others.
2. Generalisation of the simulations. Most of the simulations have been prepared for specific ore-process systems. If the effort committed to the development of simulations is not to approach that devoted to testwork programmes it is essential to have simulations that can be applied to a variety of metals, ores and reagents.
3. Development of methods for independently measuring the input variables. The methods ought to be capable of measuring not only mean values but also the distribution of values. Similarly, the simulations ought to be in a form which can use the data produced.
4. Preparation of a simulation package that can be used by people other than the original developers. The package requires not only the program but also supporting material about the ore-process systems which can be dealt with, the required data and how to obtain them, the various purposes for which the simulation can be used and the interpretation of the output data.

The stage has been reached where some responsibility for further development should pass from research workers (where it is at present) to others more concerned with the applications. One purpose of this article is to encourage potential users to start becoming involved in the developments.

Simulation selection

For those who are contemplating using one of the simulations for any of the above purposes the selection of the best simulation is an important matter. There are a few disguised traps for the unwary. This is not the place to review critically each of the simulations described in the literature, but some selection guidelines can be laid down.

There are two extreme types of simulation. There is the one that uses values of defined properties of the ore or the reagents, that can be measured in a few days in the laboratory or obtained from tables. *The measurements are completely independent of the process.* At the other extreme there is the simulation that uses values that are obtained empirically by curve-fitting from the full-scale process itself or a pilot test involving the actual material in large quantities and extending over a period of time comparable to that of the full-scale process. In this latter simulation the values are not necessarily related to any defined property. Most simulations fall between these two extremes with some input data obtained from independent measurements and some from the results of process testwork. The reports describing the simulations should be read carefully to ascertain how the data are actually obtained. Often a particular parameter is defined as a basic independent property but the value used is obtained by curve-fitting.

It was stated above that the difference between the simulated results and the actual results of the full-scale process is attributable to three errors, viz., the phenomena omitted from the simulation, the accuracy of the equations used to represent the phenomena and the accuracy of the values used for the parameters. Clearly, this difference is expected to be a minimum with the simulation that includes the most phenomena and uses the curve-fitting method for obtaining several input data. However, this benefit is obtained at the price of having to make long-term tests using large quantities of material.

If the simulation is to be used to help plan process testwork the type that requires only values determined from independent measurements or tables has an advantage. Not only does it provide a quick and easy guide to the effects of several variables but it also gives unambiguous guidance as to which variables ought to be measured accurately, i.e. those to which the result is most sensitive. For example, the simulation developed by the writer and his colleagues can be used with data obtainable from small portions of drill cores.[5,6]

Again, if the purpose is extensive extrapolation from existing data, the simulation using only independent data is probably better than another including the same phenomena that relies on curve-fitting. The advantage is far from obvious and is illustrated by the following hypothetical example.

Consider a rock which contains two different components that yield the valuable metal; the proportions of the valuable metal in each are a and b respectively; the recovery from each as a function of time is given by a relation of the form

$$R = 1 - \frac{1}{1 + kt} \qquad (4)$$

The actual recovery of metal from the rock mass is given by

$$R = c\left(1 - \frac{a}{1 + k_1 t} - \frac{b}{1 + k_2 t}\right) \qquad (5)$$

Suppose that in this case $c = 0.80$, $a = 0.25$, $b = 0.75$, $k_1 = 0.6y^{-1}$ and $k_2 = 0.1y^{-1}$.

The process is operated for six months and the cumulative recovery is determined periodically by measuring the concentration and flowrate of the pregnant solution. The results, with a small, random measurement error (approximately 5% and decreasing with increasing recovery) are given in the first row of Table 1.

Two simulations are available; Simulation A includes *two* groups of phenomena, related to the ultimate recovery and the rate of recovery, and depends on the equation

$$R = \alpha\left(1 - \frac{1}{1 + \beta t}\right) \qquad (6)$$

The values of α and β are obtained from the best fit of this equation to the data collected over six months. Simulation B includes only one group of phenomena represented by the equation

$$R = 1 - \frac{1}{1 + \beta t} \qquad (7)$$

(The group of characteristics leading to the ultimate recovery are omitted from B). In this latter simulation β is obtained from independent measurements. The results of applying the two simulations are contained in Table 1.

Using Simulation A the best fit between the measured recoveries and equation 6 corresponds to $\alpha = 0.37$ and $\beta = 0.492y^{-1}$. The calculated recoveries in the second row were obtained from these values and equation 6. Combinations of $\alpha = 0.50$, $\beta = 0.348y^{-1}$ and $\alpha = 0.30$, $\beta = 0.635y^{-1}$ fit the measured data almost as well and the corresponding calculated recoveries are given in rows 3 and 4 respectively. Thus, the predicted recovery after 10 years by Simulation A is between 25 and 40% with the most likely result about 30%.

If Simulation B is selected, the independent measurement of β on ten drill core samples gives a mean value of $0.25y^{-1}$ with a minimum value of $0.12y^{-1}$ and a maximum value of $0.50y^{-1}$. The calculated results in rows 5, 6 and 7 were obtained from these values respectively and equation 7. In this case the predicted recovery after 10 years is between 54 and 84% with the most likely result of about 70%.

The recovery that will be achieved after 10 years, calculated from equation (5), is in the last row of Table 1. (Remember this value is not known at the time of the calculations). Both simulations give most likely results some way from the reality; both indicate a range that *excludes* the real value; Simulation A is no better than Simulation B in spite of allowing for an ultimate recovery less than 100% and the curve-fitting procedure.

In terms of these results alone there is little to commend one simulation over the other for the purpose of extensive extrapolation. However, the measurements and the calculations will not cease after six months. (Unless the operation has been closed as a result of the poor recovery predicted by Simulation A!) The application of Simulation A after six months appears to have been most successful and there is no evidence to suggest that any modification is necessary. After one year the calculated range for the recovery at 10 years would change to about 30-43%. Perhaps then the question might be asked why the range was shifting upwards rather than just converging.

However, after six months, the independent measurements of β for Simulation B clearly indicate an unacceptably wide range of values for that parameter. Furthermore, the mean value of β is giving a consistently higher recovery than that measured over six months. Further measurements of β are clearly necessary and would, presumably, be made in the next few weeks. The least that would happen is that the mean value of β would approach the true weighted mean of $0.225y^{-1}$ and it would continue to be clear that Simulation B was predicting recoveries about 40% too high. Another feasible consequence of further measurements of β would be recognition that the values occurred in two groups — most near $0.1y^{-1}$ and a few about $0.5y^{-1}$. This would be one vital step forward in understanding, hence simulating, this particular operation. It is a simple matter to modify equation 7 to the form of equation 5 with C = 1 and values for a and b estimated from the distribution of β values. In the end, in this example, Simulation B is superior to A.

Table 1: Cumulative percent recoveries of valuable metal measured over six months and extrapolated to ten years.

Row	Origin	Time (years) 0.1	0.2	0.3	0.4	0.5	10
1	Measured	1.9	3.1	5.1	5.8	7.3	—
2	Simulation A; best fit	1.74	3.32	4.76	6.08	7.30	30.8
3	,, acceptable high	1.68	3.26	4.73	6.11	7.41	38.8
4	,, acceptable low	1.71	3.38	4.80	6.08	7.23	25.9
5	Simulation B; mean β	2.44	4.76	6.98	9.09	11.11	71.4
6	,, lowest β	1.19	2.34	3.47	4.58	5.66	54.5
7	,, highest β	4.76	9.09	13.04	16.67	20.00	83.3
8	True (equation 5)	—	—	—	—	—	47.1

This hypotehtical example has been dealt with in some detail because it illustrates the need for thoughtful selection of the method of simulation. The data were chosen to illustrate the various points, but there is nothing unrealistic about the example. The small random error in the recovery measurements and the existence of two different types of metalliferous material in the rock were the basic causes of the erroneous predictions illustrated in Table 1. Those are normal, not exceptional, characteristics of mineral processing.

References

1. BARTLETT, R. W. A combined pore diffusion and chalcopyrite dissolution kinetics model for in situ leaching of a fragmented copper porphyry. *International Symposium on Hydrometallurgy.* Ed. D. J. I. Evans and R. S. Shoemaker, New York: American Institute of Mining, Metallurgical and Petroelum Engineers, 1973. p.331-374.
2. BRAUN, R. L., LEWIS. A. E. and WADSWORTH, M. E. In-place leaching of primary sulfide ores: laboratory leaching data and kinetics model. *Metallurgical Transactions, Part B,* vol. 5B, 1974, p.1717-1726.
3. ROMAN, R. J., BENNER, B. R. and BECKER, G. W. Diffusion model for heap leaching and its application to scale-up. *Transactions of the American Institute of Mining, Metallurgical and Petroleum Engineers,* vol. 256, 1974, p.247-252.
4. CATHLES, L. M. and APPS, J. A. A model of the dump leaching process that incorporates oxygen balance, heat balance and air convection. *Metallurgical Transactions, Part B,* vol. 6B, 1975, p.617-624.
5. ROACH, G. I. D. and PROSSER, A. P. Prediction of rates of chemical processes for treatment of low grade materials: theory and tests for mass-transfer controlled reactions. *Transactions of the Institution of Mining and Metallurgy, Section C,* vol. 87, 1978, p.C129 C138.
6. BOX, J. C. and PROSSER, A. P. Development of general correlations for making rapid forecasts of the efficiency of dump and *in-situ* leaching processes. *Extraction Metallurgy '81.* Ed. M. J. Jones, London: Institution of Mining and Metallurgy, 1981. p.291-298.
7. MURR, L. E. Theory and practice of copper sulphide leaching in dumps and *in-situ. Minerals Science and Engineering,* vol. 12, 1980 p.121-189.
8. PROSSER, A. P. Introductory remarks to "Development of general correlations for making rapid forecasts of the efficiency of dump and *in-situ* leaching processes." To be published in Supplementary Volume to *"Extraction Metallurgy '81"* See ref. 6.
9. PROSSER, A. P., BOX, J. C. and BEAVIS, F. C. Comprehensive models of *in-situ* and dump leaching. *Australasian Institute of Mining and Metallurgy Conference, Sydney, 1981,* Melbourne: Australasian Institute of Mining and Metallurgy, 1981, p.317-327. ■

$$\Delta h = k \cdot (t - t_i)^n \qquad (1)$$

where: k = proportionality factor
n = the temperature
t_i = the initial temperature (17°C)

Taking logarithms, we obtain

$$\lg \Delta h = A + n \lg \Delta t \qquad (2)$$

where: A = log k.

Fig. 1 shows the results from measurements of the height of the deposit in suspensions of natural molybdenite (a) and galena (b) modified by treatment in a 10^{-3} M solution of potassium butyl xanthate and of barytes (c) modified by treatment in a solution of sodium oleate at the same concentration. These results confirm the temperature dependence of the hydrophobic interactions.

The stability of the volume-hydrophilic colloidal systems is determined according to Ostwald's law, a mathematical interpretation of which has been given in the form:

$$dx/dm = k(a - x) \qquad (3)$$

where: x = the amount of peptised (coagulated) substance
a = the maximum amount of the substance which can be present in t form of a sol with a given volume of electrolyte
m = the total amount of the substance introduced into the system
k = a constant (positive on the peptisation branch and negative on th coagulation branch)

Under certain influences the characteristics of the suspension can be tran formed from one class to another, and the characteristics of volume-hydro phobic suspensions of the electrolytic class can be easily transformed to th characteristics of the nonelectrolytic class. In fig. 1 the straight line d repr sents the results from measurement of the height of the column of deposit i suspension of natural galena with a partially oxidized surface, while the stra ght line f corresponds to the same galena but pretreated in a solution of so sulphide and then washed with distilled water. The sign of the temperature dependence of the column height is reversed, and the suspension changes fr "electrolytic" to "nonelectrolytic". Treatment with flotation collector rea- gents leads to analogous results. The properties of suspensions of electro lytic character are also transformed to the properties of nonelectrolytic character in the transition from weak solutions of inorganic electrolytes to concentrated solutions, in which the temperature coefficient of the stabilit of the suspension becomes positive. Corresponding results for a suspensi of barytes are given in fig. 2.

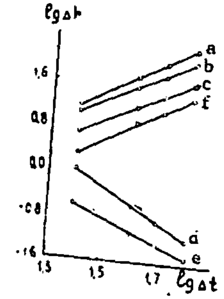

Fig. 1

The results from measurement of the column height of the deposit in a suspension of minerals. Grain size 0.10-0.25mm.

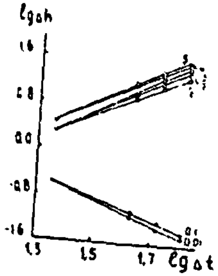

Fig. 2

The results from measurement of the column height of the deposit in a barytes suspension with various concentrations of sodium chloride in the solution. The figures by the straight lines correspond to the normalities of the salt. Grain size 0.10 - 0.25mm.

Sov. Non-Fe.
1979 v.7 N3

2 articles

UDC 669.053.4

Simulation of hydrometallurgical reactions and reactors

G N Dobrokhotov (Leningrad Mining Institute - Department of the Metallurgy f Heavy and Noble Metals)

The modern state of hydrometallurgy, as a technical science, is character- sed by a gradual replacement of the descriptive interpretation of the proces- es and equipment by more objective categories of physicochemical and math- ematical content. This replacement leads to better unification of the technical formation, secures a high degree of reliability in the technological charac- eristics, and corresponds in the best possible way to the tasks of improving etallurgical production.

One of the directions where methods of descriptive interpretation of the tech- ology and equipment are successfully replaced by analysis of the kinetics of e operations is the determination of the operating efficiency of hydrometal- urgical reactors. At the present time their designs are extremely varied, d the choice of schemes is often based on subjective considerations. Many ydrometallurgical processes occur under diffusion control, and their tech-

nological characteristics therefore depend substantially on the intensity of agitation and aeration of the suspensions. In the descriptive interpretation of the technology allowance for the effect of these and other factors and their generalisation encounter certain difficulties. Extremely complex also is the problem of simulation of the processes and equipment, since, for example, a simple geometric proportionation of the dimensions of the reactors is not accompanied by the attainment of unambiguous technological results. These problems can only be solved correctly by means of the modern theory of physicochemical similarity.

The main considerations in the simulation of diffusion processes and the analytical methods of calculation and construction of the respective equipment emerging from them are set out below. The development of these methods became possible on the basis of theoretical and fundamental investigations which were only carried out recently[1-6]. In particular, they make it possible to give some additional information about the kinetic features of the known production reaction $ZnO + H_2SO_4 = ZnSO_4 + H_2O$ proposed in discussion[5e].

In this analysis we dwell first on the points which determine the kinetics of mass transfer. As known, the rate of steady-state diffusion processes is characterised by the following equations for the intensity of mass exchange:

In the dissolution regime,

$$-\frac{dq}{d\tau} = \frac{V}{a}\cdot\frac{dC_\tau}{d\tau} = \frac{DS}{a\delta}(C_S - C_\tau) = \frac{KS}{a}(C_S - C_\tau) \qquad (1)$$

and in the reaction regime

$$-\frac{dC_\tau}{d\tau} = \frac{KSC_\tau}{V} \qquad (2)$$

where: $dq/d\tau$ and $dC_\tau/d\tau$ = the mass exchange rates
V = the volume of the reactor m^3
a = the fractional content of the active substance in the dissolving material
D = the diffusion coefficient m^2/sec
S = the reaction surface m^2
δ = the thickness of the boundary diffusion layer m
C_S and C_τ = the saturation and current concentrations kmole/m^3 H_2O

The constant K has the dimensions of linear velocity (m/sec) and is only used in such a context for simulation. It is usually determined with an arbitrary motivating force for the process $(C_S - C_\tau)$ or C_τ, equal to 1 M/100g H_2O (with the corresponding expressions for C_S and C_τ in molal concentrations and this makes it possible to unify the characteristics of the various substances with respect to their individual solubility. Another noteworthy characteristic of the rate constant K is its invariance with the dimensions of the reacting surface. This means that the values of K observed, for example, in the dissolution of whirling particles keep constant in value throughout the whole contact time. This point, while taking account of the usual anisotropy of the characteristics of crystalline materials and the electrochemical nonuniformity of the surface, appears somewhat strange and as yet only finds explanation in the formal averaging of the surface characteristics of the particles. As shown below, the point about the invariance of the rate constant K greatly simplifies all the calculations based on the change in the geometry of the dissolving material.

Integration of equations (1) and (2) gives

$$\lg\frac{C_S - C_0}{C_S - C_\tau} = \frac{KS\tau}{2.303V} = K_{obs}\,\tau \qquad (3)$$

$$\lg\frac{C_0}{C_\tau} = \frac{KS_\tau}{2.303V} = K_{obs}\,\tau \qquad (4)$$

where C_0 is the initial molal concentration of the substance and K_{obs} is the observed rate constant of the process, sec^{-1}. When S = const, the unknown values of K are easily determined by graphical representation of the observed concentrations. Accordingly, experimentation with samples having a constant surface is the most convenient and simple method of laboratory investigation.

During the dissolution of a disperse material the reaction surface is variable. For regular spheres, taking their surface to be generally accessible, we obtain

$$q = \frac{\pi x^3 \rho n}{6} \qquad x = \left(\frac{6q}{\pi\rho n}\right)$$

from which:

$$S = \pi x^2 n = \pi n\left(\frac{6q}{\pi\rho n}\right)^{2/3} = a_1 q^{2/3}$$

where x is the equivalent diameter of the spheres m; α_1 is a coefficient which takes account of the geometry and density of the particles; q is the mass of the material kg. The subsequent description of the mass-exchange rate depends on the experimental conditions. Most frequently laboratory experiments are realised by a simplified procedure with the reagents loaded in a single batch and with a variable concentration C_τ. As applied to Eqs. (1) and (3), the latter is determined by the expressions

$$C_\tau = C_0 + \frac{a(q_0 - q_\tau)}{V}$$

and

$$C_\tau = C_0 - \frac{a\,\alpha_2(q_0 - q_\tau)}{V}$$

where the subscripts 0 and τ denote the initial and current states, and α_2 represents the stoichiometric coefficient of the reaction.

Substitution of the S and C_τ values, for example, in the dissolution equation (3) gives

$$-\frac{a\,dq}{a_1 q^{2/3}\left[C_S - C_0 - a(q_0 - q_\tau)/V\right]} = K d\tau$$

and this then makes it possible to obtain the integral form of the corresponding kinetic relationship. Unfortunately, this form is very complex and is unsuitable for practical use. However, the particular unsoundness of the laboratory experiments with variable C_τ values lies in the technological nonconformity of this regime to industrial conditions. Modern hydrometallurgical undertakings mainly operate on continuous technological schemes, in which the concentrations of the reagents in the equipment are kept constant. If $(C_S - C_\tau)$ and C_τ are constant, in view of the fact that $S = \alpha_1 q^{2/3}$ integration of Eqs. (1) and (2) gives:

For dissolution processes

$$q_\tau^{1/3} = q_o^{1/3} - \frac{a_1 K(C_S - C_\tau)\tau}{3a} = q_o^{1/3} - K_{obs}\,\tau \tag{5}$$

and for reaction processes

$$q_\tau^{1/3} = q_o^{1/3} - \frac{a_1\ a_2 K C_\tau \tau}{3a} = q_o^{1/3} - K_{obs}\tau \tag{6}$$

As known, Eqs. (5) and (6) agree well with experiment and are currently known as "the cube root law". Experimentation with a constant concentration simplifies the diagnosis of the regimes and the determination of the rate constants K. Equations of type (5) and (6) are also more suitable for approximation of the dissolution kinetics in the case of the treatment of materials with complex granulometric and mineralogical composition.

Dividing Eq. (5) or (6) by $q_o^{1/3}$ and bearing in mind the fact that $x_\tau = x_o - 2K_{obs}$ and $x_o = 2K_{obs}\ \tau_o$, we obtain

$$\frac{q_\tau^{1/3}}{q_o^{1/3}} = \omega^{1/3}(\tau, T) = \frac{x_\tau}{x_o} = 1 - \frac{\tau}{\tau_o} = 1 - T$$

or

$$\omega(\tau, T) = \frac{q_\tau}{q_o}\left(\frac{x_\tau}{x_o}\right)^3 = \left(1 - \frac{\tau}{\tau_o}\right)^3 = (1 - T)^3 \tag{7}$$

where $\omega(\tau, T)$ or the "dissolution function" gives the fraction of undissolved material in the charge. The specific form of this function, determined for example analytically by the method set out above or in more simple cases experimentally, has great practical significance, since it is the main working relationship required for calculation of continuous technological processes [7])[8]). These calculations are based on the use of differential function $E(\tau)$ of the distribution of the particles of the charge with respect to the time they spent in the system. In practice the $E(\tau)$ function represents the fraction of particles leaving the n-th reactor of the system and having "ages" between $\tau + d\tau$. For ideal mixing equipment, the operation of which is characterised by insignificant longitudinal agitation, it can be obtained analytically, but in more complex constructions it is determined by a comparatively simple experimental method. The product of the functions $\omega(\tau)$ and $E(\tau)$ represents the differential output of undissolved material, and the integral of this product over the whole range of possible values of τ, i.e., from 0 to τ_o:

$$R_n = \int_0^{\tau_0} \omega(\tau)E(\tau)d\tau$$

characterises the quantitative output of the charge into the leaching residues [9]). Simpler mathematical equations are obtained with the dimensionless argument of time $T = \tau/\tau_o$ and with replacement of the constant ratio τ_c/θ by the quantity b. Here τ represents the time spent by the particles in the reactor or their "age", τ_o is the time for complete dissolution of the particles, and θ is the nominal (average or calculated) time spent by the pulp in the reactor. The final calculated equations have the following form[10]): For a number of reactors in a cascade

$$\left.\begin{aligned}
&1.\ H_1 = 1 - b\int_0^1 (1-T)^3 \exp(-bT)dT \\
&2.\ H_2 = 1 - b^2\int_0^1 (1-T)^3 T \exp(-bT)dT \\
&3.\ H_3 = 1 - \frac{b^3}{2}\int_0^1 (1-T)^3 T^2 \exp(-bT)dT \\
&4.\ H_4 = 1 - \frac{b^4}{6}\int_0^1 (1-T)^3 T^3 \exp(-bT)dT \\
&\quad \cdots\cdots\cdots\cdots\cdots \\
&n.\ H_n = 1 - \frac{b}{(n-1)!}\int_0^1 (1-T)^3 T^{n-1} \exp(-bT)dT
\end{aligned}\right\} \tag{8}$$

where H_n is the fraction of the valuable component passing into solution, obtained in the n-th reactor of the system. If the analytical form of the function $\omega(T)$ is complex, the integrals in Eqs. (8) are solved graphically from its initial (numerical) determinations.

A further practical problem is the choice of the type and the hydrodynamic regime of the reactor. Here, in most cases the requirement to reproduce the rate constants obtained under laboratory conditions is put forward as the main condition. Correctly, this problem is solved on the basis of similarity theory. The corresponding calculations involve a series of methodical limitations, which must be taken into account during experimentation.

As known[8]), the main concepts of similarity theory in mass-exchange processes are expressed by a criterial relationship of the following type:

$$Sh = A + B\,Re^m\,Sc^n\,\Gamma_g^p \Gamma_p^q \ldots \tag{9}$$

or in expanded form

$$\frac{Kl}{D} = A + B\left(\frac{\omega l \rho}{\mu}\right)^m \left(\frac{\mu}{\rho D}\right)^n \Gamma_g^p \cdot \Gamma_p^q \ldots \tag{10}$$

where A, B, m, n, p, and q are constant coefficients determined experimentally; Γ_g is the simplex of geometrical similarity; Γ_p is an additional simplex of physical similarity of the suspension; l is the determining dimension of the system m; ω is the flow rate m/sec; ρ is the density of the solution kg/m³; μ is the dynamic viscosity of the solution Pa · sec. In equipment with linear motion of the flows and freely whirling or attached particles the equivalent diameter of the particles x or the diameter of the channel (apparatus) d_e is taken as the determining dimension. The determining dimension of the rotating disc is its diameters d_m. The schemes of circulation of the flows in reactors with mixers are more complex. For example, direct observations on the rate of motion of fine spheres of naphthalene ($x = 110\mu$, $\rho = 1010$ kg/m³), aluminium ($x = 80$-90μ, $\rho = 2690$ kg/m³), and iron ($x = 80$-90μ, $\rho = 7280$ kg/m³) in a reactor with a turbine-type mixer[11]) showed that the fine particles of suspensions and the elements of the liquid move almost synchronously. Since the rate of slip is low (about 3-4%) and is incommensurable with the free settling rate, this rules out the possibility of normal description of the kinetics of mass exchange on the basis of the dimensions and physical characteristics of the particles themselves. Therefore, the diameter of the mixer d_m (or more accurately the diameter of the surroundings swept by the mixer). Since $\omega = \pi d_m n$, corresponding substitution in Eq. (10) gives:

$$\frac{Kd_m}{D} = A + B\left(\frac{nd_m^2\rho}{\mu}\right)^m\left(\frac{\mu}{\rho D}\right)^n \Gamma_g^p\cdot\Gamma_p^q\ldots \qquad (11)$$

Equations (10) and (11) select one or the other constructional prototype respectively. Essentially they fully exhaust the known types of production equipment. The only exceptions are a few original designs of oscillating, pulsating, and ultrasonic type or models with unorganised agitation of suspensions, in which criterial estimates of the intensity of agitation have not yet been worked out. The characteristics established on such models are not therefore susceptible to objective comparison and are incompatible with industrial planning.

The possible structures of Eqs. (10) and (11) and the values of the experimental coefficients A, B, m, n, p, and q have been investigated and determined many times. Initially the experiments were carried out on samples of readily soluble inorganic salts and, mainly, chlorides, sulphates, and nitrates[19]). More recently it was shown that certain organic substances and, in particular, benzoic and salicylic acid dissolve with approximately equal values for the rate constants K under similar hydrodynamic conditions with an equal motivating force for the diffusion processes (1 mole/100 g H_2O). This remarkable observation evidently reflects the related mechanism of dissolution with similar values for the diffusion coefficient D. The tested organic substances (particularly benzoic acid, table) proved more suitable materials. In particular, they permit the preparation of quite uniform samples of various forms and dimensions by simple and convenient methods such as pressing and casting. The working surface of the samples is easily polished. The solutions, from the variation in the composition of which according to Eq. (1) the observed rate constant K is assessed, are easily analysed by titration of samples against phenolphthalein. Since the solubility of the organic substances C_S is low (e.g. the solubility of benzoic acid at 20°C amounts to only 2.9 kg/m³), the low rate

Table 1: The properties of standard organic substances recommended for the simulation of mass exchange kinetics

Properties	Benzoic acid	Salicylic acid
Formula		
Molecular weight	C_6H_5COOH	$C_6H_4OHCOOH$
Density kg/m³	122.12	138.12
Melting point °C	1266	1443
$pK_{25}{}^{o}$	122	159
Solubility in water at 20°C, g/1000 g H_2O	4.20	2.97
Diffusion coefficient coefficient in water at at 20°C, m²/sec · 10⁹	2.9	2.2
	0.951	0.954

of mass exchange increases the length of the experiments and thereby reduces the possible errors in sampling. The above-mentioned advantages at present make it possible to reject tests with model designs on the original (technological) materials and to regard benzoic acid as the most convenient standard material. Its diffusion coefficients in water are usually calculated by means of the formula of Wilke and Chang[13])

$$D = \frac{1.17\cdot10^{-16}(a\cdot M)^{1/2}T}{\mu V^{0.6}} = \frac{3.26\cdot10^{-16}T}{\mu}\ \mathrm{m^2/sec}$$

where a is a parameter of the association of the molecules of the solution and is equal to 2.6 for water; M is the molecular weight of the solvent (18.016); μ is the dynamic viscosity of the solvent at temperature t, Pa · sec; V is the molecular volume of the dissolving substance and in this case is equal to 122.12/1266 = 0.09646 m³/kmole.

The criterial relationships (10) and (11) have been investigated under various experimental conditions. Here the effect of the hydromechanical characteristics of the various designs have been mostly studied. For example, the rates of diffusion dissolution of rotating discs[8])[14]), packings[12]), freely whirling and fixed spheres in uniform flows[2])[15])[16]), freely whirling spheres and fixed samples in reactors with various types of mixers[17-21]), rotating cylinders[22]), fixed cylinders in rotating vessels[23]), tubes[24]) etc. have been determined. Certain systems, such as the cathodic reduction of $Fe(CN)_6^{3-}$ or the anodic oxidation of $Fe(CN)_6^{4-}$ in a packing of platinised brass spheres[25]) also proved to be fully diffusion processes with mass exchange rate constants approximately equal to the rate constants for dissolution of the spheres of benzoic acid. Conclusions of similar scope were also obtained during comparison of the kinetics results from the cathodic reduction of oxygen[26]) and the cementation rate in the Cu/Zn, Cu/Cd, and Cd/Zn systems[48]) at rotating discs. All these investigations covered the range of Schmidt criteria in the approximate range between 1000 (water at 20°C) and 10⁶ (sugar and glycerine syrups), and this corresponded to various industrial solutions and to suspensions with various physical characteristics. The final conclusions from these investigations, which correspond to Sc = 1000, are shown in fig. 1 (the top group of curves). The following comments can be made.

In an absolutely quiescent liquid (Re = 0) A = 2[27]). However, the unavoidable appearance of concentration-type convection always leads to an increase of Re and to the appearance of the second term in Eq. (9)[12]). Objective treatment of this phenomenon is complex, and the reports by various authors are noticeabl contradictory in the region of low Re values (Re < 20). These features complicate the simulation of industrial installations. Observed small values of the S criterion do not always correspond to low values of K. For instance, in "fluidized-bed" equipment low values for the determining parameter 1 = x secure fairly high specific mass transfer rates.

In this region the coefficient m entering into the similarity equation is small. With decrease in the velocity the Sherwood number approaches 2 asymptotically, and the coefficient m approaches zero. In the range of average Re values of ~500 - 50 000, which corresponds to the transitional hydrodynamic region and to normal laboratory designs with mechanical agitation, the data fro various authors agree well with each other. This applies in particular to investigations by the rotating disc method[c]). With respect to the apparatus the rotating disc method is the simplest, and it is evidently most reliable in its results. Here, in full agreement with theory[28]), the coefficient $m \approx 0.5$. Ther fore, with K = idem the transformation of Eqs. (10) and (11) gives:

$$\omega_n \approx \frac{\omega_m d_{en}}{d_{em}} \qquad (1$$

$$n_n \approx n_m \qquad (1$$

where the subscripts *n* and *m* denote the natural and model parameters. Co sequently, with a moderate intensity of agitation the rates of the flows/or t frequencies of rotation of the stirrers in the natural devices must be appro mately equal to those of the model devices. In constructional respects such a solution is usually unsatisfactory.

High Reynold's numbers (Re > 10⁶) correspond to regimes with a stably de oped turbulence and to apparatus of fairly large dimensions. These conditi are the closest to production conditions, and the expected characteristics a therefore more interesting. In the only work on such a scale, realised wit whirling grains of galena and boric and benzoic acids in a reactor with a turbine-type mixer ($V = 0.25\ m^3$)[17]), the power index n of the Schmidt num was taken as 0.5, which gave m = 0.833. As seen from fig. 1, the results the power index n of the Schmidt number was taken as 0.5, which gave m As seen from fig. 1, the results[17]), were somewhat higher than the data of other investigators.

According to modern ideas about the nature of the boundary diffusion lay the index n should be equal to 0.33[29]), and such a value is indeed used by

majority of investigators. In the paper[21]) possible variants of analogous correlations were analysed, and it was shown that the experimental data on the kinetics of diffusion mass exchange in reactors with mixers correspond more satisfactorily to n = 0.33 and that the appropriate substitution leads to some decrease in the Sh and m values. With allowance for these corrections the data[17]) become quite comparable with the results from the other works. Here the coefficient m can be taken as equal to 0.65.

With a high intensity of agitation (Re > 10⁶) Sh >> 2, and the first term in Eqs. (10) and (11) can then be omitted, this gives:

$$\frac{Kl}{D} = B\left(\frac{\omega l \rho}{\mu}\right)^m \left(\frac{\mu}{\rho D}\right)^n \cdot \Gamma_g^p \cdot \Gamma_p^q \ldots \qquad (14)$$

$$\frac{Kd_m}{D} = B\left(\frac{nd^2_m \rho}{\mu}\right)^m \left(\frac{\mu}{\rho D}\right)^n \cdot \Gamma_g^p \cdot \Gamma_p^q \ldots \qquad (15)$$

If the aim of simulation is to obtain single-valued rate constants $K_n = K_m =$ idem, the conditions of kinetic similarity are more readily obtained with full geometrical similarity in the designs and with identical physical characteristics in the suspensions. Then for example, from Eq. (14) we obtain:

$$\frac{l_n}{l_m} = \left(\frac{Re_n}{Re_m}\right)^m = \left(\frac{\omega_n l_n}{\omega_m l_m}\right)^m$$

$$\omega_m = \omega_m \left(\frac{l_n}{l_m}\right)^{\frac{1-m}{m}}$$

Accordingly, when m = 0.65

$$\omega_n = \omega_m \left(\frac{l_n}{l_m}\right)^{0.54} \qquad (16)$$

Similarly, from Eq. (15) we obtain:

$$n_n = n_m \left(\frac{d_{m\cdot n}}{d_{m\cdot m}}\right)^{\frac{1-2m}{m}}$$

$$n_n = n_m \left(\frac{d_{m\cdot m}}{d_{m\cdot n}}\right)^{0.46} \qquad (17)$$

Further analysis of Eqs. (16) and (17) (with the experimental limitations mentioned above) makes it possible to reach the following conclusions.

For the simulation of the operation of industrial equipment an essential and ficient condition is the determination of two main parameters: For reacrs with a linear flow of pulp, e.g., the reactors of Vishnevskii[30]), ω_m and ; for reactors with mixers, n_m and d_m. Determination of only one of these not satisfactory.

Production equipment with a linear pulp flow must have somewhat higher locities for the suspensions than the models, and industrial designs with ers must be characterised by much lower frequencies of rotation in the ing devices.

Since the characteristics of the suspensions do not enter into the final simi- larity equations, the simulation of equipment can be realised with any liquid, e.g., with water at 20°C. This eliminates the need to determine the physical characteristics of suspensions under working conditions, since the analogous hydrodynamic regime of the natural device can in this case be reproduced by the water regime of the model.

Most of the systems shown in fig.1 were investigated in comparatively nar- row ranges of Reynold's numbers with various forms of the Re, Re_m, and S functions. These facts gave the results a hint of noncomparability. It was n clear how the similarity criteria of mass exchange at a rotating disc ($Re_m = nd^2$ while the rate constants for the dissolution of attached spheres (surfaces) w used to determine the rate of dissolution of whirling spheres in reactors wi mixers, and so forth. The investigations were characterised by models wit different geometry and by experiments with different levels of reliability a scale. The dimensions of the models did not usually exceed the scales of th laboratory equipment.

A comparison of the results of previous investigations, which is given in fig.1, makes it possible to generalise the existing observations. According the point that the different forms of the Reynold's and Sherwood's numbers are quite identical forms which permit objective conversion of one system another can be considered proved. The idea of the existence of a single fu tion, indicating the reliability of the presented partial determinations and possibility of some extrapolation of them, also seems correct. For liquid with Sc = 1000 the correlation curve, which gives the results from previo investigations, can be expressed by the approximate relationship:

$$Sh = 25 + 2.5\,Re^{0.66}$$

which corresponds to the conditions $Re = 1\text{-}10^6$. In a general assessment can be considered that with the experimental limitations mentioned above investigations on simulation can be reduced to only a small number of exp ments on the dissolution of the standard material in the adopted design m In vessels with *mixers* the *most convenient form* of standard sample may a casting in a recess in the bottom of the reactor. Here the conditions of etic similarity of mass exchange are calculated by means of Eqs. (14) an Since the designs of industrial chemical reactors are standardised, for la atory investigations it is necessary to select models with a similar geo profile. This condition is well satisfied by the previously presented 31) sta dard model (fig. 2).

Similarity theory also makes it possible to investigate the effect of an important factor temperature. The corresponding acceleration of diffusi [illegible]

As known the relation between D and μ is given by the Stokes-Einstein equa- tion:

$$D\mu = AT \qquad (18)$$

here A is a constant. Since the diffusion coefficients reflect the individual aracteristics of the substances, it can be expected that the activation energy diffusion for various compounds will also differ. On the other hand, since dimensions of the water molecules are considerably smaller than the dim- ions of the ions, the diffusion of electrolytes can be regarded as a process flow around large and immobile ions and their displacement by more active ater molecules. Since the nature of the latter is almost the same in moder- ely concentrated solutions, the energy of activation must be constant. Here must correspond to the energy of activation of viscous flow of pure water 32). e the numerical values of the diffusion coefficient for various materials extremely varied, it is more convenient to check these hypotheses by the ative temperature variation of D_{rel}, assuming that $D_{293} = 1$. We chose tions of NaOH, H_2SO_4, NaCl, and O_2, for which the viscosity and diffus- coefficient have been investigated over a wide range of temperatures and eement with Stokes law (for OH^- and H^+) is least likely. For dilute solu- the diffusion coefficients were calculated also from the limiting equiva- conductivities of the ions 33). The results from the comparison, in the of normal Arrhenius curves, are shown in fig. 3. The temperature vari- of D_{rel}, obtained from the variation of the viscosity of pure water, is n by the continuous line. The straight lines for the determination of D_{rel} many inorganic compounds, the diffusion characteristics of which are only n in comparatively narrow temperature ranges, agree quite satisfactorily this graph. (These data are not given in fig. 3 on account of the complex- of representation). In a general assessment the second hypothesis about etermining effect of single-valued characteristics of water agrees well the final determinations of D_{rel} and can be used for practical conclusions.

the range of 0-200°C the observed activation energy of diffusion cannot garded as a stable constant. In fact, it varies smoothly from approxim- 18 kJ/mole (4.3 kcal/mole) in processes occurring at 0-50°C (compara- Arrhenius curves with activation energies of 18, 16, and 14 kJ/mole are n the top right corner of fig. 3) to approximately 14 kJ/mole (3.3 kcal/ characteristic of temperatures above 100°C. This conclusion can be ed to all aqueous solutions of inorganic compounds.

will consider to what extent the temperature variations of the diffusion ient D affect the variation in the general rate of diffusion mass exchange. ion of Eqs. (14) and (15) with respect to K for n = 1/3 gives:

$$[illegible]\; l^{a-1}\,\varepsilon^{m-1/3}\mu^{1/3-m}D^{2/3}$$

$$[illegible]\; \rho^{m-1/3}\mu^{1/3-m}D^{2/3}$$

uation of the effect of temperature the first factors in the equations are constant. Therefore, in the general form

$$K = B_{gen}\, \mu^{1/3-m} D^{2/3}$$

and after combination with the Stokes-Einstein equation (18):

$$K = B_{gen}\, T^{1/3-m} D^{1/3+m} \qquad (19$$

Let us take the following practical equations (fig. 1): $Re<10$ (bed and fluidized-bed leaching, $m \approx 0$); $Re = 10\text{-}100$ (mass exchange of a disperse material in the free whirling of particles. $m = \frac{1}{3}$); $Re = 100\text{-}10\,000$ (dissolution a rotating discs and cylinders $m = \frac{1}{2}$); $Re > 10\,000$ (dissolution in reactors with mixers $m = \frac{2}{3}$). Substitution of the adopted values of m in Eq. (19) gives:

$$K_0 = B_{gen}\, T^{1/3} D^{1/3}; \quad K_{1/2} = B_{gen}\, T^{-1/6} D^{5/6}$$

$$K_{1/3} = B_{gen}\, D^{2/3}, \quad K_{2/3} = B_{gen}\, T^{-1/3} D$$

where the subscripts at K denote the adopted values of m.

The form of these functions (in the form of normal Arrhenius curves) is shown in fig. 4. All the curves for K are variable and they all lie below the curve for D_{rel}. The particularly small temperature acceleration with $E \approx 8$k mole (1.9 kcal/mole) is characteristic of diffusion mass exchange occurring in beds and in a fluidized bed. It is highest with an approximate E value of 14 kJ/mole (3.4 kcal/mole) during leaching in reactors with mixers. According to the specified equipment conditions, increase in temperature from, for example, 0 to 100°C (shown by the dotted line) will be accompanied by an acceleration of the mass exchange by 2.4, 4.2, 5.8, and 7.8 times. Consequ tly, technological operations realised with a high degree of turbulence in the medium will be characterised by the highest temperature acceleration.

The presented explanations explain the reasons for the various values of th activation energy observed under various experimental conditions.

The principles of the physicochemical simulation of diffusion reactions an reaction equipment set out above correspond more fully to modern scientifi ideas and better guarantee the search for optimum solutions of production operations. We will now explain the foregoing by the following examples.

In a discussion review describing the kinetics of the dissolution of zinc ox in dilute sulphuric acid (36.41) it was stated that there is a considerable discrepancy in the experimental determinations of the rate constants K and th activation energies E. The reasons for the obvious contradictions were unclear. Systematic treatment of experimental data (dissolution of fixed samp of zinc oxide in a reactor with a mixer[37]), fixed samples in a flow of reag [38]), rotating discs[39,41]), and dispersed material in apparatus with agitatio [40]) in terms of similarity theory (fig. 1, the lower group of curves) shows they all in fact agree satisfactorily with each other. Consequently, the diff ent results from the initial determinations were a simple consequence of the insufficient consideration of the observed hydrodynamic circumstances.

As follows from the experimental data, the dissolution of zinc oxide occurs at rates approximately two orders of magnitude lower than the dissolution of other substances which react fully by diffusion. This indicates the existence of additional chemical retardation. Another argument for the existence of a mixed diffusion-kinetic regime is provided by the increased values of the activation energy and by the character of their variation from 3.0[38]) to kcal/mole[40]) with increase in the intensity of agitation. Here the obvious decrease in the diffusion retardation helped to shift the reaction into the kinetic region. The character of these changes is similar in type to the changes in fully diffusion processes (fig. 4) but differs in its more progressive character. This observation also agrees with the conclusion about the existence of a mixed regime. Complex processes with an even larger shift into the kinetic region [41]) have even lower values of the Sherwood number (fig. 1).

It has been shown that the leaching of zinc calcine in fluidized-bed equipment occurs at much higher rates than in Pachucas or mechanical reactors[43]). The theory of physicochemical similarity makes it possible to compare these designs and to propose a simple method for the testing of models.

According to the literature[43]), fluidized-bed equipment operates with a velocity of 0.168 m/sec in the ascending flow of solution. For a zincite density of 5650 kg/m^3, a solution density of 1280 kg/m^3, and a dynamic viscosity of $2.77 \cdot 10^{-3}$, and a dynamic viscosity of $2.77 \cdot 10^{-3}$ Pa·sec this parameter determines the necessary size of the calcine particles ($0.44 \cdot 10^{-3}$ M). Accordingly, the finer particles are carried into the bed, and the coarser particles remain at the end of the reactor and are slowly eroded.

With a pulp density of 1380 kg/m^3 and a viscosity of $6.25 \cdot 10^{-3}$ Pa·sec[44]) the obtained particle size determines a Reynold's number of 16. According to fig. 1 (the lower graph), this Re value corresponds to a Sh number of 0.83 and to a rate constant in the technological process of $K_{fb} = 0.83 \cdot 0.44^{-4} \cdot 10^{?} \cdot D \approx 1900D$, where D is the diffusion coefficient of sulphuric acid.

A reactor with mechanical agitation has a propellor diameter of 1.3 m and a mixer rotation rate of 0.833 sec^{-1} (50 rpm). These parameters correspond to a modified Reynold's number of 310 000. Accordingly, from fig. 1 we obtain Sh = 78 and the expected rate constant of the technological process $K_{mp} = (78/1.3)D = 60D$ m/sec. Consequently, in its productivity the first variant exceeds the second by $1900/60 \approx 30$ times.

The simulation and comparison of the efficiency of these equipments can be considerably simplified with the choice of benzoic acid as standard material. In both cases it is necessary to select geometrically similar models, the parameters of which are calculated as follows: In the first variant, from the equal linear rate of the outgoing flows; in the second case, according to Eq. (17) also from the equal rate of dissolution of the benzoic acid sample.

For example, the isokinetic and geometrically similar model of a reactor with mechanical agitation having a volume of 0.014 m³ (scale 20:1, d_m = 0.065m, Re_m = 3100) must have a frequency of rotation of 3.32 sec^{-1} (200 rpm) in the mixing device. The technological productivity of the designs is assessed from the observed dissolution rate constants K.

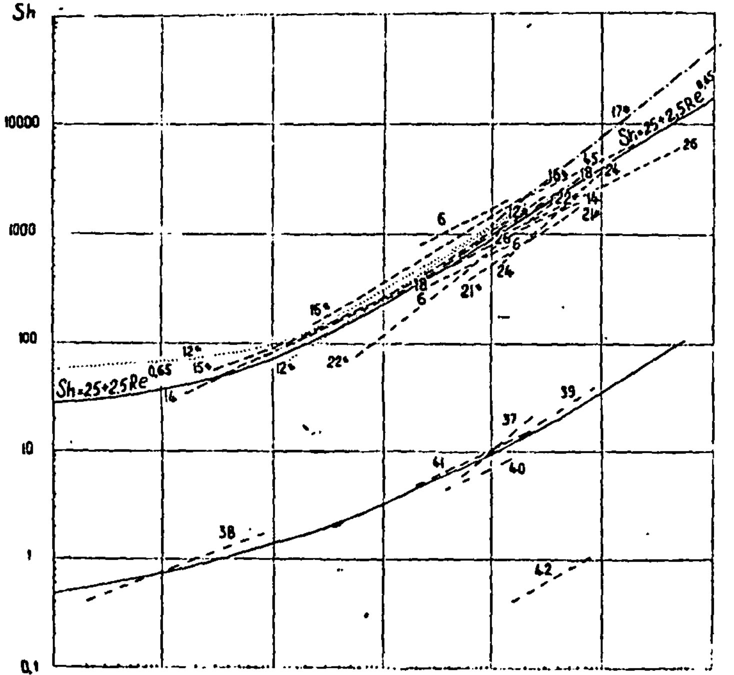

Fig. 1 The effect of the intensity of agitation on the intensity of diffusion exchange. Dissolution conditions: The dotted line represents grains beds and whirling spheres with forced convection, the dash-dot lines represent whirling spheres in reactors with mixers, and the dashed lines represent samples with a constant surface (discs, spheres, flat surfaces, tubes). The figures on the curves are the references: re data are denoted by asterisk.

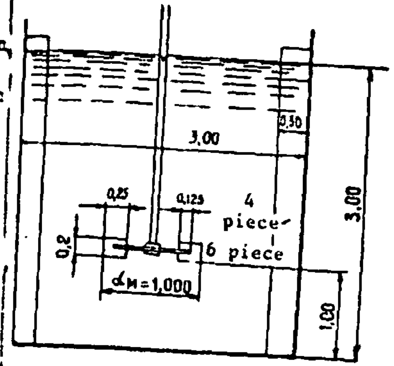

Fig. 2

The profile of the laboratory model (reactor) recommended for hydrometallurgical investigations.

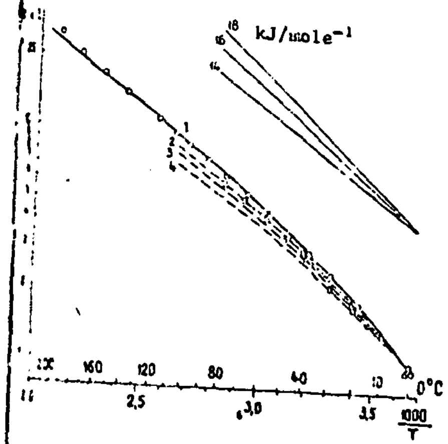

Fig. 3

The relative variation of the diffusion coefficient with temperature. Calculated from the variation of: 1 - the viscosity of pure water; 2 - the limiting equivalent conductivity of a solution of NaCl 3 - NaOH; 4 - H_2SO_4. Viscosities of solution: a)(o) - 9.6%NaOH; b)(Δ) - 10% H_2SO_4; c)(□) - 20% NaCl. x = experimental determinations for O_2 with P_{O_2} = 0.21 atm [34)] [36)]).

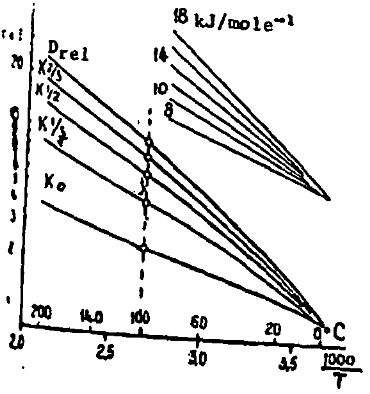

Fig. 4

The relative variation of the diffusion coefficient and rate coefficient of mass exchange with temperature

References

1) V V Dolivo-Dobrovol'skii: Zapiski LGI 1963, 42, (3), 3.
2) A D Pogorelyi et alia: Izv. Vuz. Tsvetnaya Metallurgiya 1960, (2), 54.
3) A D Pogorely et alia: Izv. Vuz. Tsvetnaya Metallurgiya 1962, (4), 60.
4) N M Demido: Izv. Vuz. Tsvetnaya Metallurgiya 1965, (1), 52.
5) N M Demido and A D Pogorelyi: Izv. Vuz. Tsvetnaya Metallurgiya 1966, (6), 41.
6) I A Kakovskii and Yu M Potashnikov: Kinetics of dissolution processes. Metallurgiya, Moscow 1975.
7) Ya M Braines: Introduction to the theory and calculation of chemical and petrochemical reactors. Khimiya, Moscow 1976.
8) P G Romankov and M I Kurochkina: Hydromechanical processes in chemical technology. Khimiya, Leningrad 1974.
9) R V Mattern et alia: A I Ch E J 1957, 3, (4), 497.
10) G N Dobrokhotov: Hydrometallurgical processes and equipment. RIO LGI Leningrad 1976.
11) D M Levins and J R Glastonbury: Trans. Instn. Chem. Engrs. 1972, 50, (1), 32.
12) G A Aksel'rud and A D Molchanov: Dissolution of solids. Khimiya, Moscow 1977.
13) C R Wilke and P Chang: A I Ch. E J., 1955, 1, (2), 264.
14) M Litt and G Serad: Chem. Engng Sci., 1964, 19, (11), 867.
15) G Tripathy et alia: Indian J Technology 1971, 9, (8), 285.
16) R L Stenberger and R E Treybal: A I Ch E J., 1960, 6, (2), 227.
17) J J Barker and R E Treybal: A I Ch E J., 1960, 6, (2), 289.
18) R K Jha and M Raja Rao: Indian Chem. Engng., 1969, 11, (4), 143.
19) A I Johnson and C J Huang: A I Ch E J., 1956, 2, (3), 412.
20) J Marangozis and A I Johnson: Canad. J. Chem. Engng., 1961, 39, (4), 1
21) J Marangozis and A I Johnson: Canad. J. Chem. Engng., 1962, 40, (6), 1
22) G Tripathy et alia: India J. Technology 1971, 9, (7), 237.
23) J A R Bennett and J B Lewis: A I Ch E J., 1958, 4, 418.
24) P Harriot and R M Hamilton: Chem. Engng. Sci 1965, 20, (12), 1073.
25) A J Karabelas and T H Wegner: Hanratty. Chem. Engng. Sci 1971, 26, (10), 1581.
26) I Cornet et alia: Chem. Engng., 1969, IX, (231), 222.
27) I Langmuir: Phys. Rev., 1918, 12, 368.
28) Yu V Pleskov and V Yu Filinovskii: Rotating disc electrode. Nauka, Moscow 1972.
29) A M Rozen et alia: Modern state of mass transfer. In: J Astartit, Mas transfer in chemical reactions. Khimiya, Leningrad 1971, p. 169.
30). N E Vishnevskii et alia: Machines and apparatus with airtight electr drive. Mashinostroenie, Leningrad 1977.
31) F Holland and F Chapman: Chemical reactors and mixers for liqui phase processes. Khimiya, Moscow 1974.
32) S Glasstone et alia: Theory of absolute reaction rates. IL, Moscow 1
33) Ya I Gerasimov et alia: Course of physical chemistry. Khimiya, M 1966.
34) Z Zembura and H Kolny: Poszniki Chemii Annates Societatis Chem

Polonorum 1969, 41, (9), 1629
35) R E Davis et alia: Electrochemica Acta 1967, 12, (3), 287.
36) A D Pogorelyi et alia: Izv. Vuz. Tsvetnaya Metallurgiya 1973, (5), 21.
37) A N Krestovnikov and E A Davydovskaya: Zh. Fiz. Khim., 1936, 8, (1), 77.
38) A N Vol'skii and E M Sergievskaya: Izv. Vuz. Tsvetnaya Metallurgiya 1958, (1). 76.
39) I A Vishnyakov et alia: Izv. Vuz. Tsvetnaya Metallurgiya 1972, (3), 56.
40) I A Vishnyakov et alia: Izv. Vuz. Tsvetnaya Metallurgiya 1972, (4), 22.
41) I A Kakovskii and B D Khalezov: Izv. Vuz. Tsvetnaya Metallurgiya 1977, (2), 26.
42) G N Dobrokhotov and E V Maiorova: Tsvetnye Metally 1963, (8), 31.
43) F I Barotitskaya and I V Sandulova: Metallurgy of nonferrous metals. Metallurgiya, Moscow 1969, (29), p.123.
44) A D Mayants and F I Barotitskaya: Metallurgy of non-ferrous metals. Metallurgiya, Moscow 1959, (15), p. 511.
45) E C Lee et alia: Hydrometallurgy 1978, 3, (1), 7, RZh Metallurgiya 1978, 8G285.

UDC 669.334.22

Pilot-plant trials on the hydrometallurgical treatment of chalcopyrite concentrates

I S Naboichenko, V I Neustroev, and I F Khudyakov (Urals Polytechnical
stitute - Department of the Metallurgy of Heavy Nonferrous Metals)

The preliminary treatment of chalcopyrite concentrates with acidified solu-
ons of copper sulphate at 170-180°C makes it possible to transfer a consider-
le part of the iron selectively into solution and to obtain an enriched sul-
de residue, from which the copper is leached at a much higher rate than
om the initial concentrate[1-3]. In the pilot-plant trials we used copper con-
ntrates obtained during the concentration of ores from the Madneul'sk
posit containing in the first test, wt.%: 28.8(22.7)Cu, including 1.34(1.07)
the form of secondary sulphides; 0.54(1.66)Zn, 29.5(29.6)Fe, 33.5(34.7)S,
4(11.34) others, including 2.02(8.6)SiO_2. The main minerals of the con-
ntrates were chalcopyrite and pyrite, and in concretions with them there
re small amounts of bornite, covellite, sphalerite, and silica.

The investigations were carried out on the previously described apparatus[4];
activation of the concentrate and hydrogen deposition of the copper we
ed 25 dm³ vertical titanium autoclaves, and leaching was carried out in a
dm³ horizontal autoclave. The development of the process was judged
m the composition of periodically taken samples and from the chemical
phase composition of the solid products.

Preliminary experiments on the activation of the concentrates confirmed
data from laboratory investigations[3]) to the effect that at temperatures

below 160°C and with a molar ratio of copper in the solution and K<1.1 in the concentrate the characteristics of the process deteriorate and the adequate length of the operation is greater than 1h. With increase in the acid consumption rate or with increase in K>1.3 the degree of opening of the chalcopyrite increases, but here the deposition of copper from the s ution deteriorates (table 1). We recommended the following activation parameters: 170-180°C, K = 1.2-1.3, $[H_2SO_4]^\circ$ = 10-20 g/dm^3, liquid-solid ra (4-5):1, τ = 0.8-1.0h. Under these conditions the chalcopyrite is opened up to the extent of 73-80%, and the degree of deposition of copper from the sol tions amounts to more than 98%. The filtration rate on a pressure filter [P = 0.118-0.137 MPa (1.2-1.4 atm), belting or cloth, thickness of cake lay 8-12mm] amounted to 17-25 dm^3/m^2·min and the moisture content of the ca was 11-14%. Since the cake was directed for leaching, it was industrially unsuitable. During the washing operation back dissolution of copper was observed, and this indicated that the obtained residue had high activity. The main phases in the activated product were chalcosite (more accurate, digenite) and undisclosed chalcopyrite, and interlayers of bornite and also individual grains of covellite were encountered. The pyrite grains remained practically unchanged.

During autoclave oxidative leaching (160-170°C, P_{O_2} = 0.382-0.784 MPa 4-8 atm) in the first 10-15 min intense heat removal was secured by the delivery of water to the tubular condensers of the apparatus. Subsequently the process occurred in a stabilized temperature regime. Effective mass exchange in the autoclave (K_c = 2.1 M Na_2SO_3/dm^3 · atm · h and liquidation of stagnant zones) was achieved by the installation of three-blade stirrers with a diameter of 90mm, α = 45°. The pulp density and the acid consumption rate were selected with due regard to the composition of the activated product, the degree of oxidation of sulphur during its leaching, and possible complete conversion of iron into a precipitate.

The characteristics of the leaching, realized in a closed cycle, with respec to the copper-containing solution with activation of the concentrate are give in table 2. The obtained results confirmed the laboratory data to the effect that at 170°C and P_{O_2} = 0.392-0.784 MPa (4-7 atm) in 2-3h more than 95-97% of the copper and not more than 2-3% of the iron are extracted into solution and 93-96% of the sulphur is oxidized.

The sulphuric acid leaching regime was preferred from the standpoint of the closed nature of the leaching-copper deposition operations with respect to the solution; however, preliminary experiments did not give positive results; after 3h at 102°C and P_{O_2} = 1.86 MPa (19 atm) about 90% of the copper had been extracted into solution and almost 50% of the iron passed into solution. Deposits of a sulphur-containing sulphide product were observed on the internal components of the autoclave. The search for the optimum co ditions for sulphuric acid leaching will be the subject of separate investigations.

The settling rate of the pulp (γ = 1.16 g/cm^3) from the oxidative leaching

Table 1: Characteristics of the activation of chalcopyrite concentrates at 180°C

Trial conditions				Content in obtained solution g/dm^3			Composition of cake %				Copper precipitated from solution %	Extracted into solution %		Degree of activation %
K	$[H_2SO_4]^\circ$ g/dm^3	τ h	l:s	Cu	Fe	H_2SO_4	Cu	Cu primary sulphides	Fe	S		Fe	S	
	Test 1													
1.20	20.0	0.75	5.3	2.0	29.2	69.9	56.6	6.2	8.63	26.2	97.0	90.0	24.9	77.5
1.20	10.0	0.75	3.7	1.1	54.0	75.3	52.2	7.5	10.5	26.9	99.8	67.2	22.9	72.7
1.23	10.0	0.75	4.1	2.4	61.3	80.8	53.4	6.8	9.1	25.1	97.5	85.7	27.9	75.6
1.28	10.0	0.75	3.9	-	-	-	55.4	5.7	8.2	-	-	69.0	-	79.0
1.44	20.0	0.75	4.1	9.3	59.5	74.0	61.3	6.1	6.9	26.3	91.5	82.2	24.7	78.0
1.40	11.5	1.00	5.0	0.8	39.4	35.7	62.9	4.2	7.9	25.6	99.1	66.8	22.2	84.0
	Test 2													
1.1	12.2	0.75	5.0	0.2	28.0	42.8	44.9	-	14.3	29.1	99.6	47.3	34.3	70.3
1.1	12.2	0.75	5.0	0.5	28.0	42.3	43.8	-	15.0	28.6	99.0	47.3	20.0	70.1
1.3	9.8	1.00	5.0	0.4	32.0	53.5	56.4	-	7.9	24.8	99.5	54.0	49.4	80.0
1.3	15.1	1.00	5.0	1.0	30.0	72.7	47.6	-	14.6	29.3	98.3	50.7	31.0	75.0
1.3	18.9	1.00	4.0	0.03	40.0	70.5	55.1	-	9.5	24.7	99.96	54.1	53.2	80.0

Table 2: Characteristics of the leaching of the activated product

Trial conditions								Composition of sol. g/dm^3			Yield of cake %	Composition of cake %			Extraction into solution %		
Composition of activated product %			t °C	P_{O_2} MPa	$[H_2SO_4]_0$ g/dm^3	l:s	τ h										
Cu	Fe	S						Cu	Fe	H_2SO_4		Cu	Fe	S	Cu	Fe	S
43.2	14.6	28.5	170	0.392	9.8	7.7	2.0	54.0	0.5	21.1	29.1	6.4	36.6	10.3	96.1	2.6	95.6
50.2	11.8	26.9	170	0.392	9.8	6.0	2.0	71.0	0.55	2.8	27.0	6.2	42.0	8.6	95.8	3.1	95.8
47.6	14.5	29.3	170	0.392	15.0	11.0	3.0	40.0	0.1	20.0	25.9	7.4	36.2	7.6	94.7	0.8	93.3
56.4	7.9	24.8	170	0.784	9.8	10.0	3.0	56.3	0.2	2.7	22.7	7.0	34.1	5.6	97.2	2.5	94.9
53.6	9.6	25.5	170	1.784	22.0	7.5	3.0	70.0	0.3	23.0	-	5.1	51.7	4.5	97.9	2.2	96.9
63.0	9.6	25.6	102	1.86	76.0	10.4	3.0	46.0	3.85	7.5	-	20.8	15.8	50.3	89.5	42.0	-

Table 3: Composition of flotation products and distribution of metals nd sulphur

Product	Yield % on weight of cake	Composition %			Extraction %		
		Copper	Iron	Sulphur	Copper	Iron	Sulphur
Concentrate	30.4-30.5	16.7-18.4	24.4-24.6	30.5-33.4	7.2-82.4	20.0-20.1	88.3-90.6
Intermediate product 1	8.6-13.1	1.8- 3.4	34.0-36.1	1.6-1.8	.5- 4.3	8.2-11.5	1.9- 2.2
Intermediate product 2	3.7- 5.7	6.5- 8.8	33.8-36.5	6.1-8.5	.6- 7.7	3.6- 5.3	2.0- 4.6
Tailings	51.7-52.8	1.3- 1.4	45.5-47.0	1.0-1.2	0.6-10.8	64.5-66.4	4.9- 5.0

amounted to 4.76 m/h, which corresponds to a specific thickening surface of 7.6 $m^2 \cdot h/t$; the settling was considerably accelerated by the addition of pol acrylamide. The filtration rate of the thickened pulp (vacuum 700mm Hg, belting, cake layer thickness 5±0.5mm) was determined as 4-4.2 dm^3/min. Thus, the thickening and filterability of the obtained pulps are satisfactory.

According to the data from mineral-petrographic and Xray crystallographic analyses, the main phases in the cake are hydrated iron oxides of the $Fe_2O_3 \cdot nH_2O$ type, pyrite, undisclosed copper sulphides (chalcopyrite, covellite), and single grains of sphalerite. The yield of the purified solution amounted to 90-94% of the initial volume, and the average composition of the solution was as follows, g/dm^3: 56-72Cu, 0.3-0.5Fe (including not more than 16-2 Fe^{2+}), 5-23 H_2SO_4. Part of the solution was used in the activation of the cha copyrite concentrate, and the remaining solution was passed to copper deposition.

The characteristics of the autoclave deposition of copper were refined on depleted batch of solution containing g/dm^3: 67.5Cu, 1.0Fe, 13.8H_2SO_4. Th experiments were carried out at 140-150°C with P_{H_2} = 2.74 MPa (28 atm) w 0.4 g/dm^3 of an anticoating additive. After 60 min the residual copper conte amounted to 6-8 g/dm^3, which corresponded to 90-92% deposition. To impro the copper deposition characteristics it is advisable to have not more than 45-55 g/dm^3 of Cu and 5-8 g/dm^3 of H_2SO_4 in the initial solution, and this c increase the direct extraction of copper and simplify the aggressive situati in the autoclave. After dehydration and heating in a stream of hydrogen (55 we obtained a powder which conformed to the standard GOST 4968-75 in co position: bulk density 1.85 g/cm^3; specific surface area 0.072 m^2/g; conte of fractions, μ%: 140, 0.34; 74, 0.24; 44, 2.44; -44, 96.98.

The decoppered solution was combined with the solutions from activation of the concentrate, and the obtained mixture containing (g/dm^3) 2.48Cu, 22. and 21.8Fe^{2+} was passed on for cementation with pieces of transformer iro After 10-15 min more than 99% of the copper had been deposited, and the l solution contained 18-30 mg/dm^3 Cu and up to 28.5-29.0 g/dm^3 Fe. The hig consumption rate of the precipitant (calculated 2.5-2.8) was due to the significant acidity of the initial solutions. In the cemented deposit the copper content was 82-87%, and the iron content was 2-3%.

The phase composition of the cake from neutral leaching predetermined t expediency of separating the remaining sulphides by flotation. Data on flotation of the cake containing 6.4%Cu, 42.2%Fe, 10.3%S (rough flotation: pH = KBX 15 g/t, T-66 9 g/t, τ = 5 min; control flotation: KBX 5 g/t, T-66 9 g/t, τ = 5 min; recleaning of tailings: τ = 5 min, soda 500 g/t), are given in table 3. In the light of the composition of the concentrate and the increasin content of gold it is expedient to direct it to the converting cycle. Thus, th flotation treatment of the cake made it possible to reduce the losses of cop to 0.2-0.6 and to resolve rationally the question of the extraction of precio metals.

Conclusions

1. A scheme is proposed for the hydrometallurgical treatment of chalcopy-ite concentrates (fig.), in which more than 99% of the copper is extracted nto the powder (~91.5%) and into a secondary concentrate. It is proposed o neutralise the acid iron-containing solutions which form and into which 0% of the iron and 90% of the sulphur pass, depending on the specific con-itions, with lime or rich manganese ores or to use them for the leaching copper from local wastes. The remainder of the iron and sulphur is dis-ributed between the waste hydrate cake (41 and 0.5%) and the secondary con-entrate (10.1 and 8.8%).

2. The technology developed forms the basis of semi-industrial trials.

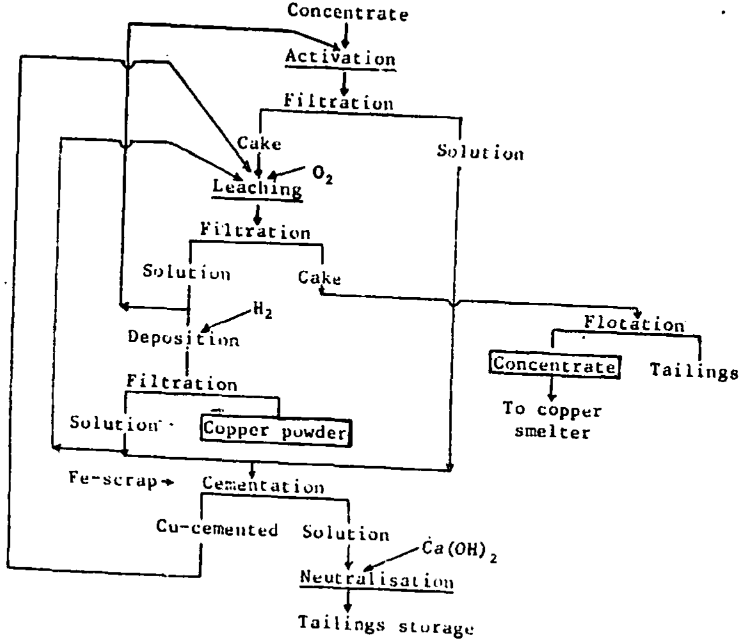

gram of the hydrometallurgical treatment of chalcopyrite concentrates.

ferences

S S Naboichenko et alia: Investigation of the autoclave sulphuric acid treatment of complex copper-containing concentrates. Papers at first all-union conference on hydrometallurgy. Nauka, Moscow 1974, p. 18.
U S Patent No. 3816105, Published 11.6.1974.
S S Naboichenko et alia: Tsvetnye Metally 1976, (6), 20.

4) S S Naboichenko et alia: Production of copper powder by the autoclave method. Ts IIN Tsvetnaya Metallurgiya 1976, (24), p.21.

UDC 669.

Problem of the complex treatment of bauxites of the Northern Urals

S I Kuznetsov (Urals Polytechnical Institute - Department of the Metallurgy of Light Metals)

Our country has a vigorous aluminium industry. In recent years some disproportion has arisen in the aluminium industry; the construction and extension of alumina plants and factories have been determined by the construction of electrolysis plants. Most of the alumina production in the USSR is concentrated at the Urals and Bogoslovsk aluminium works, since the Urals have large reserves of high-grade bauxites. The production of alumina in the Ur has been extended through the construction and introduction of a new BAZ-2 alumina plant. With the opening of this plant the disproportion will be eliminated. However, according to the tenth Five-Year plant, the production of aluminium must be increased by 1.2-1.3 times. Consequently, new facilities for the production of aluminium and alumina are necessary.

The aluminium plants of the Urals are already coming up against difficulties due to the deterioration in the quality of the raw material. There have been periods of deterioration in the grade of the aluminium, increase in the alkali consumption, and increase in the corrosion of the steel equipment in the alumina plants. The factories and institutes have found some ways of overcoming these difficulties. With increase in the depth of the bauxite deposits, however, the content of harmful impurities will increase. Whereas the ores from the northern Urals now contain a little more than 1% of sulphide sulphur and 3% of carbonates (as CO_2), according to data provided by the Gipronikel' Institute the sulphur content in 1990 will increase to 2.1%, and the carbonate content (as CO_2) will increase to 3.8%. In some mines, e.g., in the 14-14 and Cheremukhovo, the sulphur content will increase to 1.3 and the carbonate content (as CO_2) to 4.4%. It is therefore necessary to solve the problem of the struggle with the harmful impurities in the raw material. It is quite clear that on account of the harmful impurities it is inexpedient to replace the Ba process by a more expensive method. There remains the conditioning of the bauxites - the purification of the raw material by one or the other method of concentration.

In recent years the Urals Polytechnical Institute has been successfully engaged in the development of techniques for the concentration of the bauxites the northern Urals. At the Department of Metallurgy of Light Metals the technology of the flotation of bauxites of the northern Urals in order to separate the sulphides and carbonates from them is being studied under the guidance of assistant professor F F Fedyaev. The technique was first investigated

under laboratory conditions and then
al scale at a pilot plant at the Uni
ested. The carbonate content varied
lphur content varied between 0.8 a
nd carbonates was realised by flota
productive capacity of 40 kg/h. The
the first stage pyrite flotation was
e concentrate. The cell product was
t the sulphides. Copper sulphate,
ere used as flotation reagents. The
tation in order to remove the carbo
age involved three primary and two
collector, and sodium silicate was
ing minerals and to activate the flo

During semi-industrial trials a pyrit
5% Al_2O_3 was obtained. The carbon
18.5% Al_2O_3. The pyrite concentra
phuric acid or as a sulphidiser in th
concentrate can be used in the prod
nd and in the production of alumin

The main flotation product is the cell
bulk of the harmful impurities. In t
industrial conditions the content of
tent of sulphur was not higher than
nted to 85-89%. Better technical c
processing of this product to alumi
ite. The extraction of alumina was
3-4% lower. The use of flotation of
make it possible to extend the raw
n of high-sulphur and high-carbona
or the bauxites of the Ivdel' deposi
bauxites cannot be used for the pr
tration.

technology for the concentration o
At the present time the Mekhanol
esium Institute have developed the
que for the production of alumina f
tration and have demonstrated the
ieve that a concentration plant sh
tur'insk in order to provide the c
being constructed.

onstruction of a concentration pla
ks are already experiencing enor
from bauxites with increased ca
ation has been found by F F Fedy

1976 v.17 N2

METALLURGY

HEAVY NON-FERROUS METALS

STUDY AND INDUSTRIAL ASSIMILATION OF HYDROMETALLURGICAL PROCESSING FOR ZINC CAKE

UDC 669.73: 542.61

L. S. Getskin, V. A. Grebenyuk, A. S. Yaroslavtsev, A. U. Usenov, and Yu. M. Mironov

Zinc cake, into which up to 25% Zn, 30% Cd, and 50-60% Cu from the zinc concentrates and practically all the Pb, Au, and Ag pass, is the main by-product in electrolytic zinc production.

The following zinc cake composition (%) is typical of a new zinc plant: 18-22 Zn, 1.4-1.8 Cu, 0.2-0.24 Cd, 4-4.5 Pb, 20-24 Fe, 0.05-0.06 As, 0.04-0.06 Sb, 8-12 SiO_2.

The substantial zinc content of the cake is due to ferrite formation in the calcining process. According to rational analysis, 53% (rel.) of the 20.2% Zn present in the cake is in the form of zinc ferrite, 15% (rel.) is sulfide, 10% (rel.) is relatively insoluble aluminosilicate, and the remainder is oxide and sulfate.

Various methods are used to process zinc cake: sintering and smelting in the lead plant charge, smelting in vertical electrically heated retorts and producer furnaces, the Waelz process, etc.

The choice of a method of processing depends mainly upon the composition of the zinc cake and the actual working conditions at the enterprise. Until recently some 20% of the zinc cake in the world has been stockpiled, waiting for a more effective processing technology to be developed.

Hydrometallurgical methods have not been introduced, mainly because of difficulties in precipitating the iron and in separating the iron residue from the solution with the minimum loss of valuable constituents.

Research at the beginning of the fifties by B. A. Ryazanov [1] showed that crystalline deposits of jarosite and a binary iron and potassium sulfate with the composition $KFe(OH)_6[SO_4]_2$ practically insoluble in sulfuric acid solutions were formed when ferric sulfate reacted with caustic potash at pH 1.4. The conditions which ensure more complete deposition of iron as jarosite were ascertained later [2]: temperature 85-95° C and pH ≈ 1.5. It was also shown that sodium [3], rubidium, and ammonium ions might be present in addition to potassium ions.

Zinc cake from Soviet plants has a remarkably high lead (3-6%), precious and rare metal content, and the various processing methods described in the papers and patents[1] do not give a high level of extraction of all the valuable constituents from zinc cake of this composition.

Research workers and plant staff[2] have therefore developed a method of zinc cake processing giving a high level of lead, gold, and silver extraction along with zinc, copper, and cadmium. Calculations by the State Non-Ferrous Metals Research Institute have shown that the capital outlay in processing zinc cake by this method is 30% lower than in the Waelz process, the period of recoupment is almost halved, adjusted expenditure is reduced by 15%, and the profit increases by 20%. In addition, the extent of material utilization is increased. The new method is recommended primarily for the processing of zinc cake containing high concentrations of lead, gold, and silver.

The scheme provides for single-stage leaching of zinc calcine, which yields solutions of higher quality and releases some of the equipment for the processing of zinc cake.

Since the limiting stage in the cake leaching process is the speed of ferrite decomposition by the sulfuric acid solution, a study was made of the effect of leaching time upon the completeness of dissolution of zinc, copper, and cadmium, ferrites and zinc sulfide. It was established that at 90°C 97-98% of the cadmium ferrite dissolves in 5-6 hr of leaching; the corresponding figures for copper ferrite, zinc ferrite, and zinc sulfide are 95-97%, 90-94%, and 70-80%.

The speed of zinc sulfide dissolution is almost linearly dependent upon leaching time. The sulfuric acid concentration does not affect the completeness of sulfide decomposition.

---

[1] Norwegian Pat. No. 108047, 1965; Australian Pat. No. 401724, 1965.

[2] V. M. Piskunov, B. K. Plastinkin, P. I. Aidarova, B. A. Sysoev, and A. N. Zhaksybaev participated in the work.

The identical kinetic relationships for zinc sulfide dissolution and trivalent iron reduction in the solution indicate that these processes are interlinked, i.e., zinc sulfide dissolves due to its reaction with ferrisulfate. The extent of transfer of zinc from sulfide into solution increases from 70 to 90% when leaching temperature rises from 90 to 100°C. When the sulfide sulfur content of the zinc calcine increases from 0.3 to 0.6% and there is a corresponding increase from 1 to 1.8-2.5% in the zinc cake sulfide sulfur content, the bivalent iron concentration in the solutions after cake leaching rises from 1-3 to 6-8 g/liter; this causes difficulties in the subsequent processing of the solutions. Roasting the zinc concentrates until the calcine sulfide sulfur content does not exceed 0.2-0.3% is therefore a vital factor, giving a minimum Fe(II) content in the solutions after high-temperature zinc cake leaching.

Percentage extraction into the zinc-bearing solutions after high-temperature cake leaching is as follows: 94 Zn, 93 Cu, 90 As, 65 Ni, 93 Cd, 79 Fe, 16 Sb, and 60 Co.

The high-temperature leaching solutions contain up to 25 g/liter Fe (mainly in trivalent form) and considerable amounts of arsenic and antimony; their purification is therefore one of the principal operations in the scheme.

Deposition of iron and impurities in a special routine without using a neutralizer is the distinguishing feature of the method; this yields an iron deposit which is practically free from lead and precious metals. The iron deposition time depends upon the initial concentration of higher oxide iron ion in the solution, and usually amounts to 3-4 h. During this period practically all the Fe(III) and up to 90% As and Sb are deposited to form an iron cake which contains only 1-1.5% Zn.

After precipitation of the iron cake, the solution is purified hydrolytically to oxidize and then precipitate the lower oxide ion in the form of hydrosulfates and goethite. According to [6], the speed of Fe(II) oxidation by atmospheric oxygen rises with an increase in solution pH from 2-3 to 4-5, copper ions acting as catalysts in the process.[3] Under production conditions, the solutions are purified until the residual Fe content is 50 mg/liter or less.

The solutions from zinc cake processing are practically indistinguishable from the calcine cycle solutions as regards As, Sb, Mn, F, Cl, and other elements present, except for the nickel and cobalt content; the concentrations of these metals rise to 5-7 mg/liter. With this nickel and cobalt content, these impurities can be removed in the usual way with some increase in the reagent consumption; this causes no difficulty.

Zinc plant practice has shown that the introduction of a hydrometallurgical method of zinc cake processing has helped to remove K, Na, F, Cl, Pb, and other impurities coprecipitated with iron from the production solutions. Thus the solution fluorine content became < 10 mg/liter, the lead content < 0.2 mg/liter, and the chlorine content < 50 mg/liter. Thus the hydrometallurgical processing of zinc cake ensured the removal of a number of undesirable impurities from the zinc solutions.

According to industrial tests, the new hydrometallurgical method of zinc cake processing gives the following percentage extractions from zinc concentrates: 96-97 Zn and Cd into ingot metal, 90 Cu into copper cake, and 94-97 Pb, Au, and Ag into lead residues (cake).

The jarosite process [7] used, for example, at Nordenheim and Kokkolo extracted 92-93% Zn from the concentrates, and the jarosite residues, which were dumped, contained 8-9% Zn as well as up to 30% of the Pb, Au, and Ag present in the zinc concentrates.

The principal advantages of the hydrometallurgical method of zinc cake processing are:

a high degree of utilization of zinc-bearing material;

94-97% extraction of lead and precious metals into lead residues (cake);

production of iron residues which contain no impurities introduced by a neutralizer, so that they can be used for iron extraction.

REFERENCES

1. B. A. Ryazanov, Zh. Organ. Khim., No. 9, 1477, 1954.
2. G. Steintveit, Erzmetall, 23, 532-539, 1970.
3. M. A. Orekhov, Tsvetnye Metally, No. 11, 11-13, 1974.
4. Mike Mealey, Eng. Min. J., 1, 82-84, 1973.
5. C. J. High and R. W. Pickering, AIME World Symposium of Mining and Metallurgy of Lead and Zinc, 11, 423-448, 1970.
6. L. S. Getskin and E. V. Margulis, Byull. Tsentr. Nauchno-Issled. Inst. Tsvet. Met., No. 6, 23, 1955.
7. T. L. Huggare, S. Fugleberg, and J. Rastas, World Mining, 27, No. 2, 36-42, 1974.

---

[3] Editor's Note: this is confirmed by many years' practical experience in cobalt shops.

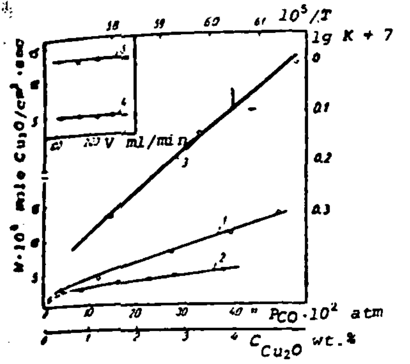

Fig.2 *The concentration dependence of the rate of reduction of cuprous oxide at 1350°C: 1 - with 3.7% Cu_2O; 2 - with $P_{CO} = 19.5\cdot10^{-2}$ atm; 3 - temperature dependence of the reaction rate constant; 4 and 5 - the process rate as a function of the intensity of the blast with the following pressures of the reducing agent: (4) $12.5\cdot10^{-2}$; (5) $50\cdot10^{-2}$ atm.*

Since we know the values of P_{CO} and P_{CO_2} in the reaction zone, by calculating the equilibrium constant (K_e) we can obtain the concentration of cuprous oxide at the interface (C) and also its variation for various contents of the reducing agent in the blast. With regard to the foregoing (with constant $C_0 = 0.017$), we determine the number of times by which the rate of reaction (1) increases with increase of P_{CO} from $4\cdot10^{-2}$ to $50\cdot10^{-2}$ atm. With the adopted CO pressures P_{CO_2} amounts to $0.6\cdot10^{-3}$ and $3.9\cdot10^{-3}$ atm respectively. At 1350°C the K_e value calculated from published data [6]) is 407. Substituting the obtained values in the equation

$$a_{Cu_2O} = \frac{P_{CO_2}}{P_{CO}K_1}$$

and assuming that the activity coefficient for Cu_2O is equal to unity, we find that $C \approx 2\cdot10^{-6}$ in the first case and $C \approx 2\cdot10^{-6}$ in the second. Neglecting these values in Eq.(4), we can conclude that the rate of mass transfer of cuprous oxide to the interface under the adopted conditions only depends on the volume concentration of the oxide:

$$W = \beta \frac{\rho}{M} C_o$$

In other words, in the case of diffusion control the rate of reaction (1) should be practically independent of the partial pressure of the reducing agent and should be determined wholly by the initial concentration of Cu_2O in the slag. However, experiment gives the opposite behaviour; the W values increase by more than six times with variation of P_{CO} from $4\cdot10^{-2}$ to $50\cdot10^{-2}$ atm (line 1, fig.2). Thus, as follows from the foregoing, mass transfer of cuprous oxide from the volume to the interface does not retard the reaction; in view of the fact that diffusion limitation in the gas phase is absent we come to the conclusion that the limiting stage in our case is the kinetic stage.

Sov. Non-Fe
1978 v.6 N 2

Since reaction (1) is far from equilibrium under our conditions, by neglecting the rate of the reverse reaction we write the following equation for W:

$$W = K(Cu_2O)^{n_{Cu_2O}}\ P_{CO}^{n_{CO}} \qquad (5)$$

where K is the rate constant of the process. The concentration of cuprous oxide in Eq.(5) is not expressed in volume units (mole/cm³) but in practically proportional values (for the investigated conditions), i.e., in weight percentages. The apparent reaction order, determined from the experimental data, is fractional: $n_{Cu_2O} = 0.6$, $n_{CO} = 0.85$. This can be explained [7]) if it is supposed that the reaction takes place through the stage of adsorption of CO on the surface of the melt. The fractional order obtained in the calculations then arises by virtue of the fact that the fact that the volume concentrations and not the surface concentrations are substituted in the kinetic equations.

We obtain the rate constants of the process for each temperature from Eq.(5), using the obtained values of the reaction orders:

$$K = \frac{W}{(Cu_2O)^{0.6}P_{CO}^{0.85}}$$

Plotting a graph for the relation between log K and 1/T (fig.2), we then obtained the apparent activation energy of the process, which amounted to 172kJ/mole (41kcal/mole). Thus, the kinetic equation for the reduction of cuprous oxide by carbon monoxide can be written in the following form:

$$W = 1.32\cdot10^{-2}\exp(-20600/T)(Cu_2O)^{0.6}P_{CO}^{0.85}$$

Thus, indirect reduction of the metal from the slag by a gaseous reducing agent can take place under control close to kinetic.

References

1) S L Kiperman: Introduction to the kinetics of heterogeneous catalytic reaction. Nauka 1964.
2) Yu G Medvedevskikh et alia: Proceedings of Symposium on Metallurgy and Physical Metallurgy (14-18 May 1968). Nauka, Moscow 1971, p.58.
3) B A Kukhtin et alia: Izv. Vuz. Tsvetnaya Metallurgiya 1971, (2).
4) T M Makhmadiyarov et alia: Izv. Akad. Nauk SSSR Metally 1974, (4), 34.
5) A B Lipin: Izv. Vuz. Tsvetnaya Metallurgiya 1961, (6).
6) Thermodynamic characteristics of inorganic materials. Handbook, Atomizdat, Moscow 1965.
7) G M Panchenko et alia: Chemical Kinetics and catalysis. Khimiya, Moscow 1974, p.408.

UDC 661.183+546.4

Sorption of the ions of elements of Group 2 of the periodic system from MeF_6-HF($NH_4F\cdot HF$, NH_4F)-H_2O solutions by the carboxylic cation-exchange resin KB-4P-2

L I Andrianova, V S Pakholkov and V P Ganyaev (Urals Polytechnical Institute. Department of the Metallurgy of Rare Metals)

Summary

The sorption of cations of group 2 of the periodic system and, for comparison, of copper (II), manganese (II), cobalt, and nickel by the weakly acidic carboxylic ion-exchange resin KB-4P-2 was investigated as a function of its salt form and of the concentration of HF, NH_4F, and $NH_4F\cdot HF$ in the initial solutions. On the basis of the obtained experimental data and of IR spectroscopy it was shown that copper and mercury form complexes with the carboxyl groups of the resin during sorption.

The difference in the behaviour of the ions of heavy metals and beryllium during sorption was used for the separation and purification of beryllium from impurities in solutions of $(NH_4)_2BeF_4$ by means of the KB-4P-2 resin in the NH_4^+ form.

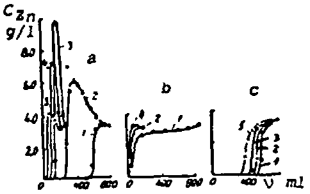

Fig.1 The output curves for the sorption of zinc from 0.1N solution of ZnF_2 containing HF 9a,b) and NH_4F (c) by the KB-4P-2 resin in the NH_4^+ (a,c) and H^+ (b) forms. Concentration of HF (NH_4F) mole/l: 1 - 0.0; 2 - 0.1; 3 - 0.3; 4 - 0.5; 6 - 1.0.

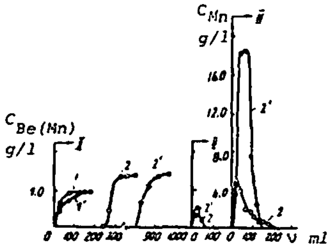

Fig.3 Separation of beryllium (1) and manganese (II) (2) ions in a 0.1M BeF_2 + 0.05N MnF_2 + 0.2M NH_4F + H_2O solution by KU-2 x 8 (curves 1 and 2) and KB-4P-2 (curves 1' and 2') resins in the NH_4^+ form. Solutions: I - Initial; II - H_2O; III - 1N HCl.

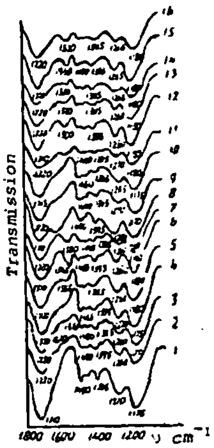

Fig.2 The infra-red spectra of the resin KB-4P-2 in the H^+ form before (1) and after sorption of copper (2,3), zinc (4,5), cadmium (6,7), mercury (8), beryllium (9,10), manganese (11,12), cobalt (13,14), and nickel (15,16) ions from 0.1N MeF_2 (2,4,6, 8,9,11,13,15) and 0.1N MeF_2 + 0.1N NH_4F (3,5,7,10,12,14,16) solutions.

UDC 669.2

Phase transformations in Moa Laterite ore during heating of the aqueous pulp for leaching

S I Sobol', E I Bogoslovskaya Nad V A Isaev (State Scientific-Research Institute of Nonferrous Metals (Ginstsvetmet)
Moscow Mining Institute

Summary

The dehydration of iron hydroxides in water at temperatures up to 250°C under the appropriate pressure is characterised by the same phase transformations and takes place at the same temperatures as during heating of an air-dry sample but is distinguished by high reversibility. Dehydration is accompanied by decomposition of the hydroxides, which increases the number of particles of solid in the volume of the pulp. This leads to a sharp increase in its viscosity.

The formation of maghemite from the iron hydroxides was not observed when they were heated rapidly. The final samples only contained the natural mineral.

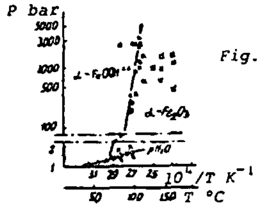

Fig.1 The Fe_2O_3-H_2O system, according to K Wefers. The region of growth of goethite (Δ) and hematite (x); o - direction of reaction undetermined.

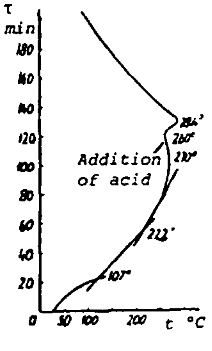

Fig.3 Section of the heating diagram for the aqueous pulp of MoA laterite ore in a laboratory autoclave with subsequent addition of sulphuric acid to leach the nickel and cobalt.

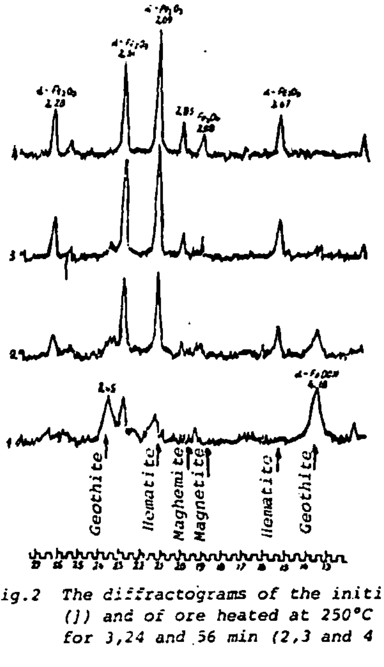

Fig.2 The diffractograms of the initial MoA laterite ore (1) and of ore heated at 250°C in the aqueous pulp for 3,24 and 56 min (2,3 and 4 respectively).

STUDY OF IRON OXIDATION BY OXYGEN IN ZINC HYDROMETALLURGY

UDC 542.943:546.722:669.536

A. G. Pus'ko, O. A. Khan, and L. S. Gusar

Intensification and optimization of oxidation of bivalent iron ions by gaseous oxygen in zinc sulfate solutions is becoming particularly important in connection with the introduction of hydrometallurgical processing for zinc cakes.

An attempt is made in the present work to give a quantitative assessment of the general laws governing the process of oxidation of increased iron ion contents by gaseous oxygen during purification of sulfate solutions in the hydrometallurgical production of zinc. A method of mathmematical planning of extremal experiments was used in the investigations [1]. Steps were taken in the course of the investigations aimed at stabilizing oxygen mass transfer and excluding the complex relationship between process speec and time.

Preliminary experiments established that altering the initial concentration of bivalent iron ions in the 5-25 g/liter range made little contribution to the speed of the process; the iron oxidation process was therefore studied at a constant initial concentration of bivalent iron ions of 10 g/liter.

Four parameters were selected as independent variables: pH, temperature, and the zinc and copper concentration in the solution (see Table).

A constant hydrogen ion concentration was maintained in the solutions studied by additional titration with alkaline reagents. It was established that the type of neutralizer did not affect the speed of the iron ion oxidation process (various alkalis, zincates, and zinc oxide were tested). The output function was the degree of iron oxidation in three hours. A 2^4 type orthogonal plan was implemented in the course of the experiments [1]. Checking the experimental findings for reproducibility by Cochran's test led to the conclusion that the variance was uniform:

$$G_{\text{calc}} = 0{,}822 < G_{\text{tabl}} = 0{,}967.$$

Calculating the regression coefficients and the t-test for a 2.5% level of significance yielded a regression relationship for speed:

$$Y = 74{,}7 - 1{,}3X_2 + 8{,}97X_3 + 28{,}95X_4 + 0{,}96X_2X_3 - 1{,}18X_2X_4 - 3{,}58X_1^2 - 1{,}33X_2^2 - 6{,}17X_3^2 - 4{,}53X_4^2.$$

The equation adequately describes the process in the range studied, since $F_{\text{tabl.}0.025} = 14.25 > F_{\text{calc}} = 5.1$. Processing the relationship on a digital computer using the method of steepest ascent with restrictions [2] revealed the presence of an oxidation speed peak with the following coordiantes:

$$X_1 = 0{,}75\ \text{g/l},\quad X_2 = 128\ \text{g/l},\quad X_3 = 75{,}5°\text{C}\ \text{and}\ X_4 = 4{,}67.$$

The curve of the multifactorial relationship of oxidation process speed to the parameters studied was plotted from the computation results (see Figure).

Experimental checking on the ascending curve and at the peak showed that the results obtained coincided completely with the results of evaluation on the digital computer.

Magnitudes and Levels of Variation of Basic Parameters

Level	C_{Cu}, g/lit	C_{Zn}, g/lit	t, °C	pH
	X_1	X_2	X_3	X_4
Upper	1	140	80	3.5
Lower	0.5	100	60	2.5
Basic	0.75	120	70	3.0
Range of variation	0.25	20	10	0.5

Analysis of the regression equation shows that among the parameters selected the hydrogen ion concentration has a decisive effect upon the speed of iron oxidation by gaseous oxygen; this accords with the published data. The presence of quadratic terms indicates nonlinearity in the effect of all the process parameters. It was established at the same time that the speed of the oxidation process approaches zero at pH = 2.72 and t = 50°C. It cannot be regarded as pure chance that the specific statistical solution pH values at which the maximum and minimum (i.e., zero) speeds of oxidation are are achieved practically coincided with the results of the Pourbaix diagram for the start of hydrolysis reactions:

$$Fe^{+3} + H_2O \rightleftarrows FeOH^{+2} + H^+, \quad pH = 2{,}43;$$
$$Fe^{+3} + 2H_2O \rightleftarrows Fe(OH)_2^+ + 2H^+, \quad pH = 4{,}69.$$

Oxidation of iron at minimum supersaturation in terms of ferri-ion at pH = 2.72 leads to precipitation of a coarse crystalline hydrogoethite residue with a solubility product $L_S = 4.4 \times 10^{-}$ [3]. Here the equilibrium ferri-ion concentration at which the solid phase begins to form is assessed at 1.8×10^{-12} moles/liter. Raising the pH to 4.67 and the temperature to 75.5°C leads to preciptation of amorphous finely dispersed hydrogoethite with $L_S = 1 \times 10^{-36}$, *for which the equilibrium ferri-ion concentration* is 0.66×10^{-12} moles/liter. However, compared with the coarse crystalline residue for which $L_S = 4.4 \times 10^{-44}$ the equilibrium concentration of ferri-ion at pH = 4.67 is 2.2×10^{-20} moles/liter, which is 10^8 times lower than the actual concentration. In other words, oxidation of iron at elevated pH values creates conditions for substantial supersaturation in terms of ferri-ion, which gives precipitation of a more finely dispersed residue. This conclusion accords with published data on the solubility of iron hydroxide of various particle sizes [3].

Industrial testing of rapid oxidation of iron by oxygen in purification of solutions in hydrometallurgical processing of zinc cakes completely confirmed the optimum conditions found from the regression relationship for oxidation speed. The All Union Non-Ferrous Metallurgy Research Institute has issued appropriate recommendations to the zinc plants for intensifying the process of bivalent iron oxidation by oxygen.

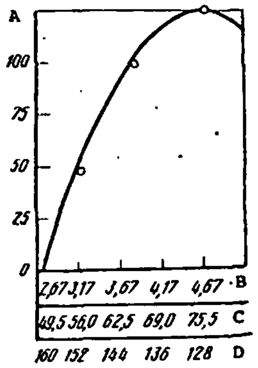

Multifactorial relationship of speed of bivalent iron oxidation by gaseous oxygen: A - nominal speed of process (% in 3 hr); B - solution pH; C - temperature °C; D - zinc ion concentration, g/l.

REFERENCES

1. V. V. Nalimov and N. A. Chernova, Statistical Methods of Planning Extremal Experiments, Moscow, Nauka, 1965, 340 pages, illustrated.
2. V. V. Kafarov, Cybernetic Methods in Chemistry and Chemical Technology, Moscow, Khimiya, 1968, 380 pp., ill.
3. D. Langmuir and D. Whittemore, Symp. Amer. Chem. Sol. Hayston, Fext., 1970, pp. 209-234.

FLOTATION SEPARATION OF COPPER AND NICKEL IONS FROM NGMK SEWAGE

UDC 622.765.5

L. D. Skrylev and F. A. Vorisov

The possibility was shown experimentally of effecting an almost complete (97.5--99.2%) flotation separation of copper and nickel ions from sewage of copper-electrolysis shops in the Noril'sk Mining-Metallurgical Combine [NGMK].

The tests were conducted on a laboratory flotation unit by passing, through a solution, air which was dispersed by porous material. The sewage under test contained 327.2 mg/l Cu, 81.8 mg/l Ni at a pH of 2.3 An aqueous solution of potassium abietate was used as the collector copper and nickel ions.

As a result of the tests, it was possible to establish the optimum flotation conditions: pH ∿ 10, collector consumption about 50 kg per t of separated metals (about 20 g/m³), and a 10 minute flotation time.

Increasing the sewage temperature from 20 to 70°C has no marked effect on the flotation separation process for copper and nickel ions.

Hydrometallurgy, 5 (1980) 207—212
© Elsevier Scientific Publishing Company, Amsterdam — Printed in The Netherlands

A STUDY OF THE LEACHING OF GOLD AND SILVER BY ACIDOTHIOUREATION

C.K. CHEN, T.N. LUNG and C.C. WAN*

Mining Research and Service Organisation, Taipei (Taiwan)

(Received February 1st, 1979; accepted June 27th, 1979)

ABSTRACT

Chen, C.K., Lung, T.N. and Wan, C.C., 1980. A study of the leaching of gold and silver by acidothioureation. *Hydrometallurgy*, 5: 207—212.

The method of thiourea leaching for the extraction of gold and silver from ore in acidic medium was studied. The effect of various amounts of oxidant was also investigated. It was found using a rotating disk experiment that when the leaching solution contained 1.0% thiourea, 0.5% sulfuric acid and 0.1% ferric ions, the rate of gold and silver dissolution was over 10 times faster than in a solution containing 0.5% sodium cyanide and 0.05% calcium oxide.

Preliminary studies of leaching gold and silver from actual thiourea solution were also encouraging.

INTRODUCTION

Gold is traditionally extracted from its ore by cyanidation. However the process is handicapped by its slow rate, being susceptible to interference by other metal ions and the poisonous nature of cyanide compounds. With appropriate oxidants, Preisler [1] found that thiourea can dissolve gold effectively in acidic solution and could thus be a potential substitute for cyanide leaching solution. Its overall reaction is

$$Au + 2\,CS(NH_2)_2 \rightarrow Au[CS(NH_2)_2]_2^+ + e \qquad (1)$$

The charged complex is positive in contrast with the negatively charged gold complexes formed in most other systems.

The choice of oxidant and acid was investigated by many workers [2—5]. Generally, it was recognized that the ferric ion can best speed up the reaction and as for the acid, sulfuric acid is more effective than nitric or hydrochloric acids. Furthermore it was also accepted [2, 6, 7] that the dissolution of gold by acidothioureation was much faster than by cyanidation. Dutrizac and MacDonald [11] wrote an excellent review on the ferric ion as a leaching

---

*C.C. Wan is at Tsing Hua University in Taiwan and serves as a consultant for MRA SO.

medium but relatively little information directly deals with gold or silver.

Most of the published results have so far concentrated on the dissolution of gold only. The dissolution of silver along with the gold is actually of great industrial importance as it is usually a very valuable by-product of many gold mines. It is the object of this research to study the simultaneous dissolution of gold and silver by acidothioureation.

EXPERIMENTAL PROCEDURE

(1) Rotating disk experiment

A pure gold (99.9%) or silver (99.9%) disk (1.8 cm diameter) was rotated by a precision speed motor (Heildoph Co.) to study its dissolution rate.

For every experiment, a 200 ml solution was prepared from reagent grade thiourea, ferric sulfate and sulfuric acid. The metal content was measured by an atomic absorption method (Zeiss FMD 3) and the thiourea was titrated with standard iodine solution according to Gupta's method [10].

(2) Ground ore concentrate leaching test

Copper concentrate from Chin-Kua-Shia Mine in Taiwan, which contains 50 ppm gold, 250 ppm silver and 6.02% copper was first washed with 5% sulfuric acid solution to remove soluble impurities. The ore was then immersed in prepared leaching solution and shaken to measure the actual dissolution of gold and silver from the ore.

All experiments were carried out at room temperature.

RESULTS AND DISCUSSION

(1) Rotating disk

The dissolution of gold and silver under various ferric ion concentrations are summarized in Figs. 1 and 2. If the dissolution rate is defined as the average dissolution rate for the first 20 min of reaction time, then Figs. 1 and 2 can be condensed to Fig. 3. It is obvious that the dissolution rate of both gold and silver increase with the increase in ferric ion concentration. The increase rate is most pronounced at low concentrations of ferric ions. This is probably because the dissolution is dependent on the diffusion of thiourea and ferric ion to the disk. At low ferric ion concentration, the reaction is controlled by the mass transfer of ferric ions. Therefore the dissolution rate is almost proportional to the concentration of ferric ions. When the concentration of ferric ions is fairly high, the process becomes controlled by the transfer of thiourea. Hence the mere increase of ferric ions will not affect the dissolution rate significantly.

The result is also consistent with Levich's [8] theory on the rotating disk system according to Fig. 4. It is known that the dissolution rate J of a rotating disk is governed by

$$J = 0.62\, D^{2/3}\, \nu^{-1/6}\, \omega^{1/2}\, C_0 \qquad (2)$$

where C_0 is the bulk concentration of the active ion, ω is the rotation speed and D is the diffusion coefficient of the active ion. When the system is controlled by the ferric ion as in our case, the active ion is the ferric ion.

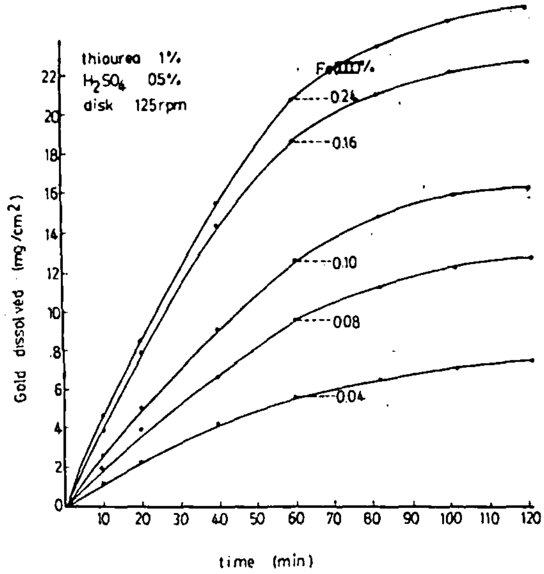

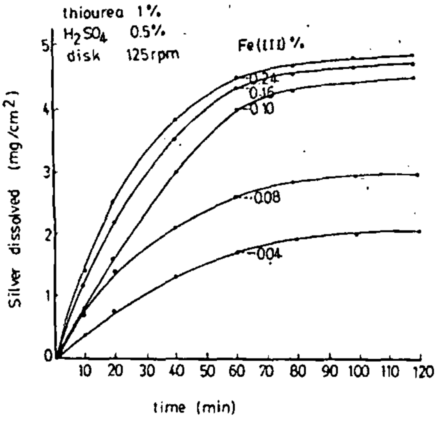

Fig. 1. Dissolution of rotating gold disk in thiourea solution with different ferric ion concentration.

Fig. 2. Dissolution of rotating silver disk in thiourea solution with different ferric ion concentration.

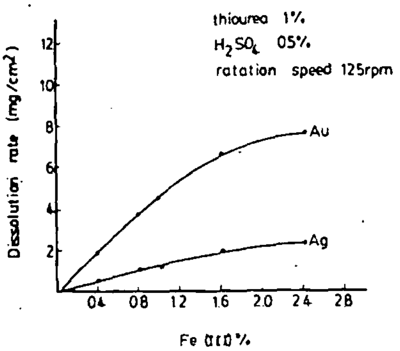

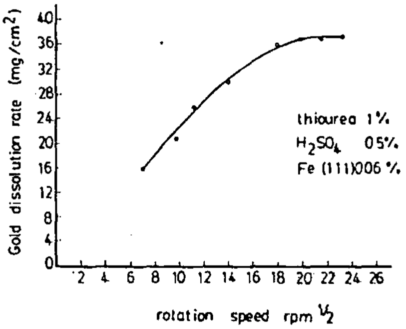

Fig. 3. Average dissolution rate of rotating gold and silver disks versus ferric ion concentration.

Fig. 4. Effect of rotation speed of disk on gold dissolution.

It is apparent when the fluid is in the laminar flow region, that the dissolution rate is proportional to the square root of rotation speed as predicted by Eqn. (2). But when the rotation speed exceeds 327 rpm, (i.e. $\omega^{1/2} = 18.1$), the results deviate from eqn. (2), since the fluid becomes turbulent. Calculated from

$$Re = \gamma^2 \omega / \nu$$

where γ is the radius of the disk, the Reynolds number (Re) is 2×10^5 for 327 rpm. Since Riddiford [9] found that the critical Reynolds number of a rotating disk in aqueous solution was around 10^4—10^5, our results seem reasonable.

Given $\nu = 0.092$ cm^2 sec^{-1}, $\omega = 125$ radians sec^{-1}, $C_0 = 1.0$ g l^{-1} of ferric ion and the dissolution rate J equal to 4.34×10^3 mg cm^{-2} sec^{-1}, the diffusion coefficient of ferric ion was calculated to be 1.8×10^{-7} cm^2 sec^{-1}, which is much smaller than the diffusion coefficient of most ions being usually in the 10^{-5}—10^{-6} cm^2 sec^{-1} range. Hence this may suggest that the system is not completely controlled by the diffusion of ferric ions and may also be kinetically influenced.

Figure 5 shows the dissolution of gold and silver in cyanide solution for comparison. The dissolution rate for gold and silver was 3.54×10^{-4} and 1.29×10^{-4} mg cm^{-2} sec^{-1}, respectively. In comparison, when the leaching solution contains 1% thiourea, 0.5% sulfuric acid and 0.1% ferric ion, the gold dissolution rate is 12.2 times faster than in the cyanide solution and the silver dissolution rate is 10.8 times faster.

(2) Ground ore leaching

A comparison study of the leaching effect of acidothioureation and

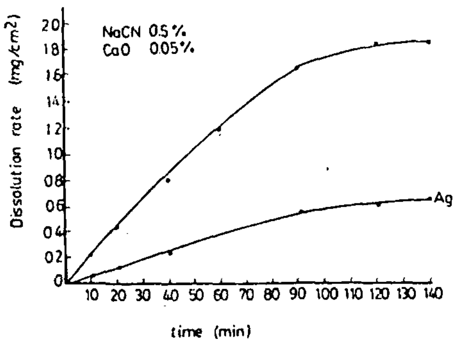

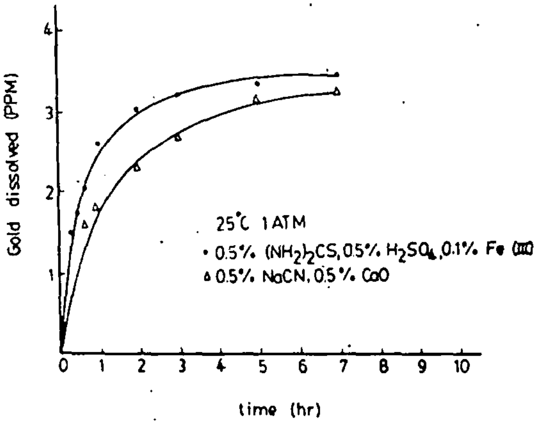

Fig. 5. Dissolution of gold or silver in cyanide solution by rotating disk method (125 rpm).

Fig. 6. Extraction of gold from ground ore by acidothioureation and cyanidation.

cyanidation of actual ground ore supplied by the Taiwan Mining Corp. is summarized in Figs. 6, 7 and 8. From Figs. 7 and 8, it is noted that the dissolution of gold and silver is somewhat faster by thiourea than by cyanide. Since copper is usually leached out simultaneously as an undesirable side reaction, the dissolution rate of copper is also an important criterion of the feasibility of acidothioureation. Figure 8 shows that the dissolution of copper by acidic thiourea solution is much less than that by cyanide solution, which is obviously an additional advantage of the acidothioureation process.

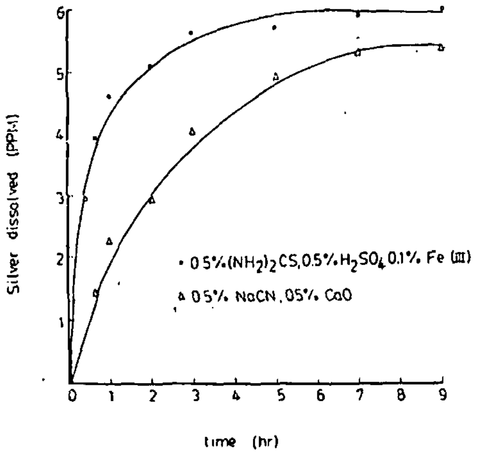

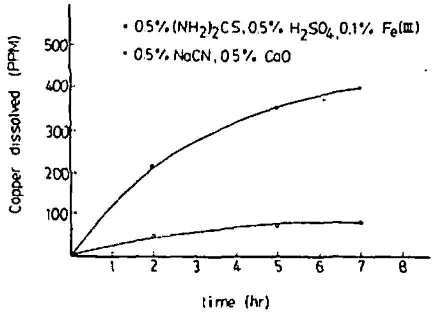

Fig. 7. Extraction of silver from ground ore by acidothioureation and cyanidation.

Fig. 8. Dissolution of copper from ground ore by acidothioureation and cyanidation.

CONCLUSIONS

From the experimental results it can be concluded that the future adoption of acidothioureation to replace traditional cyanidation method looks very promising. The dissolution of both gold and silver in suitable thiourea medium is over ten times faster than in the cyanide solution. Also the dissolution of copper by thiourea is in contrast much less than that by cyanide, which makes thiourea an ideal leaching agent for the extraction of gold and silver.

The dissolution reaction is mainly mass transfer controlled by the diffusion of ferric ions at low ferric ion concentration.

ACKNOWLEDGEMENT

The authors are indebted to the Taiwan Mining Corporation for their financial assistance and the supply of ground ore for testing.

REFERENCES

1 Preisker, P.W. and Berger, L., J. Am. Chem. Soc., 69 (1974) 322.
2 Groenewald, T., J. Appl. Electrochem., 5 (1975) 71.
3 Groenewald, T., Hydrometallurgy, 1 (1976) 277.
4 Plaskin, I.N. and Kozhukhova, M.A., Sb. Nauchn Tr., Inst. Tsevt., Metal., (1960) 33.
5 Songina, O.A., Ospanov, Kh.K., Muldagalieva, I.Kh. and Salnikova, S.D., Izv, Akad. Nauk. Kaz. SSSR. Ser. Khim (1971) 17.
6 Groenewald, T. and Jones, B.M., Anal. Chem., 43 (1971) 1968.
7 Habashi, F., Bulletin 59, Montana College of Mineral Science and Tech, April, 1967.
8 Levich, V.G., Physicochemical Hydrodynamics, Prentice Hall, 1973.
9 Kiddiford, A.C., Advanced Electrochemistry and Electrochemical Engineering, Interscience, 1966, Vol. 4, p. 47.
10 Gupta, P.C., Z. Analyst. Chem. Bd., 196 (1963) 412.
11 Dutrizac, J.E. and MacDonald, R.J.C., Minerals Sci. Engng., 6 (1974) 59.

In-Situ Leaching of Nonferrous Metals

Donald H. Davidson

In-situ leaching (ISL) of minerals has the potential of opening up resources which currently are uneconomical to mine by conventional methods with less disturbance to the local environment. The basic principle involves the recovery of metal values by transporting fluids through rock, as contrasted with mining and processing rock by conventional mining. This type of process is best suited for minerals that are deep-lying, lower grade and water saturated, with high flow conductivity and mineral contact with water..

Significant progress has been made over the past decade in the development of ISL technology for recovery of uranium and copper. Specific activities over this time period include:

- Commercialization of uranium production in south Texas.[1]
- Pilot operations for uranium in Wyoming and Colorado.[1]
- Kennecott's development project for copper sulfide leaching in Arizona.[2]
- Occidental Minerals development of copper oxide leaching in Arizona.[3]

The purpose of these remarks is to review technical and economic aspects of the ISL process and briefly discuss three of the key engineering tasks: selection of metal concentrations, oxygen injection (uranium and sulfide operations), and well pattern design considerations.

An ISL operation consists of surface and sub-surface facilities (fig. 1). Summarizing the major activities:

- Chemicals required to dissolve and maintain metals in solution are first processed through the surface facility.
- A set of injection wells is used to force the solvent into the pores or fractures of the rock by using a pressure in excess of the hydrostatic pressure in the deposit.
- Solvent travels through the rock and reacts with the solid mineral, transferring the metal value to the liquid phase.
- A set of production wells is used to create a low pressure sump where the metal enriched solution can be collected for transport to the surface.
- The produced solutions are processed for both metal recovery and solution make-up for an additional trip through the pores in the rock.

Successful implementation of these five activities requires an integration of mineral geology, and oil field and extractive mineral technologies. Although specific technical aspects of ISL can vary widely, uranium versus copper leaching, or wellfield operations ranging from massive rubblization of rock to water flooding deposits with natural permeability, most ISL systems have in common the following (fig. 2):

- The majority of the capital investment is tied up in the surface facility, where technology is somewhat standard and controlled, unlike the sub-surface component.
- A number of sub-surface mining strategies are likely to achieve a given production capacity.
- Limited or no prior industrial experience exists.

Therefore, it is important to develop mining strategies which minimize risk, and this requires understanding the interactions of key technical and economic parameters.

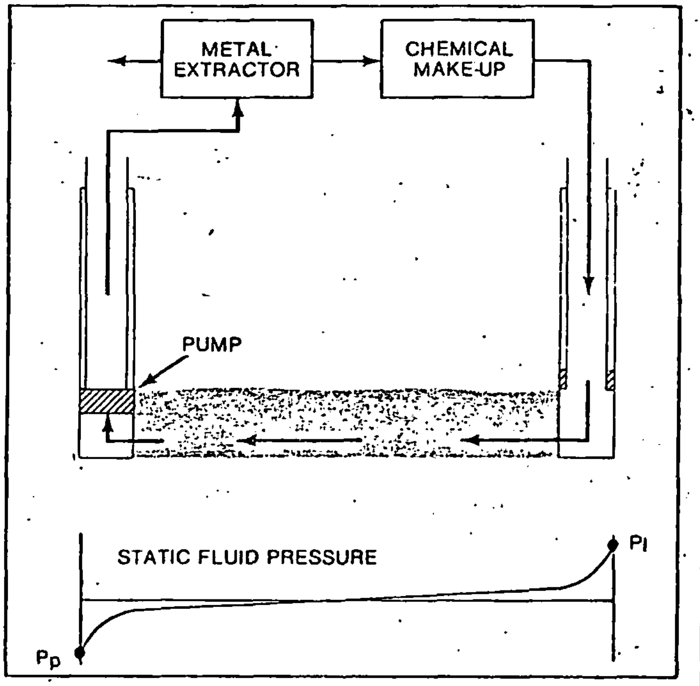

Fig. 1. Overview of in situ leaching

Solution volumes, flow rates determine performance

The economic performance of an in-situ operation is governed by the following:

- The volume of solution processed through the system.
- Rates of fluid injection and production from wells.
- The rate of mineral solubilization in the liquid phase.
- The volume of rock swept by the fluid.

Relating the above to site-specific capital investments and operating costs requires gathering, evaluating, and integrating technical data on deposit and solvent characteristics.

- Deposit characterization
  - —Depth
  - —Ore grade
  - —Total contained metal
  - —Ore thickness
  - —Flow conductivity (permeability)
  - —Void space in rock (porosity)
  - —Mineral distribution in rock
  - —Natural groundwater flow.
- Solvent characterization
  - —Composition
  - —Rate of metal solubilization
  - —Interaction with gangue minerals
  - —Impact on rock permeability
  - —Impact on materials of construction used in wells and surface facilities
  - —Trace metal solubilization and impact on surface processing and environmental requirements.

A final design requires specification of the following sub-surface parameters: effluent metal concentration, number of wells, well spacing and frequency of future well pattern additions.

For a given operation, it is likely that several combinations of the above, involving trade-offs of initial capital versus cash flow, will provide an acceptable economic performance.

Metal concentrations impact process economics

As would be expected, the level of the metal concentration in the produced solutions has a major impact on the economics of ISL. The four major capital investments that are impacted by the level of produced metal concentration are the surface facility, wells, pumps, and solution inventory for well pattern start-up.

Surface facility investment. This has two components, one related to total production capacity (tons per year), the other to the total rate (gpm) at which solution is circulated through the system. At a fixed level of production capacity, the gpm related investment declines as metal concentration increases, as smaller volumes of solution can be processed to obtain a fixed tonnage per year of metal. The product of gpm and metal concentration is proportional to tons per year production capacity. At a fixed level of production capacity, the volume of solution continually being handled (total gpm) decreases as the concentration of metal in solution increases. Thus, from the standpoint of surface facility capital, it is desirable to achieve a high effluent metal concentration.

Wells. Total well costs are related to individual well costs, which increase with depth, and the number of wells. Since the individual production capacity of a well is proportional to the product of flow rate and metal concentration in solution, it is desirable to have a high metal concentration to achieve a high level of individual well capacity, which in turn keeps the number of wells at a minimum level.

Pumps. Pump investments usually increase with both the volume of solution processed and the pressure head against which the fluid must be pumped. High effluent metal concentration results in low solution volumes, while the pressure head is proportional to both well depth and rock permeability. If the rock is tight, high pressure differentials in the wells must be used to move fluids between wells.

BASIS 250,000 LB/YEAR 0.1% ORE-GRADE,
50% RECOVERY, 30% POROSITY, 50 GPM PER WELL
PLANNED WELL LIFE 1 YEAR

50 PPM URANIUM	300 PPM URANIUM
• 1250 GPM FLOW	• 210 GPM FLOW
• 10 MILLION GALLONS FLUID IN ROCK PORES BETWEEN WELLS	• 10 MILLION GALLONS FLUID IN ROCK PORES BETWEEN WELLS
• 5 1/2 DAYS TO DISPLACE PORE FLUID	• 33 DAYS TO DISPLACE PORE FLUID
+ 1 1/2% OF OPERATING WELL LIFE START-UP TIME NEGATIVE CASH FLOW	– 9% OF OPERATING WELL LIFE START-UP TIME NEGATIVE CASH FLOW
– 25 WELL UNITS	+ 4 WELL UNITS
– MOVE FLUID AROUND 66 TIMES	+ MOVE FLUID AROUND 11 TIMES

Table 1. Opposing effects in systems handling 50 and 300 ppm uranium concentrations

Start-up. The pores of the rock in the well pattern are initially filled with water. Each time a well pattern operation is initiated the solubilized metal is diluted by the pore fluid, requiring at least one exchange of the volume of water in a well pattern (one pore-volume) to attain full production capacity. Prior to this time, operating costs are likely to exceed revenues resulting in a negative cash flow. Since the time required to achieve this one-pore volume displacement increases as the total flow rate of the system is reduced, the negative cash flow of start-up will be higher at increased levels of effluent metal concentration, as the product of total gpm and metal concentration is a constant for a given production capacity.

Table 2. Design parameters affecting major capital investments for in situ leaching

- SURFACE FACILITIES
  - PRODUCTION CAPACITY
  - TOTAL PLANT GPM
- WELLS
  - DEPTH
  - FLOW RATE PER WELL
  - METAL CONCENTRATION
- PUMPS
  - TOTAL PLANT GPM
  - DEPTH }
  - PERMEABILITY } PUMPING HEAD
- START-UP
  - OPERATING COST
  - TIME TO EXCHANGE PORE FLUID
    - WELL LIFE }
    - POROSITY } VOLUME OF PORE FLUID
    - GRADE }
    - TOTAL PLANT GPM

Three of the four major investments (surface facility, wells, and pumps) decrease with increasing metal concentration. However, since the negative cash flow associated with start-up is higher for a system designed for high metal concentration (low gpm), it is likely that an optimum concentration exists at which the initial total cash outlay is minimized. Putting it simply, even if it is possible to technically achieve very high metal concentrations, it may not be economically desirable. Table 1 illustrates these opposing effects, and table 2 summarizes the design parameters affecting each of the four major investments.

Sub-surface engineering considerations

In-situ leaching of uranium and copper sulfide deposits requires an oxidizing agent for metal solubilization, with direct oxygen injection being the least expensive. Oxidants can be grouped into two categories; those that are totally liquid soluble, such as chlorate, and those that are oxygen based, such as hydrogen peroxide and oxygen. Peroxide probably decomposes to oxygen and water on contact with rock.

Economically speaking, hydrogen peroxide is five to 10 times more expensive than gaseous oxygen. Although it probably provides equivalent leaching performance in the rock, as it decomposes to oxygen and water on contact with rock, peroxide injection avoids the difficulties of mixing and transporting downhole a gas-liquid mixture. The added cost of using peroxide in uranium operations is tolerable, as peroxide operating costs are in the $1 to $2 per lb uranium range. In leaching copper sulfides, gaseous oxygen is the only choice, as even at minimum consumption oxygen costs are 5¢ per pound of copper and use of peroxide would approach the selling price of the metal. The handling and transport of gaseous oxygen-liquid mixtures in injection wells is described in two patents.[4, 5] and has been demonstrated to be a safe and stable operation.

Free oxygen gas impacts injection and leaching

When the back pressure of the water table is not sufficient to maintain oxygen in solution, free oxygen gas will form in the rock. This leads to the possibility of reducing the efficiency of well pattern operations by reducing permeability at the point of injection, and/or venting gas in an unproductive manner in the vertical direction, or fingering through the solvent in the horizontal direction. In a uranium operation, free gas formation will be related to a combination of the ore-reducing capacity and water table (oxygen requirements versus solubility). To achieve copper loadings above 4 lb per 1000 gal (1/2 gpl) in a sulfide deposit, well pattern operations must be designed to handle free gas flow, as free gas will exist even at depths of 3000 ft. The presence of free gas in the rock affects both the rate of liquid injection and the operation of the well pattern.

As the oxygen concentration in the injected liquid is increased to achieve higher metal concentrations, some level is reached at which free oxygen gas forms. This free gas increases the resistance of liquid flow in the rock (reduces permeability). The productivity of the well unit (lb per day of metal), being the product of flow rate and concentration, will continue to increase, although at a lower rate than with a soluble oxidant, until a point is reached at which the free gas caused reductions of flow rate exceed the added oxidizing power. Beyond this point additional wells must be used to achieve higher metal concentrations.

Uneven flows of oxygen and solvent will occur in both the vertical and horizontal directions. Well separations and injected oxygen concentrations have to be balanced when free gas is present in the deposit to insure that an adequate oxidizing condition can be maintained within the well pattern.

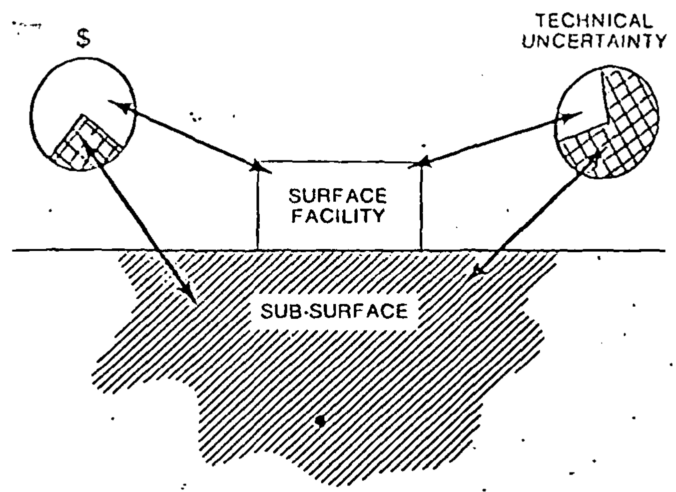

Fig. 2. Although the technical aspects of in situ leaching can vary widely, most ISL systems have in common high capital investment in the surface facilities, where the technology is standard and controlled, unlike the sub-surface component

Free gas can vertically segregate in an unproductive manner in the leach zone. The vented oxygen is not available to oxidize minerals in the bulk of the rock between wells. Two actions can be taken to compensate for gas venting.

- Increase the level of oxygen injection. This will reduce injection permeability and increase chemical and operating costs. Too much excess free gas could lead to mineral blinding, reducing the rate of leaching.
- Reduce well spacing. This will increase the number of wells and their total cost and may not provide sufficient time for oxygen to react with the mineral of interest.

The frequency at which well patterns are brought into production have significant economic and technical impact on operation of the process. Frequent replacement or addition of wells relative to the life of the operation increases the present worth of future investment, which in turn reduces the initial investment that can be allocated for wells. This places a significant burden on the technical performance of the well pattern, requiring the production capacity associated with an operation using a minimum of wells in service at any one time.

The selection of well spacing also has both economic and technical significance. Should the well spacing be made too large, then the time required to displace the water from the well pattern with enriched metal solution is high, resulting in negative cash flow impact on overall economic performance. Short well spacings provide only a limited time for the solvent to react with mineral

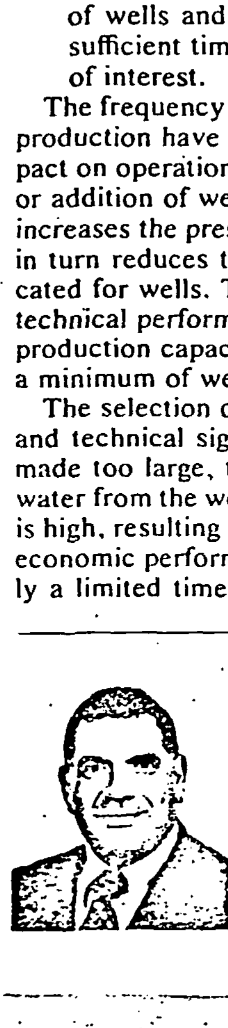

Donald H. Davidson is deputy manager of project development at TRW's Resource Development Organization. He was employed from 1971 until 1978 by Kennecott Copper Corp., where he worked on the development of in-situ leaching, and from 1967 to 1971 he was affiliated with Shell Development Co. Davidson holds a PhD in chemical engineering from New York University.

and enrich the metal value in solution to the desired level.

The local geology and its relationship to structural implications must be accounted for to insure high flow capture. In many cases fluid moves more rapidly in one direction versus another. Adequate hydrological testing of the deposit can provide sufficient data such that well separations can be adjusted to insure equal travel times of fluids in the deposit. This avoids uneven mining and premature loading declines.

In conclusion, in-situ leaching of non-ferrous metals has developed to a considerable extent over the last decade. As experience is gained in dealing with subsurface operations, it is likely that additional quantities of the large U.S. resource of low grade non-ferrous ore can be brought into economic production. ◆

References

[1] Bureau of Mines Information Circular/1978, IC-8777.

[2] Tucson Daily Citizen, July 22, 1975, "*Kenniecott Trying Mining by Liquid.*"

[3] Simpson J. Wall Street Journal, "*New Ways to Extract Metals Are Found as Deposits Thin Out and Prices Stay Up.*" June 7, 1979:

[4] Hsueh, L; R. A. Hard, D. H. Davidson, and R. V. Huff, U.S. Patent 4,045,084 (Aug. 30, 1977), "*In-Situ Mining of Copper and Nickel.*"

[5] Hsueh, L., R. A. Hard, D. H. Davidson, and R. V. Huff. U.S. Patent 4,116,488, "*In-Situ Mining Method and Apparatus.*"

---

continued from p. 25

er that we're paying no attention to the debate. One just has to learn how to listen to two conversations at the same time. While the legislative chamber is an interesting place, it is also chaotic. Remember that the people there are remarkably representative.

When you're looking at a legislature, the first thing to figure out is whether you're dealing with a professional legislature or a part time legislature. Most of your Western mining states have part-timers, but California, for instance, has a full-time legislature. Again, you're going to get an incredibly different kind of person running in those two kinds of states.

Do's and don'ts of communication

First of all, try to be informed, and if you are asked a question when you don't know the answer, say you don't know. Above all, try not to give misinformation. We're tremendously dependent on other people. I don't know very much about insurance and have to ask other people about it: if I'm told the wrong thing, I remember that. Don't be defensive about saying you don't know something. Just make sure that what you're saying is correct.

Another thing is, be honest. When I'm dealing with lobbyists, I will often ask them about other bills to see from where they are coming. Legislators want someone with whom they can communicate, so if there are some negative things about a bill you want a legislator to sponsor, for instance, explain those negative aspects, too. Someone is bound to know them and ask the lawmaker questions about them, so the bill's sponsor must be well prepared. It's like being honest with your lawyer; you've got to be honest with legislators.

Tact and common sense essential

Another point to remember is that courtesy really counts. There are a lot of unwritten conventions in any legislature. In Utah, one of them is smoking. If you're going up to a group of people who don't smoke at all, or at least aren't smoking, be careful about lighting up a cigar. You may find that they vote against your bill just because they don't like the smell of your cigar.

Another thing is that legislators are very careful about the power they have. Don't try to be a legislator when you're lobbying one. Concerning access to the legislative floor, lobbyists sometimes do themselves more harm by speaking on the floor than just staying in the wings and being a resource. So be sensitive to that, because you may think you're helping your cause by standing up and giving a speech, while it may be just the opposite.

It is particularly important for a lobbyist to try to like the folks he is dealing with. You can't be very effective if legislators think you're talking down to them, if they think you don't respect them, if they think that you don't like them. If you really don't like the people that you're being asked to talk to, don't talk to them. You'll be making a negative impression.

Remember, different strokes for different folks. It might be difficult for lobbyists to approach each person differently when there are a lot of new legislators, but it is necessary. We approach every mining property differently; you've got to approach every legislator differently. At the same time, never lay on a heavy concept the first time you meet somebody. It would be best to be introduced by someone who knows the new legislator and wait at least until the second meeting to introduce whatever concept you want them to understand or act on.

In terms of what it costs, mostly what getting to know your legislature costs is your time. And that's sometimes the most precious thing we have.

The other thing I'd warn you about is shows of force. A legislator doesn't like to be cornered into doing something. He is likely to become resentful and take an opposite stand. When people feel that they "own a legislator," the lawmaker almost has to turn around and show his constituency that he isn't owned.

As for when to communicate with your legislator, there are two things to keep in mind. One is access to the legislator; and two, you want to influence what he's doing. Access to a legislator you can get any time. Contributing to a campaign gives almost automatic access. It doesn't have to be a lot, either—ten, fifteen dollars. My whole campaign costs $1000 a year. It's not expensive in dollars; it is expensive in time, but get to know your legislator if you can in the off-season. Then, when you have to influence the legislator, at least you have access. Then, use positive reinforcement in dealing with the official.

The last thing I would suggest is that if you're really unsuccessful in dealing with legislators and you really want to change your local legislative policy, run for the legislature. You may be surprised if you win, but you won't be nearly as surprised as your opponent. ◆

Genevieve Atwood has been a senior geologist for Ford, Bacon and Davis Utah Inc. since 1975. Earlier experience includes two years as staff officer, Energy Studies Board at the National Academy of Sciences, and a year as field geologist for the government of Honduras. Atwood has been a member of the Utah House of Representatives for five years.

United States Patent [19] [11] **3,823,981**
Lewis [45] **July 16, 1974**

[54] SITU LEACHING SOLVENT EXTRACTION-PROCESS

[75] Inventor: Arthur E. Lewis, Los Altos, Calif.

[73] Assignee: The United States of America as represented by the United States Atomic Energy Commission, Washington, D.C.

[22] Filed: Apr. 4, 1973

[21] Appl. No.: 347,757

[52] U.S. Cl. 299/4, 166/247
[51] Int. Cl. E21b 43/28
[58] Field of Search 299/4, 5

[56] References Cited

UNITED STATES PATENTS

2,161,800	6/1939	Cross	299/4 X
3,640,579	2/1972	Lewis	299/4

OTHER PUBLICATIONS

Rawling, "Commercial Solvent Extraction Plant Recovers Copper From Leach Liquors," World Mining, December, 1969, pp. 30–33.

Primary Examiner—Ernest R. Purser
Attorney, Agent, or Firm—John A. Horan; F. A. Robertson; Irene S. Croft

[57] ABSTRACT

A nuclear explosive is detonated in an ore deposit below the water table to provide fragmented ore disposed in a nuclear chimney which serves as an in situ pressure vessel. The vessel is filled with water from external sources or by flow from the formation and oxidizing gas is bubbled through the ore to oxidize and dissolve metal values therein. An organic extractant solution is then contacted with the aqueous phase in the vessel and is circulated to the surface where the metal values are recovered therefrom. Following makeup the organic phase is recycled into the nuclear chimney.

9 Claims, 1 Drawing Figure

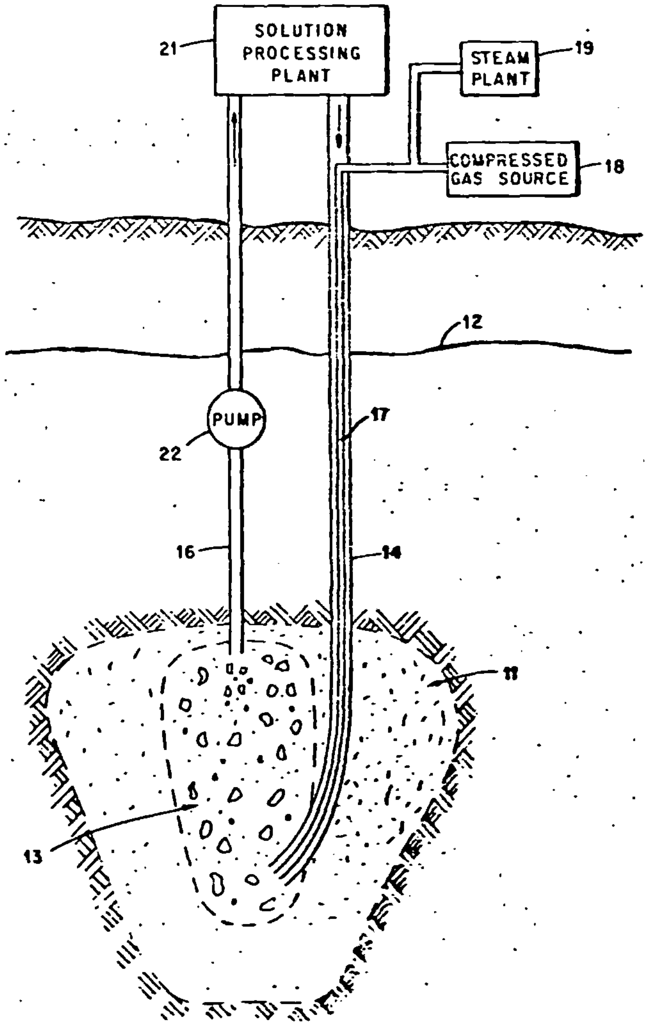

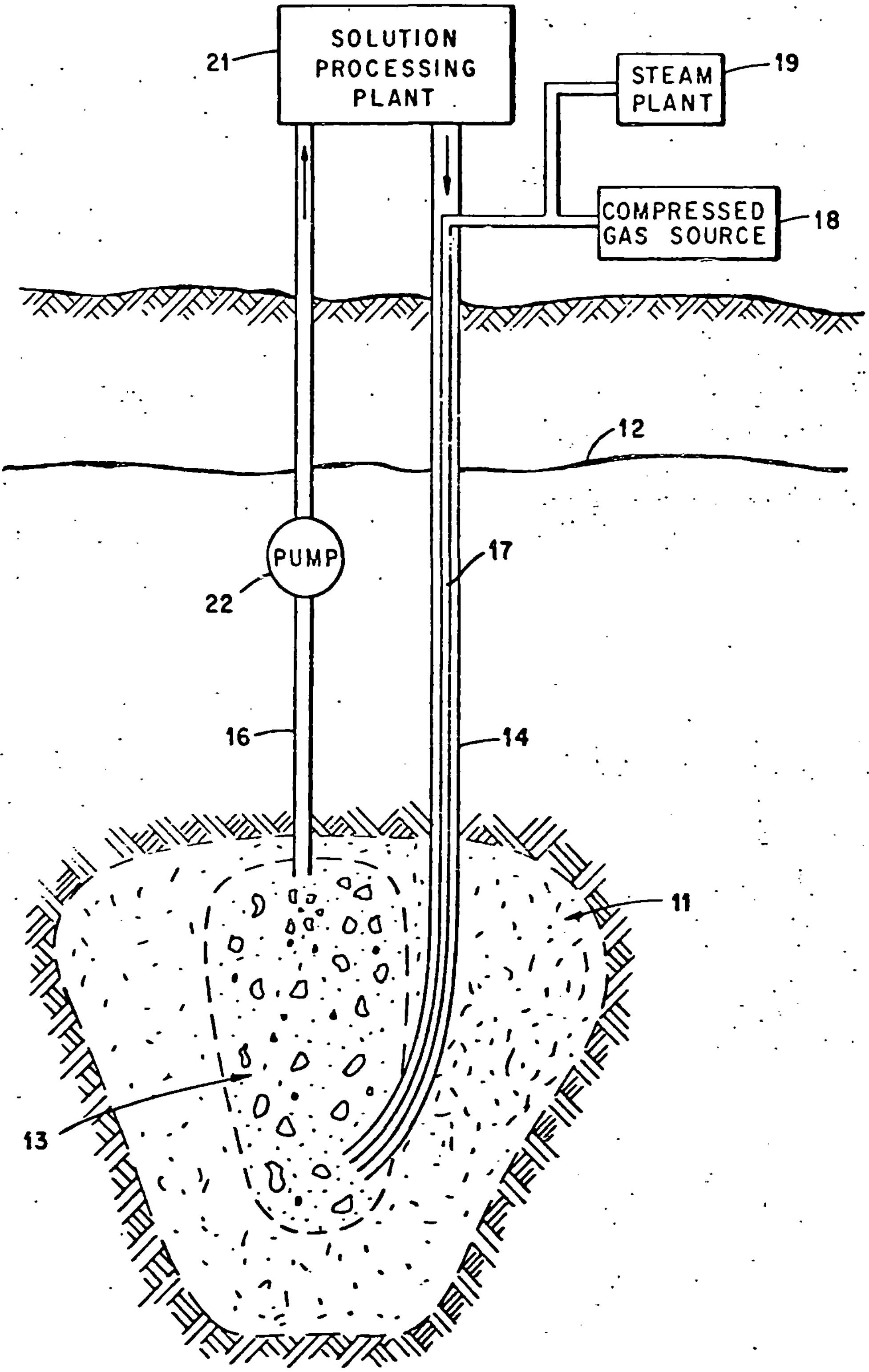
SOLUTION PROCESSING PLANT
21
STEAM PLANT
19
COMPRESSED GAS SOURCE
18
12
PUMP
22
17
16
14
11
13

SITU LEACHING SOLVENT EXTRACTION-PROCESS

BACKGROUND OF THE INVENTION

The invention disclosed herein was made in the course of or under Contract W-7405-ENG-48 with the United States Atomic Energy Commission.

Large ore deposits, particularly copper ore deposits, typically have a relatively shallow oxidized secondary ore zone above the water table and a much deeper unoxidized primary ore zone below the water table. Many of such primary deposits have been upgraded by processes of oxidation and supergene enrichment to concentrations that make them economically feasible to mine. The enrichment process is a near-surface process. Most ore deposits have been developed by mining the enriched and oxidized zone thereof. Only where the primary ore is rich enough has it been economical to mine at depth or, with large and efficient earth-moving equipment, to mine large deposits in open-pit mines. Leaching techniques have been applied economically to the oxidized parts of ore deposits or to those that can be oxidized by alternate solution and weathering or bacterial oxidation, generally by vat, heap or dump leaching procedures applied to waste or low grade material which has been excavated to the surface, or is disposed in abandoned mine workings, block caving areas, etc. Because of low permeability leaching procedures generally cannot be applied to undisturbed ore bodies. Historically, copper has been recovered from leach solutions by the cementation process. However, in recent years the copper has also been recovered by extraction with liquid ion exchange or solvent extraction techniques using reagents such as LIX-64 a product of General Food Corporation and Kelex-100 of the Ashland Chemical Company (c.f. pages 254, 255 of Supplementary Volume (1971) of The Encyclopedia of Chemical Technology, Second Edition). Primary ores, e.g., sulfides such as chalcopyrite of a sufficiently high grade are generally processed by sulfide concentration, e.g., flotation, roasting, acid treatment and electrolysis. However, large deposits of such ores remain undeveloped because they lie too deep to mine economically, their size is too small to allow the economics of large-scale mining operations, the grade is too low, or various combinations of these factors. Reserves of copper and other elements would be considerably increased if an economical process of obtaining such elements from deep primary ore deposits were available.

With a view towards economic recovery of elements from deep ore deposits, various nuclear explosive mining methods have been heretofore proposed. In this regard, it has been contemplated to employ a contained nuclear explosion to break up a deep ore deposit and form a rubble chimney therein. A leach solution is then percolated through the chimney to oxidize the broken ore and cause the desired element to go into solution. The solution is pumped to the surface and the desired element recovered therefrom by conventional processes. However, it has been found that at the low pressures, such as atmospheric pressure, various ores, e.g., chalcopyrite and most other primary sulfide minerals, are not effectively dissolved by the leach solution, or the rate of solution is so slow that any such process is impractical. It is known that the oxidation process and rate of solution are accelerated by the addition of an

oxidizing agent, such as oxygen, chlorine, ferric sulfate, or the like, to the solution and ore. However, many of such agents are too expensive or corrosive to use. Moreover, although oxygen is relatively inexpensive and non-corrosive, it is not very soluble in a leach solution and otherwise reacts only very slowly with ore minerals at atmospheric pressure.

However, as disclosed in my U.S. Pat. No. 3,640,579 issued Feb. 8, 1972, relating to an in situ leaching procedure, the rate of oxidation is dramatically increased using oxidizing gases at the elevated hydrostatic pressures occurring at depth below the water table in buried deposits and at somewhat elevated temperatures caused by the exothermic oxidation process and by heating of a leach solution which is recirculated to the surface. While such procedure is advantageous in several respects, other improved in situ leaching procedures may provide additional advantages.

SUMMARY OF THE INVENTION

The present invention relates to the economic recovery of valuable elements from their primary ores, and is more particularly directed to in situ leaching of primary ore using aqueous solutions under pressure and wherein the desired values are recovered from the leaching solution, in situ, by contact with an organic extractant.

In operating the process of the present invention, well known nuclear technology is employed to form a rubble chimney by underground nuclear detonation in a subterranean ore deposit to serve as an in situ leaching reaction vessel. Generally, according to the present invention it is preferred to provide and utilize a flooded nuclear chimney formed beneath the water table which provides an environment uniquely beneficial to the economic mining of the ore. More particularly, in accordance with the method of the present invention a contained nuclear explosive is detonated in a primary ore deposit well below the water table to provide a mass of fragmented ore in a flooded chimney subjected to substantial hydrostatic pressure, the chimney thereby serving as an in situ pressure vessel suitable for pressure leaching of the ore. The hydrostatic pressure increases the solubility of an oxidizing gas introduced into the chimney sufficiently to allow the primary ore compounds to be oxidized and dissolved into the leach solution in a relatively short time, such leach solution usually being formed by the aforesaid oxidizing reaction. Similar in situ pressure leaching cavities or vessels suitable for practice of the invention may be created by block caving, hydrostatic fracturing, by using conventional explosives or by other methods.

Thereafter, as a salient feature of the invention, an organic extractant phase is contacted with the leach solution in the nuclear chimney pressure vessel to extract the mineral values therefrom. Usually the extractant phase is introduced proximate the bottom of said chimney to disperse and rise upwardly through the leach solution and fragmented rock to collect at the top of the chimney. The loaded extract solution is withdrawn therefrom to a surface processing plant which can be of a design similar to those used to treat similar type extractant phases as employed in conventional leaching systems. Certain advantages such as the necessity of circulating lesser volumes of fluids, more selective extraction, and others are obtainable.

BRIEF DESCRIPTION OF THE DRAWING

The invention is illustrated in the accompanying drawing wherein the single FIGURE is a cross section of a geological formation with a nuclear chimney formed in a primary ore deposit and adapted to the conduct of a solvent extraction-leaching method in accordance with the present invention.

DETAILED DESCRIPTION OF THE INVENTION

Referring now to the drawing in detail, there is shown a primary ore deposit 11 which includes compounds of a valuable element which is desired to be obtained. Certain of the procedural operations and condition may be generally similar to or in a modified form of those disclosed in my aforesaid U.S. Pat. No. 3,640,579. For example, in the case of copper the ore may comprise primary copper sulfides such as chalcopyrite, bornite, chalcocite, etc. In accordance with the particularly salient aspects of the present invention, such a deposit 11 is first located which exists well beneath the water table 12. Thereafter, a nuclear chimney 13 of broken ore is formed in the deposit entirely beneath the water table, preferably at a substantial depth thereunder. Formation of the chimney is accomplished in general accordance with well established nuclear technology by emplacing and detonating a nuclear explosive having a predetermined yield, at a predetermined depth commensurate with a contained explosion in the ore deposit productive of a rubble chimney of broken ore having a predetermined height above the detonation point selected to not exceed the water table 12. It is particularly important to note that although fracturing into a water bearing formation is usually to be avoided in the detonation of some contained underground nuclear explosions in order to prevent flooding of the resulting rubble chimney, in accordance with the present mining method, the nuclear explosive is deliberately emplaced and detonated beneath the water table. As a result, if adequate permeability exists, the chimney 13 is flooded by the natural inflow of water under the hydrostatic head of its vertical displacement below the water table 12. Otherwise, water may be introduced to provide a similar situation. The broken ore in the chimney is thus subjected to hydrostatic pressures which are dependent upon the prevailing water head. In this regard, the hydrostatic pressure acting on a given point is approximately 435 psi or 30 bars for each 1,000 ft it is below the water table.

The hydrostatic pressure acting on the nuclear chimney 13 is utilized to good advantage to promote leaching of the broken ore contained therein. More particularly, the chimney 13 is employed as an in situ pressure vessel for accelerating the dissolution of the contained broken primary ore minerals. In this regard, an oxidizing gas is introduced into lower portions of the chimney at high pressure and thereby percolates through the contained broken ore and water mixture which has a substantially infinite permeability compared to that of the surrounding unbroken wall rock. By virtue of the high pressure, the solubility of the gas is increased such that it readily dissolves and more rapidly oxidizes the ore minerals particularly sulfides to form an acid leach solution as a result of the reaction. The acid solution aids the oxidation of the ore minerals by the gas and the desired ore element goes into solution at a relatively rapid rate.

For purposes of the present invention, introduction of the oxidizing gas is continued until a concentration of the desired mineral component, e.g., copper, suitable for recovery is achieved in the leach solution. Thenceforth the desired material is recovered from the pregnant leach utilizing a solvent extraction or liquid ion exchange solution as described hereinafter.

The foregoing leaching operation of the process is preferably accomplished by drilling at least one shaft 14 which is provided with a casing to communicate with the bottom of the chimney 13 and at least one shaft 16 to communicate with top portions thereof. Often times a void space of considerable volume is formed in the upper portion of the chimney (not shown) in which event shaft 16 communicates with the void space. The oxidizing gas is then introduced to the bottom of the chimney via cased shaft (or well bore) 14, as by means of a pipe 17 extending therethrough in spaced relation to the shaft wall and connected at its upper end to a suitable compressed gas source 18, such as a gas supply and compressor, at the ground surface. The gas thus rises upward through the chimney to the top portion or void space and any excess not reacting will rise to the ground surface through the shaft 16. In the event that oxygen is being employed as the oxidizing gas any excess rising to the surface may of course be recycled. If air is being employed the residual gas which would mainly be nitrogen may be discarded. The rate of reaction and attendant leaching of the desired value from the ore is significantly accelerated at elevated temperatures as well as by the increased oxygen pressure provided as discussed above. Some increase in temperature is provided by the normal geothermal gradient. The energy of the detonation provides a relatively small increase in temperature and oxidation of the sulfides also provides heat to increase the temperature of the leach solution and chimney rubble; however, where total sulfide content is low this effect may not be adequate to provide an effective temperature increase. Where leach solution is processed at the surface it may be heated and recirculated to heat the chimney contents; however, such a procedure is not particularly suitable in the present process. Accordingly, it is preferred herein to introduce the additional heat which may be required by injecting steam or superheated steam through pipe 17 as from a surface steam plant 19. Mixtures of steam and oxidizing gas may, of course, be injected simultaneously if desired. Chimney content temperatures somewhat above 100° C with oxygen pressures above several hundred psi, e.g., above 500 psi are considered advantageous. (c.f. "Chemical Mining of Primary Copper Ores," A. E. Lewis, pp. 909–917, Proceedings of Symposium on Engineering with Nuclear Explosives, held January 14–16, 1970 at Las Vegas, Nevada). The maximum temperature will usually be determined by the thermal stability of the extractant but may be at least as high as 200° C or more. It may be noted that control of the chimney temperature can be achieved by regulating the rate of oxidizing gas and/or rate of steam injection. Also, as the solvent extraction procedure provides an increase in the acid content of the aqueous phase and concentration of the extracted value is decreased the rate of leaching may be accelerated.

The leaching operation outlined hereinbefore is particularly applicable to the economic recovery of copper from deep deposits of primary copper sulfides, such as chalcopyrite ($CuFeS_2$). In this case, oxygen is employed as the oxidizing gas introduced to the chimney containing broken ore and water at least in initial phase of the operation. Other suitable oxidizing agents are also operable. Various other materials may also be contained therein such as iron sulfate in varying proportions together with trace amounts of silver, gold, molybdenum, etc. To provide conditions suitable for recovery of the copper as described hereinafter the pH (acidity) of the leach solution should preferably be of the order of 1.0 – 3. The LIX-64 type extractant is operable with about zero to several grams, i.e., 10 grams/liter of H_2SO_4. Leaching in the initial period is continued until a sufficient content of copper is leached to afford economic recovery. Such a content may range from at least about 1 gram per liter to 20 or more grams per liter in the loaded leach solution.

For recovering the metal value, e.g., copper from the loaded leach solution, in accordance with the present invention, a suitable extractant phase, i.e., a solvent extraction or liquid ion exchange phase as such phases may variously be known, is bubbled through the pregnant leach solution in the nuclear cavity and which is then drawn to the surface for recovery of the desired value. More particularly, an organic extractant solution or phase may be injected from a solution processing plant 21 situated at the surface as through the clearance space between the casing of shaft 14 and pipe 17 into the lower portion of the chimney vessel. The extractant is dispersed thereat and being of a lower density than the loaded leach solution, rises with significant turbulence and along circuitous paths through the fragmented ore to contact the leach solution so as to extract the desired value, i.e., copper therefrom. The loaded extractant phase eventually collects in the upper portion of the chimney to a depth at which the lower end of the casing of shaft 16 is immersed therein. As this operation is initiated some of the leach solution may be displaced upwardly through shaft 16 and may be treated in plant 21 for the recovery of copper therein, if of sufficient economic value, by conventional cementation, extraction, ion exchange, or other procedure.

Thereafter, loaded extractant phase may be withdrawn through shaft 16 as by means of a pump 22 and fed into the solution processing plant for recovery of the mineral value (copper).

It may be desirable in order to increase extraction efficiency to increase the interface area, contact time and dispersal of the extractant in some manner to assure adequate contact with all portions of the pregnant leach solution over an appropriate period of time. This can be accomplished in several ways. However, it may be noted that the rising current of extractant tends to cause some circulation of the leach solution as would convection currents caused by heating effects of injected steam. Also, injected oxidizing gas or injection of air or nitrogen simultaneously with the extractant phase can also assist in dispersing the extractant phase and circulating the leach solution to improve interphase contact. Also, the lower end of the casing of shaft 14 may be perforated over a length extending across the bottom of the cavity (not shown) so as to disperse the oxidizing gas and/or extractant phase more effectively.

The solvent extraction medium or phase is generally comprised of a fluid organic solvent containing an extraction agent, of which several are known in the art. The organic solvent may be a hydrocarbon in which the extractant agent and extracted species are soluble. Low cost petroleum fractions having a relatively high boiling point to reduce volatility are generally suitable and are preferred on an economic basis.

Kerosene, diesel fuel, stove oils, fuel oils and the like having a low content of lower boiling materials may be used. High gravity relatively low viscosity crude oils from which the lower boiling fractions have been removed could also be used as an economical solvent.

LIX-64, a product of the General Mills Corporation, is an extraction agent which is selective with regards to extraction of copper from leach solutions of the character described. This reagent is an α-hydroxyoxime for which the general formula is $RR''C(OH)CR'NOH$ where R, R' and R'' may be any of a variety of organic hydrocarbon radicals such as aliphatic and alkyaryl radicals. These extractants and the copper complexes have a solubility of at least about 2% by weight in a solvent such as kerosene and are insoluble in water (c.f. page 254, Supplement Volume (1971), "Encyclopedia" cited above. Also D. W. Agers et al., Trans. Soc. Mining Engrs. 235, 191–198 (1966) Kelex-100.) LIX-64N is an improved extractant from the same source. Kelex-100 type reagent from Ashland Chemical Company may be used similarly. This reagent operates best in a pH range of about 1.5 to 2.8; however, extraction still occurs at a pH of about 0.5 (c.f. Hartlage, I. A., Kelex-100 - "A New Reagent for Copper Solvent Extraction," SME Fall Meeting, Salt Lake City, Utah, September, 1969). Such reagents in amounts of about 0.5 to 7% or more determined by solubility by weight may be used with acidity conditions disclosed hereinbefore to effectively and preferentially extract copper from the aqueous leach liquor yielding the loaded extractant solution.

For recovering the copper from the loaded extractant solution the surface processing plant which may be of a modified conventional design may include copper value stripping circuits which yields a sulfuric acid solution suitable for processing in an electrolytic circuit. The copper anodes produced therein are of relatively high purity. More particularly, such plant may include at least a pair of tandem mixer-settler stripper units wherein the copper is stripped from the pregnant extractant phase using an aqueous sulfuric acid containing about 100 to about 200 grams/liter of H_2SO_4. The copper loading of the stripper solution may range from about 2 to as high as 50 grams per liter depending on operating conditions. The stripper solution is then treated in an electrowinning circuit and is recycled to the mixer settler circuit. Conventional solution processing plants are discussed in "World Mining," October, 1970, pages 38–44 and in references cited therein. An accessary circuit corresponding to the leach liquor treating circuit of such a plant may, of course, be used to treat any overflow aqueous leach liquor, if desired. The depleted extractant phase may then be refurbished and recycled into the chimney.

Further details of the process of the invention will be set forth in the following illustrative example:

EXAMPLE

Consider the case of a deep deposit having an ore grade of 0.5% copper, bulking factor of 0.15, and rock density of 2.7 g/cc in an area where the water table is at 50 meters. The lower limit of copper content which may be treated can be considerably lower while higher contents can even more readily be treated. From well established nuclear explosive technology, it can be shown that a nuclear explosive with a yield of 100 *kt* emplaced and detonated in the ore deposit at a burial depth of 750 meters is productive of a cavity or nuclear chimney with a radius of about 41 meter and volume of 2.9×10^5 cubic meters. Assuming a chimney wall slope of 3° from the vertical, it can be calculated that the chimney has a height of 250 meters above the shot point and contains 1.6×10^6 cubic meters of broken ore. The total void space may be about 25 to 50%. With the chimney thus positioned and proportioned, the hydrostatic pressure acting thereon when filled varies from 1,000 psi at the bottom of the chimney to 650 psi at the top. Steam is generally injected together with oxygen at a pressure of about 1,000 psi which is introduced to the chimney at a rate of 5,000 ft^3/hr for a time sufficient to provide a concentration of at least about 0.5 g/liter in the pH of the order of 1.5 to 04.0 therein. An organic extractant phase comprising a high boiling petroleum hydrocarbon solvent with about 2 percent of LIX-64 or LIX-64N dissolved therein may then be injected with a flow rate, e.g., 5,000 gals/min to extract copper from the leach liquor, in situ, in the nuclear chimney. Thereafter the extraction and oxidizing treatments may be alternated dependent on copper content of the leach liquor and to regulate chimney temperature. In general, the oxidizing agents and extractant are not introduced simultaneously when oxidation of the solvent or explosive mixtures may be produced. Copper contents of the extractant phase may range from about 2 to 10 grams or higher/liter under varying conditions in the chimney. The loaded extractant phase is then circulated to a surface plant and is passed through at least two mixer-settler units to contact a sulfuric acid stripping solution containing about 100 to 200 grams/liter of H_2SO_4 yielding an aqueous copper sulfate H_2SO_4 solution which is treated in an electrowinning plant. Following makeup of the organic extractant phase it is recirculated as above.

It is considered that a similar in situ pressure leaching procedure can liberate other metal values from a sulfide ore deposit and that an organic extractant solution of appropriate character may be used to strip desired values therefrom by manipulation similar to those set forth above. For example, amine extractants, alkyl phosphate extractants and others are known to be effective for extracting various metal values from acid leach liquors.

Although the invention has been hereinbefore described and illustrated in the accompanying drawing with respect to specific steps of the method thereof, it will be appreciated that various modifications and changes may be made therein without departing from the true spirit and scope of the invention, and thus it is not intended to limit the invention except by the terms of the following claims.

What I claim is

1. A leaching solvent extraction method for the recovery of a desired mineral value from a primary sulfide ore deposit containing same comprising the steps of:

locating a primary ore deposit containing a desired element existing beneath a water bearing subterranean formation;

creating a subterranean chamber containing said primary sulfide ore in a fragmented form at a substantial depth beneath the upper level of said water bearing formation so that the contents thereof are subjected to the hydrostatic pressure head of said water bearing formation;

introducing oxidizing gas to said chimney at substantially the pressure of said hydrostatic head with said gas being therefore more highly soluble in the water contained in said chimney to oxidize said ore to form an acid leach solution effective in the presence of the dissolved gas to dissolve said ore and cause said desired element to go into solution therein;

then contacting said leach solution in the chamber with an organic extractant phase to extract the desired mineral value therein yielding a loaded extract phase; and

circulating said loaded extract phase to the surface and stripping the desired mineral value from the loaded extract phase.

2. A leaching-solvent extraction method as defined in claim 1 wherein said chamber is created by emplacing and detonating a nuclear explosive in said primary ore deposit.

3. A leaching-solvent extraction method according to claim 2 wherein steam is injected along with said oxidizing gas to heat the chimney contents and accelerate oxidation and dissolution of said ore.

4. A leaching-solvent extraction method according to claim 3, further defined by said desired element being copper, said ore being primary copper sulfides, and said gas being oxygen.

5. A leaching-solvent extraction method according to claim 4, wherein the oxidizing gas and steam are injected into said chimney until a predetermined concentration of said copper is attained in the leach liquor prior to extraction of said copper therefrom.

6. A leaching-solvent extraction method according to claim 5 wherein the ore is oxidized with heating until the pH of the leach solution is in the range of about 0.5 to about 4.0 and said extractant phase comprises an organic solvent together with an α-hydroxyoxime dissolved therein and wherein the copper is stripped from the loaded extract using an aqueous phase containing about 100 to 200 gram/liter of H_2SO_4.

7. A leaching-solvent extraction method according to claim 6 wherein the pH of the leach solution is in the range of about 1.5 to 2.8.

8. A leaching-solvent extraction method according to claim 7, wherein the copper content of the leach liquor is at least 0.5 gram/liter prior to initiation of extraction of the copper therefrom.

9. A leaching-solvent extraction method according to claim 6, wherein the introduction of oxidizing gas and extractant phase to said chimney is effected by drilling at least one first shaft to communicate with the bottom of said chimney, and delivering said gas and extractant phase to the bottom of said chimney via each first shaft wherein the removal of the loaded extract phase from said chimney is effected by drilling at least one second shaft to communicate with the top portions of said chimney, and pumping said loaded extract phase from said chimney to the ground surface via each second shaft.

* * * * *

Solution Mining

David D. Rabb
Metallurgist
Lawrence Radiation Laboratory

With the increased emphasis on pollution and environmental engineering, the mineral industries are turning more and more to chemical mining. The increased availability of less expensive sulfuric acid and or sulfur in the near future will lend impetus to leaching activity. The year 1971 will be remembered as a turning point in metallurgy.

Some chemical processes promise to be competitive, if not better, than the old-fashioned smelting, particularly in the winning of copper from sulfide ores. The hydrometallurgical approach is becoming more attractive because the economics are more favorable and the problem of sulfur dioxide pollution must be considered. Instead of roasting sulfide concentrates and then smelting, reducing and electrorefining the metal, chemical processes feature leaching, then reduction of the metal from the resulting solutions.

In a cooperative effort to lessen environmental pollution, the copper industry joined in the formation of a new research group, the Smelter Research Association, Inc. Its members are: The American Smelting & Refining Co., The Anaconda Co., Cities Service Co., Copper Range Co., Inspiration Consolidated Copper Co., Kennecott Copper Corp., Newmont Mining Corp., Phelps-Dodge Corp.

These eight companies were the source of practically all newly-mined copper produced in the United States in 1971. In addition, separate efforts are underway, such as the Phelps-Dodge Division of Environmental Engineering and Research.

The adoption of leaching schemes to replace smelting generally faces the problem of high operating costs and the disposal of quantities of soluble salts. Hydrologic pollution may, in the next decade, replace atmospheric pollution as a major problem.

Hydrometallurgy is that field of metallurgical endeavor in which the chemical processes involved in the extraction of metals from their ores take place in solutions. It is the art or service of selectively dissolving and or separating metals or their compounds from solutions primarily aqueous in nature. The term solution mining is beginning to find wider acceptance in the industry and is being expanded to include the recovery of industrial minerals as well as metals. It may be more accurate to define this subject as a sequence of operations.

Preparation may include size-reduction, concentration, roasting or enhancement of availability to processing. Dissolution may be carried out at elevated temperatures, elevated pressures, in acid or alkaline solvents and it generally involves a liquid-solid separation. Recovery could include ion exchange, solvent extraction, chemical precipitation or electrolysis.

In some cases hydrometallurgy is the most important, if not the only, means of recovering the metal (e.g., aluminum, magnesium, cadmium, cobalt, uranium) or mineral (salt, potash); in other cases it accounts for a considerable percentage (copper, gold, molybdenum, nickel tungsten, zinc, and many rare earths). Only lead, of the major nonferrous metals, has resisted the hydrometallurgical approach. Pilot tests by the Bunker Hill Co. to produce lead and zinc directly from sulfide ores by high pressure leaching followed the system developed by Dr. Frank Forward and Sherritt Gordon Mines, Ltd., and gave some promise of successful commercial production.

In-situ leaching can be divided into two categories. The first is flooding or saturated leaching as practiced by Kennecott at Ray, Ariz., a pilot-plant field test initiated near the mined-out Kimbley pit of Kennecott's Nevada Mines Division, and a Utah Construction and Mining operation. Solutions are introduced or pressure-injected at one point in the ore zone and then pumped from one or more extraction wells. (This can be done from the same hole, as is the practice in solution-mining for brines.) The second is unsaturated leaching or film percolation, examples of which are Miami Copper and some of the uranium mines in the Grants district. Leach solution is sprayed lightly (on the order of one gal per sq ft per hr) over the old mined-out area and collected below in a system of old mine workings. The factors involved in this second category are practically the same as in dump leaching.[1]

At Bagdad Copper, a copper sulfate solution from the leaching of cement copper is reduced with hydrogen gas. The copper powder and regenerated sulfuric acid are sent to a settling tank, where the solution is decanted and returned to the leaching system. The copper-powder slurry is pumped to a centrifuge, separated from the remaining liquid and washed. It is then dried under a controlled atmosphere, sintered and, if desired, copper briquettes prepared.

At the Blue Bird mine of Ranchers Exploration and Development Corp., and also at Bagdad, a bulk of their production comes from amine solvent extraction. A typical agent, LIX-64, is very selective for copper ions. It rejects all the iron and other metal impurities in the solution.[2] The copper-rich solvent is then stripped to get a very high grade, pure, copper sulfate solution for subsequent precipitation of the copper by electrowinning or hydrogen reduction.

Sherritt Gordon Mines has also been working on a chemical route to win copper from sulfide concentrates. Eighty-five percent of the sulfur is recovered in elemental form and 98% of the copper as follows:

Bagdad Copper has two systems, hydrogen precipitation and solvent extraction. The latter is shown here: center and right are LIX mixing and separation cells and the tank house is at left.

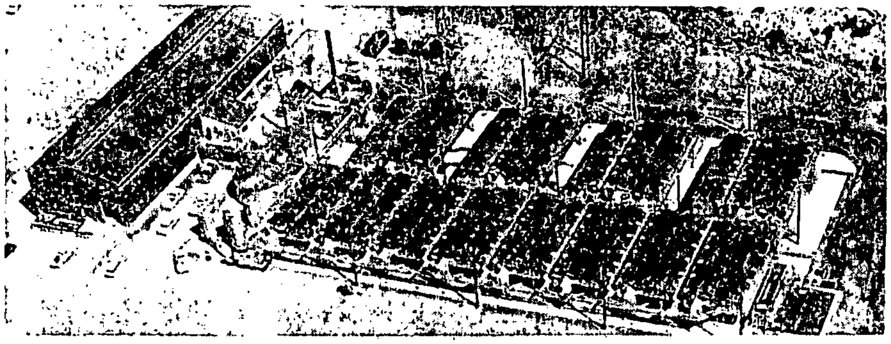

The finely-ground concentrate is treated with dilute sulfuric acid in an autoclave, with oxygen, at a pressure of 500 psi for 2½ hours at 240°F to form copper sulfate and sulfur. A 50% stoichiometric excess of concentrate gives the best results. After the copper sulfate solution is filtered off, the sulfur, excess concentrates and tailings are separated by flotation. The tailings (iron oxide and insol) are rejected, the sulfur is separated from the concentrates by hot filtration, or solvent extraction or other means, and the concentrate is recycled. The copper sulfate solution can be treated by any of the copper winning routes.

Kennecott's Utah Copper Division is adding ammonium bisulphite (a product obtainable from the neutralization of sulfur dioxide in smelter gases) to copper leaching solutions on an experimental dump to determine if dump permeability and copper extraction can be improved.

Leach-precipitation-flotation is being considered as a means of processing some 80 million tons of old gravity tailings and flotation concentrator tailings in the Miami, Ariz., area. The tailings average about six lb of copper per ton, half of it soluble in acid. With the possibility of cheap sulfuric acid from copper smelters which are now installing equipment to meet new emission standards, the copper industry is considering previously unattractive low-grade ores. Anaconda, for example, has some leachable but relatively high-acid consuming ore in their Twin Buttes mine. The material is not amenable to heap leaching but can be handled successfully in an air-lift Pachuca style leaching tank, at least on a lab scale. In some instances older time-proven methods of treatment are an aid to the treatment of heretofore difficult ores.

Recent investigations at the New Mexico Tech Research Foundation indicated that a high SO_2-ion concentration inhibits the dissolution of chalcocite and that the movement of leaching fluid across a surface being dissolved is an important factor.[3] A two-year project is underway on the rate of solution penetration into rock above the water table and techniques for determining and controlling leach solution containment in a small deposit near Socorro.

The Anaconda Co. is testing the Anatread process, based on a patent and patent application owned by Treadwell Corp. (New York). The test facility has the capacity to process 6 tpd of sulfide concentrates resulting in 2 tpd of relatively pure copper metal. The concentrates are leached with 90% sulfuric acid, then the purified metal-sulfate solution is treated with hydrogen cyanide to form a solid cuprous cyanide. Hydrogen gas reduces the cuprous cyanide briquettes at an elevated temperature to metallic copper and hydrogen cyanide gas, which is subsequently recycled. Elemental sulfur, a by-product of the leaching step, is more salable and easily transported than sulfuric acid. Treadwell-developed technology permits the plant to operate at atmospheric pressures. Ninety percent of the contained sulfur in the feed is recovered as elemental flowers-of-sulfur.

Injection leaching is being employed to improve leaching in place in some of the old underground mines at Anaconda's operations in Butte. Old waste-filled stopes are leached by acid mine water introduced through drifter holes (called Finnegans) through drift and cross-cut walls into the gob which still contains considerable leachable copper minerals.

The millions of pounds of copper recovered represent some of the cheapest copper ever produced in this country, plus the fact there was no sulfur emission problem involved in subsequent treatment.

A new method of laying down mine-waste from the Berkeley pit is in a series of long narrow fingers about 50 ft high instead of in a single conventional dump. The resulting dump (composed of many fingers) is expected to be more permeable to leaching solutions because the finger mode allows for segregation of coarse rock between each individual finger and, therefore, improved solution flow. Furthermore, layers compacted by trucks are blasted as the dumps are built up so that solution flow is improved throughout the entire dump. In a conventional dump emplacement, good solution is normally possible only at the bottom edges of the dump.

Several agencies have studied solution systems that might be employed for dissolution of copper sulfide minerals. Oxygenated pressure-leaching of deeply-buried chalcopyrite (such as would be found under the water table) has been successful in laboratory bench scale tests.[4] Another USBM report discusses percolation cyanide leaching for extraction of gold from mine strip material and marginal ores.[5]

The pilot concentrator of the Hecla Mining Co. at the Lakeshore property is capable of treating over 900 tpd of ore. A pilot roast-leach-electrowinning plant is nearly completed, and will process a portion of the concentrates which will be produced from the pilot concentrator. The sulfide ore feed for the pilot concentrator will be supplied from underground development headings which are scheduled to be in ore during the third quarter of this year.

A method for the cementation of copper from aqueous solutions was presented at the 1970 TMS-AIME Annual Meeting.[13] The copper solution is reduced by divalent chromium. The chromium is an intermediate reducing agent and is continuously recycled during the process. Nickel can also be reduced to the metal during the electrolytic reduction of the trivalent chromium to the divalent state. The reactions are rapid, high-purity copper is produced, nickel can also be recovered and no waste effluents are produced which require pollution control.

Kennecott and the USBM used a radioactive tracer to study the hydrology and permeability characteristics of a very large copper leach dump at the company's Chino Mines Division in New Mexico. The tracer was obtained from the Lawrence Radiation Laboratory, a USAEC contractor, at very little expense.

One significant engineering feat in solution mining was the washing of two large caverns in a salt bed near Eminence, Miss., and their utilization for the storage of high-pressure natural gas.[7] The feasibility and economics of this method of commercial gas storage is becoming an accepted fact. There are currently three solution mining operations in the state of Arizona forming storage cavities in deep salt deposits.

The trend is more and more toward hydrometallurgy. For example, Ranchers Exploration and Development decided upon a leaching operation at the Big Mike copper mine near Winnemucca, Nev., in place of a milling process the company originally considered. Kennecott also engaged in some large scale in-situ leaching tests in the walls of the Kimbley pit, a new approach which may lead the way to new leaching operations in the fringe areas of other existing pits.[2]

Research in general has become more and more complex, technically sophisticated and elaborately equipped. This research, on the other hand, is what is needed to keep copper production at the required levels under the increasingly demanding environmental controls that we must work under today.

References

[1] Armstrong, F. E. and Evans, G. C., et al, "Tritiated Water as a Tracer in the Dump Leaching of Copper," *USBM Report of Inv.*, Vol. 7510, May 1971, 39 pp.

[2] Spedden, H. R. and Malouf, E. E., et al, "In-Situ Leaching of Copper—Pilot Plant Test," presented at AIME Annual Meeting, New York, N. Y., Mar. 2, 1971, 32 pp.

[3] Fletcher, James B., "In-Place Leaching—Miami Mine, Miami, Ariz.," Preprint No. 71-AS-40, presented at AIME Annual Meeting, New York, N. Y., Feb. 26-Mar. 4, 1971, 13 pp.

[4] Rosenbaum, Joe B. and McKinney, W. A., "Dissolution of Copper Sulphide Minerals from Fractured Ore Bodies," Reprint No. 70-AS-329, presented at SME Fall Meeting, St. Louis, Mo., Oct. 21-23, 1970, 15 pp.

[5] Potter, George M., "Recovering Gold from Stripping Waste and Ore by Percolation Cyanide Leaching," *Tech. Prog. Rept. 20*, Dec. 1969, 5 pp.

[6] Boughton, L. D., "Solution Mining Well, Completion Service and Techniques," AIME Preprint No. 71-AS-36, 1971.

[7] Allen, Kermit, "Eminence: Natural Gas Storage in Salt Comes of Age," AIME Preprint No. 71-AS-60, 1971.

[8] Hunkin, G. G., "A Review of In-Situ Leaching," AIME Preprint No. 71-AS-88, 1971.

[9] Bhappu, Roshan, private communication.

[10] "Chemical Route to Copper," *Chemical Engineering*, Apr. 20, 1970.

[11] *Mining Engineering*, May 1971, pp. 47-49.

[12] *Mining Engineering*, June 1971, p. 38.

[13] Ford, J. H. and Rizzo, F. E., "Liquid Phase Cementation of Copper," *Journal of Metals*, September 1971, pp. 41-44.

[14] Lewis, A. E. and Brown, R. L., et al, "Nuclear Chemical Mining of Primary Sulphide Ores," *UCRL* 73357, Joint Meeting of AIME and Japanese Metallugical Society, Tokyo, May 1972.

Rock Mechanics

J. F. T. Agapito

Colorado School of Mines

Progressing from an art of ground control into a branch of engineering, rock mechanics is slowly finding more applications in mining engineering. The profusion of papers from many national and international symposia continues to deal mainly with theory. Reports on field applications are still scarce. The gap between practice and theory has created somewhat of a communication problem between the researcher and the field engineer, but the demand for more rational design procedures has provided an impetus which will eventually result in more exact and tangible field applications. The problem is how to direct more of the current proliferation of research into an applied path to achieve this goal as quickly as possible. Additional industry participation on rock mechanics work and increased industry representation on rock mechanics meetings and committees is needed to help balance the research effort.

In November 1970, the Intersociety Committee on Rock Mechanics merged with the United States Committee on Rock Mechanics under the name of the latter. This national body will represent the United States on the International Society of Rock Mechanics.

An understanding of the mechanical behavior of rocks is of paramount importance in mine design. A better understanding of rock failure was made possible with the introduction of servo-controlled and stiff-testing machines. Laboratory experiments made with conventional testing machines cause the rock specimen to fail violently as soon as the peak load is reached. This violent disintegration is not a rock property, but is due to uncontrolled release of energy from the testing machine into the rock. If the energy release from a testing machine is controlled the post-failure behavior of rock can be examined. Such study is very important because *in-situ rock very often is in a failed but stable condition.* A high degree of rock failure control has been achieved by a closed-loop servo-regulated testing machine.[1] Failure control is attained when the most

Chapter 6

SOLUTION MINING - ITS PROMISE AND ITS PROBLEMS

D. A. Shock and F. R. Conley

Continental Oil Company
Research and Development Department
Ponca City, Oklahoma 74601

ABSTRACT

Solution Mining or In Situ Mining has received increasing attention in the past few years because the method offers many attractive possibilities in improving the environmental impact of mining as well as making feasible the extraction of deeper, low value mineral reserves. This paper will present a brief discussion of the state-of-the-art in total solution, slurry removal and leach mining.

As a specific example of utilizing the method, the uranium deposits of South Texas are a type of deposit which have been considered as being amenable to in situ leach mining. The parameters required to ascertain the amenability of such a deposit for in situ leaching will be presented. The hydrological factors which influence the production of the soluble uranium solutions and their displacement will be discussed. Mathematical models for various well configurations have been made and graphic representation will be presented to illustrate various production methods and the resultant hydrological consequences.

INTRODUCTION

Solution mining, as a descriptor of a mining process, has been increasingly used in the literature over the past few years. A more accurate description of the general process possibly would be "bore hole mining." The operation we are considering is that of removing a mineral value by drilling into the ore body, circulating an extractive fluid and removing the mineral value, possibly separating the mineral value from the fluid, and then recycling the fluid. The operations in this system have much in common with the techniques of oil production; therefore, it is not surprising that there is a definite trend on the part of oil technologists to enter the field of bore hole mining. It is interesting to note, however, that the Frash Process of mining sulfur is an outstanding example of bore hole mining. This process dates back to the early 1900's. Unfortunately, there is a dearth of information in the literature on which one can ascertain the problems encountered, the efficiency of the method, the reservoir characteristics for successful operation, etc. Certainly the many years of successful production of sulfur by the Frash process is a demonstration that bore hole mining has its place as a viable mining system. It is hoped that in extending the method of bore hole mining we can build a body of technology that is documented and will find broad application in time to come.

Bore hole mining can be considered in three main types; (1) complete solution mining, (2) slurry mining, and (3) leach mining. Complete solution mining has become a significant method in its own right in the production of brines for the chemical industry and perhaps more important, in the building of petroleum storage capacity, e.g., salt cavern storage for natural gas, LPG, petroleum products and crude. The slurry mining category remains largely experimental as a means of producing phosphate rock, coal and others, and as yet has not reached a point more than the experimental stage.

Leach mining is concerned with dissolving the mineral values in an extracting fluid, leaving the gangue minerals behind in the ground and producing the solubilized mineral out of a bore hole. Thus, Frash Sulfur is an established process of this type. Much of the current leach mining research has been aimed at leaching of uranium, copper, and nickel.

The specific discussions on the extractive mechanism of this paper will concern themselves about leach mining of South Texas uranium ores. The more general remarks can be applied to all the types.

THE PROMISES

Three major assets can be envisaged by use of the bore hole mining system: (1) the environmental, (2) the mineral utilization, and (3) the economic strategy. Needless to say, we have become very aware of the environmental factors which inhibit the mining industry in many of its developments. The mining method which leaves the earth undisturbed is an impossible goal; however, the method which violates the earth the least surely should be rigorously considered. Bore hole mining fulfills this potential to a great degree. It should be pointed out, however, that the method is not without its environmental problems. The reservoir extraction system must be operated so that the solutions are held within the ore body. Thus, containment in the reservoir and contamination of ground water can be a problem. While surface disturbance may be minimized, subsidence must be considered in some cases. For instance, ground movement in sulfur mining was noticeable and sometimes very troublesome causing collapse and shearing of the tubing. The Long Beach Field subsidence problem gave evidence that withdrawal of fluid without adequate replacement can be a serious problem. The massive movement of earth during a strip mining operation should be eliminated by *in situ* extraction; and thus, this undesirable feature would be eliminated by the *in situ* system.

In the area of mineral utilization, bore hole mining should be able to reach our deeper reserves and hopefully would be applicable to lower mineral values. The reserves of South Texas uranium for instance, increase by more than another order of magnatitude if we consider lowering the minable grade average from 0.10% to 0.05%. There is little or no data to judge how much the reserves could be extended by increasing the economic depth limitations; however, it is obvious that this also would make a major increase in the uranium available in the future.

The bore hole mining system portends some advantage as an economic strategy. If the production of mineral values can be realized early in the life of the development of a mineral deposit and if the refining process is no more complex than the normal metal winning process, the bore hole mining method can have a major advantage over the conventional mining systems because of the earlier return on investment. In other words, the high development costs required in opening a mine and starting the ore preparation plants, in a usual mining project, gives a very unsatisfactory cash flow. In the high initial investment mine, the cash flow does not begin for a long time; thus the payout time is long, the time value of money requires a larger profit return, and the attractiveness of the venture is decreased. In the bore hole mining system, the development of wells should be relatively inexpensive (compared to stripping, tunneling, etc.) and if sufficient production can be maintained, and if the concentration or separation of mineral value is not overly expensive, the cash return starts in a much shorter time. Thus, the payout period is shorter and the return on investment is better. Production rates are more flexible with a well system as they depend on the rate of development of a field. Field development can be scheduled by the cash generated by the profit from the operation. If the cost of capital is high, as it is today, a less capital intensive mining system is important.

PROBLEMS FOR CONSIDERATION - URANIUM LEACH MINING

Geology

One of the primary factors in successfully performing any bore hole extraction is to obtain thorough understanding of the geological status of the ore and the ore body. The secondary uranium depositions of the U.S. are similar; however, for the discussions of this paper, we will examine more specifically the deposits of South Texas. Figure 1, taken from Eargle, et al (1), locates the band of exposures of these principal uranium bearing formations. The deposits ring the Gulf Coast inland approximately 100 miles. Known deposits sweep from western Starr County to Duval County through McMullen and Live Oak County and proceeds diagonally on up the state. At the moment, the largest number of active mines are in Karnes County. The deposits which have been worked first were relatively shallow. Typically, they are narrow in width and stretch along a distance many times the width. This band is termed the "roll front". Figure 2, (photo of area), is a view from the air showing how these long trenches extend through the county as the mines are developed.

Eargle (1,2,3) describes the rock characteristics as follows: "Host rocks of the South Texas region are chiefly sands and sandstones that contain volcanic ash and are of relatively high permeability. The sands are interbedded with bentonitic clays and tuffaceous silts that locally are almost pure volcanic ash. Most of the volcanic material has been diagenetically altered by weathering and soil-forming processes that probably took place during periods of dry climate (Weeks and Eargle, 1963).

"The Eocene rocks of the Karnes area contain considerable amounts of carbonaceous material and thin beds of impure lignite. The sands there are shallow-marine, deltaic-lagoonal, and strand-plain barrier-bar deposits laid down near the shores of gentle slopes and extending out to continental shelves. These are cyclic deposits, however, interbedded with near-shore carbonaceous swamp deposits and with beds of almost pure ash of acid volcanics, generally water laid and of fine texture. The sands are generally fine to very fine grained; only a few beds of medium or coarse grains--generally channel deposits--are found. They have a relatively high percentage of lithic (volcanic-rock) fragments and contain quartz, feldspar, and a small amount of mica.

"The host rocks of the Live Oak district are fluvial sands, which, interbedded with silts and clays, extend laterally along the strike from a central alluvial system (Klohn and Pickens, 1970). The system, about 300 feet thick, extends southeastward through central Live Oak County, nearly normal to the strike of the Oakville Sandstone. Thus the host rocks are flood-plain deposits that grade laterally into finer grained deposits. It is believed that the circulation of ground water is restricted in this stratigraphic setting, giving ample opportunity for the precipitation of uranium from solution."

The classical roll front configuration of uranium ores consists of an interface separating oxidized (hematite and goethite-bearing) arkosic sandstone from material containing a reduced (pyrite + uraninite + coffinite + jordisite) mineral assemblage. The roll con-

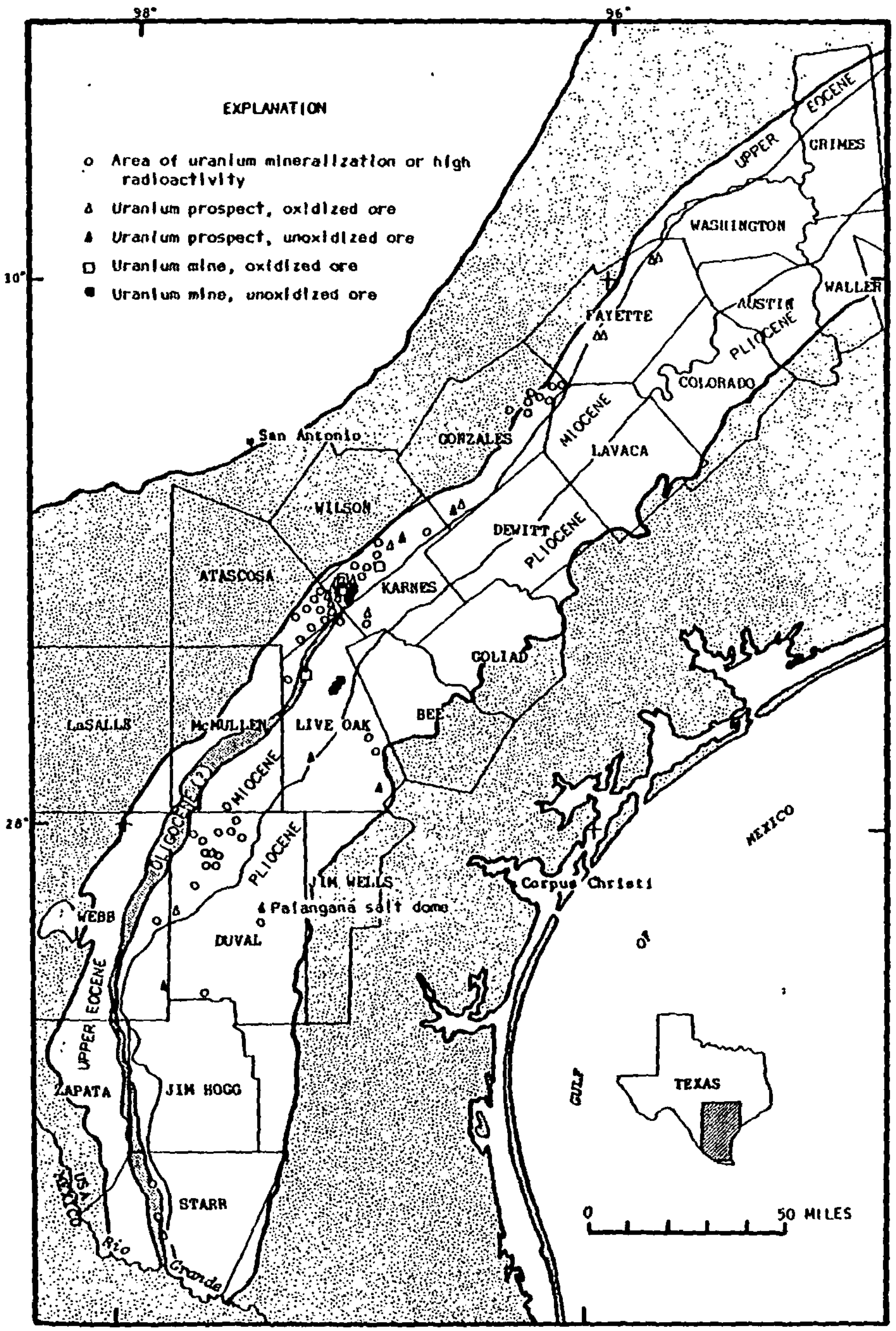

FIGURE I SOUTH TEXAS URANIUM MINERALIZATION

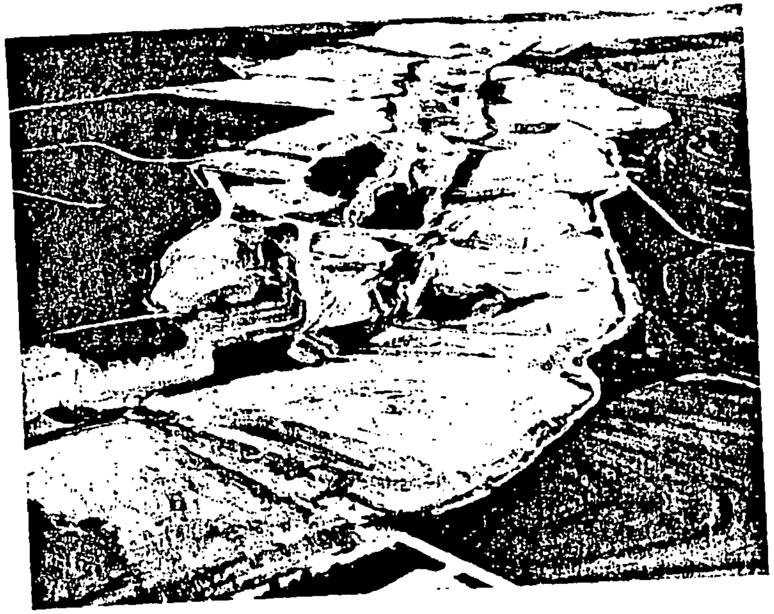

FIGURE 2 AERIAL PHOTOGRAPH OF URANIUM AREA

figuration is rather complex because the sandstone aquifer in the mineralized area is fine grained and contains numerous clay-rich intervals which act as permeability barriers and tend to split the sandstone into relatively thin parallel transmissive zones. In general, the updip portion of the sandstone is oxidized and barren; whereas, the downdip portion is pyritic and reduced. Mineralization is localized at the interface between the oxidized and reduced zones.

The sands are usually lenticular in cross-section, and both thins and becomes silty to the northwest and southeast. Groundwater transmissivity is dominantly parallel to the strike of the lens - in a southwest to northeast direction parallel to the trend of surface outcrops and of the coastline. The downdip position of mineralization is related to a geochemical front, and this in turn is related to stratigraphic position within the lens. The geochemical front appears to be localized at least in part by loss of permeability on the downdip side resulting from thinning of the sandstone and appearance of a greater proportion of clay in the sandstone interval.

Mineralization along the redox interface has a strike length of at least 10,000 feet, but is highly variable as regards grade over this distance. Figure 3 gives an idea of the nature of the ore zones, the oxidized and residual zones, and the comparative permeabilities which can be experienced along the roll. Permeability variations in the sands varies from 1000 md to impermeable streaks (less than 10 md). In addition, it has been observed that the permeability decreases due to uranium deposition within the permeable sands. Thus one can encounter a wide range of permeabilities through the ore zone.

Figure 4 illustrates the elonganted nature of the roll front. From the complex nature of the ore deposits it is obvious that the maximum of data as to location of the mineralization, type of clays, occurrence of pyrite and carbonaceous material, carbonate content, identification of the uraniferous minerals, state of oxidation, ground water analysis, ground water movement and level should be obtained. Thus it is highly important that the geological parameters of a deposit should be thoroughly investigated in the preplanning of any in situ mining operation. Flawn (4).

Recovery Factors

In planning the in situ leach program three important factors related to recovery are evident; (1) the injectivity response, (2) the solution kinetics to solubilize the uranium, and (3) the displacement mechanism which will optimize the concentration of uranium in the produced solution. For the purposes of this paper, the recovery of uranium from the solutions and purification techniques will not be discussed. It is assumed that the existing techniques of solvent extraction, ion exchange, etc., can be used. The importance of maintaining a high uranium concentration in the extracting liquor is obvious, however, to an economical extraction process. Consequently,

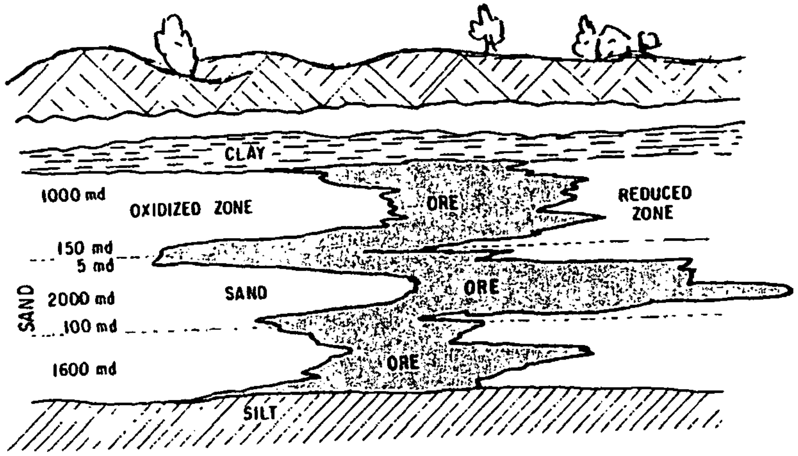

FIGURE 3 ROLL FRONT MINERALIZATION

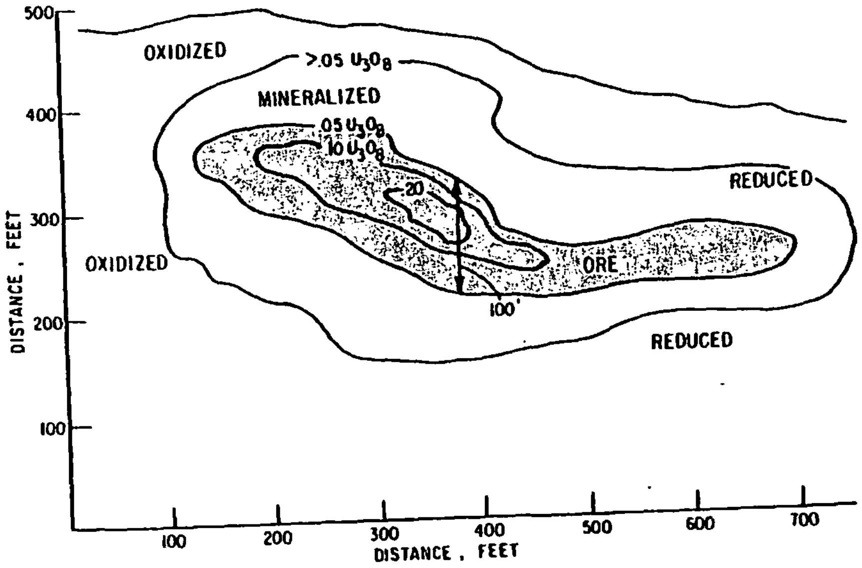

FIGURE 4 PLAN VIEW - ROLL FRONT

one of the primary objectives in the production practice is to operate so that maximum concentration uranium solution is produced with a minimum volume of injected fluid.

Injectivity Response: Considerable literature exists in the petroleum technological literature which is applicable to the problems of injectivity. The work done on the compatability of injection water in water flooding, and in the operation of brine and waste water disposal wells should be in hand in order to evaluate the parameters of handling and producing satisfactory injection solutions. The tendency of the injection fluid to plug, due to precipitation at the well face, or to cause a decline due to interaction with the clay minerals is important to know before flooding. Proper selection of solvent and composition of the extraction solution should be made to minimize these injection problems. Gupta and Jessen (5) investigated the response of several solutions as well as dissolution rates on Texas Uranium Ore showing that there was a definite decline with both acid and alkaline leachments due to interaction with the clay minerals. Their data indicated that the addition of sodium chloride aided the injectivity without decreasing uranium recovery. For these reasons, it is felt that injectivity response to a representative number of cores is important to planning a successful *in situ* fluid.

Kinetic Factors: For optimum recovery of uranium, rapid and complete dissolution of the uranium minerals and no subsequent precipitation of uranium compounds is necessary. Thus, the knowledge of the rates of solution of the various soluble minerals present and their solubility in the extracting solution is essential. The choice of extractant solutions are similar to the choice in the hydrometallurgical processes in use in the present agitation leach extraction systems. While the agitated leach data is useful for determining the response of the ore to acid or alkali leaching solutions, the problems encountered by depositional plugging, variations in oxidation of the uranium minerals, and interaction with reducing compounds (sulfides, carbonaceous material, etc.) can only be estimated by core flooding experiments.

The techniques of meaningful core flooding experiments are important. Sievert, Martin and Conley (6) describe their method used in North Dakota sandstone. Representative samples of South Texas ore are very difficult to obtain due to the unconsolidated nature of the formation. Care also should be made to maintain both the rock and contained fluid as close to reservoir conditions as possible as difference in oxidation state are important in the response of the uranium mineral to extraction.

A typical extraction curve using sulfuric acid is shown in Figure 5. The solubilized mineral values and pH is shown in relationship to the volume throughput in relation to pore volume. This type of information is important as it gives some idea of the composition of the solution which could be produced at various times of injection

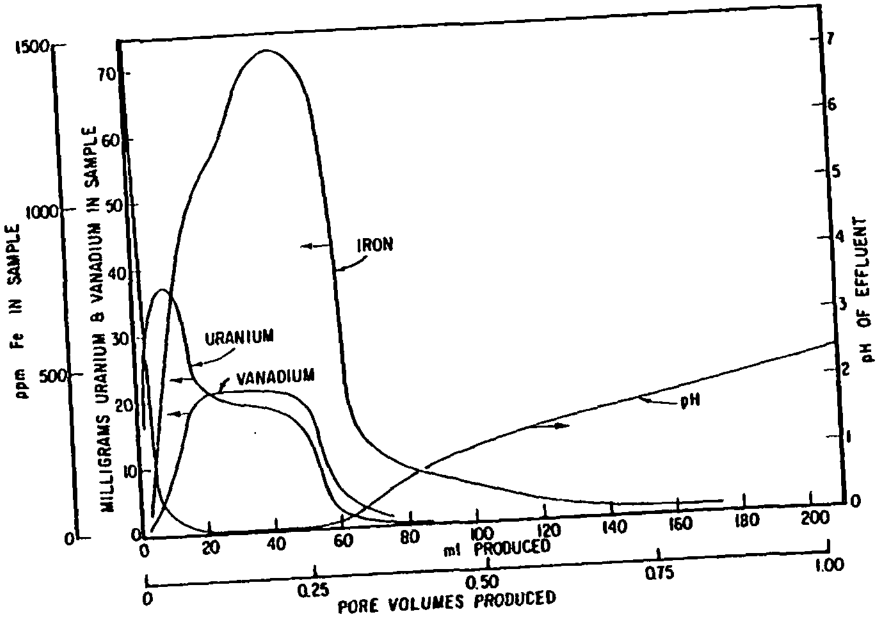

FIGURE 5 TYPICAL RECOVERY CURVES FOR AN ACID LEACH OF A URANIUM BEARING SANDSTONE

history, the possible mixtures and possible concentration. In this particular case, practically all uranium recovery is complete by the time one-half a pore volume is swept through the core. The values for iron and vanadium come to a maximum at considerably different places than the uranium, so one could expect quite a variable concentration difference if the solubilizing sweep contained only the composition of the produced fluids. These concentrations would be those seen if the displacement were a line drive. As will be discussed later, these are not the concentrations which can be expected in a radial displacement extraction system. The limit of concentration of an individual extractant can become quite complex if the solubility is exceeded and secondary deposition occurs. Also, since the other metallic constituents are varying in concentration, there can be double salts formed which limit solubilities or rates of extraction. The object of the investigations of the linear displacement or kinetic studies, therefore, is to ascertain what can happen under the optimum displacement conditions.

Displacement Studies: When a fluid is injected into a porous rock which is fluid filled and the fluid has internal reservoir pressure, the fluid flow and extractive concentrations become considerably different than those represented by the linear extraction experiments. The pore volumes increase rapidly with distance from the well until the radius becomes quite large. Thus at 1 ft from the injection well at 30% pore space, the pore volume is approximately 1 cu ft per foot height. At 50 feet this pore volume per foot is 93 cu ft. The zone of concentrated liquid thins considerably due to this radial expansion. If the wells are in an unconfined reservoir, as is the case of all water filled ore bodies, the problem of suitable displacement recovery becomes one of choosing the optimum well spacing and configuration. As pointed out by Sievert, et al (6), the usual five spot flood pattern in an unconfined reservoir will produce a thin high concentration zone, the displacement liquids break through quite rapidly, and then the wells produce a solution which decreases rapidly in uranium concentration. The sweep drives the concentrated liquid zones on beyond the producing wells.

In dealing with various recovery processes and predictive reservoir recovery methods, our production research group has evolved the capability of mathematically modeling the system and obtaining printouts via the data plotter so that various recovery gains can be compared. Uranium extraction by leaching is similar enough to the removal of oil by imiscible displacement, that it was felt that the oil recovery methodology would be applicable. The extraction curves determined by Sievert, et al, were used as the typical extraction and displacement values which would be expected in the flood. The permeability of the entire zone was considered to be the same and the rate of production from the injection wells was held to be equal from each of the production wells. Thus if 100 gal/min were injected in the center of a five spot, the four production wells would produce 25 gal/min each.

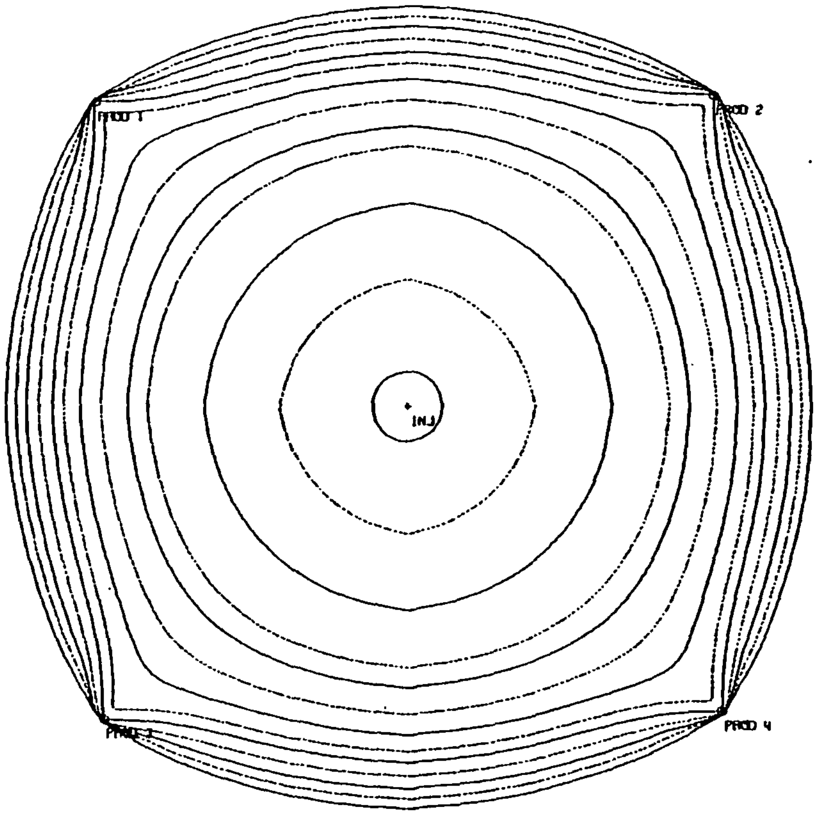

FIGURE 6 DISPLACEMENT PATTERN-UNCONFINED 5-SPOT

Figure 6 is the computer printout showing the advance and drain of the uranium solution front. The printout clearly shows the usual cusping effect at the producing wells. Taking the values for the extraction experiment and the dilution factors from the flow calculation, the recovery from the four wells are plotted in Figure 7. This curve illustrates how the passage of the front gives produced solution of maximum concentration and then the concentration tails out for a long period. The economic recovery becomes quite problematical. The recovery up to two pore volumes is estimated at 55% by integrating the values under the curve. It is clear that this recovery system should be improved.

By drilling two additional wells on the sides of a five spot we create a thirteen spot flood. Figure 8 shows the computer printout on what may be termed a thirteen spot pattern. The recovery calculation is very interesting in that the edge wells contribute to the early production of uranium solution. A double maximum exists by virtue of the front passing these edge wells. The recovery calculation showed some 68% by this technique as shown in Figure 9.

This computer routine is capable of producing an unending series of cases with interesting implications. One of the most interesting results was the case of the confined five spot. In this situation, it was assumed that a rigid barrier exists along the edges. The injection fluid proceeds to break through, but rather than the high concentration solution passing and diluting the uranium, the edge concentration zone is forced to the producing wells. Figure 10 displays the computer printout and Figure 11 the recovery curve calculated from the computer printout. It is noteworthy that the concentration curve comes to a peak value considerably higher than the other two cases and falls to a very low value at only 1.7 pore volumes of injected solution. It is also worthy of note that the system yields approximately 100% displacement recovery.

It is realized that the maintenance of a true confined barrier is probably impossible; however, these theoretical values makes it quite evident that the manipulation of this extracted zone is important to recovery and worthy of considerable consideration in planning an in situ recovery test for the fluid.

CONCLUSIONS

Bore hole mining holds considerable attraction as a possible method of recovering values from lower grade ores than now workable, at greater depths, with less disturbance to the environment. The in situ method should be considered as a possible method in mining the secondary uranium of South Texas. In order to accomplish this, a considerable effort must be made to design the floods properly. Much research work needs to be done to determine the critical variables necessary for a successful extraction system. Besides the

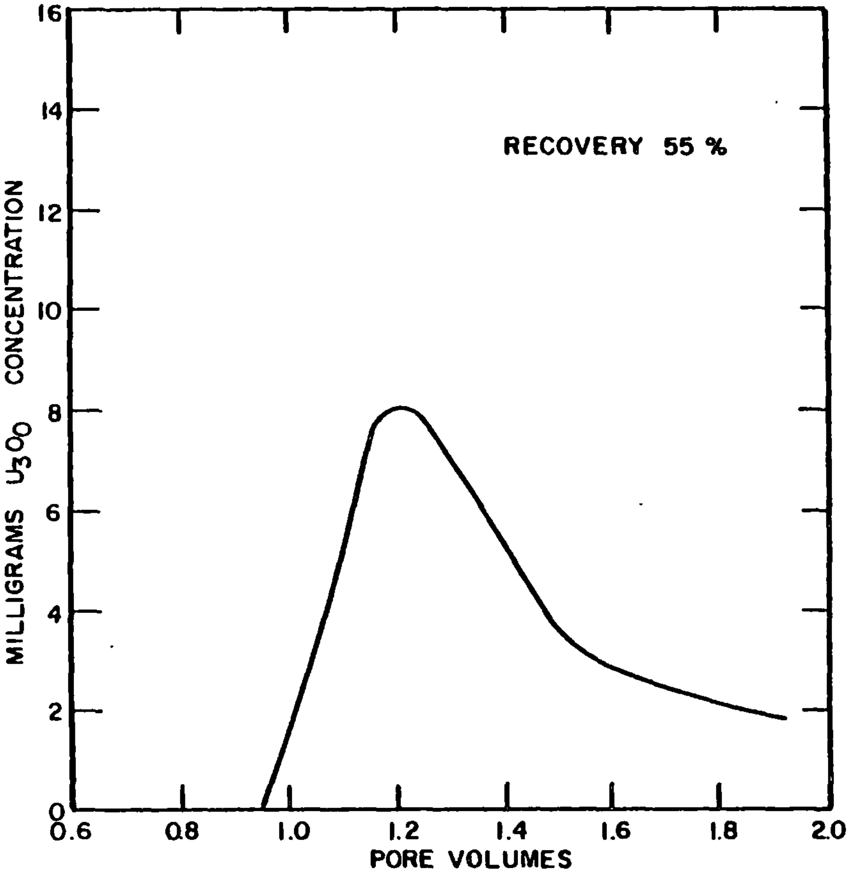

FIGURE 7 RECOVERY FROM UNCONFINED 5-SPOT

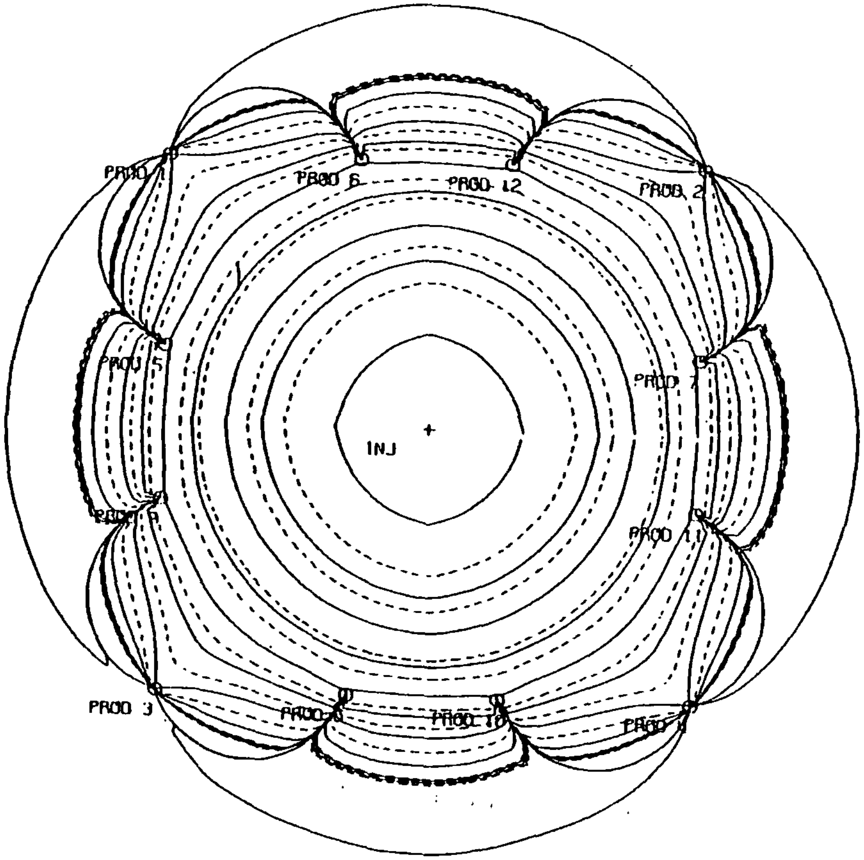

FIGURE 8 DISPLACEMENT PATTERN –UNCONFINED 13-SPOT

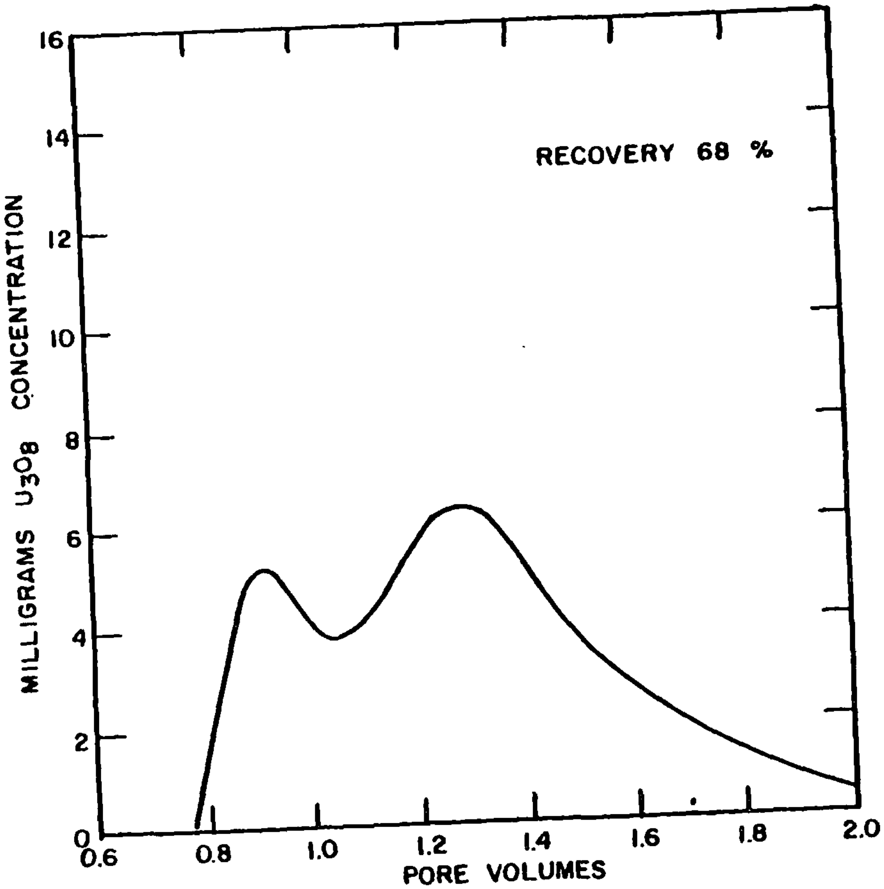

FIGURE 9 RECOVERY FROM UNCONFINED 13-SPOT

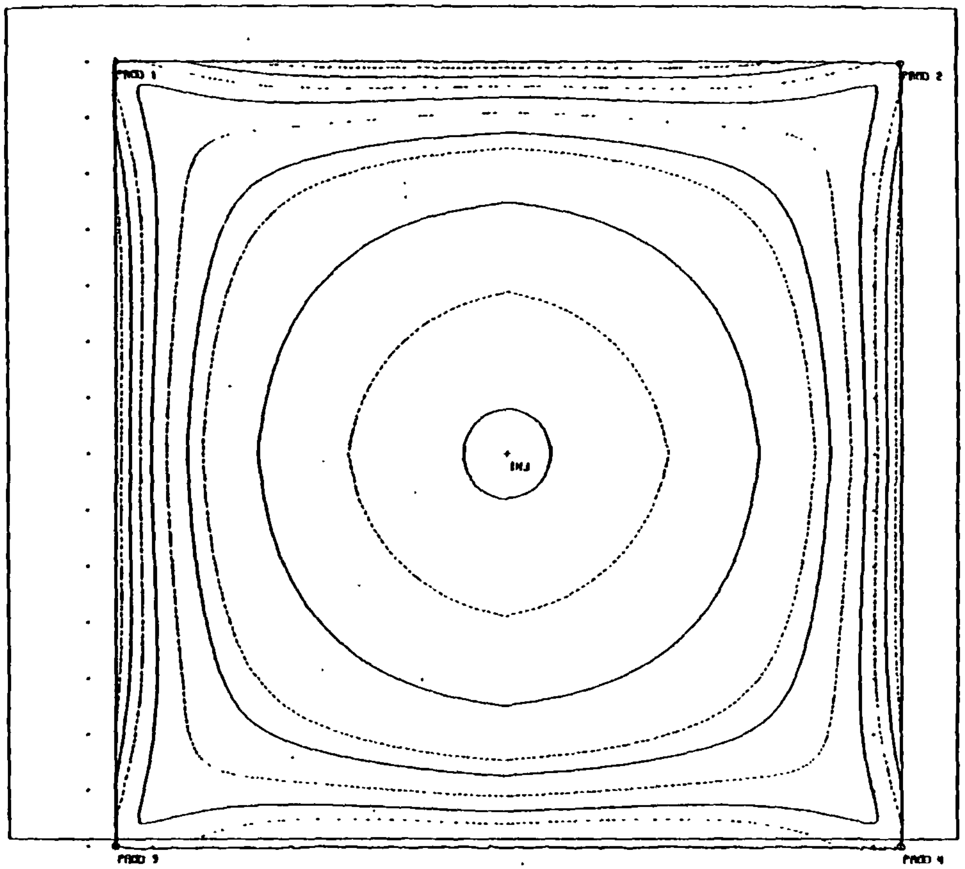

FIGURE 10 DISPLACEMENT PATTERN - CONFINED 5-SPOT

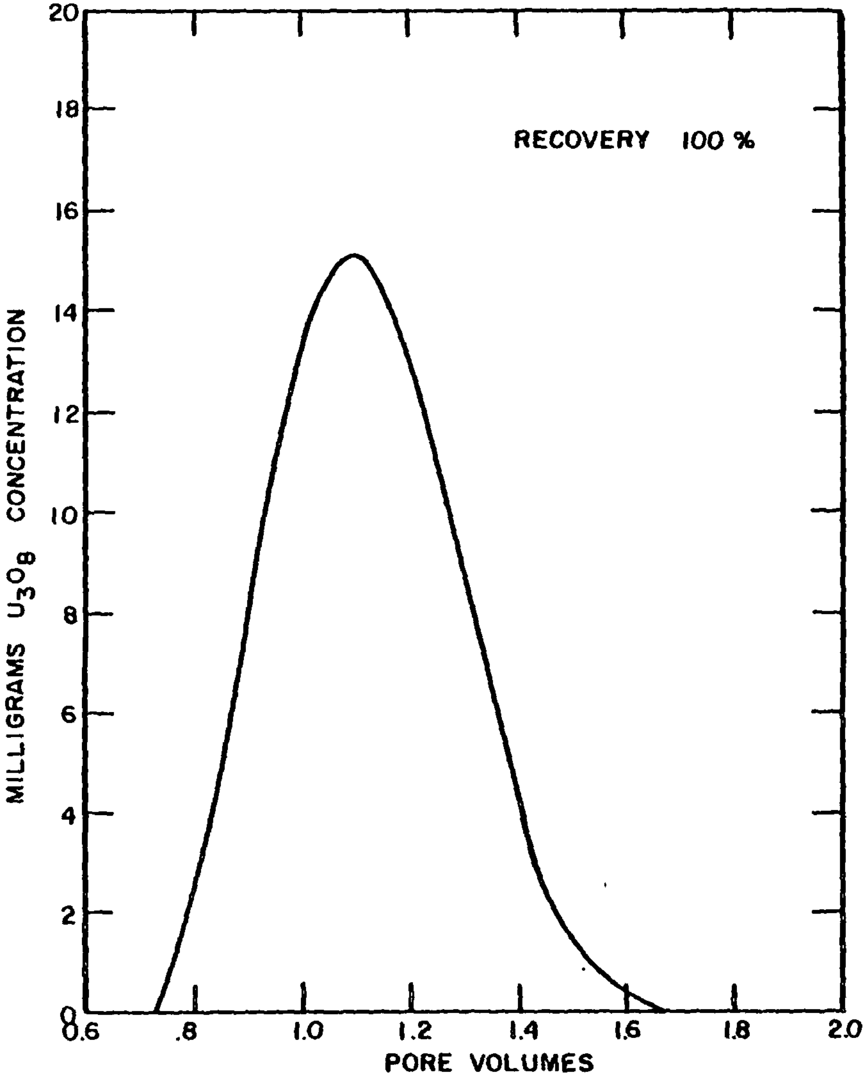

FIGURE II RECOVERY FROM CONFINED 5-SPOT

factors normally examined in ore extraction methods, the in situ extraction method must consider the geological parameters, a detailed reservoir study, injectivity tests, extraction tests, and finally a careful study of displacement methods.

REFERENCES

1. Eargle, D. H., Hings, G. W., Weeks, Alice M. D., "Uranium Geology and Mines, South Texas," Guidebook Number 12, University of Texas at Austin, Bureau of Economic Geology (1973).

2. Eargle, D. H., "Geology of The Karnes County Uranium Area South Central Texas," U. S. Geological Society, Vol. 7, No. 4, (Aug. 1959).

3. Eargle, D. H., and Snider, J. L., "A Preliminary Report on The Stratigraphy of The Uranium Bearing Rocks of The Karnes County Area, South Central Texas," Report of Investigation No. 20, State of Texas, Bureau of Economic Geology.

4. Flawn, P. T., "Uranium in Texas," Texas Bureau of Economic Geology, Geological Circular No. 67-1 (1967).

5. Gupta, B. S., and Jessen, F. W., "Batch Leaching of A Texas Uranium Ore," M.S. Thesis, The University of Texas at Austin, July, 1971.

6. Sievert, J. A., Martin, W. L., and Conley, F. R., "In Situ Leaching of Uranium," Presented at the SME Fall Meeting, St. Louis, Missouri, October, 1970.

Chapter 7

FLUID FLOW AND MASS TRANSPORT IN FRACTURED ROCKS

Hossein Kazemi and John F. McElhiney

Marathon Oil Company
Littleton, Colo.

ABSTRACT

This chapter is a review of fluid flow and mass transport in fractured rocks. The topics include: single-phase and multiple-phase flow theory, formation productivity or injectivity improvement by artificial fracturing, and mass transport associated with fracture acidizing. Possible extension and application of such ideas to in situ mining in fractured rocks are presented.

The full text of this chapter is available
as SME Preprint No. 74AS53.

Chapter 8

FLUID RETENTION IN LEACH DUMPS BY CAPILLARY ACTION

Dr. William A. Kennedy and Jonathan R. Stahl

Department of Minimg and Petroleum Engineering
New Mexico Institute of Mining and Technology
Socorro, New Mexico 87801

ABSTRACT

This paper deals with the phenomenon of water held in a leach dump due to capillarity. Water is shown to be retained in the fine pores of the ore as well as in the interstices between the rock and soil particles. Upon drainage, Chino leach dump material shows two distinct capillary systems and a double capillary curve is often obtained.

Both the igneous and the sedimentary rocks composing the leach material are shown to have appreciable porosity but little permeability. Fluid flow is, therefore, restricted to the interstices between the rock and soil particles. The irreducible water saturation for the aggregate is found to be 88% for the -48 mesh material and 23% for the +48 mesh to one inch material. The composite sample of minus one inch dump material had an irreducible water saturation of 52 percent. The irreducible water saturation in the fine pores of the ore was found to be between 73 and 76 percent. Very coarse pores or channels between large rocks exhibit essentially zero capillary retained water.

The presence of fine material in a dump can cause high water saturations to be retained and these saturations may be mistaken for perched water tables. Perched water tables can be drained but capillary water will be retained. Capillary pressure data can aid in distinguishing between perched water tables and capillary retained water.

SUBJ
MNG
SMIS

SOLUTION MINING (*IN SITU* LEACHING)

A Literature Survey

by

J.A. Lackey

Abstract

The current state-of-the-art of solution mining or 'in situ' leaching is reviewed and the major aspects of technology and techniques described. This method has received increasing attention in the last few years as it offers attractive possibilities in improving the environmental impact of mining, utilisation of the whole of the ore, and cost of savings in comparison with conventional mining and treatment of ore. While the extraction of evaporites, sulphur, etc., by solution mining is well-established, emphasis is placed in this review on the extraction of metals from their ores — in particular, uranium.

1. INTRODUCTION

Solution mining, or *in situ* leaching, is defined as the use of solutions in extracting metal values from broken or unbroken ores within the mine. This technique has been applied commercially at a number of locations and has received increasing attention in the past few years. The reason for the upsurge in interest is that the method offers attractive possibilities in improving the environmental impact of mining, utilisation of the whole of the ore, and cost-savings in comparison with conventional mining and ore-treatment.

Awareness of environmental factors which inhibit the mining industry has been growing over the last few years. The mining method which leaves the earth undisturbed is an impossible goal; however, the method which violates the earth the least surely should be rigorously considered. Solution mining fulfils this potential to a great degree; however, it should be pointed out that this method is not without its environmental problems.

Leaching solutions must be controlled so that they are held within the orebody, otherwise ground-water contamination could be a problem.

In situ leaching appears to be a promising possibility for smaller, lower-grade orebodies and deeper reserves, or in difficult-to-mine areas, provided the nature and disposition of the mineralised and surrounding rock meet certain conditions.

Solution mining also potentially offers some advantage from an economic viewpoint. If the production of minerals values can be realised early in the life of the development of the deposit, this method can have a major advantage over conventional mining systems because of the earlier return on investment. In other words, the high initial investment associated with opening a mine by conventional methods requires high financial returns to cover the investment, and this generally requires continuous processing over many years. *In situ* leaching, on the other hand, should be relatively inexpensive as regards capital cost and, provided operating costs are not excessive, return on investment should occur in a relatively short period of time.

2. THE PROCESS

In solution mining, as in other leaching operations, there are four factors that are normally necessary for the successful leaching of ores (Hardwick, 1967):

(1) A solution that will attack the valuable minerals must be brought into contact with the particles of ore.

(2) The minerals must be dissolved by chemical action of the solution.

(3) The solution must find its way out of the voids of the rock and be recovered in a collecting system.

(4) The valuable element in solution must be recovered from the solution.

A variety of techniques have been tried, described or proposed in the literature to achieve these four steps. Different types of solution mining operations have used different treatment methods for these steps; these operations can be separated as follows:

(1) Unfractured orebodies.

(2) Fractured orebodies.

(3) Stope leaching — leaching of both unfractured ore and ore piles (fractured) in the mine.

2.1 Unfractured Orebodies

Methods of applying solution mining to unfractured orebodies rely on the natural permeability of the native ore to ensure solution dispersal. A number of patents have been issued on this subject, of which the earliest of interest is by Livingston (1957). He proposed a system for leaching mineral values *in situ* in which the leaching solution was injected into the native ore through boreholes or wells. His process recognised the need for controlling the flow of the underground leach solution so that the mineral values could be recovered. The approach was to drill a multiplicity of wells for injecting and producing the fluids and to interchange rates of the various wells from time to time in order to control the fluid behaviour within the orebody. To keep the fluid from escaping to the surrounding barren rock, he suggested emplacing a grout curtain around the entire orebody.

Dew and Martin (1960) proposed an *in situ* combustion scheme for the oxidation of uranium to the hexavalent state and simultaneous removal of the carbonaceous material associated with the mineral values. Following this oxidation process, a hot *in situ* leach was suggested to recover the uranium values. Again, injection and production wells were proposed as the method of solution dispersion and withdrawal respectively.

A method proposed by Martin (1964) made use of fluid-flow technology to inject water or a mixture of gaseous carbon dioxide and water, perhaps in the presence of surface active agent, as the leaching solution.

Hurd and Fitch (1966) and Fitch and Hurd (1966) recognised the problem of formation plugging in their patent for subterranean leaching of minerals (in particular, the leaching of phosphate ores). To circumvent the problem, they considered generating the acid leach solution *in situ*. Initially, water was to be injected to fill the formation, followed by an acidifying gas. The solubilised mineral was then to be propelled to a producing well bore. Such a process is closely allied to gas injection methods used to recover petroleum.

Fitch and Hurd (1967) also recognised the containment and flow-control problem which can occur in a permeable deposit that is initially dry. Their solution to the problem involved filling the orebody and part of the surrounding formation with an inert fluid, so that both vertical and horizontal fluid-control was maintained during the subsequent leaching step by controlling the relative injection rates of the inert fluid and the solvent.

Gardner and Ritchie (1967) specified that for their control system to work, the orebody had to be below the natural water table. They suggested using the natural water in much the same manner as Fitch and Hurd (1967) used injected water. Flow-control within the area of interest was to be obtained by surrounding a producing well with several injection wells. Monitor wells were to be placed beyond the injection wells to indicate where the fluids were going and to help control the pressure in the area surrounding the injection pattern. The process also involved a complete filling of the flooded area with leach solution, after which injection and withdrawal rates were to be kept equal.

While these procedures are generally technically feasible and some of the inventors have recognised problems that are peculiar to *in situ* leaching — e.g., plugging of the pores in the orebody (Hurd and Fitch, 1966) — they do not offer anything sufficiently substantial to commercialise this technique. However, *in situ* leaching has been commercialised at one location — Shirley Basin Uranium Mine, Wyo (Anderson and Ritchie, 1968). Basically, this operation consisted of inflow and production wells as has been previously proposed. However, the following criteria were considered to exist for the process of solution mining to be successful:

(1) The mineral values should occur in a generally horizontal bed underlain by a relatively impermeable stratum.

(2) The ore must occur below the static water table.

(3) Direction and velocity of regional water flow must be known.

(4) Mineralogy of the ore should be determined so that its amenability to the proposed leaching process may be assessed. Material recovered by core drilling was considered to be normally sufficient to make this determination.

In situ leaching of copper was tested at pilot-plant scale at Kennecott's Kimbley pit — Anon. (1971a). The section of orebody remaining from an open-cut mining operation had a steep face that allowed an adit to be driven under the orebody for the collection of leach solution. Liquor was injected into holes from above and collected in a dam in the adit. This operation was not successful because overall solution recoveries were very low, probably due to high strata permeability in the vicinity of the adit.

Laboratory testing involving leaching slabs of ore (to simulate solution mining) has been carried out by Sievent, Martin and Conley (1970). While these tests indicated good metal extraction efficiencies, they did not indicate what sort of solution recoveries could be expected. Mathematical modelling to simulate solution mining was used to investigate various geometric patterns for injection and production — Sievent, Martin and Conley (1970) and Shock and Conley (1974). Solution injection into liquid-saturated and dry reservoirs was studied and, in general, overall recoveries were found to be low except for the case of confined orebodies — i.e., similar to the findings of Anderson and Ritchie (1968).

While solution injection and recovery are important to the successful mining operation, the chemical environment must also be carefully studied. Precipitation of any species in the orebody must be discouraged, as this will tend to block or plug the cracks and fissures in the orebody, greatly reducing the percolation rate. This problem was recognised by Hurd and Fitch (1966). For many systems, precipitation is inevitable (e.g., leaching of most sulphides) and this could mean that solution mining of the unfractured orebody is not likely to be successful. Where sulphuric acid is used as the leachant, it is important that operations commence with dilute acid (1 to 1.5 *g/l*) so that dissolution of calcium from limestone (which generally is preferentially attacked) will not exceed the solubility product of $CaSO_4$ (Anderson and Ritchie, 1968). When free acid appears in the effluent, this indicates that any deposition of gypsum will be minimal and acid strength in the inflow well can be increased. Care must also be taken to avoid the precipitation of basic iron sulphates by ensuring that sufficient acid will remain in the production well to keep pH <2.5. If an oxidant is needed for the leaching of the valuable mineral (e.g., uranium) a water-soluble oxidant such as ferric ion or sodium chlorate must be used.

Many orebodies have natural permeabilities that are too low for *in situ* leaching operations. For these orebodies, there are a number of techniques that can be applied to increase solution throughout — for example, addition of flocculants to the injection fluid (Anderson and Ritchie, 1968) and introduction of a high-pressure water jet into the injection wells (Anderson and Ritchie, 1968; Anon., 1971b; Daneshy, 1974). In the former method, synthetic flocculants such as the polyelectrolytes have been found to be suitable at dosages of 5 to 10 mg/*l*. The latter method is hydraulic fracturing of the orebody and will be described more fully in a later section.

In conclusion, the basic criteria considered by Anderson and Ritchie (1968) to exist for the success of an *in situ* leaching operation appear still to hold (i.e., the ore must occur below the static water table and must occur in a generally horizontal bed underlain by a relatively impermeable stratum).

2.2 Fractured Orebodies

If natural permeability is insufficient to allow satisfactory percolation rates through the orebody, fracturing may provide an economic alternative. There are a number of techniques for accomplishing ore fracturing:

(a) Hydraulic fracturing.

(b) Blasting — chemical or nuclear.

(c) Ore subsidence due to conventional mining in adjacent areas.

2.2.1 Hydraulic Fracturing

Hydraulic fracturing is a well-established and extensively-used means of stimulating oil and gas wells. It has been commercially used since 1949 with approximately $^3/_4$ million fracturing treatments being completed by the oil industry throughout the world (Daneshy, 1974).

The first stage of a fracturing treatment is initiation of the fracture. To achieve this, fluid is pumped into the well until the resulting pressure exceeds the resistance of the formation, at which point a hydraulic fracture initiates. Fracture initiation is identified by either a sudden sharp drop in the fluid pressure or an increase in the ability to pump fluid. This stage of the process may be absent in cases of refracturing or when the well-bore is already naturally fractured.

The next stage of the process is extension of the initiated fracture. Fluid injected after initiation will flow into the fracture and force its extension. The extent of fracture propagation depends on the volume of fluid pumped plus formation and fluid properties. At a certain point during fracture extension a propping agent is mixed with the treatment fluid and pumped into the fracture. The purpose of this operation is to keep the fracture open and conducive to fluid flow after the treatment termination.

The flow-rate of a fluid into or out of a hydraulically fractured well is normally much larger than that from a well without a fracture. Two reasons can be given for this (Daneshy, 1974): (a) the fracture establishes contact with more of the formation than the well-bore alone; (b) the flow-mode is almost linear in the presence of the fracture and radial in its absence.

The hydraulic fracturing technique has been partially applied at Shirley Basin (Anderson and Ritchie, 1968) using a high-pressure jet of water to increase solution throughput without using a propping agent for fracture extension. It was considered (Anon., 1971b) for the pilot-scale *in situ* leaching of copper. Hydraulic fracturing has also been very effective in exploiting salt bodies (Daneshy, 1974).

Since the fracturing is simply created from the pumping of high-pressure water through a formation, this technique has the advantage that there are no location restrictions as there would be with blasting (e.g., near buildings, etc.).

The restrictions placed on the shape of the orebody (ground water level, ore being underlain by relatively impermeable strata as detailed by Anderson and Ritchie (1968), and the chemical environmental restrictions of no precipitation in the orebody) will be as applicable to hydraulically fractured orebodies as to unfractured orebodies.

While there is little quantitative information as to the effectiveness of hydraulic fracturing in promoting solution throughput for *in situ* leaching the wide acceptance of the method in the oil industry indicates that it should be seriously considered for *in situ* leaching. It is considered that this method should give marked improvement over *in situ* leaching of unfractured orebodies provided that fracturing occurs at moderate pressures. Also, it would be unnecessary to consider this technique for naturally fractured, highly permeable formations.

2.2.2 Blasting

There are two types of explosives that warrant consideration for the fracturing of deposits — chemical and nuclear.

The consideration of using controlled nuclear explosives for the breaking of ore and subsequent *in situ* leaching has received a great amount of attention in the literature (Hansen, 1965; Wilson, 1965; Anon., 1967b, c; Hardwick, 1967; Jackson, 1967; Chopey, 1968; Lewis *et al.*, 1974) although this method is yet to be used commercially. The use of chemical explosives (ammonium nitrate; fuel oil) has, however, been used at two locations in the USA (Anon., 1972; Longwell, 1974; Ward, 1974).

A considerable amount of research has taken place into studying the effects of buried nuclear explosions on the surrounding rocks (Hansen, 1965; Wilson, 1965; Hardwick, 1967; Jackson, 1967; Chopey, 1968; Lewis *et al.*, 1974). From deeply buried nuclear explosions, vaporised rock and metal at temperatures greater than 10^6 degrees centigrade and at pressures of several million atmospheres surround the explosion centre at the instant of detonation. The gas-filled cavity expands nearly spherically until its internal pressure decreases to a level approximately equal to the weight of the overburden. The cavity reaches its full diameter in a few hundred milliseconds.

A shock-wave, passing through the rock surrounding the nuclear explosion, expands radially, but much more rapidly than the cavity boundary. This shock-wave travels initially at velocities of hundreds of thousands of metres per second, but decreases to a level of between 2000 to 6000 m/sec within 300 metres or less of the centre of detonation. Initially, the stresses associated with the shock-wave so far exceed the rock yield strength that the rock responds like a fluid. As the shock-front moves further outward from the explosion centre, the peak stresses in it attenuate rapidly. When peak shock-stresses have dropped to within 10 times the rock's dynamic yield strength, the rock begins to respond in a plastic manner. At greater distances, the stresses decrease to the elastic range.

Initially, the walls of the cavity are lined with a few centimetres of molten rock which flows and drips under the influence of gravity to the bottom of the cavity, where it collects in a puddle. After cooling, the molten rock forms a hard, slag-like, non-water- and non-acid-soluble glass which contains up to 95% of the radioactive fission products.

The roof of the cavity collapses shortly after the explosion in most types of rock and progressive collapse continues upwards above the cavity, until the swell of broken rock equals the volume of the original cavity and the broken rock mass supports the upward arch. The roughly cylindrical-shaped mass or 'chimney' of broken rock develops above the shot point to a height about 4.5 cavity radii, although its exact height is a function of the energy of expansion, the depth of burst, and the characteristics (including the water content) of the rock.

Fractures produced by the explosion and subsequent subsidence extend outward from the cavity and chimney boundaries into the surrounding rock. A zone of substantially increased fracture permeability has been measured laterally out to almost two cavity radii beyond the chimney and up to three cavity radii above the top of the chimney. However, extensive fracturing in rock beneath the bottom of the cavity has been observed only within about ½ cavity radii of the lower boundary. A zone of compacted rock with reduced permeability has been shown to exist, surrounding the lower hemisphere of the cavity.

At intermediate sealed depths of burst shallower than containment, the force of explosion shatters the overlying rock and imparts sufficient velocity to hurl the rock nearly vertically upward from the crater. A mound of rubble in the crater results from the bulking of the explosion — broken rock that has fallen back into the crater.

The voidage from these controlled explosions has been found to be about 25%. Curves have been developed to show the cavity radius as a function of the depth of burial (Fig.1), the chimney height as a function of the depth of burial (Fig.2) and the tonnages of rock broken as a function of the depth of burial (Fig.3) for different yields.

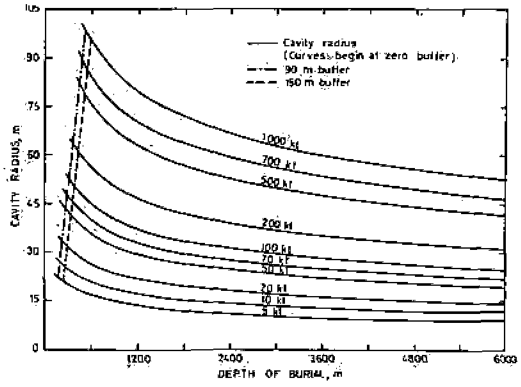

FIG.1: CAVITY RADII FOR CONTAINED UNDERGROUND NUCLEAR EXPLOSIONS IN GRANITIC ROCK
Reproduced from *Hardwick (1967)*

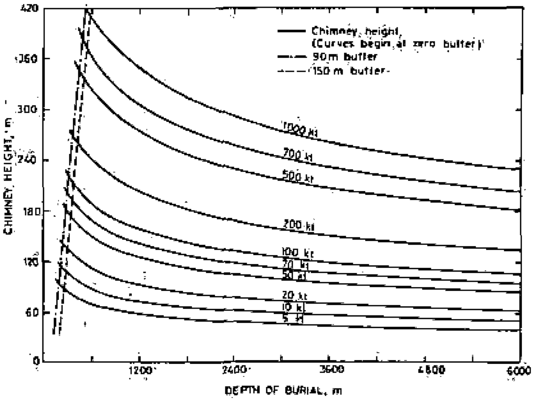

FIG.2: CHIMNEY HEIGHTS FOR CONTAINED UNDERGROUND NUCLEAR EXPLOSIONS IN GRANITIC ROCK
Reproduced from *Hardwick (1967)*

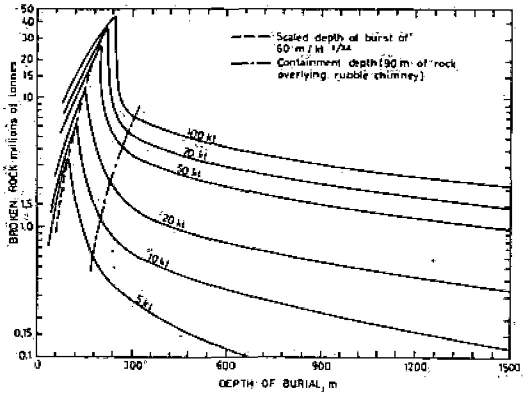

FIG.3: TONNAGE CURVES OF ROCK BROKEN BY INTERMEDIATE UNDERGROUND NUCLEAR EXPLOSIONS
(Reproduced from *Hardwick (1967)*

While chemical explosions, by comparison, produce initial pressures about one order of magnitude lower than nuclear explosions, it is expected that similar explosive energy yields will produce similar tonnages of rock breakage. Table 1 compares the cost of explosive energy for TNT, dynamite, ammonium nitrate-fuel oil (ANFO) with the kiloton nuclear explosives. Table 2 gives the projected charges for thermonuclear explosives and includes AEC charges for nuclear explosives and their arming and firing; emplacement and related engineering costs for site development and support and other miscellaneous costs. Not included are direct costs for safety studies which vary greatly and are highly dependent on the region in which the project is located. In many cases the cost of safety studies could equal that of total costs given in Table 2. These methods of rock breakage are in general only economically viable for the breaking of relatively large quantities of rock, as the cost of explosives has to be recouped from the operation. These costs indicate that nuclear explosives are probably cheaper for blasts greater than 10 kilotons but ANFO is cheaper for smaller blasts.

TABLE 1: COMPARISON OF EXPLOSIVE ENERGY COSTS*

Explosive	US$ Cost/10^6 Btu
TNT	115.00
Dynamite	100.00
Ammonia nitrate-fuel oil	30.00
10 kiloton nuclear explosive**	8.75
100 kiloton nuclear explosive**	1.12
1 megaton nuclear explosive**	0.145
2 megaton nuclear explosive**	0.075

* USAEC cost 1964.

** A kiloton is defined as a prompt release of 4×10^9 Btu or about the same amount of energy as 1000 tons of TNT. (Reproduced from Hardwick, 1967).

TABLE 2: COST OF NUCLEAR EXPLOSIVES

Explosive Yield kiloton	Cost US$*		
	Explosive	Other	Total
10	350 000	200 000	550 000
20	390 000	225 000	615 000
50	425 000	250 000	675 000
70	450 000	275 000	725 000
100	475 000	300 000	775 000

* USAEC cost 1964.
(Reproduced from Hardwick, 1967).

The approaches to breaking orebodies with explosives for *in situ* leaching can be divided into two categories. The first is the use of deeply buried (contained) explosions to produce chimneys of highly permeable rubble surrounded by fracture zones. This approach is applicable to relatively deeply buried mining deposits, overlain by a capping of barren rock or alluvium. The basic layout of such an operation is illustrated in Fig.4.

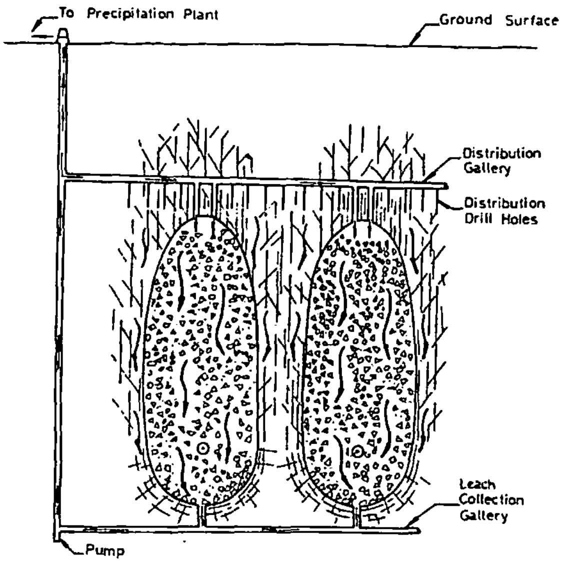

FIG.4: PRINCIPLES INVOLVED IN DEEP *IN SITU* LEACHING
Reproduced from *Hansen (1965)*

The second approach is to use explosives buried at intermediate-scale depths of burst, so that the mass of explosion-broken rock is exposed at the surface. This method produces substantially greater tonnages of broken rock for the same energy yield compared to explosion at greater depths. The utilisation of mineral deposits outcropping at the surface or buried at shallow depths for *in situ* leaching is illustrated in Fig.5.

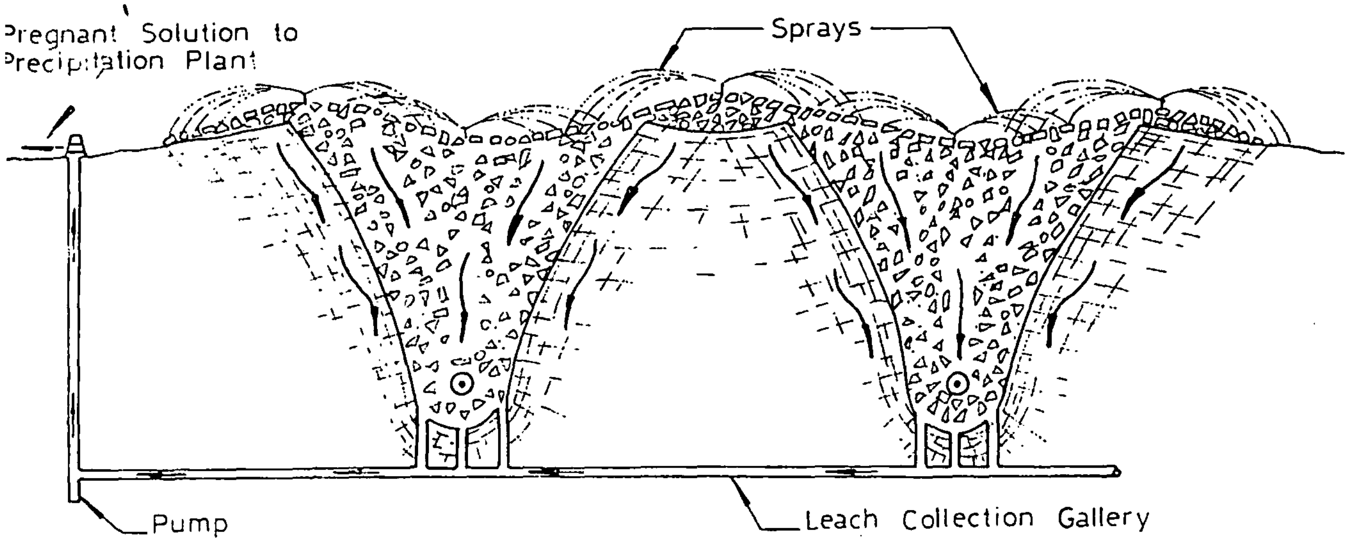

FIG.5: PRINCIPLES INVOLVED IN SHALLOW *IN SITU* LEACHING
Reproduced from *Hansen (1965)*

Safety Problems. The handling of explosives must be accomplished safely and the effects of the explosion anticipated and controlled. Nuclear explosives, because of the large amount of energy involved, amplify the safety problems connected with air-blast and ground-shock and introduce a new problem — radioactivity.

Air-blast from a surface explosion results from the rapid expansion of hot gases. The explosion causes a shock-wave to form in the air and move outward at high velocity. Waves move radially along the surface of the ground or may rise and be ducted and refracted by atmospheric conditions. The air-blast wave from a buried explosion may consist of two pulses, one resulting when ground-shock reaches the surface and one resulting when gases are vented. Both pulses decrease with charge burial, and the pulse caused by venting gases becomes zero when the explosion is completely contained. The zone of air-blast damage is normally inside the region of ground-shock damage.

Ground-shock results when the shock-wave caused by an explosion is transmitted outward through the rock. Particle velocity or acceleration in terms of gravity are used to measure particle motion. Damage appears as cracks and as structural deformation. It has been established (Hardwick, 1967) that a particle velocity of 5 cm/sec is a reasonable point of demarcation between shock levels in the safe zone and the damage zone. Because controlled chemical and nuclear explosions result in a significant air-blast and ground-shock in the immediate vicinity of the blast, they are limited to locations away from population centres.

The above two factors are important in considering the safety of chemical explosions. For nuclear explosions, radioactivity also has to be considered. For the purpose of fracturing, the explosive charge would have to be placed at a depth such that the radioactive products are completely contained or, at most, only an insignificant fraction escapes. When the explosion is completely contained, radiological safety problems encountered from activity will be introduced in the ore from the following sources:

(1) Radionuclides resulting from fission or fusion products of explosion.

(2) Radionuclides resulting from the activation by bombardment of the ore and materials in the nuclear explosive with neutrons released in the explosion (neutron activation products).

The radioactivity of a given radionuclide decays exponentially with time but the activity of daughter products may increase before decaying. Hansen (1965) gives a general rule for the decrease of radioactivity in the solidified melt (which contains essentially all of the radioisotopes) as follows: 'As the time increases by a factor of seven the level of radioactivity will decrease by a factor of ten'. For example, the solidified slag will be only one-tenth as radioactive seven months after detonation as it was at one month. It can thus be seen that advantage will be gained by postponing mining into the radioactive area for several months after detonation, but little further advantage will accrue from waiting several additional months.

The possibility of ground-water contamination by radioactive fission products has been studied (Hardwick, 1967). For deeply buried nuclear explosions, most of the radioactive fission products are trapped in the solidified glass in a non-water-soluble form and are thus prevented from contaminating ground water. The mechanisms of ion exchange, radioactive decay, dilution, and the typical slow movement rate of ground-water tend to limit spread of any radioactivity which does find its way into mobile water. Nevertheless, a study of ground-water movement and solution disposal will be mandatory.

Radiation hazards from radioactivity in recirculating solutions and through development openings in the shattered ground are not likely to be excessive (Hardwick, 1967). Similarly, contamination of the products in the case of copper is not expected to be a serious problem (details of the recovery of other elements are not available so it is not possible to pass comment).

Fracturing of the orebody by explosives produces broken ore of a similar size range to that used in heap leaching. Hence technology developed for heap leaching should be applicable to this type of operation. Heap leaching operations, which are outside the scope of this article, are well-documented (Rosenzweig, 1967; Robinson, 1972; Bruynesteyn and Cooper, 1974; Pizzaro *et al.*, 1974). The *in situ* leaching operation of solution inflow and outflow is illustrated in Figs 4 and 5 for two types of explosions.

The restriction of no chemical precipitation in the orebody during leaching is not so critical for fractured ores as for unfractured orebodies because of the substantially higher voidage (about 25%), so sulphide ores can be treated by this method. The *in situ* leaching of sulphide minerals justifies special comment because of the natural bacterial breakdown that occurs for the extraction of the valuable minerals. Investigators (Hansen, 1965) of bacterial leaching under conditions similar to those expected to exist in the environment of a nuclear chimney have indicated that *Ferrobacillus ferrooxidans* and *Thiobacillus ferrooxidans* can be expected to grow under these conditions. The small quantities of radioactive-explosion by-products present do not inhibit bacterial leaching, and the residual heat left in the rock surrounding the nuclear explosion, in most cases, should tend to stimulate, rather than inhibit, growth of the bacteria.

While the leaching characteristics of the fractured orebody should be similar to that of heap leaching, one basic difference between the techniques will be in the collection and recovery of solution. Heap leaching practice is to place the broken ore on an impervious prepared pad. This allows solution collection and recovery pipes to be laid on the pad under the ore. The *in situ* leaching technique has to rely on the rock strata to provide the boundary for solution distribution. Nuclear explosives create a relatively impervious dish of glassy solidified rock at the bottom of the rubble chimney. As has been previously stated, this solidified rock should aid in solution collection by forming an impenetrable boundary to the solution. Chemical explosions, not being nearly so intense as nuclear explosions, probably do not form significant quantities of glassy solidified rock.

However, the rock underneath the explosion should have low permeability in comparison to the broken rock and should act as a natural barrier, allowing at most a small leakage of leach solution. As there is insufficient information available on solution losses from producing *in situ* leaching operations (the above discussion is yet to be proved experimentally), the possibility has to be considered that the operation may be successful only if the ore is underlain by a relatively impermeable strata (as for unfractured orebodies).

While the use of chemical explosives for the shattering of orebodies does not appear to present any technical problems (Anon., 1972), there are still unanswered technical questions regarding nuclear explosions. As this latter method is at present untried, it needs further development before it can be recommended for commercial use.

2.2.3 Ore Subsidence Due to Conventional Mining in Adjacent Areas

This type of operation cannot be described as a technique because the subsidence (resulting in rock fracture) or caving-in of an area above old underground workings is generally not intentional. In other words, the subsidence can represent a bonus to other aspects of deposit exploitation. The type of leaching for this operation would be very similar to heap leaching or *in situ* leaching from broken ore by blasting. Solution inflow would be pumped into the deposit through pipes or sprays, and solution outflow would be through bore-holes sunk into the lowest points of the old workings below the broken ore. These old workings — tunnels, shafts, etc. would act as a sump for collecting the solution, and solution recovery should be high unless there are porous walls or faults in the workings.

This type of operation would represent a very low capital cost method of recovering values from the broken ores.

2.3 Stope Leaching

In mined-out areas of underground mines, significant quantities of low-grade material generally remain which cannot be recovered economically by more conventional methods. Many of these mines contain sulphides which readily oxidise on contact with air and water, producing acidic iron sulphate liquors. These liquors, or liquors with sulphuric acid added, when passed through the low-grade unfractured ore and broken ore left lying in the stopes, will leach-out a portion of the values. Solution recovery can generally be arranged by having the liquors drain into other stopes, tunnels or haulageways at lower levels in the mine. This solution is pumped to the surface for recovery of the valuable elements.

This type of operation, as with fracturing by ore subsidence, would represent a low capital cost method of recovering values from the residual and broken ore.

3. LEACHANTS

Because of solution recovery problems, the range of solvents used in solution mining is much more restricted than for other hydrometallurgical processes. In particular, reagents not dependent on recycle for economy of operation must be preferred. Only three leachants have been used in commercial operations — water (e.g., extraction of sylvite and evaporites), dilute sulphuric acid (uranium and copper) and acid ferric sulphate (uraniu produced by bacterial oxidation of iron sulphides in the ore. Other reagents have been recommended, e.g., ammonia-ammonium carbonate (Shoemaker, 1972), sodium carbonate (Anon., 1971a; Livingston, 1957). However, as far as is known to the author these have not been used commercially and it is probable that the potential high loss of reagents has precluded their use, though some reference has been noted to an *in situ* alkaline leach for uranium developed by Westinghouse.

Ammonia-ammonium carbonate is unlikely to be suitable under the circumstances proposed for the leaching of native copper (Shoemaker, 1972). This is an oxidation reaction (by oxygen from the air):

$$Cu^{\circ} + \tfrac{1}{2}O_2 + 4(NH_4)^+ \longrightarrow Cu\,(NH_3)_4^{++} + 2H^+ + H_2O$$

Under the conditions suitable for the above reaction to take place (cyclic flooding and drying in contact with air), free ammonia would escape with the air and would be very difficult to recover. However, an alternative would be to use ammonium carbonate for leaching with no free ammonia. This leachant has been found to be as active as ammonia-ammonium carbonate mixtures for dissolving copper (but with lower equilibria copper solubility).

It is very difficult to determine the circumstances in which ammonium carbonate, sodium carbonate and more expensive leachants could be used without extensive experimental programmes studying such factors as adsorption of reagents on the ore and overall solution recoveries.

The use of acid ferric sulphates produced by the bacterial oxidation of iron sulphides in the ore requires special circumstances. The basic oxidation process may be summarised as follows:

$$2FeS_2 + 2H_2O + 7O_2 \longrightarrow 2FeSO_4 + 2H_2SO_4$$

pyrite

$$Fe_7S_8 + H_2O + 15\tfrac{1}{2}O_2 \longrightarrow 7FeSO_4 + H_2SO_4$$

pyrrhotite

$$4FeSO_4 + 2H_2SO_4 + O_2 \longrightarrow 2Fe_2(SO_4)_3 + 2H_2O$$

or

$$6FeSO_4 + 1\tfrac{1}{2}O_2 + 3H_2O \longrightarrow 2Fe_2(SO_4)_3 + 2Fe(OH)_3$$

All of the above reactions use oxygen from the air, hence both oxygen and solution have to contact the ore. The best results are achieved by adopting a cyclic procedure of wetting and drying (or in contact with the air) of the ore. Two procedures are commonly used in heap leaching — cyclic flooding and draining of the orebody, and the use of water sprays to continuously spray the ore (partially soaking the ore).

Because precipitation of iron hydroxides and basic sulphates can occur, it is unlikely that the *in situ* leaching of sulphides or mixed oxide-sulphide orebodies could be carried out on unfractured orebodies.

4. EXAMPLES OF *IN SITU* LEACHING OPERATIONS

4.1 Unfractured Orebodies

The uranium-extraction operations of Shirley Basin Mines, Utah Construction and Mining Co. (Anderson and Ritchie, 1968), is unique in that it is the only *in situ* leaching operation of unbroken ore in place.

Conditions considered favourable for the use of solution mining for this operation are detailed in Section 2.1.

A pattern of inflow and outflow wells was chosen as the method for solution dispersal and recovery. The design was based on the assumption that natural ground-water could be made to act as a containment shell for the leaching solutions. An experimental programme of various test drill-hole patterns showed that, provided the optimum pattern geometry was used, solution recovery was very high.

The optimal design is based on the fact that inflow between wells in an aquifer having regional flow can be controlled by varying inflow-effluent rates, by distances between wells, and by aligning wells at specific angles to the direction of ground-water flow. The present pattern used at Shirley Basin Mines consists of three inflow wells upstream from a production well, with the centre inflow well directly upstream of the regional ground-water flow direction. The remaining two inflow wells are located on radii diverging at an angle of 75° from one another, equally spaced from the centre inflow well. Distances from inflow wells to the production wells are about 6 metres (see Fig.6).

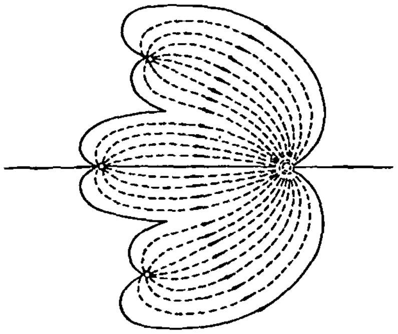

FIG. 6: THE WELL PATTERN CURRENTLY USED AT SHIRLEY BASIN MINES CONSISTS OF THREE INFLOW WELLS LOCATED UPSTREAM IN THE REGIONAL GROUND-WATER FLOW FROM *A PRODUCTION WELL. THE CENTRE WELL IS DIRECTLY* UPSTREAM AND THE OTHER TWO WELLS ARE ON RADII DIVERGING AT AN ANGLE OF 75° FROM ONE ANOTHER. INFLOW WELLS ARE 6m FROM THE PRODUCTION WELL.

Reproduced from Anderson & Ritchie (1968)

Well drilling and development was found to be important for satisfactory operation of the solution mining pattern. Except for the finished diameter, the procedure for drilling and completion of inflow and production wells is the same. Wells are first pilot-drilled and probed, after which they are reamed to take the required casing. Inflow well casing is 75-mm diameter stainless-steel and production well casing is 0.2-m diameter with stainless-steel on the bottom 12 m. Screens are placed in the ore zone in all wells. The wells are developed by means of a high-pressure jet, this treatment being continued until the wells are capable of a satisfactory rate of inflow by water test.

Pattern operation starts with the introduction of leaching solution to the three inflow wells and simultaneous pumping in the production well at a rate which barely exceeds total input to the inflow wells. Patterns start with an acid inflow of 1 to 1.5 g/*l* until titratable acid is measured in the effluent, at which time the concentration of sulphuric acid is increased in increments to a maximum of 5 g/*l*. After an acid condition has been established in the pattern network, uranium leaching is enhanced by the addition of small quantities of sodium chlorate. Flocculant addition (5 to 10 ppm) has been infrequently used to promote solution flow in less permeable formations.

Uranium values generally have been found to appear in the effluent in less than 48 h and the uranium concentration continues to build up for about a week before remaining constant at about 0.2 to 0.3 g/*l*. Towards the end of the life of the well (greater than one month), the uranium concentration drops off. A number of patterns are operated simultaneously. After a pattern has been finished, pumps,screens and casings are salvaged.

Uranium is recovered from pregnant solution by means of ion exchange columns. Stripping of uranium from the ion exchange resin is by a mixture of nitric acid, sodium nitrate and sulphuric acid. The strip solution is precipitated with dolomitic lime or magnesia slurry. The barren solution emanating from the top of the column is discarded as waste, since while it contains some acid it cannot be recycled underground because of its dissolved calcium content.

4.2 Nuclear Blasting

While this technique has received considerable publicity in the sixties (Hansen, 1965; Wilson, 1965; Hardwick, 1967; Jackson, 1967; Chopey, 1968) and a submission by Kennecott Copper Corporation (Anon., 1967b,c) to the USAEC for a joint US$13 million* contained nuclear blast and solution mining experiment at its Safford Arizona Copper porphyry deposit, no proposals have reached fruition. One probable reason for this is the pressure on the US government by environmentalists who do not share the overall view expressed by researchers in the field that, if the proper precautions are taken, then it is most unlikely that radiation levels from adjacent ground-water, etc., will be hazardous.

---

* 1967 Costs.

4.3 Chemical Blasting

Chemical blasting is a very common practice in the mining industry; however, it appears that there are only two cases where this technique has been used to fracture an orebody for *in situ* leaching.

Ranchers Exploration and Development Co. detonated 2000 tonnes of ANFO (ammonium nitrate-fuel oil) to fracture 4 million tonnes of 0.8% copper ore located in an area 120 m in diameter and 100 m deep (Anon., 1972). The orebody is remotely located in Arizona so that damage from the blast was minimal. As the orebody was located near the surface, it was possible to fracture the whole orebody with a moderate amount of explosive. The orebody had been partially worked as an underground operation and it was possible to use old shafts and adits to place the charge at three different levels. About 590 tonnes were located at the bottom level, 950 tonnes at the middle level and 370 tonnes at the upper level.

Preliminary measurements of the effects of the blast indicate that breakage of the rocks resulted in fragments measuring 220 mm or less.

The area above the deposit was terraced, and perforated pipes were laid on the terraces for irrigation of the orebody. Recovered solution from percolation was led to a storage area for pumping to a precipitator plant. About 4 million kg of copper was estimated to be recoverable in the form of cement copper over a period of five years.

Soakage of the complete orebody with liquor acidified to pH 2 took about six months to complete (Longwell, 1974). Following this period, solution recovery averaged about 97%. Production of copper started after four months and reached plant design level eight months later. Acid consumption for the production of copper for the first ten months of operation was 5.17 kg/kg Cu. However, the acid consumption is expected to decrease with time as the acid-consuming gangue materials in the orebody are depleted and acid generation by the bacterial action on the sulphides present in the ore is initiated. Ferric iron first appeared eight months after soakage of the ore commenced (this is evidence of bacterial action in the ore).

Ranchers Exploration and Development Co. detonated 200 tonnes of explosives (ANFO) to fracture 600 000 tonnes of low-grade copper ore (mixed oxide-sulphide ore) at Big Mike, Nevada (Anon., 1972). Fracturing was considered excellent, giving an average rock size of about 220 mm. In an effort to expedite the project, sprinkling of the broken ore was started prior to completing drilling of the recovery well. This assured a saturated orebody and immediate production once the recovery well pump was made operational. Liquor of 2 g/*l* Cu concentration is being produced and recovered in a standard iron launder precipitation plant. Good overall solution recoveries are expected because of tight formation around the orebody and low-permeability material at the bottom of the deposit.

The cost of setting up the operation was US$300 000.

4.4 Ore Fractured by Subsidence

The first significant application of leaching rock *in situ* was at the Ohio copper mine, Utah, in 1922 (Anderson and Cameron, 1926). After mining by the block caving method was terminated, an inverted cone of broken rock from a cave-in containing about 38 million tons remained. Water, applied to the top of the broken rock, percolated down through the copper-bearing rock and collected in an adit below. The copper was recovered by precipitation. After the success at the Ohio copper mine, *in situ* leaching was generally attempted and often succeeded on large masses of broken copper-bearing rock remaining after large-scale mining operations were terminated.

An open drainage *in situ* leach method is successfully used for the recovery of copper at the Miami mine of Tennessee Corporation in Gilo County, Arizona (Hardwick, 1965). During the active life of the Miami mine, ore was mined by the block-caving method and subsidence resulted in a crater of about 500 m in diameter and 100 m deep. From this crater, broken rock extends downwards to the mining levels. Sulphuric acid is added to water (made up to 0.5%) and the solution flows by gravity in plastic pipes to points of application. Ponds, drillholes, and sprays are used to introduce the solution into the ground. A cyclic operation of liquor application is used; it requires three to four weeks after a spray is turned on the surface before the solution percolates through the broken rock and comes through on the 1000 level. The flow stops about two weeks after the spray is turned off. The first solution emerging is high in copper content. The spray is left in one place until pregnant solution grade drops below 1.5 g/*l* Cu. The spray is then turned off and the area allowed to dry. Drying and wetting periods are alternated. The solution is collected on the 1000 level and pumped to a precipitation plant on the surface where it passes through cells containing detinned shredded cans. About 9000 tonnes of copper per year are produced from the *in situ* leaching of broken ore at this property.

A flood leaching method is used in a combined dump and *in situ* leaching operation for the recovery of copper at Ray Mines Division of Kennecott Copper Corporation in Arizona (Thomas, 1938). During the active life of the mine, the block caving method was used and subsidence resulted in an elongated crater 300 m wide by 600 m long and 45 m deep. When a nearby open pit was stripped, material containing some leachable copper was used to fill this crater. The bottom of the ore is well below ground-water level, and the rock surrounding the broken ore in workings is tight and impermeable. The workings are maintained in a flooded condition throughout the year. Copper-bearing solution is pumped from the flooded mine at three points by submersible pumps in shafts and drillholes connected with the under-ground workings. About 500 k*l*/h is pumped and passed through a precipitation plant where the copper is removed. Spent solution is returned to the flooded mine.

4.5 Stope Leaching

Stope leaching was practised at Stanrock Mines Eliot Lake District of Ontario, Canada (MacGregor, 1966, 1969a,b; Anon., 1967a). Old mined-out stope areas were washed with high-pressure water (500 to 700 kPa) and the cycle repeated every three months. On 1200 stopes with an average of

550 m^2 floor area, the production rate has been approximately 80 tonnes/annum. During the leaching process, visible alterations occurred and these phenomena were an indication of the leaching process. In the first stage, oxidation of the sulphides to sulphates produced a dark (almost chocolate) brown colouration on the walls and floors. As uranium oxidised, a bright yellow bloom appeared through the brown coating, indicating the characteristic colour of yellow cake. Bacteria were considered to play an important part in the leaching process.

The loaded mine solution of about 0.1 to 0.2 g/*l* U_3O_8 collected in stopes below the injection points, was fed directly to mill Pachucas. Overflow from these units was transferred to clarification tanks where fine suspended silica was removed, before it was routed to an ion exchange circuit for uranium capture on resin. Uranium was eluted from the resin periodically and thereafter precipitated as yellow cake with ammonia.

Since mine waters at Stanrock contained appreciable quantities of thorium and rare earths in addition to the uranium content, their recovery was also possible.

Stope leaching is also practised at Denison Mines Ltd, Eliot Lake District, Ontario, where this operation is but a minor adjunct to its conventional mining programme. A lawn sprinkler system has been installed in the stopes.

Bacterial and sulphuric acid leaching of worked-out stopes were investigated at Milliken Mines, Rio Algon Mines Ltd, Eliot Lake District of Ontario. Over a period of one year, about 60 tonnes of U_3O_8 were produced — but the technique was discontinued.

In Australia, copper is recovered from mine waters by cementation at Peak Hill, NSW, and Wee MacGregor Mine, near Mt Isa, Queensland. There would be other operations of a similar nature producing minor quantities of copper.

5. CONCLUSIONS

The following conclusions have been drawn from the literature survey:

(1) *In situ* leaching has been applied to the recovery of copper, uranium and evaporites.

(2) *In situ* leaching operations can be divided into the following types — unfractured orebodies, fractured orebodies and stope leaching.

(3) Solution mining from unfractured orebodies consists of inflow and outflow bore-holes. Because of solution recovery and other associated problems, certain criteria have to be met for solution mining to be successful. These are that the mineral values should occur in a generally horizontal bed underlain by a relatively impermeable stratum, the ore must occur below the static water table, and the direction and velocity of regional water must be known.

Also, chemical precipitation in the orebody should not be allowed to occur. Low solution recovery and poor permeability would represent the two major reasons for this method not being widely used.

(4) Fracturing of orebodies can be accomplished by hydraulic means, by chemical or nuclear blasting or by ore subsidence due to conventional mining in adjacent areas. Solution mining operations using hydraulic fracturing techniques probably face the same restrictions as operations on unfractured orebodies. Solution recovery of the other types of fractured ores should not present the same problem as for unfractured ore or hydraulically-fractured ore operations. Similarly, chemical precipitation in the ore is probably only a problem with unfractured or hydraulically-fractured ore.

(5) Chemical and nuclear blasting of orebodies are probably only economically viable for the breaking of large tonnages of ore. Because of safety problems associated with the blast, these operations cannot be located near population centres.

(6) Because of the similar size-range of broken rock, dump leaching technology is also applicable to *in situ* leaching of ore broken by blasting and subsidence.

(7) Solution recovery from *in situ* leaching of subsided ores and stope leaching is simplified by collecting in shafts, tunnels and slopes below the area being leached.

(8) Published information on many of the different techniques of solution mining is rather sketchy and there appears to be a lack of proper understanding of many of the complexities of the operations. This is basically due to the fact that *in situ* leaching is still in the development stage.

The following aspects require evaluation:

(a) For unfractured orebodies: What is the optimum well spacing and pattern for various different orebodies? Can natural fracture systems be used as effective aids in the control and containment of leach solutions? What is the effect of natural ground-water flow on flood pattern efficiency? Can hydraulic fracturing offer a cheap method of greatly increasing the permeability of the ore? What effect does ore inhomogeneity have on the operation?

(b) For fractured orebodies: What is the optimum explosive placement, charge size and explosive type? What size of broken rock is required for an adequate leaching rate? Many of the questions in (a) are also applicable.

6. ACKNOWLEDGEMENT

This article represents part of a study supported by the Department of Mines of South Australia.

7. REFERENCES

ANDERSON, A.E., and CAMERON, F.K. (1926). Recovery of copper by leaching: Ohio Copper Co. of Utah. *Trans. AIME,* 73, 31.

ANDERSON, J.S., and RITCHIE, M.I. (1968). Solution mining of uranium. *Min. Congr. J.,* 20.

ANON. (1964). Engineering with nuclear explosive. *Chem. Engng,* 71(14), 117.

ANON. (1967a). Mining *in situ* by Nature's easy way. *Engng Min. J.,* Oct., 75.

ANON. (1967b). Kennecott proposes nuclear mining experiments of Safford deposit. *Soc. Min. Engrs,* Nov., 66.

ANON. (1967c). Kennecott sets sight on nuclear test for *in situ* recovery of copper. Engng Min. J., Nov., 116.

ANON. (1971a). Underground uranium ore leaching. *Min. Mag., Lond.,* 124, 117.

ANON. (1971b). *In situ* leaching: pilot-plant tests on copper extraction. *Min. Mag., Lond.,* 125, 27.

ANON. (1972). Rancher's big blast shatters copper orebody for *in situ* leaching. *Engng Min. J.,* April, 98.

BRUYNESTEYN, A., and COOPER, J.R. (1974). Leaching of Cananea ore in test dumps. *Solution Mining Symposium,* 103rd AIME Annual Meeting, Dallas, Texas. 268-92.

CHOPEY, N.P. (1968). Will nuclear blasts reverberate in the CPI? *Chem. Engng,* 75(6), 88.

DANESHY, A.A. (1974). Principles of hydraulic fracturing. *Solution Mining Symposium,* 103rd AIME Annual Meeting, Dallas, Texas. 15-32.

DEW, J.N., and MARTIN, W.L. (1960). *In situ* roasting and leaching of uranium ores. *US patent* 2,954,218.

FITCH, J.L., and HURD, B.G. (1966). *In situ* leaching method. *US patent* 3,278,232.

FITCH, J.L., and HURD, B.G. (1967). Method of leaching subsurface minerals *in situ.* *US patent* 3,309,141.

GARDENER, J., and RITCHIE, M.I. (1967). Leaching of uranium ore *in situ.* *US patent* 3,309,140.

HANSEN, S.M. (1965). Nuclear blasting for mining and leaching. *Wld Min.* Sept., 56.

HARDWICK, W.R. (1965). Block caving copper mining methods and costs at the Miami Mine, Miami Copper Co., Gila County, Arizona. *US Bur. Min.,* IC 8271.

HARDWICK, W.R. (1967). Fracturing a deposit with nuclear explosives and recovering copper by the *in situ* leaching method. *US Bur. Min.*, RI 6996.

HURD, B.G., and FITCH, J.L. (1966). *In situ* leaching of subterranean deposits. *US patent* 3,278,233.

JACKSON, M.W. (1967). Ten years of plowshare. *Civil Engng — ASCE*, Dec., 34.

LEWIS, A.E., BRAUN, R.L., SISEMORE, C., and MALLON, R.G. (1974). Nuclear solution mining: breaking and leaching considerations. *Solution Mining Symposium*, 103rd AIME Annual Meeting, Dallas Texas, 56-75.

LIVINGSTON, C.W. (1957). Method of mining ores *in situ* by leaching. *US patent* 2,818,240.

LONGWELL, R.L. (1974). In-place leaching of a mixed copper orebody. *Solution Mining Symposium*, 103rd AIME Annual Meeting, Dallas, Texas. 233-42.

MacGREGOR, R.A. (1966). Recovery of U_3O_8 by underground leaching. CIM Bull., May, 583.

MacGREGOR, R.A. (1969a). The bacterial leaching of uranium. *Nucl. Appl.*, 6, Jan., 68.

MacGREGOR, R.A. (1969b). Uranium dividends from bacterial leaching. *Soc. Min. Engrs*, March, 54.

MARTIN, J.M. (1964). Recovery of uranium by carbonated water and surface action agents and wetting agents. *US patent* 3,130,960.

PIZARRO, R., McBETH, J.D., and POTTER, G.M. (1974). Heap leaching practice at the Carlin Gold Mining Co., Carlin, Nev. *Solution Mining Symposium*, 103rd AIME Annual Meeting, Dallas, Texas, 253-67.

ROBINSON, W.J. (1972). Finger dump preliminaries promise improved copper leaching at Butte. *Soc. Min. Engrs*, Sept., 47.

ROSENZWEIG, M.D. (1967). New copper technology is winning the ore. *Chem. Engng*, 74(25), 88.

SHOCK, D.H., and CONLEY, F.R. (1974). Solution mining: its promise and its problems. *Solution Mining Symposium*, 103rd AIME Annual Meeting, Dallas, Texas, 79-97.

SHOEMAKER, R.G. (1972). Ammonia revival for the Keweenaw. *Min. Engng Soc.*, May, 45.

SIEVENT, J.A., MARTIN, W.L., and CONLEY, F.R. (1970). *In situ* leaching of uranium. *Soc. of Min. Engrs.* Presented at the SME Fall Meeting, St Louis, Missouri.

THOMAS, R.W. (1938). Leaching copper from worked-out areas of the Ray Mines, Arizona. *Min. metall. J.*, Nov., 481.

WARD, M.H. (1974). Surface blasting followed by *in situ* leaching, Big Mike Mine. *Solution Mining Symposium*, 103rd AIME Annual Meeting, Dallas, Texas, 243-51.

WILSON, A.R.W. (1965). Peaceful uses of nuclear explosives — an evaluation for Australian purposes of proposed civil engineering and mining application. *AAEC* (SP)/pl.

Solution Mining

William A. McKinney
Research Supervisor,
USBM

Increased pressure to develop technology for the recovery of metals and minerals with minimum pollution of the environment resulted in many new developments in solution or chemical mining in 1972. This was apparent in the number of new field applications of true solution mining or in situ leaching of copper ores.

Probably the most important development in solution mining in 1972 was the fracturing of an entire copper ore-body with conventional explosives followed by leaching of the ore in place.[1,2] On March 9, the largest nonatomic blast ever set off in the United States marked the beginning of a novel in situ leaching operation by Ranchers Exploration and Development Corp. at the previously worked Old Reliable copper mine about 50 mi northeast of Tucson, Ariz. E. I. DuPont de Nemours and Co., operating jointly with Ranchers, furnished and directed placement of 2000 tons of explosive which were detonated to fracture a compact 4-million ton pipe-like deposit of oxidized and secondarily enriched copper. Following the blast, the rubble was terraced and perforated pipes were placed on the terraces for leaching of the broken ore. A precipitation plant was constructed to recover copper from leach liquors. Leaching was started in August 1972. It is estimated that 30 million lb of copper will be recovered over a period of 5 yr. A cost of $1.7 million was given for bringing the property into production. If the expected low cost production of copper is achieved, similar ore bodies would be exploited by the technique in the future.

In another joint venture, Asarco and the Dowell Division of Dow Chemical Co. are planning to leach copper in situ from a copper oxide ore body near Florence, Ariz.[3] Dowell will use hydraulic fracturing techniques developed in oil field work to fracture the deposit. Then acid solutions will be injected through drill holes, leach liquor recovered from a producing well and copper recovered by electrowinning. Sufficient results should be available for an evaluation of the method in 1973.

Near Mountain City, Nev., Cleveland-Cliffs Iron Co. and Dupont are engaged in a project to recover copper by in situ leaching of old underground mine workings and an adjacent fractured and caved ore body. Dewatering of the underground mine is nearly complete after which the mine will be allowed to aerate. Leach solutions will be percolated downward through the chalcocite-bearing stope backfill in early 1973 to extract the copper. Future plans are to drift out from the 600-ft level of the mine shaft below an adjacent 7-million ton chalcocite-bearing ore body, fracture the ore with conventional explosives, allow broken ore to cave into the cavity created by drifting and undercutting and introduce leach solutions via holes drilled through about 300 ft of overburden to extract the copper. This latter operation will be similar to the in place leaching of the block caved Miami mine in Arizona which has been producing copper since 1941.[4]

A recent paper describes a possible method for revitalizing the native copper mines of the Keweenaw Peninsula of upper Michigan.[5] The article suggests that low grade stope fill, caved backs and crushed pillars might be leached in place using cupric ammonium carbonate and the copper recovered from the ammoniacal leach liquor by solvent extraction and electrowinning.

Improved Dump Leaching

In addition to the new in situ leaching developments, there is continued interest in improving dump and heap leaching of copper ore and open pit strip waste. Finger dump leaching as practiced at Anaconda's Butte, Mont., operations results in improved permeability to air and leaching solutions.[6] This method of dump emplacement appears to give 50% higher copper extraction than that obtained from conventional dumps.

The USBM is investigating another method for improving dump permeability and recovery of not only copper but also associated by-products.[7] The process comprises screening of enriched fines from coarsely crushed mine waste, froth flotation for prompt recovery of copper and such by-products as molybdenum, gold and silver, all of which are lost in conventional dump leaching and dump leaching of the residual coarse rock to extract some of the remaining copper. In addition to early recovery of copper and by-products, the combination of fines flotation and coarse fraction leaching has resulted in overall copper recoveries that in many cases were double those obtained by conventional leaching for one year.

Much remains to be learned about solution flow during leaching of copper waste dumps. In a recent study at the Phelps Dodge Corp.'s Bisbee operation, churn drill holes were logged with geophysical instruments to provide information on internal dump conditions.[8] Several means of directing leach solution to unleached portions of the dump were suggested.

A novel method for heap leaching of copper oxide ore was evaluated on a 1200-ton dump at Gaspe Copper Mines Ltd. in Canada.[9] Pyrite concentrate was added to the dump and acid was generated in situ by oxidation assisted by bacterial action. It was concluded that pyritic leaching offers some advantages over acid leaching.

Bacterial activity during solution mining continues to hold considerable interest. The role of microorganisms in altering minerals by oxidation or reduction during leaching was reviewed by Malouf.[10] The practical value of operating sulfide leach dumps under conditions evolving from the British Columbia Research microbiological leaching research program is being evaluated on three 6000-ton test dumps.[11]

The chemistry operative in dump leaching was treated by Wadsworth, Baur and associates in studying oxygen consumption and the kinetics of chalcopyrite dissolution.[12,13]

The other major commercial application of solution mining is the extraction of potash from bedded deposits. Conversion of Texas Gulf Inc.'s Cane Creek potash mine near Moab, Utah, from conventional mining to solution mining was completed in March 1972.[14] After terminating unprofitable underground mining operations in 1970, the mine workings, consisting of some 430 mi of tunnels, were filled with water from the Colorado River. The water dissolves the sylvanite and brine is pumped to solar evaporation ponds. After evaporation, the potash-sodium chloride salts are harvested using scrapers with depth of cut controlled by a laser beam. Harvested salts are slurried in spent brine and pumped to the original mill for processing by flotation.

Solution Mining

A simple solution mining method is outlined and methods for recovering potash from brine are discussed in a recent article by Husband.[15] The mechanism for solution of salt and mixed halides of sodium and potassium is reviewed in a report by Jessen.[16] In this paper, the parameters influencing type and shape of cavity formed with single well or multiple well systems are examined. Jacoby[17] describes and gives examples of the use of solution-mined salt cavities for storage of liquid petroleum gas, natural gas and other hydrocarbons, storage of radioactive wastes and surge vessels for air compressed by electric utilities during off-peak hours. The use of an articulated platform for offshore solution mining of sulfur, potash or salt is proposed by Dravo Ocean Structures.[18]

Fundamental research in solution mining is being carried out at New Mexico Institute of Mining and Technology. A computer model was developed and used to simulate several examples of leach solution flow through a layered leach dump.[19] The simulation studies have revealed a new method to find areas of channeling and impermeable lenses